

Augmented Control for Flexible Operation of Wind Turbines

Adam Stock

A thesis presented in fulfilment of the requirements for the
degree of Doctor of Philosophy

Industrial Control Centre
Department of Electronic and Electrical Engineering
University of Strathclyde
Glasgow G1 1XW
Scotland, UK

June 2015

This thesis is the result of the author's original research. It has been composed by the author and has not previously been submitted for examination which has led to the award of a degree.

The copyright of this thesis belongs to the author under the terms of the United Kingdom Copyrights Act as qualified by University of Strathclyde regulation 3.50. Due acknowledgements must always be made of the use of any material contained in, or derived from, this thesis.

Dedicated to Bryony, Finlay, and Eleanor

“Wisdom comes from experience. Experience is often a result of lack of wisdom.” – *Terry Pratchett*

Acknowledgements:

As with all acknowledgement lists there will be people not listed who should be, but there is definitely no one mentioned here who does not thoroughly deserve it. First and foremost, thank you to my surprisingly patient wife Bryony for her love and support over the last few years and especially during the prolonged writing up period, and thank you to Finlay, my son, and Eleanor, my daughter, for brightening my day every time I got home. Thank you to Professor Leithead for his excellent advice throughout the PhD (even when it meant hours or days more work!). Thank you must go to my mum and dad for all their love and support over the past 30 years! Thank you also, to Fraser and Lizzie, my in-laws who have provided (amongst other things) much needed child care for Finlay and pre-cooked meals for me and Bryony. Thank you to all my colleagues at Strathclyde University and throughout academia, particularly (in no particular order) Hong Yue, David Thompson, Han Yi, Sung Ho Hur, Charlie Plumley, Kamila Nieradzinska, Iain Morrison, Lourdes Gala-Santos, Saman Poushpas, Julian Feuchtwang, Simon Gill, Velissarios Kourkoulis, Alex Giles, Sheila Campbell, and Drew Smith. Finally, thanks to all my friends to whom I may have complained about work.

Abstract

In this thesis a novel controller for providing greater flexibility of operation of wind turbines known as the Power Adjusting Controller (PAC) is presented. The controller takes the form of an augmentation to a wind turbine's full envelope controller, allowing it to be applied to any horizontal axis, pitch regulated, variable speed wind turbine.

Conventional wind turbine control seeks to maximise the power output of a wind turbine whilst minimising the loads on the turbine, controlling on the error in generator speed via demands to the blade pitch actuator and generator torque actuator.

The PAC uses additions to the full envelope controller inputs and outputs to alter the power output of the turbine by an additional input value ΔP . It is ensured that the operation of the full envelope controller is not compromised by the PAC.

Testing of the PAC using lumped parameter models of wind turbines and full aero-elastic models makes clear a requirement for a wind speed estimator within the PAC that incorporates the effects of dynamic inflow. A novel wind speed estimator that accounts for dynamic inflow by redefining blade element momentum theory solely in terms of the dynamics at the rotor is therefore developed and incorporated into the PAC.

Limits are designed to ensure that the operating point of a wind turbine with the PAC is kept within a safe operational envelope, and a system of flags and sub-flags is developed to allow easy integration of the PAC into a hierarchical wind farm control structure. The effect of using the PAC on the wind turbine loads is investigated, with the ultimate loads introduced by operation of the PAC found to be within the range of normal operating loads and the impact of prolonged reduction of the power output found to reduce the lifetime damage equivalent loads in most cases.

Two applications of the PAC, namely providing synthetic inertia and providing droop control, are presented, with the PAC shown to be able to match the performance of conventional synchronous plant in both cases. It is shown that neither application causes ultimate loads outside of the range of normal operation and that providing droop control reduces the lifetime damage equivalent loads.

List of Contents

ABSTRACT	III
LIST OF CONTENTS	V
NOMENCLATURE.....	IX
CHAPTER 1: INTRODUCTION	1
1.1 OVERVIEW OF THE THESIS	1
1.2 CONTRIBUTIONS TO KNOWLEDGE	2
1.3 PUBLICATIONS.....	3
CHAPTER 2: OVERVIEW OF WIND ENERGY	4
2.1 THE DEVELOPMENT OF THE MODERN WIND TURBINE AND WIND FARM	4
2.2 CONVENTIONAL WIND TURBINE CONTROL	7
2.2.1 <i>Typical Strategies for Variable Speed, Pitch Regulated Turbines</i>	8
2.2.2 <i>Minimising Loads through Wind Turbine Control</i>	9
2.3 SEPARABILITY	11
2.4 GAIN SCHEDULING	17
2.5 WIND TURBINE AERODYNAMICS.....	19
2.5.1 <i>What is Wind Speed?</i>	19
2.6 BLADE ELEMENT THEORY	19
2.7 MOMENTUM THEORY	21
2.8 BERNOULLI’S PRINCIPLE	22
2.8.1 <i>Non-Rotating Stream Tubes</i>	22
2.8.2 <i>Rotating Stream Tubes</i>	23
2.9 BLADE ELEMENT MOMENTUM THEORY (BEM)	24
2.9.1 <i>BEM – Non-Rotating Stream Tubes</i>	24
2.9.2 <i>BEM – Rotating Stream Tubes</i>	26
2.9.3 <i>Standard BEM</i>	27
2.10 AERODYNAMIC COEFFICIENT MODELS	28
2.11 SINGLE STREAM TUBE AERODYNAMIC COEFFICIENT MODELS	30
2.12 OVERVIEW OF AERODYNAMICS DISCUSSED	31
2.13 SIMULATION ENVIRONMENTS.....	32
2.13.1 <i>Basic First Order Model</i>	32
2.13.2 <i>Control Model</i>	33

2.13.3	<i>Aero-Elastic Model</i>	35
2.13.4	<i>Examples of Each Model</i>	35
CHAPTER 3: FLEXIBLE OPERATION OF WIND PLANT		38
3.1	WHY IS FLEXIBLE OPERATION NECESSARY?	38
3.2	WIND TURBINES AND GRID FREQUENCY.....	41
3.3	DESIGN AND DEVELOPMENT OF AUGMENTED CONTROLLERS.....	43
3.4	AUGMENTED CONTROLLERS IN THE LITERATURE.....	54
3.4.1	<i>Summary of Literature</i>	68
3.5	REQUIREMENTS FOR AN AUGMENTATION TO A WIND TURBINE CONTROLLER	69
3.6	THE POWER ADJUSTING CONTROLLER CONCEPT	69
3.7	THE ROLE OF THE POWER ADJUSTING CONTROLLER AS PART OF A WIND FARM CONTROL HIERARCHY	73
CHAPTER 4: DEVELOPMENT OF THE POWER ADJUSTING CONTROLLER		76
4.1	DEFINITIONS OF VARIABLES	76
4.2	DESIGN OF THE POWER ADJUSTING CONTROLLER.....	77
4.3	PITCH CONTROLLER DESIGN.....	92
4.4	LINEARISATION OF THE PAC CONTROLLER	92
4.5	RETURNING TO NORMAL OPERATION – THE RECOVERY PROCESS.....	98
4.5.1	<i>Torque Demand Action</i>	99
4.5.2	<i>Pitch Demand Action</i>	100
4.5.3	<i>Varying the Speed of Recovery</i>	100
4.6	MODELLING OF THE POWER ADJUSTING CONTROLLER	101
4.6.1	<i>Required Variables</i>	101
4.7	TESTING OF THE PAC	102
4.7.1	<i>Change in Power Sample Signals</i>	103
4.7.2	<i>Simulink Simulations</i>	104
4.7.3	<i>Bladed Simulations</i>	134
4.8	CONCLUDING REMARKS	141
CHAPTER 5: DEVELOPMENT OF AN IMPROVED WIND SPEED ESTIMATOR		143
5.1	BEM REFORMULATED LOCALLY TO THE ROTOR DISC	144
5.2	MODELLING OF DYNAMIC INFLOW EFFECTS	147
5.3	APPLICATION OF THE DYNAMIC INFLOW MODEL TO THE SIMULINK WIND TURBINE MODEL	151
5.3.1	<i>Calculating the Steady State Induction Factor</i>	151
5.3.2	<i>Calculating the Unsteady Induction Factor</i>	151
5.3.3	<i>Calculating the Aerodynamic Torque</i>	152
5.3.4	<i>Demonstration of the implementation of Dynamic inflow to the Simulink Model</i>	152

5.4	INCORPORATING THE DYNAMIC INFLOW EFFECTS INTO THE PAC	155
5.4.1	<i>Calculating an Estimate of the Wind Speed at the Rotor in its Absence</i>	156
5.5	CALCULATION OF THE CHANGE IN AERODYNAMIC TORQUE	156
5.6	DESIGN AND ANALYSIS OF THE PAC CONTROLLER	157
5.6.1	<i>Controller Design</i>	159
5.7	EVALUATION OF THE EFFECT ON INCORPORATING DYNAMIC INFLOW ON PAC PERFORMANCE	173
5.8	CONCLUDING REMARKS	176
CHAPTER 6: EVALUATION OF THE PAC'S PERFORMANCE		177
6.1	CONTROL IN DISCRETE TIME	177
6.2	ANTI-WIND UP	180
6.2.1	<i>Rearrangement of Transfer Functions to Allow Back Calculation</i>	181
6.2.2	<i>Position Limits</i>	182
6.2.3	<i>Rate Limits</i>	183
6.3	APPLICATION OF THE PAC USING BLADED	185
6.3.1	<i>Tuning the PAC to Bladed</i>	191
6.4	PERFORMANCE COEFFICIENT TABLES	194
6.5	IMPACT OF THE USE OF THE PAC ON LOADS ON THE WIND TURBINE	195
6.5.1	<i>Ultimate Loads</i>	196
6.5.2	<i>Fatigue Loads</i>	204
6.6	CONCLUDING REMARKS	216
CHAPTER 7: PAC SUPERVISORY RULES		219
7.1	THE RECOVERY PROCESS AND THE REJECTION FLAG	222
7.2	HARD LIMITS ON THE PROVISION OF A CHANGE IN POWER OUTPUT ("BLACK LIMITS")	222
7.3	SOFT LIMITS ON THE PROVISION OF A CHANGE IN POWER OUTPUT ("TRAFFIC LIGHT LIMITS")	225
7.3.1	<i>Maximum and Minimum Change in Power</i>	226
7.3.2	<i>Response of the WFDC to Operation within the Red and Amber Zones</i>	226
7.3.3	<i>Limit to the Rate of Change of Power</i>	228
7.4	ADDITIONAL LIMITS ON THE PROVISION OF A CHANGE IN POWER OUTPUT	228
7.4.1	<i>Limiting Operation due to High Turbulence</i>	228
7.4.2	<i>Limitation due to Wind Speed</i>	229
7.4.3	<i>Limiting Operation due to Saturation of the Pitch Actuators</i>	229
7.4.4	<i>The Divergent Flag</i>	229
7.4.5	<i>Limitations due to Specific Wind Turbine Design Issues</i>	230
7.5	DESIGN OF THE FLAGS AND LIMITS	231
7.5.1	<i>Diagrams of Limits for the 1.5MW and 5MW Wind Turbines</i>	231
7.5.2	<i>Hard Limit on the Speed of the Wind Turbine</i>	232

7.5.3	<i>Hard Upper and Lower Limits on the Torque of the Wind Turbine</i>	233
7.5.4	<i>Maximum and Minimum Torque Limits</i>	236
7.5.5	<i>Summary of Flags</i>	237
7.6	DEMONSTRATION OF RECOVERY FLAG AND SUB-FLAGS.....	239
7.7	TESTING OF THE HARD LIMITS	245
7.7.1	<i>Upper Torque Limit, Maximum Torque Limit and Minimum Speed Limit</i>	245
7.7.2	<i>Lower Torque Limit, Minimum Torque Limit and the Maximum Speed Limit</i>	249
7.8	CONCLUDING REMARKS	253
CHAPTER 8: USING THE PAC TO PROVIDE GRID FREQUENCY SUPPORT		255
8.1	USING THE PAC TO PROVIDE SYNTHETIC INERTIA.....	256
8.1.1	<i>Alteration to the PAC Laws when providing Synthetic Inertia</i>	257
8.1.2	<i>Impact of Turbine Size and Operating Strategy on Provision of Synthetic Inertia</i>	258
8.1.3	<i>Synthetic Inertia Simulations</i>	259
8.2	USING THE PAC TO PROVIDE DROOP CONTROL.....	271
8.2.1	<i>The Requirements for Droop Control</i>	272
8.2.2	<i>Strategies for Implementation of Droop Control</i>	272
8.2.3	<i>Droop Control Simulations</i>	275
8.3	COMBINED DROOP CONTROL AND SYNTHETIC INERTIA.....	289
8.4	CONCLUDING REMARKS	293
CHAPTER 9: CONCLUSION		295
CHAPTER 10: REFERENCES.....		299
APPENDIX I: SAMPLE CODE		306
APPENDIX II: TURBINE AND FULL ENVELOPE CONTROLLER VARIABLES		326
APPENDIX III: LINEARISATION – WITHOUT INDUCTION		330
APPENDIX IV: LINEARISATION WITH INDUCTION		335
APPENDIX V: PAC SUPERVISORY RULES SUMMARY		343
APPENDIX VI: PI CONTROLLER GAINS AND GAIN SCHEDULING		346

Nomenclature

Symbol	Meaning
A	Swept area of the rotor
A_0	Separated discretised gain
A_B	Area of the blade element in the vertical direction
A_R	Cross sectional area of the fluid at the rotor
A_s	Nonlinear function based on the thrust coefficient
$A(s)$	Actuator transfer function
AMBER	Flag to say the turbine is in the amber “traffic light” zone
(Actuator)	Sub-flag to say the PAC cannot be turned on as the pitch demand signal from the full envelope controller has exceeded the actuator limits
a_0	Unsteady induction factor where the PAC is not used
a_1	Unsteady induction factor where the PAC is used
a_{A1}	Separated gain for the first half of the second order actuator transfer function, separated for gain scheduling
a_{A2}	Separated gain for the second half of the second order actuator transfer function, separated for gain scheduling
$a_d[n]$	Rate of change (differential) of the discrete induction factor
a_s	Steady state induction factor
$a_s[n]$	Discrete steady state induction factor
a_{s0}	Steady state induction factor where the PAC is not used
a_{s1}	Steady state induction factor where the PAC is used
B	Total wind turbine drivetrain damping

B_N	Number of Blades
b	Constant in actuator dynamics approximation
C_D	Drag coefficient
C_L	Lift coefficient
C_P	Coefficient of power
C_Q	Coefficient of torque
C_T	Coefficient of thrust
(Complete)	Sub-flag to say the wind turbine has recovered back to normal operation
\hat{C}_P	Reformulated power coefficient table
\hat{C}_Q	Reformulated torque coefficient table
\hat{C}_T	Reformulated thrust coefficient table
c	Constant in actuator dynamics approximation
c_l	Chord length
D	Drag force
DIVERGENT	Flag to say the turbine will continue to move further from the normal operating strategy unless the PAC enters recovery or a change to ΔP is made.
F_T	Thrust force
$F(s)$	Transfer function
$F(z)$	Discretised transfer function
(Fast/Slow)	Sub-flag to set the recovery speed to fast or slow
f	Grid frequency
$f_{nominal}$	Nominal (desired) frequency value
$G(s)$	Model of turbine drive train
$G(z)$	Separated discretised transfer function
$G_{A1}(s)$	Half of the second order actuator transfer function, separated for gain scheduling
$G_{A2}(s)$	Other half of the second order actuator transfer function (integrator), separated for gain scheduling
$G_{nm}(s)$	Transfer function representing the dynamics of the linearised PAC

GREEN	Flag to say the turbine is in the green “traffic light” zone
g	Second separated function for turbine torque
H	Inertia constant
$H(s)$	PAC pitch controller
h	First separated function for turbine torque
J	Total wind turbine inertia
J_A	Internal variable in gain scheduling
J_s	Total grid inertia
K_B	Tuning constant for dynamic inflow
K_{GS}	PAC Gain scheduling variable
K_I	Integral gain for $H(s)$
$K_{Inertia}$	Constant used in the provision of synthetic inertia
K_{Lower}	Constant used during torque limiting
K_{Minus}	Constant used during torque limiting
K_{Offset}	Constant used during torque limiting
K_P	Proportional gain for $H(s)$
K_R	Recovery constant
K_{Upper}	Constant used during torque limiting
K_{freq}	Constant used in droop control
K_{opt}	Gain for the max power tracking region
K_{plus}	Constant used during torque limiting
$K_{\beta I}$	PAC Pitch controller integral gain
$K_{\beta P}$	PAC Pitch controller proportional gain
k_{max}	Value used in maximum speed limit
k_{min}	Value used in minimum speed limit
$(Limit)$	Sub-flag to say the requested ΔP cannot be provided as a black limit has been exceeded
L	Lift force
\dot{M}	Mass flow rate
P_0	Power output if no increments were applied

P_{∞}	Pressure far upstream of the rotor
P_{Dem}	Demanded power
P_{Farm}	Farm power output
P_L	Power applied to the stream tube
P_R	Power applied to blade element
P_{Sup}	Supplied power
P_W	Pressure far downstream of the rotor
P_d	Pressure just downstream of the rotor
P_u	Pressure just upstream from the rotor
PAC ON	Flag to say the PAC is on
PR_{Max}	Maximum pitch rate
PR_{Min}	Minimum pitch rate
(Power)	Sub-flag to say the requested ΔP cannot be provided as it exceeds the maximum/minimum power limit
PRIORITY	Flag to say that a priority event (such as synthetic inertia) is occurring and so the traffic light limits and power rate limits are ignored
(Power Rate)	Sub-flag to say the requested ΔP cannot be provided due to the limits on the rate of change of power
Q	Rotor torque
\bar{Q}	Equilibrium operating point for rotor torque
Q_0	Rotor torque where the PAC is not used
Q_1	Rotor torque where the PAC is not used
R	Rotor radius
RECOVERY	Flag to say the wind turbine is recovering back to normal operation or has recovered
(Recovery)	Sub-flag to say the requested ΔP cannot be provided as the PAC is in recovery mode
RED	Flag to say the turbine is in the red "traffic light" zone
(Red/Amber/Green)	Sub-flag to say the requested ΔP cannot be provided as it is of greater magnitude than the limit set for the relevant traffic light zone

r_R	Radius measured at the rotor
r_W	Radius of the stream tube far downstream in the wake
S	Rated power
S_n	Flag signals from turbine n
T	Generator torque
T^*	Value used during torque limiting
T_0	Generator torque output from the full envelope controller
T_{Lower}	Lower torque limit
T_R	Recovery torque
T_{Rated}	Generator torque in above rated operation
T_{Upper}	Upper torque limit
T_{cs1}	Maximum torque of the first constant speed region
T_{cs2}	Minimum torque of the second constant speed section
T_s	Time step
T_{upper}	Upper torque limit
(Turbulence)	Sub-flag to say the PAC cannot be turned on as the turbulence level is too high
U	Input to transfer function
u	Input to gain scheduling
V	Effective wind speed
\bar{V}	Equilibrium operating point for wind speed
\hat{V}	Estimate of wind speed – the wind speed that would result in a steady state induction factor equal to the unsteady induction factor
V_∞	Wind speed far upstream from the rotor
V_A	Wind speed at the rotor in its absence
V_R	Wind velocity at the rotor
V_{Rated}	Rated wind speed
V_W	Wind speed far downstream of the rotor
$V_{cut\ in}$	Cut in wind speed

$V_{cut\ out}$	Cut out wind speed
\hat{V}_0	\hat{V} in the case where the PAC is not used
\hat{V}_1	\hat{V} in the case where the PAC is used
\hat{V}_A	Estimate of V_A
\bar{V}_R	Average axial wind speed at the rotor
v	Variable in gain scheduling of the controller
W	Resultant wind velocity
(Wind Speed)	Sub-flag to say the PAC cannot be turned on as the wind speed is too low
w	Variable in gain scheduling of the controller
w_E	Speed of wake expansion
x	PAC internal variable
Y	Output from transfer function
y	PAC internal variable
y_1	Output from separated discretised transfer function
y_2	Output from separated discretised gain
y_{max}	Maximum limit for transfer function
z	PAC internal variable
α	Resultant wind angle of attack minus the blade pitch angle
β	Actual Blade pitch angle
$\bar{\beta}$	Equilibrium operating point for pitch angle
β_0	Blade pitch angle if no increments were applied
β_{0d}	Pitch angle that would have been demanded with no increment
β_d	Blade pitch angle demand
γ	Output of gain scheduling in the controller (equivalent to β_d)
$\frac{\partial Q_+}{\partial V}$	Short hand for $\frac{\partial Q}{\partial V}(\bar{y}, \bar{\omega}_0 + \Delta\bar{\omega}, \bar{V})$
$\frac{\partial Q_+}{\partial \beta}$	Short hand for $\frac{\partial Q}{\partial \beta}(\bar{y}, \bar{\omega}_0 + \Delta\bar{\omega}, \bar{V})$

$\frac{\partial Q_+}{\partial \omega}$	Short hand for $\frac{\partial Q}{\partial \omega}(\bar{v}, \bar{\omega}_0 + \Delta\omega, \bar{V})$
$\frac{\partial Q}{\partial V}$	Short hand for $\frac{\partial Q}{\partial V}(\bar{\beta}_0, \bar{\omega}_0, \bar{V})$
$\frac{\partial Q}{\partial \beta}$	Short hand for $\frac{\partial Q}{\partial \beta}(\bar{\beta}_0, \bar{\omega}_0, \bar{V})$
$\frac{\partial Q}{\partial \omega}$	Short hand for $\frac{\partial Q}{\partial \omega}(\bar{\beta}_0, \bar{\omega}_0, \bar{V})$
ΔP_{Farm}	Increment in farm power
ΔP_{Offset}	Power offset for droop control
ΔP_{freq}	Further adjustment for droop control
ΔP_{max}	The maximum change in power allowed to be requested
ΔP_{min}	The minimum change in power allowed to be requested
ΔP_n	Increment in power for turbine n
ΔT_{High}	Value used in maximum speed limit
ΔT_{Low}	Value used in minimum speed limit
ΔT_{new}	New value of ΔT when limiting the PAC
$\Delta \beta_d$	Demanded increment in pitch angle
ΔP	Increment in power
ΔQ	Change in aerodynamic torque
ΔT	Increment in torque
$\Delta \beta$	Increment in generator speed
$\Delta \omega$	Increment in generator speed
ε	Separability function
Λ	Adjustment for inverse actuator transfer function
λ	Tip speed ratio
λ_0	Tip speed ratio if no increments were applied
λ_{∞}	Tip speed ratio (relative to V_{∞})
λ_A	Tip speed ratio corresponding to V_A
λ_R	Tip speed ratio (relative to V_R)
$\hat{\lambda}$	Tip speed ratio corresponding to \hat{V}

τ	Separability function
τ_c	Time constant for recovery
ρ	Density of air
φ	Resultant wind angle of attack
Ω	Rotor speed
$\bar{\Omega}$	Equilibrium operating point for rotor speed
Ω_0	Rotor speed if no increments were applied
ω_0	Generator speed if no increments were applied
ω_{cs1}	Minimum operational generator speed
ω_{cs2}	Maximum operational generator speed
ω_d	Rotational velocity of the wake just downstream of the rotor
ω_{max}	Maximum generator speed limit
ω_{min}	Minimum generator speed limit
ω_{offset}	Offset from minimum speed at which limiting starts
ω_r	Rotational velocity of the wake
$\bar{\omega}$	Equilibrium operating point for generator speed
$\bar{\omega}_R$	Average rotational wind speed at the rotor

Chapter 1:

Introduction

THIS THESIS DETAILS the development of a novel controller that acts as an augmentation to a wind turbine's full envelope controller, allowing the power output to be adjusted via an input ΔP provided from outwith the controller. Also included in this chapter are a description of the contribution to knowledge of the thesis, and a list of publications from the work herein.

1.1 Overview of the Thesis

Here, in chapter 1, a brief introduction to the thesis is provided.

In chapter 2, an overview of the aspects of wind turbine technology relevant to the later sections of the thesis is provided. This includes overviews of standard wind turbine control practices, separability, blade element momentum theory, and wind turbine modelling.

In chapter 3 the concept of flexible operation of wind plant is introduced and a review of techniques and controllers in the literature designed to provide flexible operation is presented. The chapter concludes by introducing the concept of the Power Adjusting Controller (PAC), which is the focus of the rest of the thesis.

In chapter 4, the PAC concept is developed into a fully realised controller, which is tested on lumped parameter models of wind turbines. At the end of chapter 4, a requirement for an improved wind speed estimator to ensure accurate performance of the PAC is identified.

Chapter 1: Introduction

Chapter 5 details the development of a novel wind speed model and estimator capable of including the effects of dynamic inflow. The wind speed estimator is incorporated into the design of the PAC. The dynamics of the PAC are thoroughly investigated to ensure that it does not have a detrimental effect on the operation of the wind turbine full envelope controller. The PAC, with the new wind speed estimator, is tested using a lumped parameter model of a wind turbine with dynamic inflow modelled.

In chapter 6 the PAC is converted from continuous time to discrete time for application in the aero-elastic modelling software GL Bladed. The discretisation of the PAC is discussed in detail. The effect of using the PAC on the wind turbine loads is assessed through simulations using GL Bladed.

Chapter 7 details the development of measures put in place to prevent the PAC from causing the wind turbine operating point to move outside of a designated safe working envelope. The design of the limits is discussed, with the limitations split into two types; soft “traffic light” limits set by the wind farm operator and hard, “black” limits designed to protect the turbine, set by the turbine manufacturer.

In chapter 8 two applications of the PAC are presented – using the PAC to provide synthetic inertia and using the PAC to provide droop control. An assessment of the impact on energy capture and turbine loads of each of these techniques is presented.

Chapter 9 summarises the results of the work presented in this thesis, draws conclusions and discusses the future work that may be undertaken in this area of research.

Chapter 10 contains a list of references and is followed by the appendices.

1.2 Contributions to Knowledge

The contributions to knowledge of this thesis are:

- A novel augmentation to a wind turbine controller that allows the power output of the turbine to be accurately adjusted by a change in power demand ΔP , known as the power adjusting controller (PAC). The PAC is

Chapter 1: Introduction

generic in that it can be applied to any asynchronous variable speed horizontal axis wind turbine without alteration to nor knowledge of the turbine's full envelope controller. The PAC does not affect the normal operation of the wind turbine.

- A novel wind speed estimator that accounts for dynamic inflow effects, derived from a reformulation of blade element momentum theory based solely on the properties at the rotor.

1.3 Publications

A. Stock and W. Leithead, "Providing Frequency Droop Control Using Variable Speed Wind Turbines with Augmented Control," in Proc. European Wind Energy Conference 2014, Barcelona, 2014, pp.68-72.

A. Stock and W. Leithead, "Providing Grid Frequency Support Using Variable Speed Wind Turbines with Augmented Control," in Proc. European Wind Energy Association Conference 2012, Copenhagen, 2012, pp. 152–156.

Chapter 2:

Overview of Wind Energy

The wind industry has seen rapid growth in recent years and is becoming a mature industry. This chapter provides an overview of the aspects of wind energy relevant to the thesis.

The development of modern wind turbines and farms is discussed. An overview of the current control techniques used is then completed, followed by an in depth review of the blade element momentum theory of wind turbine aerodynamics.

2.1 The Development of the Modern Wind Turbine and Wind Farm

The content of this thesis pertains to the control of modern wind turbines and wind farms; a brief overview of the development of wind turbines is therefore given.

In 1887, the first machine for generating electricity from the wind was built by Professor James Blyth of Anderson's College (later to become the University of Strathclyde) in the garden of his holiday cottage in Marykirk Scotland [1]. This first wind power machine generated electricity, to power the electric lights in Blyth's house. Whilst wind energy continued to develop in the intervening years it was only in the 1980s that wind energy began to become a significant producer of electrical power.

Whilst wind turbines have taken many forms in the intervening years, the preference amongst the vast majority of manufacturers of large (that is greater than

1MW) wind turbines is for horizontal axis, variable speed, pitch regulated machines. These wind turbines vary their speed in lower wind speed conditions to maximise their power output. In order to do this, back to back converters are utilised, resulting in asynchronous electricity generation – that is to say that the speed of the generator is decoupled from the grid frequency.

With the threat of climate change largely caused by CO_2 emissions, it has become increasingly important for governments to reduce their carbon footprint. Energy supply contributes over a quarter of the world's total greenhouse gas emissions and so the “decarbonisation” of the sector is a key requirement to prevent large increases in the average global temperature [2].

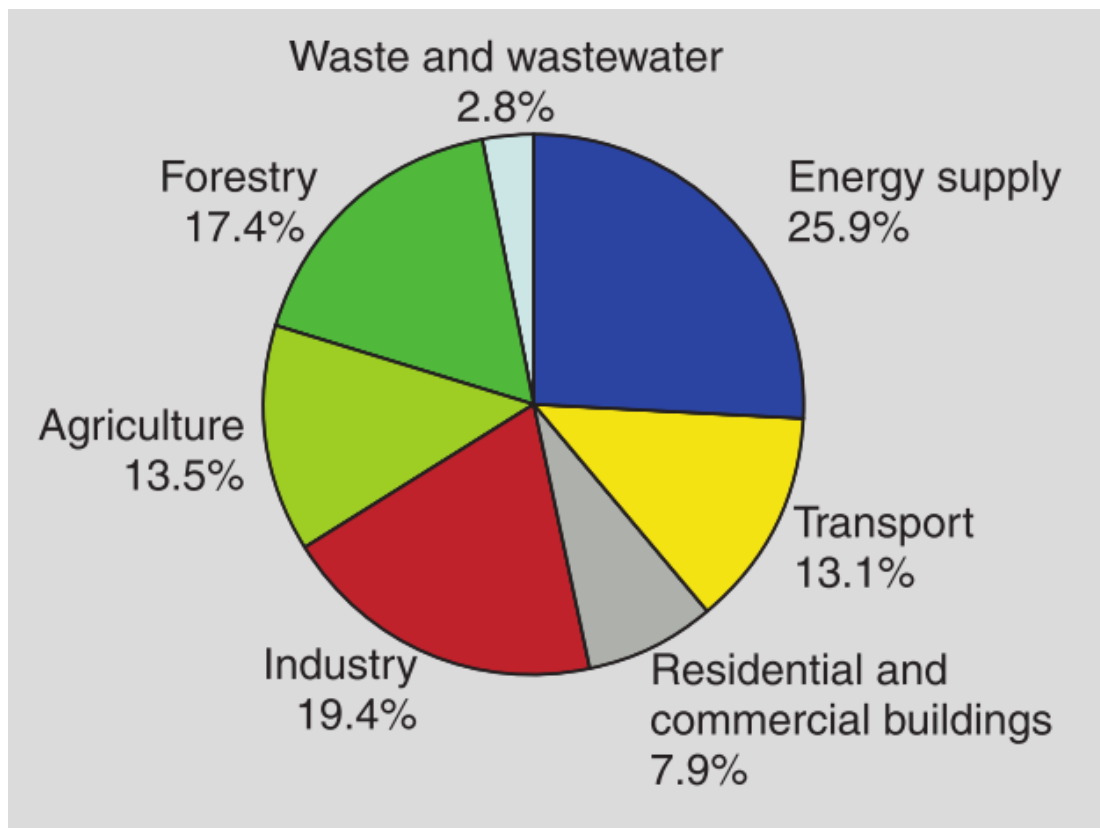


Figure 1: Share of Different Sectors in Total Anthropogenic Greenhouse Gas Emissions in 2004 (Adapted from [2])

In light of this, the UK has committed to reducing its carbon output to ensure that “the net UK carbon account for the year 2050 is at least 80% lower than the 1990 baseline” [3]. This policy has led directly to the installation of large numbers of

Chapter 2: Overview of Wind Energy

wind turbines, with the installed capacity of wind energy rising from 3410 MW in 2008 to 8888 MW in 2012 [4].

In order to provide the large amounts of capacity required, wind turbines and wind farms have increased in size year on year. The first wind farm in the UK, (Delabole, built in 1991) consisted of ten 400 kW machines. By contrast, the recently completed phase one of the London Array consists of one hundred and seventy five 3.6 MW machines. These machines are of a typical size and design, with most modern machines now being upwind, horizontal axis wind turbines (HAWTs), grid connected and with rated power outputs of up to 7.5MW.

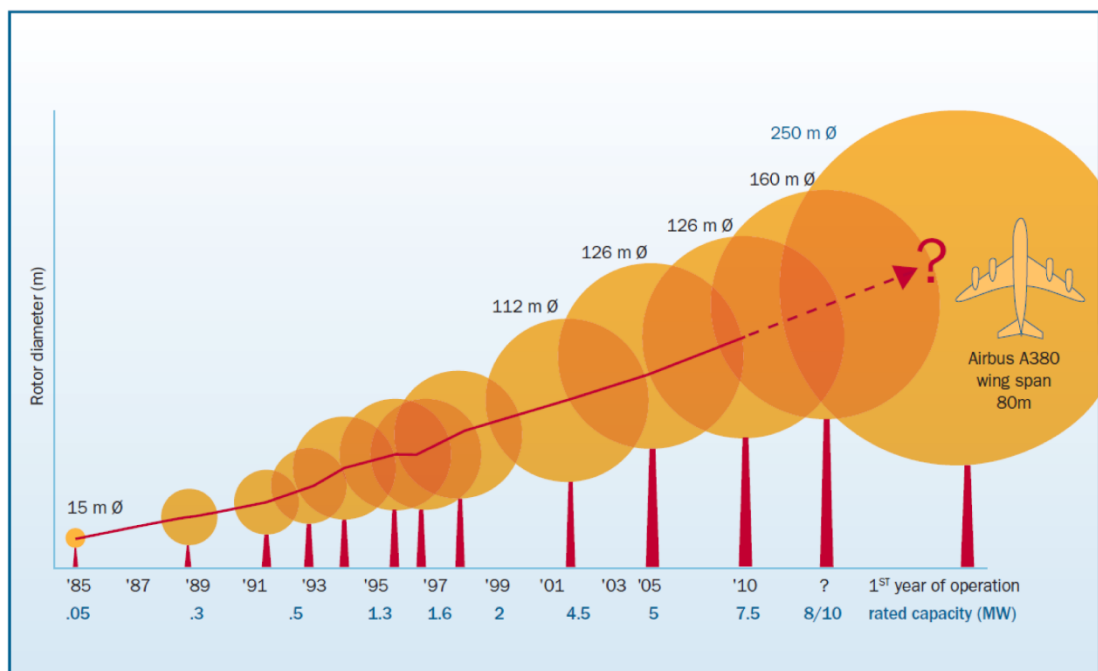


Figure 2: Increase in Typical Wind Turbine Size Over Time [5]

Whilst in recent years direct-drive wind turbines have increased in popularity, the majority of multi-megawatt wind turbines in production feature a gearbox which increases the speed of rotation and decreases the torque between the input and output shafts, commonly known as the low speed shaft (LSS) and high speed shaft (HSS) respectively. The majority of large wind turbines are three Bladed machines with towers made from either concrete or, more commonly, steel.

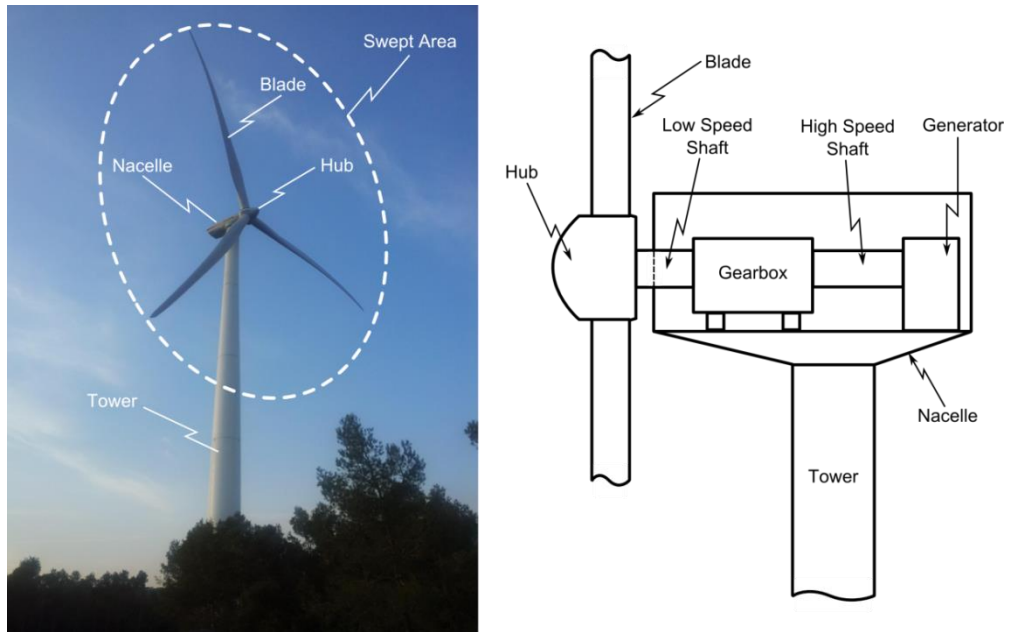


Figure 3: Basic Configuration of a Modern Three Bladed Wind Turbine and its Drive-Train Components

2.2 Conventional Wind Turbine Control

Wind turbines are typically operated when the wind speed is between a minimum value, $V_{cut\ in}$, and a maximum value, $V_{cut\ out}$. Outside of these bounds, the wind turbine is shut down and does not generate electrical power.

Between $V_{cut\ in}$ and $V_{cut\ out}$ the wind turbine is operated using a full envelope controller to control the generator speed. At wind speeds higher than V_{rated} the turbine utilises blade pitch control to control the rotational speed of the machine. Below V_{Rated} the generator reaction torque is used as the control mechanism. The full envelope controller typically controls the turbine based on a measurement of the generator speed ω .

In addition to the requirement of capturing as much energy from the wind as possible, controllers are increasingly being required to ensure that the loads on the wind turbine do not become too great. As wind turbines have rapidly increased in size this requirement has become increasingly important.

There are four types of horizontal axis wind turbine:

- 1- Constant Speed, Stall Regulated

Chapter 2: Overview of Wind Energy

- 2- Constant Speed, Pitch Regulated
- 3- Variable Speed, Stall Regulated
- 4- Variable Speed, Pitch Regulated

Constant speed machines operate at a single rotational speed, with a varying the generator torque in below-rated operation. In contrast, variable speed machines may operate at different rotational speeds depending upon the wind conditions. Stall regulated machines use the properties of aerodynamic stall to limit their aerodynamic torque above the rated wind speed, whereas pitch regulated machines use actuators in the blade to vary the pitch angle and hence vary the aerodynamic torque of the rotor in order to control their speed in above-rated wind speeds.

Whilst constant speed machines are still manufactured by some companies, the majority of large multi-megawatt machines produced by the main wind turbine manufacturers in recent times have tended to be variable speed, pitch regulated machines.

2.2.1 Typical Strategies for Variable Speed, Pitch Regulated Turbines

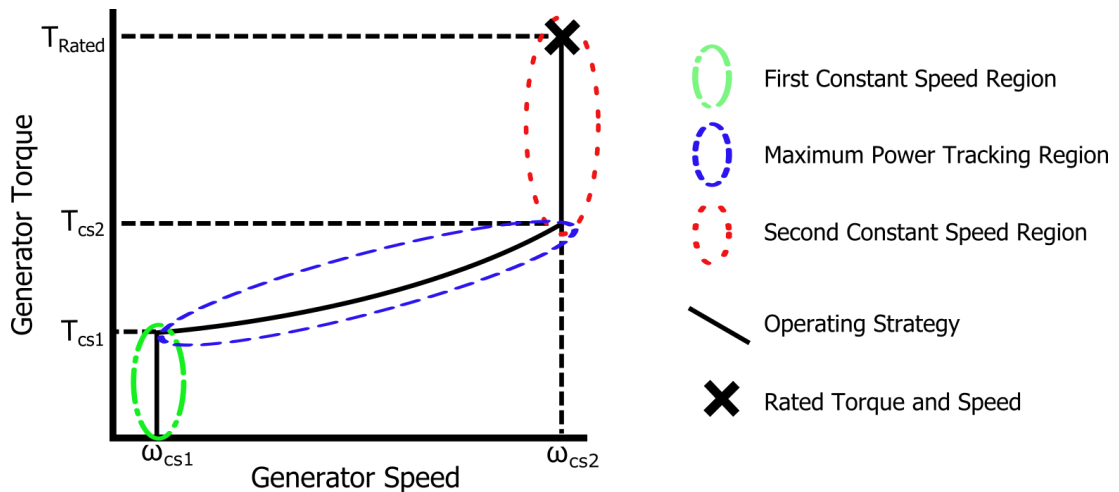


Figure 4: Typical Operating Strategy for a Modern Variable Speed Wind Turbine

A typical operating strategy for a variable speed, pitch regulated wind turbine is shown in Figure 4. When the wind speed rises above $V_{cut\ in}$, the wind turbine is operated at a constant generator speed ω_{cs1} . If the wind speed is large enough such that the generator torque increases above T_{cs1} , the controller switches to the

maximum power tracking region. In this region the wind turbine varies the generator torque with the generator speed via the relationship:

$$T = K_{opt}\omega^2 \quad (2.1)$$

where T is the generator torque, ω is the generator speed and K_{opt} is a constant found such that the total power output is at a maximum for the given wind speed. K_{opt} is dependent upon the physical properties of the wind turbine.

If the wind speed is high enough such that the demanded generator torque is above T_{cs2} , then the controller will enter the second constant speed region. The controller does not continue tracking the maximum power curve, as to do so would result in a generator/rotor speed that would cause large loads due to excitation of structural frequencies.

The controller continues to control the wind turbine via the generator torque up to a torque value of T_{Rated} . T_{Rated} is the rated torque of the machine, with the product of ω_{cs2} and T_{Rated} the rated power output. The value for T_{Rated} is reached at a wind speed V_{Rated} . Above V_{Rated} the wind turbine utilises blade pitch control to regulate the aerodynamic torque.

2.2.2 Minimising Loads through Wind Turbine Control

With the increasing size of wind turbines it is increasingly important to ensure that the controller minimises the loads on the wind turbine. Whilst a well-designed strategy avoids excitation of the structural modes, further additions can be made to the controller to minimise the loads on the turbine.

These additions take a number of different forms, and not all are used on every turbine. The four most common techniques, as identified in a review of such methods [6], are:

- Joint control of pitch and torque.
- Using torque control to dampen drive-train resonances.
- Reducing tower loads through the addition of a nacelle mounted accelerometer and a tower feedback loop.

- Reduction of asymmetric loads through individual pitch control.

The first of these options has been explored by Leithead and Dominguez [7], [8], and Chatzopoulos and Leithead [9], with the resulting controller known as a “coordinated controller”. In normal control of pitch regulated machines the controller maintains the torque demand at a set value during above-rated operation and just uses the pitch demand. Coordinated control uses torque control as well as pitch control in above-rated wind conditions to remove a right half plane zero from the dynamics, reducing the fatigue loads on the tower.

The second option (using torque control to dampen drive-train resonances) is commonly used for most large wind turbines via a drive-train filter.

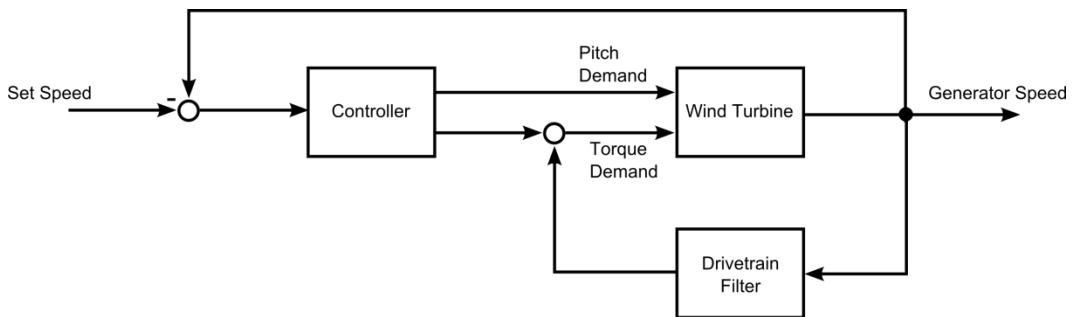


Figure 5: Drive-Train Filter

The concept of the drive-train filter is to increase the damping at the drive-train frequency by the addition of a feedback loop with a band pass filter centred at the drive-train frequency as shown in Figure 5.

The third option (the addition of a tower feedback loop) is commonly used on larger wind turbines to reduce the fore-aft fatigue loads on the wind turbine tower.

Descriptions of methods to achieve this appear in [6] and [10].

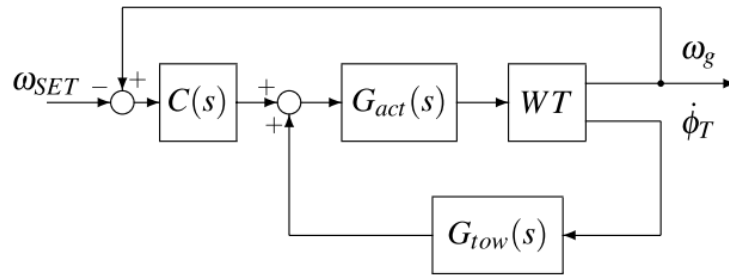


Figure 6: Tower Feedback Loop Design (From [10])

The tower feedback loop is designed in a similar manner to the drive-train filter, albeit with the input of tower speed (itself an integral of the tower acceleration from an accelerometer in the nacelle). The layout used in [10] is shown in Figure 6.

The final option for reducing the wind turbine loads is the use of individual pitch angles for each blade. There are two popular methods used, individual pitch control (IPC) [11], [12] and individual blade control (IBC) [13], [14]. Both methods reduce the asymmetric loads on the turbine by adjusting the pitch demand for each blade of the turbine in response to measurement of the loads on the blades or rotor.

Using IPC in its standard form, the out-of-plane root bending moments for each blade are measured. The blade bending moment measurements are sent to a central controller that uses this information to set an individual pitch angle for each blade. This technique is capable of reducing the unbalanced lifetime out-of-plane fatigue loads on a rotor.

IBC utilises an actuator, sensor, and controller on each blade. Load reduction is separated from the central speed control and is instead conducted locally at each blade. This increases the flexibility of the controller as the blade loads are directly controlled. Unlike IPC, IBC is completely separated from the central controller and is not model dependent.

2.3 Separability

The aerodynamics of wind turbines when using pitch control in above-rated operation are highly non-linear. As such, either non-linear control methods, or some form of linearization of the dynamics is required to achieve satisfactory

control of a turbine. Separability is discussed in [15]–[18], a brief overview of separability based on these works is presented in this section.

In the case of wind turbine control, a disturbance rejection problem, gain scheduling is often used. Gain scheduling utilises the state of a system in order to obtain information about how the controller must alter as the disturbance (in this case the wind speed) changes [15], [19]. This technique changes the structure of the controller continuously based on scheduling variables that are measured or constructed based on local set points. Whilst some methods of gain scheduling use an estimation of the wind speed as the scheduling variable, this is not common, and typically the blade pitch angle is used as the scheduling variable.

This technique is a sound approach due to the surprising but useful characteristic of wind turbine aerodynamics known as separability, described in detail in [15]. The dynamic relationship between pitch, effective wind speed and torque is shown diagrammatically as in Figure 7:

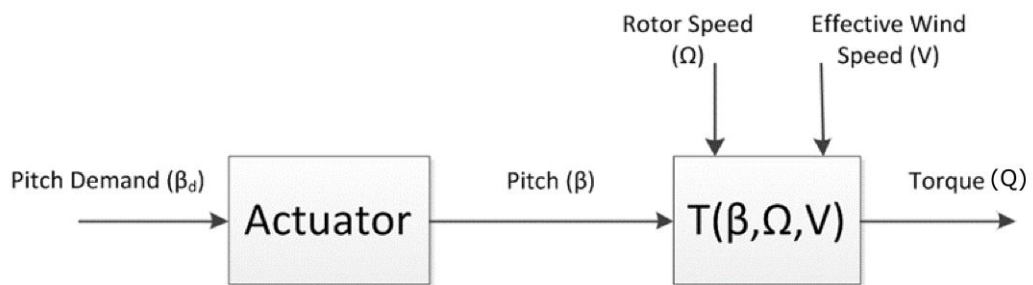


Figure 7: Dynamic Relationship Between Pitch, Rotor Speed, Effective Wind Speed and Torque
(Adapted from [15])

Separability theory states that the aerodynamic torque, a function of the rotor speed, effective wind speed and the blade pitch angle, can be separated into two components,

$$Q(\beta, \Omega, V) = h(\beta, \Omega) - g(V) \quad (2.2)$$

enabling the diagram shown in Figure 7 to be reformulated as shown in Figure 8.

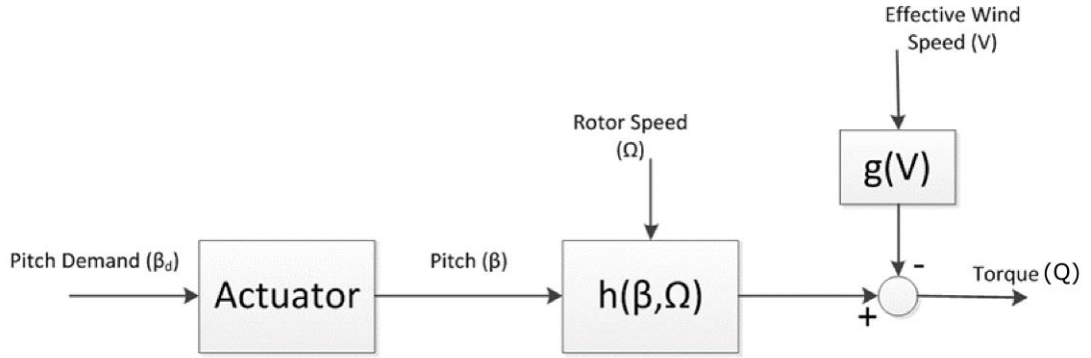


Figure 8: Dynamic Relationship between Pitch, Rotor speed, Effective Wind Speed and Torque after the Application of Separability (Adapted from [15])

It can therefore be stated that for every set of $(\bar{\Omega}, \bar{V})$ the aerodynamic torque \bar{Q} can only be obtained at a unique pitch angle $\bar{\beta}$. The nonlinearity is then linearised within these specific operating points by the use of a Taylor expansion.

Taylor's expansion assures that it is possible to linearise around the equilibrium point, so in the worst case there would be a local separability, although this is not useful from the operational point of view of the wind turbine. So a more useful description comes from the relationship of the partial derivatives [16],

$$\frac{\partial Q}{\partial V}(\bar{\beta}, \bar{V}) = -\frac{d\bar{\beta}(V)}{dV} \frac{\partial Q}{\partial \beta}(\bar{\beta}, \bar{V}) \quad (2.3)$$

When talking about separability in constant speed wind turbines, the aerodynamic torque will only be dependent on two variables, pitch angle and wind speed, while operating at fixed rated rotor speed, $\bar{\omega}$. Thus Separability for $Q(\beta, V, \omega)$ at $\bar{\omega}$, on the locus, has the form,

$$Q(\beta, V, \omega)|_{\omega=\bar{\omega}} = \tau_{\bar{\omega}}(\varepsilon_{\bar{\omega}}) = \tau_{\bar{\omega}}[\bar{Q} + (h_{\bar{\omega}}(\beta) - g_{\bar{\omega}}(V))] \quad (2.4)$$

$$\tau_{\bar{\omega}}(\varepsilon_{\bar{\omega}})|_{\varepsilon_{\bar{\omega}}=\bar{Q}} = \bar{Q} \quad (2.5)$$

$$\tau_{\bar{\omega}}'(\varepsilon_{\bar{\omega}})|_{\varepsilon_{\bar{\omega}}=\bar{Q}} = 1 \quad (2.6)$$

This effectively means that in a neighbourhood of the whole range of operating points, the aerodynamic torque dependence on the pitch demand is represented by $h_{\bar{\omega}}(\beta)$ and the function $g_{\bar{\omega}}(V)$ holds the time-varying, non-linear dependence on

Chapter 2: Overview of Wind Energy

wind speed, while the function $\tau_{\bar{\omega}}$ represents the non linear dependence on displacement from the locus of equilibrium operating points. Hence, the wind turbine can be viewed as a non-linear system with non-linearity $h_{\bar{\omega}}(\beta)$ (dependant on the pitch angle) with an additive external disturbance which is the wind speed, represented by function $g_{\bar{\omega}}(V)$ ¹.

There are underlying physical reasons as to why the representation in (2.4) should hold for all constant wind speed wind turbines, as discussed in [16].

In the outer third of the rotor, the region from which aerodynamic torque largely stems, the wind velocity is many times less than the blade velocity. Relative to the blades, the change in direction of the wind velocity therefore has an almost linear relationship as the wind speed varies but its magnitude varies little.

As such, the aerodynamic torque is largely a function of the angle of attack of the wind on the outer third of the blades. This is simply the difference in the pitch angle and the direction of the relative velocity of the wind.

For separability in variable speed wind turbines, the foregoing physical argument in support of separability of the aerodynamics for constant speed wind turbines cannot be directly extended to the variable speed case. The tangential component on the rotor speed typically dominates the magnitude of the wind velocity over the blades in the outer third of the rotor. Hence, the aerodynamic characteristics of the rotor are extremely sensitive to the rotor speed.

Despite this, there is a suggestive indication that separability may apply and be of a broad enough range to be useful – the torque to rotor speed contour lines with constant wind speed at constant pitch angle of 0° , are relatively parallel within the normal operating envelope away from stall.

¹ Functions $h_{\bar{\omega}}(\beta)$ and $g_{\bar{\omega}}(V)$ are unique for each $\bar{\omega}$ and rotor

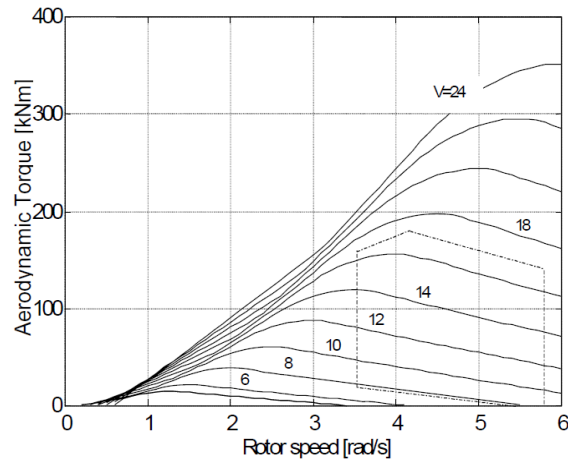


Figure 9. Aerodynamic Torque Versus Rotor Speed for a 300 kW Variable Speed Machine at Pitch Angle of 6 Degrees (Rated Torque is 71.75 kNm and Rated Speed is 4.64 rad/s) [16]

In [17], the torque aerodynamics separability on the locus, is more generally expressed as:

$$Q(\beta, V, \omega) = \bar{Q} + (h(\beta, \omega) - g(V, \omega)) \quad (2.7)$$

where, when the rotor speed is fixed and equal to rated,

$$h(\beta, \omega)|_{\omega=\bar{\omega}} = h_{\bar{\omega}}(\beta) \quad (2.8)$$

$$g(V, \omega)|_{\omega=\bar{\omega}} = g_{\bar{\omega}}(V) \quad (2.9)$$

The separated form $Q(\beta, \omega, V) = h(\beta, \omega) - g(V, \omega)$ has the correct gradients at the operating points. That is, all three partial derivatives are correct since the gradients in β and V are correct by construction.

Interestingly, Figure 10, which shows a collection of $g(V)$ functions for varying rotor speeds, ω , strongly suggests that the function $g(V)$ remains unchanged with broad variations of rotor speed, and by extension that separability could have a simplified form with $g(V, \omega)$ only dependent on V ;

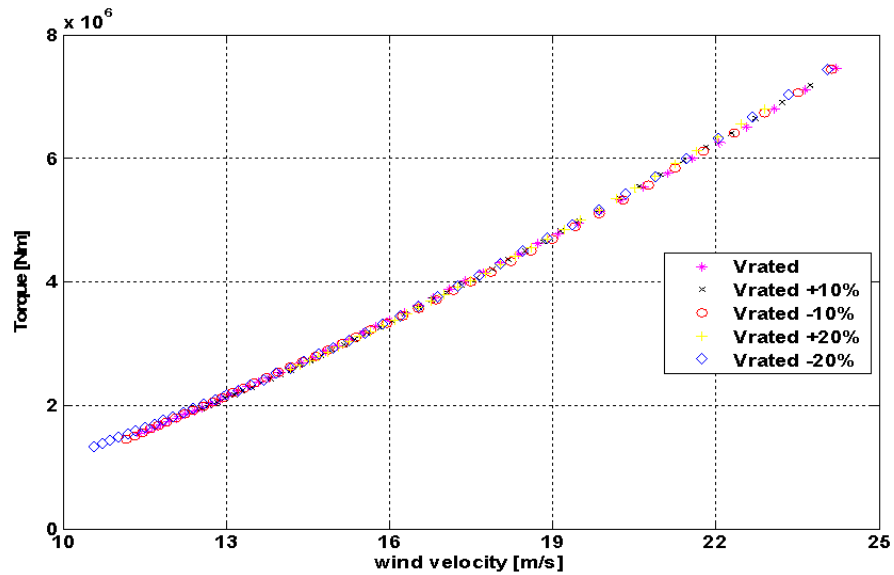


Figure 10: Function $g(v)$ for a Rotor with Different Rated Rotor Velocities (From [17])

that is, on the locus of equilibrium operating points:

$$Q(\beta, V, \omega) = \varepsilon(\beta, \omega) = \bar{Q} + (h(\beta, \omega) - g(V)) \quad (2.10)$$

Figure 11 shows separability for a rotor operating at 100% of rated rotor speed. It can be appreciated that separability easily holds for values beyond 2.5 times rated torque.

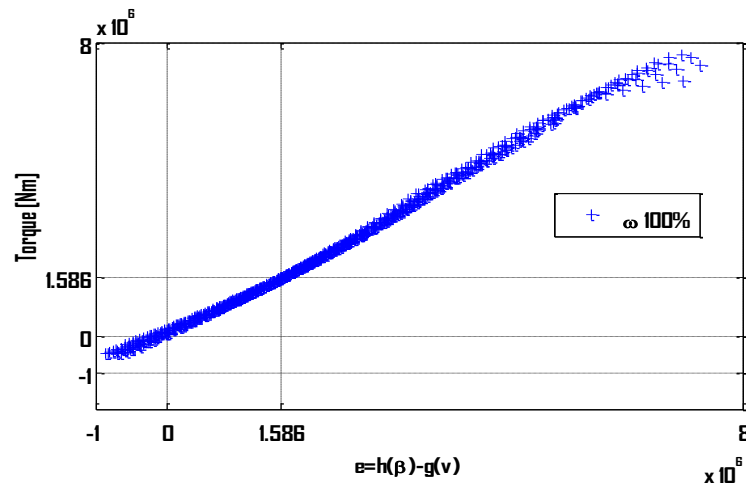


Figure 11: Torque Separability for a Rotor at 100% of Rated Rotor Speed [18]

It should be noted that, although separability does not yet have a mathematical proof, the empirical evidence that it is a highly accurate (within a margin of error of well under 1%) approximation is overwhelming [17], [18].

2.4 Gain Scheduling

The concept of separability outlined in the previous section is used to gain schedule a wind turbine's pitch control in [15].

Firstly, the partial derivative of aerodynamic torque with respect to wind speed (h) is calculated numerically and a linear approximation made. Hence, an estimate of the inverse function of h is made.

The inverse function of h is utilised as shown in Figure 12 to schedule the output of the pitch controller (note that $A(s)$ represents the actuator dynamics, typically a second order transfer function).

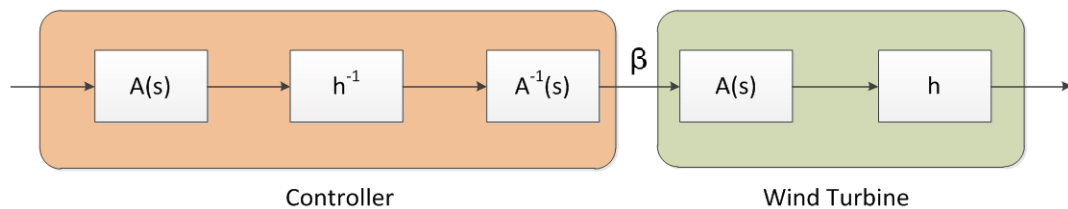


Figure 12: Implementation of Gain Scheduling (adapted from [15])

Following Figure 12 from the left, the non-scheduled pitch demand passes through the actuator dynamics and then an approximation of the inverse of the turbine dynamics h . The signal then passes through the inverse of the actuator dynamics. As such, the value β takes into account the dynamic effects of the actuator dynamics and the rotor dynamics and is appropriately adjusted.

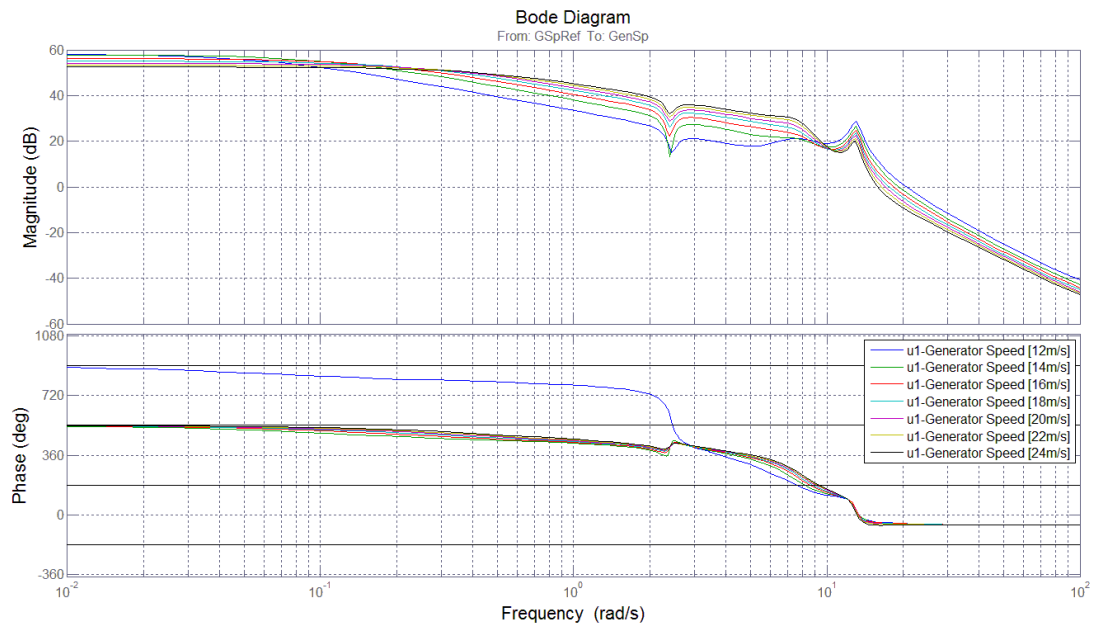


Figure 13: Bode Plot of Wind Turbine Plant without Gain Scheduling

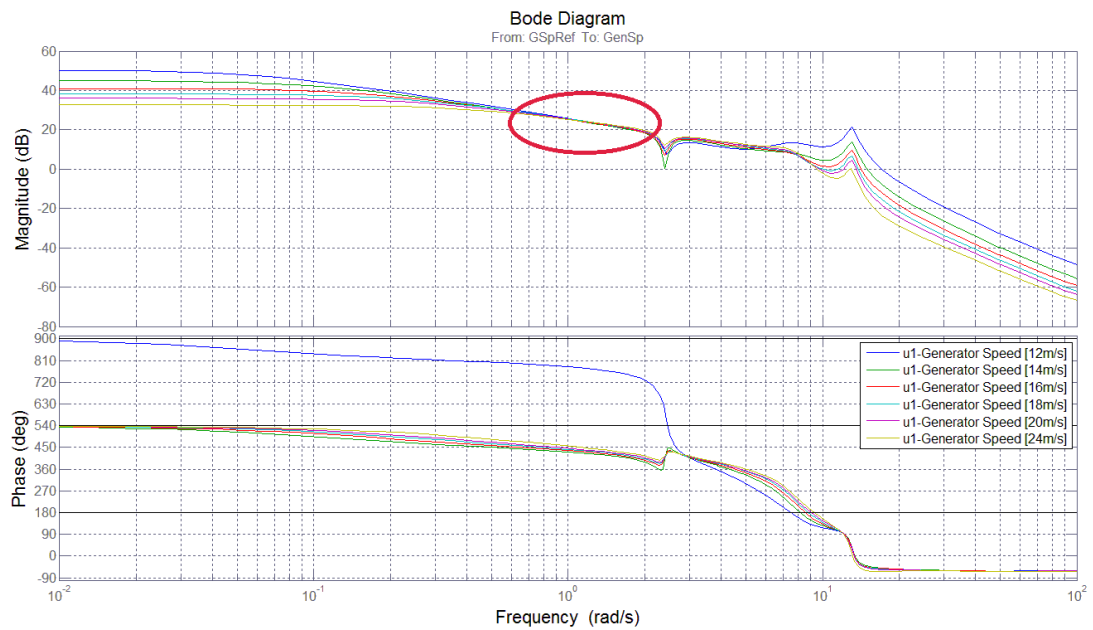


Figure 14: Bode Plot of Wind Turbine Plant with Gain Scheduling

The effect of gain scheduling on the plant dynamics is shown in Figure 13 and Figure 14.

2.5 Wind Turbine Aerodynamics

In order to control wind turbines, knowledge of how they operate is essential. Much of the work in this thesis is concerned with the aerodynamics of the wind turbine, particularly the work presented in chapter 5. As such, an in depth overview of blade element momentum (BEM) theory is presented in this section. Blade element momentum theory is the most common theory used for modelling wind turbine dynamics and is detailed in the vast majority of wind energy text books (e.g. [20], [21]).

2.5.1 What is Wind Speed?

Whilst the question “what is wind speed?” may at first seem facile, it is in fact extremely important. Fundamentally, wind speed is the speed at which air in the atmosphere moves in relation to the surface of the Earth. The wind speed at any particular point in the Earth’s atmosphere (known as the “point wind speed”) can therefore be defined fairly simply as the speed of the air at an exact, infinitesimally small point.

A wind turbine rotor is obviously not infinitesimally small however, and so it would clearly be incorrect to state that a wind turbine interacts with a point wind speed. Instead, it can be correctly stated that the wind turbine rotor interacts with a wind field comprising a (theoretically infinite) number of point wind speeds.

Standard models for the aerodynamics of wind turbines utilise momentum theory, blade element theory, and Bernoulli’s principle to model the interaction of the rotor with the wind. These models are explored in the following section.

2.6 Blade Element Theory

Blade element theory uses the conditions at the rotor to calculate the thrust and torque acting on it. Consider B_N blade elements sweeping out an annulus at a distance r_R from the rotational centre. The velocity of the wind at the rotor is V_R , the tangential velocity of the blade element is Ωr_R , and the tangential velocity of the fluid at the rotor is $\omega_R r_R$, where ω_R is the angular velocity of the fluid at the blade

element. The blade element velocities and forces are represented as shown in Figure 15.

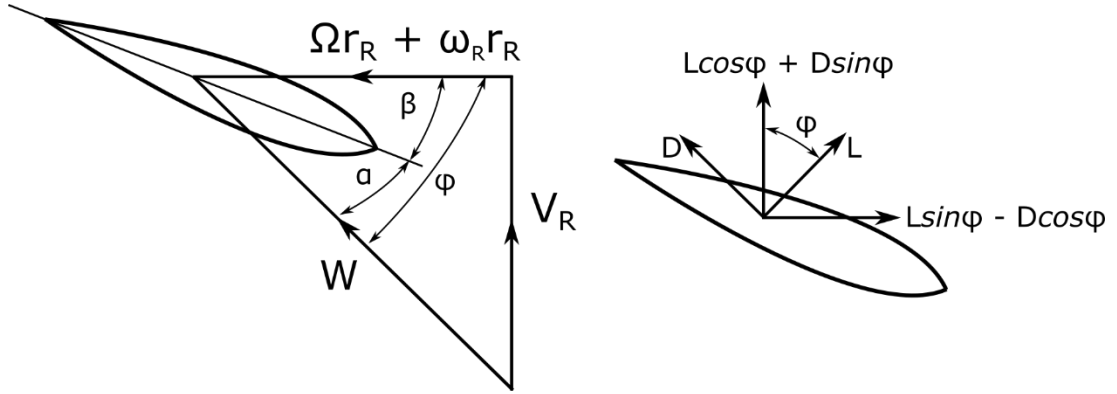


Figure 15: Blade Element Velocities and Forces

The resultant relative velocity of the wind W is therefore given by,

$$W = \sqrt{V_R^2 + (\Omega r + \omega_R r_R)^2} \quad (2.11)$$

the thrust on the blade elements is given by,

$$dF_T(V_R, \omega_R) = \frac{1}{2} \rho B_N W ((\Omega r + \omega_R r_R) C_L + V_R C_D) dA_B \quad (2.12)$$

(note that in this thesis the notation F_T is used for the thrust force rather than the usual T , as T is used later in the thesis to denote the generator torque) and the torque on the blade elements is given by,

$$dQ(V_R, \omega_R) = \frac{1}{2} \rho r_R B_N W r_R (V_R C_L - (\Omega r + \omega_R r_R) C_D) dA_B \quad (2.13)$$

where ρ is the density of air, V_R is the axial wind speed at the position of the rotor blade elements, C_L is the lift coefficient of the aerofoil section, C_D is the drag coefficient of the aerofoil section, and A_B is the area of the blade element in the vertical direction as observed in Figure 15.

Finally, the power applied to the blade elements is found via,

$$dP_R = dQ \Omega \quad (2.14)$$

2.7 Momentum Theory

Separately from blade element theory, which considers the forces acting on the blade elements, momentum theory can be applied to the fluid flow with reference to Figure 16.

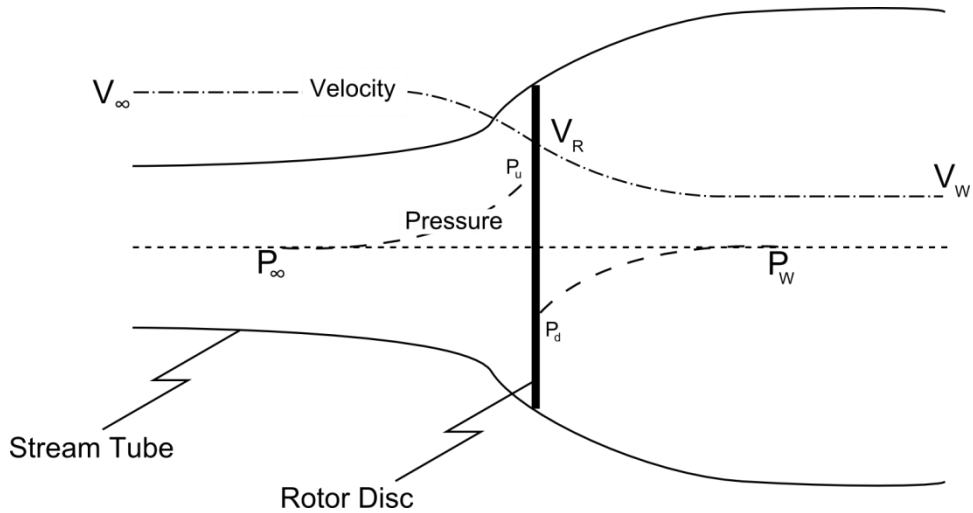


Figure 16: Stream Tube Interacting with a Rotor

Note the use of subscripts whereby a subscript ∞ denotes conditions far upstream, subscript R denotes conditions at the rotor (with subscript u being just upstream from the rotor and subscript d being just downstream of the rotor), and subscript W denotes conditions far downstream of the rotor.

Considering the rotational motion of an annular stream tube as it passes through the rotor disc, Newton's second law is applied to find the torque:

$$dQ = d\dot{M}r_R^2\omega_d \quad (2.15)$$

where \dot{M} is the mass flow rate of the fluid, r_R is the radius from the rotational centre, and ω_d is the rotational speed of the fluid just downstream. The rotational speed of the fluid just upstream, ω_u is assumed to be zero.

Newton's second law is also applied to the linear motion of the stream tube from far upstream to far downstream,

$$d\dot{M}(V_\infty - V_W) = (p_u - p_d)dA_R + (p_W - p_\infty)dA_W \quad (2.16)$$

where A_R is the cross sectional area of the fluid at the rotor.

Further, the velocity of the centre of mass of the stream tube is given by,

$$\frac{1}{2}(V_\infty + V_W) \quad (2.17)$$

and so the power applied to the annular stream tube is,

$$dP_L = \frac{1}{2}d\dot{M}(V_\infty - V_W)(V_\infty + V_W) = \frac{1}{2}d\dot{M}(V_\infty^2 - V_W^2) \quad (2.18)$$

It should be noted that this expression was derived entirely separately from the blade element theory equation for dP_R and that there is no direct relationship between dP_L and dP_R . For example, the rotor could be such that dQ is zero even though Ω and dF_T are not.. As such, it cannot be assumed that $dP_L = dP_R$.

2.8 Bernoulli's Principle

The stream tube can also be assessed using Bernoulli's principle applied to a series of annular stream tubes. Bernoulli's principle dictates that, for an inviscid flow (i.e. assuming an ideal fluid with no viscosity) along a steady streamline, the change in speed of a fluid occurs at the same time as an opposite change in the fluid's pressure and/or potential energy.

When assessing the stream tube using Bernoulli's principle, an assumption must be made about the motion of the fluid in the stream tubes after they have interacted with the rotor. Specifically, an assumption is made that they are either rotating or non-rotating.

2.8.1 Non-Rotating Stream Tubes

Applying Bernoulli's principle separately to the upstream and downstream parts of the stream tube yields the following equations. For the upstream part of the stream tube (between far upstream and just before the rotor),

$$p_\infty + \frac{1}{2}\rho V_\infty^2 = p_u + \frac{1}{2}\rho w_E^2 + \frac{1}{2}\rho V_K^2 \quad (2.19)$$

where w_E is the radial speed due to the wake expansion. For the downstream part of the stream tube (between just after the rotor and far downstream),

$$p_W + \frac{1}{2}\rho V_W^2 = p_d + \frac{1}{2}\rho w_E^2 + \frac{1}{2}\rho V_R^2 \quad (2.20)$$

Combining these equations gives,

$$\frac{1}{2}\rho(V_\infty^2 - V_W^2) = (p_u - p_d) - (p_\infty - p_W) \quad (2.21)$$

Using (2.21) with (2.16) along with the relationship between mass flow rate and wind speed,

$$d\dot{M} = \rho V_R dA_R = \rho V_W dA_W \quad (2.22)$$

where A_R and A_W are the swept area at the rotor and far down stream respectively.

It follows that,

$$(p_u - p_d) = \frac{\frac{1}{2}\rho V_R (V_\infty - V_W)^2}{V_R - V_W} = \frac{1}{2}\rho \frac{V_R \left(V_R - \frac{1}{2}(V_\infty + V_W) \right)^2}{V_R - V_W} \quad (2.23)$$

and

$$(p_\infty - p_W) = \frac{\rho V_W (V_\infty - V_W) \left(\frac{1}{2}(V_\infty + V_W) - V_R \right)}{V_R - V_W} \quad (2.24)$$

2.8.2 Rotating Stream Tubes

Applying Bernoulli's principle separately to the upstream and downstream parts of the stream tube yields the following equations. For the upstream part of the stream tube (between far upstream and just before the rotor),

$$p_\infty + \frac{1}{2}\rho V_\infty^2 = p_u + \frac{1}{2}\rho w_E^2 + \frac{1}{2}\rho V_R^2 \quad (2.25)$$

For the downstream part of the stream tube (between just after the rotor and far downstream),

$$p_W + \frac{1}{2}\rho V_W^2 + \frac{1}{2}\rho r_W^2 \omega_W^2 = p_d + \frac{1}{2}\rho w_E^2 + \frac{1}{2}\rho V_R^2 + \frac{1}{2}\rho r_R^2 \omega_d^2 \quad (2.26)$$

Combining these equations gives,

$$(p_u - p_d) - (p_\infty - p_W) = \frac{1}{2}\rho(V_\infty^2 - V_W^2) + \frac{1}{2}\rho(r_R^2\omega_d^2 - r_W^2\omega_W^2) \quad (2.27)$$

and, using (2.27) with (2.16) and (2.22), it follows that,

$$(p_u - p_d) = \frac{\frac{1}{2}\rho V_R (V_\infty - V_W)^2}{V_R - V_W} + \frac{\frac{1}{2}\rho V_R (r_R^2\omega_d^2 - r_W^2\omega_W^2)}{V_R - V_W} \quad (2.28)$$

and

$$(p_\infty - p_W) = \frac{\rho V_W (V_\infty - V_W) \left(\frac{1}{2}(V_\infty + V_W) - V_R \right)}{V_R - V_W} - \frac{\frac{1}{2}\rho V_W (r_R^2\omega_d^2 - r_W^2\omega_W^2)}{V_R - V_W} \quad (2.29)$$

Note that equations (2.28) and (2.29) are similar to equations (2.23) and (2.24), with an additional term to account for the rotation of the stream tube.

2.9 Blade Element Momentum Theory (BEM)

By using Bernoulli's principle, combined with blade element theory and momentum theory, "blade element momentum theory" is obtained – the assumptions, on which BEM depend, are highlighted.

2.9.1 BEM – Non-Rotating Stream Tubes

In this case the assumption is made that $\omega_R = 0$. It therefore follows from (2.12) that,

$$dF_T(V_R, \omega_R) = \frac{1}{2}\rho B_N W ((\Omega r_R + \omega_R r_R)C_L + V_R C_D) dA_B \Big|_{\omega_R=0} \quad (2.30)$$

where dA_B is the area of the blade over which the force acts. Since dF_T is due to the pressure difference across the rotor disc however, it can also be stated that,

$$dF_T = (p_u - p_d) dA_R \quad (2.31)$$

Additionally with the assumption,

$$V_R = \frac{1}{2}(V_\infty + V_W) \quad (2.32)$$

Chapter 2: Overview of Wind Energy

when (2.31) is combined with (2.23),

$$dF_T = \frac{\frac{1}{2}\rho dA_R V_R (V_\infty - V_W)^2}{V_R - V_W} = 2\rho dA_R V_R (V_\infty - V_R) \quad (2.33)$$

Combining (2.33) with (2.30), the relationship $dA_B = c_l dr$ and the relationship $dA_R = 2\pi r dr$ yields,

$$V_R(V_\infty - V_R) = \frac{B_N W c_l}{8\pi r R} ((\Omega r_R + \omega_R r_R)C_L + V_R C_D) dA_B \Big|_{\omega_R=0} \quad (2.34)$$

Given V_∞, V_R can be determined from (2.34). Using (2.13) and (2.14), it follows that the power applied to the element is,

$$dP_R = \frac{1}{2}\rho r_R c_l B_N \Omega W (V_R C_L - (\Omega r + \omega_R r_R)C_D) \Big|_{\omega_R=0} dr_R \quad (2.35)$$

From (2.24), whose derivation is based on Bernoulli's Theorem applied to non-rotating stream tubes, an equivalent assumption to (2.32) is that $p_W = p_\infty$.

Furthermore, noting that $\rho dA_R V_R (V_\infty - V_R)$ is the rate of change in stream tube linear momentum occurring upstream, (2.33) simply states that the rate of change in stream tube linear momentum occurring upstream is due to half of the force applied by the blade element to the stream tube, that is; a further equivalent assumption to (2.23) is that the rate of change in stream tube linear momentum occurring upstream is due to half of the force applied by the blade element to the stream tube. Note that of the three equivalent assumptions underlying the derivation of (2.34), only one needs to invoke Bernoulli's Theorem. Of course, it might be more convenient to provide arguments to support the latter assumption but that would need to be supported in a wider fluid-dynamic context and would depend on further assumptions regarding the characteristics of the rotor. Hence, confined solely to the context of BEM, all three possible assumptions are logically equally valid, in that each can be derived from the others.

2.9.2 BEM – Rotating Stream Tubes

A similar process is utilised for the case of rotating stream tubes.

Using (2.12), (2.28), and (2.31),

$$\begin{aligned} \frac{1}{4}V_R(V_\infty - V_R) + \frac{4V_R\left(V_R - \frac{1}{2}(V_\infty + V_W)\right)^2 + V_R(r_R^2\omega_d^2 - r_W^2\omega_W^2)}{4(V_R - V_W)} & \quad (2.36) \\ = \frac{B_N W c_l}{8\pi r_R} ((\Omega r_R + \omega_R r_R)C_L + V_R C_D) & \end{aligned}$$

and, by combining (2.13) and (2.15),

$$V_R r_R \omega_d = \frac{B_N W c_l}{4\pi r_R} (V_R C_L - (\Omega r + \omega_R r_R) C_D) \quad (2.37)$$

(Note that $r_R \omega_d$ is the fluid tangential wind speed just downstream of the rotor). By making the assumption that $\omega_d = 2\omega_R$ and given V_∞ , V_R and ω_R are determined from (2.36) and (2.37). The variables V_W , ω_W , r_W , and p_W are related to r_R , ω_R , V_∞ and p_∞ by (2.29) and the relationships for conservation of angular momentum, conservation of mass flow rate, and Euler respectively,

$$\omega_W r_W^2 = \omega_d r_R^2 \quad (2.38)$$

$$r_W V_W \frac{dr_W}{dr_R} = r_R V_R \quad (2.39)$$

and

$$\frac{dp_W}{dr_R} = \rho \omega_W^2 r_W \frac{dr_W}{dr_R} = \frac{\rho \omega_W^2 r_R V_R}{V_W} \quad (2.40)$$

Finally, the power applied to a blade element is derived from (2.13) and (2.14) as,

$$dP_R = \frac{1}{2} \rho r_R B_N W c_l \Omega (V_R C_L - (\Omega r_R + \omega_R r_R) C_D) dr_R \quad (2.41)$$

In this version of BEM, it is assumed that $\omega_d = 2\omega_R$. Noting that $\rho dA_R V_R r_R^2 \omega_R$ is the rate of change in stream tube angular momentum occurring upstream, an equivalent assumption to $\omega_d = 2\omega_R$, which underlies the derivation of (2.37), is that the rate of change in stream tube angular momentum occurring upstream is due to

half of the torque applied by the blade element to the stream tube. As before when discussing the assumptions underlying (2.34), it might be more convenient to provide arguments to support the former assumption but, confined solely to the context of BEM, both possible assumptions are logically equally valid..

It should be noted that this is not in agreement with the non-rotating stream tubes case, as $p_W \neq p_\infty$ and $V_R \neq \frac{1}{2}(V_\infty + V_W)$. As a consequence, the change in stream tube linear momentum occurring upstream is not half the total change.

2.9.3 Standard BEM

The standard approach to BEM combines blade element theory and momentum theory to give,

$$V_R(V_\infty - V_R) = \frac{B_N W c_l}{8\pi r_R} ((\Omega r_R + \omega_R r_R)C_L + V_R C_D) \quad (2.42)$$

and

$$2V_R r_R \omega_R = \frac{B_N W c_l}{4\pi r_R} (V_R C_L - (\Omega r_R + \omega_R r_R)C_D) \quad (2.43)$$

Given V_∞ , V_R and ω_R , determined from (2.42) and (2.43), the power applied to a blade element is,

$$dP_R = \frac{1}{2} \rho r_R B W c_l \Omega (V_R C_L - (\Omega r_R + \omega_R r_R)C_D) dr_R \quad (2.44)$$

Comparing (2.43) to (2.44), $\omega_R = 0$ only for the uninteresting situation in which the power applied to the rotor is zero.

In the textbook justification for (2.42), the left-hand side is obtained as in Section 2.9.1, i.e. on the basis of non-rotating stream tubes with underlying assumptions that $\omega_R = 0$ and $p_W = p_\infty$. The right-hand side is strictly speaking that of (2.36) on the basis of rotating stream tubes. Nevertheless, the extra terms present in the left-hand side of (2.36) can be neglected by arguing that they are relatively small.

However, confined solely to the context of BEM, this amounts to an extra assumption that would need to be supported in a wider fluid-dynamic context and

would depend on further assumptions regarding the characteristics of the rotor, such as its solidity and the blockage it induces. Of course, when the latter conditions apply, BEM is known to be a good approximation.

An alternative to the textbook justification for (2.43), is to apply to the rotating stream tube case the equivalent assumption from Section 2.9.1 for the non-rotating stream tube case, namely the assumption that the rate of change in stream tube linear momentum occurring upstream is due to half of the force applied by the blade element to the stream tube. Of course, this assumption is not strictly correct, since, as observed in Section 2.9.2, the equivalent assumptions, $p_W = p_\infty$ and $V_R = \frac{1}{2}(V_\infty + V_W)$, are no longer valid in the rotating stream tube case. Nevertheless, the discrepancies are the same as those that are argued to be negligible in the textbook justification. Hence, to obtain (2.42) on the assumption that the rate of change in stream tube linear momentum occurring upstream is due to half of the force applied by the blade element to the stream tube is equally valid to the textbook justification and the assumptions contained therein.

The textbook justification for (2.42) follows that of Section 2.9.2, i.e. on the basis of non-rotating stream tubes with underlying assumption that $\omega_d = 2\omega_R$. As discussed above an equally valid assumption would be that the rate of change in stream tube angular momentum occurring upstream is due to half of the torque applied by the blade element to the stream tube.

Note, in all three versions of BEM, the non-rotating stream tube, the rotating stream tube and standard version, V_R and ω_R are obtained as functions of V_∞ .

2.10 Aerodynamic Coefficient Models

The aerodynamic coefficient models for thrust and torque are given by,

$$F_T = \frac{1}{2}\rho AV_\infty^2 C_T \quad (2.45)$$

and

$$Q = \frac{1}{2} \rho A R V_\infty^2 C_Q \quad (2.46)$$

where A is the swept area of the rotor, R is the radius of the rotor C_T is the thrust coefficient and C_Q is the torque coefficient.

As such, using (2.12) and (2.13),

$$F_T = \frac{1}{2} \rho A V_\infty^2 C_T = \frac{1}{2} \rho B_N \int_0^R c_l W ((\Omega r_R + \omega_R r_R) C_L + V_R C_D) dr_R \quad (2.47)$$

and

$$\begin{aligned} Q &= \frac{1}{2} \rho A R V_\infty^2 C_Q \\ &= \frac{1}{2} \rho B_N \int_0^R c_l r_R W (V_R C_L - (\Omega r_R + \omega_R r_R) C_D) dr_R \end{aligned} \quad (2.48)$$

In terms of the coefficients,

$$C_T = \frac{B_N}{\pi R^2 V_\infty^2} \int_0^R c_l W ((\Omega r_R + \omega_R r_R) C_L + V_R C_D) dr_R \quad (2.49)$$

and

$$C_Q = \frac{B_N}{\pi R^3 V_\infty^2} \int_0^R c_l r_R W (V_R C_L - (\Omega r_R + \omega_R r_R) C_D) dr_R \quad (2.50)$$

For each of the three BEM cases (rotating stream tubes, non-rotating stream tubes and standard BEM), V_R and ω_R are determined in the appropriate manner as functions of V_∞ . Hence C_T and C_Q are functions of Ω , β , and V_∞ ; equivalently β and the tip speed ratio far upstream $\lambda_\infty = \Omega R / V_\infty$.

Let the thrust coefficient be defined by,

$$C_T = 4 \bar{V}_R (V_\infty - \bar{V}_R) / V_\infty^2 \quad (2.51)$$

For both the non-rotating stream tubes BEM case (see (2.34)) and for standard BEM (see (2.42)) \bar{V}_R defines a weighted average axial wind speed over the rotor disc such that,

$$\frac{1}{2}R^2\bar{V}_R(V_\infty - \bar{V}_R) = \int_0^R r_R V_R (V_\infty - V_R) dr_R \quad (2.52)$$

For the rotating stream tubes case (see (2.36)) however,

$$\begin{aligned} \frac{1}{2}R^2\bar{V}_R(V_\infty - \bar{V}_R) = & \quad (2.53) \\ \int_0^R \frac{r_R}{4(V_R - V_W)} & \left(V_R (V_\infty - V_W)^2 + V_R (r_R^2 \omega_d^2 - r_W^2 \omega_W^2) \right) dr_r \end{aligned}$$

and, in this definition, it is not appropriate to interpret \bar{V}_R as a weighted average axial wind speed. In this case, it is possible that \bar{V}_R is greater than V_R .

Similarly, let the torque coefficient be defined by,

$$C_Q = \frac{4}{3} \bar{V}_R \bar{\omega}_R / V_\infty^2 \quad (2.54)$$

Using this definition, for both the rotating stream tubes case (see (2.37)) and the standard BEM case (see (2.43)), $\bar{\omega}_R$ defines an average rotational wind speed at the rotor such that,

$$\frac{1}{3}R^3\bar{V}_R\bar{\omega}_R = \int_0^R r_R^2 V_R \omega_R dr_R \quad (2.55)$$

However, for the non-rotating stream tubes case, ω_R is assumed to equal zero and so it is not appropriate to interpret $\bar{\omega}_R$ as an average rotational fluid speed.

2.11 Single Stream Tube Aerodynamic Coefficient Models

The final aerodynamic model of a wind turbine to be considered is that of a single stream tube with both V_R and ω_R constant over the rotor.

For the non-rotating stream tube case, from (2.31) and (2.34),

$$F_T = \frac{1}{2} \rho B_N \int_0^R \left(W c_l ((\Omega r + \omega_R r_R) C_L + V_R C_D) \right) \Big|_{\omega_R=0} dr \quad (2.56)$$

$$= 2\rho\pi R^2 V_R (V_\infty - V_R)$$

from which V_R is determined and, hence,

$$C_T = 4V_R(V_\infty - V_R)/V_\infty^2 \quad (2.57)$$

For the standard BEM case, from (2.42),

$$F_T = \frac{1}{2} \rho B_N \int_0^R \left(W ((\Omega r + \omega_R r_R) C_L + V_R C_D) \right) dr \quad (2.58)$$

$$= 2\rho\pi R^2 V_R (V_\infty - V_R)$$

and from (2.43),

$$Q = \frac{1}{2} \rho B_N \int_0^R \left(W R c_l (V_R C_L - (\Omega r + \omega_R r_R) C_D) \right) dr \quad (2.59)$$

$$= \frac{1}{2} \rho \pi R^4 V_R \omega_R$$

From these equations, V_R and ω_R are determined and C_T is again related to V_R by (2.57). In both of the cases discussed, F_T differs from that determined using a multiple stream tube model.

2.12 Overview of Aerodynamics Discussed

In the preceding Sections BEM is discussed with particular emphasis on the assumptions supporting its derivation. Logically equivalent assumptions are suggested, namely, that the rate of change in stream tube linear momentum occurring upstream is due to half of the force applied by the blade element to the stream tube and that the rate of change in stream tube angular momentum occurring upstream is due to half of the torque applied by the blade element to the stream tube. An interesting observation is that these assumptions are concerned only with the upstream section of the stream tube.

In the context of the single stream tube model, directly combining the aerodynamic coefficient model with BEM, specifically that the rate of change in stream tube linear momentum occurring upstream is due to half of the force applied by the rotor,

$$\rho A_R (V_\infty - V_R) V_R = \frac{1}{2} F_T = \frac{1}{4} \rho A_R V_\infty^2 C_T(\lambda_\infty, \beta) \quad (2.60)$$

There is a direct relationship between V_∞ , the far upstream axial wind speed of the stream tube, and V_R , the axial wind speed at the rotor. Both V_∞ and V_R are constant over the stream tube cross-section. There is, thus, a one-to-one relationship between them. By contrast, in the context of the multiple stream tube model, V_R varies over the stream tube cross-section and so, for certain purposes, a weighted average, \bar{V}_R , must be used instead.

2.13 Simulation Environments

When modelling wind turbines the complexity of the model must be carefully considered. If the model is not complex enough then vital dynamics may be missing. If the model is overly complex however, then calculation time increases and it is more difficult to implement changes. There are three broad categories of wind turbine model that are typically used. In order of increasing complexity these are:

1. A basic model
2. A control model
3. A full aero-elastic simulation

In the following sections each type of model is described and a sample output from a model typical of each type provided.

2.13.1 Basic First Order Model

A basic first order model is the simplest model in common usage for the simulation of wind turbines. The general layout of such a system is given in Figure 17.

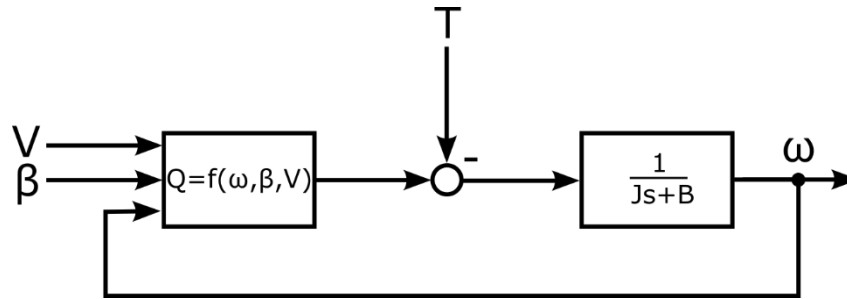


Figure 17: Basic Wind Turbine Model

The model is supplied with the following inputs:

- Effective wind speed, V
- Blade pitch angle, β
- Generator Torque, T

The aerodynamic torque Q is calculated as a function of V , β , and the rotational speed ω . The difference between Q and T is then used as an input to a first order model of the wind turbine drive-train, consisting of an inertia term J and a damping term B , in order to generate a value for ω .

The values of T and β are supplied either from a basic PI controller or, more commonly, as a function of the wind speed, ensuring that the power curve is correct.

Whilst design of controllers or assessment of loads is not possible with a basic model, this model is useful in cases where the wind turbine dynamics are not a concern.

2.13.2 Control Model

A control model is a far more detailed model that can be used as a design tool for developing controllers. A control model is a lumped parameter ordinary differential equation model, with the aerodynamics based on blade element momentum theory summed across the actuator disc with a single stream tube. Using this method, the thrust on the rotor is found and the tower dynamics can therefore be modelled. The rotor dynamics are also modelled, however, as the model considers the whole rotor disc rather than each blade; individual blade

dynamics are not easily modelled. This shortcoming is overcome through the derivation of a single blade model using Lagrange's equations [18], [22]. The drive-train and generator are modelled as a two or three lumped inertia model.

The control model contains enough detail that the rotational loads on the machine (cyclic components of the dynamics at multiples of the rotor speed referred to as " nP ", where n denotes the number of repetitions per rotation) up to $3P$ are modelled. This level of detail is required for controller design.

A control model allows full design of wind turbine controllers as it contains validated models of all the major dynamics of a wind turbine, allowing comparison of the relative loads on the turbine for each controller design. The model is not considered accurate enough however, for the measurement of absolute loads.

A diagram showing the dynamic relationships of the control model is given in Figure 18.

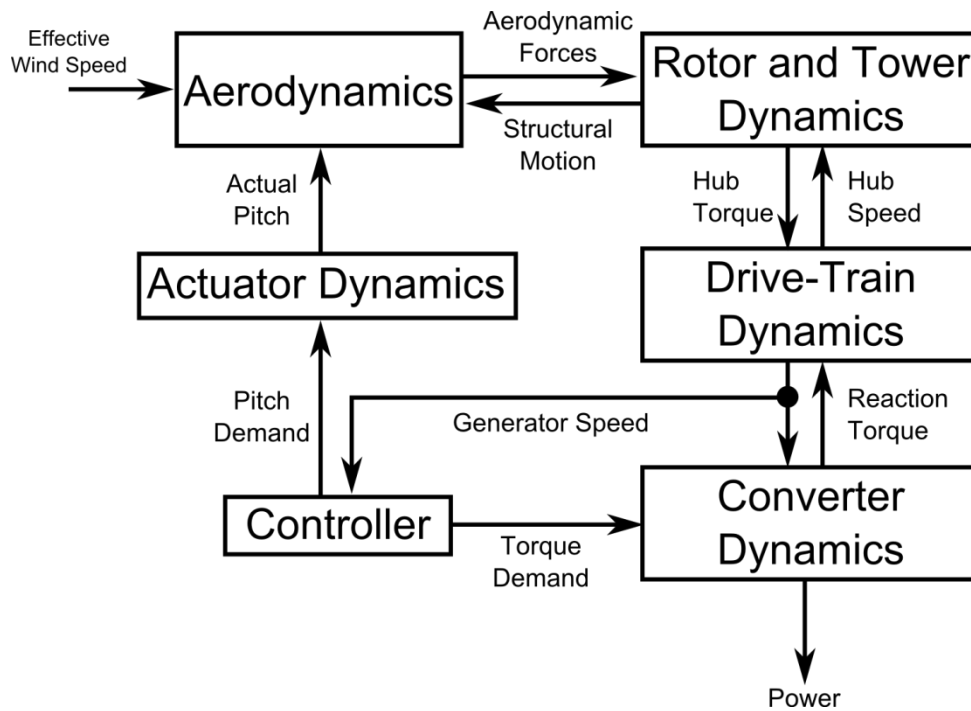


Figure 18: Dynamic Relationships of the Control Model (Adapted from [22])

2.13.3 Aero-Elastic Model

The final type of model commonly used is a full aero-elastic model such as Germanischer Lloyd's Bladed or the National Renewable Energy Laboratory developed FAST (Fatigue, Aerodynamics, Structures, and Turbulence) [23], [24].

Both use blade element momentum theory to model the aerodynamics of the wind turbine, along with full, multi-body models of all the major components of the wind turbine; allowing the dynamics across the machine, including the tower and blades to be modelled. The model uses a full three dimensional wind field and is a distributed model rather than a lumped parameter model.

The aero-elastic model allows the design and testing of a full wind turbine controller and the measurement of the absolute loads on the turbine. As aero-elastic models are used for certification of wind turbines prior to installation and are the current industry standard.

2.13.4 Examples of Each Model

In order to highlight the difference between the models, a sample simulation of the same wind turbine modelled in each way is completed and the results presented below. Plots of the power output, generator torque and generator speed are given. In addition, a plot of the power spectral density of the generator speed is given in order to show the frequency content.

The basic first order model and the control model are implemented using Matlab Simulink, whilst the aero-elastic model is designed and operated using GL Bladed. The wind turbine used is a generic 1.5 MW machine, the parameters for which can be found in appendix II. The basic and control models use the same effective wind speed input, however, for the full aero-elastic model a three dimensional turbulent wind field is required. As such, the wind experienced by this model is not identical; never the less, the turbulence level is similar.

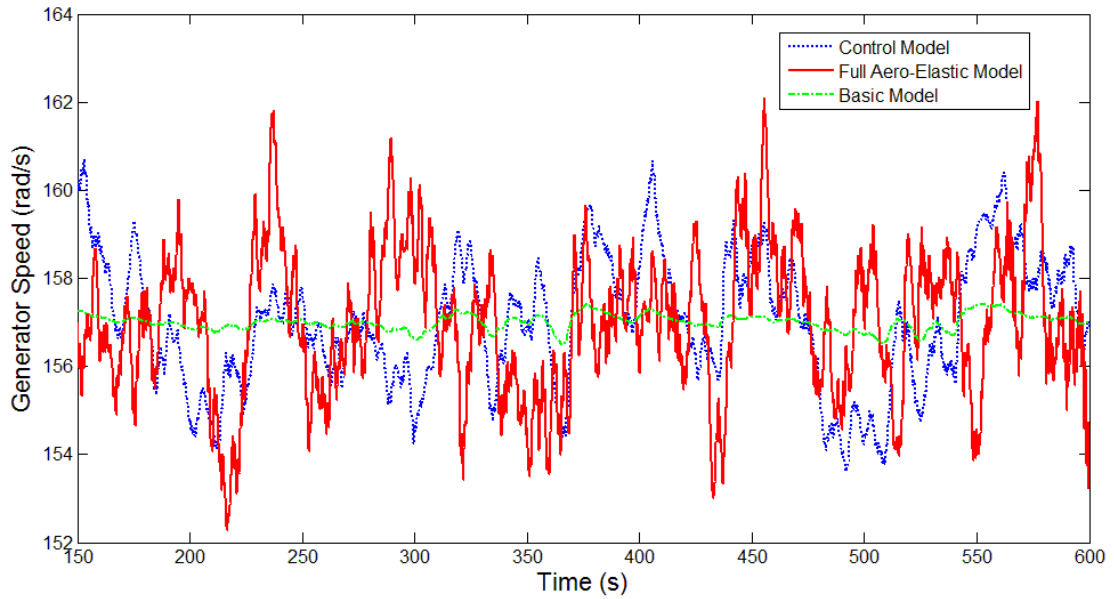


Figure 19: Generator Speed for Three Types of Wind Turbine Model - Basic, Control and Full Aero-Elastic

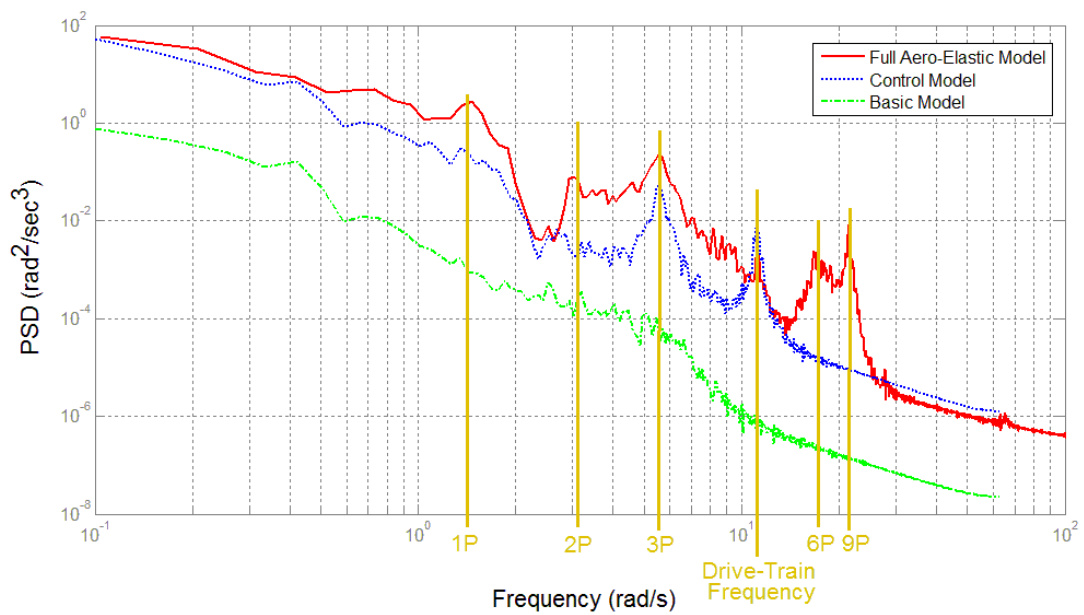


Figure 20: Power Spectral Density for Three Wind Turbine Models - Basic, Control and Full Aero-Elastic

The different levels of complexity are clear in Figure 19 and Figure 20. The basic model does not include any modelling of the wind turbine structural dynamics, and so the generator speed is held more constant and the resulting spectra is fairly flat with no large peaks. The control model contains a higher level of detail, and so the peaks at 1P, 3P and the drive-train frequency are clearly observed in Figure 20. In

Chapter 2: Overview of Wind Energy

addition, the generator speed has more variation about the set value (157 rad/s).

Finally, the full aero-elastic model has the highest level of detail. The generator speed is seen to vary at a greater variety of frequencies, though the maximum and minimum variations are consistent with the control model. These additional frequencies (6P and 9P) are visible in the power spectral density plot in Figure 20.

Chapter 3:

Flexible Operation of Wind Plant

THE CONVENTIONAL MANNER in which to operate a wind turbine is to maximise the power output within certain operational constraints, whilst minimising the loads on the turbine, as discussed in Chapter 2. These constraints usually consist of a maximum and minimum rotational speed and a rated output power. Turbines are typically operated in this manner to maximise their profitability. As more turbines connect to the grid, and as wind turbines and wind farms get larger, it may be desirable or even a requirement to operate them in a different, more flexible manner.

This chapter provides some background as to the motivation for the development of an augmented controller for more flexible operation of wind turbines and sets out the requirements for a new controller to achieve this.

3.1 Why is Flexible Operation Necessary?

Conventional operation of wind turbines maximises their power output whilst minimising the loads on the turbine. There may however, be a number of reasons for an operator to operate their wind turbines in a more flexible manner. The foremost reason is if the Transmission Service Operator (TSO) required them to do so. Currently, the grid code set out by National Grid for wind turbine operators in the UK gives no requirement that would force wind farm/turbine operators to

operate their plant in any specific manner with regards to their active power [25]. This approach is becoming less common amongst countries with high levels of wind energy connected to their grids. The requirements on active power in a variety of international grid codes are reviewed in detail in [26]. Curtailment of active power is required in four grid codes:

- In Germany, where an active power ramp rate of 10% of grid connection capacity per minute is required.
- In Ireland, where a ramp rate of 1-30MW/min is required.
- In the Nordic grid code, where a ramp rate of 10% of rated power per minute is required.
- In Denmark, where a ramp rate of 10-100% of rated power per minute is required.

The German grid code also requires curtailment of wind farm power output in over frequency events, whilst the Irish and Danish grid codes also have requirements for wind plant to vary their power output in response to grid frequency [27], [28]. The authors of [26] go as far as to comment that “As a general remark, it is clear that most grid codes require wind farms (especially those of high capacity) to provide frequency response, that is to contribute to the regulation of system frequency”.

The Danish grid code offers very clear explanations of the “regulation functions” required from wind farms, with the farms required to be able to perform seven different functions if requested. The seven functions are:

1. Absolute production constraint.
2. Delta production constraint.
3. Balance regulation.
4. Stop regulation.
5. Power gradient regulation.
6. System protection.
7. Frequency controlled regulation of the power production.

Chapter 3: Flexible Operation of Wind Plant

Function 1 requires restricting the maximum power to a set value that is less than the rated power output. Function 2 requires the operator to reduce the power output by a set constant, maintaining that constant offset. Function 3 requires the operator to be able to rapidly reduce the power output at a set speed (MW/min) and to a set value (+/- MW change). Stop regulation (function 4) requires the operator to hold the value of the power output at its current value until instructed otherwise. In the event of a reduction in wind speed the power is allowed to reduce. Function 5 requires the operator to limit the gradient of the power change (set a MW change/min limit). Function 6 is a requirement in the case of a fault, which demands that the operator must be able to rapidly curtail the output of the farm at a pre-set speed. The farm must be able to be completely shut down in 30 seconds. The final function, function 7, requires the operator to provide frequency support for the grid in the form of droop control, whereby additional power is provided when the frequency drops below the reference frequency and power is reduced when the frequency rises above the reference frequency. The capability of wind farms and/or wind turbines providing frequency control is explored in more depth in the section 3.2.

Beyond requirements dictated by the TSOs, there are other reasons why a wind farm operator may wish to vary the power output of the farm and/or the individual turbines. One possible application of flexible operation is to increase the total power captured by the wind farm by reducing the power capture of upwind turbines so as to increase the power capture of downwind turbines. The benefits in increased power production were explored in a range of studies. In [29] and [30], Johnson et al. reported increases in power production of up to 6%, in [31] Horvat and Spudic reported increases of 2.85%, Schepers and van der Pijl reported the increase to be somewhat lower at around 0.5% [32], whilst Machielse et al. claimed that 4.1% is the maximum achievable increase for two wind turbines with one in the other's wake [33]. Whilst the increase in power achievable is clearly under some dispute, the general strategy is well supported.

Reducing the power output (and hence a reduction in the axial induction factor) of a wind turbine is also postulated to reduce the fatigue loads on the machine. Use of this approach to reduce loads across a wind farm has been investigated in the literature. In [34], a wind farm control technique based on a parametric programming technique [35] was presented, with the goal of reducing loads whilst maintaining the same power output. The authors claimed to reduce the shaft damage equivalent loads by between 5 and 8%, with small reductions of 1% in the tower damage equivalent loads, whilst the total power output is maintained, albeit with a “wind farm” of just two wind turbines.

Madjidian et al. [36] presented an approach whereby the wind farm power output was first reduced to a level lower than the capacity. This approach was expanded in Biegel et al. [37]. The reduced power level was then maintained whilst the power output of each turbine in the farm was optimised to reduce loads. Tower and shaft fatigue load reductions of 15-20% were claimed by the authors.

Whilst there is no source in the literature that investigates operation and maintenance cost reductions when using wind farm control, the exact magnitude of the likely reduction in loads on the turbines is disputed, and the impact on the power output is also in question, there is still potential to reduce operation and maintenance costs through wind farm control to reduce loads.

A review of the state of the art for wind farm control techniques for increasing power capture and/or reducing loads was presented by Knudsen et al. in [38].

3.2 Wind Turbines and Grid Frequency

Electrical grids are operated at a set reference frequency, usually either 50Hz (in Europe, Asia, Africa, and Australasia) or 60Hz (in the USA and much of the Americas). Conventional power plant, such as coal or gas fired power stations run synchronously with the grid, that is to say that the generators in the plant rotate at a multiple of the grid frequency. Power supplied to the grid and power demanded from the grid must be kept equal at all times, else the grid frequency will either rise (in the case of supply being greater than demand) or fall (in the case of demand

being greater than the supply). The relationship between the power supply, power demand and grid frequency is expressed in mathematical form as,

$$J_s f \frac{df}{dt} = P_{sup} - P_{dem} \quad (2.1)$$

where J_s is the combined inertia of all the synchronous plant, f is the grid frequency, P_{sup} is the power supplied and P_{dem} is the power demanded. If the value of J is high, then the frequency will change more slowly than if the value of J_s is low, assuming the same difference between P_{sup} and P_{dem} . As such, in order to maintain the grid frequency at the reference value a high inertia is useful.

Conventional synchronous plant also provide primary response in the case of a drop in frequency via a process called droop control. Droop control is the provision of additional power in proportion to the difference between the measured grid frequency and the reference grid frequency. This response is used to stabilise the grid frequency.

As discussed previously in chapter 2, the majority of modern wind turbines use back to back converters and are therefore asynchronous to the grid. Because the wind turbine's speed is not linked to the grid frequency in any way they do not contribute to the combined inertia of the grid. As such, in grid systems with large numbers of wind turbines the system inertia is often low, resulting in a less stable grid frequency [39].

With the EU targets for 20% of energy to be supplied from renewable sources by 2020 [40], and with the possibility of further targets of 30% of energy to be supplied from renewable sources by 2030 [41], it is highly likely that the proportion of electricity supplied by wind turbines to the grid will increase. In Denmark 27.1% of electricity in 2012 was supplied from wind energy averaged across the whole year [42]. Clearly at times of high wind and low demand, wind energy will have supplied a significantly higher proportion than this.

As modern variable speed wind turbines are not directly connected to the grid, they do not naturally provide inertia to the power system like synchronous power plant

do. An alternative way to provide a similar reduction in the rate of change of frequency by using wind turbines is therefore required if wind turbines are to contribute to grid frequency support. If this is not done then the grid frequency is more susceptible to large drops following a sudden peak in demand or drop in supply as discussed in [39].

One method used to mitigate this problem is commonly called synthetic inertia. Synthetic inertia works by temporarily increasing the power output of the wind turbine proportionally to the rate of change of grid frequency. Hansen et al. [43] showed that the short-term increase in power provision required from a wind turbine to provide synthetic inertia is available in most operating conditions, though the available power for over production varies greatly with the wind speed. Provision of synthetic inertia has been shown to reduce both the speed of the drop in grid frequency and the minimum frequency in the case of a sudden peak in demand or drop in supply [44]–[46], however the best control method to supply synthetic inertia is not clear, with many different options available within the literature (see section 3.3).

When operated in the conventional manner, asynchronous wind turbines also do not provide any droop control, which is a requirement of conventional plant. Droop control is the provision of additional power from a power plant proportional to the change in grid frequency from the reference value. The UK grid code for example, requires that conventional power plant must provide droop capability of 3-5% [25], i.e. a change in frequency of 3-5% must result in a change in the power output of 100%. As with synthetic inertia, whilst the provision of droop control from wind turbines has seen significant interest in the literature [45]–[52], the best control method to provide it is not clear (see section 3.3).

3.3 Design and Development of Augmented Controllers

There are three basic ways in which the power output of a wind turbine can be altered. These are,

1. Changing the pitch angle demand.

2. Altering the torque demand.
3. Utilising a change to the locus of set points (i.e. the operational strategy) of the full envelope controller.

These methods all suffer from drawbacks that limit their effectiveness. All the papers reviewed later in section 3.4 use one of, or a combination of these methods.

Using method 1, an addition is made to the pitch demand signal from the full envelope controller. By increasing the pitch angle in below-rated operation the aerodynamic torque is reduced. This leads to a reduction in the rotor speed and the full envelope controller therefore reduces the torque demand. Hence, the power output of the turbine is reduced.

Method 1 has the following issues:

- 1a. The speed of the response depends greatly on the controller and the operating point and so it is not consistent across the operational envelope.
- 1b. A given change in pitch angle results in a different change in power at different operating points, so the pitch angle used must be scheduled in some way.
- 1c. By introducing a pitch angle outwith the full envelope controller, the gain of the controller may no longer be at an appropriate value, especially close to rated wind speeds.
- 1d. In above-rated operation, without further alterations, this approach is ineffective as any change in the pitch angle is countermanded by the action of the full envelope controller in response to the change in generator speed.

To illustrate these limitations, a simulation is run using a Simulink model of a 1.5MW wind turbine with a full envelope controller. An increment of 2, 4, or 6 degrees is made to the pitch demand outwith the full envelope controller at ten seconds simulation time. Note that the model used does not account for losses in the power electronics (of approximately 5%) and so the power at rated wind speed is 1.58MW

Plots of the resulting power output (graph *a*), change in power relative to no addition to the pitch angle (graph *b*), pitch angle (graph *c*), and change in pitch angle relative to no increment (graph *d*) are given in Figure 21. The wind speed used is a turbulent wind with an average close to the rated wind speed for the turbine.

Figure 21 shows that the increase in pitch angle does produce a reduction in the power output in below-rated conditions (between 18 and 34 seconds, when the simulation with no increase in pitch has a pitch angle of -2 degrees), albeit varying with wind speed. With some scheduling of the pitch angle it may be possible to obtain a fairly accurate change in power via this method in below-rated conditions. Scheduling the pitch angle is not simple however, as the controller must be designed so as to not introduce any feedback loops around the full envelope controller as this would adversely affect the full envelope controller's performance.

In above-rated conditions however there is little to no change in the power output. This is due to the full envelope controller detecting the change in generator speed caused by the increment in pitch angle and counteracting it via an equal and opposite change in pitch angle. In addition, because there is a pitch angle applied to the wind turbine outwith the full envelope controller, which the full envelope controller has no information regarding, the gain scheduling of the pitch angle by the full envelope controller is no longer correct. This results in a reduction in stability and large oscillations in both the pitch angle and the generator speed, seen towards the end of the simulation from 40 seconds onwards. The larger the change in pitch angle, the greater the oscillations; as the gain of the full envelope controller is incorrectly set and so it is unaware of the increment to pitch angle being provided. In some cases this may lead to instability of the controller, as may be observed in the simulation with a 6 degree increase in pitch.

At wind speeds close to rated (such as at simulation time of approximately 12 to 17 seconds), the power is reduced; however this reduction is not as large as the

reduction in above-rated conditions. Note that gain scheduling the pitch response would not improve this error.

Finally, the change in power is not quickly achieved, with a delay of approximately three seconds between the reduction in power being demanded (at 10 seconds) and the reduction being achieved in Figure 21. The speed of the response is limited by the speed of the full envelope controller, the limitations of the pitch actuator, and the delays inherent in aerodynamics, as can be seen in Figure 22, in which the same set of simulations are shown, completed at a lower wind speed in the max power tracking section of the wind turbines operational strategy. When operating in this part of the operational strategy the response speed is even slower.

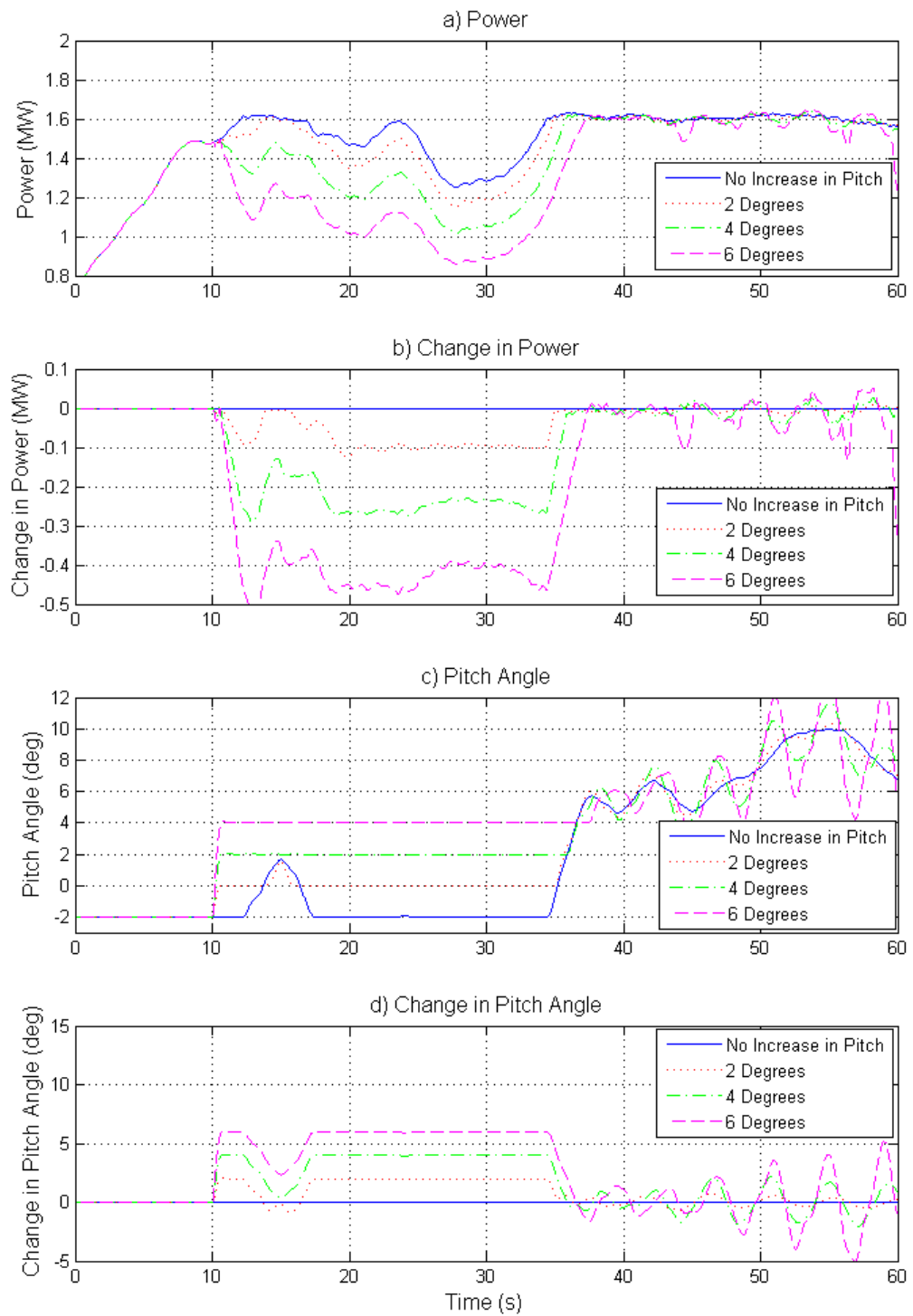


Figure 21: 1.5MW Turbine with Various Requested Changes in Pitch

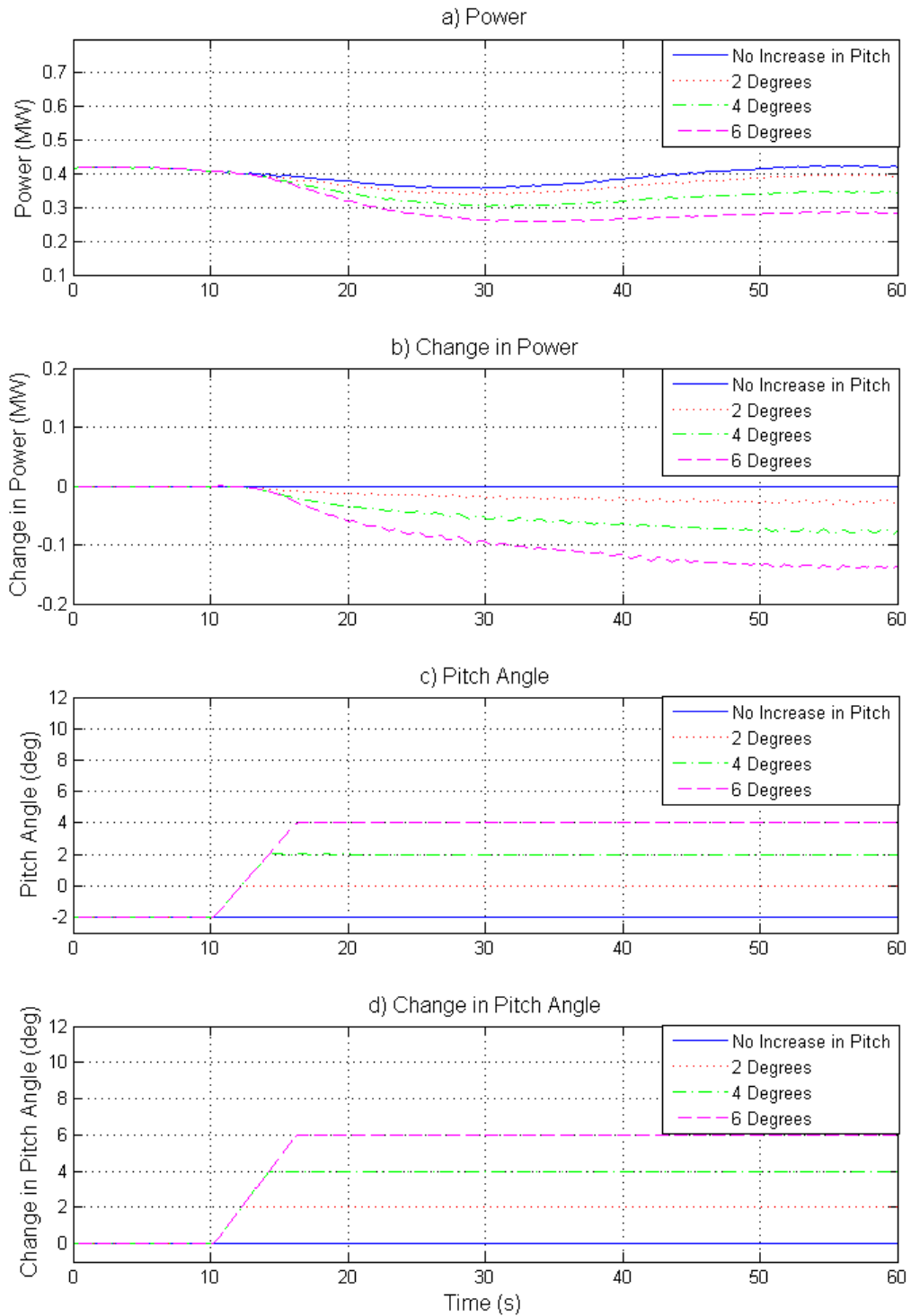


Figure 22: 1.5MW Turbine with Various Requested Changes in Pitch (Maximum Power Tracking Region)

Using method 2, an addition to the torque demand sent to the wind turbine is made in order to alter the power output of the machine. In above-rated wind conditions this is an effective way of altering the power output. The change in the torque leads

to a change in the rotor speed, which is counteracted through an adjustment to the pitch angle made by the full envelope controller. However, this approach has the following issues:

- 2a. Without additional alterations, in below-rated wind conditions the change in rotor speed is counteracted by the full envelope controller via an adjustment to the torque demand, eliminating the change in power requested. The speed with which the increment in torque is countermanded is dependent on the speed of the full envelope controller at the operating point.
- 2b. The change in torque required to produce a given change in power changes dependent upon the generator speed. This is not an issue at above-rated wind speed as the rotor/generator speed is constant, however in the maximum power tracking region the speed varies and so this issue becomes a concern.

An example of this style of controller is designed and operated via simulation in Simulink for a 1.5MW wind turbine with a full envelope controller. An increment is made to the torque demand. The magnitude of this increment is defined by a demanded change in power divided by the generator speed. Three different increments are used, a reduction of 0.1MW, 0.2MW, and 0.4 MW, as well as a simulation with no increment. The results are shown in Figure 23.

The increment is applied at 10 seconds simulation time, at which point the turbine is in below-rated operation. The power instantly drops by the desired amount, however, the full envelope controller responds to the ensuing change in generator speed and counteracts the change in speed via torque, bringing the power back to value of that with no increment. When the turbine enters above-rated operation (between 32 and 35 seconds), the desired change in power is achieved, as the change in generator speed caused by the increment is counteracted via pitch action rather than generator torque.

At close to rated wind speeds the increment in torque acts as a reduction in the rated torque of the turbine. As such, the turbine enters above-rated operation at a

different wind speed. When the turbine has exceeded this wind speed but is still below the rated wind speed without the increment (for example between 25 and 32 seconds in Figure 23), the change in power output is not accurate as is clearly seen in the (graph *b*) of Figure 23.

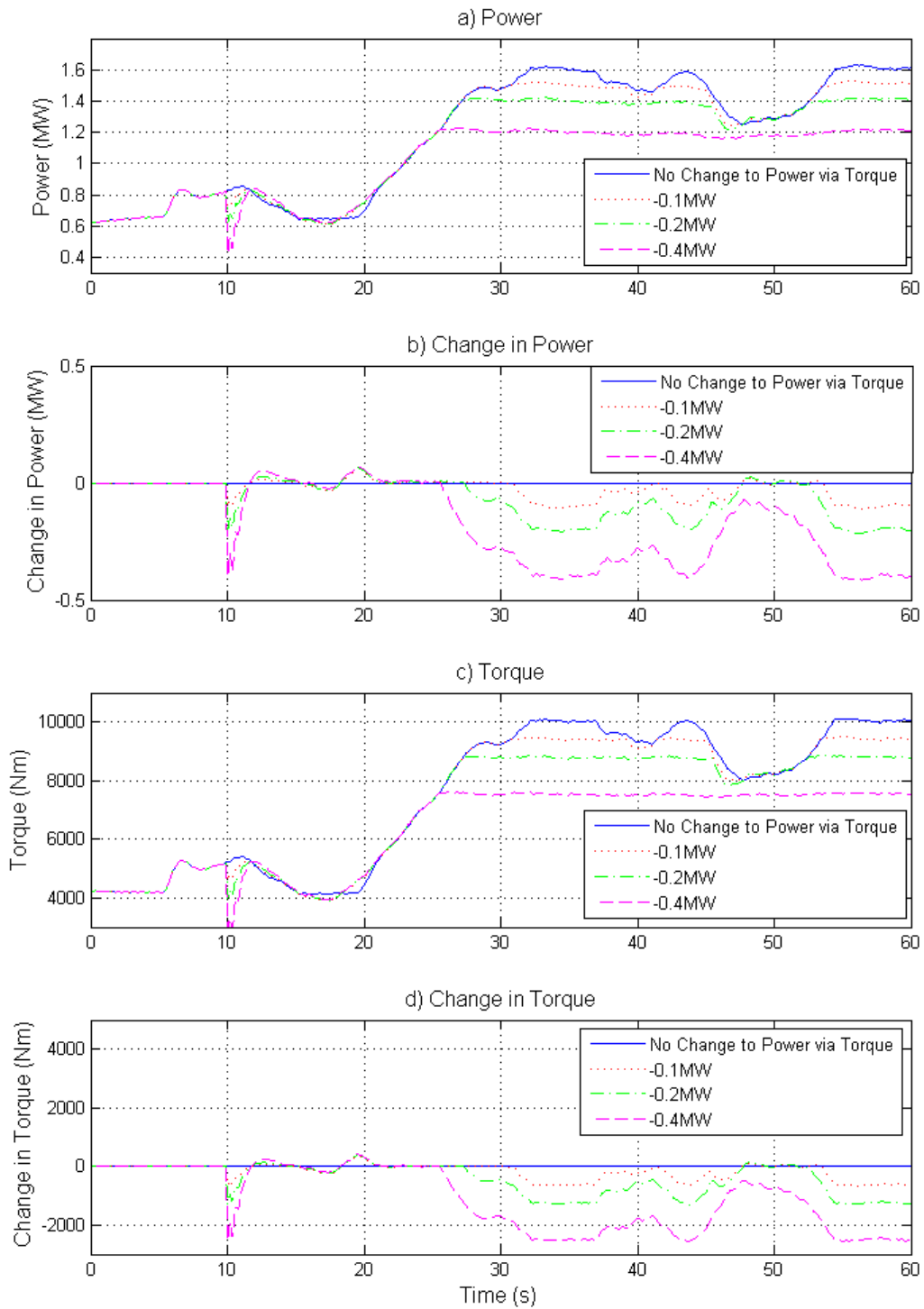


Figure 23: 1.5MW Turbine with Various Requested Changes in Power via Torque

Chapter 3: Flexible Operation of Wind Plant

As method 1 is suitable for use in below-rated wind conditions and method 2 is suitable for use in above-rated conditions, the two methods can be combined, so that the method used is switched between above and below-rated operation. Doing this may lead to many implementation problems at close to rated wind speeds however, as the controller needs to switch between the modes smoothly, possibly many times in a short time period.

Method 3 uses an alteration to the locus of set points (operational strategy) of the full envelope controller in order to vary the power output. This requires the design of more than one operational strategy for the wind turbine. The wind turbine can then be switched between these operational strategies to vary the power output.

This approach has the following issues:

- 3a. The power can only be altered to follow a previously set strategy; that is to say that the number of possible requested changes in power output are restricted to a small number.
- 3b. The full envelope controller must often be significantly altered in order to incorporate this method. As such, applying the controller to a machine would often require either in depth knowledge and access to the original controller and/or the complete redesign of the controller. For example, moving the operating curve alone alters the gain of the controller for a given wind speed. This can lead to a poorly tuned controller if not redesigned.

If the pitch angle in below-rated operation is not altered then the strategy can be altered in a variety of different ways, as shown in Figure 24.

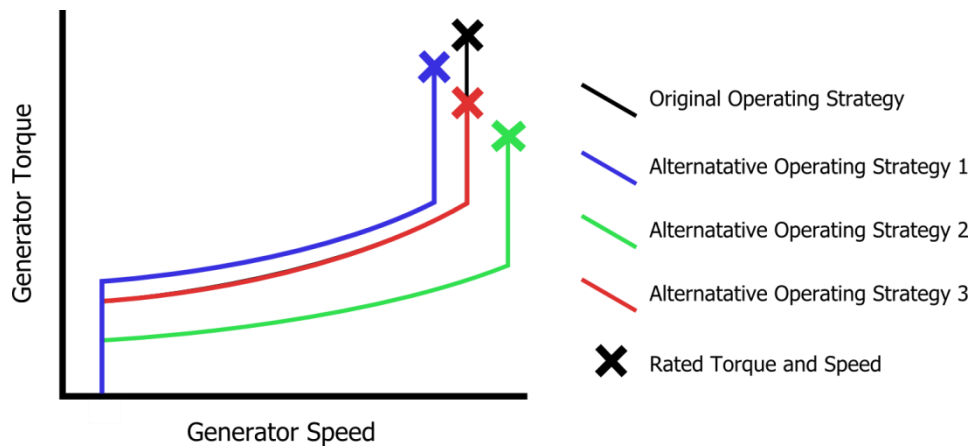


Figure 24: Alternative Operating Strategies

The operating strategy can either be moved upwards and to the left (alternative operating strategy 1) or downwards and to the right (alternative operating strategy 2). In addition, the strategy could be altered by solely reducing the rated torque (alternative strategy 3). The first option moves the operating strategy of the turbine further towards the stall region, and so is unlikely to be chosen. The second alternative strategy also has limitations. Whilst it reduces the power output in all wind conditions and does not move the operating strategy closer to the stall region, there is an upper limit to the rotor speed, either due to structural resonant frequencies or due to the wind turbine's over-speed limit. This upper limit would soon be reached. For example, for a typical 1.5MW wind turbine with a rated rotor speed of 1.87rad/s, a reduction in power of just 5% would require the rated rotor speed to increase by 23% to 2.42rad/s.

Strategy 1 and 2 suffer from the major limitation that the change in power cannot be consistent for all wind speeds. A consistent change in power can be achieved for all wind speeds in the maximum power tracking region, however for the constant speed region this is not the case.

The third strategy only reduces the rated power and so, whilst it is useful for reducing power in above-rated wind conditions it does not have any effect below-rated wind speeds. In addition, at close to rated wind speeds the reduction in power output is not accurate for the same reasons as explained previously for method 2 in close to rated wind speeds. Also, strategy 3 may reduce the length of

the second constant speed region, which can cause problems for the controller switching between modes and for the gain scheduling. This method can also cause the cross-over frequency of the full envelope controller to be reduced, reducing the effectiveness of the controller.

An example is given in Figure 25 of the open loop Bode plot from controller input to generator speed for a 1.5MW machine, the same turbine de-rated to 1MW and the same turbine de-rated to 750kW, all using the third alternative strategy. This plot shows that the cross-over frequency is significantly degraded, from approximately 1.2rad/s, to approximately 0.65rad/s for the 1MW de-rated machine and 0.55rad/s for the 750kW de-rated machine at rated wind speed in each case. A cross-over frequency (the frequency at which the gain crosses zero magnitude) of half the original value has a highly detrimental effect on performance that can only be rectified via redesign of the controller.

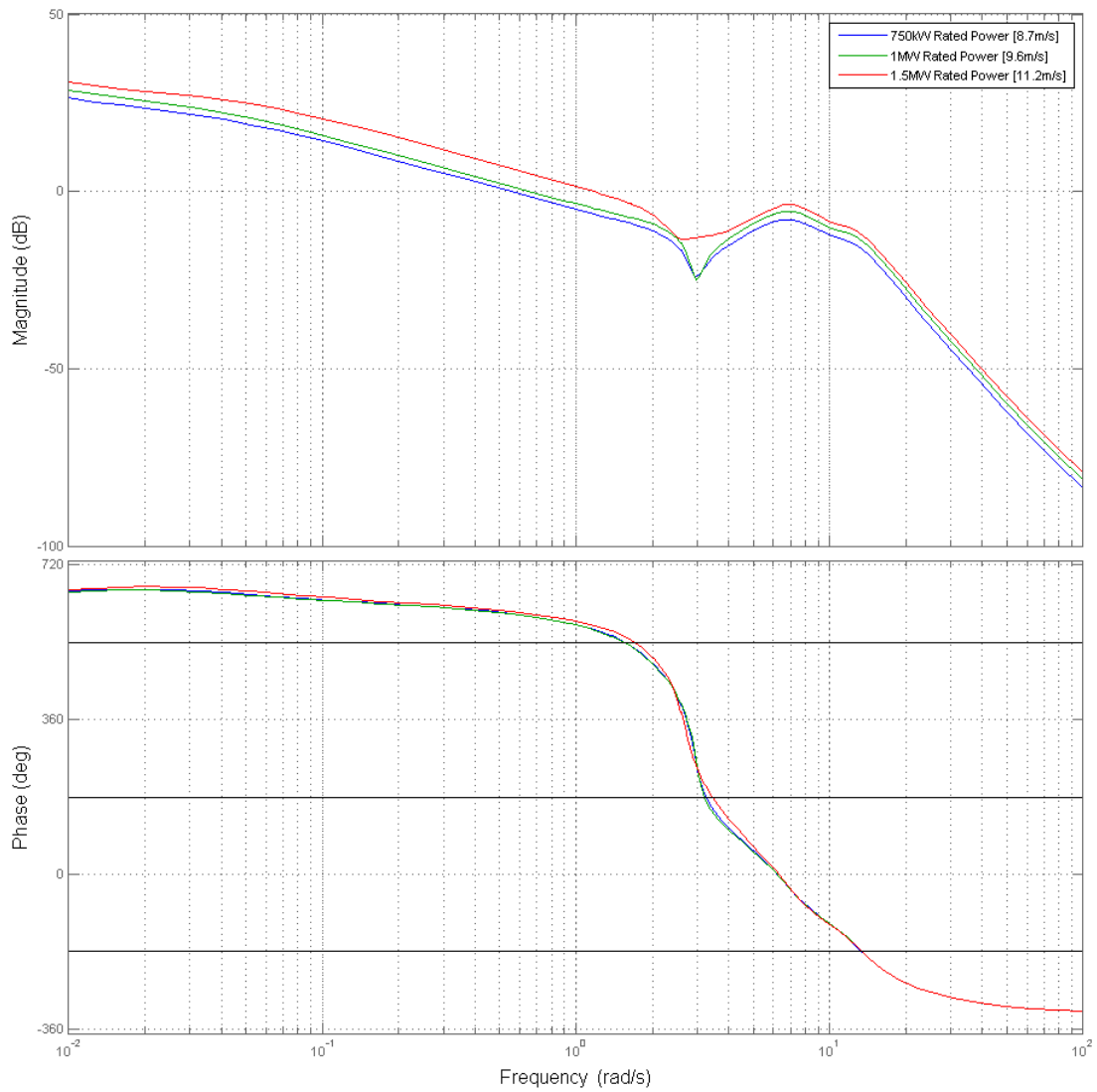


Figure 25: Bode Plot of Controller and Turbine Open Loop Dynamics at Rated Wind Speed for 3 Different Rated Powers

3.4 Augmented Controllers in the Literature

Various proposed designs for an augmentation to a controller to vary the power output are discussed in the literature. Several of these controllers are proprietary systems developed by wind turbine manufacturers such as Siemens, Mitsubishi, and Vestas [53]–[55] and so there is no in depth description of how these controllers achieve the proposed aims.

The Siemens patent [53] is a US patent for “frequency responsive wind turbine output control”. The patent focusses primarily on wind farm control to provide the frequency response, with the tacit assumption that the power output of individual

wind turbines can be altered. Only the application of changing the output power in response to a demand from the grid operator is presented.

The Mitsubishi patent [54] is a US patent for altering the power output of a wind turbine. The power output is claimed to be altered with a maximum and minimum rate of change in power applied. The power is altered via a change to the power set point, which in turn alters the blade pitch angle and the torque demand. It is assumed that the full envelope controller operates based on a power set point.

The Vestas patent [55] is a US patent relating to “a method for curtailing electrical power supplied from a wind turbine”. The patent details three general methods of achieving this, changing the pitch angle, changing the rotor speed, and changing both the pitch angle and the rotor speed. No detail beyond the general methods outlined is given. The patent claims that the “only way to reduce the power production at low wind speeds is to switch the wind turbine into a nominal power control algorithm”. The patent requires that the current available power be known and suggests one method of achieving this is through “measurement of the actual wind speed”. Later in the patent the authors suggest a system whereby measurements from the wind turbine’s anemometer are used to provide the measurement of the wind speed. Such a system relies upon the anemometer providing accurate data. No mention is made in the patent of utilising a direct adjustment to the torque demand sent by the controller to the generator without a direct alteration of the power set point.

None of the patents offer detail as to how the power output of a wind turbine would be altered beyond words to the effect of “altering the power set point” or “changing the blade pitch angle”.

Work on the development of augmented controllers to provide frequency support and/or curtailment has also been presented in the open literature, with more detail regarding the design of the controllers available than in the industrial patents.

Many (though not all) of these papers approach the problem from a power systems perspective however, and use very simple wind turbine models, causing the

controller design to be simplistic. An overview of the papers on the topic of the design of augmented controllers follows.

A controller for providing synthetic inertia and droop control was proposed by Morren et al. [48], [56]. The controller was a form of "method 2" defined in section 3.3. The wind turbine used had a DFIG (Directly Fed Induction Generator). The wind turbine model was not described in detail, but did include modelling of the drive-train, rotor, and tower dynamics. As such, it was similar to the control model described in section 2.7.

This controller was designed solely with the purpose of providing synthetic inertia and droop control. Curtailment was not considered. The full envelope controller that was later adapted used a "speed controller", which simply used a look up table, provided with the measured power output and output a reference speed as a set point. A PI controller was then used to control to that set point.

To supply synthetic inertia an input of the rate of change of frequency filtered with a low pass filter to remove noise was provided. A gain of $2H$ was applied and this value was added to the torque sent to the converter. The schematic for this controller is shown in Figure 26.

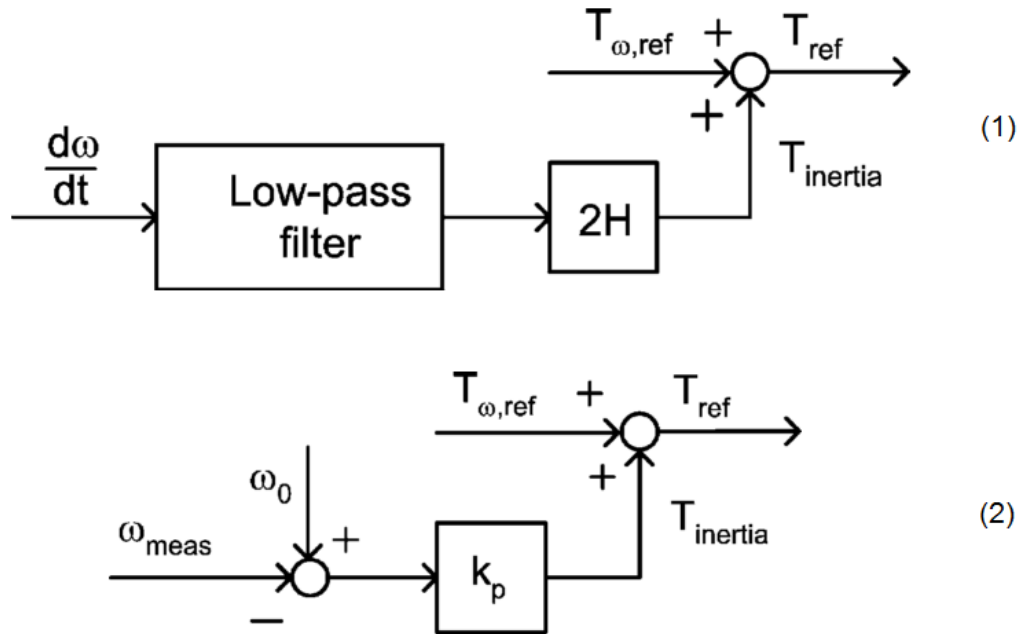


Figure 26: Controller used by Morren et al. (Adapted from [56]), with the Alteration to the Turbine Torque Demand Shown for Synthetic Inertia (1) and for Droop control (2)

For the droop controller the deviation from the desired grid frequency was measured and a simple proportional gain was used to give an increase in the torque to be added to the torque demand.

Issue 2a raised with method 2 in section 3.3 was not addressed in the paper. No alteration was provided to prevent the PI controller counteracting the increment to torque. As such, the increment is likely to be eventually eliminated.

The second problem; that of the required change in torque changing as the generator speed changes, was partially addressed by setting the change in torque to be equal to the desired change in power divided by the generator speed. This approach does not account for the reduced power from moving the operating point. For example, if the original operating torque is T_0 , the original generator speed is ω_0 , the new torque is $T_0 + \Delta T$ and the new generator speed is $\omega = \omega_0 + \Delta\omega$, then the required change in torque to affect a change in power of ΔP is,

$$\Delta T = \frac{\Delta P}{\omega} - \frac{\Delta\omega}{\omega} T_0 \quad (3.1)$$

Chapter 3: Flexible Operation of Wind Plant

The second term of this equation accounts for the change in power output caused solely by the change in the generator speed. This term was not included in the proposed augmented controller.

Both the proposed "droop control" and the proposed "synthetic inertia" control were only investigated for use in the case of a large frequency drop. As there was no use of the pitch control, neither method proposed is suitable for sustained reductions in power output such as those required for curtailment. This issue was not addressed, as only a short term change in the grid frequency was simulated.

No investigation was conducted into the impact of the proposed technique on the wind turbine loads.

A controller designed to provide synthetic inertia was proposed by Zeni et al. in [57]. To provide synthetic inertia, the authors used an approach of the form of "method 2" defined in section 3.3. The wind turbine model used was a basic model as defined in section 2.7. A look up table was used to provide a power reference based on the generator speed. An additional term proportional to the rate of change of grid frequency was added to this power reference and the total value was then fed into the mechanical model of the wind turbine. A simple aerodynamic model provided an aerodynamic power. The mechanical model used assumed that the requested generator power was delivered and then found the resulting change in generator speed using a first order model.

Neither issue *2a* nor issue *2b* raised with method 2 in section 3.3 was addressed.

Only constant wind speed simulations were conducted and there was no investigation into the loads induced on the turbine. The paper focussed mainly on the impact of the proposed provision of synthetic inertia on grid frequency and concludes that wind turbines capable of providing synthetic inertia have the potential to offer better inertial characteristics than synchronous machines.

Ramtharan et al. [51] used a combination of method 2 and method 3 defined in section 3.3. The wind turbine model used was a DFIG turbine modelled in GL

Bladed; a full aero-elastic simulation package. The standard operating curve was “de-loaded” in order to allow head room for sustained droop control. The authors state that "The de-loading was achieved by shifting the operating curve towards the right" as shown in Figure 27. This is an example of method 3 defined in section 3.3. The de-loading of the turbine was 90% of the maximum power in the variable speed region; however, in the constant speed region the de-loading necessarily varied as discussed in section 3.3.

To achieve droop control, a change in torque was used to provide the change in power in a similar manner to [56] (discussed previously) and the same comments regarding issues 2a and 2b apply. Because the wind turbine strategy was altered, the controller was capable of maintaining an increase in power of up to 10% indefinitely, however, in wind speeds in the constant speed section the maximum increase in power was less than 10%. Changing the strategy however, raises the issues discussed in section 3.3. Issue 3a was addressed, as the controller does not switch between strategies per se, it instead operates following a non-optimum strategy before using method 2 to affect the change in power. Issue 3b was not addressed; the method proposed requires a redesign of the wind turbine strategy and controller.

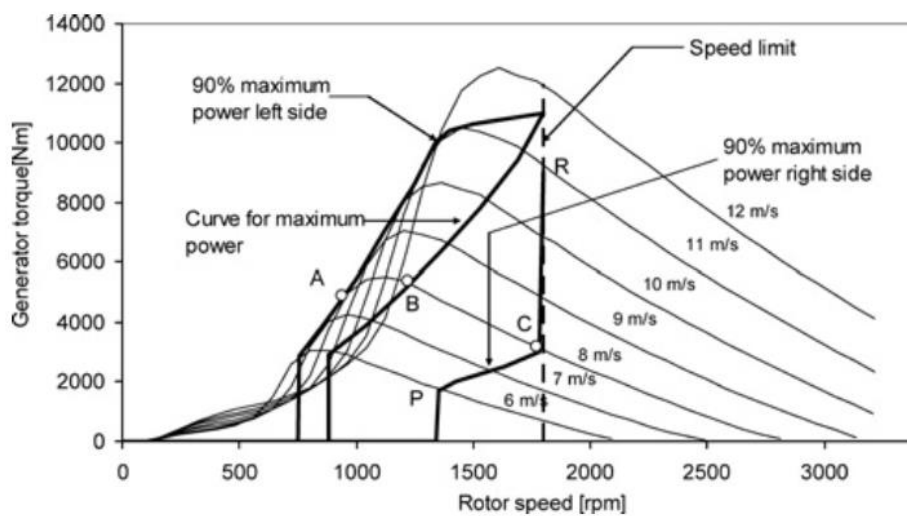


Figure 27: Alteration to the operating strategy proposed in [51]

Whilst the simulations were conducted using GL Bladed, no investigation was made into the impact on loads and only constant wind speed simulations were undertaken, which are not representative of real conditions.

In the work by de Almeida et al. ([58], [59] and [52]), a controller was proposed to provide droop control and changes in power as defined by a separate “supervisory wind farm control system”. For each wind turbine a “de-loaded optimum power extraction curve” was defined, in which the power for a given wind speed and rotor speed was 20% lower than the optimum value. This curve was used as a look up table to provide a power reference P_{del} . The authors made no comment on how the wind speed would be measured in order to achieve this. Change in power values ΔP_1 and ΔP_2 were then subtracted from the reference value P_{del} , where ΔP_1 was proportional to the change in grid frequency (droop control) and ΔP_2 was provided from a “supervisory wind farm control system”. The “supervisory wind farm control system” was designed to optimise the power output of the turbines in a wind farm to “obtain a minimum deviation between the total active and reactive powers delivered by the wind farm to the grid as required by the system operator”.

The new reference value ($P_{del} - \Delta P_1 - \Delta P_2$) then had the measured power subtracted from it, to find the error in power, which was then processed through PI control to provide changes in generator torque.

Simultaneously, the value P_{del} was divided by the measured mechanical torque of the turbine, which was assumed to be known, to find a speed reference ω_{ref} . This was subtracted from the measured speed to find a speed error. Simple PI control was then used to provide pitch control. There was no mention of any scheduling of the gain of this controller.

For the wind turbine model itself, a very simple aerodynamic model was used, similar to the basic model described in section 2.7. A wind farm and power system consisting of five wind turbines, with a conventional generator also connected to the system, was modelled, with each wind turbine controlled in the manner discussed.

Chapter 3: Flexible Operation of Wind Plant

Constant wind speed simulations were conducted wherein a sudden change in the load on the power system was simulated. No simulations with variable wind speeds were performed. The authors were mainly concerned with the impact on the grid frequency. No assessment of the loads on the turbines was made.

The controller presented was a combination of all methods 2 and 3 described in section 3.3. Method 3 was used to define a de-loaded power curve. Changes in the electrical power were then affected by means of a change in the torque demand (method 2). Although pitch control was then used to control the generator speed, it was not used to directly alter the power output of the turbine and so method 1 is not applicable.

Because the change in torque resulted from a change in the set point of the controller, the torque change was not rejected and so issue *2a* is not a concern. Issue *2b* is not addressed.

As method 2 was only used to de-rate the turbine, and not to affect the subsequent change in power, issue *3a* is not a concern. Issue *3b* is not addressed.

Because the controller used a measure of the wind speed, and no explanation of how this measure was obtained was provided, the controller cannot be applied to an actual wind turbine.

Chowdhury et al. [60] and Ma and Chowdhury [50] also proposed an augmented controller to provide synthetic inertia and droop control.

As in [58] and [61], the authors were mainly concerned with the effect on the grid frequency of providing frequency support from wind turbines and as such, the wind turbine model used was equivalent to the basic model described in section 2.7. Simulations were only presented for a single, constant wind speed.

Three methods for altering the power output of the turbine were presented – “Inertial Control”, “Pitch Angle Control”, and “Rotor Speed Control”. “Inertial Control” was used to provide inertial response to a change in grid frequency and is

similar to that presented in [48], discussed previously; hence the same comments apply here.

“Pitch Angle Control” was used to supply droop control through the action of the pitch actuator. An additional pitch angle was first applied to allow head room for increased power production. The pitch angle was then altered dependent upon the deviation of the grid frequency from the desired value. This is an example of method 1 defined in section 3.3. The work presented only considered a single wind speed, with the controller and model designed specifically for that wind speed. In order to work at alternative wind speeds the controller needs to be redesigned. As such, it is unsuitable for use in a variable wind. This was not discussed by the authors and only simulations at the single constant wind speed for which the controller was designed were performed. None of the issues raised in section 3.3 were addressed.

“Rotor Speed Control” (RSC) is an example of method 3 defined in section 3.3 and was used to provide droop control. The operational strategy was redefined at 90% of the strategy for optimum power output in below-rated wind conditions. There was no constant speed region used and so issue 3*b* is avoided. When the grid frequency changes, a change in power output was requested proportional to the change in frequency. This change in power was then added to the set point defined by the operational strategy. Changing the power output of the wind turbine altered the rotor speed, which in turn altered the set point derived from the operating strategy (P_0 in Figure 28). Because the set point was altered the desired power output was not obtained. The authors suggested that the value for P_0 could be held constant to alleviate this problem, however this is not a valid solution in variable wind conditions. The authors did not present any discussion regarding solving this issue.

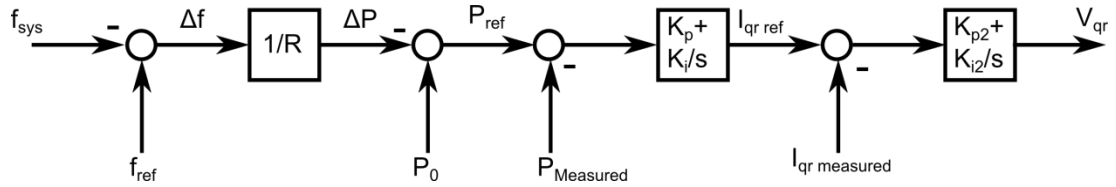


Figure 28: Adaptation of "RSC Schematic" from [60]

Results were presented for "Pitch Angle Control", "Inertia Control", a combination of both, and for RSC. As "Pitch Angle Control" and RSC couldn't be applied in varying wind speeds, and as the former couldn't be applied at more than one constant wind speed without redesign of the controller, only a single constant wind speed was considered. The results presented showed improvements in the grid frequency for a hypothetical power system through application of the presented controllers on wind plant, however no discussion was presented regarding changes required to allow the controllers to work in varying wind speeds.

Erlich and Wilch [49] investigated three different strategies for supplying grid frequency support via augmented control. All the methods required redesign of the whole controller. The first of these methods used method 1 as defined in section 3.3. Issue 1a, variation in the speed of response dependent upon operating conditions, was not addressed by the authors, though they did conclude that this method was generally slower than other methods. Issue 1b was addressed in part, with the authors stating that the calculation of a suitable change in the pitch angle to down regulate the wind turbine power "needs extensive knowledge of the behaviour of the wind turbine's mechanical system, since this offset has to be calculated and changed for nearly every new operating point". The methods used to achieve this were not given. Issue 1c does not appear to have been addressed. The standard pitch controller (i.e. that of the full envelope controller without augmentation) did not have any gain scheduling and no information was provided as to how the gain of the controller was altered when the augmented value is added. Issue 1d was not addressed by the authors.

The second method investigated was similar to that used by Morren et al. [48], [56] (discussed earlier) and involved altering the turbine set point to provide additional

power. No de-loading of the turbine was used and so the length of time for which the increased power can be provided was limited as the rotor was slowed when this technique was utilised. Similar limitations to [48], [56] (see previous discussion) apply here.

The third technique involved initially accelerating the turbine when the frequency dropped by reducing the power output to increase the kinetic energy in the rotor. The power output was then rapidly increased to limit the frequency drop via a change in the torque demand. This had the advantage of being able to supply a larger increase in the power output, albeit at a later time. It is unclear as to how the decision on when to transition from accelerating phase to the increased power phase was made, though the simulation results indicate a period of approximately 5 seconds of acceleration. It is also unclear how the decision to begin accelerating was made. Using this technique the pitch actuators were not used and the length of time that the increased power could be maintained was therefore limited.

As in [52], [58] and [60], the paper focused on the electrical side of the turbine and very simple wind turbine models similar to the basic model defined in section 2.7 were used that did not model more complex aspects of wind turbine dynamics. As such, there was no investigation of the loads on the turbine brought about from the techniques investigated. In addition, only constant wind speed simulations were conducted, which are not representative of real conditions.

Diaz de Corcuera et al. investigated the possibility of altering the wind turbine strategy to provide head room for droop control in [61], with a GL Bladed wind turbine model of the 5MW Upwind machine using an augmentation to a controller developed in [62]. Whilst the work showed that for constant, above-rated wind speeds the controller allowed a wind turbine to deliver droop control, no simulations were completed with turbulent wind.

The change in power was achieved by altering the reference torque and reference generator speed used to calculate the control error; an example of Method 3 defined in section 3.3. Because the operating strategy was not fully redefined for a given

change in the power output and only the reference values were altered issue 3a was avoided. This does however, mean that the forward gain of the controller was changed by the change in power output (issue 3b). Issue 3b was not directly addressed, however the very low cross-over frequency of the controller used (as low as 0.1rad/s for some wind speeds) meant that this issue was not apparent in the results as the controller already had a bandwidth an order of magnitude lower than the frequency content of the wind field.

An analysis was performed of the impact of providing grid frequency support on the loads on the wind turbine; however only a single, constant above-rated wind speed was modelled, severely limiting the conclusions drawn.

A team at the National Renewable Energy Laboratory (NREL) in Colorado, USA, have developed a controller for "Active Power Control" (APC)[47], [63]–[66]. In [63], Aho et al. reviewed the literature surrounding APC and presented their concept for an APC controller, which was further developed in [64]. The controller was "developed as an augmentation to [an] industry standard blade pitch controller". They classified three modes of operation. In mode 1 the output of the turbine was limited to a set maximum - i.e. the power was curtailed if the power output in normal operation would have exceeded a set value. In mode 2 the turbine was operated with an offset applied to the power output. In mode 3 the turbine was set to capture a given percentage of the available power in the wind.

A diagram of the controller is shown in Figure 29.

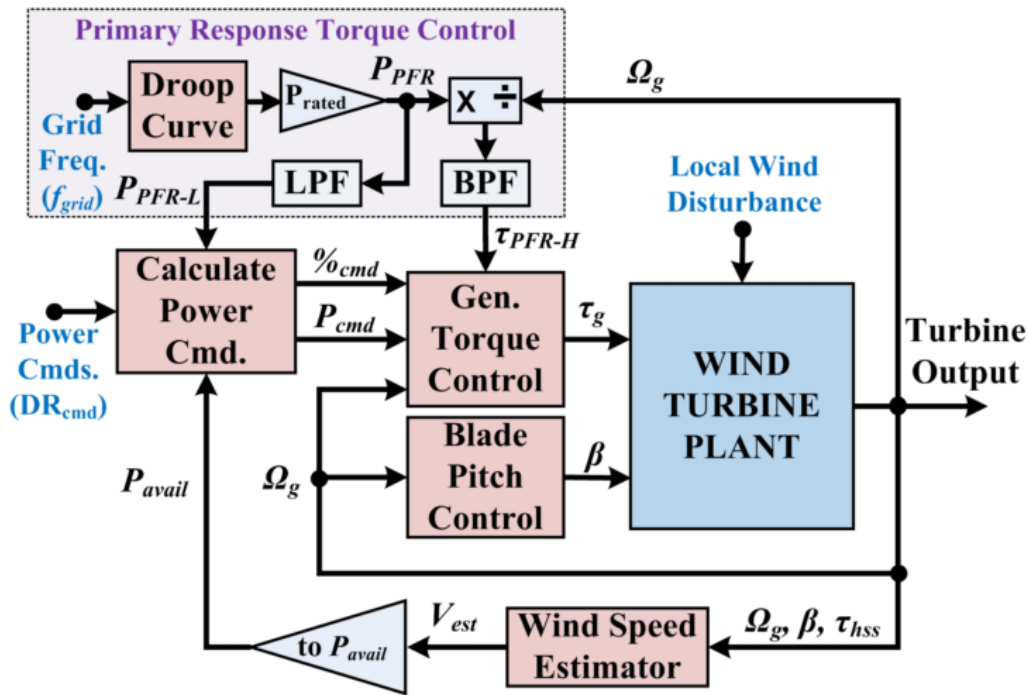


Figure 29: Schematic of the Controller Used by Aho et al. [64]

The controller shown in Figure 29 acted as a full envelope controller capable of providing changes in power output. In the max power tracking region the pitch angle was set to the minimum pitch and torque control was used via the relationship $T_g = K\omega_g$, where T_g is the generator torque, K is a constant and ω_g is the generator speed.

Once rated generator speed was reached, the torque controller changed its method for calculating T_g . Instead of the method described previously, the controller used an estimate of wind speed (estimated using the method described in [67]) to calculate the maximum power available. This value was then divided by the measured generator speed to give a torque demand. The torque demand was bounded to a maximum of the rated power divided by the rated generator speed. In order to maintain the generator speed at the set maximum, the blade pitch control was switched on. The input to the blade pitch control was the error in generator speed, which was fed through a gain scheduled PI controller to calculate the demanded pitch angle β .

Chapter 3: Flexible Operation of Wind Plant

To switch between the max power tracking region and the rated generator speed region a switching method that interpolates between the two methods was used at close to rated generator speeds. This was referred to as "mode 2.5".

In order to provide a change in the power output, one of two methods was used, depending on whether the turbine was in the max power tracking region or the rated generator speed region. If the turbine was in the max power tracking region then the power output was adjusted via alteration to the value of the gain K . The required value was found using a look up table with the percentage of the maximum power as an input. When in the rated generator speed region the power was altered by multiplying the power available signal by the percentage of that power that was desired.

The controller used two inputs to regulate the power output - a grid frequency measurement and a power command. The grid frequency measurement was utilised to provide droop response, whilst the power commands were used to specify any curtailment of the power output. The "LPF" and "BPF" blocks in Figure 29 are representative of a low pass filter and a band pass filter respectively.

Simulations were completed using the FAST aero-elastic simulation package (a full aero-elastic model as defined in section 2.7), modelling a wind turbine rated at 550kW, which is small by modern standards. Whilst the controller provided correctly altered power output much of the time, there were issues when switching through "mode 2.5" that sometimes resulted in a large drop in power output. An analysis of the damage equivalent loads (DELs) was performed, comparing performance with normal operation - i.e. no curtailment nor frequency response. The tower side to side and low speed shaft loads showed consistent reductions, however there was often an increase in the tower fore-aft loads and/or the blade root flap loads of up to 7%. This increase in loads was found to be worse if the droop response was made to be more aggressive, though the figures for the increased loads in this instance were not presented.

It was noted in [64] that “the bandwidth of the wind speed estimator is set very low (to prevent unstable feedback through the torque control loop)”, which implies that there was at least some feedback introduced by the wind speed estimator. The increased tower fore-aft loads may have been a by-product of this feedback.

The stability of the controller used in below-rated operation (named mode 2) was investigated in [65]. No similar work has yet been published regarding the stability of the above-rated (named mode 3) controller, nor the “mode 2.5” controller though this is suggested as possible future work.

A report on the project [66] was also published, giving results of field testing of the controller on a real wind turbine – a 550kW machine. The field testing results presented showed two examples of de-rating the turbine in above-rated wind speeds. Also presented were the output of the wind speed estimator for a different, below-rated wind speed, which was compared with wind measurements from a nearby met mast. These tests showed good results, with fairly accurate power tracking and good wind speed estimates, however they were limited in scope as the number of cases investigated was small. The authors aim to complete further testing and evaluation in future work.

3.4.1 Summary of Literature

All of the methods for providing augmented control in the papers reviewed in this section required that the full envelope controller for the wind turbine be fundamentally altered in order to vary the power output. Most of the papers focussed on the power systems aspects of the controllers, mainly the effect of said controllers on the grid frequency when providing grid frequency support. Only one of the papers investigated the loads on the turbine from utilising more flexible operation strategies in turbulent wind conditions, however the turbine modelled in that study was small by modern standards and not representative of the large multi-megawatt machines that are currently favoured by the vast majority of wind turbine manufacturers. None of the papers reviewed fully addressed all the relevant issues from section 3.3. All the papers reviewed tended to focus on specific applications

for varying the power output of a wind turbine, most notably to regulate the grid frequency, as opposed to developing a general controller for a variety of applications.

3.5 Requirements for an Augmentation to a Wind Turbine Controller

A case is made for the development of an augmentation to a wind turbine controller that fulfils the following requirements:

- 1- The augmentation must be applicable to variable speed, pitch regulated machines without alteration to the turbine's full envelope controller
- 2- No knowledge of the design of the wind turbine's full envelope controller must be required.
- 3- The augmentation must allow the operator to vary the power output of the wind turbine by an increment ΔP , however defined.
- 4- The augmentation must allow the power output of the wind turbine to be altered quickly and accurately.
- 5- The augmentation must be capable of switching smoothly between any different modes of operation.
- 6- The performance of the full envelope controller must not be compromised through the addition of the augmentation, including taking into account any gain scheduling.

An augmentation to a conventional wind turbine's controller that fulfils the requirements laid out above is the focus of the work presented here. This augmentation is called the Power Adjusting Controller (PAC).

3.6 The Power Adjusting Controller Concept

An overview of the concept for the power adjusting controller is presented in this section.

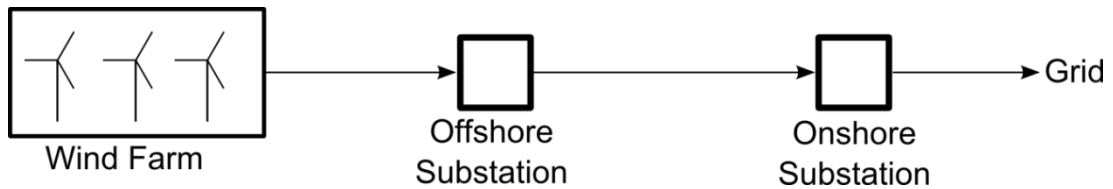


Figure 30: Connection of a Wind Farm to the Grid

For the majority of wind farms there are three possible points at which the power output can be changed; at the onshore substation, at the offshore substation, or at the converter for each individual turbine (see Figure 30). Initiating the change in power at either of the substations would give rise to an imbalance between the aerodynamic power at the wind turbine and the electrical power transmitted. This imbalance must be quickly removed. Coordinated control action is therefore required at multiple points in the system. If, instead, the power alteration is initiated at the wind turbines, say by altering the aerodynamics, then the power at the substations would naturally follow the change and so no additional modifications to the system are required. Changes to the wind farm power output can be achieved by distributing the total change in power between the turbines in the farm.

In order to change the power output of a wind turbine it must be moved off its normal operating curve. In above-rated wind speeds it is possible to do this by adjusting the torque demand with a simple increment, ΔT . Because in above-rated operation the full envelope controller regulates the rotor speed through pitch action, this change in torque gives rise to a disturbance in the rotor speed that is counteracted through pitch action. As such, the power output is altered whilst the rotor speed is still controlled. In below-rated wind speeds however, the full envelope controller regulates the rotor speed through alteration of the generator torque demand. As such, the disturbance caused by the ΔT input is counteracted by a torque response equal but opposite to ΔT , eliminating the change in torque and hence eliminating the change in power output. An alternative approach in below-rated wind speeds is therefore to either provide an increment to the pitch angle $\Delta\beta$

or alter the full envelope controller operational strategy to provide the required change in power output.

Controllers using these principles have been explored in the literature (see section 3.4); however, as discussed, these are not complete solutions. Introducing a variety of strategies within the full envelope controller is both complicated and requires knowledge of the composition of the full envelope controller, whilst providing an increment to $\Delta\beta$ is not accurate, is relatively slow to respond and does not allow an increase in power output in below-rated operation. Additionally, if the method of operation differs in above and below-rated wind speeds, there can be problems switching between them.

The scope for development of a turbine controller that allows fast, accurate alteration of a wind turbine's power output without switching between different methods in above and below-rated wind speeds is therefore clear.

The power output is required to be altered in below-rated wind speeds by adjusting the torque, without altering the full envelope controller. Suppose therefore, that an increment to the torque demand sent to the converter, ΔT , is added to the output from the full envelope controller. In addition, suppose a speed adjustment $\Delta\omega$ is added to the input of the full envelope controller, where $\Delta\omega$ is the change in speed caused by the increment in torque. The full envelope controller no longer counteracts the torque increment and so the power output is successfully altered. In this scenario however, there is now a disparity between the generator torque and the rotor torque. As such, dependent upon the sign of ΔT , the rotor either speeds up or slow down. An increment to the pitch angle, $\Delta\beta$ can therefore be introduced to adjust the aerodynamic torque and bring the rotor speed back to its normal operating value. This value must be adjusted in such a manner as to avoid altering the forward gain of the pitch control.

In some circumstances it may not be possible to obtain a pitch angle that balances the aerodynamic and generator torques, e.g. when a positive ΔP is requested in below-rated operation. In scenarios such as these the rotor therefore slows down or

speed up unless provision of the requested ΔP is curtailed. It is therefore necessary to prevent the operating point of the wind turbine moving outside of a safe operating envelope bound by a maximum torque and a minimum torque (which may vary with generator speed) and a maximum and minimum generator speed.

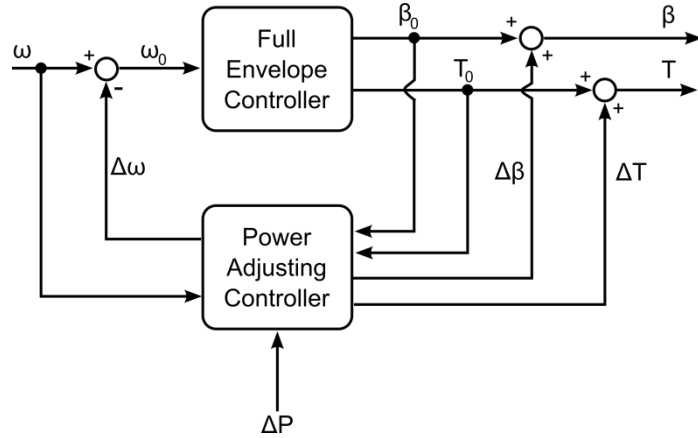


Figure 31: General Layout of the Power Adjusting Controller

A schematic of the proposed controller, named the “Power Adjusting Controller” is shown in Figure 31. So long as the input ΔP is provided by some external agency and therefore, consequent $\Delta\omega$, ΔT , and $\Delta\beta$ are not dependent upon the current state of the turbine, the controller does not contain feedback.

Figure 32 shows an example of a reduction in output power, assuming a constant wind speed. The generator torque is rapidly reduced (in a fraction of a second) from A to B via an increment ΔT . This causes the aerodynamic torque (the torque at the rotor) to exceed the generator torque and so the rotor/generator speed increases. As the rotor/generator speed increases, the generator torque must follow a constant power curve in order to maintain a constant power output (blue line), whilst a gradual change in the pitch angle of $\Delta\beta$ reduces the aerodynamic torque (green line). At point C the aerodynamic and generator torque are equal, after which the pitch angle alters further, such that the rotor/generator speed is reduced, eventually settling at an equilibrium point B.

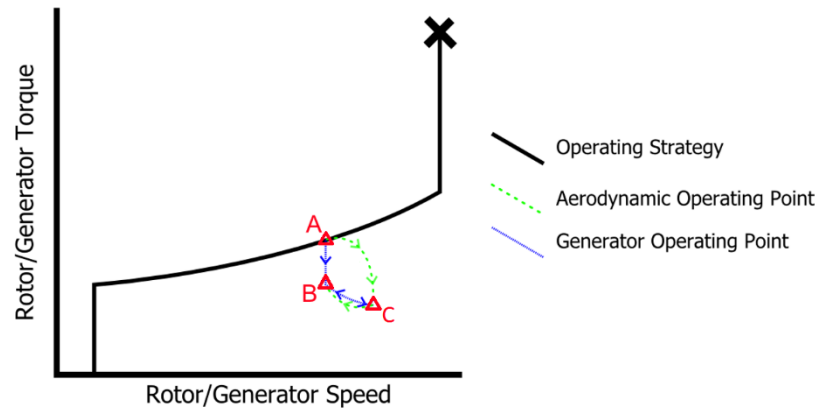


Figure 32: Movement of the Operating Point on the Torque-Speed Plane

Because the power adjustment is made using an adjustment to the generator torque, the change in power can be quick, limited only by the speed of response of the power electronics. The same method can be used in both above and below-rated wind speeds with no switching between modes of operation required. In addition, no knowledge of the design of the full envelope controller is required and so the controller could be implemented on any wind turbine, including retrofitting to older machines.

3.7 The Role of the Power Adjusting Controller as Part of a Wind Farm Control Hierarchy

It is important to highlight at this stage that the PAC can be used as part of a system for wind farm control, by utilising a hierarchical structure such as that shown in Figure 33.

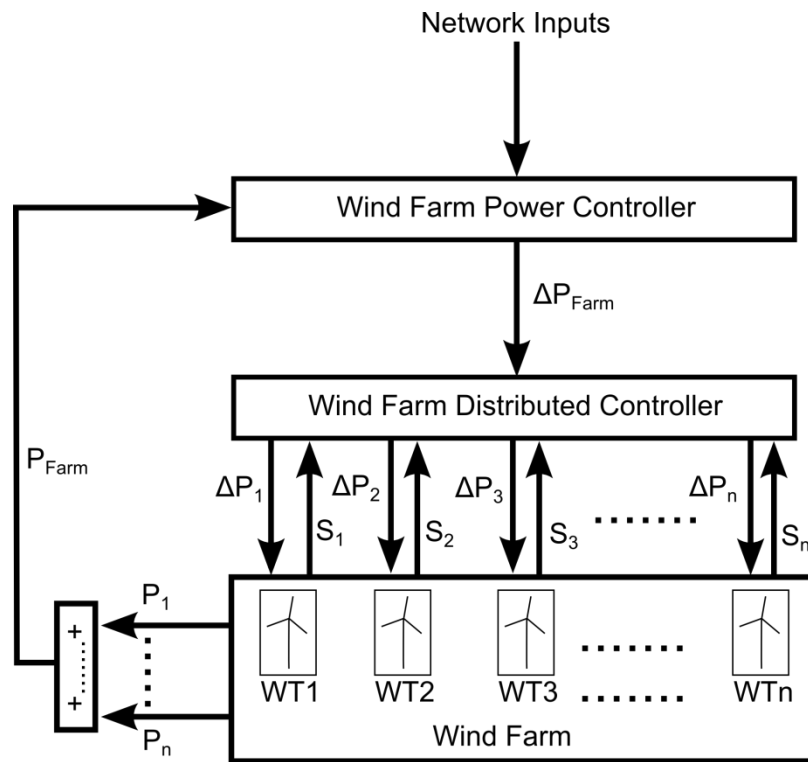


Figure 33: Wind Farm Control Hierarchy

Within such a structure there are three levels of control:

- 1- Wind Farm Power Controller (WFPC)
- 2- Wind Farm Distributed Controller (WFDC)
- 3- Power Adjusting Controller (PAC)

The WFPC utilises network inputs, market information, and information regarding the requested and delivered power output from the farm, to calculate a given change in power request to be sent to the turbine wind farm controller. The WFDC then uses this signal, along with signals and flags from each wind turbine, and information regarding the state of each turbine, to distribute the requested change in power amongst the wind turbines in the farm. The PAC's role is to deliver the change in power requested at a turbine level.

By setting up the system in the hierarchical manner shown it is possible to distribute a given change in power for the farm amongst the turbines in any manner, so long as the total change in power output meets the requirement. There are advantages of this method over simply distributing the change in power evenly between all the

Chapter 3: Flexible Operation of Wind Plant

turbines. Firstly, if a wind turbine is unable to produce its requested change in power for whatever reason its share of the change in farm power output can be distributed to other wind turbines and the change in wind farm power output is not affected. Secondly, the changes in turbine power can be more sensibly distributed across the farm. Thirdly, the solution is highly decentralised and is therefore easily scalable to large wind farms. Finally, the approach given here gives great autonomy to wind farm control designers.

This thesis is concerned with the design and operation of the PAC and so there are no complete descriptions of the wind farm level controllers. Where applicable however, a description of the requirements of the wind farm level controllers is provided.

Chapter 4:

Development of the Power Adjusting Controller

AS DISCUSSED IN Chapter 3, it is often desirable to be able to adjust the power output of a wind farm rather than simply generate the maximum power available from the wind. In this chapter, the development of the “Power Adjusting Controller” (PAC) from the concept presented at the end of chapter 3 to a controller suitable for use in wind turbine control models is presented.

4.1 Definitions of Variables

When discussing the design of the PAC, it is useful to refer to two separate cases:

1. The conditions at the wind turbine with the PAC in use
2. The conditions at the wind turbine if the PAC had not been used.

By considering these two cases it is possible to calculate the effect that the PAC has had on operation by subtracting the second case from the first. For example, if the power output without the PAC would have been 2MW and the power output with the PAC is 1.8MW then the change in power is simply found as 0.2MW. Computer simulations using software such as Simulink or GL Bladed allows both cases to be simulated, which in turn enables the accuracy of the PAC to be estimated.

When discussing the two cases the notation used is,

$$\xi = \xi_0 + \Delta\xi \quad (4.1)$$

where ξ is a variable in a case where the PAC is being used, ξ_0 is a variable in the case that the PAC is not being used and $\Delta\xi$ is change in the variable required to be added to ξ_0 to make it equal to ξ .

The values most commonly referred to in this manner are the generator torque, T , generator speed, ω , and blade pitch angle, β . For clarity the relationships of these values when the PAC is in use compared to their value without the use of the PAC are,

$$\omega = \omega_0 + \Delta\omega \quad (4.2)$$

$$T = T_0 + \Delta T \quad (4.3)$$

$$\beta = \beta_0 + \Delta\beta \quad (4.4)$$

4.2 Design of the Power Adjusting Controller

There is a requirement for the PAC to be able to adjust the power output of the wind turbine quickly. There are two control inputs to the wind turbine available, torque demand, T , and pitch demand, β . The torque actuator has very fast dynamics, whereas the pitch actuator is comparatively slow. The PAC alters the turbine power by means of an adjustment to the torque, ΔT . As discussed in chapter 3, if only an adjustment to the torque is made, then the wind turbine full envelope controller would counteract it. To avoid this happening, an estimate of the change in generator speed $\Delta\omega$ caused by the change in torque, ΔT , is made and fed forward into the generator speed input to the full envelope controller, as shown in Figure 34. The estimate of the change in generator speed is made by feeding the change in torque through a simple first order model of the wind turbine's drive train $G(s) = \frac{-1}{Js+B}$, where J is the total inertia of the rotor, drive shafts, and generator and B is the damping of the same system. It should be noted that the control strategy shown in Figure 34 is purely feed-forward and so does not interfere with the wind turbine's full envelope controller.

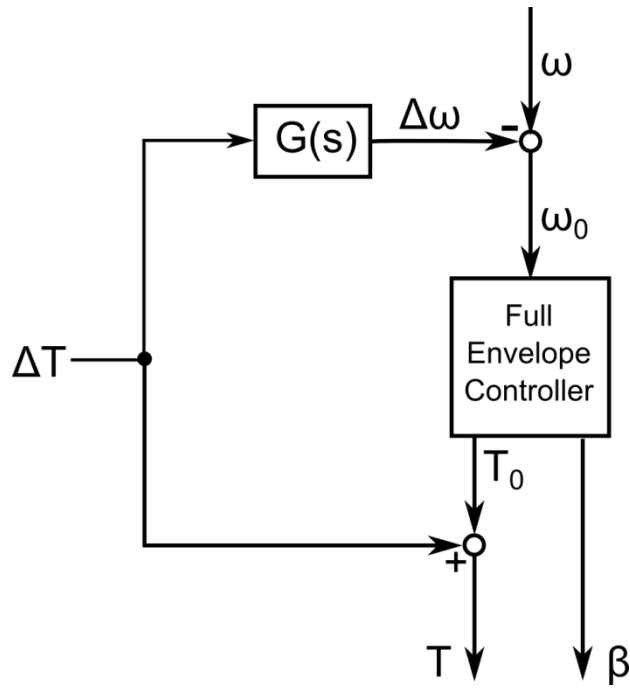


Figure 34: Addition of a Change in Torque with an Accompanying Estimate of the Change in Generator Speed

For small changes in $\Delta\omega$ the above system works well. However, for larger changes the estimate of $\Delta\omega$ becomes inaccurate and so ΔT is at least partially counteracted by the full envelope controller. The inaccuracy is due to changes in the wind turbine's operating point, causing the aerodynamic torque at the rotor to change. The change in the aerodynamic torque is not accounted for in the above model. The equation of motion for the turbine with the PAC is,

$$J\dot{\omega} = -B\omega + Q(\omega, V, \beta) - T \quad (4.5)$$

where Q is the aerodynamic torque as a function of generator speed, wind speed, and pitch angle. When the PAC is not in use it becomes,

$$J(\dot{\omega} - \dot{\Delta\omega}) = -B(\omega - \Delta\omega) + Q(\omega - \Delta\omega, V, \beta) - (T - \Delta T) \quad (4.6)$$

Hence, from (4.5) and (4.6),

$$J\Delta\dot{\omega} = -B\Delta\omega - \Delta T + \Delta Q(\omega, \Delta\omega, V, \beta) \quad (4.7)$$

where ΔQ is the change in aerodynamic torque, which is a function of ω , $\Delta\omega$, V , and β .

Chapter 4: Development of the Power Adjusting Control

The change in aerodynamic torque is the difference between the aerodynamic torque with the PAC in use and the aerodynamic torque without the PAC; that is,

$$\Delta Q = Q(\beta, \Omega, V) - Q(\beta, (\Omega - \Delta\Omega), V) \quad (4.8)$$

where Ω is the rotor speed. From (2.12) in chapter 2,

$$P = \frac{1}{2} \rho AV^3 C_p(\lambda, \beta) \quad (4.9)$$

and so,

$$Q = \frac{\frac{1}{2} \rho AV^3 C_p(\lambda, \beta)}{\Omega} = \frac{\rho}{2} AR^3 \Omega^2 C_Q(\lambda, \beta) / \lambda^2 \quad (4.10)$$

Hence,

$$\Delta Q = \frac{\frac{1}{2} \rho AV^3 C_p(\lambda, \beta)}{\Omega} - \frac{\frac{1}{2} \rho AV^3 C_p(\lambda_0, \beta)}{\Omega_0} \quad (4.11)$$

A and ρ are constants and the values of Ω , Ω_0 , and β are available to the PAC. Hence, as λ is a function of Ω and the rotor radius, only an estimate of the wind speed is required.

An alteration to Figure 34 is therefore made to include the effect of the change in aerodynamic torque, with the new system shown in Figure 35.

Note that the system is further refined in chapter 5 via modification to the wind speed estimator.

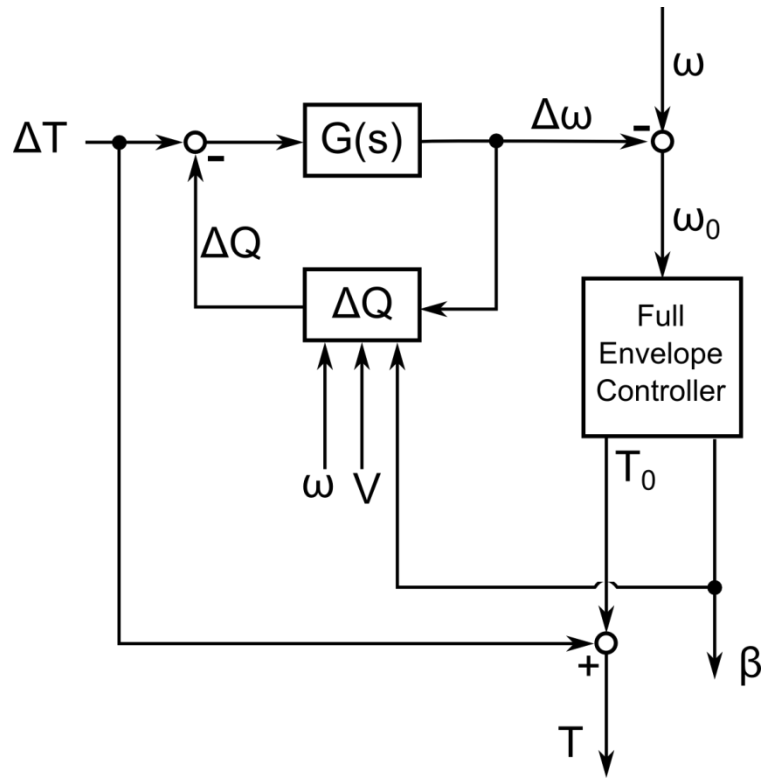


Figure 35: Development of the PAC to Incorporate the Change in Aerodynamic Torque

From separability (shown diagrammatically in Figure 36), the change in the wind turbine's aerodynamic torque due to action by the PAC is,

$$\Delta Q \approx g(\beta, \Omega) - h(V) - g(\beta, \Omega - \Delta\Omega) + h(V) \quad (4.12)$$

As the wind speed is the same for each case, the $h(V)$ terms cancel.

As the PAC may cause the wind turbine to operate across a far greater range of operating points, the turbine may be operating far from an equilibrium point. In these conditions the tau function $\tau(\varepsilon)$ (see (2.4) in section 2.3) is not exactly 1 and so the $h(V)$ terms in (4.12) do not exactly cancel. However, the tau function is very weakly non-linear and hence in (4.8) the dependence of ΔQ on wind speed is extremely weak. Therefore any reasonable estimate of wind speed is sufficient. Since the rotor inertia is very large, any feedback introduced through the dependence of ΔQ on ω and β should be very weak.

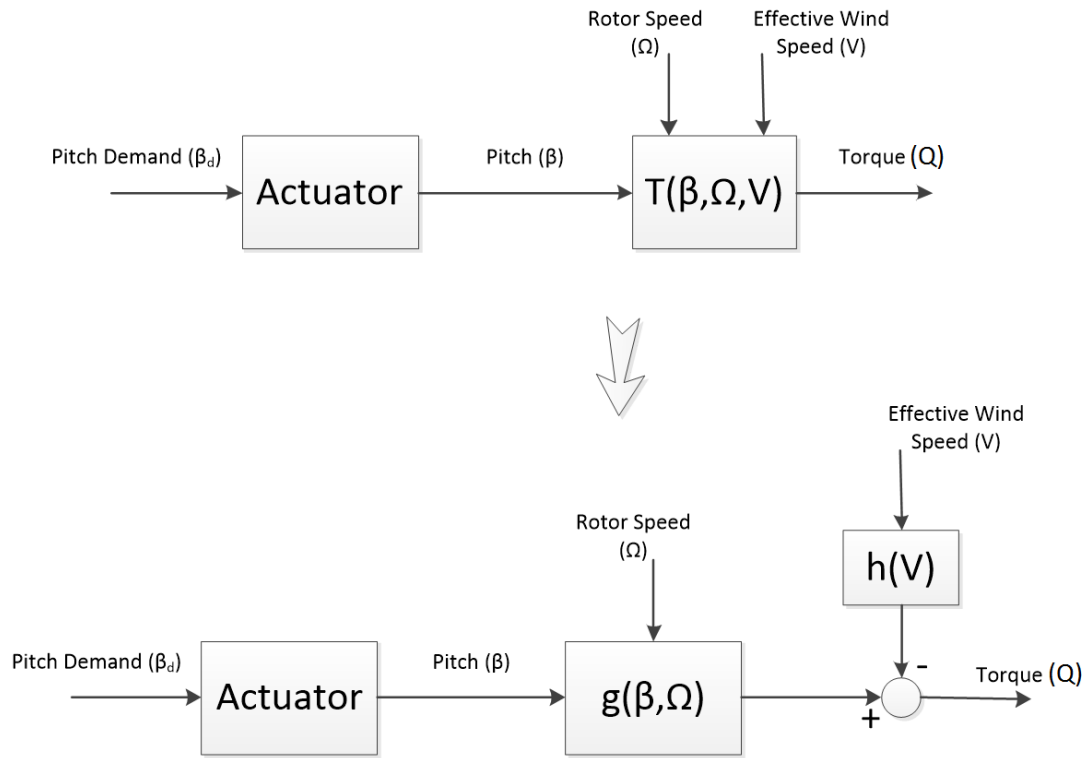


Figure 36: Using Separability to Separate the Functions of Rotor Speed and Pitch Angle from that of Wind Speed

The wind speed is estimated using a method similar to that used in [67]–[69]. The aerodynamic torque for the wind turbine in its current state is estimated, i.e. with the PAC in use. As aerodynamic torque is not directly measured, an indirect method must be used to obtain the estimate. A simple first order model of the drive-train dynamics is used whereby

$$\hat{Q} = NT + (Js + B)\Omega + Q_{loss} \quad (4.13)$$

where \hat{Q} is the estimated aerodynamic torque, T is the measured generator torque, N is the gearbox ratio, J is the inertia of the entire drive-train and rotor, B accounts for the viscous damping in the drive-train, Ω is the rotor speed, and Q_{loss} is any other losses. All of the variables required can be easily measured in a real wind turbine. The generator torque can be assumed to be equal to the demanded generator torque from the controller as the dynamics of the generator are comparatively very fast.

As (4.13) contains a differentiator it is not a proper transfer function and is likely to be highly noisy. As such, a low pass filter of the form $\frac{a}{s+a}$ where a is a constant is

used. The value of a must be selected carefully to balance noise cancellation against the delay that results from such a filter.

Once the estimate of the aerodynamic torque is calculated the tip speed ratio is found by solving

$$\hat{Q} = \frac{\rho}{2} AR^3 \Omega^2 C_Q(\lambda, \beta) / \lambda^2 \quad (4.14)$$

Hence the estimated wind speed is found using

$$\hat{v} = \frac{\Omega R}{\lambda} \quad (4.15)$$

The wind speed is then utilised in (4.11) to give an estimate of the change in aerodynamic torque ΔQ .

Note that this method can be thought of as the application of a basic wind turbine model (akin to that discussed in section 2.7) to estimate the dynamic behaviour.

The wind estimator described is incorporated into the PAC as shown in Figure 37.

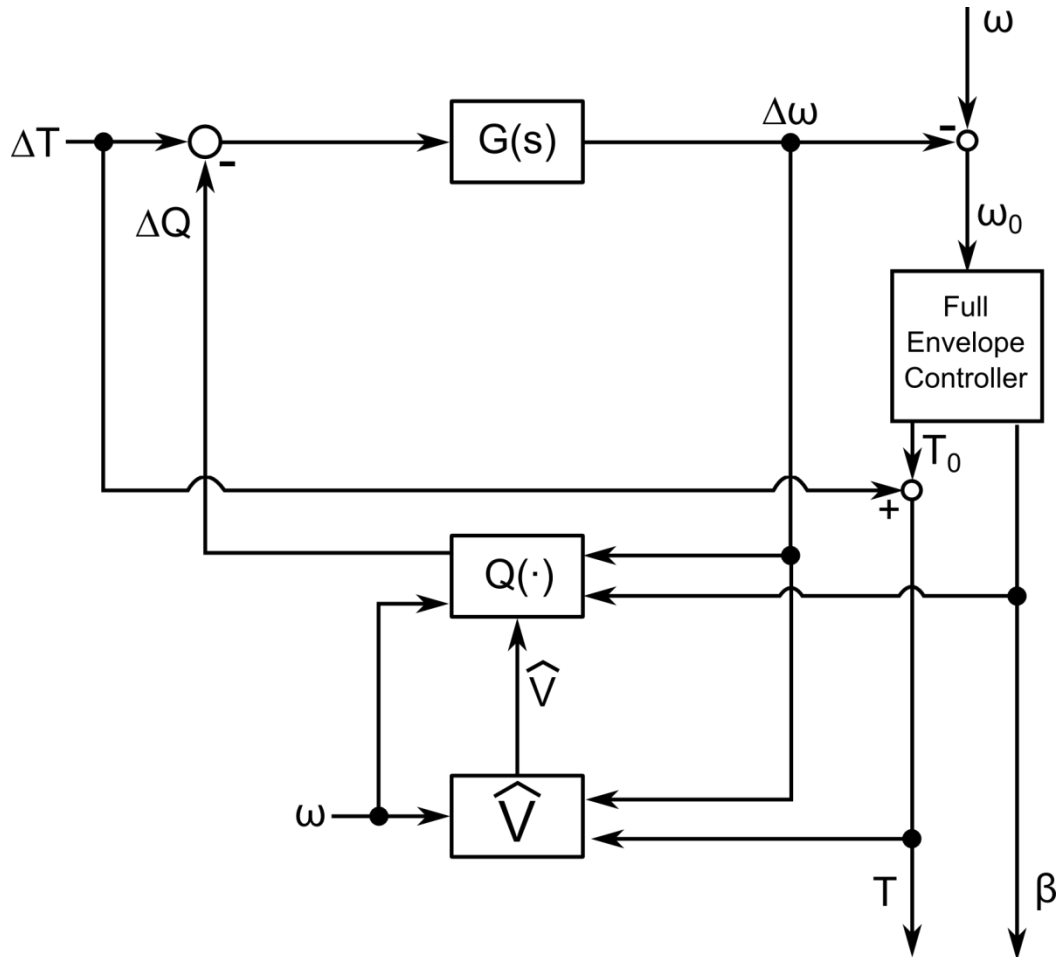


Figure 37: Development of the PAC to Incorporate the Wind Speed Estimator

With the PAC designed as shown in Figure 37, it is possible to alter the power output of the wind turbine using a torque input ΔT , without the full envelope controller countermanning this input, resulting in a change in the rotor speed. If the change in the torque is negative (i.e. a reduction in power is required) then the generator torque reduces to a lower value than the rotor torque, resulting in an increase in rotor speed. The increase in rotor speed is minimised through an addition to the pitch demand from the full envelope controller, denoted $\Delta\beta$. A schematic of the PAC with $\Delta\beta$ added is shown in Figure 38.

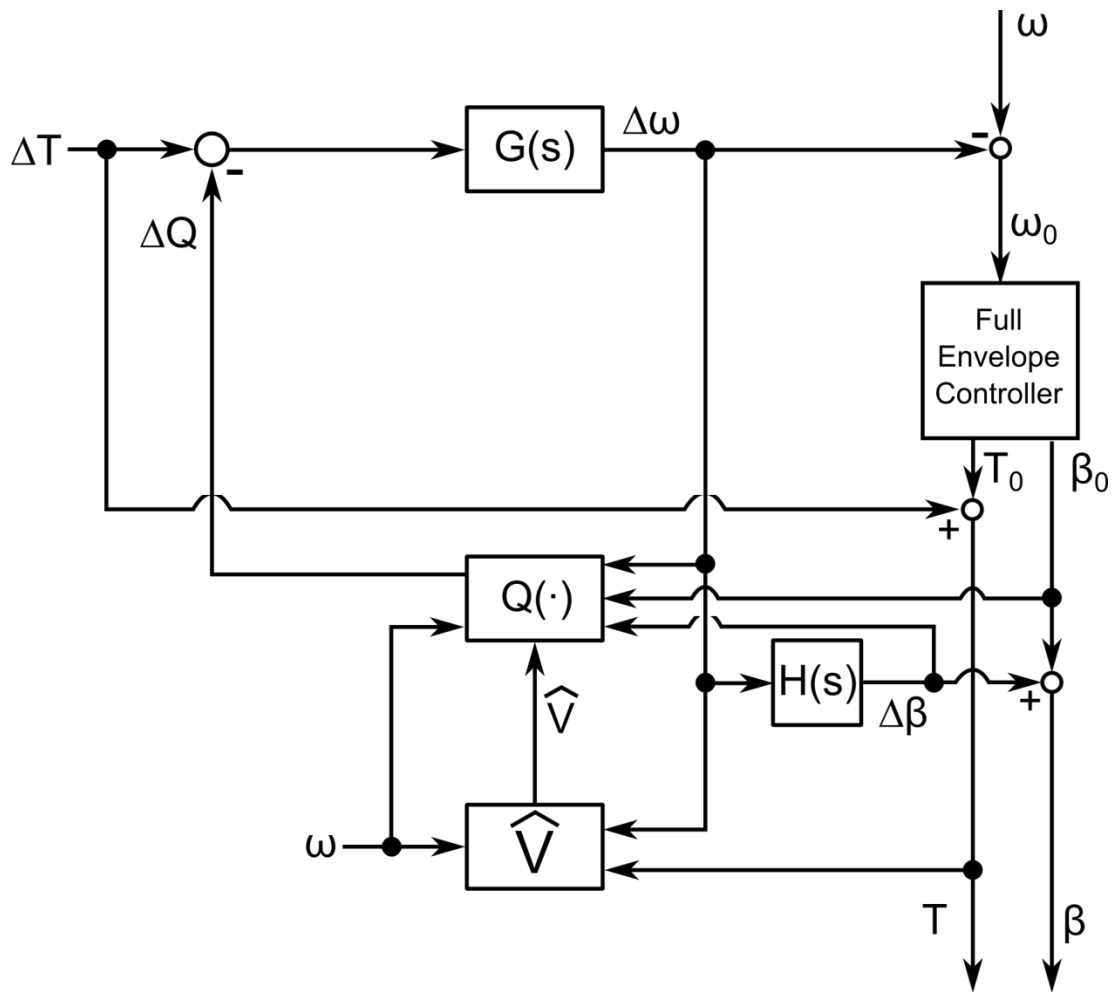


Figure 38: Development of the PAC to Incorporate an Increment to the Pitch Angle

The $\Delta \beta$ output from the PAC; designed to minimise the output $\Delta \omega$, is generated by designing a controller with integral action on $\Delta \omega$ to drive it to zero, as shown in Figure 38. The controller, $H(s)$, is designed to be sufficiently weak that little feedback is introduced to the PAC. The wind turbine dynamics between pitch demand and generator speed include the non-linear aerodynamics, and the adjustment to the pitch demand by adding $\Delta \beta$ significantly changes the gain and so affects the full envelope controller, perhaps even destabilising it. It is essential that the PAC counteracts this change in gain.

By separability theory (see section 2.3 in chapter 2) the dynamics of the wind turbine are considered to be the sum of two components, one dependent on β and Ω , $g(\beta, \Omega)$, and the other dependent solely on the wind speed, $h(V)$. In above rated wind speeds, for pitch regulated wind turbines, the rotor speed is usually held at a

set value and so the function h becomes dependent solely on β . The inverse of $g(\beta)$ can, thus, be included in the controller to cancel out these dynamics.

Gain scheduling is implemented as shown in Figure 39; where $A(s)$ is a model of the actuator dynamics and $g(\beta)$ is related to the turbine aerodynamics as discussed above. The input u is the demanded pitch angle from the full envelope controller prior to gain scheduling. Separability implies that gain scheduling as in Figure 39 is general and not local; that is it counteracts the aerodynamic non-linearity over a wide area and not only in a local neighbourhood of an operating point [18].

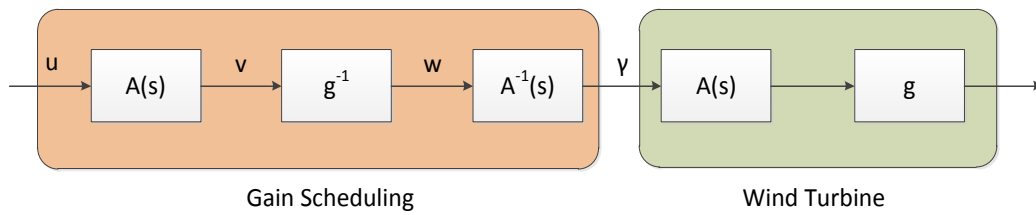


Figure 39: Implementation of Gain Scheduling (adapted from [15])

In order to avoid an improper transfer function for the inverse of the actuator dynamics the system must be reformulated as shown below.

The dynamics of the actuator are modelled by the second order system,

$$A(s) = \frac{c}{s^2 + bs + c}$$

for which a realisation explicitly providing v and \dot{v} is as shown in Figure 40.

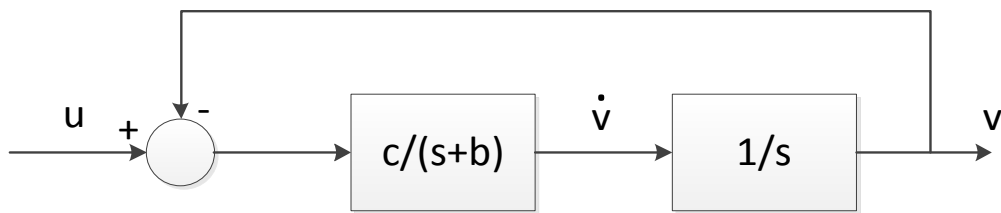


Figure 40: Splitting the Actuator Transfer Function into Two Transfer Functions

From Figure 39 it follows that,

$$\ddot{v} + b\dot{v} + cv = cu \tag{4.16}$$

$$v = g(w); \quad \dot{v} = g'(w)\dot{w}; \quad \ddot{v} = g''(w)\dot{w}^2 + g'(w)\ddot{w} \tag{4.17}$$

$$c\gamma = \ddot{w} + b\dot{w} + cw \quad (4.18)$$

$$c\gamma = \frac{\dot{v} - g''(w)\dot{w}^2}{g'(w)} + \frac{b\dot{v}}{h'(w)} + cw \quad (4.19)$$

$$\gamma = \frac{(u - v)}{h'(w)} - \frac{(h''(w)\dot{v}^2)}{c(h'(w))^3} + w \quad (4.20)$$

Hence the schematic diagram for the gain scheduling approach of Figure 39 is that of Figure 41. It should be noted that no explicit differentiation is required.

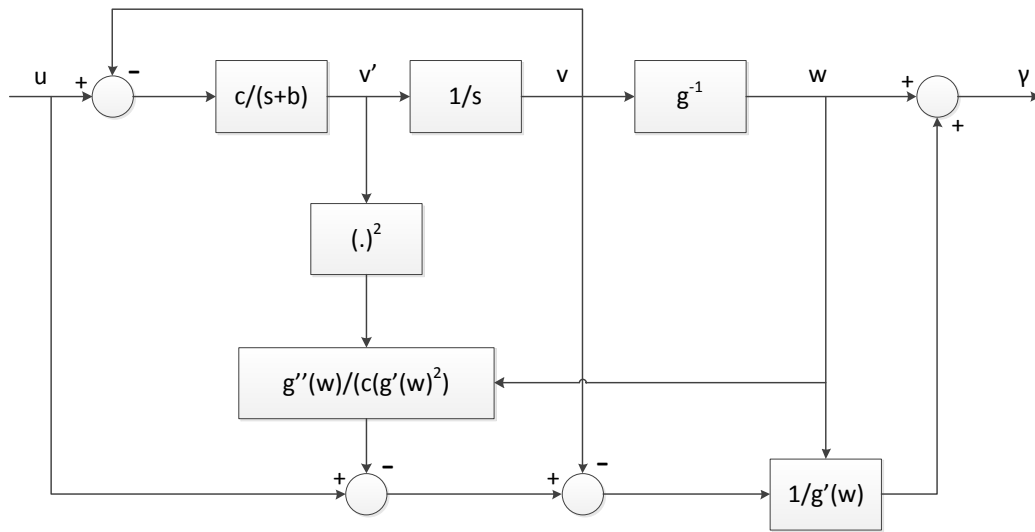


Figure 41: Schematic Diagram for Gain Scheduling

In the case of the PAC, the $\Delta\beta$ output cannot simply be gain scheduled and added to the (already gain scheduled) output from the full envelope controller. Instead, the total values of β , that is the value of $\beta_0 + \Delta\beta$, *without* gain scheduling must first be found. β is then gain scheduled and β_0 (which has already been gain scheduled) subtracted, leaving the correctly gain scheduled $\Delta\beta$ to be output from the PAC.

The gain scheduling process in the PAC may also be considered as being a correction to the gain scheduling of the full envelope controller accounting for the adjustment $\Delta\beta$.

The appropriate procedure is depicted in Figure 42. The gain scheduling scheme of Figure 41 is applied to β . The scheme to remove the gain scheduling is implemented similarly, with the exception that the function $g(\cdot)$ and its derivatives

are replaced with the function $g^{-1}(\cdot)$ and its derivatives. Note that $A(s)$ represents the actuator dynamics. For a real wind turbine, the actuator dynamics can be easily obtained via simple tests and measurements.

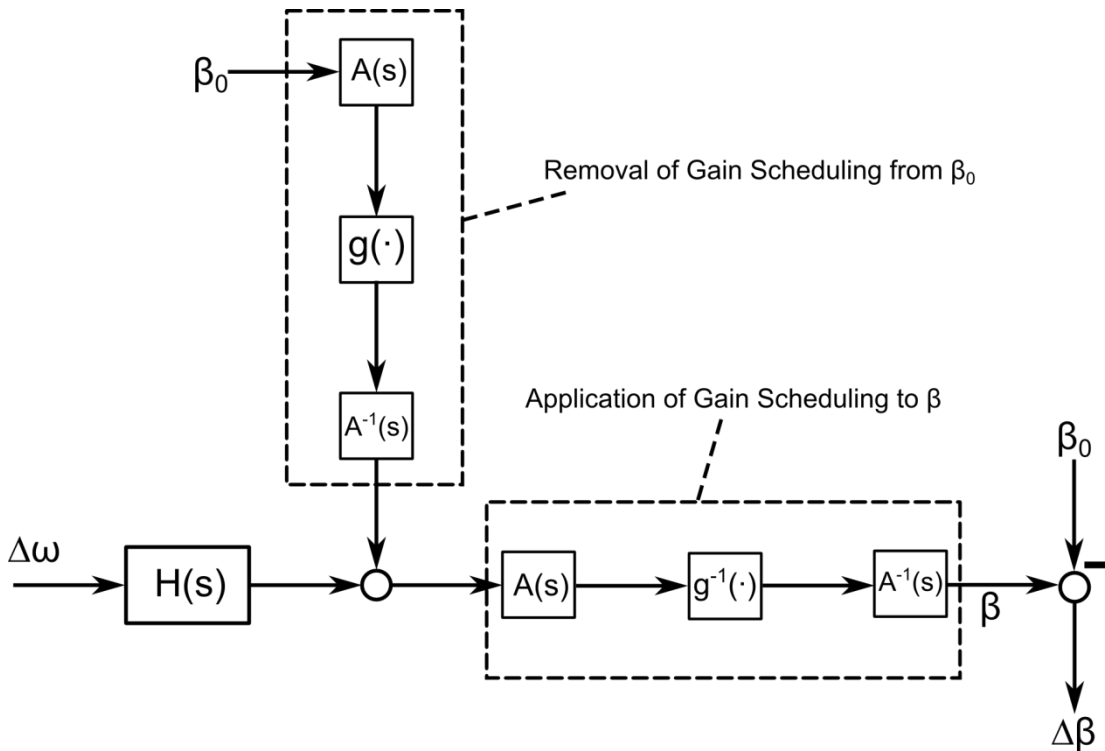


Figure 42: Gain Scheduling of $\Delta\beta$

If a positive change in power is requested then the situation may arise whereby there is no equilibrium point for the generator and aerodynamic torques, that is, the required aerodynamic torque to prevent a change in rotor speed is higher than the maximum possible aerodynamic torque given the current tip speed ratio. In these conditions the rotor speed will necessarily slow down.

In this situation, the change in pitch angle is allowed to reduce the total pitch to the minimum pitch for the machine to enable the largest possible aerodynamic torque to be achieved. The change in pitch angle is not permitted to cause the total pitch angle to exceed this value.

The gain scheduling is incorporated into the PAC, see Figure 43. Note that in Figure 43 the wind turbine full envelope controller is removed for clarity and a negative

$$P_e = P_m E_f \quad (4.21)$$

where E_f is the efficiency of the converter (typically around 0.95).

As such, when the PAC is first activated, the change in torque required is found simply as,

$$\Delta T = \frac{\Delta P_e}{\omega E_f} \quad (4.22)$$

Once a value for ΔT is produced however, it brings about a change in the generator speed $\Delta\omega$. As the value of ω has now changed compared to its value if the PAC had not been used, but the torque output from the full envelope controller has not, the value of ΔT required must be adjusted to achieve the required ΔP . Since,

$$\Delta P_e = P_e - P_{e0} = (T_0 + \Delta T)\omega E_f - T_0(\omega - \Delta\omega)E_f = \Delta T\omega E_f + T_0\Delta\omega E_f \quad (4.23)$$

the corresponding ΔT is,

$$\Delta T = \frac{\Delta P}{\omega E_f} - T_0 \frac{\Delta\omega}{\omega E_f} \quad (4.24)$$

So long as the value of $\Delta\omega$ remains accurate, using ΔT as in (4.24) gives rise to the requested ΔP .

Note that, since ΔT is dependent upon T_0 there is some feedback through $\Delta\omega$.

However, this feedback is weak, due to the low bandwidth of $G(s)$. The PAC with ΔP as an input is depicted in Figure 44.

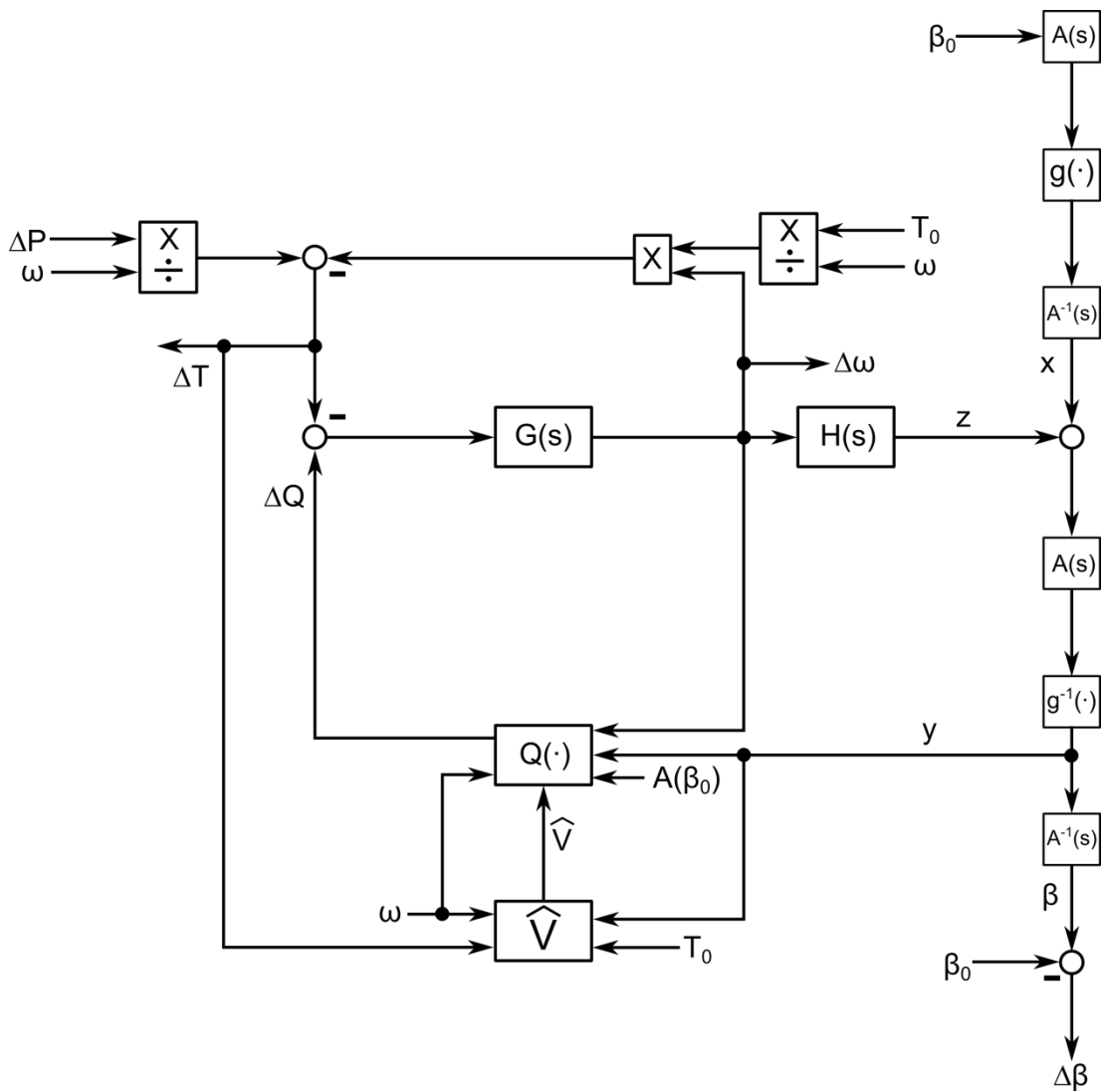


Figure 44: Structure of the PAC

The legend for Figure 44 is given in Table 1.

Table 1: Legend for Figure 44

Variable Symbol	Variable Description
ΔP	Requested Change in Power
Ω	Generator Speed
T_0	Torque Demand from the Full Envelope Controller
β_0	Pitch Demand from the Full Envelope Controller
ΔT	Change in Torque output from the PAC
$\Delta\beta$	Change in Pitch Angle Output from the PAC
$\Delta\omega$	Estimated Change in Generator Speed Output from the PAC
\hat{V}	Estimated Wind Speed
$A(s)$	Actuator Transfer Function
$A^{-1}(s)$	Inverse Actuator Transfer Function
ΔQ	Change in Aerodynamic Torque
$G(s)$	Approximation of Turbine Dynamics from Torque to Generator Speed
$H(s)$	$\Delta\beta$ Controller
$Q(\cdot)$	Function to Estimate the Change in Aerodynamic Torque
$g(\cdot)$	Non-Linear Turbine Dynamics
$g^{-1}(\cdot)$	Inverse of the Non-Linear Turbine Dynamics
x, y, z	Internal Variables

4.3 Pitch Controller Design

The PAC Pitch controller $H(s)$ takes the form of a simple proportional-integral (PI) controller, which is manually tuned to give a $\Delta\beta$ output without large overshoot with a pitch rate below one degree per second to avoid overworking the pitch actuators, as this could result in higher blade loads. The design of this controller is discussed in greater detail in section 5.6.

4.4 Linearisation of the PAC Controller

Although the basic schematic of the PAC shown in Figure 31 may appear to include feedback loops around the full envelope controller, the PAC is predominantly feed forward as discussed in its development in section 4.2. To confirm this, the transfer functions in the linearised system from ω , β_0 , and T_0 to $\Delta\omega$, $\Delta\beta$ and ΔT are all very low gain.

Linearising the PAC about an equilibrium operating point, the dynamics in the s-domain are

$$\begin{bmatrix} \delta\Delta\omega \\ \delta\Delta\beta \\ \delta\Delta T \end{bmatrix} = \begin{bmatrix} G_{11}(s) & G_{12}(s) & G_{13}(s) & G_{14}(s) \\ G_{21}(s) & G_{22}(s) & G_{23}(s) & G_{24}(s) \\ G_{31}(s) & G_{32}(s) & G_{33}(s) & G_{34}(s) \end{bmatrix} \begin{bmatrix} \delta\omega \\ \delta\beta_0 \\ \delta T_0 \\ \delta\Delta P \end{bmatrix} \quad (4.25)$$

where $\delta\Delta\omega$, $\delta\Delta\beta$, $\delta\Delta T$, $\delta\omega$, $\delta\beta_0$, δT_0 , and $\delta\Delta P$ are the perturbations in each variable relative to the equilibrium operating point. From the diagram in Figure 44,

$$\Delta\omega = G(s) \left(\Delta Q + \frac{T_0}{\omega_0 + \Delta\omega} \Delta\omega - \frac{\Delta P}{\omega_0 + \Delta\omega} \right) \quad (4.26)$$

$$\Delta Q = Q(\beta_0 + \Delta\beta, \omega_0 + \Delta\omega, V) - Q(\beta_0, \omega_0, V) \quad (4.27)$$

and,

$$z = H(s)\Delta\omega \quad (4.28)$$

In addition, with the subscript d used to indicate a value demanded from an actuator,

$$x = A(s)^{-1}g(A(s)\beta_{0d}) \quad (4.29)$$

$$A(s)\beta = g^{-1}(A(s)z + g(A(s)\beta_{0d})) \quad (4.30)$$

and,

$$\Delta\beta_d = A^{-1}(s)y - \beta_{0d} \quad (4.31)$$

that is,

$$A(s)\beta = A(s)(\Delta\beta_{0d} + \beta_{0d}) \quad (4.32)$$

Let

$$y = A(s)\beta \quad (4.33)$$

then

$$\Delta Q = Q(y, \omega_0 + \Delta\omega, V) - Q(\beta_0, \omega_0, V) \quad (4.34)$$

and

$$\Delta\omega = G(s) \left(Q(y, \omega_0 + \Delta\omega, V) - Q(\beta_0, \omega_0, V) + \frac{T_0}{\omega_0 + \Delta\omega} \Delta\omega - \frac{\Delta P}{\omega_0 + \Delta\omega} \right) \quad (4.35)$$

Linearising (4.34) yields,

$$\begin{aligned} \delta\Delta Q &= \frac{\partial Q}{\partial \beta} (\bar{y}, \bar{\omega}_0 + \bar{\Delta\omega}, \bar{V}) \delta y + \frac{\partial Q}{\partial \omega} (\bar{y}, \bar{\omega}_0, \bar{V}) (\delta\omega_0 + \delta\Delta\omega) \dots \\ &+ \frac{\partial Q}{\partial V} (\bar{y}, \bar{\omega}_0 + \bar{\Delta\omega}, \bar{V}) \delta V - \frac{\partial Q}{\partial \beta} (\bar{\beta}_0, \bar{\omega}_0, \bar{V}) \delta\beta_0 - \frac{\partial Q}{\partial \omega} (\bar{\beta}_0, \bar{\omega}_0, \bar{V}) \delta\omega_0 \dots \\ &- \frac{\partial Q}{\partial V} (\bar{\beta}_0, \bar{\omega}_0, \bar{V}) \delta V \end{aligned} \quad (4.36)$$

Note that a variable with a bar (e.g. $\bar{\beta}$) denotes the value at the equilibrium point.

To find δy ,

$$g(y) = A(z) + g(A(\beta_{d0})) \quad (4.37)$$

$$g'(\bar{y})\delta y = g'(\bar{\beta}_0 + \bar{\Delta\beta})\delta y = A(\delta z) + g'(\beta_{d0})A(\delta\beta_{d0}) \quad (4.38)$$

$$\delta y = \frac{A(\delta z + g'(\bar{\beta}_0)\delta\beta_{d0})}{g'(\bar{\beta}_0 + \bar{\Delta\beta})} \quad (4.39)$$

Substituting into (4.36),

$$\begin{aligned}
 \delta\Delta Q &= \frac{g'(\beta_0)}{g'(\beta_0 + \Delta\beta)} \left(\frac{\partial Q}{\partial \beta}(\bar{y}, \bar{\omega}_0 + \overline{\Delta\omega}, \bar{V}) - \frac{\partial Q}{\partial \beta}(\bar{\beta}_0, \bar{\omega}_0, \bar{V}) \right) \delta\beta_0 \dots & (4.40) \\
 &+ \frac{1}{g'(\beta_0 + \Delta\beta)} \frac{\partial Q}{\partial \beta}(\bar{y}, \bar{\omega}_0 + \overline{\Delta\omega}, \bar{V}) A(\delta z) \dots \\
 &+ \left(\frac{\partial Q}{\partial \omega}(\bar{y}, \bar{\omega}_0, \bar{V}) - \frac{\partial Q}{\partial \omega}(\bar{\beta}_0, \bar{\omega}_0, \bar{V}) \right) \delta\omega_0 \dots \\
 &+ \frac{\partial Q}{\partial \omega}(\bar{y}, \bar{\omega}_0 + \overline{\Delta\omega}, \bar{V}) \delta\Delta\omega + \left(\frac{\partial Q}{\partial V}(\bar{y}, \bar{\omega}_0 + \overline{\Delta\omega}, \bar{V}) - \frac{\partial Q}{\partial V}(\bar{\beta}_0, \bar{\omega}_0, \bar{V}) \right) \delta V
 \end{aligned}$$

For ease of notation, let,

$$\frac{\partial Q}{\partial \beta}(\bar{y}, \bar{\omega}_0 + \overline{\Delta\omega}, \bar{V}) = \frac{\partial Q_+}{\partial \beta} \quad (4.41)$$

$$\frac{\partial Q}{\partial \beta}(\bar{\beta}_0, \bar{\omega}_0, \bar{V}) = \frac{\partial Q}{\partial \beta} \quad (4.42)$$

$$\frac{\partial Q}{\partial \omega}(\bar{y}, \bar{\omega}_0 + \overline{\Delta\omega}, \bar{V}) = \frac{\partial Q_+}{\partial \omega} \quad (4.43)$$

$$\frac{\partial Q}{\partial \omega}(\bar{\beta}_0, \bar{\omega}_0, \bar{V}) = \frac{\partial Q}{\partial \omega} \quad (4.44)$$

$$\frac{\partial Q}{\partial V}(\bar{y}, \bar{\omega}_0 + \overline{\Delta\omega}, \bar{V}) = \frac{\partial Q_+}{\partial V} \quad (4.45)$$

$$\frac{\partial Q}{\partial V}(\bar{\beta}_0, \bar{\omega}_0, \bar{V}) = \frac{\partial Q}{\partial V} \quad (4.46)$$

Linearising (4.35) and substituting in (4.40),

$$\delta\Delta\omega = G(s) \left(\begin{aligned} &\left(\frac{\partial Q_+}{\partial \omega} - \frac{\bar{T}_0 \bar{\omega}_0}{(\bar{\omega}_0 + \overline{\Delta\omega})^2} + \frac{\overline{\Delta P}}{(\bar{\omega}_0 + \overline{\Delta\omega})^2} \right) \delta\Delta\omega \dots \\ &+ A(s) \left(\frac{1}{g'(\beta_0 + \Delta\beta)} \frac{\partial Q_+}{\partial \omega} \right) \delta z - \frac{1}{\bar{\omega}_0 + \overline{\Delta\omega}} \delta\Delta P \dots \\ &+ \left(\frac{\partial Q_+}{\partial \omega} - \frac{\partial Q}{\partial \omega} - \frac{\bar{T}_0 \overline{\Delta\omega}}{(\bar{\omega}_0 + \overline{\Delta\omega})^2} + \frac{\overline{\Delta P}}{(\bar{\omega}_0 + \overline{\Delta\omega})^2} \right) \delta\omega_0 \dots \\ &+ A(s) \left(\frac{g'(\beta_0)}{g'(\beta_0 + \Delta\beta)} \frac{\partial Q_+}{\partial \beta} - \frac{\partial Q}{\partial \beta} \right) \delta\beta_{a0} \dots \\ &+ \frac{\overline{\Delta\omega}}{\bar{\omega}_0 + \overline{\Delta\omega}} \delta T_0 + \left(\frac{\partial Q_+}{\partial V} - \frac{\partial Q}{\partial V} \right) \delta V \end{aligned} \right) \quad (4.47)$$

At an equilibrium point some of the terms in (4.47) cancel or are equal to zero. The δV term cancels due to separability, as $\frac{\partial Q_+}{\partial v}$ and $\frac{\partial Q}{\partial v}$ are equal. At a stable operating point $\Delta\omega$ is driven to zero and so the δT_0 and the third term of $\delta\omega_0$ are zero. Because the function $g'(\bar{\beta}_0 + \Delta\beta)$ is a normalised approximation of $\frac{\partial Q_+}{\partial \omega}$, the δz term simplifies to $A(s)K\delta z$, where K is the constant used to normalise the function. Via the same logic, the $\delta\beta_0$ term cancels.

Hence, at a stable operating point and using $\delta z = H(s)\delta\Delta\omega$,

$$\begin{aligned} \delta\Delta\omega = & \frac{G(s) \left(\frac{\partial Q_+}{\partial \omega} - \frac{\partial Q}{\partial \omega} + \frac{\Delta P}{\bar{\omega}_0^2} \right)}{1 - G(s) \left(\frac{\partial Q_+}{\partial \omega} - \frac{\bar{T}_0}{\bar{\omega}_0} + \frac{\Delta P}{\bar{\omega}_0^2} + A(s)H(s)K \right)} \delta\omega_0 \dots \\ & - \frac{G(s) \frac{1}{\bar{\omega}_0}}{1 - G(s) \left(\frac{\partial Q_+}{\partial \omega} - \frac{\bar{T}_0}{\bar{\omega}_0} + \frac{\Delta P}{\bar{\omega}_0^2} + A(s)H(s)K \right)} \delta\Delta P \end{aligned} \quad (4.48)$$

The linearised relationships for $\delta\Delta T$ and $\delta\Delta\beta$ can also be found,

$$\delta\Delta T = \frac{1}{\bar{\omega}_0} \delta\Delta P - \frac{\Delta P}{\bar{\omega}_0^2} \delta\omega_0 + \left(\frac{\bar{T}_0}{\bar{\omega}_0} - \frac{\Delta P}{\bar{\omega}_0^2} \right) \delta\Delta\omega \quad (4.49)$$

and

$$\delta\Delta\beta_d = \frac{1}{g'(\bar{\beta}_0 + \Delta\beta)} H(s)\delta\Delta\omega - \left(1 - \frac{g'(\bar{\beta}_0)}{g'(\bar{\beta}_0 + \Delta\beta)} \right) \delta\beta_{d0} \quad (4.50)$$

The second term in equation 4.50 is equivalent to correcting the scheduling of the full envelope controller. As the full envelope controller is not aware of the increment $\Delta\beta$, the scheduling of the pitch control is based on β_0 rather than the correct value of $\beta_0 + \Delta\beta$. The second term in (4.50) acts as a correction, altering the gain from ω to β_0 to account for the altered pitch angle.

The linearised relationships in (4.48), (4.49), and (4.50) contain some feedback components, specifically the $\delta\omega_0$ and $\delta\Delta\omega$ components, however, these components should be very small. In order to further validate this assertion, the system is linearised as given in Appendix III and interrogated using Matlab.

Chapter 4: Development of the Power Adjusting Control

dynamics without the PAC in use. The Bode plots for these comparisons for a range of wind speeds are given in Figure 47 and Figure 48.

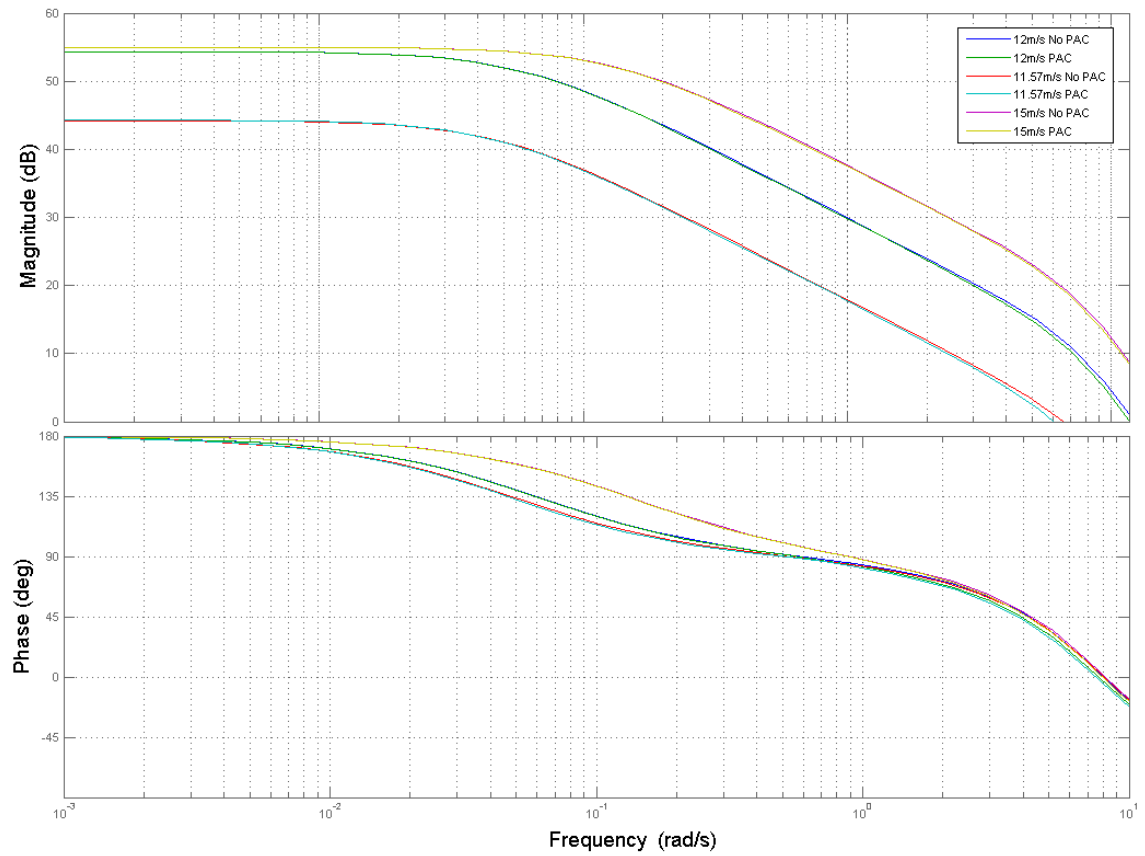


Figure 47: Bode plot of the Dynamics from the Full Envelope Controller Pitch Output to the Full Envelope Controller Input

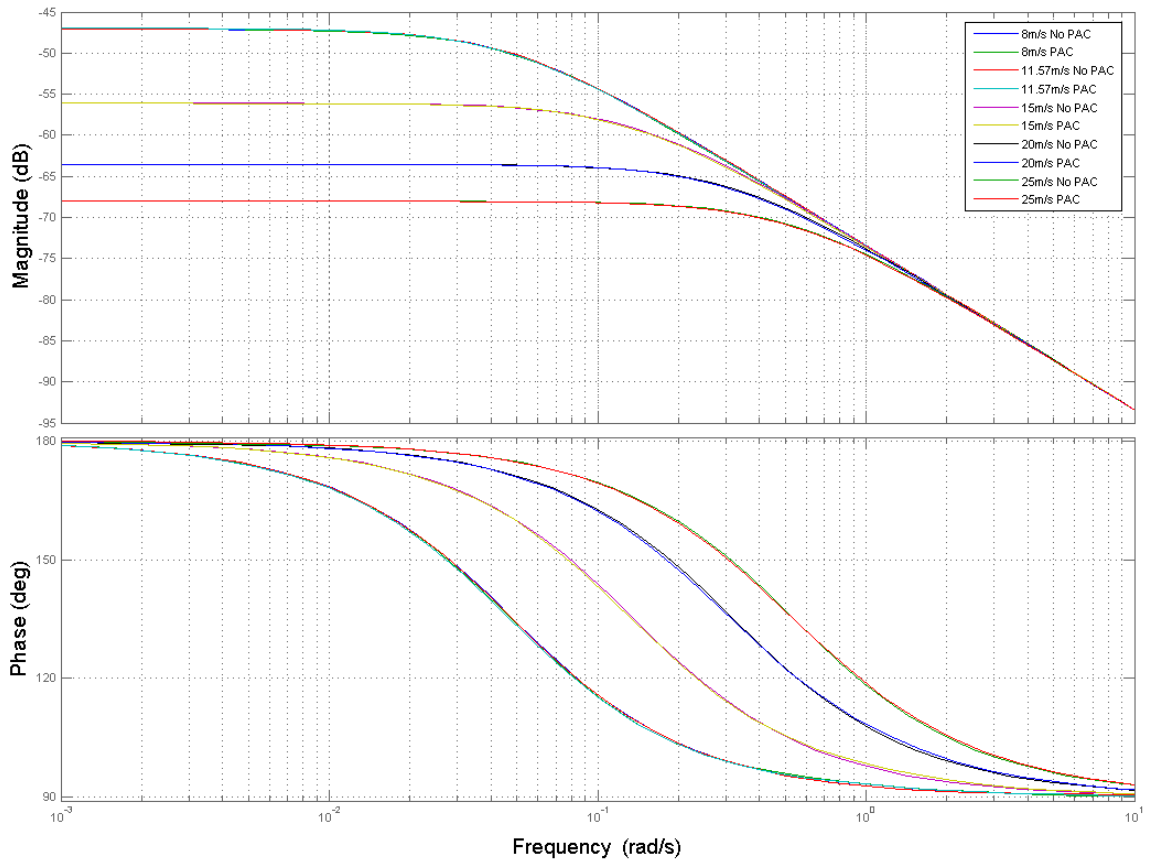


Figure 48: Bode plot of the Dynamics from the Full Envelope Controller Torque Output to the Full Envelope Controller Input

The worst case change for $\delta\beta_0$ to $\delta\omega_0$ is -0.2dB at 1 rad/s (the cross-over frequency of the full envelope controller) at rated wind speed, which is less than a 2.5% change. Note that only above-rated wind speeds have been investigated as pitch is not used in below-rated conditions.

The worst case change for δT_0 to $\delta\omega_0$ is -0.15dB at 1 rad/s (the cross-over frequency of the full envelope controller) at a wind speed of 20m/s , which is less than a 2% change. For below-rated wind speeds, the change is less than 0.5%.

Clearly, any feedback loop around the full envelope controller is very weak.

4.5 Returning to Normal Operation – The Recovery Process

When the PAC is not in use the wind turbine operates in the normal manner, controlled by the full envelope controller. When the PAC is in use the wind turbine operates with an effective change to the set points of the wind turbine. It is

important to ensure that the wind turbine can safely switch between these two modes.

Switching the PAC on is straightforward, as a ΔP request is received and the procedures described in this chapter are executed, resulting in a change in power output. Turning the PAC off is less straightforward however. If the change in power is just reduced to zero then there is no guarantee that this would return the wind turbine operating point to the normal operating strategy. For example, if the wind turbine provides additional power then the rotor speed reduces. If the change in power is subsequently reduced to zero then, because of the decrease in rotor speed, a higher torque is necessary than that used in normal operation. Hence the wind turbine will not return to the normal operating strategy. The situation becomes even more complex when the PAC is providing a change to the pitch angle.

In order to ensure that the PAC can be returned to the normal operating strategy after use of the PAC, a recovery process is required. The recovery process prevents a sudden change in the operating conditions of the turbine and controls the turbine as it returns to normal operation. Without the recovery process, the turbine is susceptible to large loads, especially if the PAC has driven operation far from the normal operating strategy.

4.5.1 Torque Demand Action

If the operating point is above and to the left of the operating strategy, then a negative torque is required to move it back towards the operating strategy. If the operating point is below and to the right of the operating strategy then the converse is true. The $\Delta\omega$ output shows which of these scenarios is true, with a negative $\Delta\omega$ showing that a negative torque is required and a positive $\Delta\omega$ showing the opposite.

It is desirable to weight the torque demand dependent upon the distance of the operating point from the operating strategy. If the operating point is far away from the strategy then a larger torque is demanded compared to if the operating point is

very close to the operational strategy. As the operating point moves closer, the torque reduces.

The recovery torque ΔT_R is therefore calculated using the relationship given in (4.54).

$$\Delta T_R = K_R \Delta \omega \quad (4.52)$$

where K_R is a constant.

It is important to avoid a step in the change in torque demand as a step change in torque demand is likely to cause increased loads on the wind turbine, so the signal is passed through a first order low pass filter when the recovery starts. The ΔT signal must not be filtered during normal operation however, as for some applications (such as synthetic inertia) a rapid response is necessary. The logic required to achieve this is given in Appendix I.

The speed of the recovery is strongly affected by the time constant of the filter. The time constant is given the symbol τ_c .

4.5.2 Pitch Demand Action

The pitch demand action in the recovery process could follow one of two options. When operating without the PAC, the change in pitch due to the PAC ($\Delta\beta$) is zero. As such, when recovering to the normal operational strategy one option is to drive the value of $\Delta\beta$ to zero. This results in the fast removal of the increment in pitch. The second option is to simply allow the pitch controller to reduce the pitch angle through the normal mechanism. As ΔT changes, $\Delta\omega$ changes, driving $\Delta\beta$ towards zero. This results in a slower reduction of the pitch increment.

4.5.3 Varying the Speed of Recovery

In order to allow the operator to vary the speed of the recovery, one of two methods can be chosen. The quickest method sets τ_c to a low value and sets $\Delta\beta$ to zero. The slower method uses a higher value of τ_c and allows the controller to reduce $\Delta\beta$ to zero through the normal mechanism.

4.6 Modelling of the Power Adjusting Controller

In order to test the power adjusting controller it is modelled in two software packages, Matlab Simulink and GL Bladed. The former incorporates a model of a wind turbine and full envelope controller based on the work in [9], [14], [70]–[73], incorporating full dynamic models for the aerodynamics and drive-train. The aerodynamics are based upon blade element momentum theory using a single effective wind speed as the input. This model is a lumped parameter ordinary differential equation model, and is classed as a “control model” using the definition outlined in section 2.7. The latter is a wind turbine simulation package, commonly used in the wind industry for validation of wind turbines. The aerodynamics in GL Bladed are based upon blade element momentum theory and a full three dimensional wind field is used as the input. This model is referred to as a “full aero-elastic simulation” using the definitions outlined in section 2.7. The same design of full envelope controller is used in each model.

The Simulink model operates in continuous time, with a user friendly block diagram interface, whereas the GL Bladed model operates in discrete time, with the controller written and then compiled from C code. The PAC is therefore initially designed and tuned using the Simulink model for ease of design.

Two wind turbines are used, each modelled in both software packages. The first has a rated power of 1.5MW, whilst the second has a rated power of 5MW.

4.6.1 Required Variables

The Physical properties of the 1.5MW wind turbine and the 5MW wind turbine, along with their operational strategy variables and controllers are given in Appendix II. In order to define the PAC the variables in Table 2 are defined.

Table 2: Variables Required to Tune the PAC

Variable Description	Variable Symbol	Variable Value (1.5MW)	Variable Value (5MW)

Inertia of the drive-train and rotor	J	738	4664
Damping of the drive- train	B	5.013	20.94
Recovery Time Constant	τ_c	5 (fast recovery) or 10 (slow recovery)	5 (fast recovery) or 10 (slow recovery)
$\Delta\beta$ Controller Proportional Gain	$K_{\beta P}$	0.025	0.04
$\Delta\beta$ Controller Integral Gain	$K_{\beta I}$	0.005	0.008

4.7 Testing of the PAC

In order to test the PAC, a set of sample signals for a change in power are used as an input. The sample signals include both positive and negative changes in power output of varying sizes, at various rates of change of power, and for various lengths of time.

In order to demonstrate that the PAC works across the operational envelope, below-rated wind speeds, wind speeds around rated, and above-rated wind speeds are used. The first tests are conducted with a constant wind speed in order to easily show the change in power output. After this, tests are completed at a variety of wind turbulence levels, with one simulation completed using the PAC and a second completed with the same wind input and no PAC used. By subtracting the second test from the first, the actual change in power output is obtained. Note that the mechanical power is used rather than the electrical power. The rated mechanical power is 1.58MW for the smaller turbine and 5.25MW for the larger turbine.

Different values are used for the recovery gain to demonstrate the effect of changing this variable.

Tests are completed first in Simulink using the control model. After this, the same tests are completed in GL Bladed (the full aero-elastic model).

4.7.1 Change in Power Sample Signals

There are three different change in power (ΔP) signals used to test the PAC. The first is for an instant increase in power output that is held for 10 seconds. The second is an instant decrease in power output that is held for 60 seconds. Finally, there is a variable change in power that requests varying values of ΔP over a 250 second time period. In all cases the PAC is turned off and recovers back to normal operation at the end of the requested change in power.

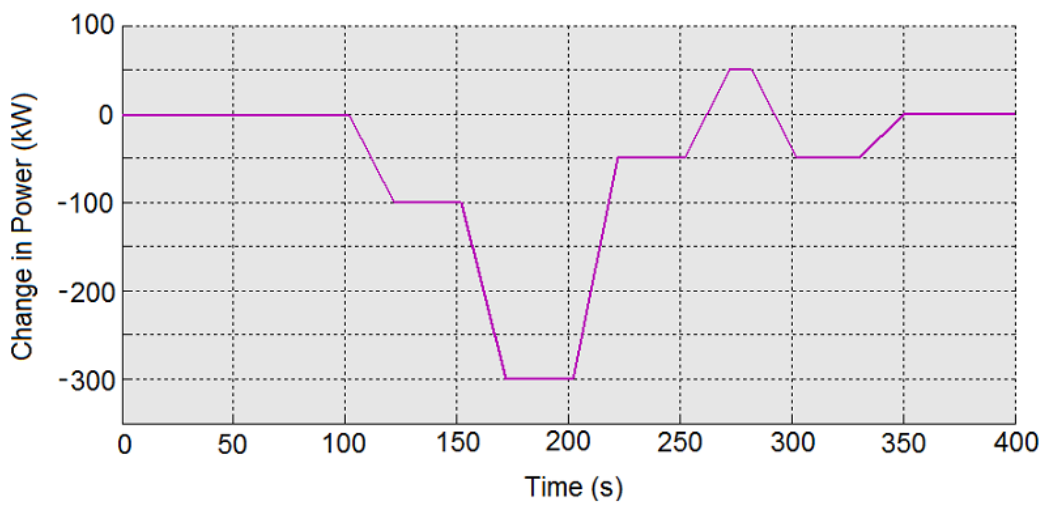


Figure 49: Variable Change in Power Signal for the 1.5MW Wind Turbine

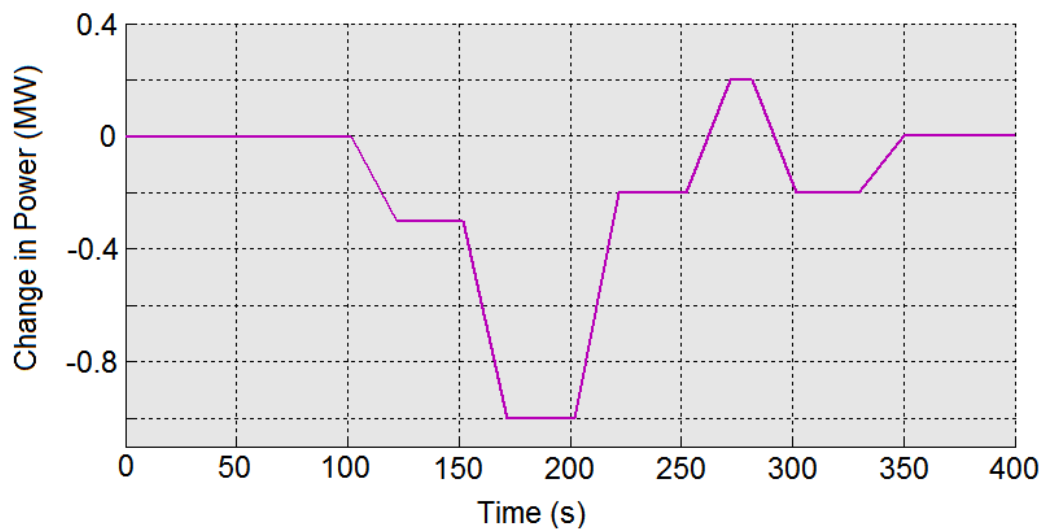


Figure 50: Variable Change in Power Signal for the 5MW Wind Turbine

4.7.2 Simulink Simulations

4.7.2.1 Reduction in Power – Constant Wind Speed

The first test is a reduction in the power output of 100kW for 50 seconds using a 1.5MW wind turbine at constant wind speeds of 10m/s and 15m/s. After 50 seconds the PAC is switched off and recovers the turbine back to normal operation.

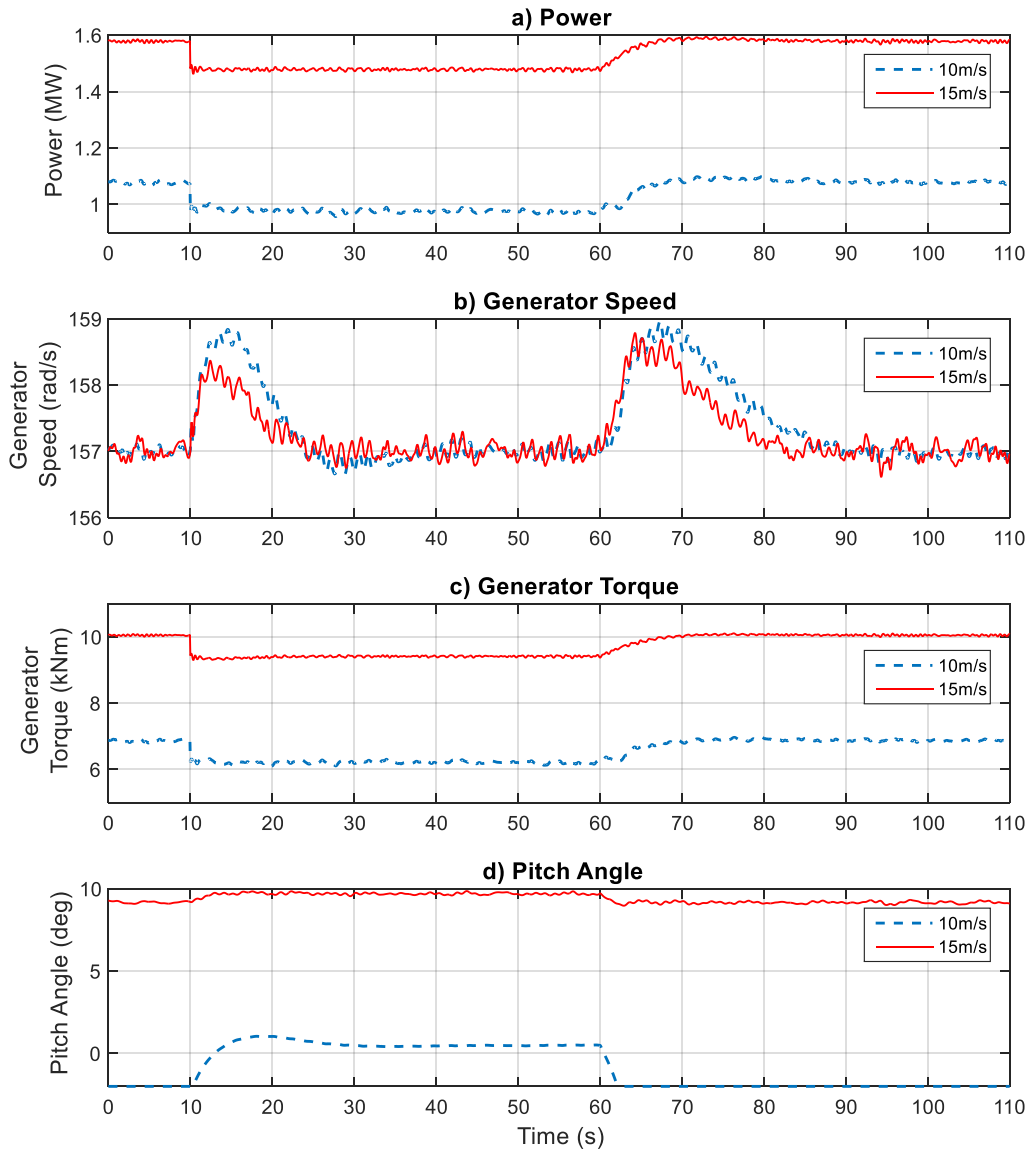


Figure 51: 1.5MW Turbine with a Requested Change in Power of 100kW held for 50s

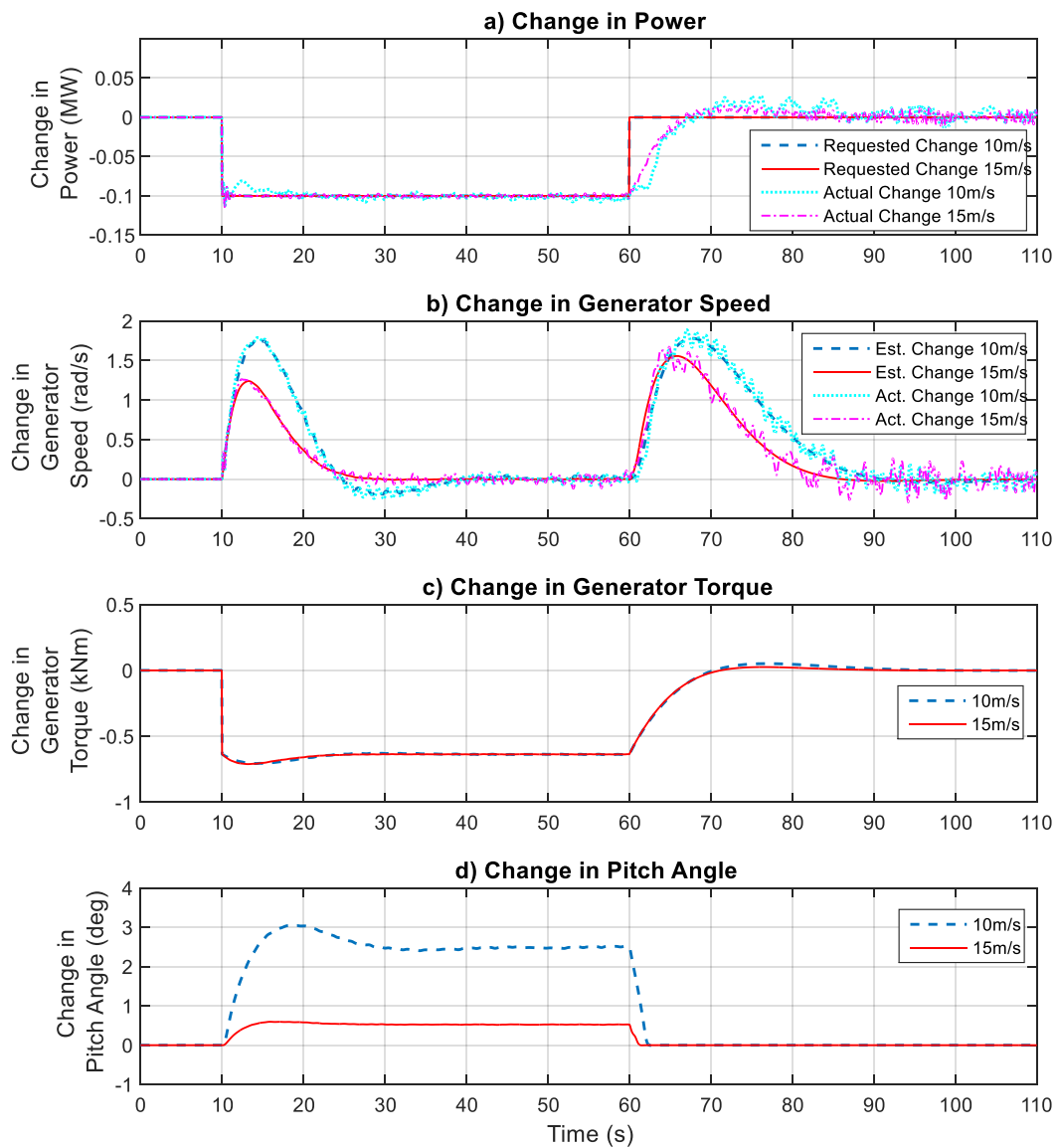


Figure 52: 1.5MW Turbine with a Requested Change in Power of 100kW held for 50s – Change in Variables

The outputs of power, generator speed, generator torque and pitch angle are shown in Figure 51. Figure 52 shows a comparison between the demanded change in power and the actual change in power, the estimated change in generator speed ($\Delta\omega$) and the actual change in generator speed, the change in generator torque (ΔT) and the change in blade pitch angle ($\Delta\beta$). The “actual” changes are found by subtracting the value from the simulation using the PAC from the value obtained from an identical simulation without the PAC.

Chapter 4: Development of the Power Adjusting Control

The primary goal of the PAC is to change the power output accurately. In graph *a*) in Figure 52 it is seen that in both above and below-rated operation the requested change in power is achieved with a high level of accuracy. In the below-rated case there is a discrepancy shortly after the initial power reduction. This is caused by the pitch action inducing tower motion. As the blades pitch, the thrust experienced by the rotor reduces, causing the tower to nod forwards. This in turn results in an increase in the effective wind speed at the rotor, increasing the aerodynamic torque. Because the simple model of the turbine used within the PAC does not have these dynamics, the estimates within the PAC are temporarily incorrect, leading to the error in the actual change in power. In above-rated conditions the pitch angle does not change as much because at higher pitch angles used at higher wind speeds smaller changes in pitch angle are required to affect the same change in torque compared to lower wind speeds with smaller pitch angles. As such, there is less change in the thrust compared with the below-rated simulation and so the error in actual change in power is far smaller. This is more noticeable using the 5MW wind turbine at low wind speeds in the power tracking region of the operational curve. An example is shown in Figure 53, with the simulation conducted with both the nominal values for stiffness of the tower and blades and with much increased stiffness for the tower and blades.

At 60s simulation time the turbine enters recovery. In this example, the blade pitch angle is driven quickly to the minimum pitch, whilst the torque demand is also increased albeit more slowly. As the pitch angle changes more quickly, the generator speed increases during this process before settling to the normal operational value.

As the generator speed and torque can change through use of the PAC, limits on the operational point at which the turbine operates must be imposed. In this chapter, the simulations keep the operating point within a safe operational envelope through sensible selection of values for ΔP . Limits that prevent operation outside of a safe working envelope, no matter what change in power is requested, are discussed in chapter 7.

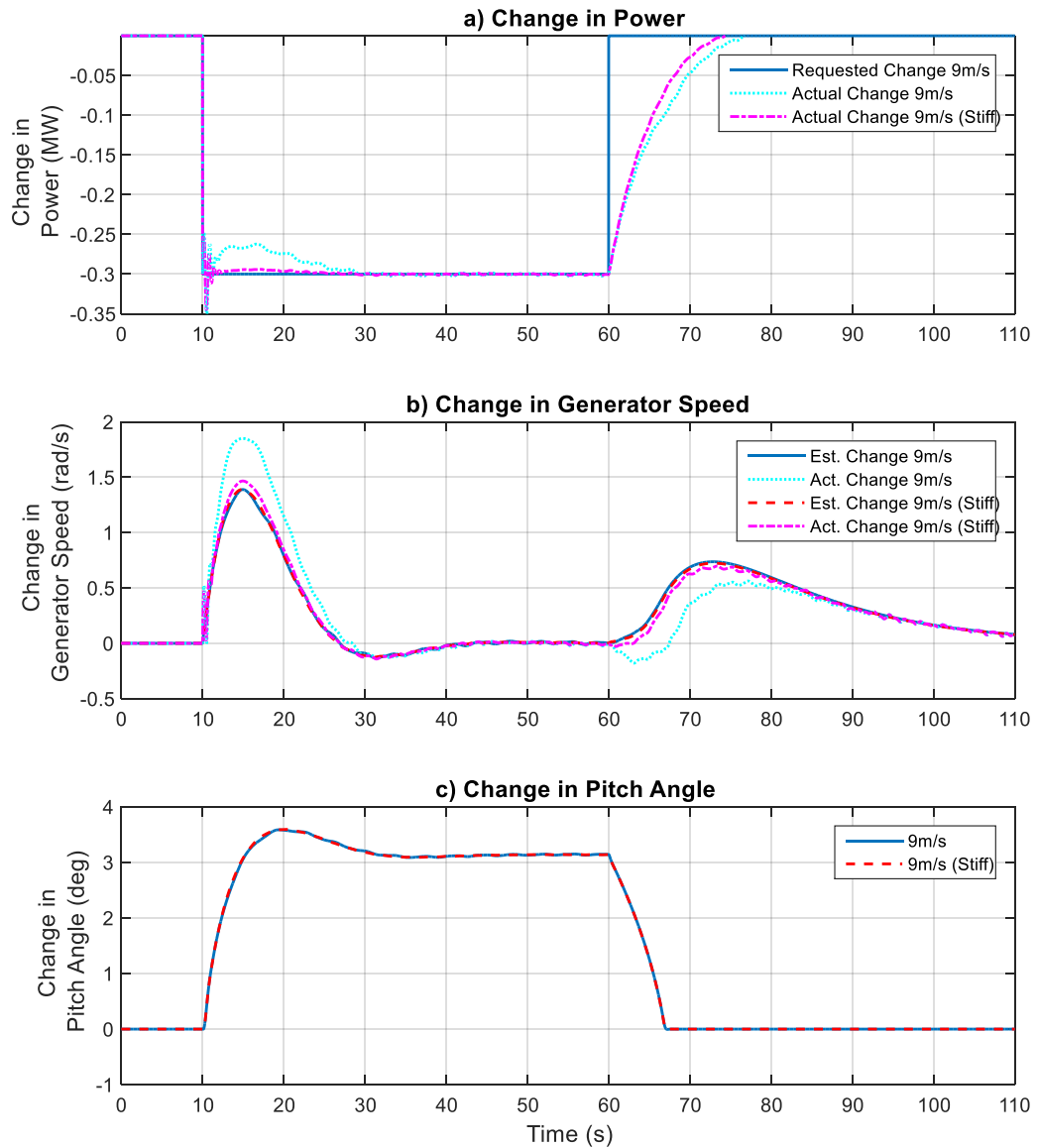


Figure 53: 5MW Wind Turbine with a Requested Change in Power of -300kW

Because of the relative size and flexibility of the 5MW tower the effect described previously is more pronounced. It leads to an error in the estimated change in generator speed (graph *b*) and an error in the change in power (graph *a*) in the case where the nominal values for stiffness are used. In the case where the blades and tower are stiffened the error is much smaller.

In graph *b*) in Figure 51 it is clear that the generator speed increases when the power is first reduced (at 10s simulation time) before returning to the original value as the pitch changes (the pitch angle given in the graph *d*). This is due to the difference in

speed between the torque control and the pitch control. When a change in power is requested the torque changes rapidly to achieve the power change resulting in a change in speed. The pitch control loop subsequently alters the pitch angle to minimise the change in generator speed. During the recovery phase, the generator speed again increases before settling back to the original value. In this case the increase in speed is due to the pitch reducing rapidly to zero. The torque control then brings the turbine back to its normal operating point.

Graph *b*) in Figure 52 shows that the change in generator speed as estimated by the simple wind turbine model within the PAC is an accurate estimate. The disparities between the estimated and the actual change in generator speed consist solely of higher frequency components from the rotational sampling or structural modes. This is expected, as because the wind turbine speed is altered during the simulation, the oscillations due to rotational sampling and structural modes are misaligned when comparing the simulation with the PAC to that without it. As such, when one signal is subtracted from the other to find the actual change in a variable some oscillations in the resultant signal will be introduced as a by-product of the calculation.

4.7.2.2 Increase in Power – Constant Wind Speed

The second test is an increase in the power output of 300kW for 20 seconds using a 5MW wind turbine at constant wind speeds of 10m/s and 15m/s (below-rated wind speed and above-rated wind speed). It is clear from graph *a*) in Figure 54 and graph *a*) in Figure 55 that, as with the previous example, the requested change in power and the actual change in power are in close agreement, that is to say that the PAC produces an accurate change in power.

In the below-rated simulation (10m/s), the increased generator torque cannot be matched by an increase in aerodynamic torque as the blade pitch angle is already at the optimum value. Therefore the pitch angle (graph *d*) in Figure 54) does not change and the generator speed (graph *b*) in Figure 54) reduces. Because the generator speed reduces, the generator torque (graph *c*) in Figure 54) must increase

Chapter 4: Development of the Power Adjusting Control

to maintain the same power output. In the above-rated simulation however, the pitch angle (graph *d*) in Figure 54) is reduced to increase the aerodynamic torque. As such, the generator speed does not continue to drop and so the generator torque does not need to keep increasing.

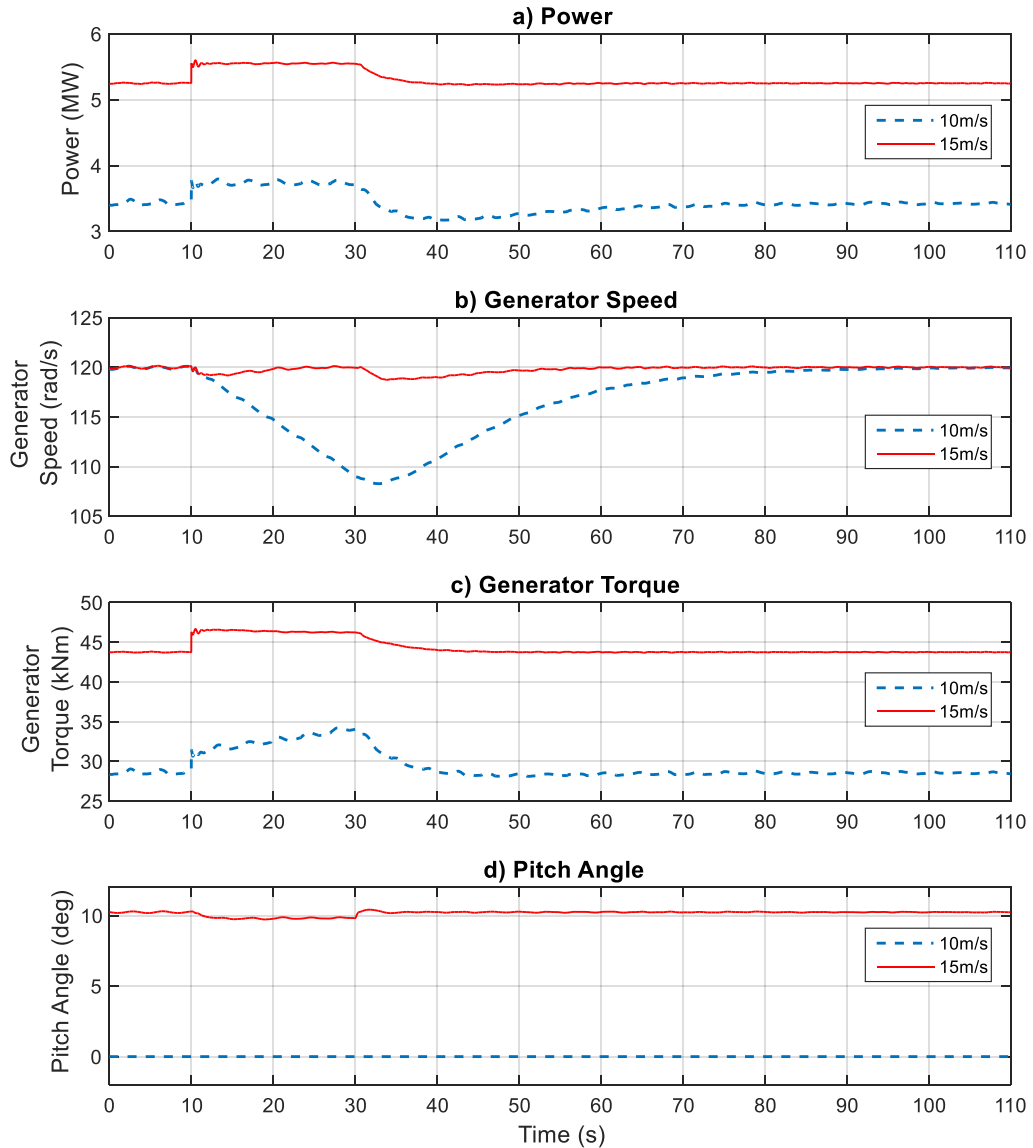


Figure 54: 5MW Turbine with a Requested Increase in Power of 300kW held for 20s

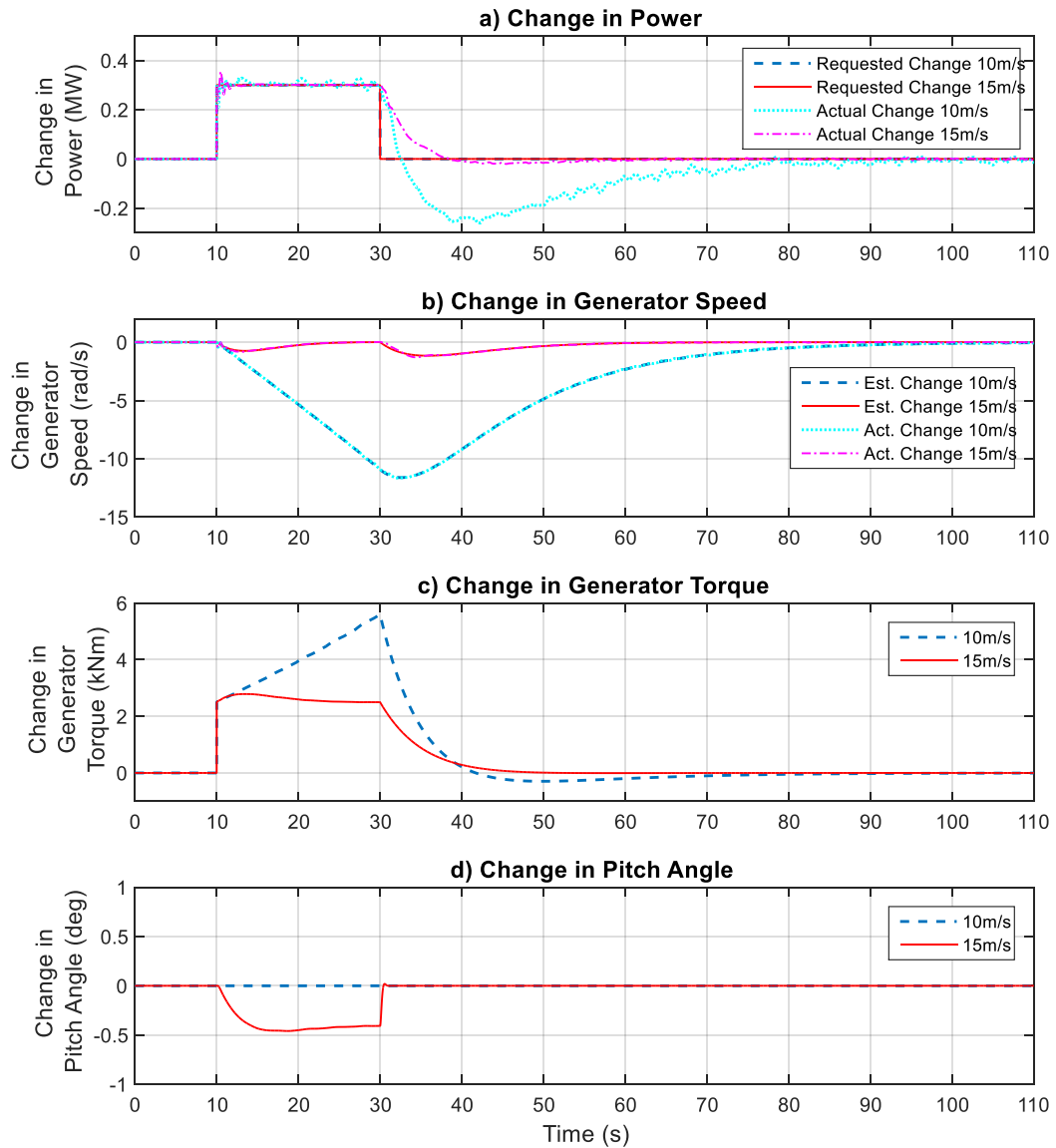


Figure 55: 5MW Turbine with a Requested Increase in Power of 300kW held for 20s – Change in Variables

4.7.2.3 Variable Change in Power – Constant Wind Speed

Simulations are conducted using constant wind speeds (one above-rated and one below) with a requested change in power as per the plot in Figure 49, using the 1.5MW wind turbine. The results are presented in Figure 56 and Figure 57.

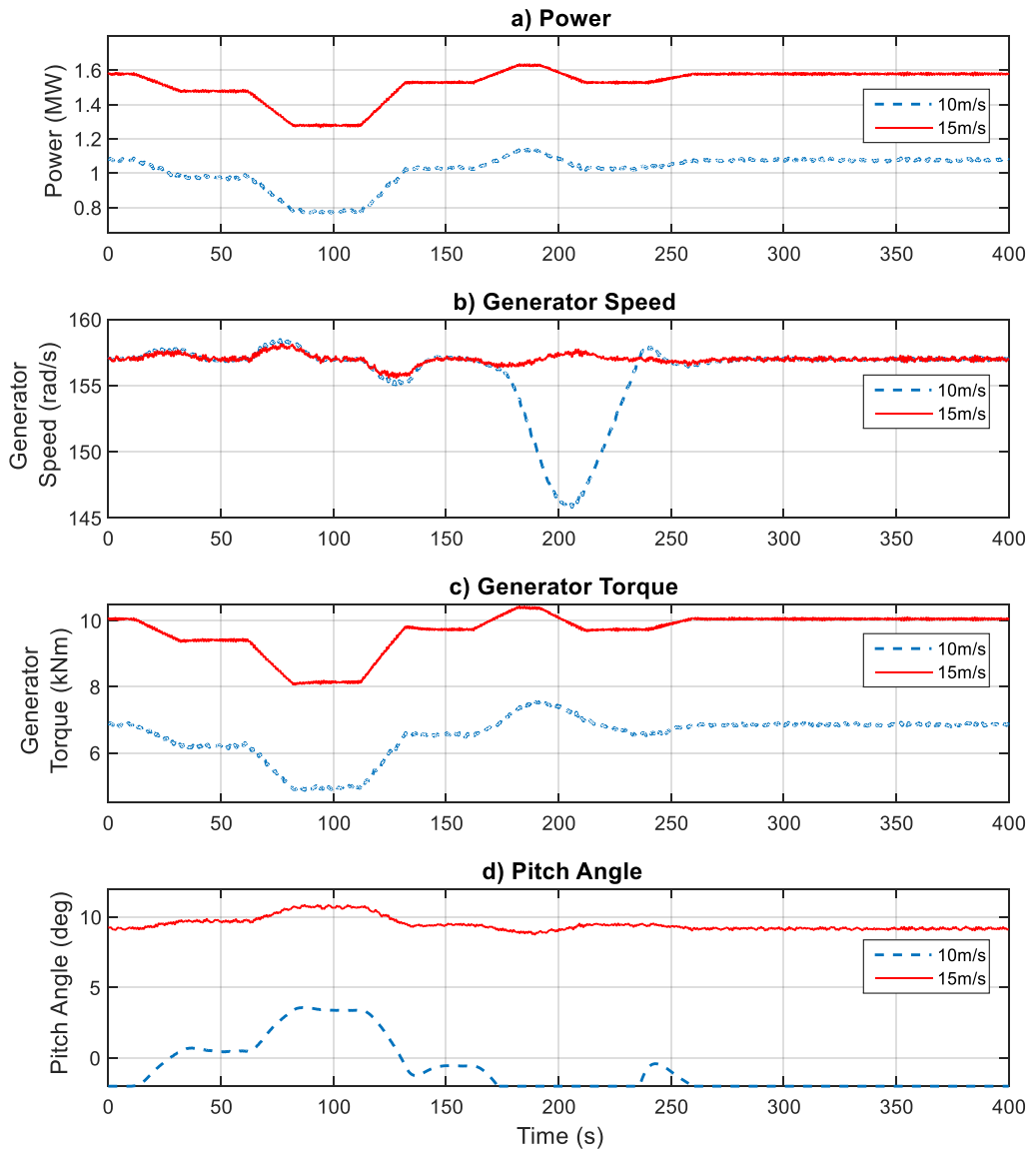


Figure 56: 1.5MW Turbine with a Variable Change in Power Requested

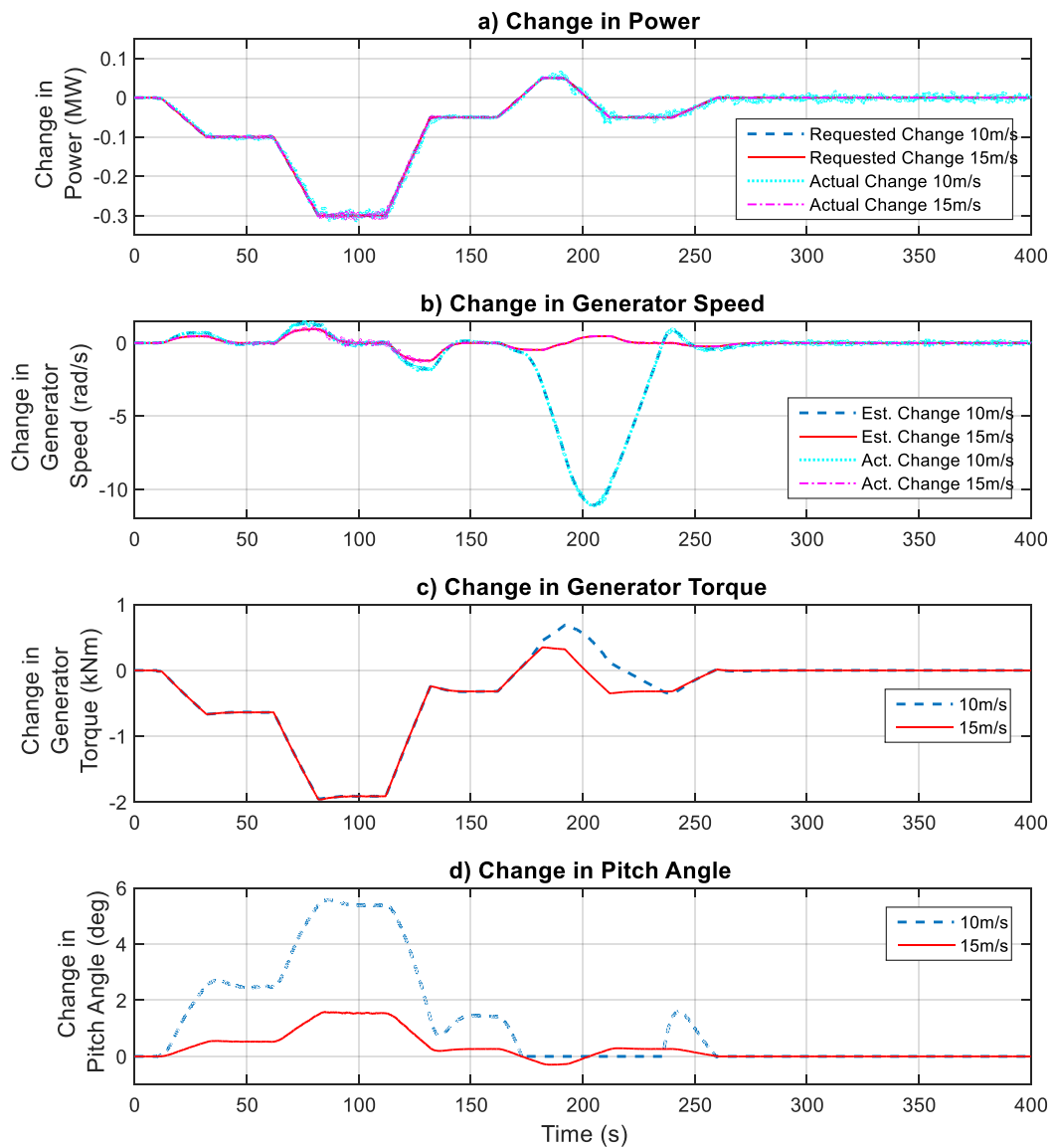


Figure 57: 1.5MW Turbine with a Variable Change in Power Requested – Change in Variables

Graph *a*) in Figure 57 shows that the PAC delivers an accurate change in power, with the actual change in power closely matching the requested change in power. There is some noise in the actual change in power signal, especially for the 10m/s plot due to misalignment of the rotational components of the signal. Because the 10m/s simulation has a larger deviation in the generator speed, the misalignment of the rotational components is greater, especially after the increased power request around 150 seconds that causes the largest change in generator speed (graph *b*) of Figure 57). In graph *a*) in Figure 56 it is clear that there is no increase in the noise of

the power signal and hence the increase in noise in graph *a*) of Figure 57 is a by-product of the subtraction of one power from another. Graph *b*) in Figure 56 and graph *b*) in Figure 57 show that the change in generator speed is well restrained by the pitch control, being kept below ± 2 rad/s except when an increase in power below-rated is requested. As discussed previously, in this situation there is no available pitch angle that will balance the aerodynamic and generator torques and so a change in generator speed is unavoidable.

As expected, the change in pitch angle (graph *d*) in Figure 57) is greater for the below-rated case as gain scheduling has been applied.

4.7.2.4 Reduction in Power – Variable Wind Speed – Low Turbulence

A reduction in power of 300kW is requested using the 5MW wind turbine in varying wind speeds of 5% turbulence, with averages of 9m/s, 11.5m/s and 15m/s. A plot of the actual wind speeds and the estimate of the wind speed produced by the PAC is given in Figure 58.

Figure 58 shows that, whilst there are fluctuations in the estimated speed due to the fluctuations in generator torque and generator speed used as a basis for the prediction, the estimate is generally accurate. The only significant deviation is seen at 10 seconds, when the PAC is switched on. At this point there is an oscillation caused by the sudden decrease in power. If the decrease in power is applied more gradually then this oscillation can be eliminated. The actual wind speed shown in Figure 58 is the effective wind speed fed into the model. It is produced using the techniques described in [22], in which a point wind speed is filtered using a Dryden filter.

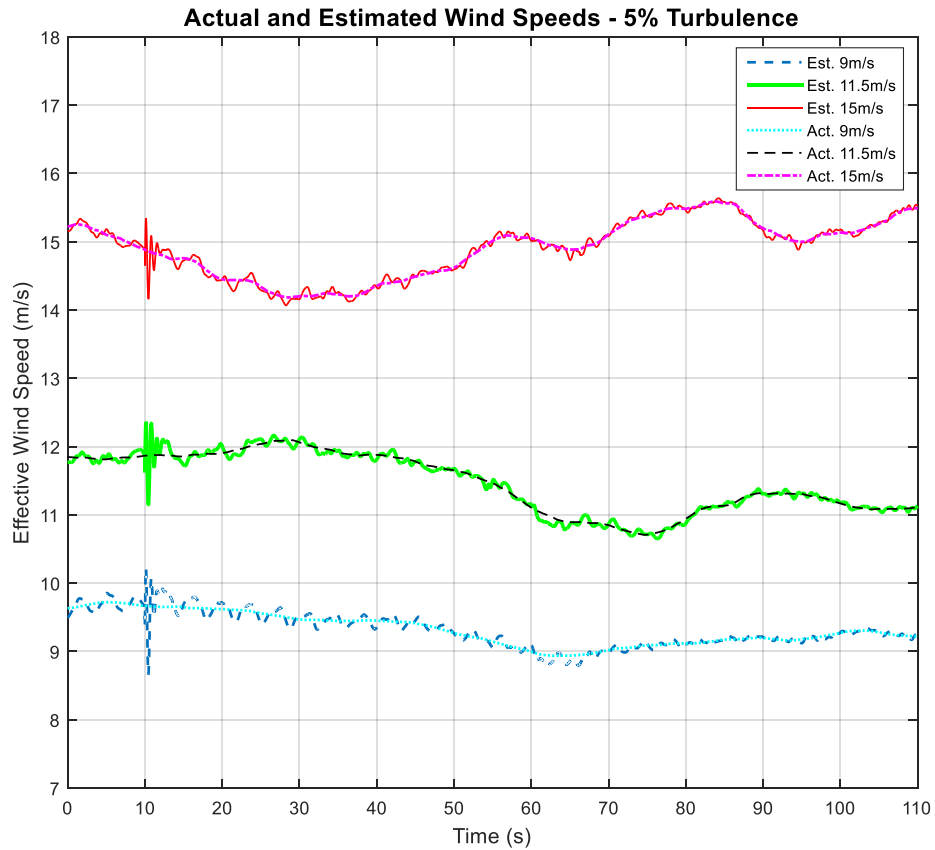


Figure 58: Actual and Estimated Wind Speeds (5% Turbulence)

The resultant changes in power, generator speed, generator torque and pitch angle are shown in Figure 59 and Figure 60 and show that for the simulation at 15m/s the actual change in power is very accurate, as is the estimated change in generator speed. For the 9m/s simulation however there are significant errors in the estimated generator speed and the change in power. This is due to the issue caused by the flexible tower and blades discussed in section 4.7.2.1. The same issue causes an oscillation in the actual change in power for the 11.5m/s simulation. In this case however it is not at the start of the reduction in power output but at approximately 50 seconds. This is due to the full envelope controller switching to below-rated operation from above-rated operation as can be seen in Figure 61. At approximately 55 seconds the pitch angle for the simulation without the PAC reaches the minimum pitch, inducing an oscillation in the power output. The simulation with the PAC does not reach minimum pitch at this time and so there is not as large an oscillation,

Chapter 4: Development of the Power Adjusting Control

resulting in the discrepancy in the actual change in power. Apart from these two issues, the PAC shows excellent performance despite the variations in the wind speed.

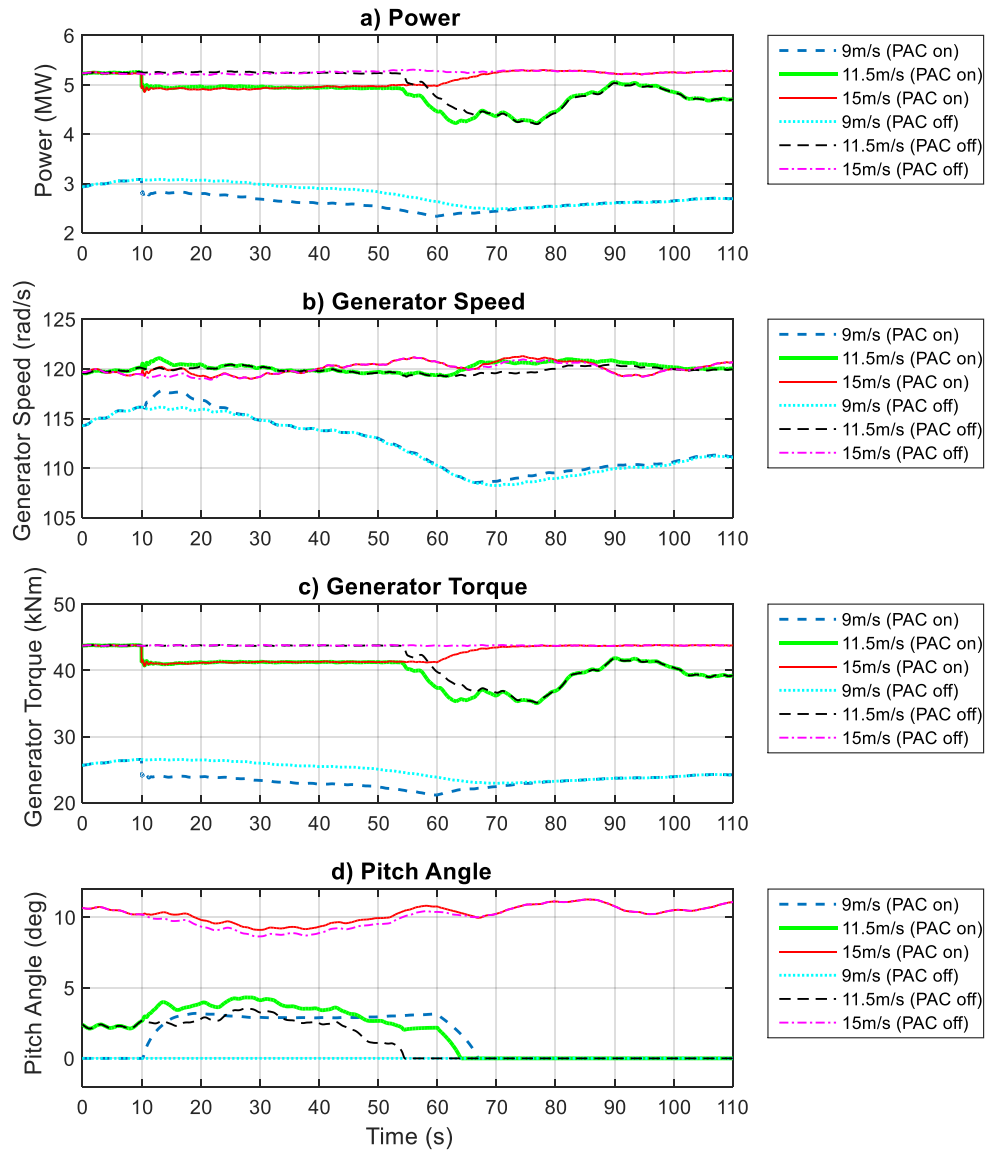


Figure 59: 5MW Turbine with a Requested Change in Power of -300kW held for 50 Seconds

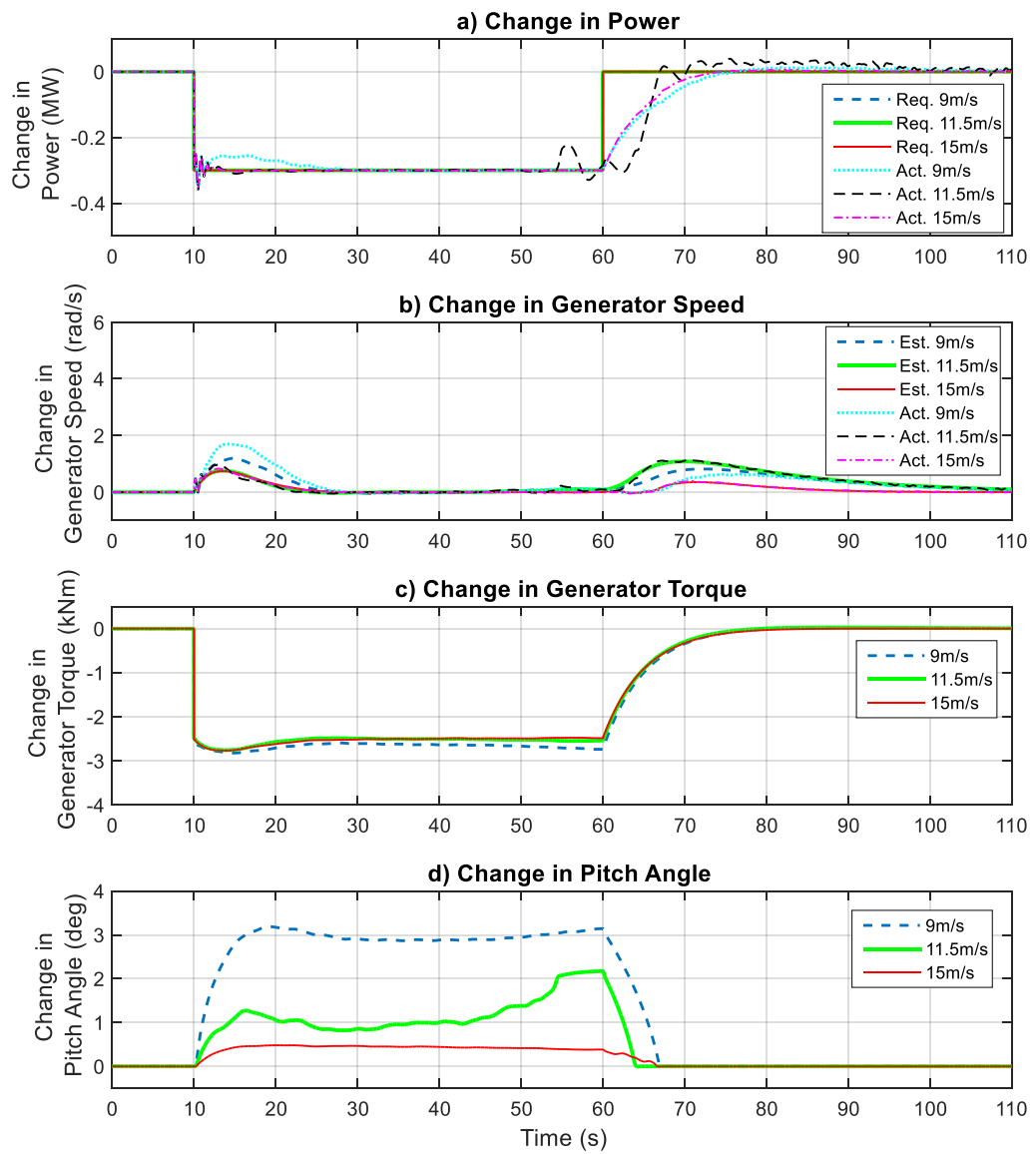


Figure 60: 5MW Turbine with a Requested Change in Power of -300kW held for 50 Seconds - Change in Variables

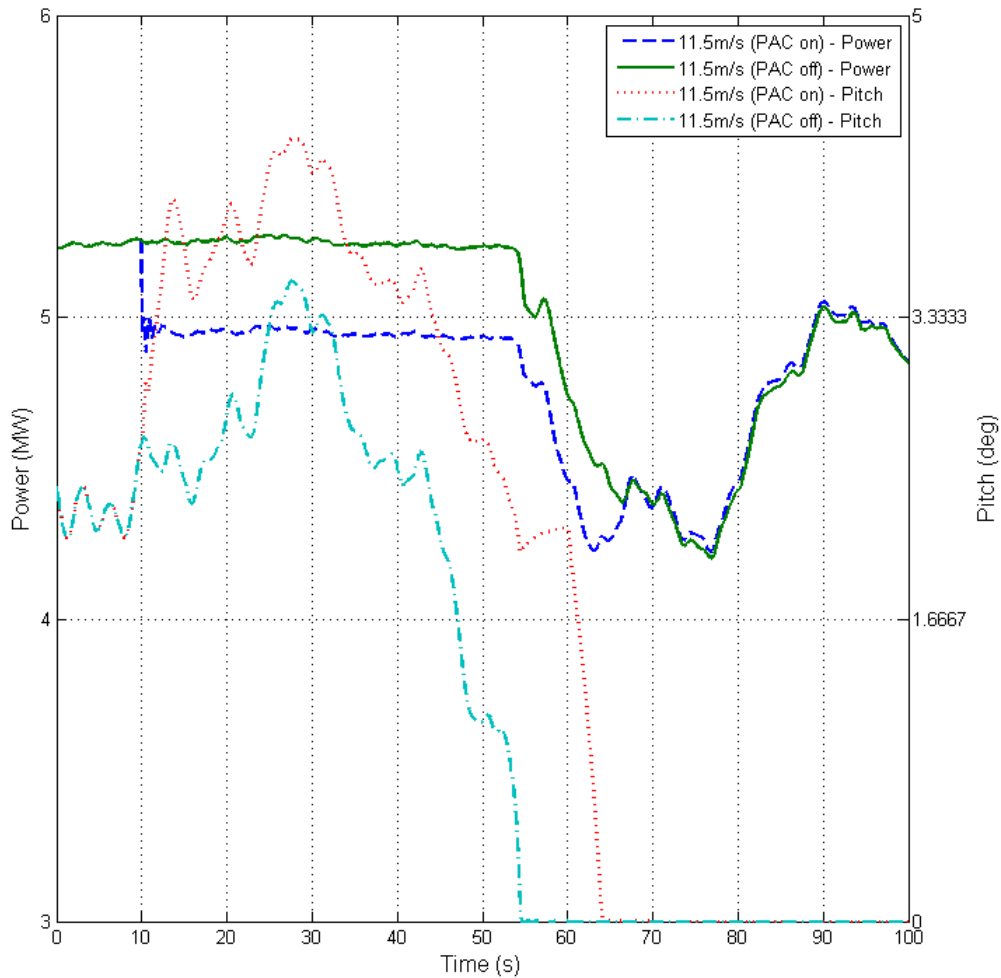


Figure 61: Power and Pitch Angle for the 5MW Wind Turbine

4.7.2.5 Increase in Power – Variable Wind Speed – Low Turbulence

The 1.5MW machine is used to simulate a requested increase in power output of 100kW in low turbulence (5%) variable wind speeds of mean values 9m/s, 11.5m/s, and 15m/s. Graphs of the outputs are given in Figure 62 and Figure 63. The simulations at 15m/s and 9m/s perform as expected, with accurate changes in the power output achieved. For the 15m/s simulation there is only a small deviation in the generator speed as the pitch angle is reduced to increase the aerodynamic torque. In the 9m/s simulation there is a larger deviation in the generator speed as the pitch angle cannot be altered to give extra aerodynamic torque as it is already at the minimum (and optimal) pitch angle.

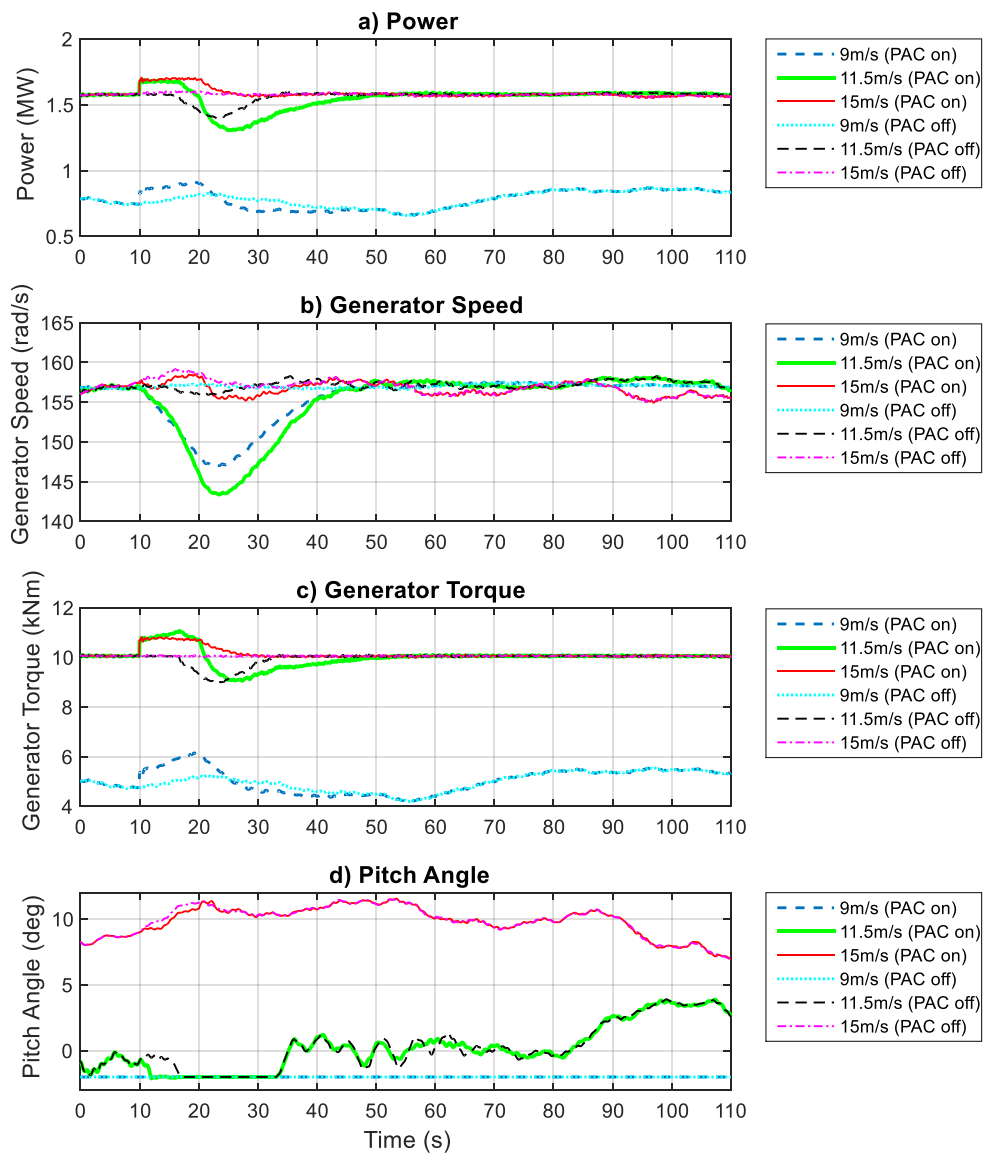


Figure 62: 1.5MW Wind Turbine with a Requested Change in Power of 100kW held for 10s

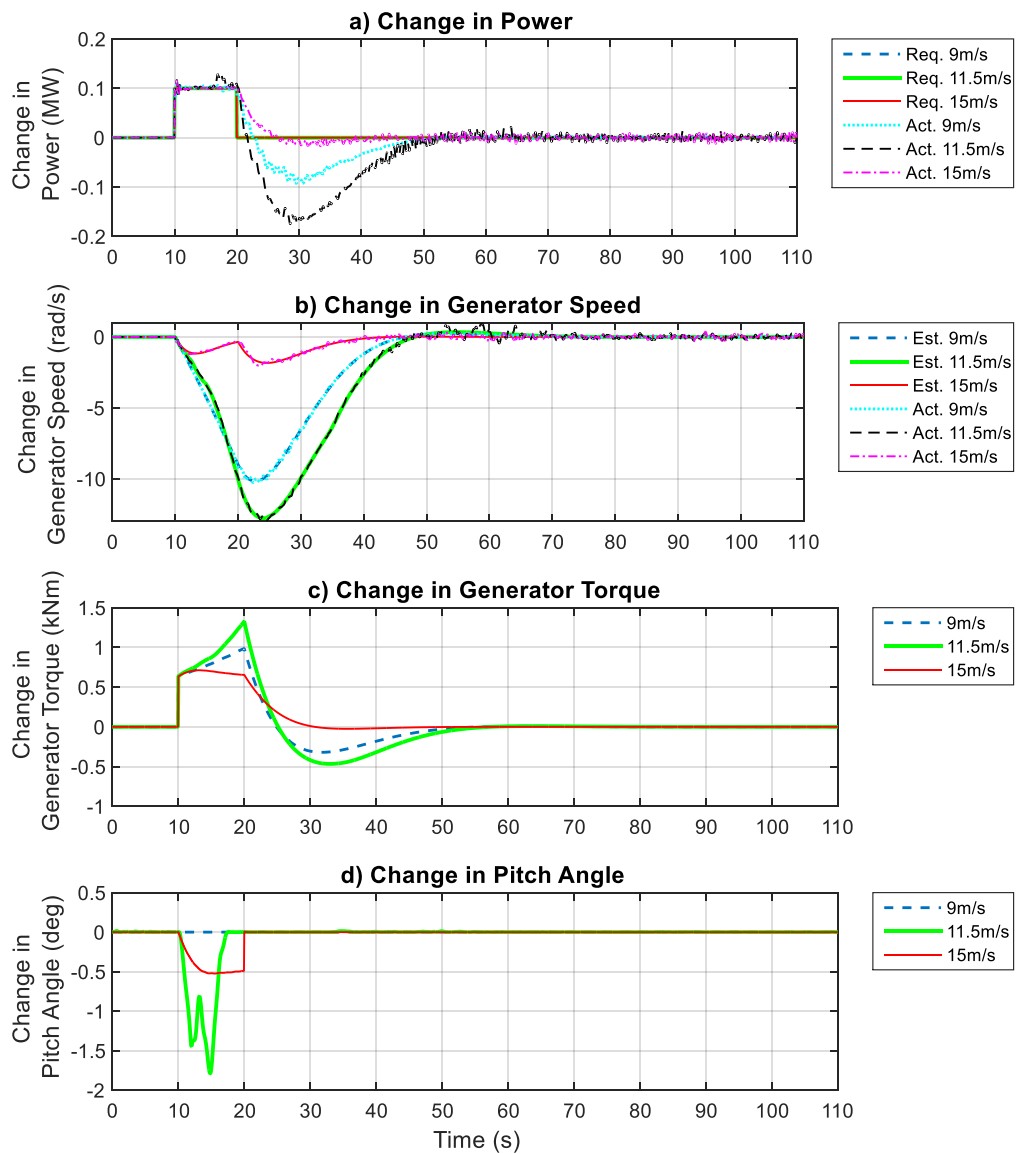


Figure 63: 1.5MW Wind Turbine with a Requested Change in Power of 100kW held for 10s – Change in Variables

The simulation at 11.5m/s has some interesting features. The wind turbine begins the simulation in above-rated operation, however, during the provision of extra power the wind speed drops so that the full envelope controller switches to below-rated operation. The graph *d*) in Figure 62 shows the total pitch angle. In the simulation with the PAC used, the pitch angle is reduced when the additional power is requested to try to minimise the change in generator speed. It quickly reaches the minimum pitch angle however, and is limited at that value. Because of the inability to reduce the pitch further, the generator speed drops.

The change in power plot (graph *a*) in Figure 63) shows a slight oscillation in the actual change in power at approximately 17 seconds. This is due to the wind turbine without the PAC enabled entering below-rated operation leading to a similar effect to that described in section 4.7.2.1.

4.7.2.6 Variable Change in Power – Variable Wind Speed – Low Turbulence

The 5MW machine is used to simulate a requested change in power output as shown in Figure 50, in low turbulence (5%) variable wind speeds of mean values 9m/s, 11.5m/s, and 15m/s. The results are presented in Figure 64, Figure 65, and Figure 66

Despite both a varying wind and a varying requested change in power, the actual change in power (the first graph in Figure 65) is generally very accurate. There are some small errors for the 11.5m/s and 9m/s simulations (accompanied by a small error in the estimated change in generator speed). These are the result of the tower motion that occurs when the pitch is changed rapidly as described previously in section 4.7.2.1.

A plot of the estimated wind speed and the actual wind speed is given in Figure 66. This is similar to that given previously for a reduction in power (Figure 58), however, because there is no sudden change in the change in power request, there is no large oscillation in Figure 66. The estimated wind speed is just as accurate, despite the varying requested change in power.

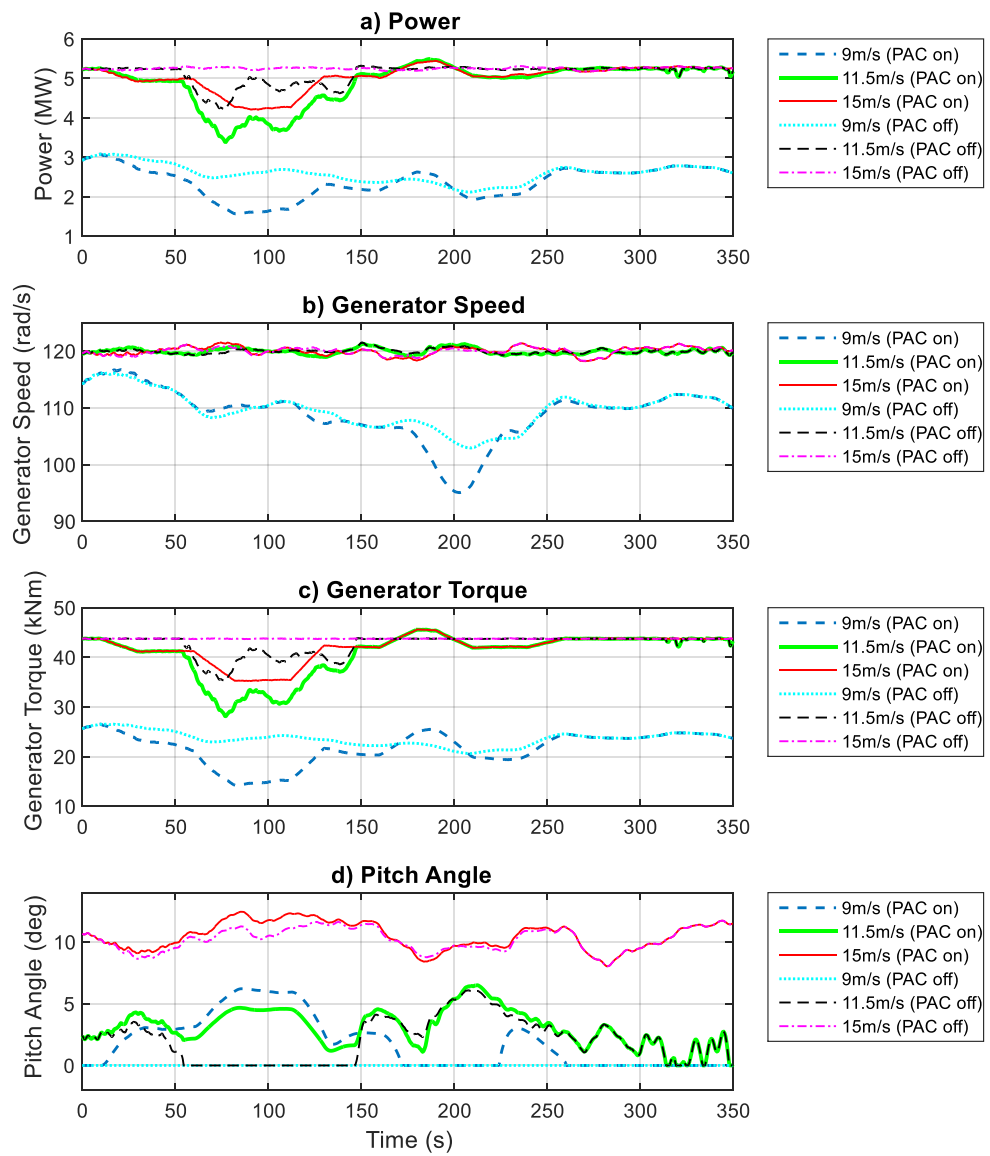


Figure 64: 5MW Wind Turbine with a Variable Requested Change in Power

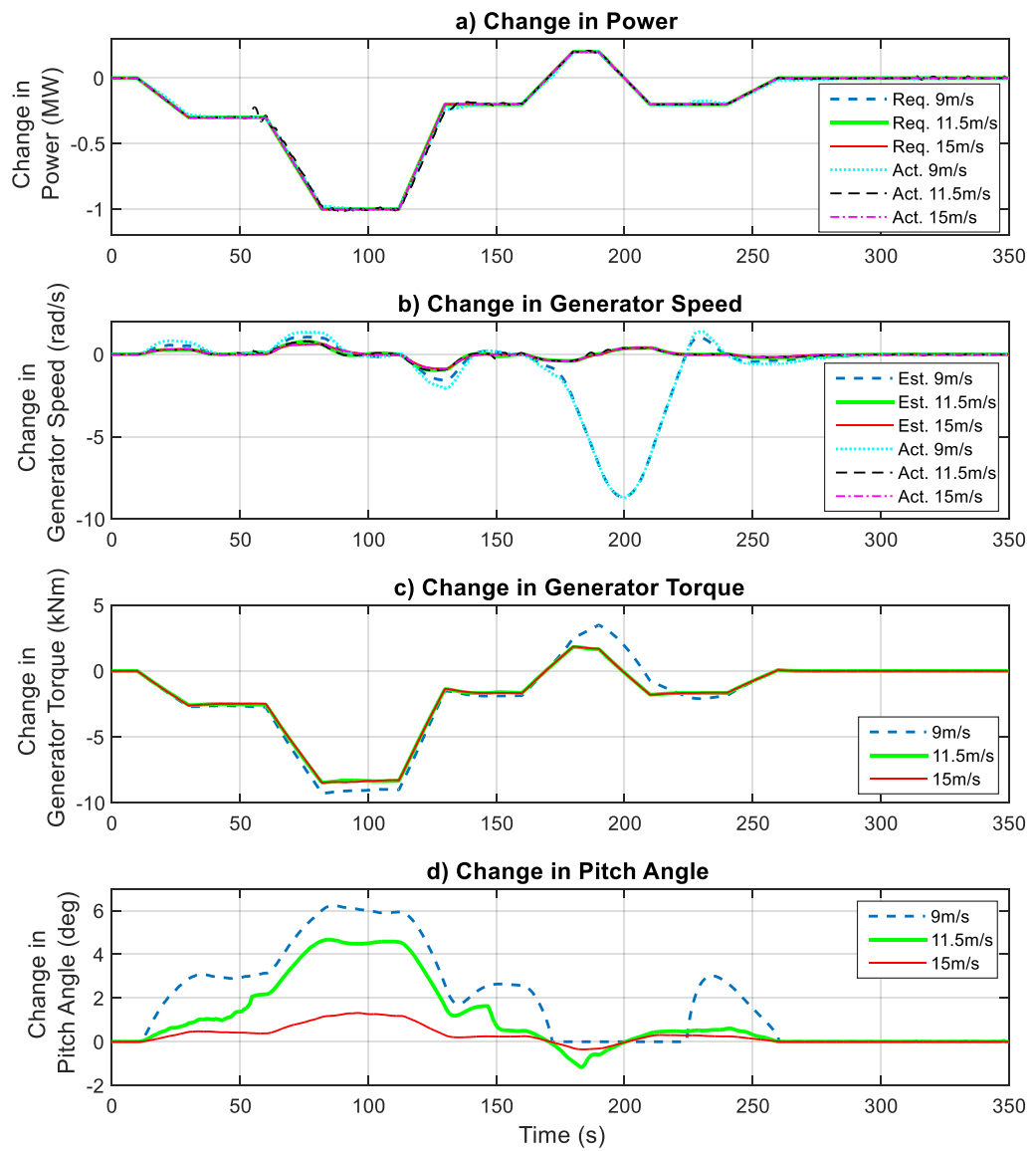


Figure 65: 5MW Wind Turbine with a Variable Requested Change in Power – Change in Variables

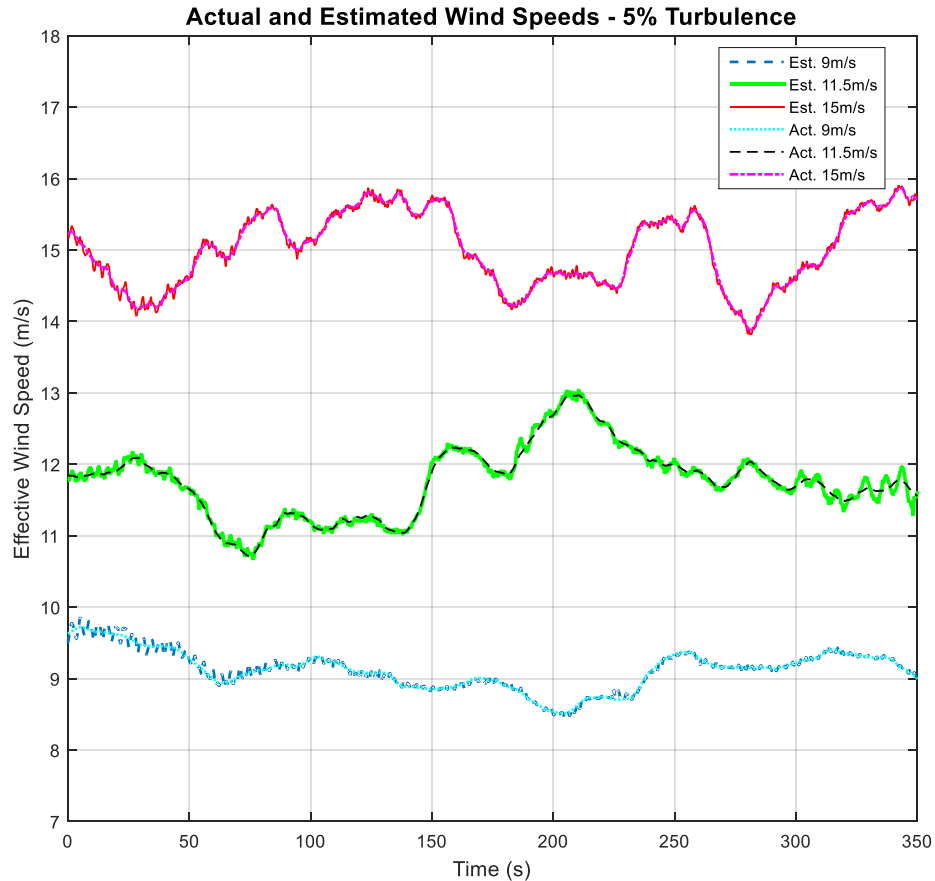


Figure 66: Estimated and Actual Effective Wind Speed - 5% Turbulence

4.7.2.7 Reduction in Power – Variable Wind Speed – High Turbulence

The 1.5MW machine is used to simulate a requested reduction in power output of -100kW in higher turbulence winds (20%) than were used in section 4.7.2.4. Mean wind speeds of 9m/s, 11.5m/s and 15m/s are used.

The results are presented in Figure 67 and Figure 68, which show that the change in power output is still accurate, despite the higher levels of turbulence. The change in generator speed caused by the PAC (graph *b*) in Figure 68) is of a similar magnitude to the simulation with lower turbulence, as is the change in pitch angle (graph *d*) in Figure 68).

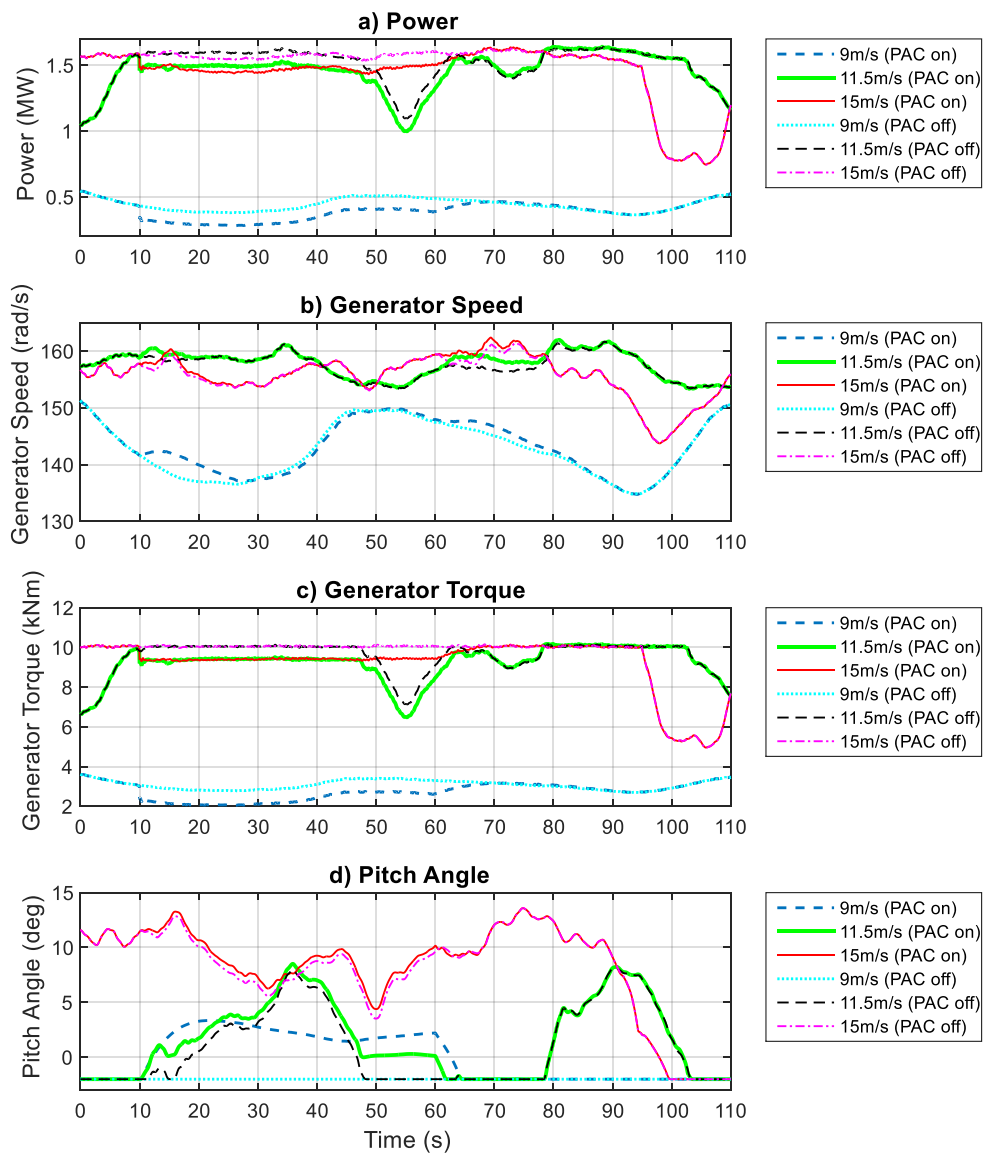


Figure 67: 1.5MW Wind Turbine with a Requested Change in Power of 100kW held for 50s (High Turbulence)

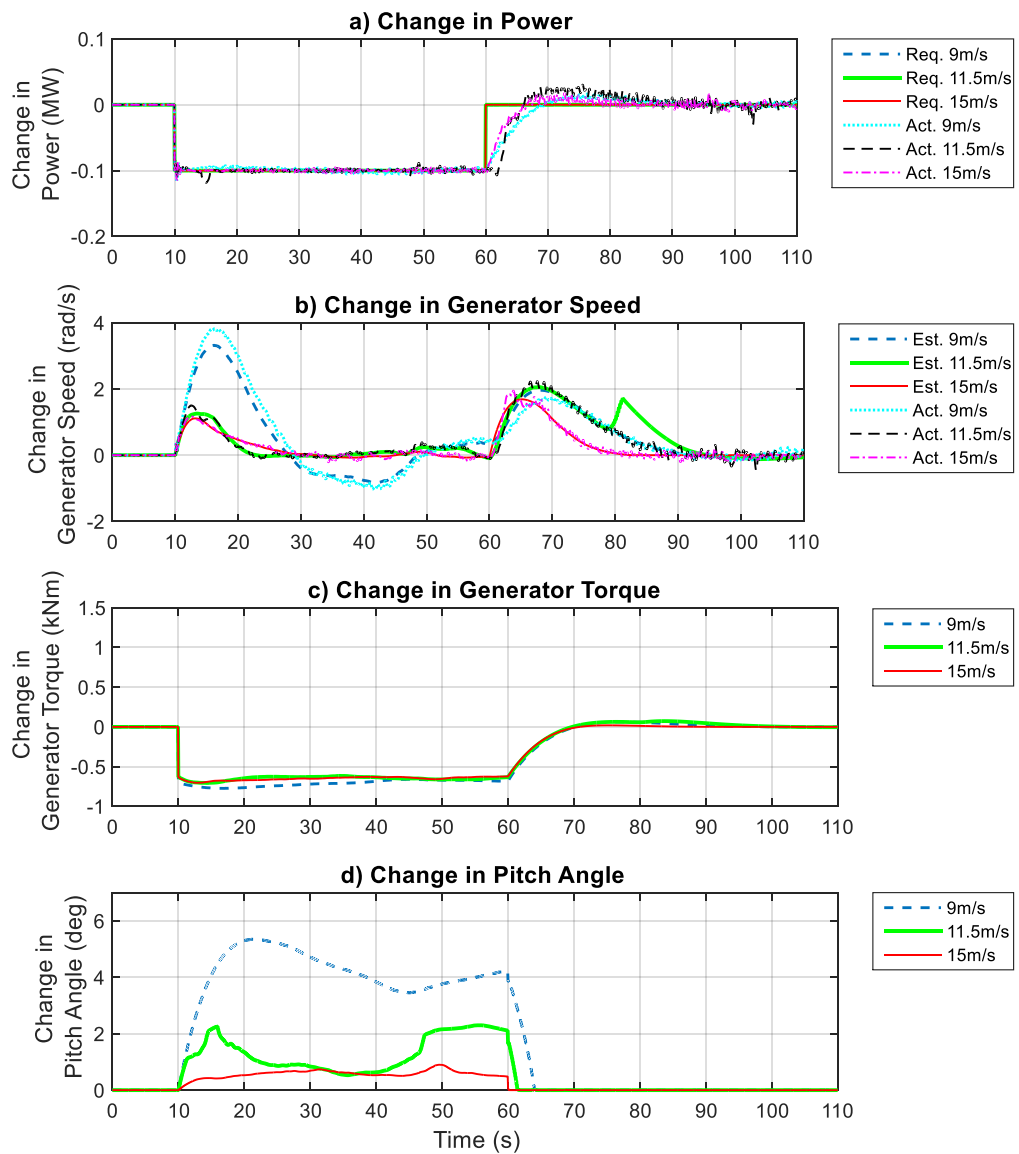


Figure 68: 1.5MW Wind Turbine with a Requested Change in Power of 100kW held for 50s (High Turbulence) – Change in Variables

Figure 69 shows the generator torque plotted against the generator speed for 3 runs both with and without the PAC enabled. This graph shows clearly that the effect of the PAC is equivalent to redefining the operational strategy such that it produces a lower power for a given wind speed. Note that a 10m/s wind speed was used rather than the 11.5m/s wind speed to give a better range of operating points. The time period covered is from the moment the PAC is switched on until the moment it is switched off. The wind turbine appears to be following an offset operational curve that gives a lower power output when the PAC is used. This shows that the PAC is

effectively altering the wind turbine’s strategy in a manner that is similar to changing the set point of the full envelope controller. It is also clear that, after the initial transient as the PAC is turned on, the generator speed is controlled equally as well with the PAC switched on as it is when the PAC is switched off.

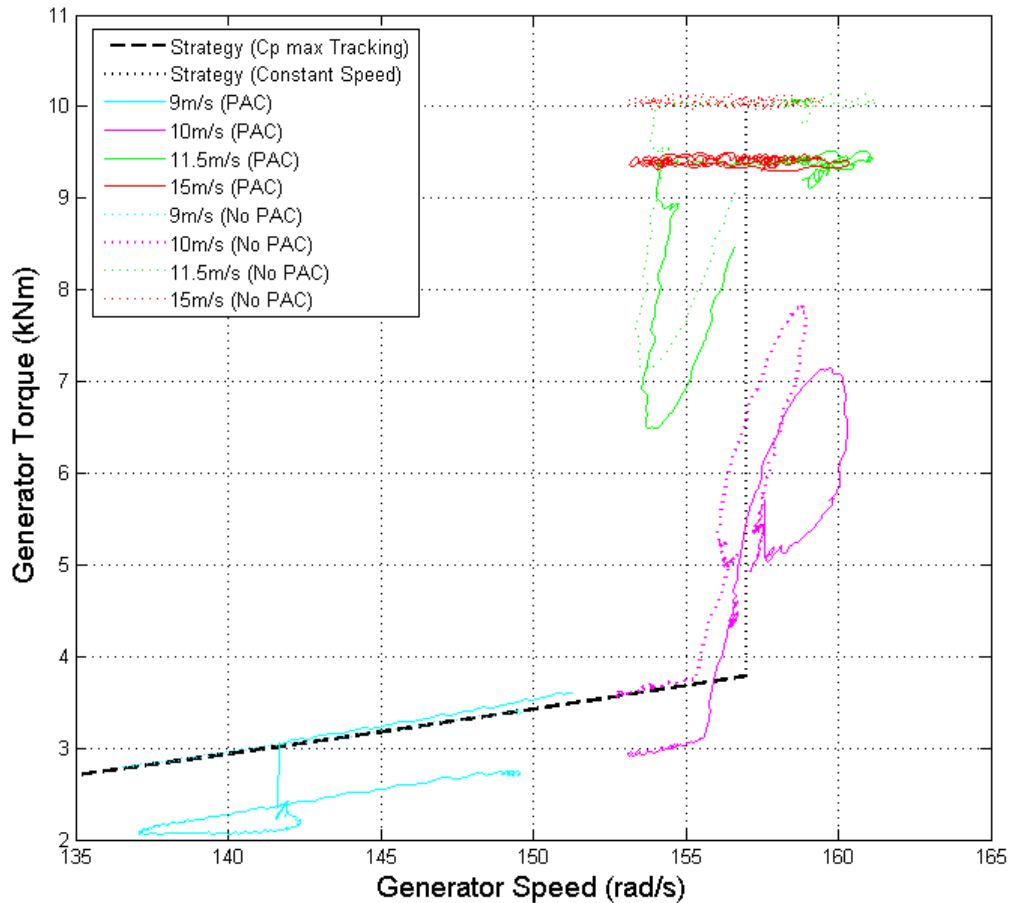


Figure 69: Torque-Speed Curve for a 1.5MW Wind Turbine Operating With and Without the PAC

4.7.2.8 Variable Change in Power – Variable Wind Speed – Higher Turbulence

The 5MW machine is used to simulate a requested change in power output as outlined in Figure 50, in higher turbulence (20%) variable wind speeds of mean values 9m/s, 11.5m/s, and 15m/s. The results are presented in Figure 70, Figure 71, Figure 72, and Figure 73

Figure 71 shows the actual change in power in graph *a*). It is clear that although the signal is slightly noisier for the 9m/s (below-rated) and 11.5m/s (around rated) simulations the actual change in power is still very accurate, with only small deviations occurring.

Chapter 4: Development of the Power Adjusting Control

Because of the higher turbulence, the below-rated simulation (9m/s) occasionally switches into above-rated operation. This is particularly notable at approximately 220 seconds, where the change in generator speed (graph *b*) in Figure 71) is still negative after the previous positive change in power. Because the turbine moves to above-rated operation, the PAC is able to demand a negative pitch angle, keeping the total pitch angle (graph *d*) in Figure 70) at zero, to help drive the change in generator speed back towards zero.

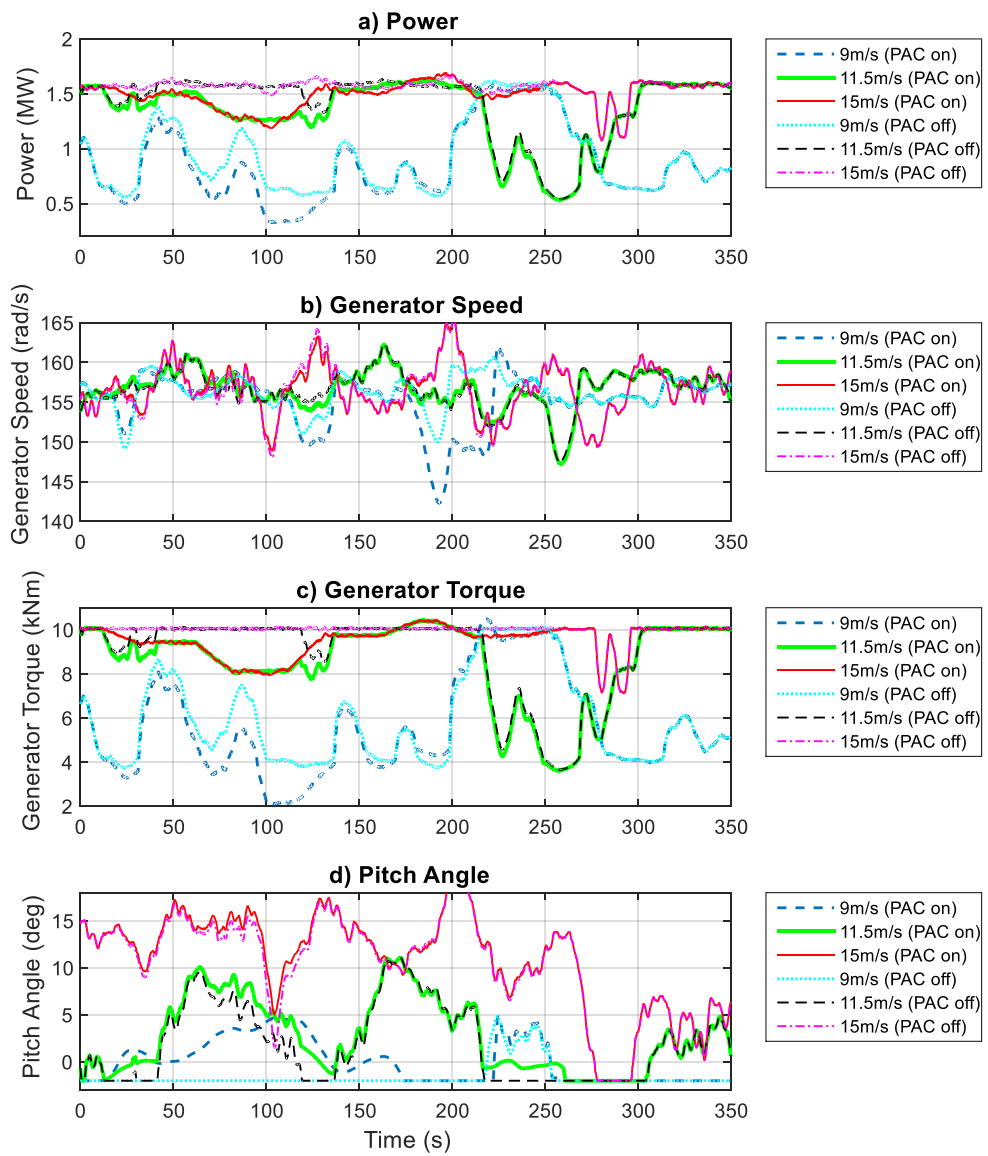


Figure 70: 1.5MW Wind Turbine with a Variable Requested Change in Power

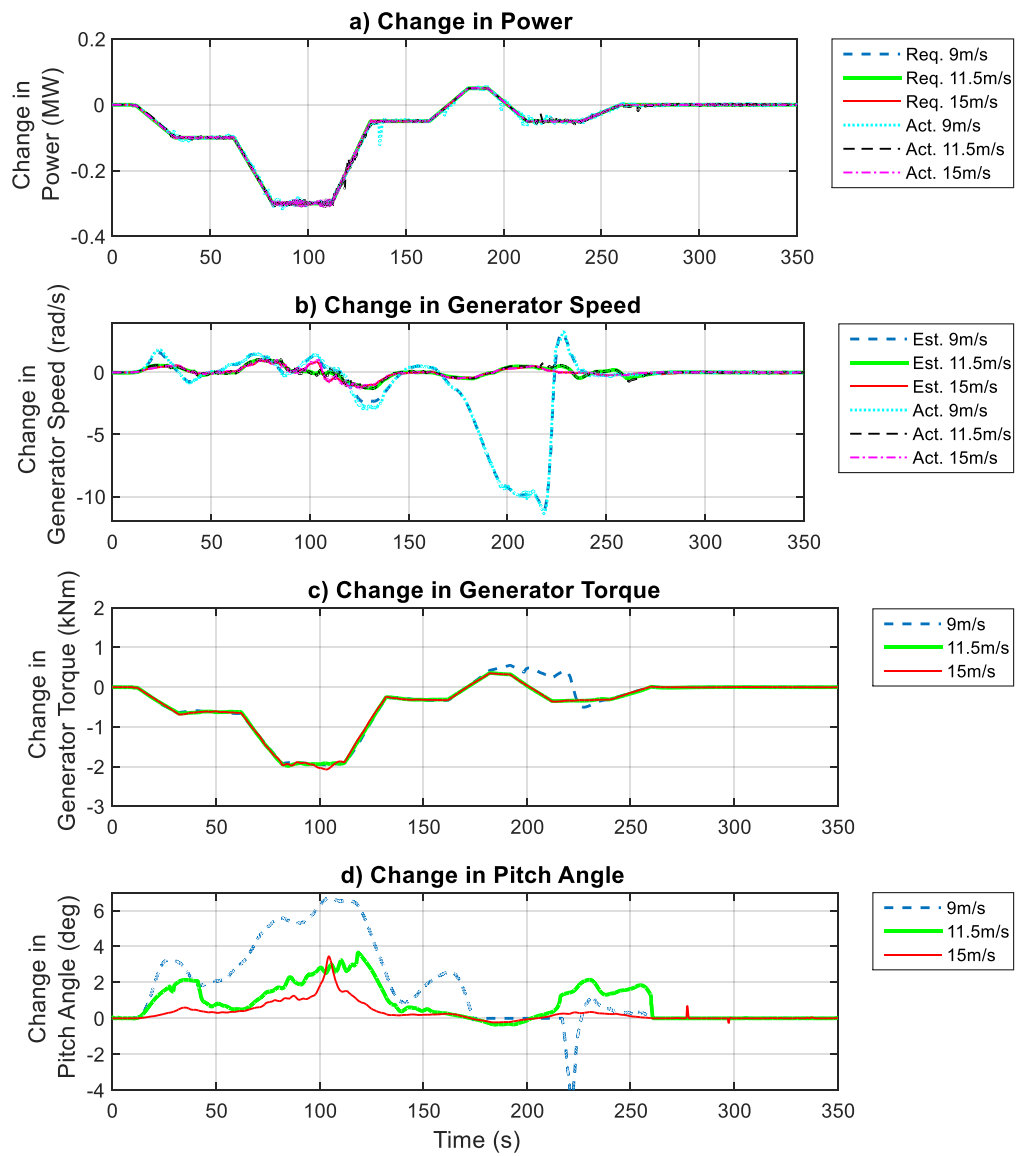


Figure 71: 1.5MW Wind Turbine with a Variable Requested Change in Power – Change in Variables

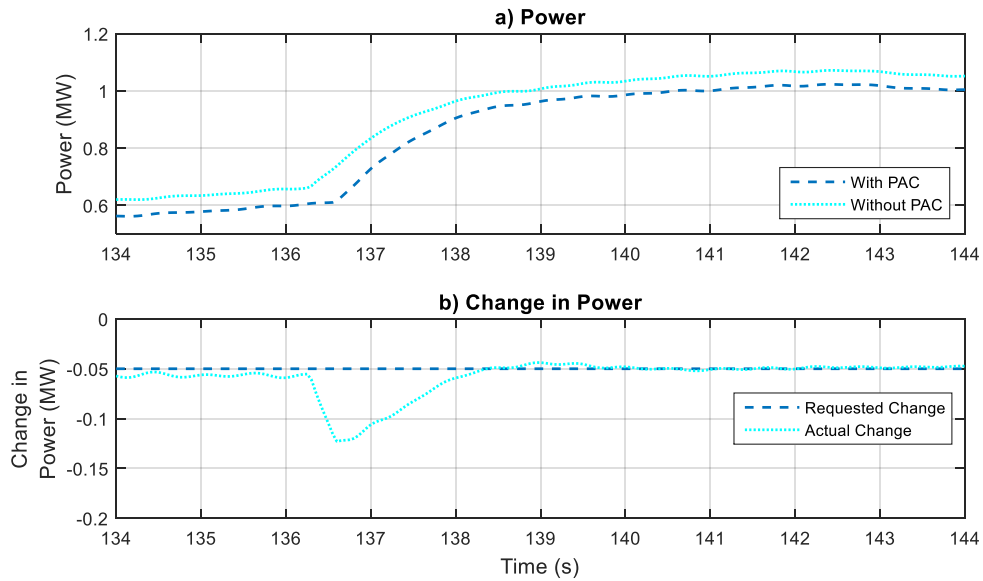


Figure 72: Magnified view of the Power Output and the Change in Power Output for the 9m/s Simulation

Figure 72 shows a magnified view of the power (graph *a*) and change in power (graph *b*) for the 9m/s simulation between 134 seconds and 144 seconds. This shows a situation where a small discrepancy in the change in power occurs. In this case it is due to the full envelope controller switching between the C_{pmax} tracking region and the second constant speed region. Because the generator speeds of the two simulations are slightly different, the full envelope controller switches between the two operating regions slightly later in the simulation with the PAC, leading to the discrepancy in the change in power. It is clear from the first graph however that this is purely a result of subtracting one simulation from another, that is to say that there is no oscillation in the total power output.

The actual and estimated effective wind speeds are shown in Figure 73, which shows that despite the increased turbulence, the estimate of the wind speed is still accurate, albeit with a small increase in noise in the signal.

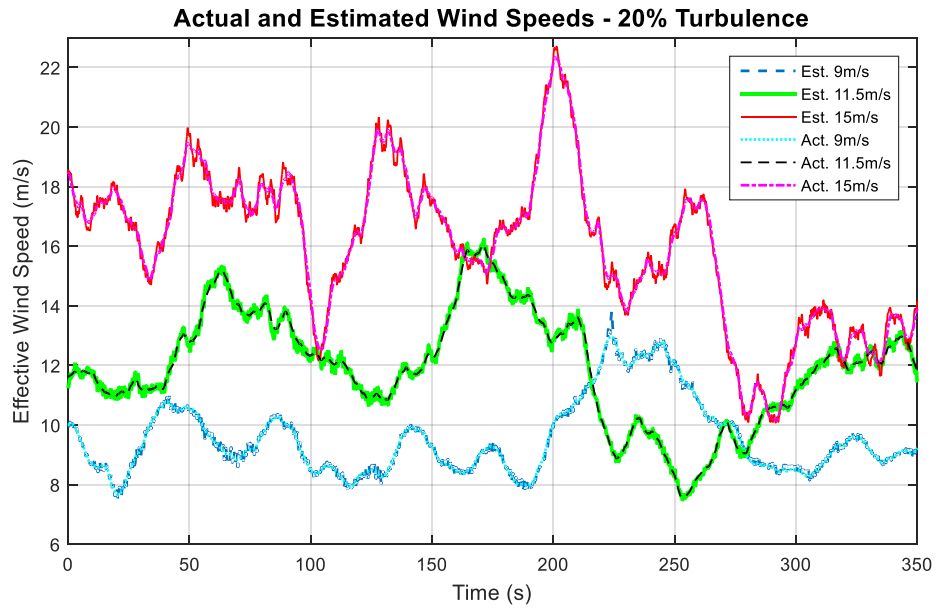


Figure 73: Estimated and Actual Effective Wind Speed - 20% Turbulence

Figure 74, Figure 75 and Figure 76 show the power spectral density of the generator speed signal for each of the simulations conducted. There are no additional peaks, nor increases/decreases in existing peaks in the power spectral density beyond very minor changes close to rated wind speed. These minor changes are due to the slight differences in timing of the switch between each operational mode by the full envelope controller, as discussed previously. This shows that the PAC is not impacting on the operation of the full envelope controller.

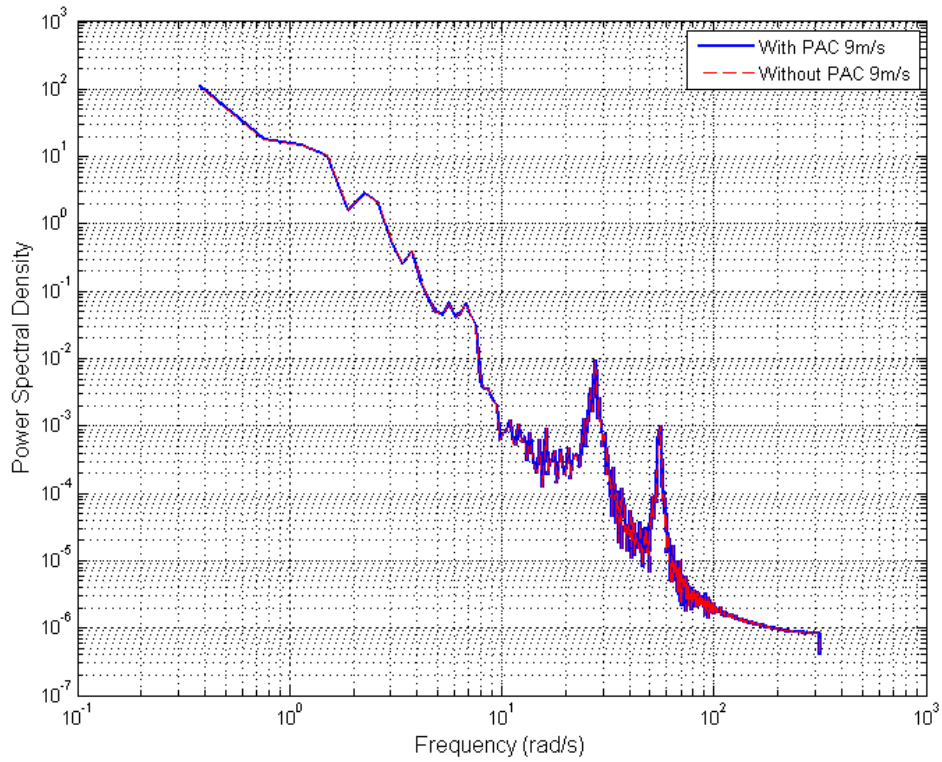


Figure 74: Power Spectral Density of Generator Speed Signal With and Without the PAC for a Variable Change in Power Output from the 1.5MW Wind Turbine at a Wind Speed of 9m/s

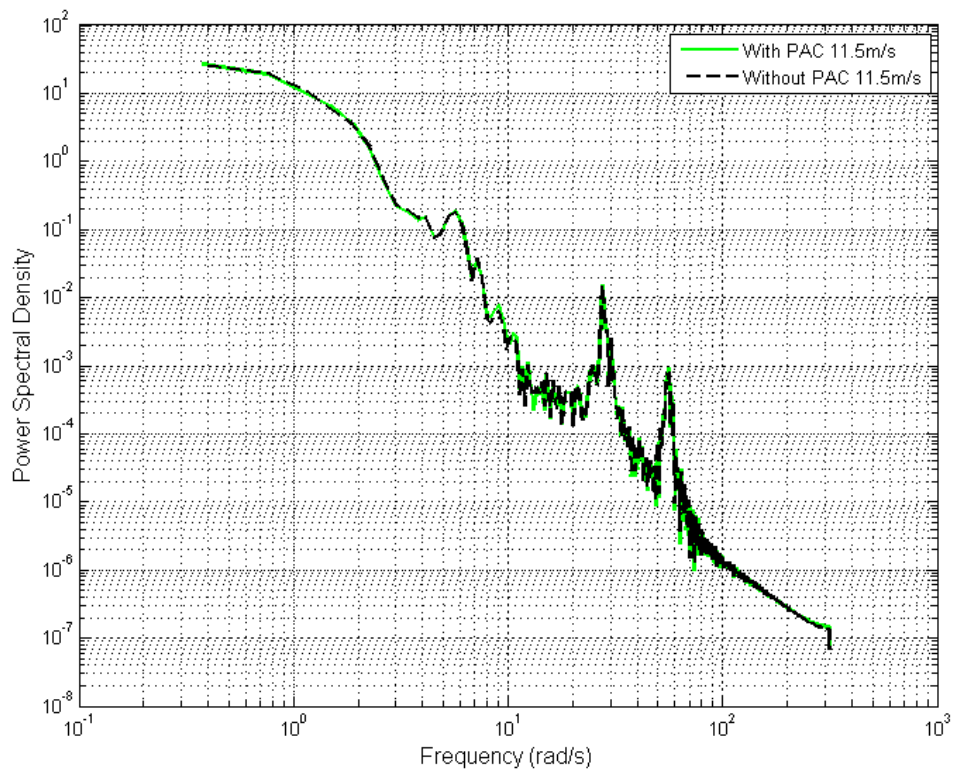


Figure 75: Power Spectral Density of Generator Speed Signal With and Without the PAC for a Variable Change in Power Output from the 1.5MW Wind Turbine at a Wind Speed of 11.5m/s

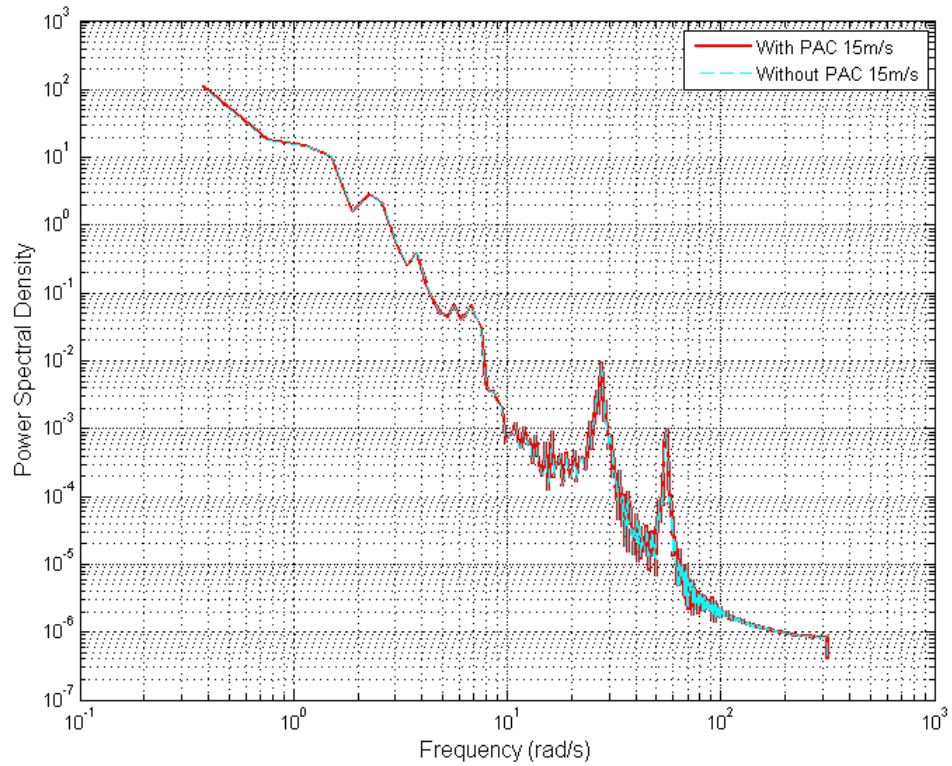


Figure 76: Power Spectral Density of Generator Speed Signal With and Without the PAC for a Variable Change in Power Output from the 1.5MW Wind Turbine at a Wind Speed of 18m/s

4.7.2.9 Varying the Speed of Recovery

The simulations shown in section 4.7.2.1 to section 4.7.2.8 use a quick recovery as defined in section 4.5.3. In Figure 77, simulations are presented at above and below rated wind speeds with varying speeds of recovery.

With the faster recovery, the wind turbine returns to normal power output within 10 seconds. The slower recovery takes between 30 and 40 seconds. Neither option causes large changes in the generator speed.

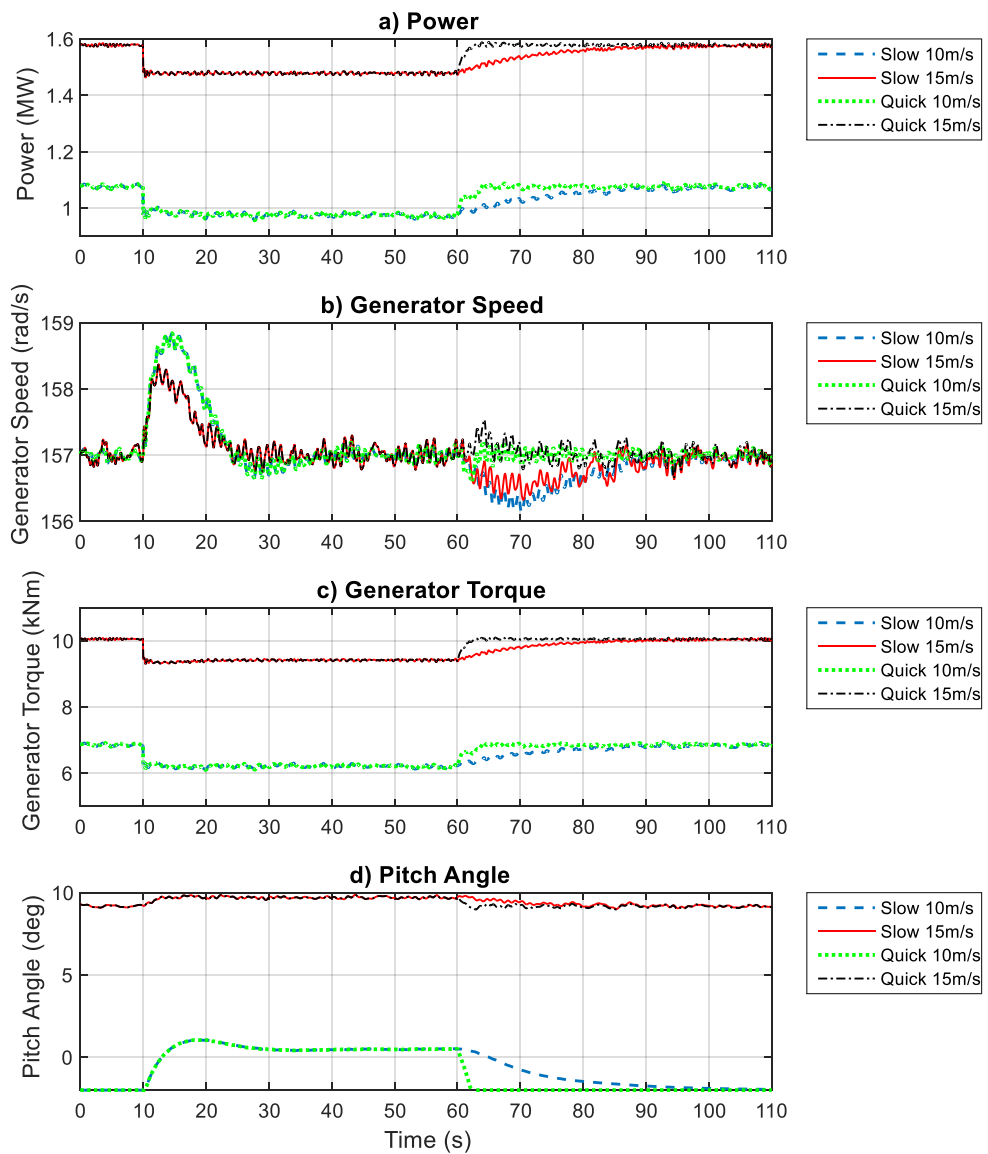


Figure 77: 1.5MW Wind Turbine with a Requested Change in Power of -100kW held for 50s Followed by a Slow or Quick Recovery

4.7.3 Bladed Simulations

The PAC is converted into C code for use in GL Bladed – a full aero-elastic wind turbine simulation package. The same full envelope controllers are used along with models of the same wind turbines – a 5MW machine and a 1.5MW machine. The conversion of the controller from the continuous form used in Simulink to the discrete form required for GL Bladed is discussed in detail in chapter 6.

4.7.3.1 Constant Speed Reduction in Power

The PAC is tested using the 1.5MW machine, with a demanded decrease in power of 100kW in above-rated (15m/s) and below-rated (10m/s) wind conditions. The results are presented in Figure 78 and Figure 79.

Whilst the results for the simulation at 15m/s are comparable with the control model simulations, the results at 10m/s show far poorer performance in attaining the requested change in power (see graph *a*) of both Figure 78 and Figure 79). A large drop in the power output below the desired value is seen between 10 and 20 seconds. The drop in power output corresponds with the pitch action (graph *d*) in each figure), with a similar oscillation in the power output when the PAC is switched off. In the 15m/s simulations this feature is not observed. Other than this, the simulation results are comparable with the control model results.

In the control model simulations there are small errors in the actual torque caused by the flexibility of the tower and blades, which is not accounted for in the simple model used within the PAC itself. Simulations are therefore conducted to ascertain if this is the same cause for the larger drops in power output seen in the full aero-elastic simulations.

Chapter 4: Development of the Power Adjusting Control

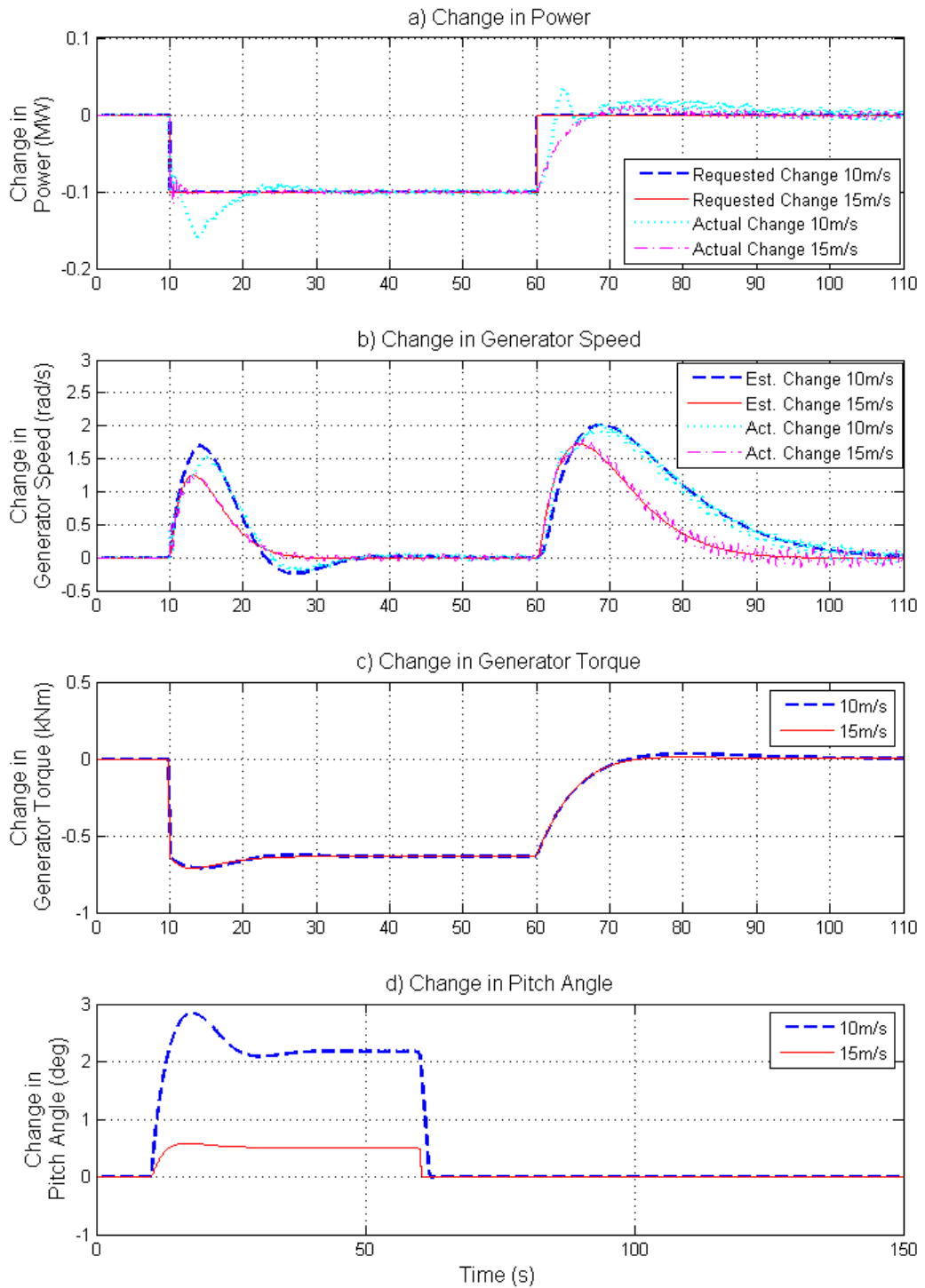


Figure 78: 1.5MW Turbine with a Requested Change in Power of -100kW held for 50s – Bladed Simulation

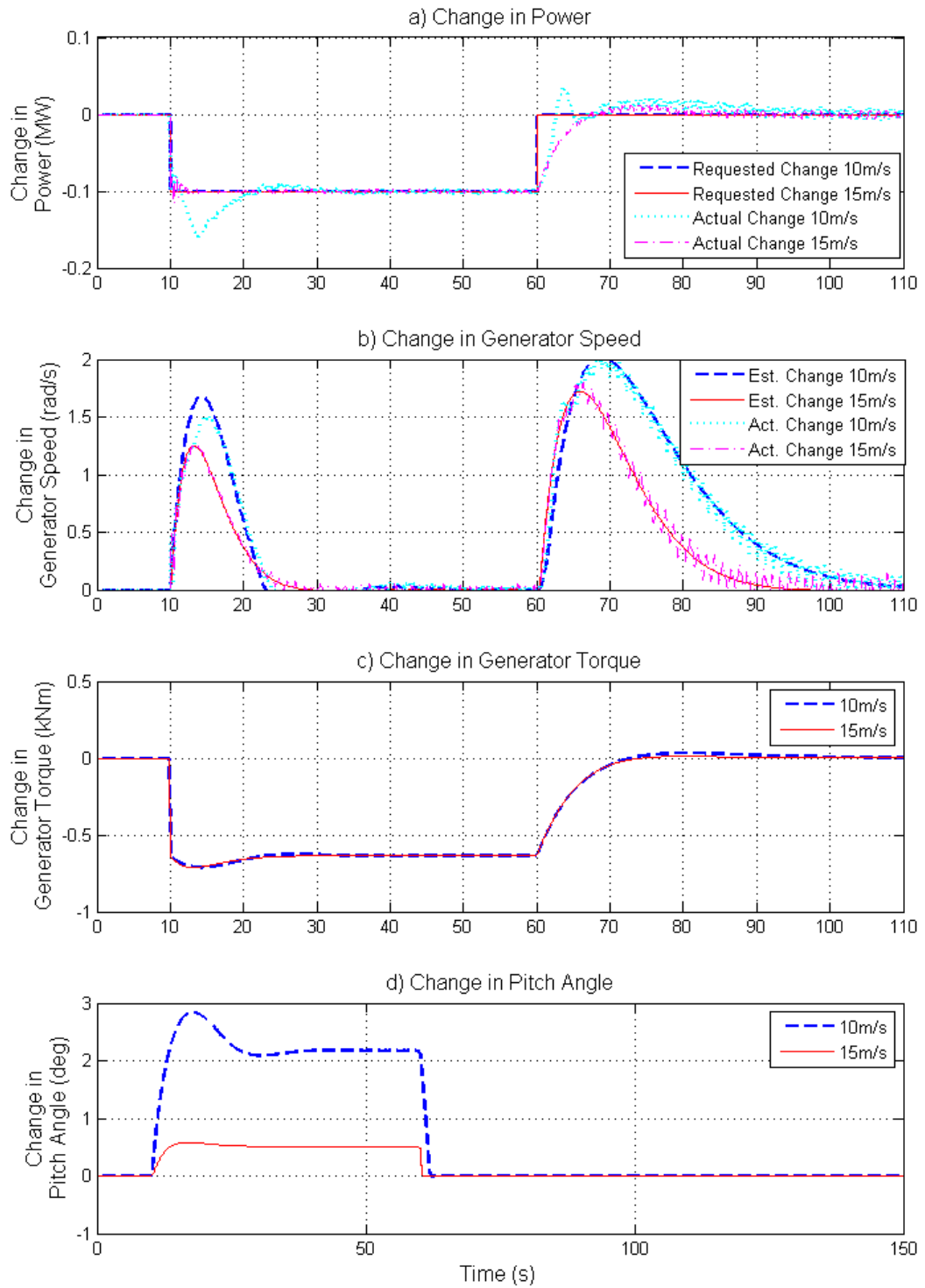


Figure 79: 1.5MW Turbine with a Requested Change in Power of -100kW held for 50s – Bladed Simulation – Change in Variables

4.7.3.2 Constant Speed Reduction in Power – Stiff Tower and Blades

The same simulation as that conducted in section 4.7.3.1 at 10m/s is repeated with the tower and blade modes turned off, resulting in a completely stiff tower and

completely stiff blades. The two sets of results are then compared in Figure 80 and Figure 81.

The error in the actual change in power compared with the requested change in power is actually increased in the simulation with the stiffened blades. This indicates that the dynamics resulting in the error are not a direct result of blade and tower motion in the full aero-elastic simulations; a different issue is causing the error.

Because the same error is not present in the control model, it can be deduced that it must be caused by dynamics that are present in the full aero-elastic model but not in the control model. It is also clear that the error is only noticeable when there is a high pitch rate. In addition, the time constant is of the order of 3 to 4 seconds, too high to be another structural mode.

The best candidate for the cause of the error is therefore induction lag. Induction lag is an aerodynamic effect whereby there is a lag between altering the aerodynamic conditions of an aerofoil and the change in resultant torque and thrust. The control model does not simulate induction lag, it would be at its zenith in high pitch rates, and the time constant is of the same order.

It is apparent therefore, that to remove the large error observed in the full aero-elastic models the simple model used in the PAC for estimation of the change in aerodynamic torque must be improved to accommodate the effects of induction lag.

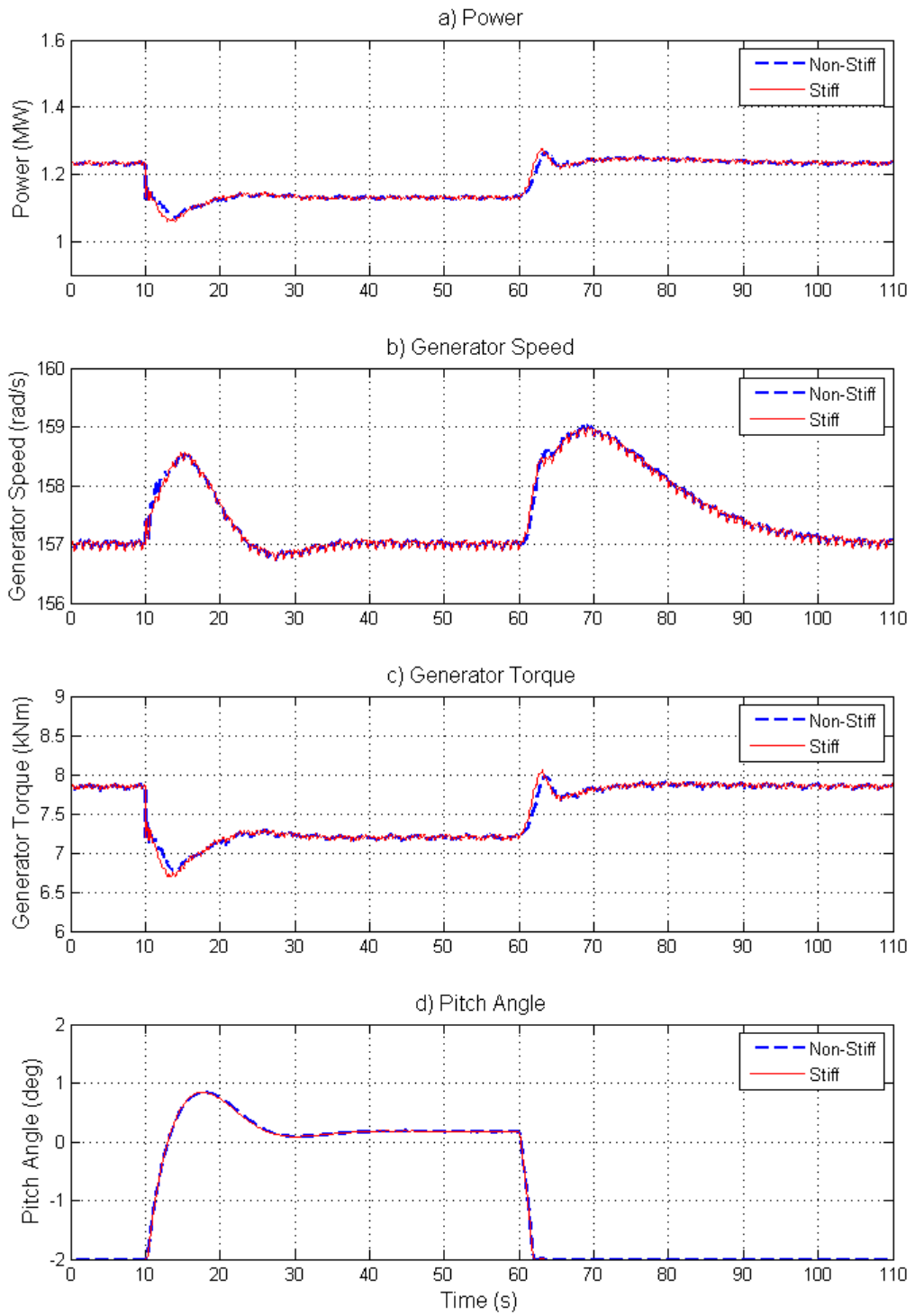


Figure 80: 1.5MW Turbine with a Requested Change in Power of -100kW held for 50s with Non-Stiff Tower and Blades and with Stiff Tower and Blades – Bladed Simulation

Chapter 4: Development of the Power Adjusting Control

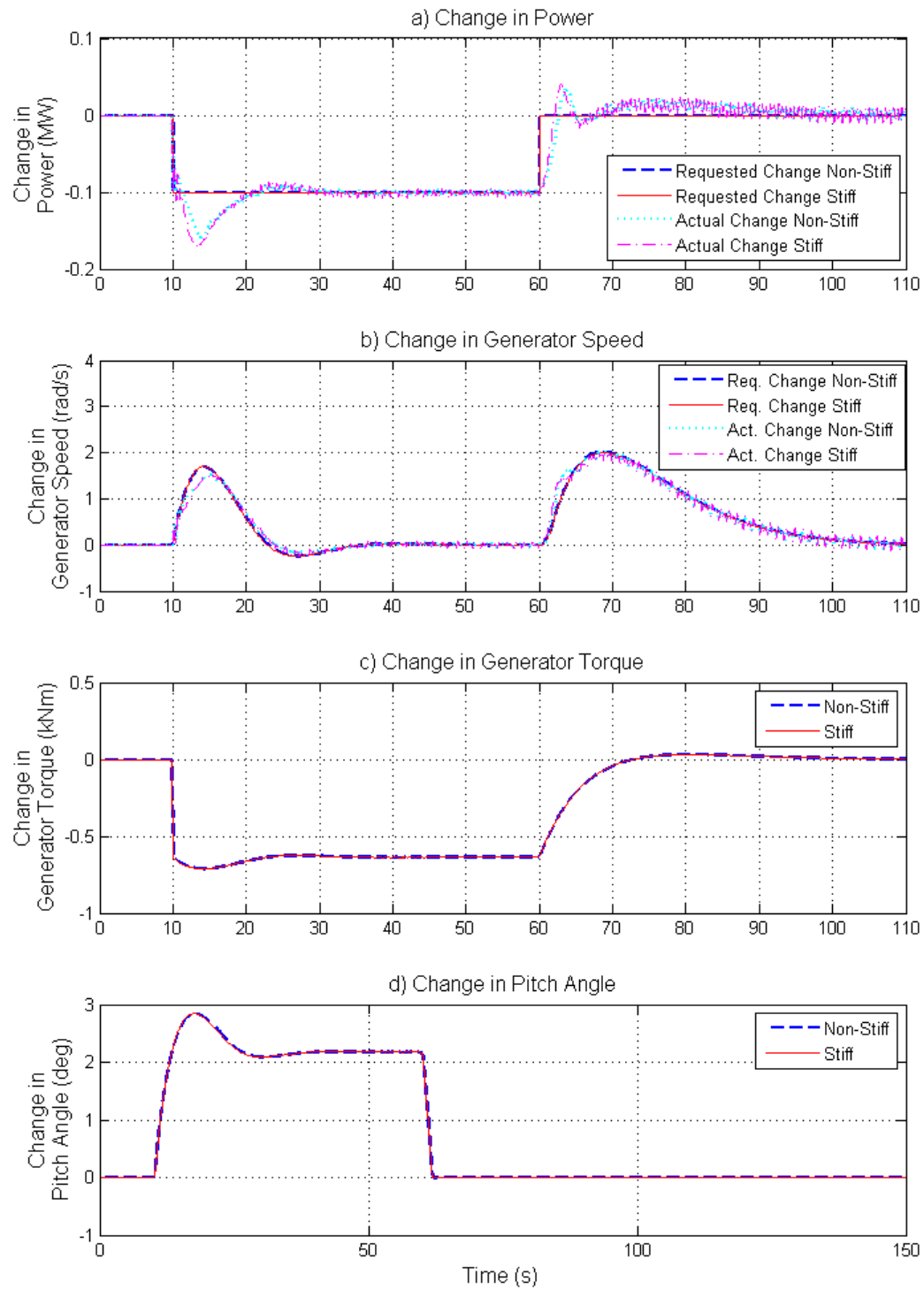


Figure 81: 1.5MW Turbine with a Requested Change in Power of -100kW held for 50s with Non-Stiff Tower and Blades and with Stiff Tower and Blades – Bladed Simulation – Change in Variables

4.8 Concluding Remarks

In this chapter, the “Power Adjusting Controller” (PAC) is presented, which allows an operator to vary the power output of a wind turbine by an increment ΔP . At the end of chapter 3, a set of requirements for the design of the PAC were specified.

The requirements are:

- 1- The augmentation must be applicable to variable speed, pitch regulated machines without alteration to the turbine’s full envelope controller.
- 2- No knowledge of the design of the wind turbine’s full envelope controller must be required.
- 3- The augmentation must allow the operator to vary the power output of the wind turbine by an increment ΔP
- 4- The augmentation must allow the power output of the wind turbine to be altered quickly and accurately.
- 5- The augmentation must be capable of switching smoothly between modes of operation.
- 6- The performance of the full envelope controller must not be compromised through the addition of the augmentation, including taking into account any gain scheduling.

The PAC development and testing shows that the PAC is capable of meeting all of these requirements. Requirements 1, 2, and 3 are satisfied during the design process. Requirement 4 is demonstrated in the testing of the PAC in section 4.7. Requirement 5 is satisfied as the PAC does not have separate modes of operation; the PAC operates the same way in all conditions. Finally, the controller is predominantly feed forward in its design and so no strong feedback loops around the full envelope controller are introduced. In addition, the increment to the pitch demand takes into account gain scheduling. As such, requirement 6 is satisfied.

When tested, the PAC shows excellent performance when used on the Simulink model of both the 1.5MW and 5MW wind turbines. When operated on the Bladed model of the same turbines however, there is a large degradation in the controller

Chapter 4: Development of the Power Adjusting Control

performance. Analysis of this issue results in a hypothesis that the degradation in performance is due to a lack of modelling of the induction lag caused by dynamic inflow effects. The hypothesis is investigated in Chapter 5.

Chapter 5:

Development of an Improved Wind Speed Estimator

CONVENTIONAL WIND TURBINE control does not use a measurement of the wind speed as an input to the controller. The controller instead acts on the error between the rotational speed of the generator and a given set point. The changes in the wind speed are then treated as a disturbance and the control system is designed as a disturbance rejection problem. It is often useful however, to have some knowledge of the wind speed experienced by a wind turbine, and, for this purpose, most wind turbines are fitted with an anemometer behind the rotor.

Typically anemometer measurements are used to measure trends in the wind speed over long periods of time. Anemometers are not reliable for wind speed estimation for control purposes for a number of reasons. Firstly, they are prone to mechanical problems that can result in either an error in their measurement or their complete inoperability. Especially for turbines operating far offshore, reliability is a concern as access to the turbine to fix the anemometer is limited. Secondly, the anemometer is typically positioned behind the rotor of the turbine, in the turbine's wake, and so the operation of the turbine affects the measurements made by the anemometer. Lastly, anemometers measure a point wind speed in a single position. The wind speed may vary considerably across the rotor disc and it cannot be guaranteed that

the wind speed measured by the anemometer is indicative of the average wind speed across the disc.

As discussed in the previous chapter, the PAC requires an estimate of the wind speed and it is therefore essential that a more accurate and reliable technique for determining the wind speed be developed. The initial method described and applied in Chapter 4 does not take into account dynamic inflow effects, reducing the accuracy of the change in power output by the PAC, and so a new technique, which accounts for these dynamics, is required. This chapter concerns the development of such a technique, which uses the wind turbine's own operational information to deliver an accurate estimate of the effective wind speed across the rotor including the incorporation of unsteady aerodynamic effects, specifically, induction lag. The new wind speed estimator is then incorporated into the PAC.

A method for modelling the dynamic inflow effects using a lead lag term has previously been explored in [74] with a similar method also used in [75]. This method is purely empirical however, both in regard to the variables used and the formulation. Additionally, data from [74] and [75] are all for fixed speed machines, and would require significant adaptation for application to a variable speed application. Furthermore, this model of dynamic inflow is applied to aerodynamic torque and so does not differentiate between changes in torque due to changes in pitch angle, rotor speed or wind speed. An alternative approach for multiple stream tube BEM is implemented in Bladed but its interpretation is not clear, particularly with regard to the choice of wind speed input. To clarify matters, a similar dynamic inflow model for the single stream tube case is independently derived.

5.1 BEM Reformulated Locally to the Rotor Disc

In this Section, BEM is reformulated in a form local to the rotor disc; that is, in terms of wind speeds at the rotor disc only without recourse to those far upstream and far down stream. It is based on the single stream tube aerodynamic coefficient model for standard BEM as discussed in Section 2.11. In this model, a uniform axial wind speed, V_R , over the rotor disc and uniform angular velocity, ω_R , are assumed. These

are determined as functions of V_∞ by solving (2.60) and (2.61) with the aerodynamic thrust coefficient, C_T , subsequently determined using (2.59). Note, that, with fixed pitch angle, there is a monotonic relationship between V_R and V_∞ because of the uniformity of both over the rotor disc.

Blade element theory is inherently local to the rotor disc (see Section 2.6), and is implicitly incorporated into BEM. Hence, as V_R and V_∞ are monotonically related, an equivalent reformulation of the single stream tube aerodynamic BEM model local to the rotor disc is possible. In the standard formulation, the thrust is given by,

$$F_T = \frac{1}{2} \rho A_R V_\infty^2 C_T(\lambda_\infty, \beta) \quad (5.1)$$

where,

$$\lambda_\infty = \frac{\Omega R}{V_\infty} \quad (5.2)$$

Equivalently, reformulated locally to the rotor disc, it is given by,

$$F_T = \frac{1}{2} \rho A_R V_R^2 \hat{C}_T(\lambda_R, \beta) \quad (5.3)$$

where,

$$\lambda_\infty = \frac{\Omega R}{V_\infty} \quad (5.4)$$

Of course, similarly to (2.49), \hat{C}_T can be determined directly from the blade lift and drag coefficients by,

$$\hat{C}_T(\lambda_R, \beta) = \frac{B_N}{\pi R^2 V_\infty^2} \int_0^\infty c_l W ((\Omega r_R + \omega_R r_R) C_L + V_R C_D) dr_R \quad (5.5)$$

However, when only C_T is available, perhaps obtained from an aero-elastic code such as GL Bladed, \hat{C}_T can be determined directly from C_T .

Let,

$$V_R = (1 - a_s) V_\infty \quad (5.6)$$

then, from (5.2) and (5.4),

$$\lambda_R = \frac{\lambda_\infty}{1 - a_s} \quad (5.7)$$

and, from (2.57), (5.6) and (5.7),

$$C_T((1 - a_s)\lambda_R, \beta) = 4a_s(1 - a_s) \quad (5.8)$$

Solving (5.8), a_s can be determined as a function of β and λ_R . Comparing (5.3) to (5.1) and using (5.8),

$$\begin{aligned} \hat{C}_T(\lambda_R, \beta) &= \left(\frac{V_\infty}{V_R}\right)^2 C_T\left(\frac{\lambda_R V_R}{V_\infty}, \beta\right) \\ &= (1 - a_s(\beta, \lambda_R))^{-2} C_T((1 - a_s(\beta, \lambda_R))\lambda_R, \beta) \\ &= \frac{4a_s(\beta, \lambda_R)}{1 - a_s(\beta, \lambda_R)} \end{aligned} \quad (5.9)$$

Similarly, the aerodynamic torque Q , and power P , can also be defined in terms of coefficients, \hat{C}_Q and \hat{C}_P , respectively, and the conditions local to the rotor.

Hence, it is possible for the usual aerodynamic relationships for thrust, torque, and power to be rewritten in terms of the local conditions at the rotor such that,

$$\hat{C}_T(\lambda_R, \beta) = (1 - a_s(\beta, \lambda_R))^{-2} C_T(\lambda_R(1 - a_s(\beta, \lambda_R)), \beta) \quad (5.10)$$

$$\hat{C}_Q(\lambda_R, \beta) = (1 - a_s(\beta, \lambda_R))^{-2} C_Q(\lambda_R(1 - a_s(\beta, \lambda_R)), \beta) \quad (5.11)$$

$$\hat{C}_P(\lambda_R, \beta) = (1 - a_s(\beta, \lambda_R))^{-3} C_P(\lambda_R(1 - a_s(\beta, \lambda_R)), \beta) \quad (5.12)$$

and,

$$F_T = \frac{\rho}{2} AV_R^2 \hat{C}_T(\lambda_R, \beta) \quad (5.13)$$

$$Q = \frac{\rho}{2} AV_R^2 \hat{C}_Q(\lambda_R, \beta) \quad (5.14)$$

$$P = \frac{\rho}{2} AV_R^3 \hat{C}_P(\lambda_R, \beta) \quad (5.15)$$

Using (5.10), (5.11), (5.12), and $a_s(\lambda_R, \beta)$ (the solution to (5.8)), tables in β and λ_∞ for C_T , C_Q , and C_P can be converted to tables in β and λ_R for \hat{C}_T , \hat{C}_Q , and \hat{C}_P , when equations (5.13), (5.14), and (5.15) can be applied in the normal manner.

The aerodynamic coefficient models, (5.4), (5.5) and (5.6), derived above, use only the conditions at the rotor, specifically the axial wind speed at the rotor, V_R ; the upstream or downstream wind speeds are not required. However, V_∞ could be derived from F_T using (5.4), (5.9) and (5.6). Since, within BEM, the upstream and downstream flow is in equilibrium, a physical interpretation of V_∞ in the context of the model local to the disc is that it is the wind speed at the position of the rotor in its absence. For clarity, V_A is used to denote V_∞ when it has that interpretation. Similarly, whilst $\rho A_R V_R^2$ is the linear momentum flow rate of the stream tube at the rotor disc, i.e. the linear momentum of the section of the stream tube passing through the rotor disc per unit time, $\rho A_R V_R V_A$ is the linear momentum flow rate at the position of the rotor in its absence (as $\rho A_R V_R$ is the mass flow rate of the fluid, the value of which is the same both with and without the rotor) and $\rho A_R (V_A - V_R) V_R$ is the difference, between the rotor being absent or present, in the momentum flow rate at the position of the rotor. The section of stream tube involved can be made local to the rotor by choosing it to be short or equivalently the time interval to be small. This rate of change, between the rotor being present or absent, in linear momentum at the rotor is, as before, caused by the rotor.

5.2 Modelling of Dynamic Inflow Effects

In reality, there is a lag between the changes to the blade loading and the effect on the induced flow field. This lag can impact significantly on the aerodynamic torque and thrust. It is identified in chapter 4 as the cause of the inaccuracy in the change in power output when using the PAC. A model for the induction lag is developed in this Section for incorporation into the PAC. Because the induction lag is a dynamic phenomenon local to the rotor disc, its model is based on the single stream tube BEM model, reformulated locally to the rotor in section 5.1.

When the stream tube is not in steady state (i.e. when the axial wind speed through the rotor is not constant) there is an additional contribution, between the rotor being present or absent, to the rate of change in linear momentum at the position of the rotor, related to the rate of change in axial wind speed.

The section of fluid contributing to the change of linear momentum in this additional contribution extends upstream and downstream from the rotor. Unlike the discussion of the local interpretation of $\rho A_R (V_A - V_R) V_R$ in section 5.1, the section of stream tube involved cannot be made local to the rotor by choosing it to be short. Consequently, the wind speed in the absence of the rotor is not simply V_A but varies over the section of stream tube. However, due to the averaging of the wind speed over the rotor disc, the effective wind speeds in the vicinity of the rotor change relatively slowly, with a time constant as high as 20 seconds when, as in this thesis, the wind turbines are large. Hence, the variation in V_A over this section of stream tube can be ignored; that is, the non-strictly locality to the rotor can be ignored. The total contribution to the rate of change, between the rotor being present or absent, in linear momentum, due to the rate of change of the axial wind speed at the rotor is then related to \dot{V}_R . Specifically, it is $m_A \dot{V}_R$ where m_A , from potential theory [74], is approximately,

$$m_A = \frac{8}{3} \rho R^3 \quad (5.16)$$

Attributing half of this contribution to the rate of change in momentum to having taken place by the time the fluid reaches the position of the rotor, the additional contribution to the rate of change, between the rotor being present or absent, in linear momentum at the position of the rotor is $4/3 \rho R^3 \dot{V}_R$. Hence, the total rate of change, between the rotor being present or absent, in linear momentum at the position of the rotor is,

$$\rho A_R (V_A - V_R) V_R - \frac{4}{3} \rho R^3 \dot{V}_R \quad (5.17)$$

In chapter 2, an interpretation of standard BEM is discussed which is based on the assumption that the rate of change of momentum in the upstream flow field is due to half the thrust applied by the rotor; that is,

$$\rho A_R (V_A - V_R) V_R = \frac{1}{2} F_T = \frac{1}{4} \rho A_R V_R^2 \hat{C}_T(\lambda_R, \beta) \quad (5.18)$$

In the context of the reformulation of BEM locally to the rotor discussed in section 5.1, the above underlying assumption for standard BEM becomes the assumption that the rate of change in linear momentum, between the rotor being present or absent, is due to half the thrust applied by the rotor to the stream tube. Extending this assumption to the unsteady state situation,

$$\rho A_R (V_A - V_R) V_R - \frac{4}{3} \rho R^3 \dot{V}_R = \frac{1}{2} F_T = \frac{1}{4} \rho A_R V_R^2 \hat{C}_T(\lambda_R, \beta) \quad (5.19)$$

that is,

$$\dot{V}_R = \frac{3\pi}{4R} (V_A - V_R) V_R - \frac{3\pi}{16R} V_R^2 \hat{C}_T(\lambda_R, \beta) \quad (5.20)$$

It is worth explaining that all the variables in (5.20) pertain to conditions at the position of the rotor, specifically V_R and V_A , the latter being interpreted as the wind speed at the position of the rotor in its absence.

Using (5.9), (5.20) becomes,

$$\frac{-\dot{V}_A}{V_A} + \frac{\dot{V}_A a}{V_A} + \dot{a} = \frac{3\pi}{4R} V_A \left(\frac{(1-a)}{(1-a_s)} \right) (a_s - a) \quad (5.21)$$

As explained, previously, the variation in V_A can be ignored. Hence,

$$\dot{a} = \frac{3\pi}{4R} V_A \left(\frac{(1-a)}{(1-a_s)} \right) (a_s - a) \quad (5.22)$$

where a_s itself is a function of a due to (5.9).

The additional assumptions used in the above formulation (that the rate of change, between the rotor being present or absent, in linear momentum is due to half the thrust applied by the rotor to the stream tube; and that half of the rate of change in linear momentum, between the rotor being present or absent, due to the rate of change of the axial wind speed at the rotor, takes place by the time the fluid reaches the position of the rotor) are straight forward extensions to the similar assumptions of standard BEM (that the rate of change of momentum in the upstream flow field is due to half the thrust applied by the rotor; and that the rate of change in stream tube

angular momentum occurring upstream is due to half of the torque applied by the blade element to the stream tube) to the non-steady state conditions.

It is useful at this stage to define the wind speed \hat{V} whereby,

$$\hat{V} = V_A \frac{(1-a)}{(1-a_s)} \quad (5.23)$$

and

$$\hat{\lambda} = \frac{\Omega R}{\hat{V}} \quad (5.24)$$

Hence,

$$V_R = (1-a)V_A = (1-a_s)\hat{V} \quad (5.25)$$

The wind speed \hat{V} can be interpreted as the steady state wind speed for which its steady state induction factor a_s has the same value as the current unsteady induction factor a .

Combining (5.25) and (5.13),

$$F_T = \frac{\rho}{2} A (1-a_s)^2 \hat{V}^2 \hat{C}_T(\lambda_R, \beta) \quad (5.26)$$

And, by (5.10),

$$\begin{aligned} F_T &= \frac{\rho}{2} A (1-a_s)^2 \hat{V}^2 (1-a_s)^{-2} C_T(\lambda_R(1-a_s), \beta) \\ &= \frac{\rho}{2} A \hat{V}^2 C_T(\hat{\lambda}, \beta) \end{aligned} \quad (5.27)$$

In this form no reformulation of the aerodynamic look up tables is required.

In the same manner, the aerodynamic coefficient models for power and torque can also be reformulated in terms of \hat{V} and $\hat{\lambda}$, using their original tables.

$$Q = \frac{\rho}{2} A \hat{V}^2 C_Q(\hat{\lambda}, \beta) \quad (5.28)$$

$$P = \frac{\rho}{2} A \hat{V}^3 C_P(\hat{\lambda}, \beta) \quad (5.29)$$

5.3 Application of the Dynamic Inflow Model to the Simulink Wind Turbine Model

The Simulink wind turbine model used in chapter 4 uses standard BEM based aerodynamic coefficient models to determine the thrust and torque at the rotor. Because the standard method assumes the equilibrium stream tube model, the effects of induction lag are not modelled.

The reformulated aerodynamic model outlined in section 5.2 is used to improve the wind turbine model and allow the dynamic inflow effects to be modelled.

5.3.1 Calculating the Steady State Induction Factor

The model is supplied with a value for the wind speed at the rotor in its absence V_A . To model the induction lag effects, a value for the induction factor for the wind turbine in its current state (a), and a value for the equivalent steady state induction factor for the turbine in its current state (a_s) are calculated.

The tip speed ratio with reference to the wind speed at the rotor in its absence is,

$$\lambda_A = \frac{\Omega R}{V_A} \quad (5.30)$$

Assuming for the moment that the induction factor a is known, the tip speed ratio with reference to the wind speed at the rotor is,

$$\lambda_R = \frac{\lambda_A}{1 - a} \quad (5.31)$$

By combining (5.7) and (5.31),

$$4a_s(1 - a_s) = C_T(\lambda_A, \beta) = C_T(\lambda_R(1 - a), \beta) \quad (5.32)$$

The look up tables utilising λ_A are equivalent to the standard look up tables utilising λ_∞ . Hence, using the standard look up table for $C_T(\lambda_\infty, \beta)$, (5.32) is solved to find a_s .

5.3.2 Calculating the Unsteady Induction Factor

Using the value of a_s calculated using (5.32), a is found by solving

$$\dot{a} = \frac{3\pi}{4R} V_A \left(\frac{(1-a)}{(1-a_s)} \right) (a_s - a) \quad (5.33)$$

The value of a is fed back to be used in (5.32). This does not cause an algebraic loop due to the integrator used to solve (5.33).

5.3.3 Calculating the Aerodynamic Torque

The values of a , and a_s are used to calculate estimates of the wind speed, \hat{V} , that would result in a steady state induction factor equal to the unsteady induction factor.

$$\hat{V} = V_A \frac{1-a}{1-a_s} \quad (5.34)$$

The corresponding tip speed ratio is,

$$\hat{\lambda} = \frac{\Omega R}{\hat{V}} \quad (5.35)$$

The rotor torque is,

$$Q = \frac{\rho}{2} A R^3 \Omega^2 C_Q(\hat{\lambda}, \beta) / \hat{\lambda} \quad (5.36)$$

and the thrust is,

$$T = \frac{\rho}{2} A \hat{V}^2 C_T(\hat{\lambda}, \beta) \quad (5.37)$$

5.3.4 Demonstration of the implementation of Dynamic inflow to the Simulink Model

The model for dynamic inflow discussed in section 5.3.1 to section 5.3.3 is applied to the Simulink model used in chapter 4. The wind turbine full envelope controller and PAC are as presented in chapter 4. This Simulink model is used to simulate a 1.5MW machine, with a demanded decrease in power of 100kW in below-rated (10m/s) wind conditions; the same below-rated simulation as that presented in section 4.7.3 using the Bladed model. The results are compared in Figure 82 and Figure 83.

The total power output in each simulation is different due to differences between Bladed and the Simulink model in the modelling of the viscous damping of the drive train resulting in differences in the losses calculated. The effect on the power output of the induction lag is best observed in graph (a) of Figure 83. The size and shape of the deviation from the requested change in power is very similar. It can also be observed that the error in the estimated change in generator speed is similar, as are all the other variables.

The results presented in Figure 82 and Figure 83 show that the inaccuracy in the change in power produced by the PAC caused by the introduction of dynamic inflow effects to the turbine Simulink model, has similar characteristics to the inaccuracy in the change in power produced by the PAC when used in Bladed. This confirms that the inaccuracy in the change in power produced by the PAC is due to dynamic inflow effects.

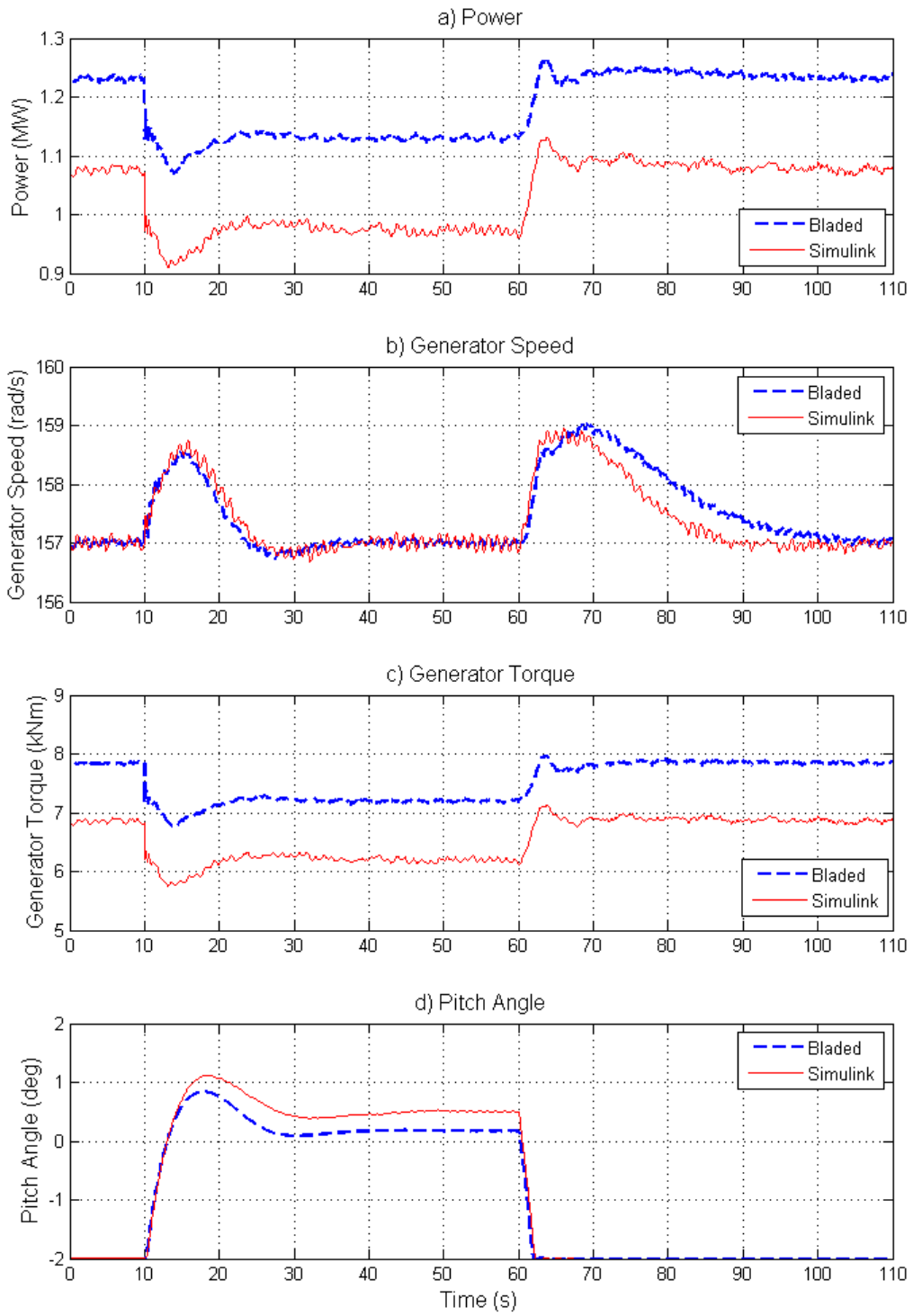


Figure 82: Comparison Between Bladed and Simulink Models

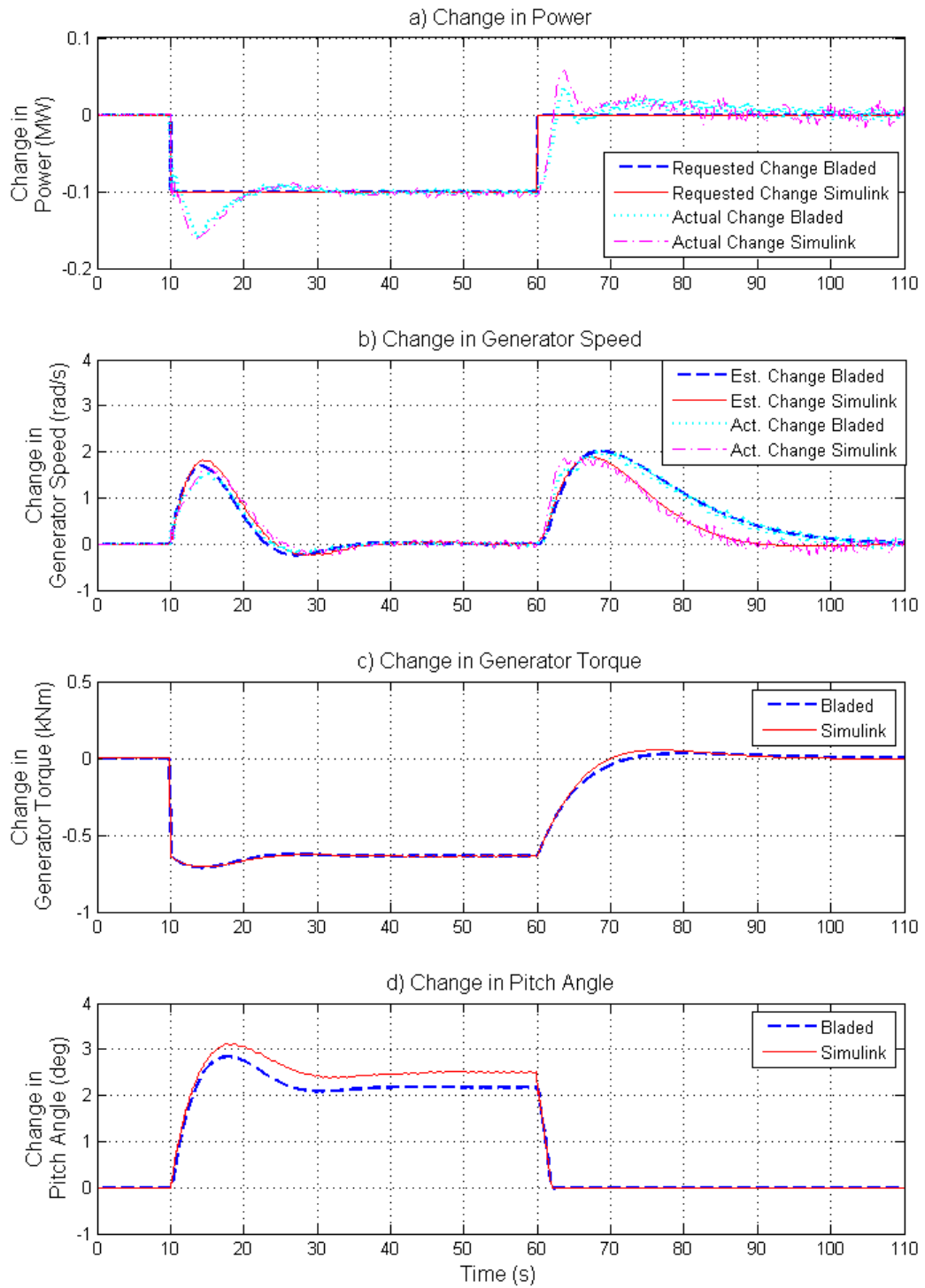


Figure 83: Comparison Between Bladed and Simulink Models

5.4 Incorporating the Dynamic Inflow effects into the PAC

The inaccuracy in the change in power produced by the PAC due to dynamic inflow effects can be mitigated through appropriate modelling of the dynamic inflow effects in the PAC's aerodynamic model. As the PAC's aerodynamic model

considers both the case where the PAC is in use and the case where the PAC has not been used, the dynamic inflow effects must also be modelled for both cases. An estimate of the wind speed at the rotor in its absence is first obtained, as this is the same in both cases.

5.4.1 Calculating an Estimate of the Wind Speed at the Rotor in its Absence

The wind speed estimator presented in section 4.2 does not take into account dynamic inflow effects, instead, the induction factor is equal to the steady state induction factor at all times. The estimated wind speed in the PAC can therefore be defined as the wind speed that would result in a steady state induction factor equal to the unsteady induction factor; the same definition as that for \hat{V} in section 5.3.3.

Using the value for \hat{V} derived from the wind speed estimator presented in section 4.2, the process described in section 5.3 is reversed to find an estimate of the wind speed at the rotor in its absence, denoted as \hat{V}_A .

First the value of $\hat{\lambda}$ is derived using (5.35) and hence a_s is determined from,

$$4a_s(1 - a_s) = C_T(\hat{\lambda}, \beta) \quad (5.38)$$

Using a_s and \hat{V} , a is determined from,

$$\dot{a} = \frac{3\pi}{4R} \hat{V}(a_s - a) \quad (5.39)$$

and finally, the estimate of V_A , \hat{V}_A , is calculated from,

$$\hat{V}_A = \frac{\Omega R (1 - a_s)}{\hat{\lambda} (1 - a)} \quad (5.40)$$

5.5 Calculation of the Change in Aerodynamic Torque

Having determined an estimate of the wind speed at the rotor in its absence, the aerodynamic torque is calculated for both the case where the PAC is used, and the case where the PAC is not used. The value of \hat{V} for each case, denoted as \hat{V}_1 and \hat{V}_0 respectively, is first calculated.

To find \hat{V}_1 , (5.30), (5.31), (5.32), and (5.33) are used to find the corresponding a_1 and a_{s1} , with \hat{V}_A used in place of V_A . The values for a_1 and a_{s1} are then used in (5.34) to

find \hat{V}_1 . To find \hat{V}_0 a similar approach is used. Again, (5.30), (5.31), (5.32), and (5.33) are used to find the corresponding a_0 and a_{s0} , using \hat{V}_A in place of V_A and using $\Omega_0 = (\omega - \Delta\omega)/N$ in place of Ω . \hat{V}_0 is calculated using (5.34).

Note that the values derived for \hat{V}_1 and \hat{V} using this approach are identical, as the calculation to find \hat{V}_1 from \hat{V}_A is the inverse of the prior calculation to find \hat{V}_A from \hat{V} . The method described is still used however so that there is a consistency of approach in calculating \hat{V}_1 and \hat{V}_0 and so that any small numerical errors in solving the equations are the same in each case.

The rotor torque for each case, with the PAC and without, is now found from (5.35) and (5.36), using the corresponding values for wind speed (\hat{V}_1 and \hat{V}_0) and rotor speed (Ω and Ω_0) respectively. Hence ΔQ is calculated by subtracting Q_0 from Q_1 .

5.6 Design and Analysis of the PAC Controller

With the effects of dynamic inflow incorporated into the PAC, the controller dynamics are analysed. In chapter 4, a simple PI controller was used to minimise the change in generator speed via a change to pitch angle. This controller is investigated further in this section. An updated schematic for the PAC is shown Figure 84. For ease of reference, the overview of the PAC and full envelope controller from chapter 4 is also repeated in Figure 85.

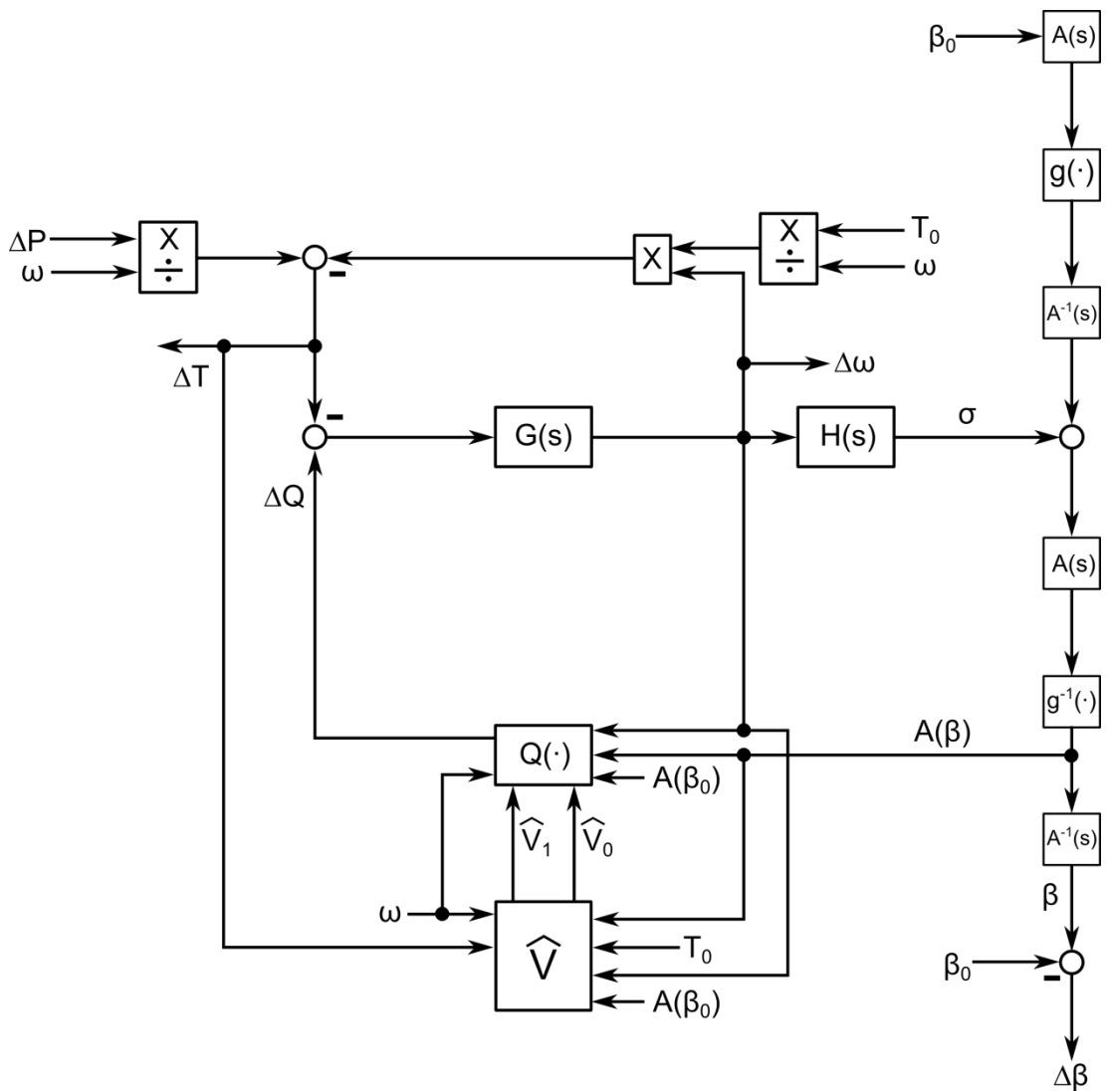


Figure 84: Schematic of the PAC with Induction Lag Effects Incorporated

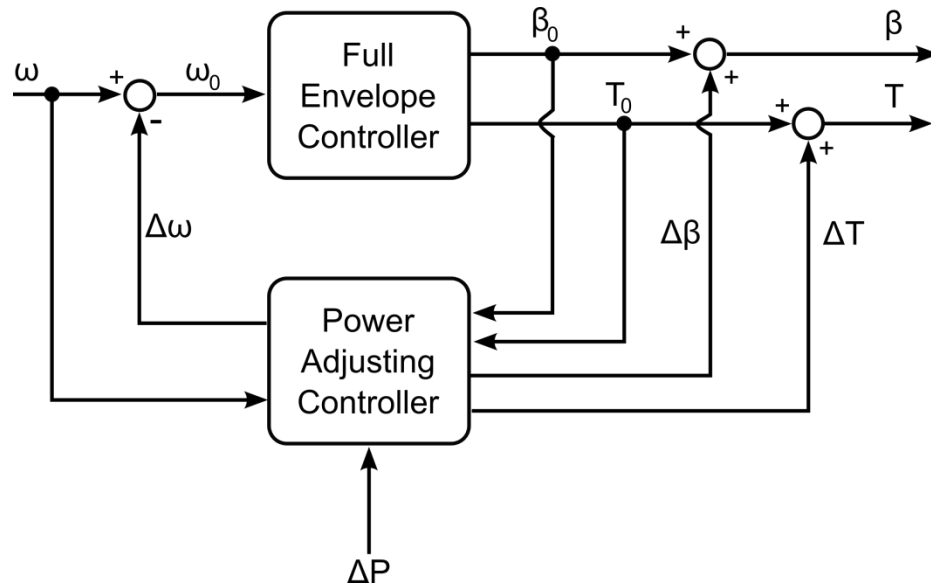


Figure 85: Arrangement of the PAC with the Full Envelope Controller

The controller is linearised about a set of operating points using Taylor series expansions, to produce a set of linearised models. Linearising the model allows standard linear control analysis methods to be used. The linearised model produced is given in Appendix IV.

5.6.1 Controller Design

In essence, $H(s)$ in the PAC acts as a controller. Its purpose is to drive $\Delta\omega$ to zero. In doing so, it adjusts the pitch angle by $\Delta\beta$ to induce a change in the aerodynamic torque, ΔQ , required to balance the change in generator torque, ΔT . The controller $H(s)$, thus requires integral action and a PI controller suffices. The bandwidth of the closed loop system needs to be kept low, firstly, to avoid the introduction of feedback around the turbine full envelope controller that would reduce its effectiveness and, secondly, to minimally utilise the pitch actuator in order that almost all of the demand on the actuator stems from the turbine full envelope controller. With regard to the latter, the rate of change of the PAC pitch adjustment, $\Delta\beta$, is restricted to being less than 0.5 deg/s.

Because the open loop system is unstable in some operating conditions the PI controller is designed in two steps, using an inner and outer feedback loop (see Figure 86). In the first step, the proportional controller is designed with the

objective of achieving closed loop stability with minimum gain K_p . Having closed the inner feedback loop, the integral controller is designed.

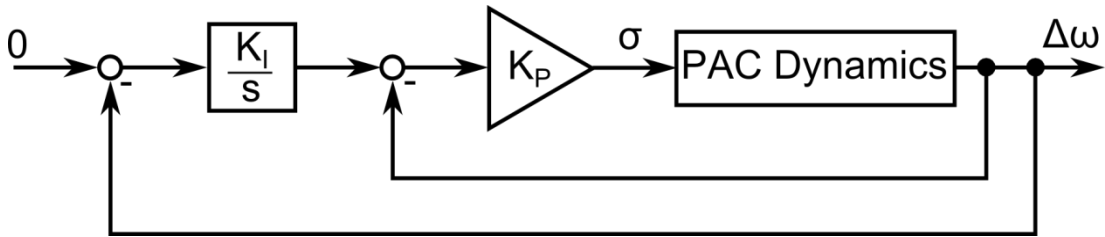


Figure 86: Design of $H(s)$ PI Controller

Although its gain, K_I , must be kept low to meet the above requirements, it must not be so low that the generator speed adjustments requested by the PAC, $\Delta\omega$, are high. The bandwidth of the closed outer feedback loop is much less than that of the inner feedback loop. Of course, because the relevant input to the system in Figure 86 is zero, $H(s)$ is simply $\left(K_p + \frac{K_I/K_p}{s}\right)$.

The PI controller is designed using the PAC linear models in Appendix IV. The Bode plot of the transfer functions for the open loop system from σ to $\Delta\omega$ for the 5MW wind turbine is shown in Figure 87.

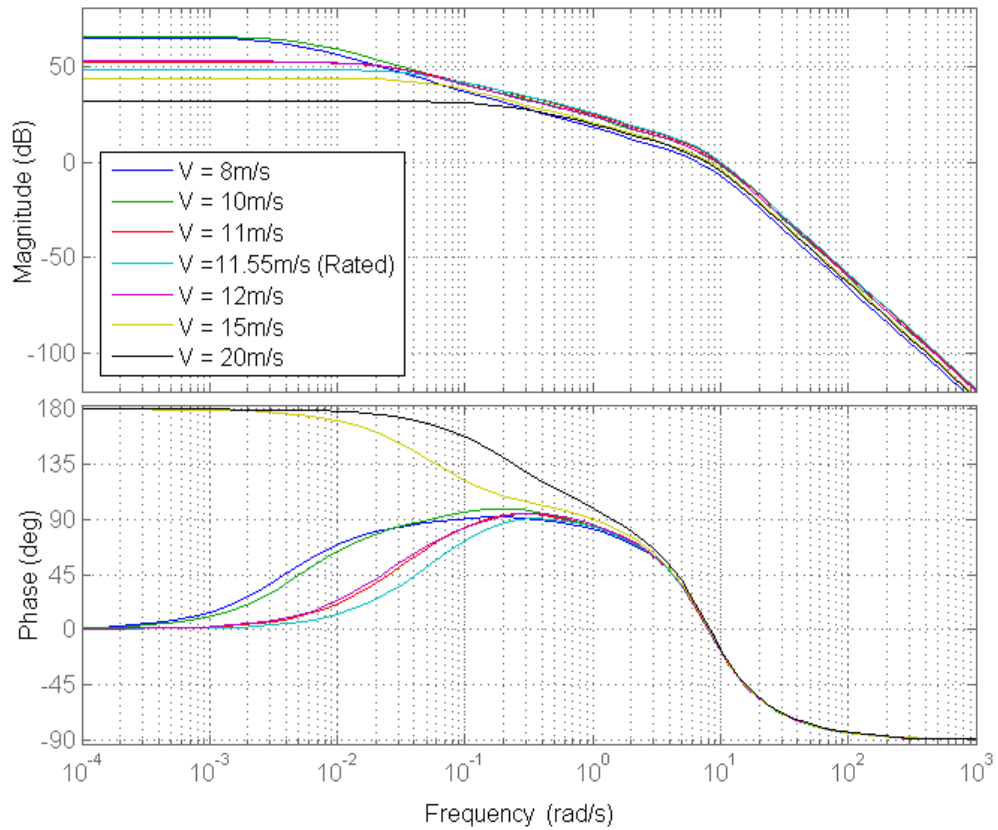


Figure 87: Bode Plot of the Open Loop System - 5MW Wind Turbine

The presence of unstable poles can be observed for all wind speeds below 15m/s. The highest frequency of the unstable pole occurs at rated wind speed. Hence the proportional gain is designed on the basis of the transfer function at this wind speed. The specific controller gain used is $K_p = 0.04$. The Bode plots for the plant, open loop system and closed loop systems are depicted in Figure 88. It can be observed that the gain is low but sufficient to stabilise the system.

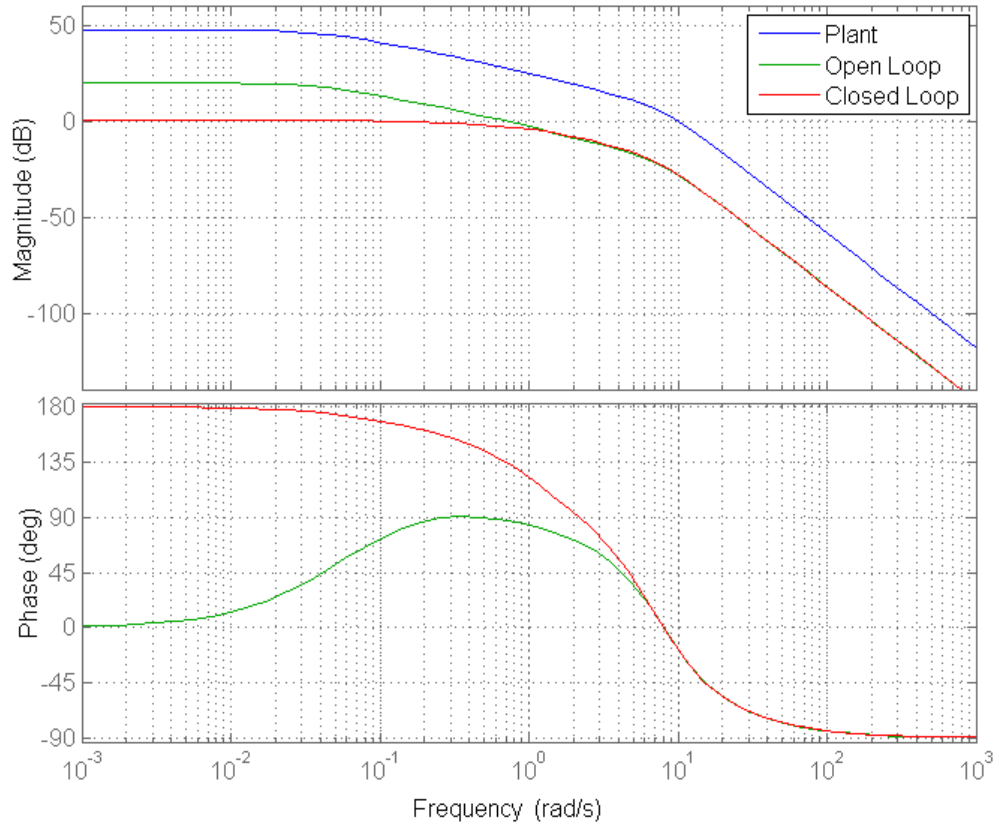


Figure 88: Plant, Open Loop and Closed Loop Bode Plots – 5MW Wind Turbine at Rated Wind Speed

With the inner feedback loop closed, the Bode plots for the plant, the system with open outer loop and the system with closed outer loop at rated wind speed are shown in Figure 89. The integral gain K_I is chosen to be 0.2. This is sufficiently high to keep the excursions in $\Delta\omega$ small and sufficiently low to maintain a low rate of change of $\Delta\beta$, as confirmed by extensive simulation with the Simulink model.

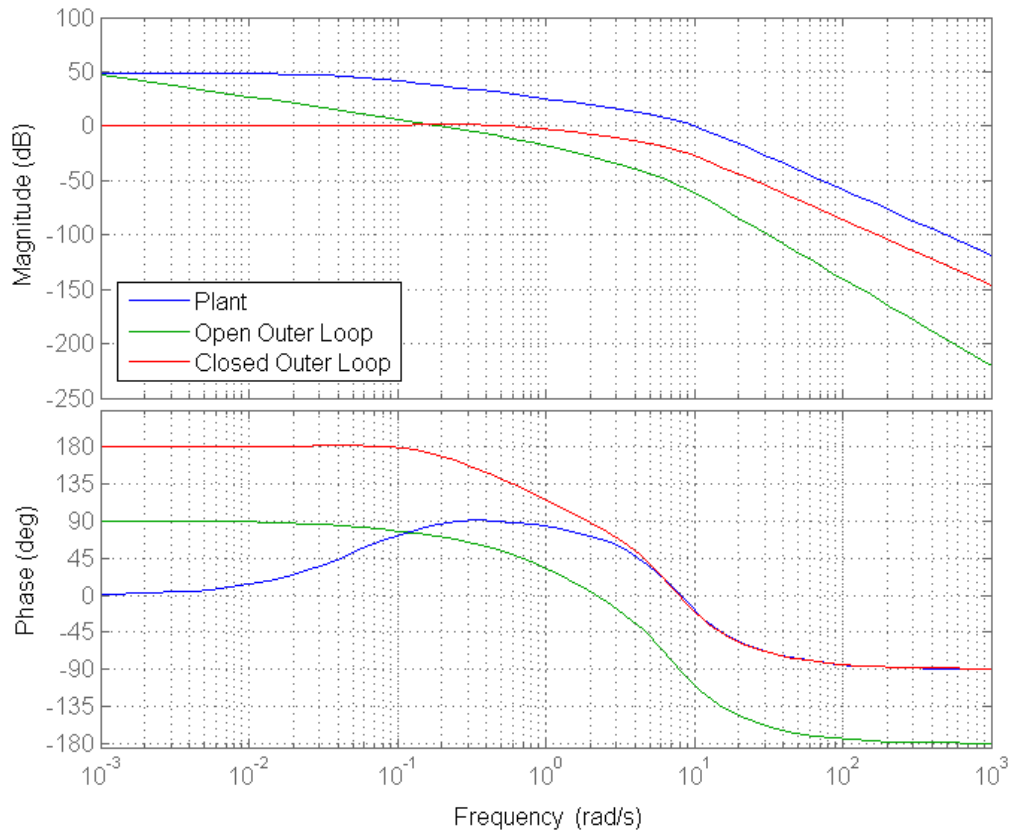


Figure 89: Plant, Open Outer Loop and Closed Outer Loop Bode Plots – 5MW Wind Turbine at Rated Wind Speed

5.6.1.1 Gain Scheduling

From Figure 87, it can be observed that the dynamics of the PAC vary with wind speed. The source of this variation is the non-linear aerodynamic calculation in $Q(\cdot)$. The non-linearities are in part counteracted by the presence of $g^{-1}(\cdot)$ before σ and $A(s)$. This is particularly effective in above rated wind speed (see Figure 87), but inevitable variation in the dynamics remain in below rated conditions. Additional gain scheduling of K_p is required.

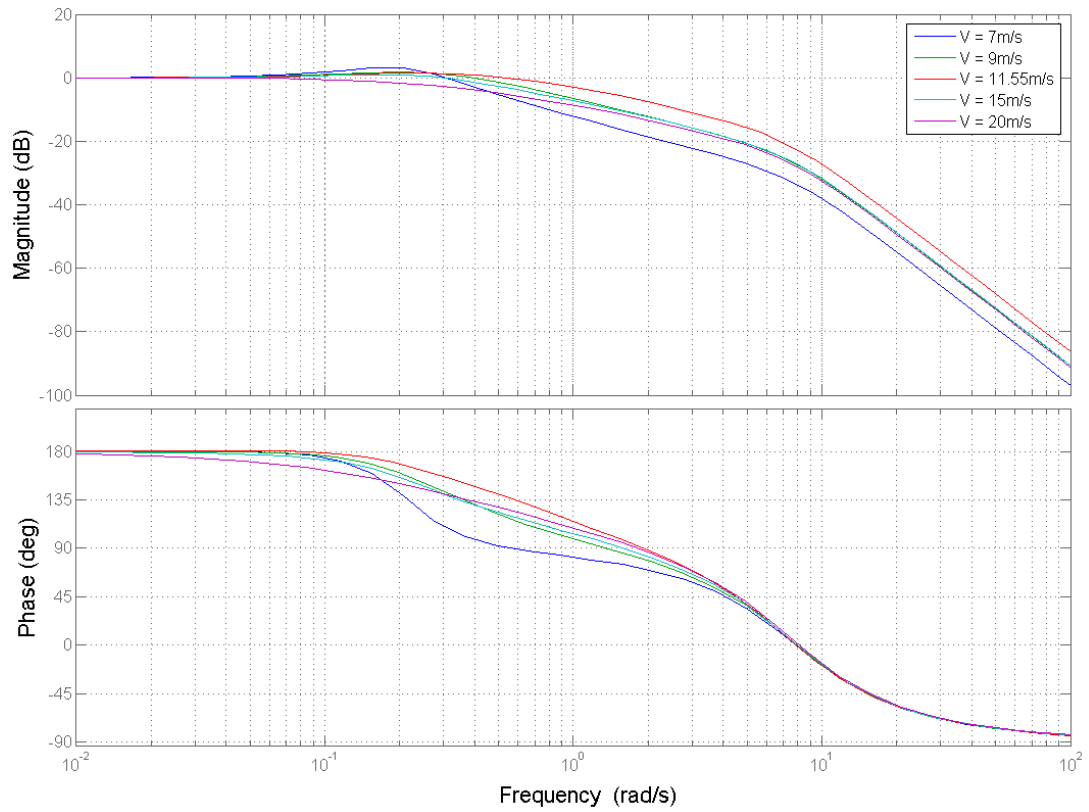


Figure 90: Closed Loop Bode Plot from $\Delta\omega$ to $\Delta\omega$ with PI Controller for a Variety of Wind Speeds

Firstly, the PI controller is gain scheduled based on the generator speed. The torque output of the turbine in the max power tracking region (the region in which the generator speed varies) is proportional to the square of the generator speed. It is sensible therefore to schedule the change in $\Delta\beta$ (itself used to affect a change in torque) by the inverse of the generator speed squared. A scheduling variable K_{GS} is therefore introduced whereby,

$$K_{GS} = \frac{\omega_{rated}^2}{\omega^2} \quad (5.41)$$

In addition, the gain is varied depending upon the wind speed estimated in the PAC. These values are tuned using the linearised model. Application of the gain scheduling to the controller yields a Bode plot of the dynamics as shown in Figure 91 and Figure 92.

The values of K_I , K_P , and the gain scheduling are given in Appendix VI.

Chapter 5: Development of an Improved Wind Speed Estimator

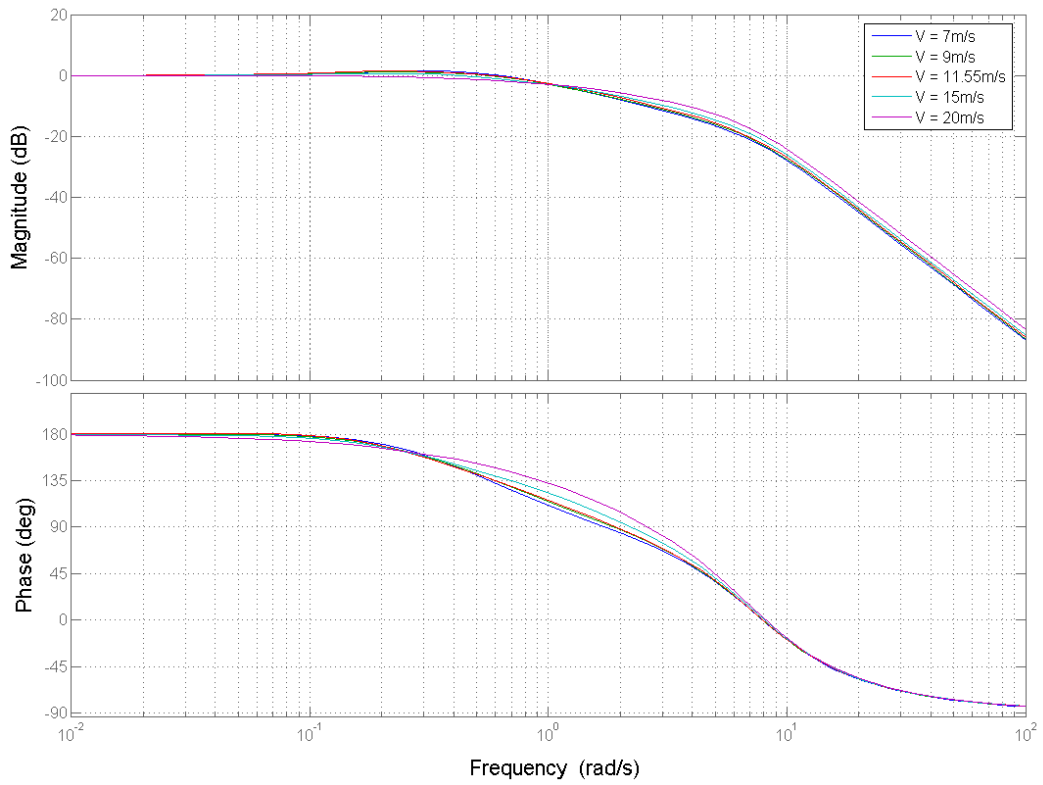


Figure 91: Closed Loop Bode Plot from $\Delta\omega$ to $\Delta\omega$ with PI Controller for a Variety of Wind Speeds with Gain Scheduling

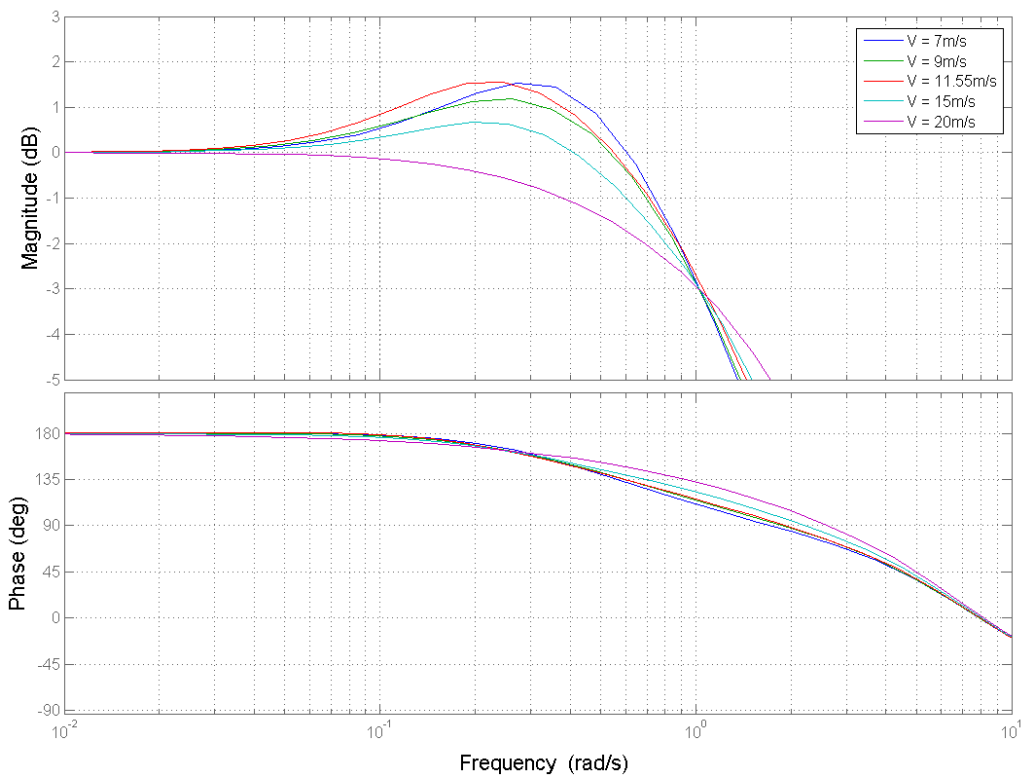


Figure 92: Closed Loop Bode Plot from $\Delta\omega$ to $\Delta\omega$ with PI Controller for a Variety of Wind Speeds with Gain Scheduling (Zoomed in View)

Due to the variation in the bandwidth caused by varying the requested change in power, it is not possible to exactly gain schedule the controller using this method for all values of ΔP . However, by gain scheduling at a representative value for ΔP (in this case 10% of rated power), the variation of bandwidth of the controller with wind speed for all values of ΔP is improved. In Figure 93, the closed loop dynamics for a reduction in power of 20% of the rated power at a variety of wind speeds are shown. Despite the 100% increase in the requested change in power, the spread of the bandwidths of the controller at each wind speed is small.

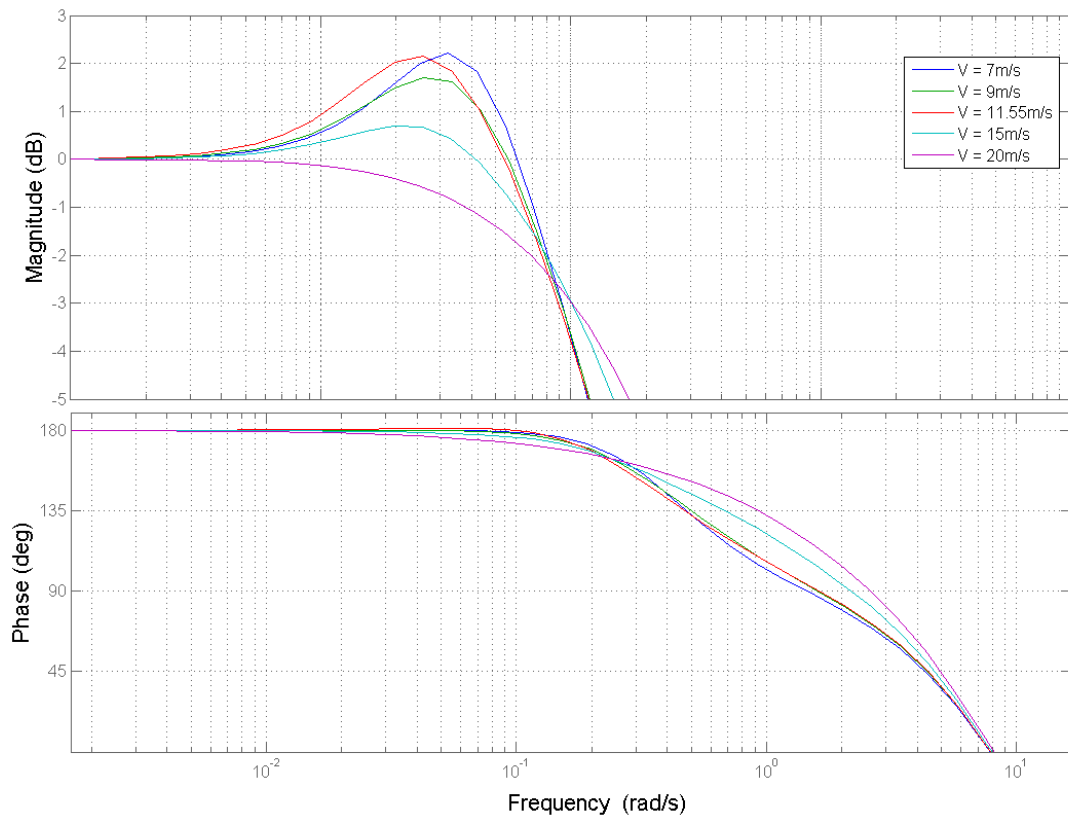


Figure 93: Closed Loop Bode Plot from $\Delta\omega$ to $\Delta\omega$ with PI Controller for a Variety of Wind Speeds with Gain Scheduling (Increased Reduction in Power Output)

5.6.1.2 Feedback Loops

It is important that the PAC does not introduce any strong feedback loops around the full envelope controller; that is to say, the dynamics from the wind turbine full envelope controller outputs to the wind turbine full envelope controller inputs should not be altered by the PAC. As discussed in chapter 4, the PAC is

fundamentally a feed forward controller, and so any feedback loops present should be very weak.

The linearised models are used to assess the dynamics from the outputs of the full envelope controller of β_0 and T_0 to $\Delta\omega$. The Bode plots of these dynamics are given in Figure 94 to Figure 97 for the 5MW wind turbine for a range of operating points, a range of values of ΔP , and at a range of wind speeds. Note that because the full envelope controller only uses pitch angle to control the wind turbine in above-rated conditions, only above-rated wind speeds are shown. Whilst torque demand is used predominantly in below-rated operation, it is also used in above-rated operation for some applications such as the drive-train filter or coordinated control. The dynamics from T_0 to ω_0 are therefore plotted for wind speeds below rated, at rated and above rated.

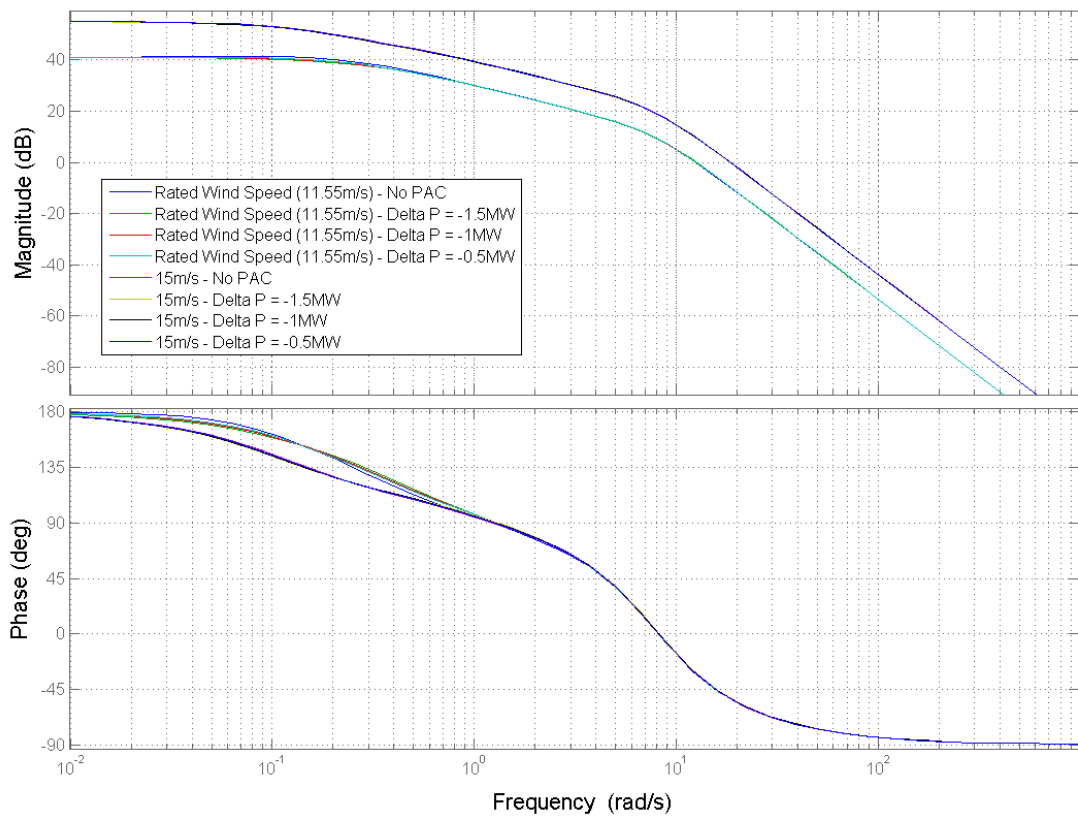


Figure 94: Dynamics from the Pitch Demand Output of the Full Envelope to the Input of the Full Envelope Controller

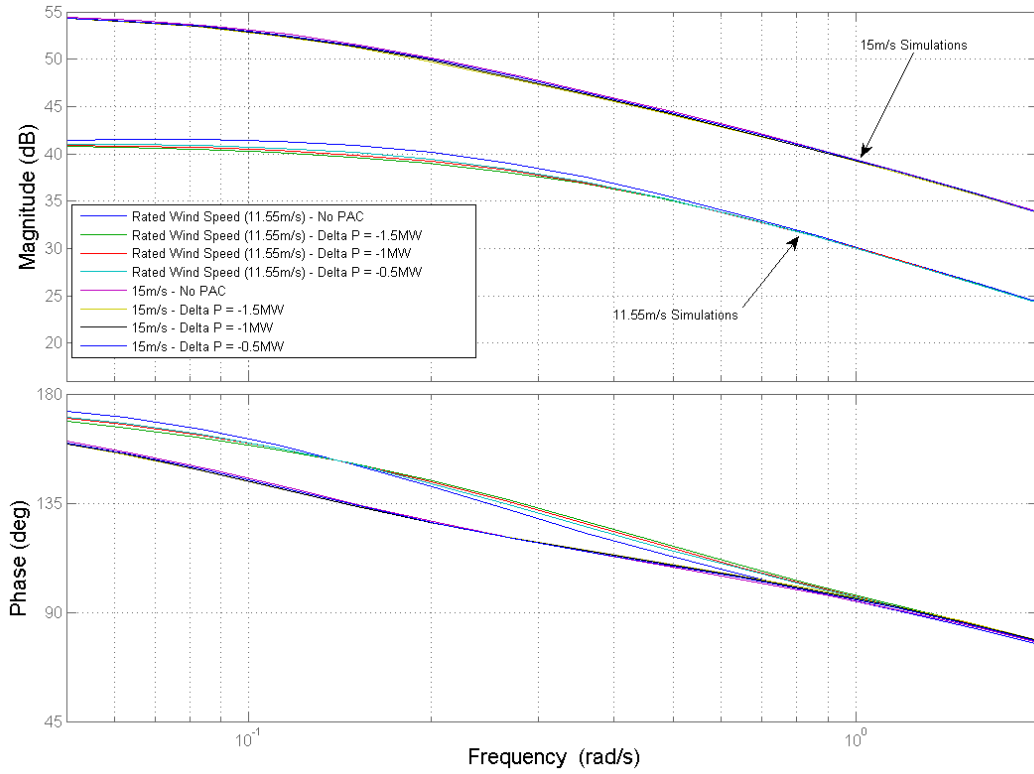


Figure 95: Dynamics from the Pitch Demand Output of the Full Envelope to the Input of the Full Envelope Controller (Zoomed in View)

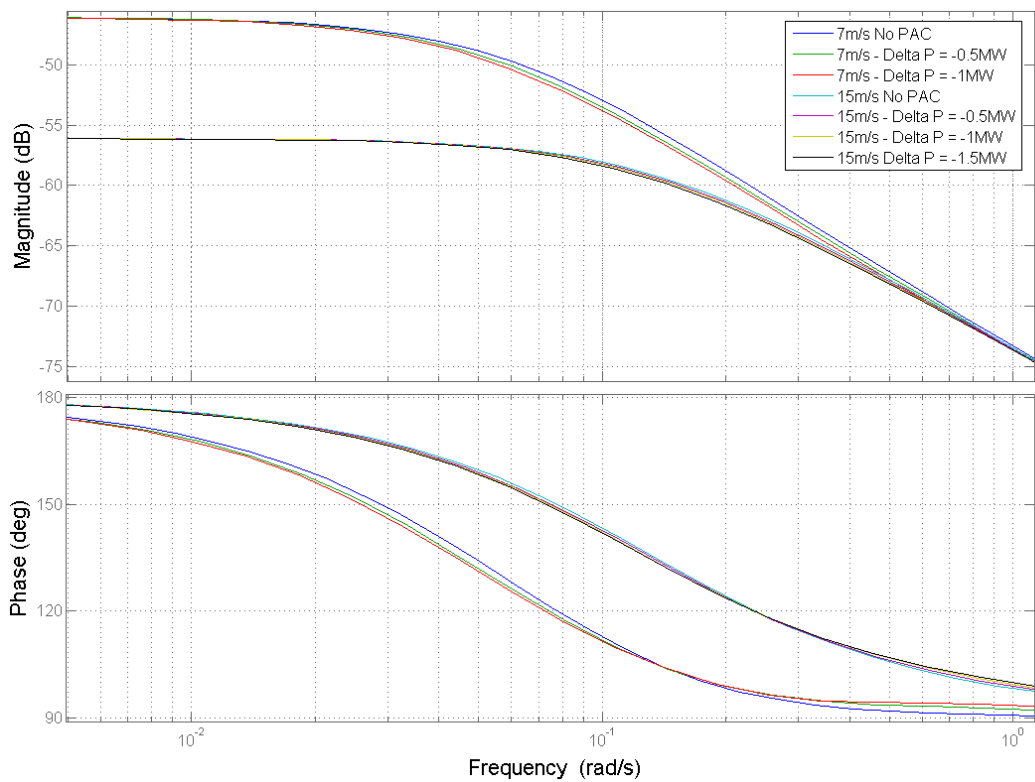


Figure 96: Dynamics from the Torque Demand Output of the Full Envelope Controller to the Input of the Full Envelope Controller (7m/s and 15m/s)

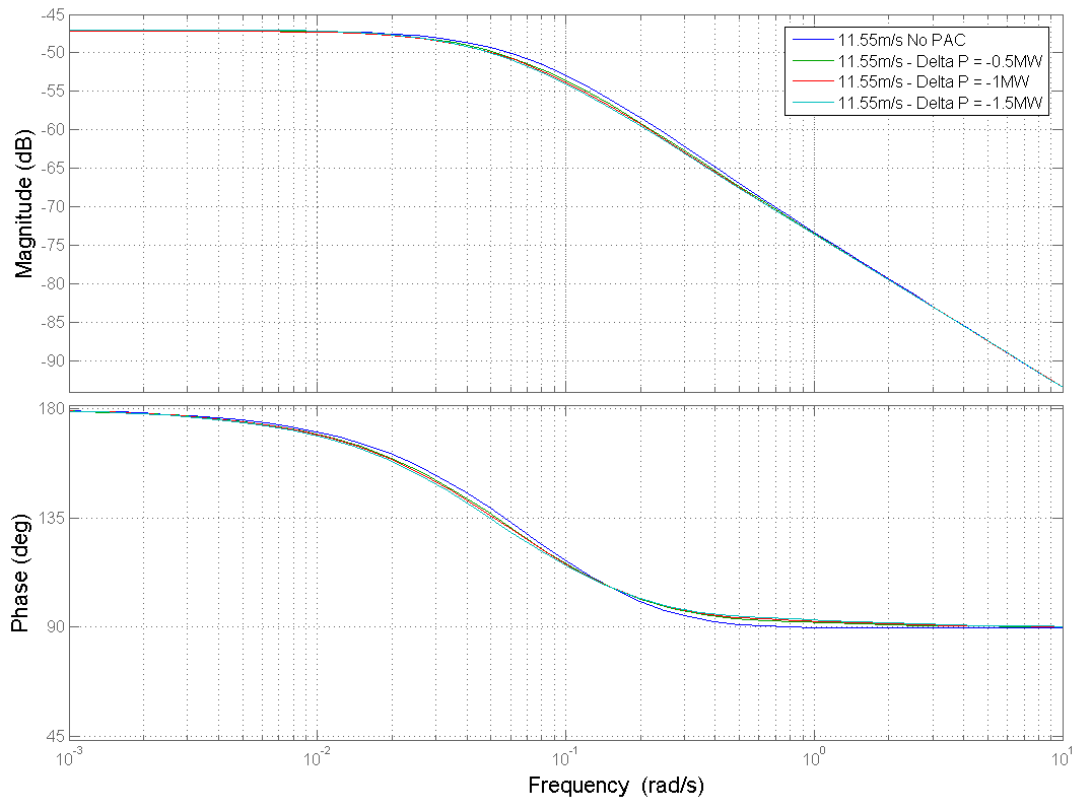


Figure 97: Dynamics from the Torque Demand Output of the Full Envelope Controller to the Input of the Full Envelope Controller (11.55m/s)

As wind turbine full envelope controllers are designed to have a cross-over frequency of 1 rad/s (see chapter 2) it is crucial that any change in gain at this frequency is not large. The largest change in gain at 1 rad/s for either the dynamics from full envelope controller pitch demand or full envelope controller torque demand to full envelope controller input is -0.2dB, less than 2.5%. As such it is clear that there is no strong feedback loop induced by the PAC and so the performance of the full envelope controller is not degraded.

The lack of impact on the performance of the full envelope controller is further shown via power spectral density plots of the generator speed (below and above-rated wind speed), pitch angle (above-rated wind speed) and generator torque (below-rated wind speed), with and without the PAC in operation in Figure 98, Figure 99, Figure 100, and Figure 101.

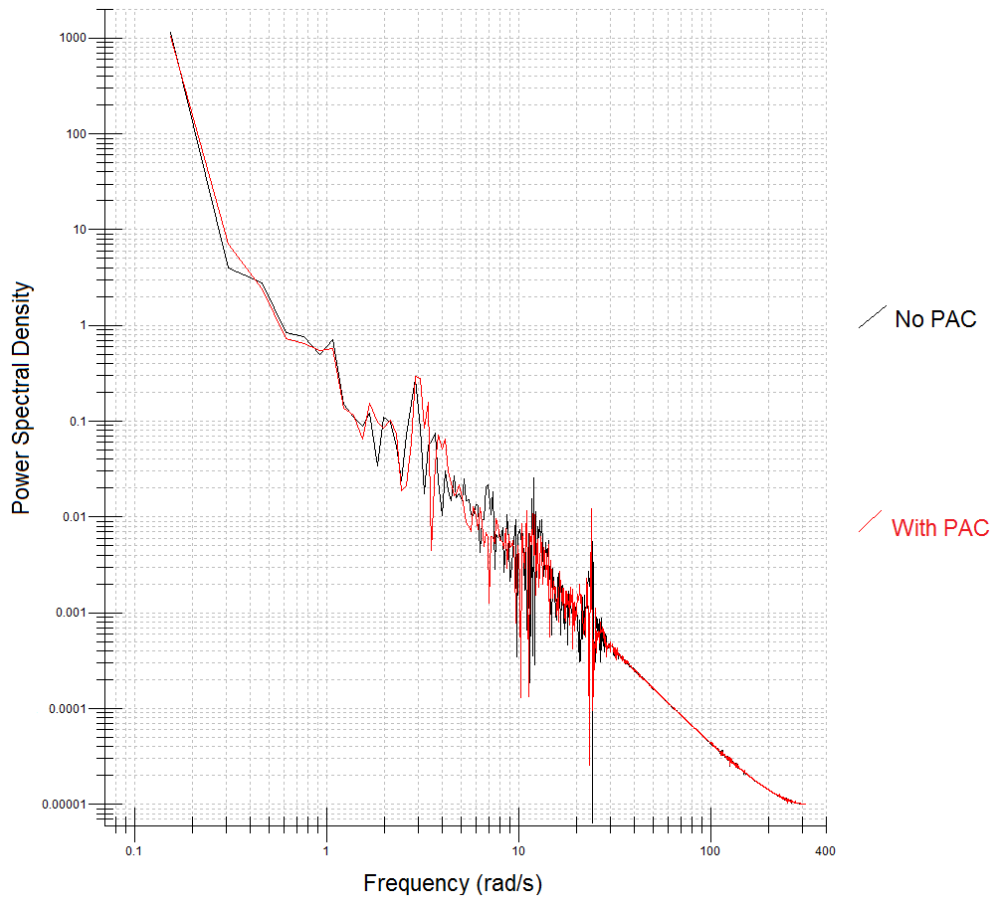


Figure 98: Power Spectral Density - Generator Speed (Below-rated Wind Speed)

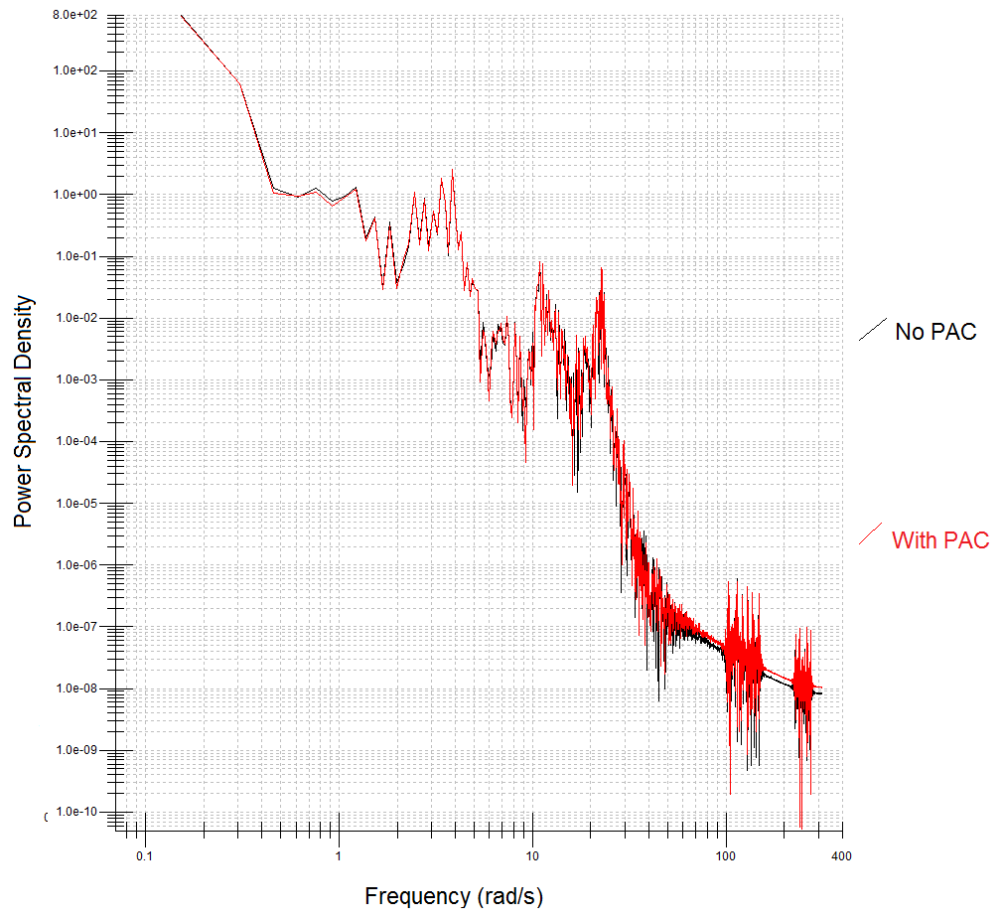


Figure 99: Power Spectral Density - Generator Speed (Above-rated Wind Speed)

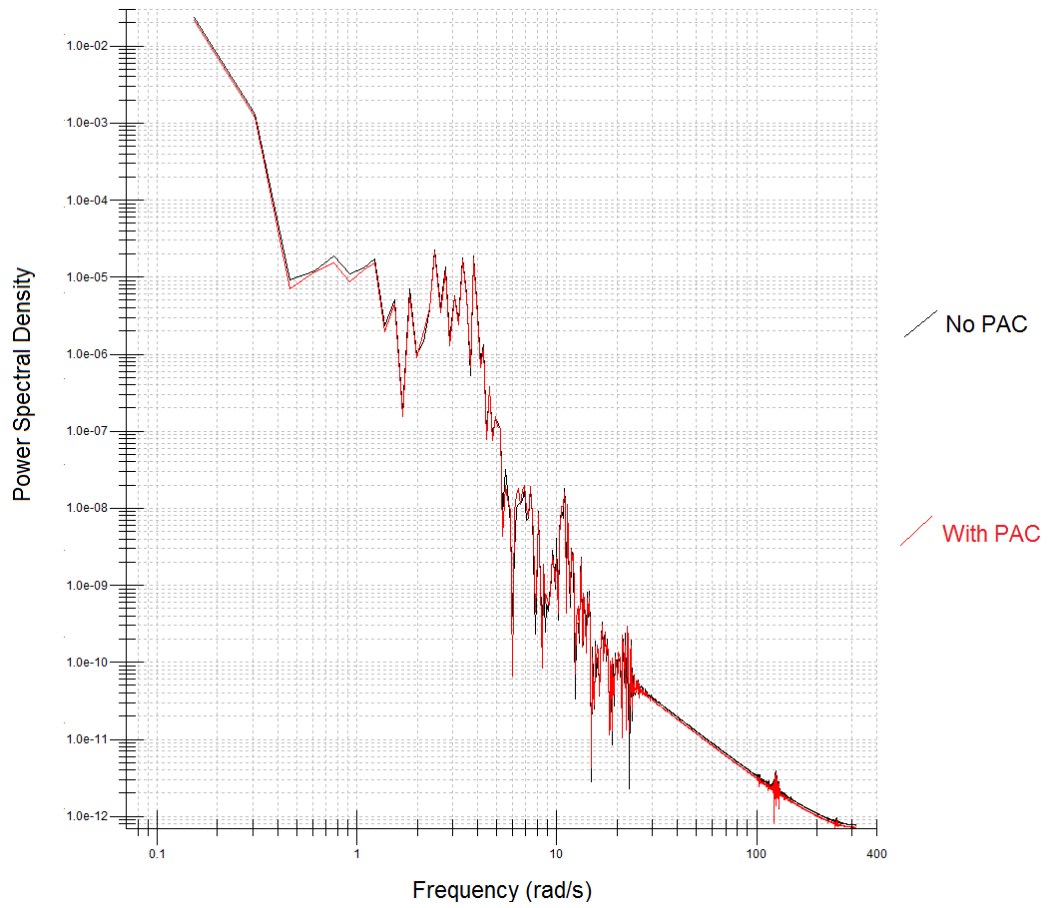


Figure 100: Power Spectral Density – Pitch Angle (Above-rated Wind Speed)

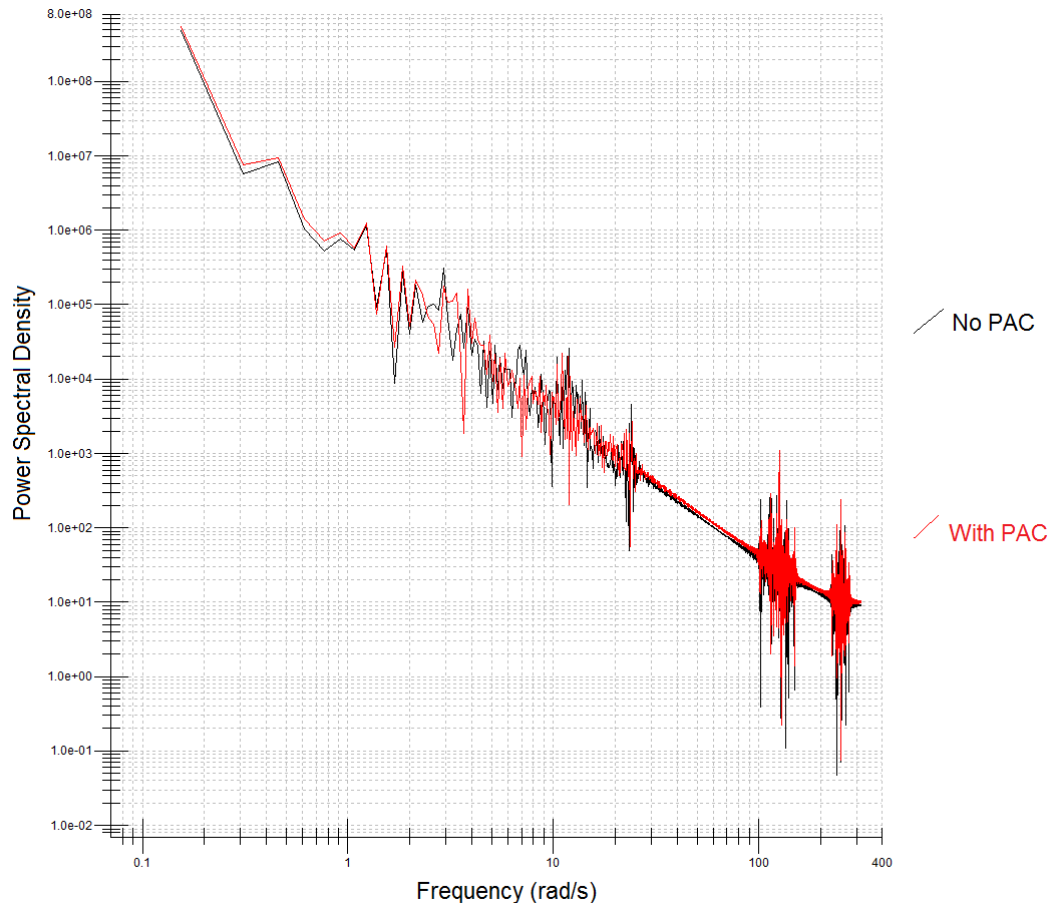


Figure 101: Power Spectral Density – Torque Demand (Below-rated Wind Speed)

These plots show that little difference in the power spectral density has been introduced by the PAC. The power spectral densities with and without the PAC are similar for all cases.

5.7 Evaluation of the Effect on Incorporating Dynamic Inflow on PAC Performance

A direct comparison is made between the PAC with dynamic inflow modelled and without. Four simulations are conducted, two at a steady wind speed of 9m/s and two with a turbulent wind at a mean of 9m/s. One of each is conducted without dynamic inflow effects modelled in the PAC and one of each is conducted with dynamic inflow effects modelled. The simulations are carried out using the Simulink model of the 5MW wind turbine, with induction lag modelled in the turbine. The results are given in Figure 102 and Figure 103. A drop in power

output of 0.5MW is requested at 10 seconds simulation time. The PAC is switched off and undergoes recovery at 60 seconds simulation time.

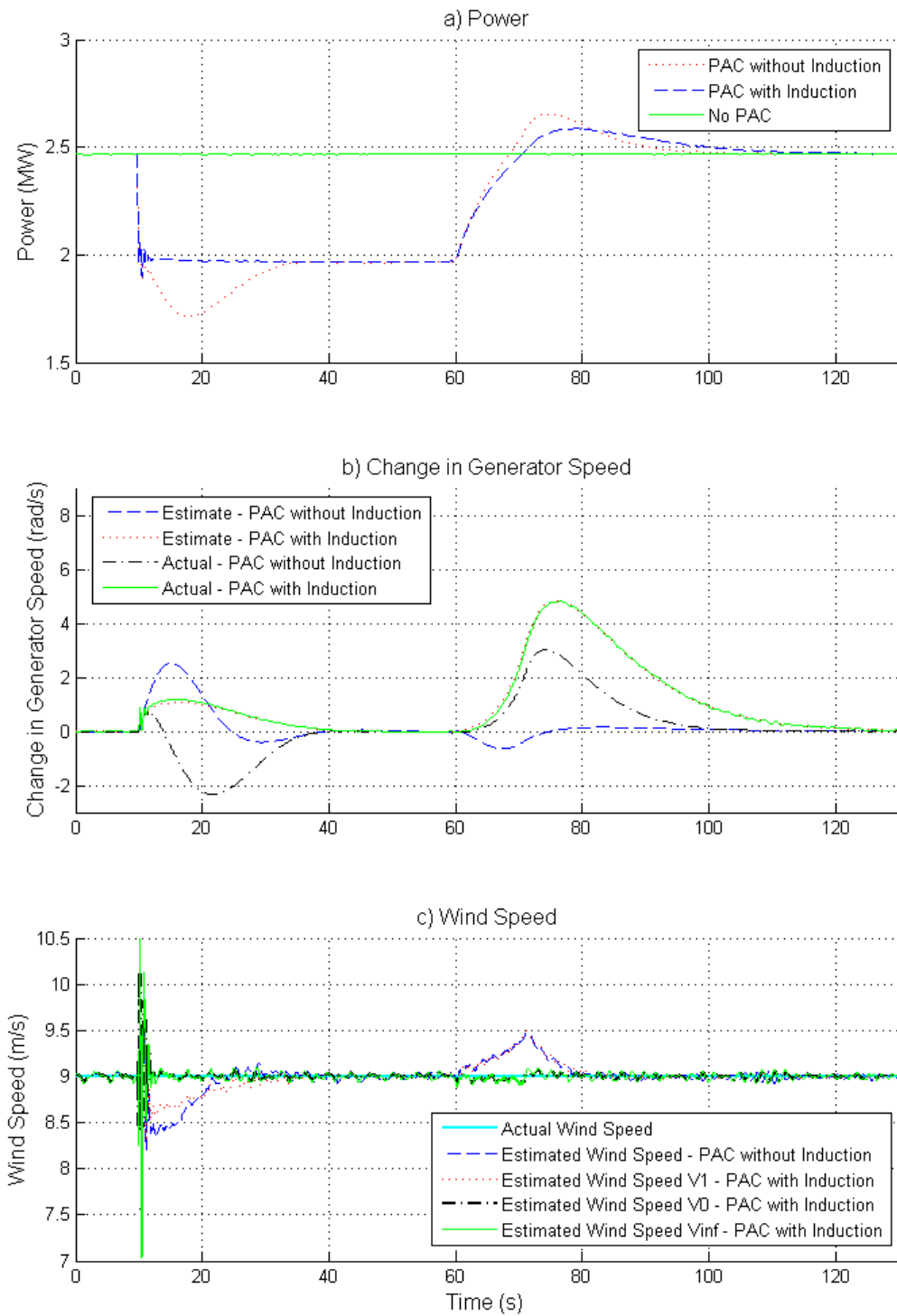


Figure 102: PAC with Induction and PAC without Induction - 5MW Wind Turbine – Constant Wind Speed

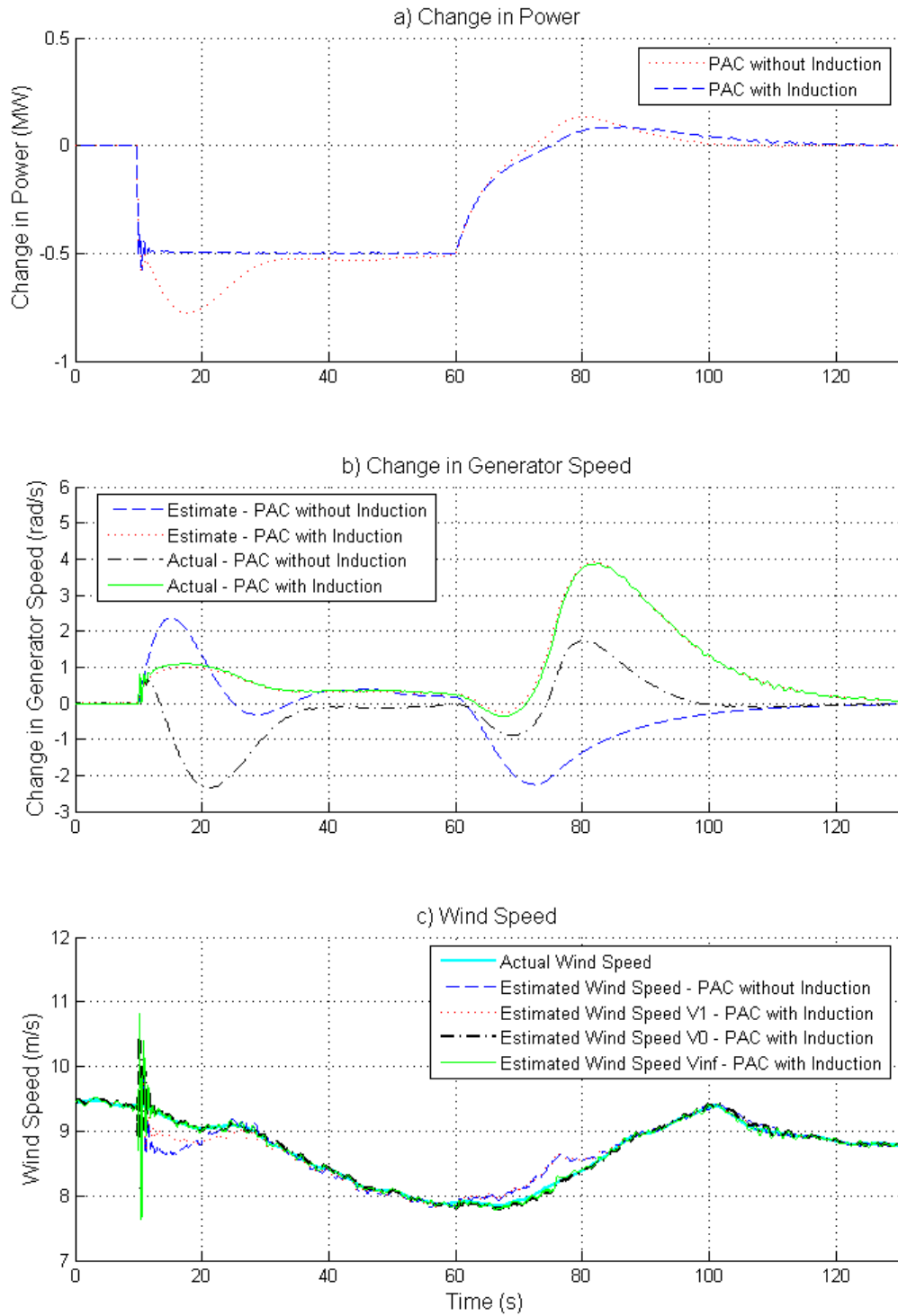


Figure 103: PAC with Induction and PAC without Induction - 5MW Wind Turbine – Variable Wind Speed

Using the PAC with the model for dynamic inflow effects produces a more accurate ΔP output. This is the case for both the constant wind speed and variable wind speed simulations. The estimate \hat{V}_A when incorporating the model for dynamic

inflow effects is an excellent estimate of the actual wind speed that is supplied to the model. The estimate \hat{V}_1 and the estimated wind without the dynamic inflow effects modelled differ from one another because the response of the PAC as a whole is different. The error in ΔP leads to errors in ΔT , $\Delta \omega$, and $\Delta \beta$, which in turn lead to differences in the wind speed estimate.

The results confirm the hypothesis that the inaccuracy in the change in power output produced by the PAC in the Bladed simulations at the end of chapter 4 is due to dynamic inflow effects. The results also confirm that modelling the dynamic inflow effects within the PAC increases the accuracy of the change in power produced by the PAC.

5.8 Concluding Remarks

In this chapter a new wind speed estimator based on a reformulation of blade element momentum theory considering only the properties at the rotor is introduced. The estimator takes into account dynamic inflow effects in order to improve the accuracy of the change in power output produced by use of the PAC. This estimator is adapted for use in the PAC, greatly improving the performance of the PAC in Simulink models when dynamic inflow is modelled.

The dynamics of the PAC with dynamic inflow effects modelled are investigated and the $\Delta \beta$ controller is gain scheduled to ensure even response across all wind speeds.

Analysis of the PAC via a linearised model shows that the PAC is highly decoupled from the full envelope controller; i.e. there are no strong feedback loops introduced around the full envelope controller. This ensures that the performance of the full envelope controller is unaffected by the use of the PAC.

Chapter 6:

Evaluation of the PAC's Performance

THE POWER ADJUSTING CONTROLLER (PAC) is developed and applied to Simulink lumped parameter models of wind turbines in chapter 4 and chapter 5. To fully evaluate the performance of the controller however, including assessment of the increase or decrease in the loads, the PAC is applied to a full aero-elastic model. GL Bladed, an industry standard aero-elastic wind turbine modelling program, is used. Bladed requires that controllers be written in discrete time rather than continuous time (used in the Simulink model in chapters 4 and 5). This is also the case for real wind turbine control systems. In this chapter, the PAC is discretised and tested with GL Bladed. An assessment of the change in loads on the wind turbine when using the PAC is made.

6.1 Control in Discrete Time

Controller design in the previous chapters is in continuous time or the “s-domain”. The PAC is converted into discrete time (the “z-domain”) for implementation in Bladed. In discrete time, the system is solved and the outputs produced once every (fixed) time step.

Converting controllers from the s-domain to the z-domain necessitates the use of some transformation method. There are several transformation methods available, with the three most common given in Table 3. Each of these transformations is a discrete time approximation of the continuous controller.

Table 3: Methods of Transforming Differential Equations from Continuous to Discrete Time
(adapted from [75])

Method	Approximation
Forward Rectangular Rule	$s \sim \frac{z-1}{T_s}$
Backward Rectangular Rule	$s \sim \frac{z-1}{T_s z}$
Trapezoid Rule (also known as Tustin's Bilinear Rule or the Bilinear Transform)	$s \sim \frac{2}{T_s} \frac{z-1}{z+1}$

All methods of discretisation can be divided into two categories, implicit methods and explicit methods. Explicit methods use the state of the system at the current time to calculate the state of a system at a later time, whereas implicit methods solve an equation using both the state of the system at the current time and the state of the system at a later time to find a solution.

Whilst implicit methods are more complicated, they are generally more numerically stable than explicit methods. In addition, compared to the time step for an explicit algorithm, the time step for an implicit algorithm can be an order of magnitude larger. When discretising the PAC, the bilinear transform, an implicit method, is used. The time step required for sufficient accuracy is dependent upon the fastest dynamics in the controller, in this case the actuator dynamics. The time step chosen is 20Hz.

Using this method presents problems however, when applied to the wind speed estimator. The calculation of a and a_s in the wind speed estimator discretises as shown:

$$a[n] = \frac{T_s a_d[n] + T_s a_d[n-1] + 2a[n-1]}{2} \quad (6.1)$$

$$a_d[n] = \frac{3\pi}{4R} V_A \frac{1 - a[n]}{1 - a_s[n]} (a_s[n] - a[n]) \quad (6.2)$$

and

$$a_s[n] = A_s \left(\frac{\Omega R}{V} \frac{1}{(1 - a[n])}, \beta \right) \quad (6.3)$$

where T is the step length, A_s is a nonlinear function based on the thrust coefficient and the subscript d denotes the differential (i.e. the rate of change) of a value. As both a_d and a_s require a value for a in order to be calculated, there is a loop that cannot be algebraically solved.

The problem is avoided by using an explicit transformation method. Using the forward difference rule, the equation for a becomes:

$$a[n] = a_d[n - 1] + a[n - 1] \quad (6.4)$$

where a_d and a_s are found as in (6.2) and (6.3). Because the value of $a[n]$ is solely reliant on prior values of a and a_d , there is no algebraic loop and so no iteration is involved.

Using an explicit method rather than an implicit method typically requires the use of a time step an order of magnitude smaller. In the PAC however, the dynamics that require the use of the explicit method are an order of magnitude slower than the fastest dynamics in the controller (the actuator dynamics). Hence it is appropriate to choose a similar time step for the actuator dynamics, which are an order of magnitude faster, using an implicit algorithm and the rest of the dynamics using an explicit algorithm.

The PAC is therefore designed using two different solvers with the same time step, as shown in Figure 104. The dynamics inside the marked area are solved using the forward difference rule, an explicit method, whereas the dynamics outside the marked area are solved using the bilinear transform method, an implicit method. Using two different solvers is simpler and easier than linearising the function A_s , which is an alternative solution.

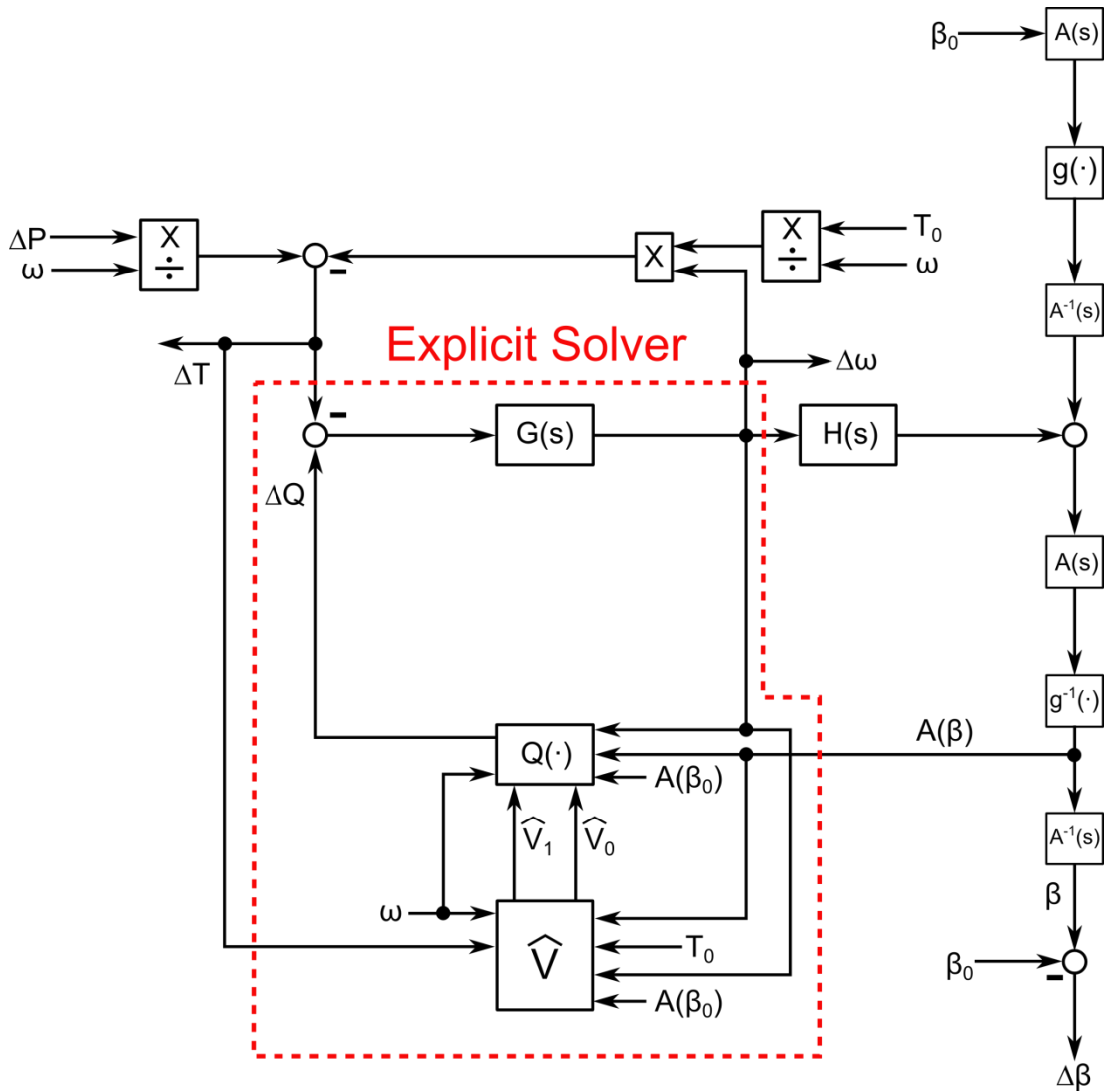


Figure 104: Section of the PAC Using an Explicit Solver

6.2 Anti-Wind Up

It is important that any pitch demand sent to the wind turbine does not exceed the limits of the actuator and cause integrator wind up. The limits to the PAC are applied with reference to the total pitch angle $\beta = \beta_0 + \Delta\beta$. As β_0 is limited by the full envelope controller the limits can only be exceeded due to $\Delta\beta$.

An anti-wind up system is therefore put in place whereby the output value of $\Delta\beta$ is not permitted to take a value that would cause the total pitch demand to exceed the limits of the actuator. The following process is used:

1. A value for $\Delta\beta$ and hence the total pitch angle β , is generated using the process described in chapters 4 and 5.

2. The rate of change of the pitch angle is calculated.
3. If the position or velocity of β exceed the limits of the actuator then the value of $\Delta\beta$ that achieves but does not exceed the limit, and the corresponding input to $H(s)$ is calculated by "back calculating" through the system.
4. The process runs in the forward direction again, resulting in an output of β that does not exceed the limits, whilst ensuring that all intervening values in the controller are also correct for the limited value of $\Delta\beta$.

6.2.1 Rearrangement of Transfer Functions to Allow Back Calculation

The first step in applying the anti-wind up method described is to discretise the transfer functions in such a manner as to split them into a component relying solely on values from previous time steps and a component that is a gain multiplied by the current value of the input. For the general case:

$$F(s) \rightarrow F(z) = \frac{n(z)}{d(z)} = \frac{A_n z^{-n} + A_{n-1} z^{-(n-1)} + \dots + A_1 z^{-1} + A_0}{B_m z^{-m} + B_{m-1} z^{-(m-1)} + \dots + B_1 z^{-1} + 1} \quad (6.5)$$

$$F(z) - A_0 = z^{-1} \frac{m(z)}{d(z)} = z^{-1} G(z) \quad (6.6)$$

so:

$$F(z) = z^{-1} G(z) + A_0 \quad (6.7)$$

Figure 105 shows this method applied to a continuous time transfer function $F(s)$.

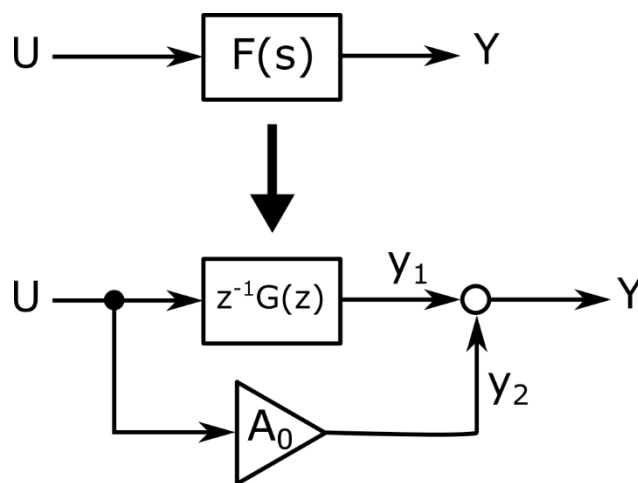


Figure 105: Transformation from Continuous to Discrete Time to Implement Anti-Wind Up

For a given maximum value of the output $y = y_{max}$ it is ensured that the limit is not exceeded by using (6.8), (6.9), (6.10), and (6.11).

$$y_1[n] = G(z)U[n - 1] \tag{6.8}$$

$$y_2[n] = A_0U[n] \tag{6.9}$$

$$Y[n] = y_1[n] + y_2[n] \tag{6.10}$$

$$\begin{aligned} \text{if } Y[n] > y_{max} \text{ then } Y[n] &= y_{max} \\ \text{and } U[n] &= \frac{y_{max} - y_1}{A_0} \end{aligned} \tag{6.11}$$

Using this method, wind up is avoided whilst limiting the output to the desired maximum. A similar method could be used for any constraint on the output value.

6.2.2 Position Limits

Figure 106 shows the section of the PAC in which anti-wind-up is applied. The dynamics from U to β are converted into discrete time using the method in section 6.2.1, as shown in Figure 107.

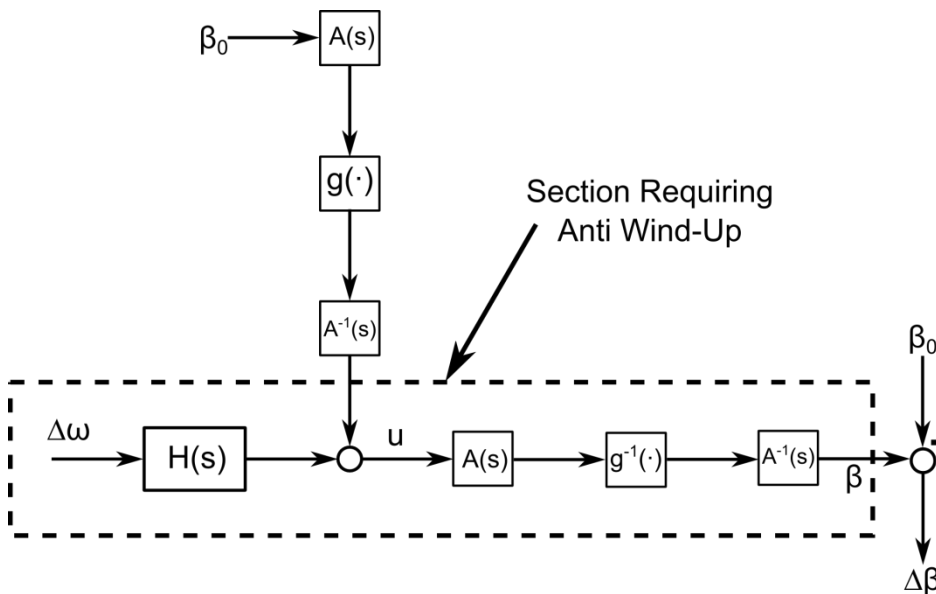


Figure 106: Section of the PAC Requiring Anti Wind-Up

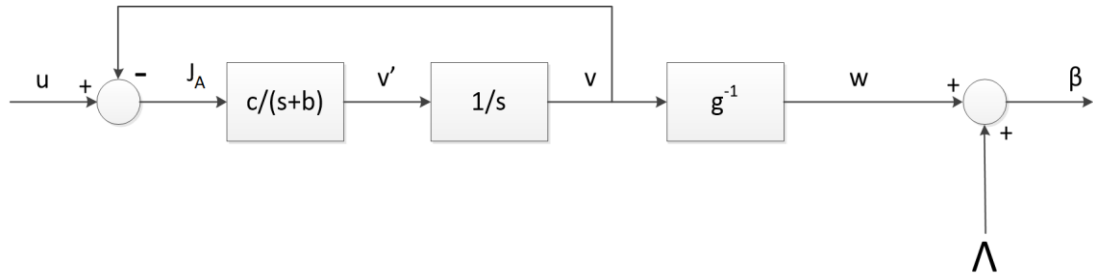


Figure 108: PAC Gain Scheduling Diagram

Where,

$$\Lambda = \frac{(u - v)}{g'(w)} - \frac{(g''(w)v'^2)}{c(g'(w))^3} \quad (6.14)$$

By utilising the back calculation method discussed in section 6.2.1, a method for limiting the value of w due to the pitch rate limitations is derived. To test whether the maximum or minimum pitch rates have been exceeded the following logic is used,

$$\begin{aligned} & \text{if } v' - \min(v', PR_{max}.h'(w)) \neq 0 \\ & \text{then the pitch rate is greater than the maximum pitch rate} \end{aligned} \quad (6.15)$$

$$\begin{aligned} & \text{if } v' - \max(v', PR_{min}.h'(w)) \neq 0 \\ & \text{then the pitch rate is greater than the maximum pitch rate} \end{aligned} \quad (6.16)$$

Where PR_{min} is the minimum pitch rate and PR_{max} is the maximum pitch rate.

It follows that, with reference to Figure 108,

$$\frac{v'}{J_A} = \frac{c}{s + b} \quad (6.17)$$

$$J_A = \frac{1}{c}(v'' + bv') \quad (6.18)$$

$$v = h(w) \quad (6.19)$$

$$v' = h'(w)w' \quad (6.20)$$

$$v'' = h''(w)w'^2 + h'(w)w'' \quad (6.21)$$

When the max pitch rate is reached it is reasonable to assume that $w'' = 0$. Hence, by substituting the equations for v'' and v' ,

$$J_A = \frac{1}{c}(M.PR^2 + bh'(w).PR) = \frac{1}{c}(M.PR^2 + b(C + Mw).PR) \quad (6.22)$$

$$v = v_1 + a_{A2}v' = v_1 + a_{A2}h'(w)w' = v_1 + a_{A2}(C + Mw)PR \quad (6.23)$$

$$v = \frac{(C + M.w)^2 - (C + M.PIT_{min})}{2M} \quad (6.24)$$

Where PR is the max or min pitch rate (depending on which has been reached) and PIT_{min} is the minimum pitch.

Hence it follows that,

$$w = \frac{-2(C - Ma_{A2}PR) + \sqrt{D}}{2M} \quad (6.25)$$

where,

$$D = 4(C - Ma_{A2}PR)^2 + 4M(PIT_{min}(2C + M.PIT_{min}) + 2v_1 + 2a_{A2}PR.C) \quad (6.26)$$

The value of u is then back calculated in the same manner as for the limit on position.

6.3 Application of the PAC Using Bladed

The PAC is discretised as set out in section 6.1, written in the C++ coding language, and compiled into a .dll file suitable for use with GL Bladed.

Simulations are completed for a drop in power of 100kW using the 1.5MW wind turbine. Three constant wind speeds and three variable wind speeds are used (one wind speed in which the operating point of the turbine is in the max power tracking region, one in which the operating point of the turbine is in the constant speed region, and one in which the operating point of the turbine is above rated). The results are presented in Figure 109, Figure 110, Figure 111, and Figure 112.

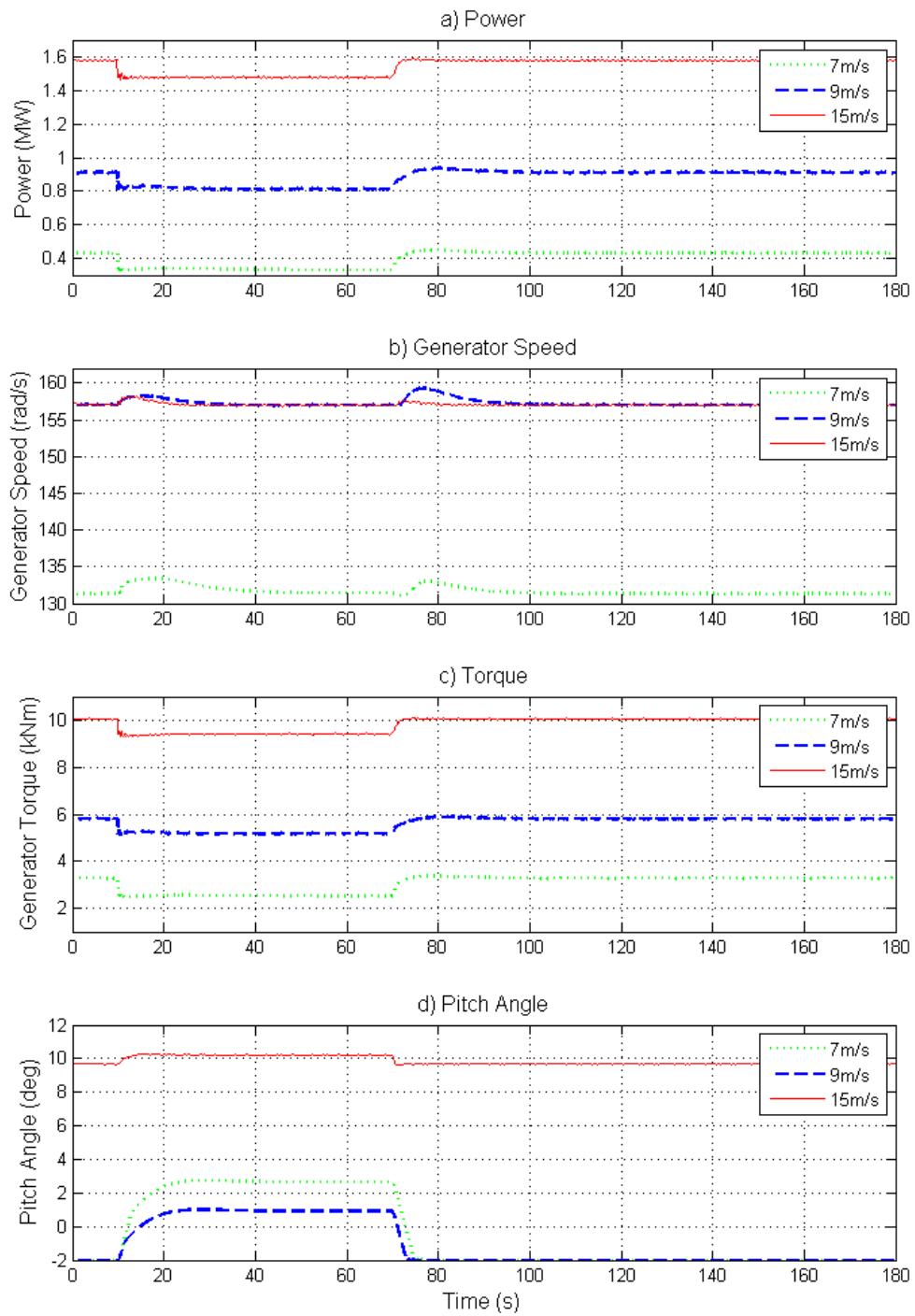


Figure 109: 1.5MW Wind Turbine with a Requested Change in Power of -100kW held for 60s

Chapter 6: Evaluation of the PAC's Performance

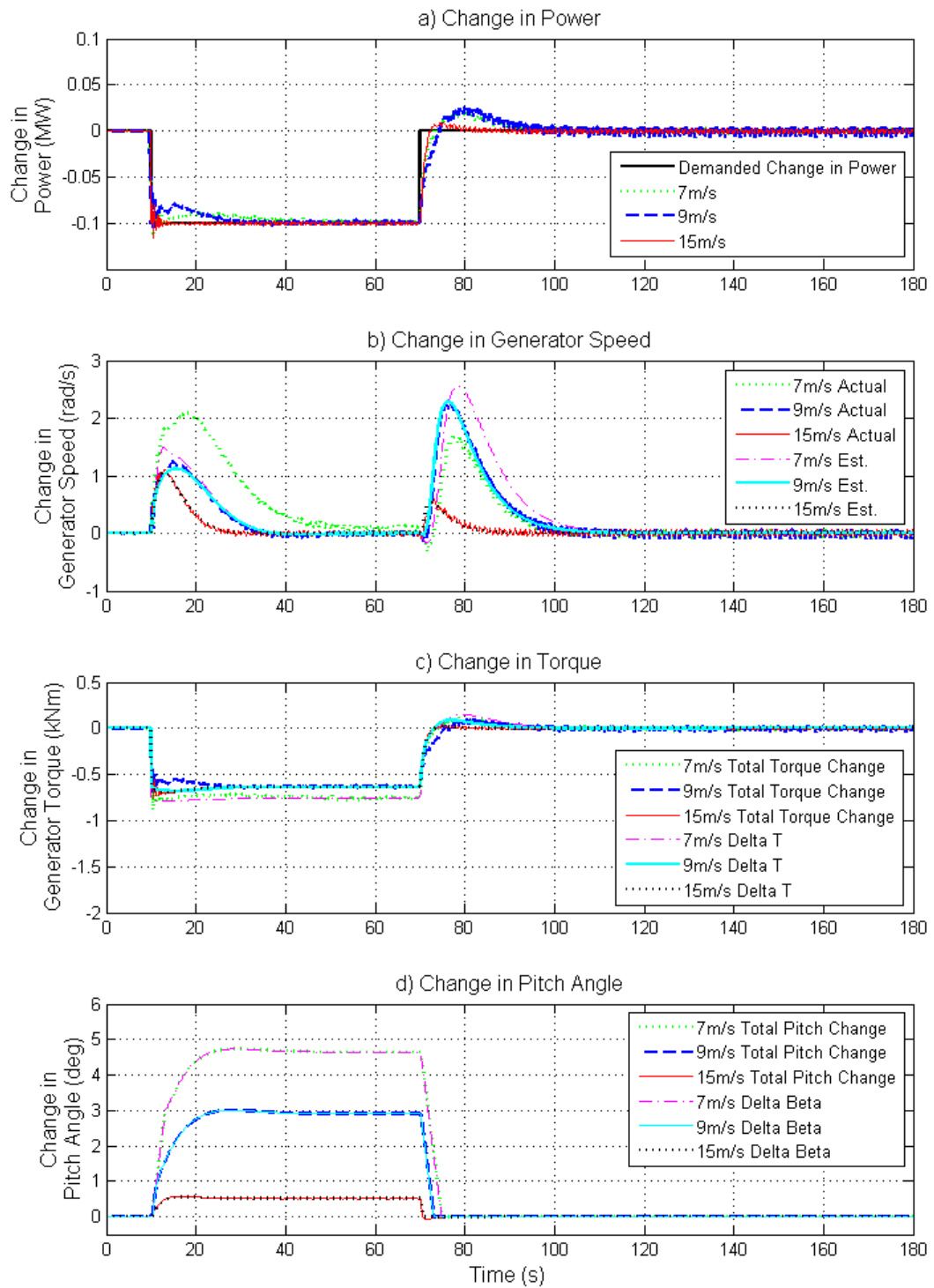


Figure 110: 1.5MW Wind Turbine with a Requested Change in Power of -100kW held for 60s – Change in Variables

Chapter 6: Evaluation of the PAC's Performance

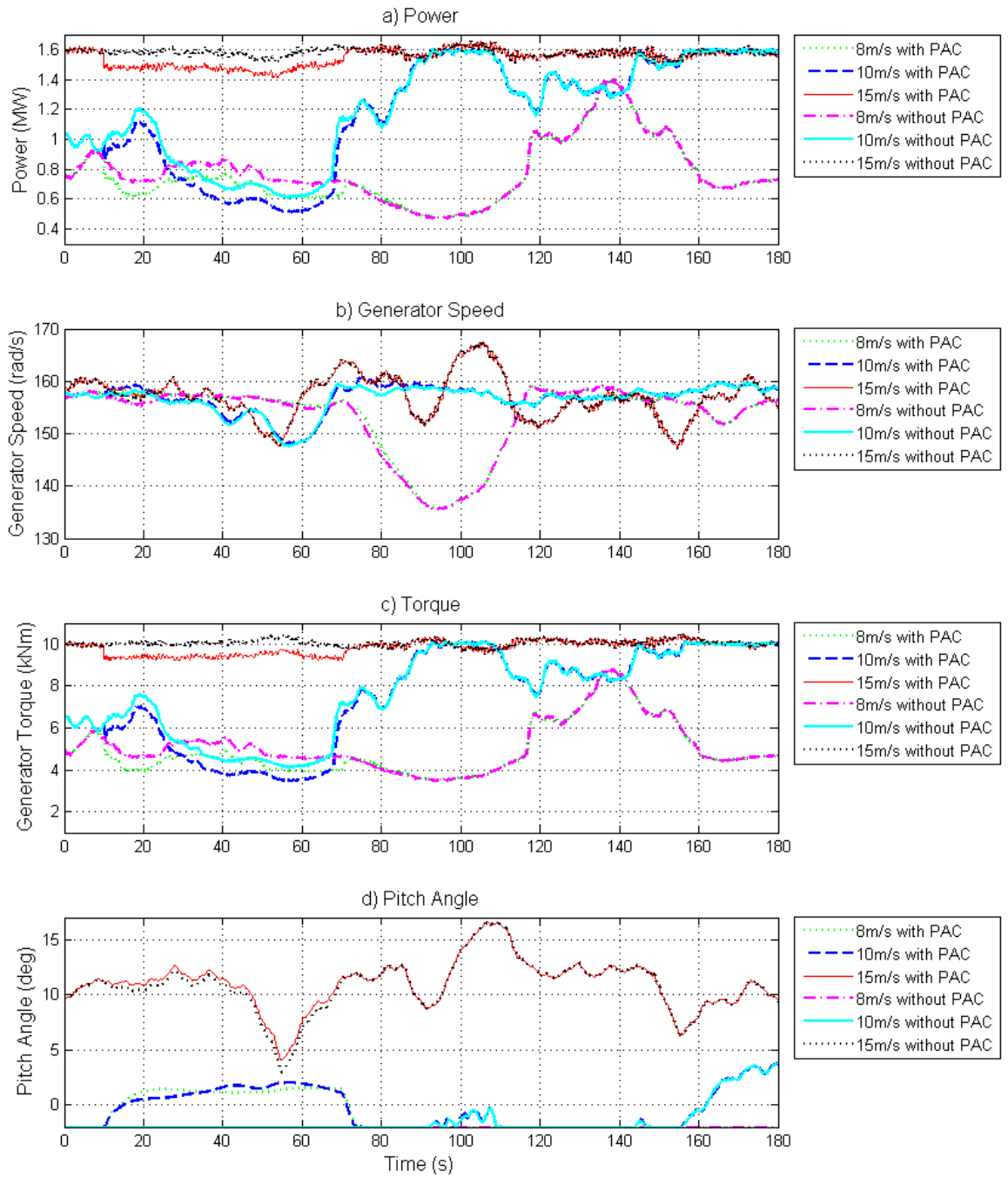


Figure 111: 1.5MW Wind Turbine with a Requested Change in Power of -100kW held for 60s

Chapter 6: Evaluation of the PAC's Performance

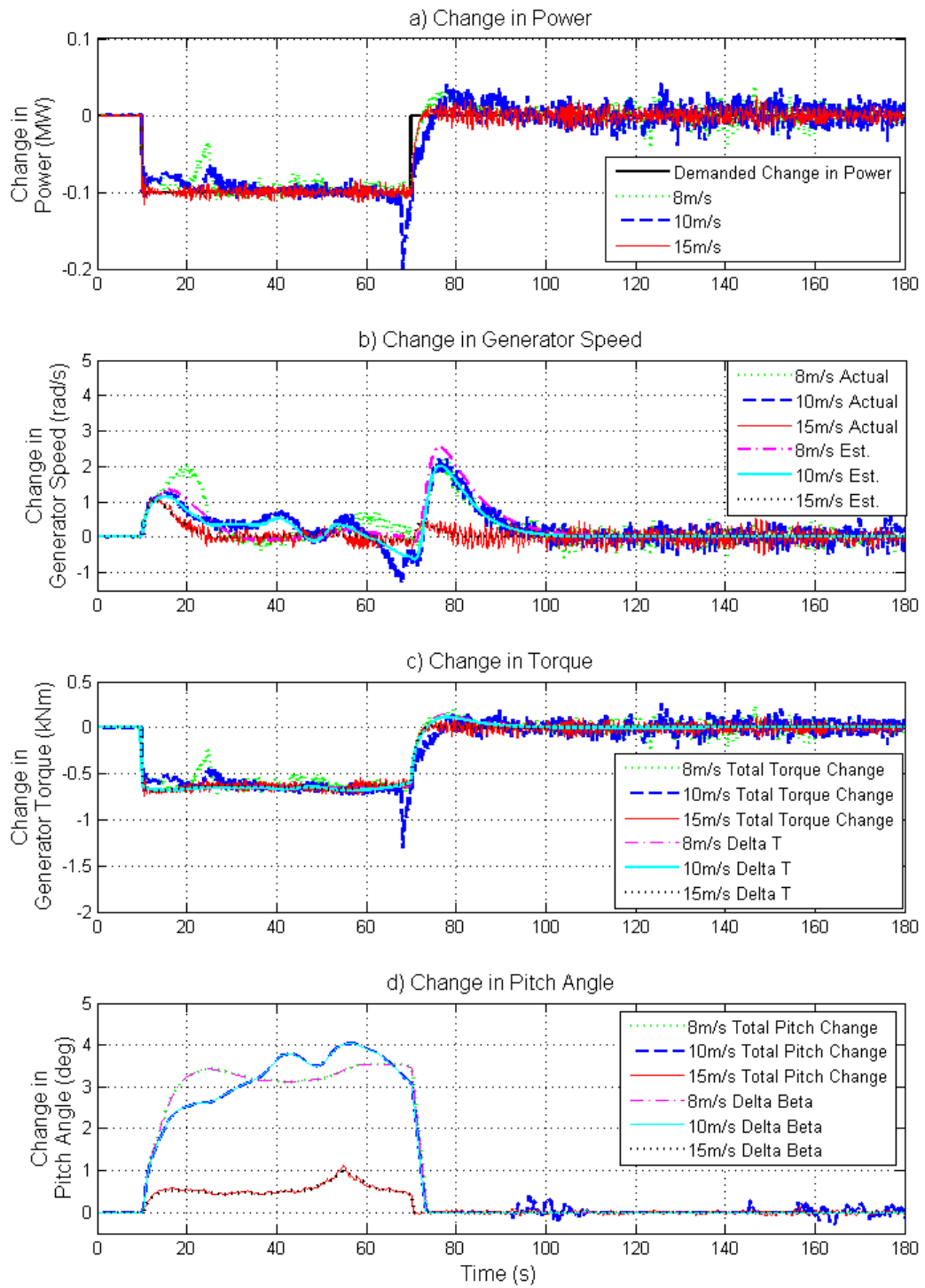


Figure 112: 1.5MW Wind Turbine with a Requested Change in Power of -100kW held for 60s – Change in Variables

Chapter 6: Evaluation of the PAC's Performance

The results of the simulations show that the accuracy of the output value of ΔP is greatly improved compared to the results where induction lag was not modelled (given in chapter 4).

Considering first the results for the constant wind speed simulations given in Figure 109 and Figure 110, the change in power (graph *a*) in Figure 110) is fairly accurate, albeit with some error for 20 to 40 seconds after the initial reduction in power output. This inaccuracy is likely still due to the dynamic inflow effects, as the error in ΔP is higher when the $\Delta\beta$ output from the PAC is greater. For the 9m/s simulation, where the turbine is in the constant speed operational region, the difference in the induction lag effect estimated by the PAC compared to that given by Bladed results in an error in the estimated change in generator speed. The error is then counteracted by the full envelope controller through generator torque in order to maintain the correct generator speed. As such, the estimated and actual change in generator speed appear very well matched (graph *b*) of Figure 110), however this is due to a change in the torque demand from the full envelope controller, as is seen by the difference between the total change in torque and the value of ΔT output from the PAC (graph *c*) of Figure 110).

In contrast, for the 7m/s simulation, where the turbine is in the max power tracking operational region, the difference between the estimated and actual change in generator speed is not counteracted in the same way by the full envelope controller. The error is seen as a change in wind speed, and in the max power tracking region this results in a change in both torque and generator speed set point. As such there is a large difference between the estimated and actual change in generator speed. There is also a change to the torque demand from the full envelope controller; however it is not as large as that produced in the constant speed region.

Similar effects are seen in the variable speed simulations. In these simulations there are also a couple of peaks in the change in power output (at approximately 23 and 68 seconds in graph *a*) in Figure 112). It should be noted that this is due to the same reasons as the peaks seen in the simulations in chapter 4 – i.e. the action of the PAC

means that the full envelope controller switches between operational modes at slightly different times, resulting in peaks when the power output without the PAC is subtracted from the power output with the PAC. It can be seen from graph *a*) in Figure 111, that there is no peak in the power output, it is merely a result of the subtraction.

The difference between the estimate of the dynamic inflow effect calculated by the PAC compared to the dynamic inflow effect calculated by Bladed is discussed in more detail in section 6.3.1.

6.3.1 Tuning the PAC to Bladed

As discussed in the previous section, there are some differences between the dynamic inflow effects calculated by the PAC and those calculated by Bladed. Bladed is a full aero-elastic model that solves the aerodynamics using annular rings, whereas the PAC models the aerodynamics using a rotor disc and this difference may have some effect on the result. The exact method used by Bladed is unknown however, as it is proprietary information belonging to Germanscher Lloyd, and as such, it is impossible to make an assessment as to the accuracy of the method used in Bladed when compared to a real turbine or compared to the method used in the PAC.

It is however, possible to “tune” the PAC to be consistent with Bladed. This is done by inserting a constant K_B into the equation for \dot{a} :

$$\dot{a} = K_B \left(\frac{3\pi}{4R} V_A \frac{1-a}{1-a_s} (a_s - a) \right) \quad (6.27)$$

Experimentation with this method using the 1.5MW wind turbine shows that a K_B value of 1.5 gives the best performance, as shown in Figure 113 and Figure 114. A similar result is found using the 5MW wind turbine, using the same value of K_B . Note that the value required is also consistent for all values of ΔP .

Chapter 6: Evaluation of the PAC's Performance

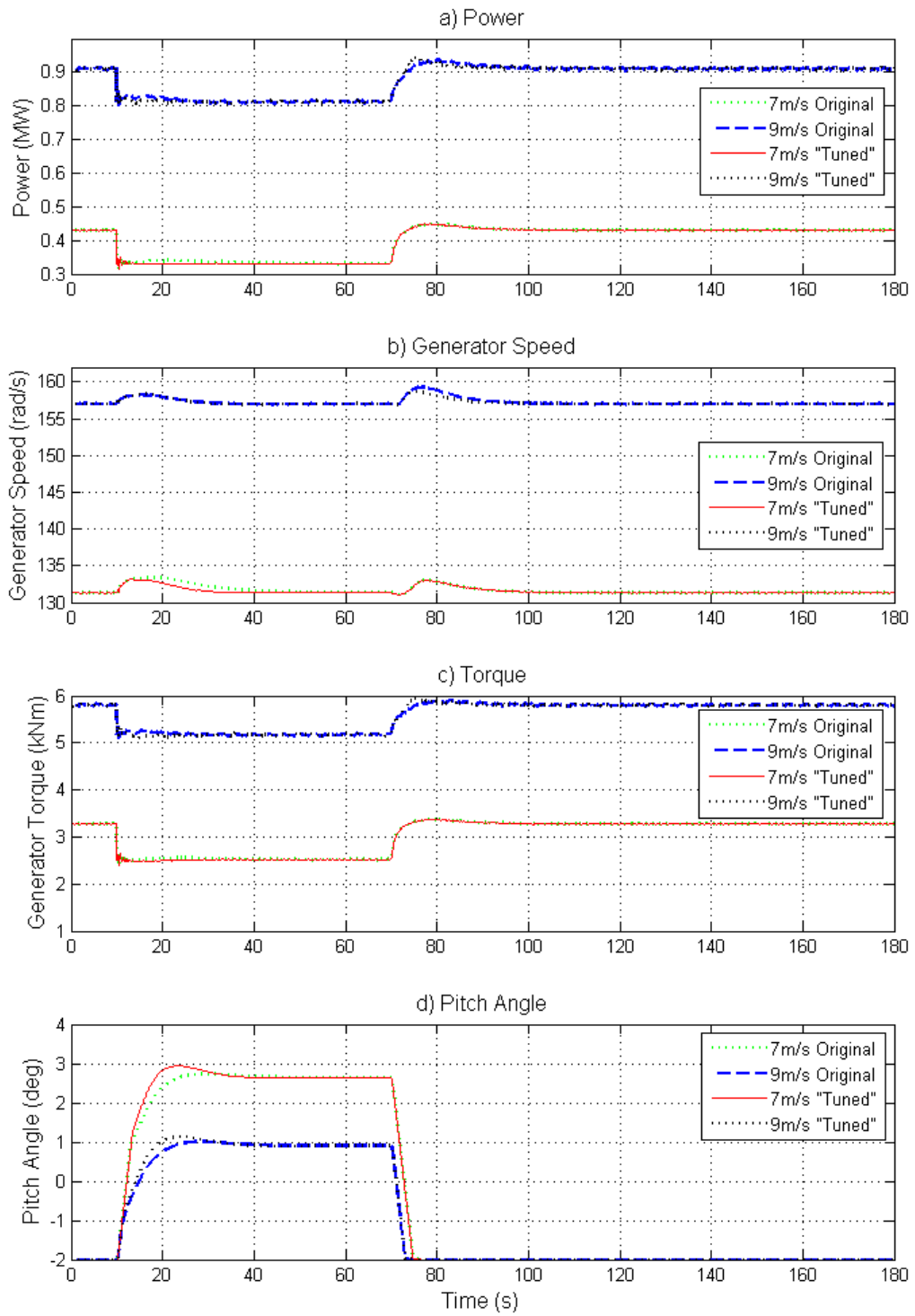


Figure 113: 1.5MW Wind Turbine with a Requested Change in Power of -100kW held for 60s - Tuned for Bladed and Original (Without Tuning)

Chapter 6: Evaluation of the PAC's Performance

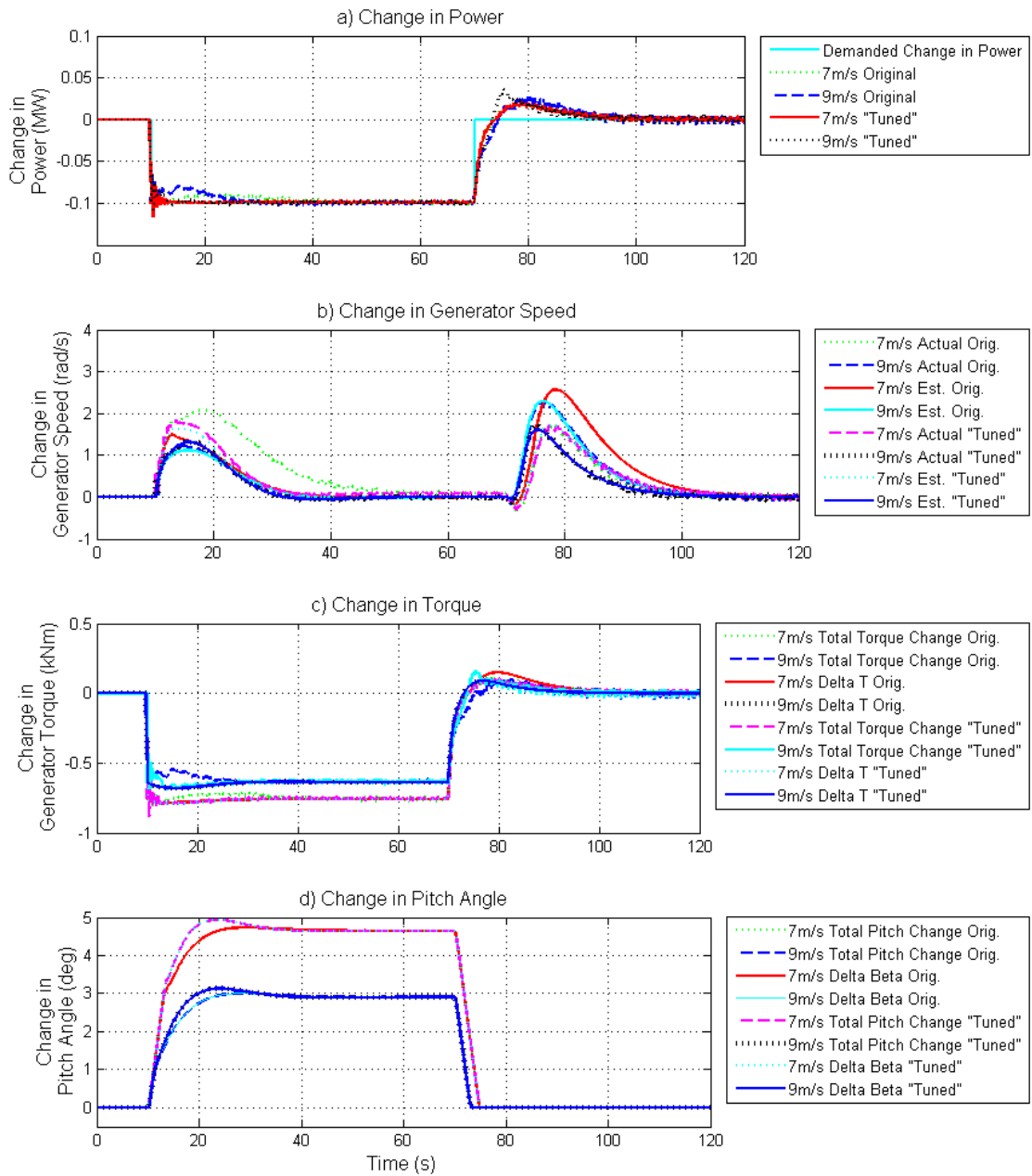


Figure 114: 1.5MW Wind Turbine with a Requested Change in Power of -100kW held for 60s - Tuned for Bladed and Original (Without Tuning) – Change in Variables

Without access to a real wind turbine, there is no way of knowing which method (that used by the PAC or that used by Bladed) gives the best approximation of the real dynamics. However, the fact that the method in the PAC can be tuned to match that used in Bladed does show that it may be possible to tune the calculation of \dot{a} to match a real turbine if required.

Future work comparing to experiments, or computational fluid dynamics could also be performed to help to tune the model.

6.4 Performance Coefficient Tables

Performance of the PAC is directly affected by the accuracy (or inaccuracy) of the performance coefficient tables used within it. An example is given in Figure 115, in which a simulation with accurate performance coefficient tables is compared with a simulation in which the performance coefficients have a consistent error of 4%.

Constant wind speeds are used for clarity of the results.

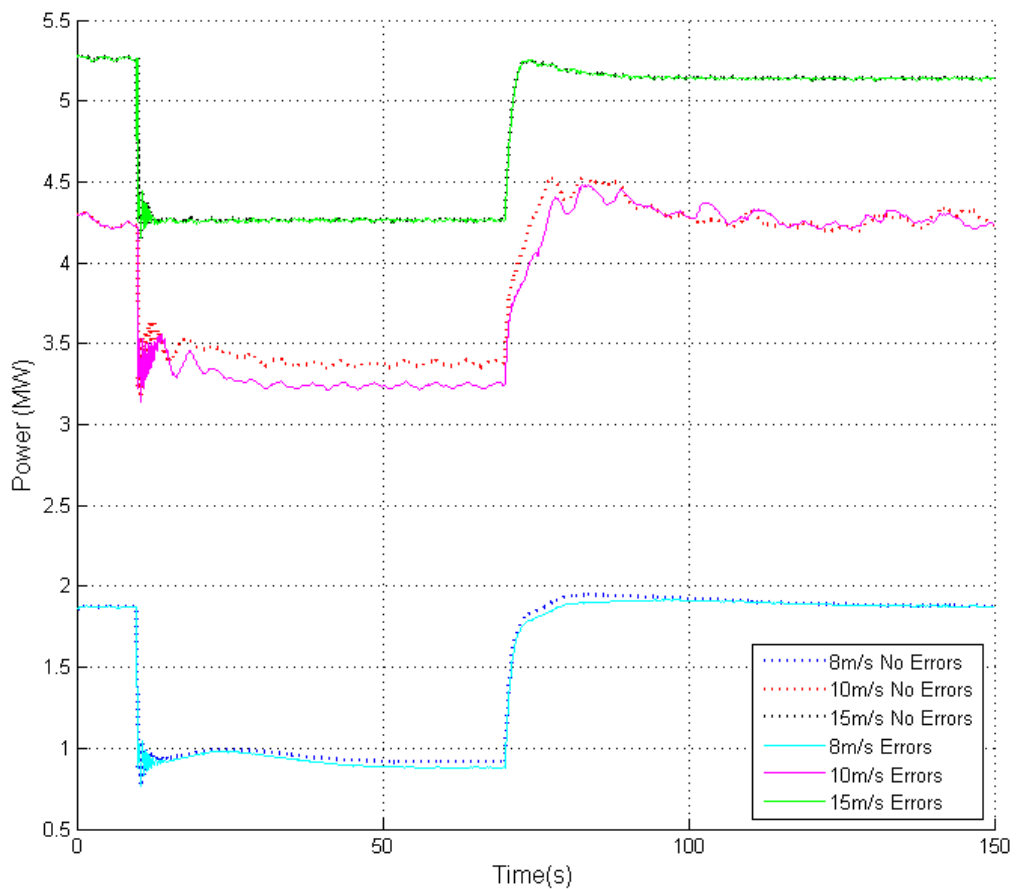


Figure 115: Errors in Power Output Caused by Errors in the Performance Coefficient Tables

Whilst the inaccuracy of the performance coefficient tables clearly leads to degradation in the performance of the PAC, the PAC still operates correctly, albeit less accurately. It is clear that the largest errors occur for the 10m/s simulation, when the wind turbine is operating in the second constant speed region below-rated wind speed. The rate of change of both the power coefficient and the thrust

coefficient is much higher in this region than in the maximum power tracking region (shown by the 8m/s simulation). This may be the reason for the particularly impaired performance. For the simulation at 15m/s (above-rated wind speed) there is little effect upon the power output. The smaller impact on performance is because any error in $\Delta\omega$ is adjusted for by the pitch demand, β_0 , from the full envelope controller, and hence the correct power output is maintained.

It should be noted that errors in performance coefficient tables would have a similar impact for all the methods proposed in the literature (see chapter 3), as all make use of performance coefficient tables.

If the coefficient tables contain errors then this could be detected through operation of the PAC and it may be possible to refine the tables through analysis of the power, generator speed, blade pitch angle, and generator torque output of the turbine.

6.5 Impact of the Use of the PAC on Loads on the Wind Turbine

As discussed in chapter 3, reducing the power output of a wind turbine is expected to reduce the loads on the turbine. Ultimately however, it is vital that the PAC should not impose *additional* loads on the turbine. Loads on a turbine can be divided into two categories, ultimate loads and fatigue loads. Ultimate loads are one off events that may damage a component/components of a wind turbine. Fatigue loads are cyclic loads that progressively damage a component/components.

The PAC may be used for a large number of different applications and so it would be impractical to attempt to model all possible uses. Instead, the following simple uses are investigated in this section:

- A sudden increase in power output (ultimate loads).
- A sudden decrease in power output (ultimate loads).
- A gradual increase in power output (ultimate loads).
- A gradual decrease in power output (ultimate loads).
- Prolonged operation with a decrease in power output (fatigue loads).

Note that as the aerodynamic and generator torques cannot be balanced for an increase in power output, prolonged operation with an increased power output is impossible and is therefore not investigated.

6.5.1 Ultimate Loads

For the ultimate load simulations, the loads on the tower, blades, and drive-train are investigated. Simulations are completed at variable wind speeds above and below-rated wind speed (8m/s and 15m/s). The turbulence level used is medium turbulence, as defined in the IEC international standard 61400-1 (third edition) [76].

6.5.1.1 Sudden Increase in Power Output

An increase in power of 100kW is requested for the 1.5MW wind turbine for 20 seconds starting at 10 seconds simulation time. The PAC is then switched off and the turbine recovers back to normal operation. The results are given in Figure 116.

It is clear that, despite a large increase in the power output being supplied, the loads on the blades in the flap direction and on the tower in the fore-aft direction during the use of the PAC are not significantly higher than the loads at other times when the PAC is not being used.

The blade flap loads decrease slightly when the PAC is first used in the 8m/s simulation (see graph *c*) in Figure 116). The reduction happens because the turbine is moving away from the maximum power tracking region and so the induction factor is necessarily reducing, resulting in a reduction in the thrust on the rotor. In the 15m/s simulation the PAC pitches the blades to increase the aerodynamic torque and hence balance the rotor and generator torques. This causes an increase in the induction factor and so a small increase in the blade flap loads is observed.

Chapter 6: Evaluation of the PAC's Performance

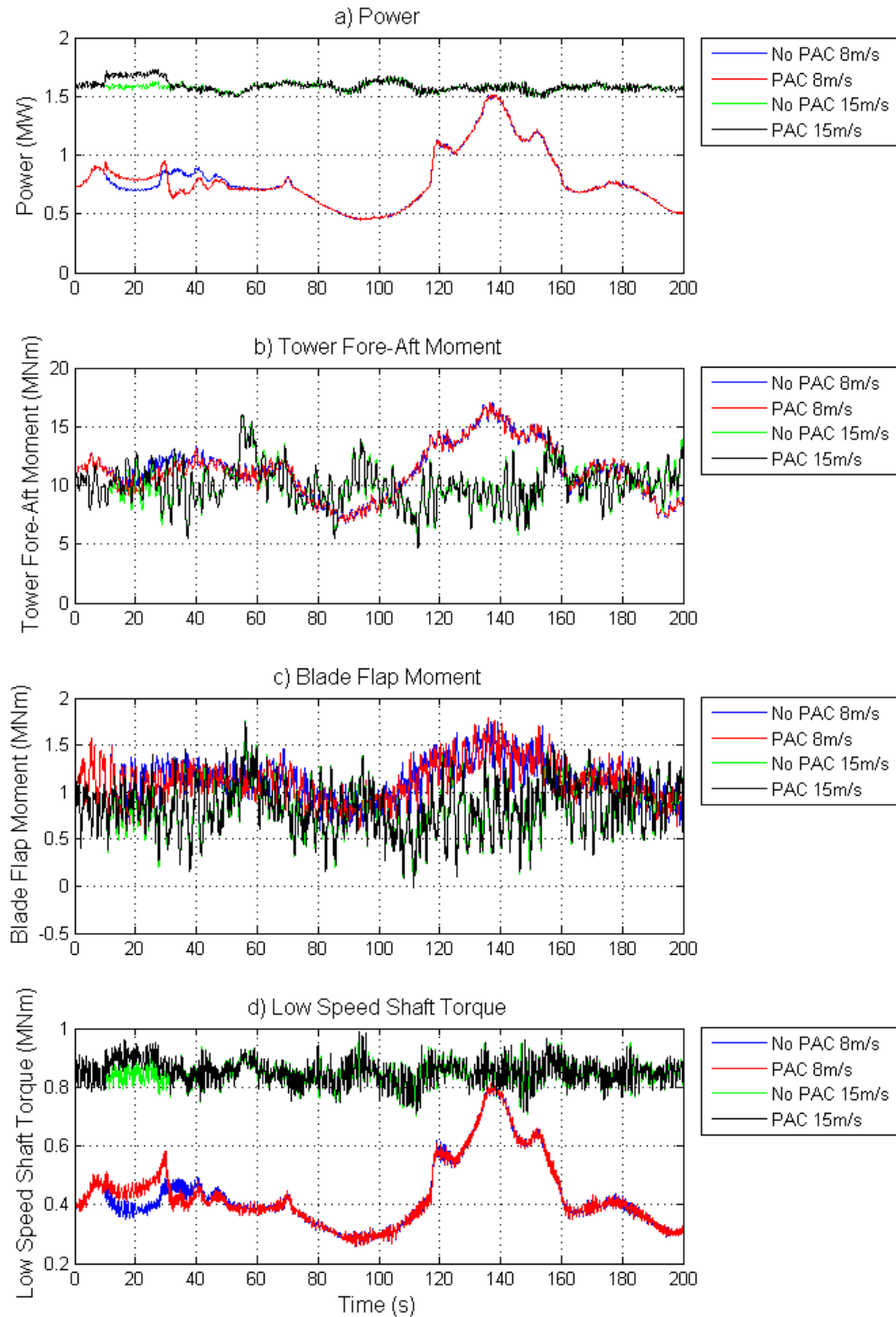


Figure 116: 1.5MW Wind Turbine with a Sudden Increase in Power of 100kW

The low speed shaft torque experiences a resonant “ringing” (i.e. a high frequency oscillation) for 2 to 3 seconds after the sharp change in torque (at 10 seconds simulation time). This is seen more clearly in Figure 117, particularly in the 15m/s simulation. Whilst the loading is not a concern as a one-off loading event, many

such events may contribute to increased fatigue. It is therefore recommended to avoid frequent sharp changes in the power output.

There is an increase in the loads on the high speed shaft when the PAC is used to provide an increase in power. The increase in loading is due to the change in the reaction torque at the generator and so a maximum torque increase could be set to limit this increase if required (limits are discussed in more detail in chapter 7). The increase is generally fairly small however and is expected to be well within the design limits of the drive train components.

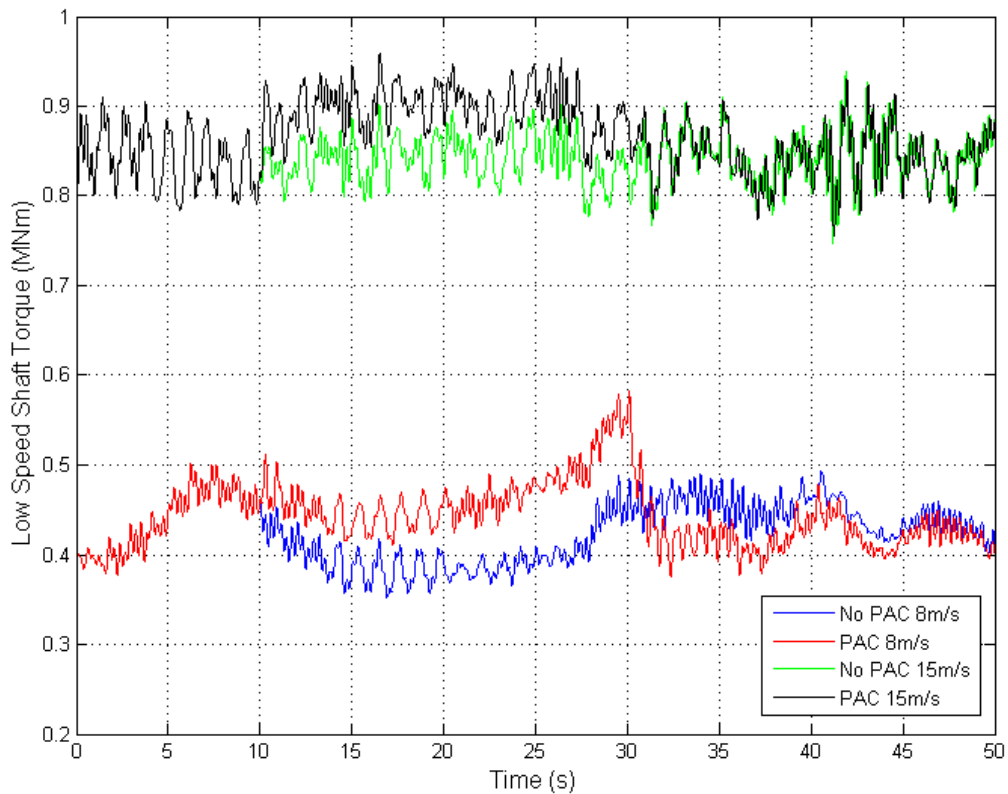


Figure 117: Zoomed in View of the Low Speed Shaft Torque During a Sudden Increase in Power

6.5.1.2 Gradual Increase in Power Output

An increase in power, linearly increasing from 0 to 100kW over 10 seconds is requested for the 1.5MW wind turbine at 10 seconds simulation time. Upon reaching 100kW, the increase is maintained at 100kW for a further 10 seconds. The results are given in Figure 118.

Chapter 6: Evaluation of the PAC's Performance

By having a gradual increase in power the rate of change of the loads on the turbine when the PAC is turned on is decreased and the “ringing” of the drive train for 2 to 3 seconds after the power increase is greatly reduced. This is seen more clearly in Figure 119.

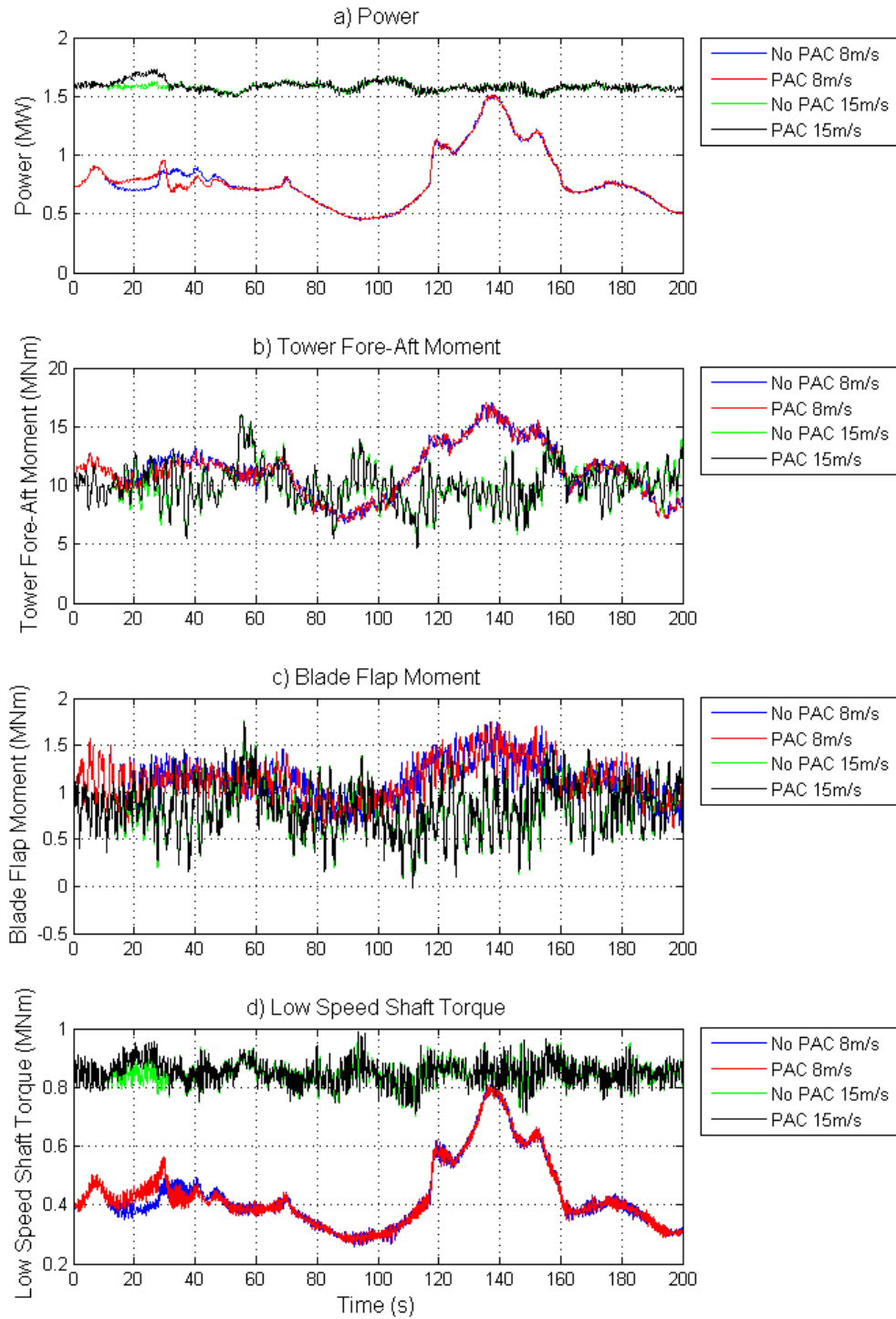


Figure 118: 1.5MW Wind Turbine with a Gradual Increase in Power of 100kW

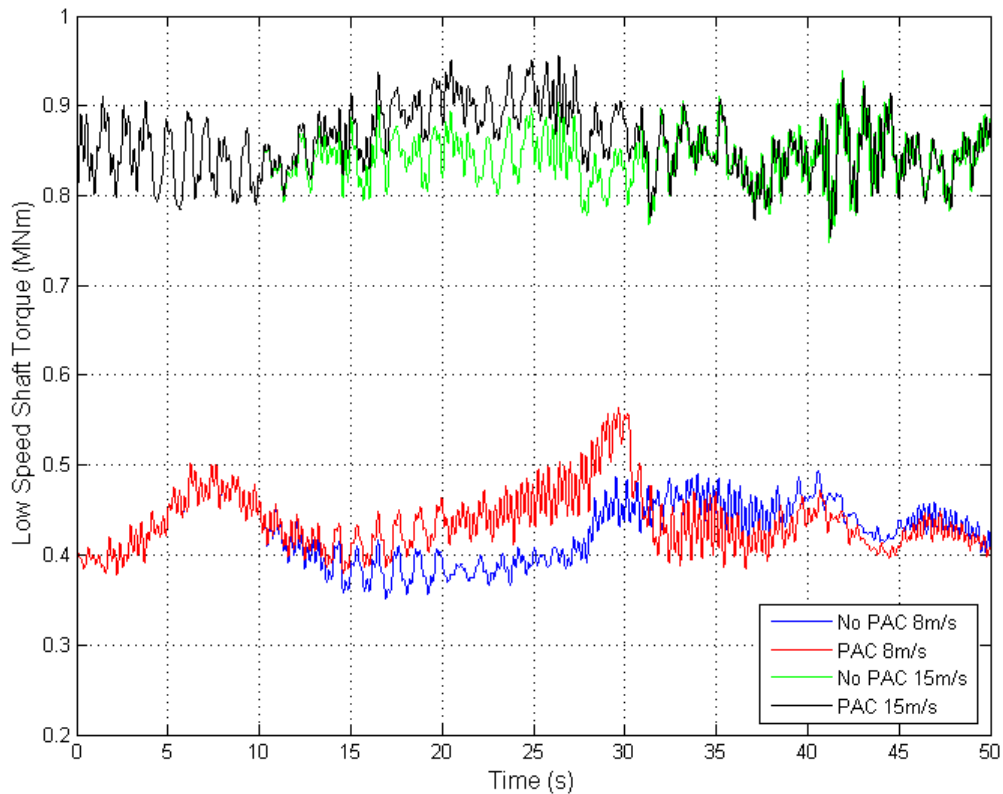


Figure 119: Zoomed in View of the Low Speed Shaft Torque During a Gradual Increase in Power

6.5.1.3 Sudden Decrease in Power Output

A decrease in power of 500kW is requested for the 5MW wind turbine at 10 seconds simulation time and held for a further 50 seconds. The PAC is then switched off and the turbine recovers back to normal operation. The results are given in Figure 120.

As with the simulations showing an increase in power demand, the loads during the use of the PAC are no worse than the loads at other times when the PAC is not being used; that is to say that the peak load is not caused by use of the PAC.

The low speed shaft torque resonates when the initial sharp change in generator torque is applied at 10 seconds simulation time. This is more clearly seen in Figure 121. The same comments as discussed for the sudden increase in torque regarding this “ringing” apply here.

Chapter 6: Evaluation of the PAC's Performance

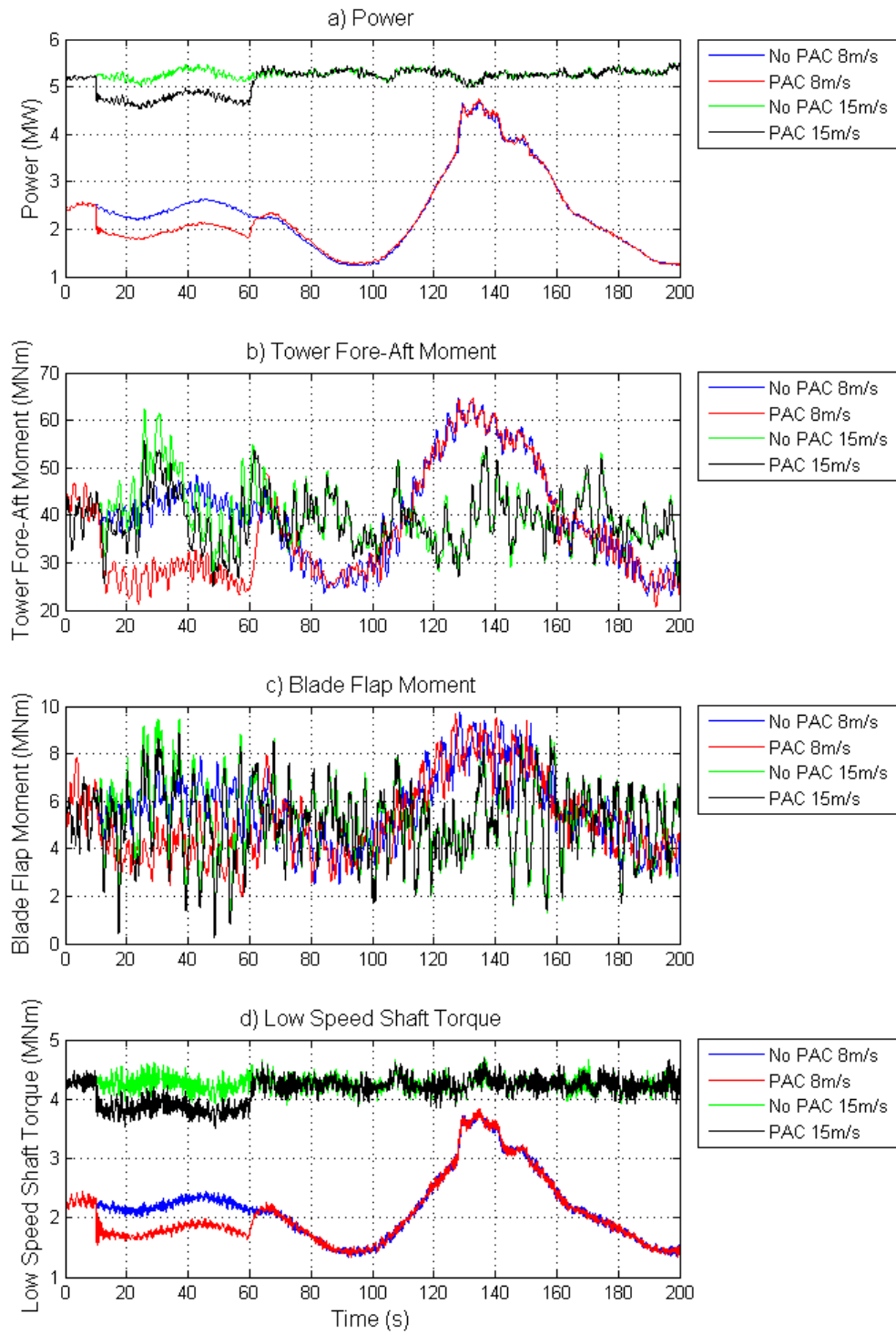


Figure 120: 5MW Wind Turbine with Variable Wind Speed with a Sudden Decrease in Power of 500kW

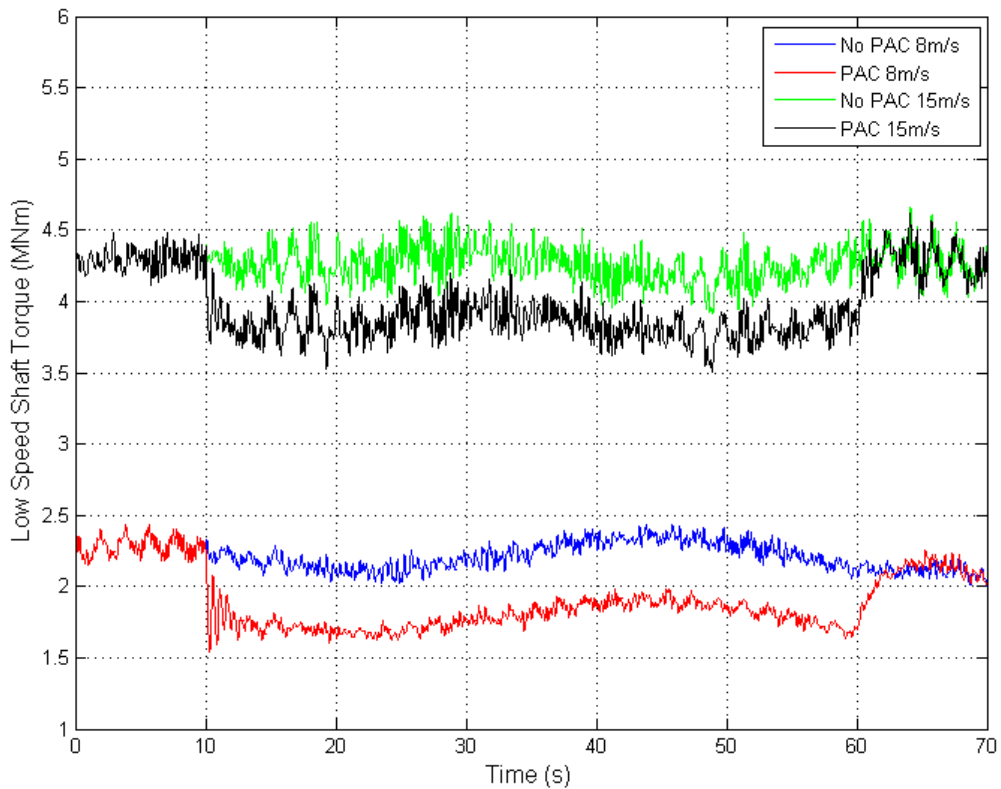


Figure 121: Zoomed in View of the Low Speed Shaft Torque During a Sudden Decrease in Power

6.5.1.4 Gradual Decrease in Power Output

A decrease in power, linearly decreasing from 0 to -500kW over 10 seconds is requested for the 5MW wind turbine. Upon reaching -500kW, it is held for a further 40 seconds. The PAC is then switched off and the turbine recovers back to normal operation. The results are given in Figure 122, with a magnified view of the low speed shaft torque shown in Figure 123.

All the loads show reductions when the PAC is operated. The resonant “ringing” present in the sudden change in power (presented in the previous section) is eliminated. The absolute value of each load when using the PAC is never higher than the highest absolute value when not using the PAC; that is to say that the peak load is not caused by use of the PAC.

Chapter 6: Evaluation of the PAC's Performance

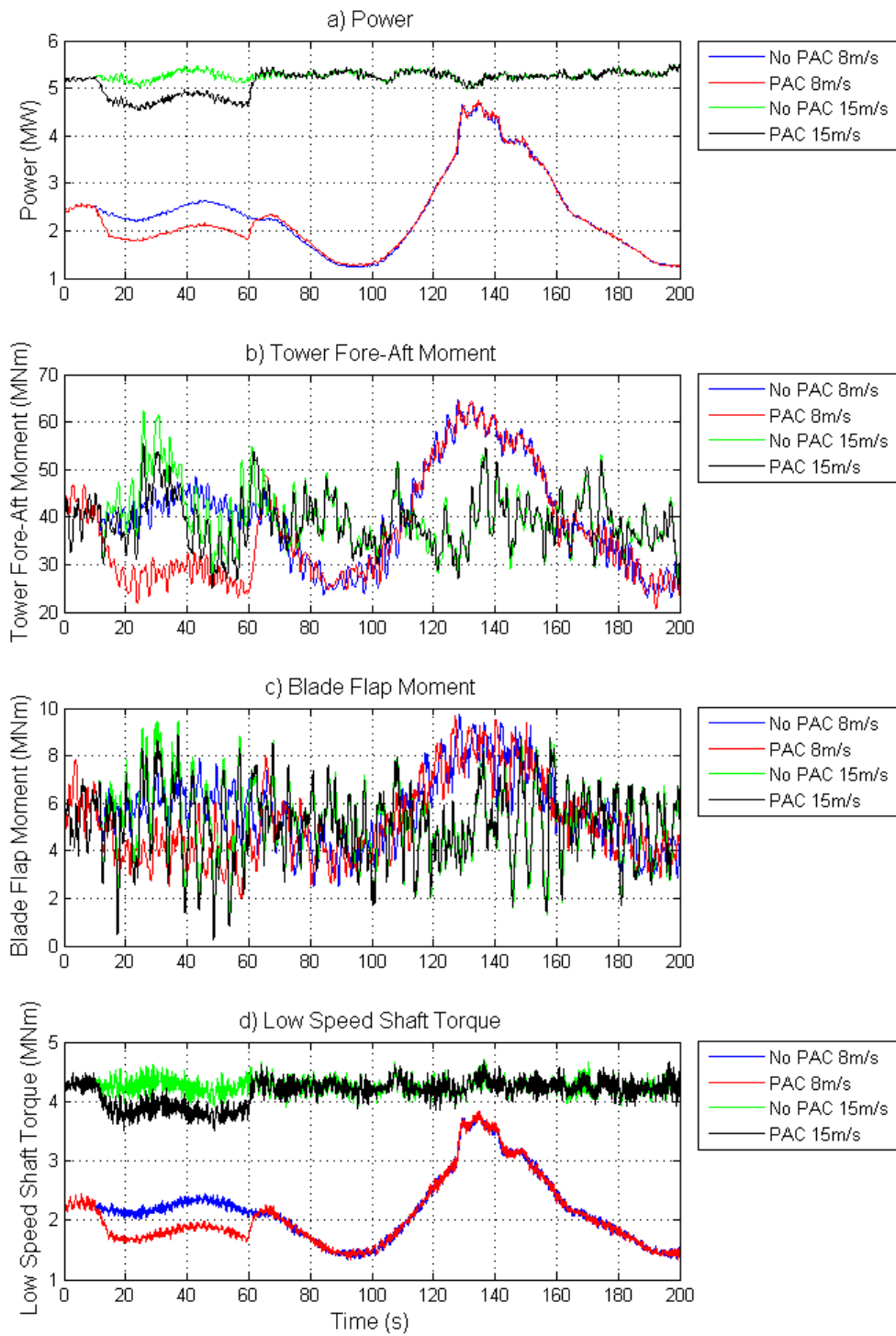


Figure 122: 5MW Wind Turbine with a Gradual Decrease in Power of 500kW

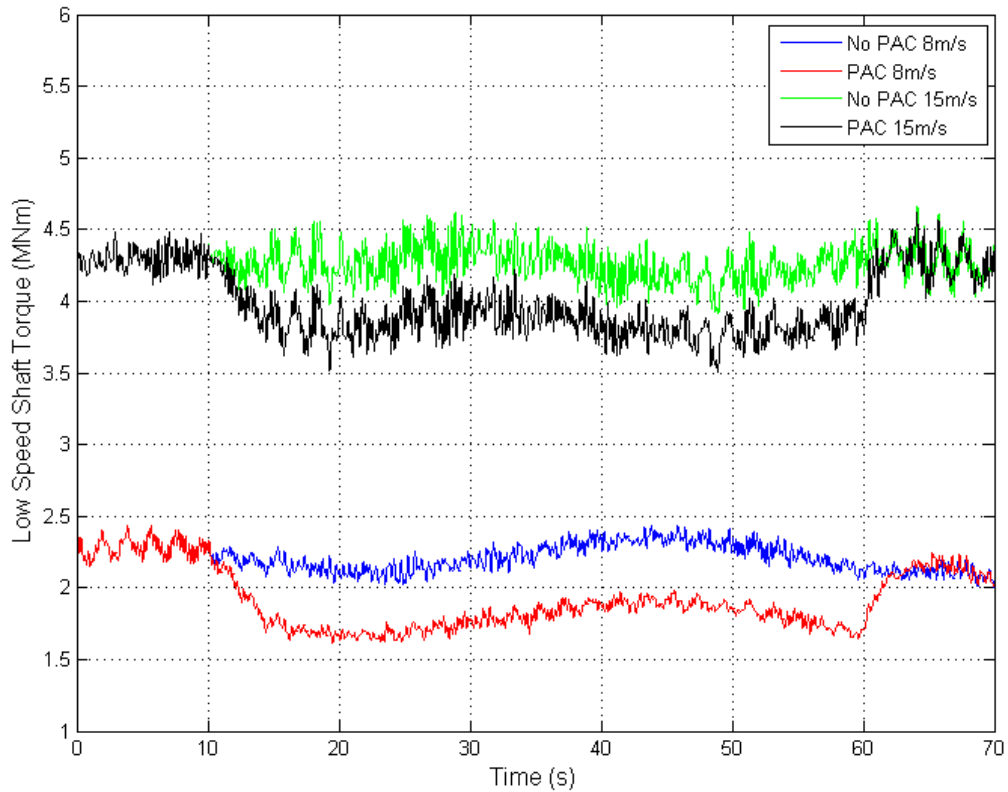


Figure 123: Zoomed in View of the Low Speed Shaft Torque During a Gradual Decrease in Power

6.5.2 Fatigue Loads

Repeated applied loads on a material causes weakening of said material and can, over time, lead to material failure. This process is known as fatigue. One method for measuring the fatigue loads of a turbine is by calculation of the Damage Equivalent Loads (DELs). DELs are calculated using rain-flow counting in the time domain in order to determine stress cycles. Wohler S-N curves and Palmgren-Minors rule are then used to convert this into a measure of material damage. The method used in this thesis is that described by Plumley [77], adapted from the work by Veldkamp [78].

For the fatigue load simulations, the loads on the tower in the fore-aft direction, blades in the flap direction, rotor hub in the yaw direction, and rotor hub in the over-turning direction are investigated. Simulations are completed at variable wind speeds across the wind spectrum from the cut in to the cut out speed.

Chapter 6: Evaluation of the PAC's Performance

Damage Equivalent Loads (DELs) are calculated for a variety of wind distributions and compared with the DELs caused by operation without the PAC.

To provide a realistic estimate of the conditions over the lifetime of the turbine, wind speed distributions and turbulence levels are defined by following the IEC international standard 61400-1 (third edition) [76]. The conditions are assumed to be class B as defined in these standards – that is medium turbulence levels. The wind speeds are assumed to follow a Rayleigh distribution as defined in the same document. There are three distributions defined, high mean wind speed (Class I, mean wind speed 10m/s), medium mean wind speed (Class II, 8.5m/s mean wind speed) and low mean wind speed (Class III, 7.5m/s mean wind speed). All of these cases are investigated. The turbulence and wind speed distribution information is tabulated in Table 4.

Table 4: Wind Speeds, Turbulence for Fatigue Load Calculations

Mean Wind Speed	Longitudinal Turbulence Intensity (%)	Lateral Turbulence Intensity (%)	Vertical Turbulence Intensity (%)
4	24.00	19.20	12.00
6	20.57	16.46	10.29
8	18.67	14.93	9.33
10	17.45	13.96	8.73
12	16.62	13.29	8.31
14	16.00	12.80	8.00
16	15.53	12.42	7.76
18	15.16	12.13	7.58
20	14.86	11.89	7.43

Chapter 6: Evaluation of the PAC's Performance

22	14.61	11.69	7.30
24	14.40	11.52	7.20

Table 5: Wind Speed Distributions for Fatigue Load Calculations

Mean Wind Speed	Percentage of Operation (Class I)	Percentage of Operation (Class II)	Percentage of Operation (Class III)
4	11.00	17.50	20.08
6	14.12	17.25	18.18
8	15.12	14.62	13.81
10	14.27	10.91	9.02
12	12.14	7.26	5.12
14	9.44	4.34	2.55
16	6.75	2.35	1.12
18	4.46	1.15	0.44
20	2.74	0.51	0.15
22	1.56	0.21	0.05
24	0.83	0.83	0.83

In order to determine the change in the fatigue loads caused by use of the PAC, a baseline measurement is made of the fatigue loads under normal operation, which is then compared to the fatigue loads when operating the PAC with a variety of different power reductions, as shown in Table 6.

Table 6: Reductions in Power for Fatigue Load Simulations

Wind Turbine	Power Reduction
1.5MW	100kW
1.5MW	200kW
1.5MW	300kW
5MW	500kW
5MW	750kW
5MW	1MW

It is assumed that the PAC is not used in mean wind speeds below 8m/s as the energy capture of the wind turbine is very low in such conditions and so a request for a reduction in power output is less likely.

6.5.2.1 Fatigue Simulation Results

The results of the fatigue load simulations described in the previous section are shown in Figure 124, Figure 125, Figure 126, and Figure 127.

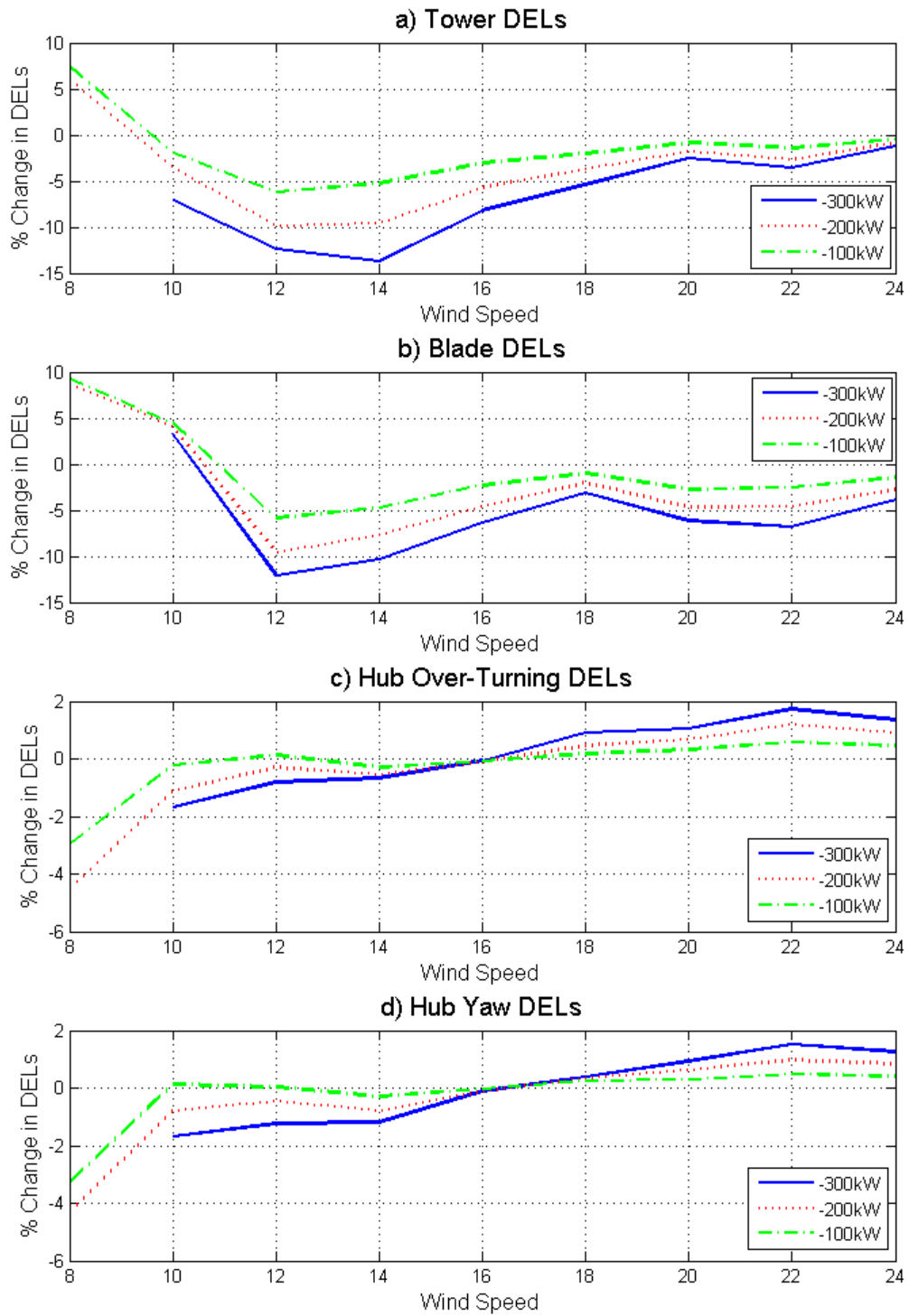


Figure 124: Percentage Change in Tower, Blade, and Hub Damage Equivalent Loads for the 1.5MW Wind Turbine

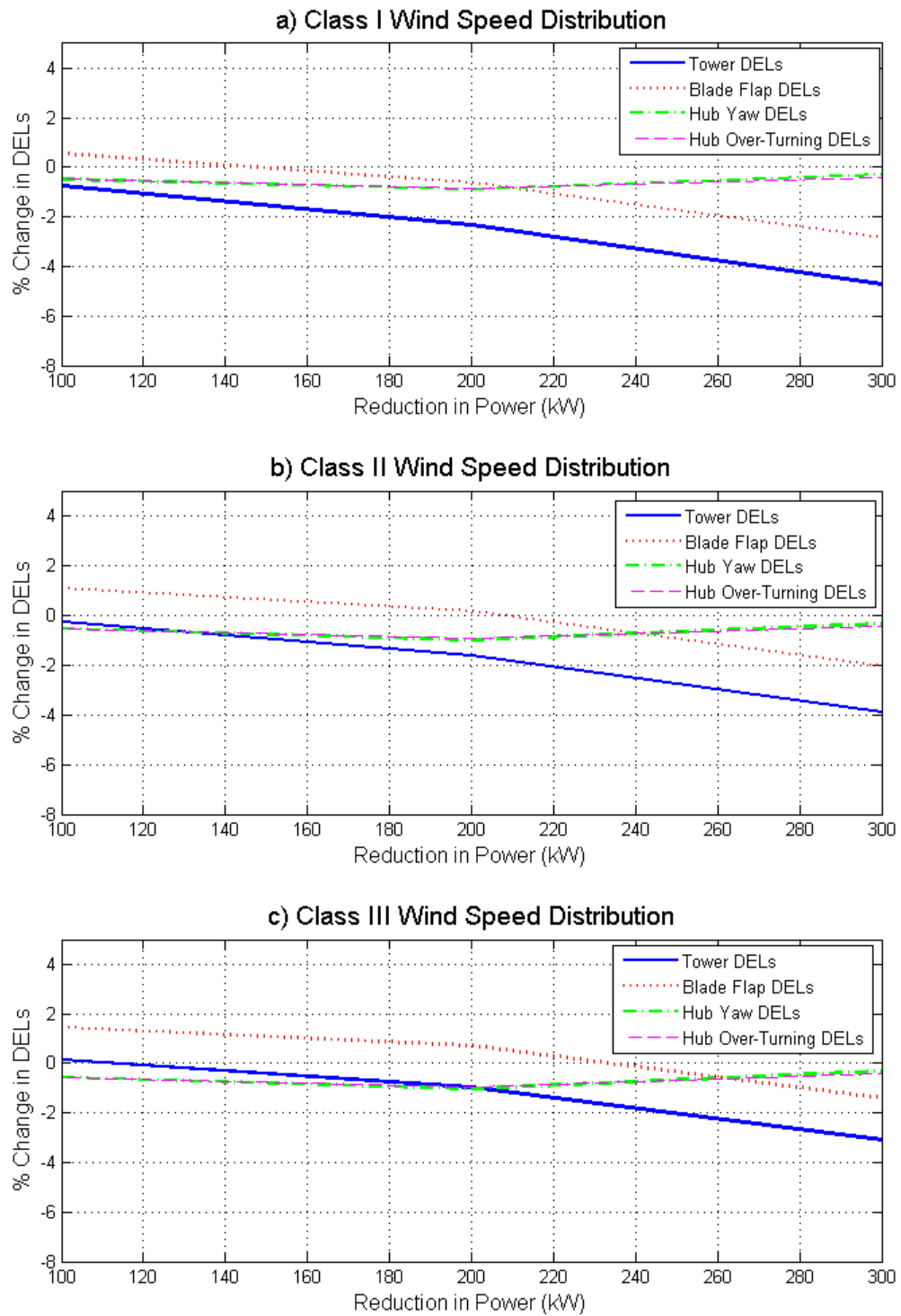


Figure 125: Percentage Change in DELs for the 1.5MW Wind Turbine

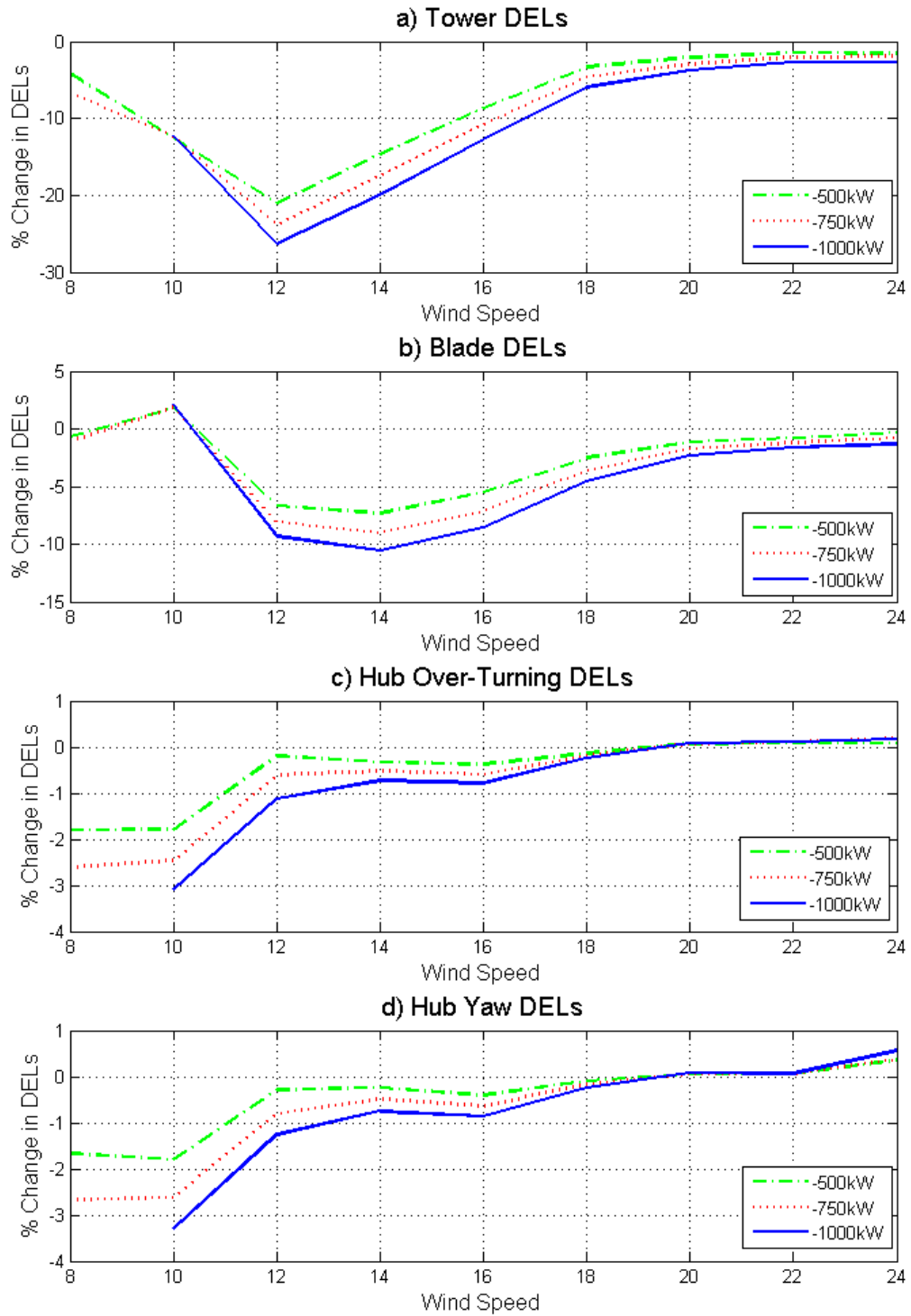


Figure 126: Percentage Change in Tower, Blade, and Hub Damage Equivalent Loads for the 5MW Wind Turbine

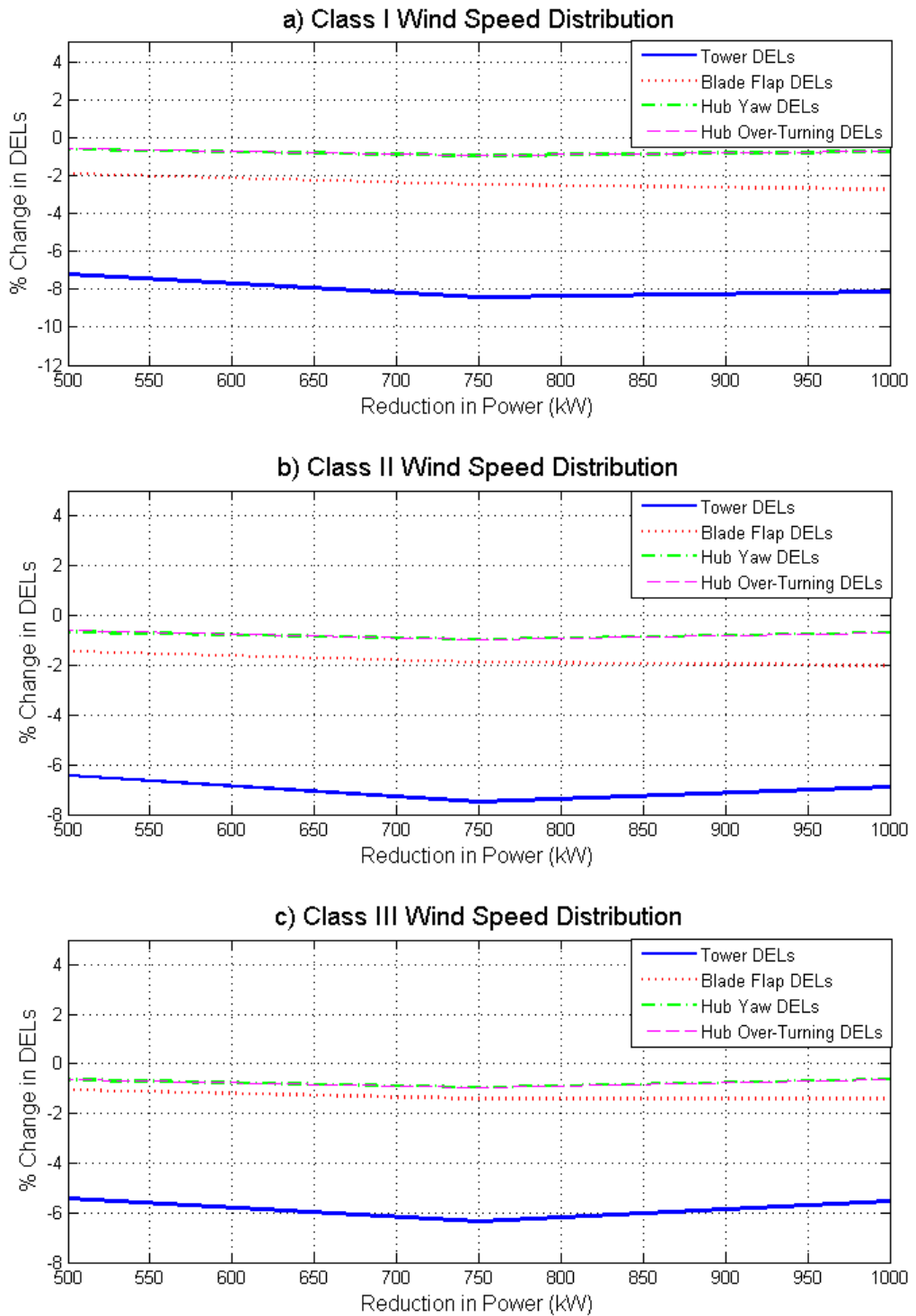


Figure 127: Percentage Change in DELs for the 5MW Wind Turbine

Simulations with the largest reduction in power in each case were not conducted for 8m/s mean wind speed, as the power output after the reduction is applied would be zero or negative for some simulations.

Chapter 6: Evaluation of the PAC's Performance

For the above rated simulations (12m/s to 24m/s) for both turbines, the damage equivalent loads for the blades and the tower are reduced for all the power reductions tested. The larger the reduction in power, the larger the reduction in the DELs. The reduction in the DELs for the tower and blades in above rated wind speeds is caused by the reduction in the induction factor due to the addition to the blade pitch angle $\Delta\beta$. The reduction in the induction factor leads to a reduction in the mean thrust on the blade, reducing the damage from each cycle and therefore reducing the DELs.

In below rated conditions however, the blade DELs for both turbines, and the tower DELs for the 1.5MW wind turbine are increased for all reductions in power.

Analysis of the spectra for blade bending moment (an example of which is shown in Figure 128) shows no added peaks from use of the PAC.

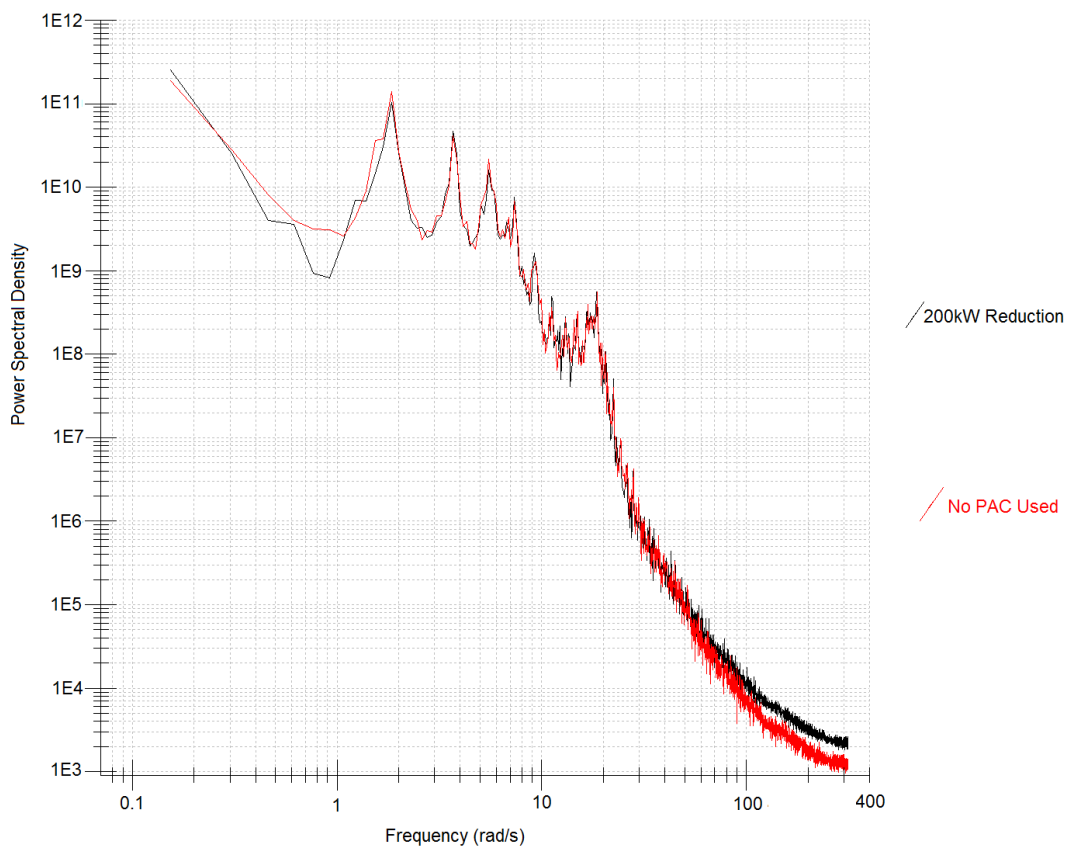


Figure 128: Power Spectral Density for Blade Bending Moment – 1.5MW Wind Turbine – Mean Wind Speed 8m/s

Analysis in the time domain (Figure 129) reveals the cause of the increase in DELs.

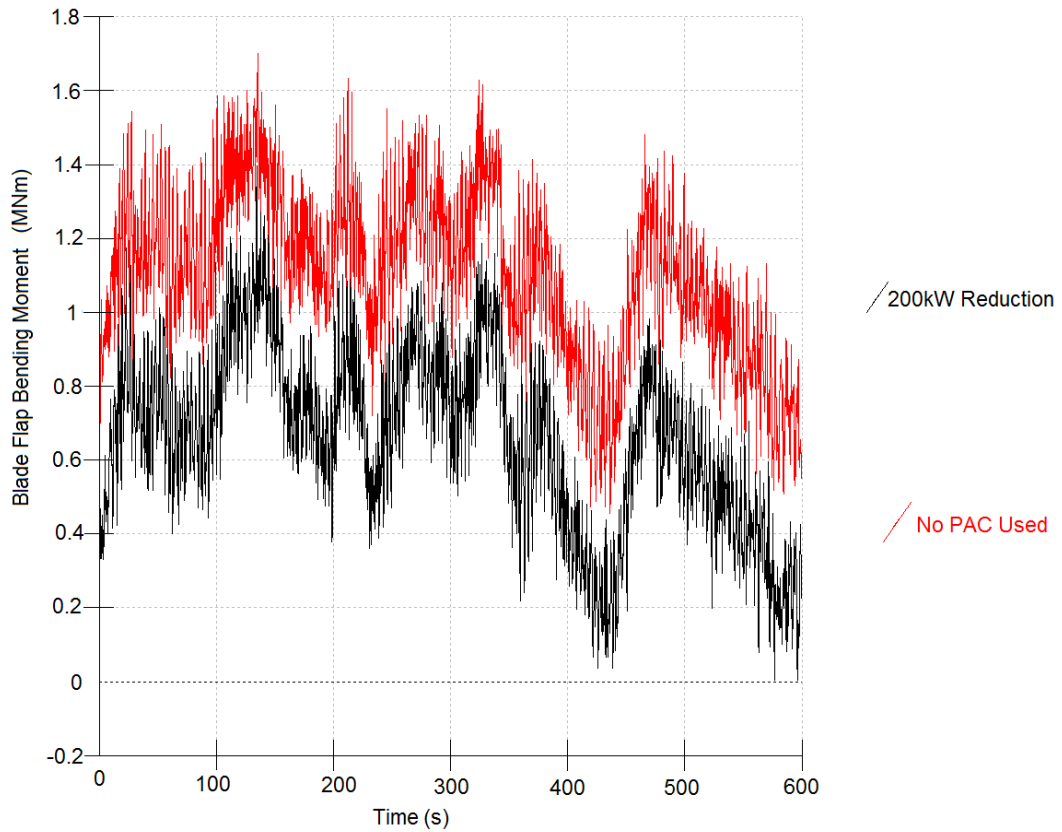


Figure 129: Blade Flap Bending Moments – 1.5MW Wind Turbine – Mean Wind Speed 8m/s

The difference between the maximum bending moment and the minimum bending moment with the PAC is approximately 1.4MNm, whereas without the PAC the difference is approximately 1.2MNm. The time between the maximum and minimum is approximately 290 seconds. The increase in the loads at very low frequencies is the cause of the increase in the DELs. The low frequency cycles can be seen in the cumulative variance graph shown in Figure 130. The offset in cumulative variance is large at the lowest frequency plotted and reduces slightly as the frequency rises.

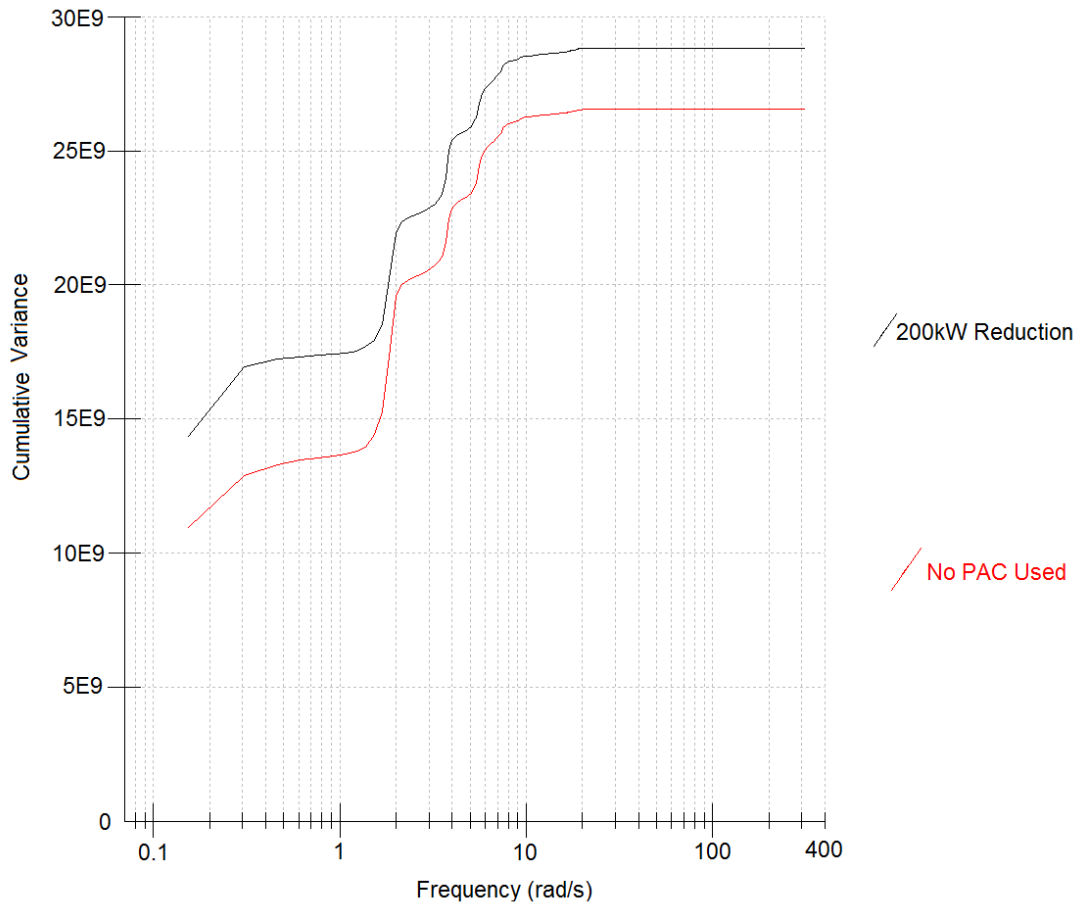


Figure 130: Cumulative Variance of Blade Flap Moment – 1.5MW Wind Turbine – Mean Wind Speed 8m/s

The underlying cause of the increase in the size of the very low frequency load cycles is the change in pitch angle, $\Delta\beta$, from the PAC. A plot of blade pitch angle and the hub longitudinal (point) wind speed, the same as that in the simulation with the PAC in Figure 129, is shown in Figure 131 (note that for the simulation without the PAC the blade pitch angle is always at the minimum pitch of -2 degrees and the wind speed is identical).

The peak in blade loads observed in Figure 129 coincides with the peak in hub wind speed, at which time the blade pitch angle is at its minimum. When the blade loads reach their minimum, the blade pitch angle is at its maximum. As the blade is pitching to feather, the loads at low wind speeds are therefore reduced by a greater amount than at high wind speeds; increasing the range of the loads across the cycle, which increases the DELs. The increase in the tower loads is a consequence of the

described blade loads, as the thrust on the blades is transmitted into the structure of the tower.

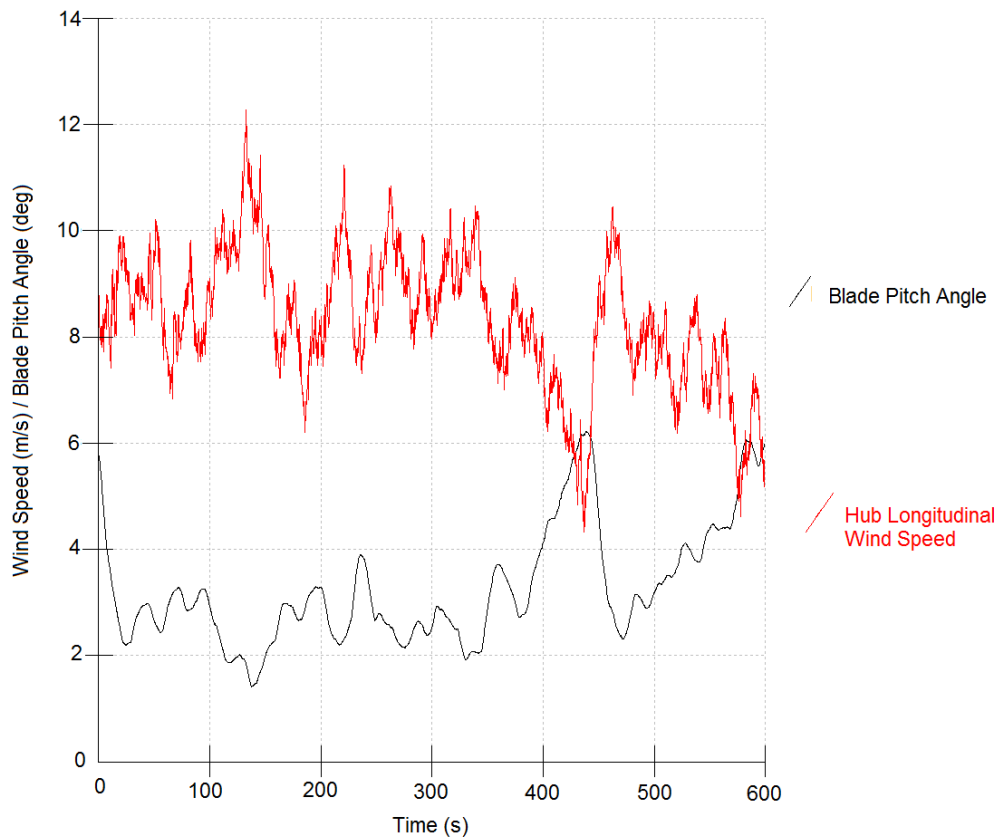


Figure 131: Blade Pitch Angle – 1.5MW Wind Turbine – Mean Wind Speed 8m/s

The reduction of the pitch angle at high wind speeds and the increase of the pitch angle at low wind speeds is a requirement to balance the aerodynamic and generator torques. As such the increase in the range of the load cycles at very low frequencies is unavoidable and is not particular to the PAC. Any controller that reduces the power output of a wind turbine and balances the torque using pitch action will encounter the same effect. A corollary of this effect can be observed in the very simple case explored in chapter 3 (Figure 21), where a constant pitch was applied. In the case of constant pitch the resultant change in power output was not constant, as operation at different wind speeds requires a different pitch angle to achieve the same change in power.

By contrast, the reduction in the mean blade loads (clearly observed in Figure 129) acts to reduce the DEL. The net change in DELs is dependent upon the cumulative effect of both the increased range of the very low frequency loads and decreased mean of the blade loads. For the 5MW wind turbine the reduction in the blade and tower DELs due to the reduced mean load outweighs the increase in DELs due to the increased range of the very low frequency cycles.

The hub DELs in both the yaw and over-turning direction are either reduced or see a small increase. The small increase only occurs at high wind speeds, whilst the decreases are larger and at more common, lower wind speeds. As such, the lifetime DELs for the hub are reduced for all cases.

In higher average wind speed distributions such as wind speed distribution class I, the wind turbine spends more time in above rated operation and less time in below rated operation than in lower average wind speed distributions and so the blade and tower lifetime DELs are reduced the most. In general, the greater the reduction in power output, the greater the reduction in blade and tower lifetime DELs. For the 5MW wind turbine the tower, blade, and hub lifetime DELs are all reduced for all wind speed distributions. For the 1.5MW wind turbine hub lifetime DELs are reduced for all wind speed distributions, the tower lifetime DELs are reduced for all but the smallest reduction in power coupled with wind speed distribution III, whilst the blade DELs either have an increase or a decrease (between -1.8% and 1.8%) depending upon the wind speed distribution.

6.6 Concluding Remarks

In this chapter the Power Adjusting Controller's performance is evaluated. First the controller is discretised for use in the full aero-elastic modelling simulation package GL Bladed. As part of the discretisation process an anti-wind up loop is applied to the pitch demand from the PAC, $\Delta\beta$.

Simulations conducted using GL Bladed show reduced accuracy compared to the simulations conducted using Simulink (presented in chapter 5). The reduced accuracy is hypothesised to be due to differences in the method used to calculate the

dynamic inflow effects in GL Bladed compared to that used in the PAC and in the lumped parameter Simulink model (discussed in chapter 5). The detail of the method used by GL Bladed to calculate the dynamic inflow effects is not publically available, and so it is impossible to compare the two methods. It is noted that including a constant multiplier in the equation used in the PAC to find the induction factor a allows the PAC to be “tuned” to more closely match GL Bladed. As the method used in GL Bladed is not clear, it is not possible to investigate this relationship further, however it does leave open the possibility of tuning the PAC to a real wind turbine if similar differences in the dynamic inflow effects are found.

The effect of consistent errors in the performance coefficient tables is investigated. Although the change in power output is found to be less accurate, no other effect on the performance of the PAC is noted.

The impact of operating the PAC on both the ultimate loads on the wind turbine and the wind turbine fatigue loads is investigated. Any increase in the the peak load on the wind turbine tower (in the fore-aft direction), the blades (in the flap direction), or the drive train (low speed shaft torque) is small and likely to be well within the design limits of the relevant components. Sudden changes in power output result in some resonant “ringing” (high frequency oscillation) of the drive train, gradually changing the power output eliminates this effect.

The DELs for both turbines are investigated for a range of power reductions and wind speeds. For the 5MW machine operating with a reduced power via the PAC, the tower fore-aft DELs are reduced for all power reductions at all wind speeds and the blade flap DELs are reduced at all wind speeds except 10m/s. For the 1.5MW turbine the tower fore-aft DELs are reduced for all power reductions at all wind speed except 10m/s and the blade flap DELs are reduced at all power reductions at all above rated wind speeds. The hub DELs in both the yaw and over-turning direction are either reduced or see a small increase. The small increase only occurs at high wind speeds, whilst the decreases are larger and at more common, lower wind speeds. As such, the lifetime DELs for the hub are reduced for all cases.

Chapter 6: Evaluation of the PAC's Performance

The cause of the lesser reduction and/or increased blade flap and tower loads in below rated operation are found to be due to very low frequency cycles in which the range of the loads is increased at low wind speeds due to the required increased use of the pitch actuator.

Chapter 7:

PAC Supervisory Rules

WIND TURBINES ARE designed to operate within a set operational envelope defined in terms of the aerodynamic torque and the rotor speed. Outside of this set operational envelope the turbine may encounter load cases that it is not designed to withstand, resulting in increased loads that may in turn lead to damage to the machine.

The PAC supervisory rules described in this chapter are a set of limits and flags designed to ensure that the wind turbine cannot operate outside of a predefined safe operating envelope on the torque-speed plane. The flags and limits applied within the PAC are designed allow the PAC to be easily incorporated into a wind farm control hierarchy such as that proposed in chapter 3. The diagram for this structure is repeated here in Figure 132 for clarity. Please see section 3.7 for a detailed overview of the reasoning behind this structure.

A summary of the PAC supervisory rules is presented in Appendix V.

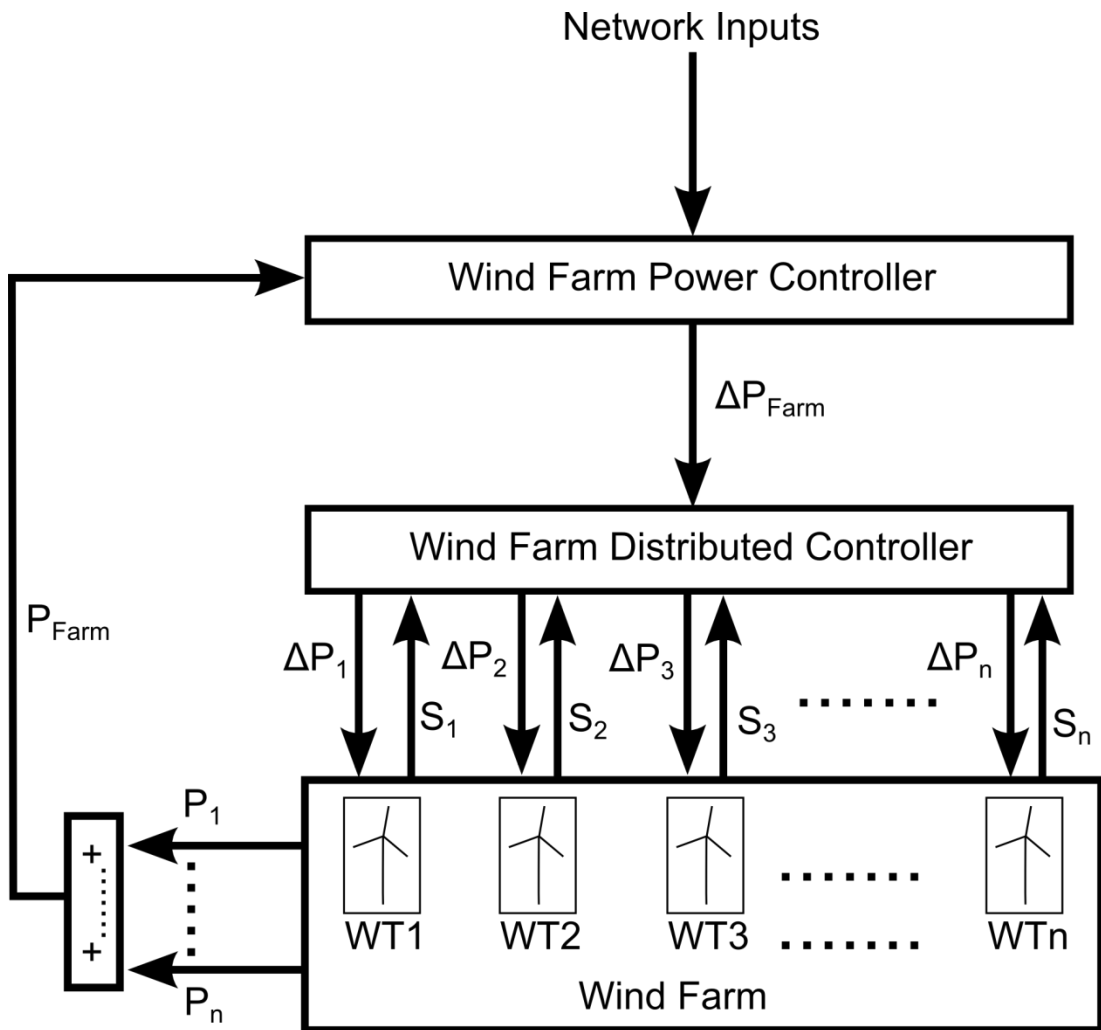


Figure 132: Hierarchical Controller Structure

Before looking in more depth at this issue, some common terms are defined:

- Torque-Speed Plane – A graph with the axis of rotor/generator speed and rotor/generator torque.
- Safe Operational envelope – The region on the torque-speed plane, defined as an acceptable region for the wind turbine to operate by the designer.
- Operating point – The specific point on the torque-speed plane at which the wind turbine is operating at a given moment in time.
- Operating Strategy – The locus of operating points that the wind turbine’s full envelope controller is tracking.

Chapter 7: PAC Supervisory Rules

- Limit – A mechanism put in place that prevents the PAC from causing the wind turbine to operate in an unacceptable region, i.e. a region outside of the operational envelope.
- Flag – A Boolean, which alerts the operator to a given behaviour. For example, the activation of a limit or movement from one area of operation to another. The notation for a flag in this chapter is the name of the flag in capitals, for example: REJECTION
- Sub-Flag – A Boolean, which is used to give additional information regarding the flag issued. The notation in this chapter is the name of the sub-flag in bracketed italics. For example: REJECTION (*Limit*).

(Note that a full list of the flags and sub-flags is given in Table 7 in section 7.5.5)

As described in chapter 4, the PAC necessarily moves the turbine's operating point away from the defined operating strategy when it is used. As a result, there is a risk that the turbine may enter an operational region on the torque-speed curve that is outside of the safe operational envelope, and, to avoid this, limits must be imposed on the operation of the PAC.

In addition, when the PAC is used as part of a larger wind farm control system it is useful for the operator to be alerted if the turbine is operating in certain regions, especially if the turbine is likely to move towards a limit. The wind farm operator then decides if action needs to be taken to move the turbine back towards the normal operating strategy.

As such, the limits placed on the turbine are broken down into two categories:

- 1- "Hard" limits that are dependent upon the physical properties of the turbine and are not allowed to be exceeded.
- 2- "Soft" limits that may give rise to action by the WFDC

If a hard limit is activated then the PAC immediately takes remedial action to prevent the limit being exceeded and sends a flag to the WFDC.

If a soft limit is exceeded then the PAC sends a flag to the turbine wind farm controller, which may or may not then take remedial action depending upon its own inputs.

It is important to also consider any supervisory control that may already be applied to the wind turbine, to ensure that operation of the PAC is not restricted by said rules and that any PAC rules do not conflict with the current supervisory control measures.

7.1 The Recovery Process and the Rejection Flag

The recovery process as described in Chapter 4 is utilised whenever the PAC is turned off. When the PAC is in recovery mode the RECOVERY flag is set by the PAC. A fast or slow recovery is requested by the WFDC. The PAC then sets either the (*Recovery Fast*) or (*Recovery Slow*) sub-flag. When the (*Recovery Fast*) sub-flag is set a fast recovery is used, when the (*Recovery Slow*) sub-flag is set a slow recovery is performed. The default setting is fast recovery. The difference between these speed settings is discussed in section 4.5. When the recovery process is completed the (*Recovery Complete*) sub-flag is set.

The recovery process is driven primarily by the PAC ON flag. The PAC ON flag is set when the PAC is switched on. The flag is reset to 0 when the PAC is switched off, which starts the recovery process. In addition, limits within the PAC may force the PAC into recovery mode, and set the PAC ON flag to 0.

In cases where the requested ΔP value from the WFDC cannot be delivered, the REJECTION flag is set by the PAC, accompanied by a sub-flag detailing the reason. When the PAC is in recovery mode, if a request for ΔP is received then the REJECTION (*Recovery*) flag and sub-flag are set.

7.2 Hard Limits on the Provision of a Change in Power Output (“Black Limits”)

The safe operational envelope of a wind turbine is bound by the hard limits, also referred to as black limits. The safe operational envelope for one wind turbine may be very different from that of another. In general however, for variable speed, pitch

regulated horizontal axis wind turbines; there are some limits that apply to every turbine.

The hard limits that define the operational envelope are divided into two categories, those that are a rotor torque limit, and those that are a rotor speed limit. These limits are displayed graphically in Figure 133. All hard limits are set in collaboration with the wind turbine manufacturer and once the boundaries are set it is not possible for the operator to alter them.

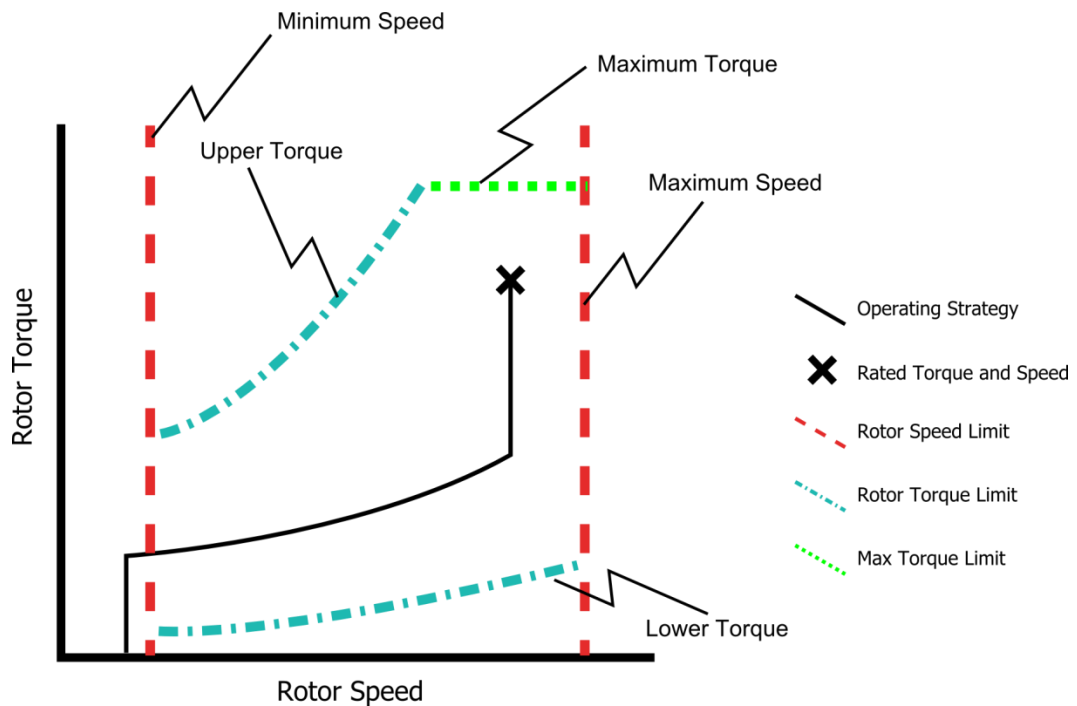


Figure 133: General Operating Envelope

The PAC imposes two limits set on the rotor speed – a maximum speed and a minimum speed. The maximum speed is set a small amount below the wind turbine’s over-speed value (the maximum speed that the rotor can rotate at without being shut down by the safety system). The minimum speed boundary should be set so that the turbine is unlikely to still be in the early stages of start-up when above it. It may not be possible to obtain the information regarding the start-up procedure for a given wind turbine and so this precaution prevents operation during the start-up process. As the energy capture is low at low rotor speeds there is little restriction in practical performance. During the recovery process, the

minimum speed limit is set to a value just below the minimum speed defined in the operational strategy as the required operating point on the operational strategy may be below the normal minimum speed. Within these limitations, the maximum and minimum speeds are defined so as to allow the largest range between them.

The upper torque limit consists of two parts, a variable section and a constant, horizontal section – labelled as the maximum torque limit. The variable section is defined in such a manner as to prevent the operating point moving into the region of aerodynamic stall, though it may incorporate other limiting factors.

Aerodynamic stall occurs when the angle of attack of the wind on the blade chord exceeds a critical aerodynamic angle. Once the critical aerodynamic angle is exceeded, the airflow separates at the rotor blade surface, which severely limits the aerodynamic torque. The aerodynamic stall region is highly non-linear and so operation in this zone by non-stall regulated turbines is avoided as the full envelope controller of such machines is not designed for operation in the stall region, so very large loads could be induced on the turbine and the controller may become unstable.

The constant, horizontal section is defined by the limitation in the reaction torque that can be produced by the generator. The limit is set a small amount below the hardware limit (in agreement with the manufacturer). If the generator torque exceeds this limit then the PAC automatically enters recovery mode. The operator receives warnings that the torque is approaching this limit as the operating point passes through the traffic light limits before reaching the maximum torque limit (see section 7.3).

The lower torque is designed in a similar manner to the upper torque limit, with the exception that only the generator torque is considered. If the aerodynamic torque falls below the minimum limit then this it is not of concern. A constant horizontal minimum torque limit may also be added that operates in the same manner as the horizontal maximum limit.

If the wind turbine operating point moves within a set offset from a hard limit it is limited to prevent the hard limit from being exceeded. If no remedial action is taken then the operating point moves towards an equilibrium point between the black limit and the offset. The wind turbine continues to remain on the boundary for a set period of time, defined by the manufacturer, after which the PAC is turned off and the recovery process is completed. The timer for this time limit is started when the limit is first reached. If the operating point subsequently moves away from the limit then a second timer is started. The first timer is held constant until either the limit is reached again or the second timer reaches a set value. In the former case the second timer is set back to zero and the first timer restarted, in the latter case the two timers are reset. In the case of the maximum and minimum torque limits the offset and the time limit are set to zero, the PAC will recover if the limit is exceeded. As soon as the turbine exceeds the offset it is inevitably unable to deliver the requested ΔP from the WFDC. As such the REJECTION (*Limit*) flag and sub-flag are set.

7.3 Soft Limits on the Provision of a Change in Power Output (“Traffic light Limits”)

The soft limits on the wind turbine’s operation are defined by the wind turbine operator. The limits themselves are defined within the PAC on each turbine. When a limit is reached a flag is sent to the WFDC. The response to reaching a limit is then decided by the WFDC.

The soft limits take the form of a “traffic light” system. In this system there are three defined zones; a green zone, an amber zone and a red zone. Flags are sent to the WFDC to identify which zone each turbine within the farm is in. The flags are the GREEN flag, the AMBER flag and the RED flag. The WFDC uses this information to inform the distribution of the total change in power amongst the turbines in the farm. An example of the traffic light zones for a wind turbine is given below in Figure 134.

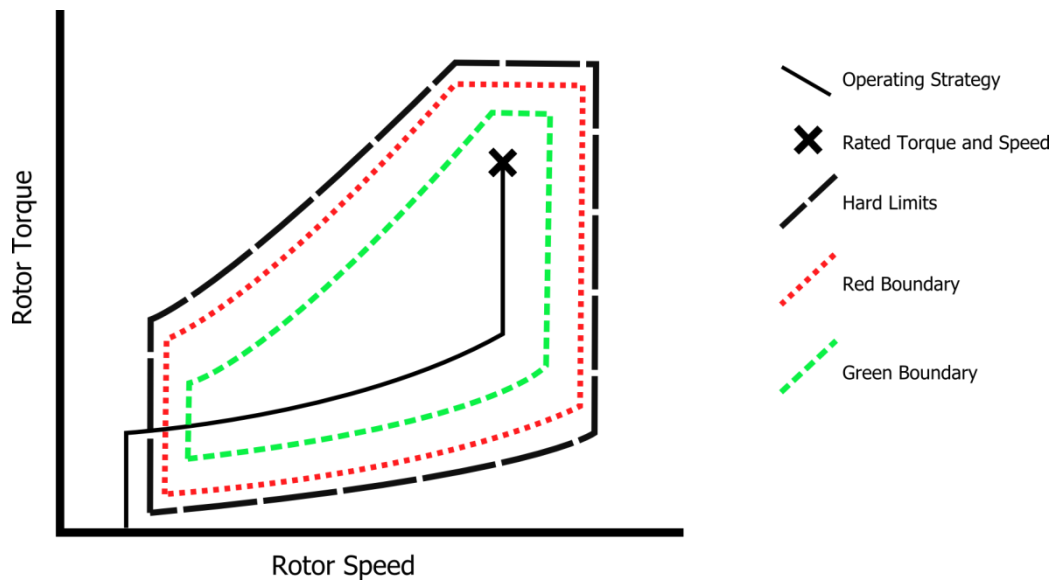


Figure 134: "Traffic Light" Zones

7.3.1 Maximum and Minimum Change in Power

Any ΔP less than the defined maximum and greater than the defined minimum for the turbine may be requested by the turbine wind farm controller. Any requested change in power outside these limits will result in the REJECTION (*Power*) flag and sub-flag being set to 1 and the value of ΔP being limited to the relevant value.

7.3.2 Response of the WFDC to Operation within the Red and Amber Zones

The response from the WFDC to turbines moving into the amber or red zones is left to the operator to decide, however a suggested response would be as follows.

When a turbine is in the amber zone, the WFDC is set to alter the change in power requested in order to move the turbine's operating point back towards the green zone. In order to do this whilst maintaining the correct farm change in power, other turbines in the farm that are within the green zone are required to accommodate the difference.

When turbines are in the amber zone, the total change in power from the wind farm takes precedence over the operational point of the turbine. That is to say, if the change to the wind turbine's ΔP required to move it back to the green zone cannot be absorbed by the other turbines within the farm whilst maintaining the correct

change in power from the wind farm, then the wind turbine is allowed to continue operating in the amber zone.

If a wind turbine crosses into the red zone then it is required to change its ΔP output in order to move back towards the green zone. In this situation the wind turbine operating point takes precedence over the change in the wind farm power output and so if the necessary change to the wind turbine's ΔP cannot be absorbed by other turbines in the farm then the farm's change in power output is compromised.

Whilst the correct operation of the red zone should ensure that turbine operating points do not stray into unwanted operational areas, it is important to still have the hard limits described previously as well as the red limits. The hard limits are still important as the traffic light zones are set by agreement with the operator and are soft limits, whereas the black limits are hard limits, are set by agreement with the manufacturer, and are put in place to protect the turbine.

The WFDC can set maximum and minimum ΔP values for each of the traffic light zones. If a ΔP outside of the set bounds for the traffic light zone that the operating point is in is requested then the REJECTION (*Red/Amber/Green*) flag and sub-flag are set.

For some turbines there may be very little space between the hard limit and the normal operating strategy, especially close to the upper limit on generator speed. In this situation it may be useful to only use one boundary, i.e. include a green zone and a red zone with no amber zone between, as otherwise the zones may be very small, with any wind turbine in the green zone having to curtail its provision of ΔP almost immediately as it quickly passes outside of the green zone.

It is reiterated at this point that the farm control strategy presented in this section is only a suggested strategy and any strategy may be defined by the operator as the black limits ensure that the operating point is kept within a safe operating envelope.

7.3.3 *Limit to the Rate of Change of Power*

Fast changes in power output result in fast changes in torque demand. Whilst a one off fast change in power output is unlikely to cause damaging loads for a wind turbine (see section 6.5), the fatigue loads of a great number of such events may have an impact over the life-time of the turbine. As such, a limit on the maximum and minimum rate of change of power is included in the PAC. This rate is set in agreement with the turbine manufacturer. If the requested rate of change of power is outside of the limits then the REJECTION (*Power Rate*) flag and sub-flag are set. For some applications, such as synthetic inertia (see chapter 8), it is necessary to request a very fast change in power output in order to protect the power system. The stability of the power system is given precedence over the turbine loads and so in these situations the PRIORITY flag is set to 1 and the usual rate limits on power are rescinded.

7.4 **Additional Limits on the Provision of a Change in Power Output**

7.4.1 *Limiting Operation due to High Turbulence*

Whilst wind turbines follow a set operating strategy as closely as possible, it is impossible for the turbine operating point to always be exactly on the strategy. Disturbances caused by variation in the wind speed, i.e. turbulence, cause the operating point to deviate from the strategy for a limited time whilst the controller works to bring it back; the higher the turbulence, the larger the deviations from the strategy. If the turbulence level is very high, then it is prudent to limit the use of the PAC.

The level of turbulence at which this limit is applied is decided by the operator and is dependent upon a number of factors such as:

- The design of the wind turbine and its controller
- The reason for the desired change in power output
- The typical atmospheric conditions at the wind farm site

If the turbulence level is exceeded then the PAC ON Flag is reset to zero, the PAC ON (*Turbulence*) sub-flag is set, and the PAC recovers. The PAC ON flag is latched to 0 until the turbulence level reduces.

7.4.2 Limitation due to Wind Speed

In very low wind speeds, because of the low levels of energy capture, use of the PAC is limited and so the PAC is turned off. If the wind speed (estimated within the PAC) drops below a pre-set value then the wind turbine enters recovery. The PAC ON flag is reset, the PAC ON (*Wind Speed*) sub-flag is set, and the wind turbine recovers to normal operation. The PAC ON flag can only be set again once the wind speed is above the defined minimum, at which point the PAC ON (*Wind Speed*) sub flag will be reset.

7.4.3 Limiting Operation due to Saturation of the Pitch Actuators

A well designed full envelope controller includes appropriate anti-wind up to prevent the pitch actuators from being saturated. When applying the PAC to a wind turbine however, no knowledge of the full envelope controller is required and, as such, it may be the case that there is no information about the design of the full envelope controller available. It is possible therefore, that appropriate measures to prevent actuator wind up have not been taken. If this is the case then it may be dangerous to run the PAC.

A limit is therefore imposed that prevents the PAC from operating if the pitch demand output from the full envelope controller exceeds the actuator limitations for velocity or position. If the pitch demand output from the full envelope controller exceeds the limits then the PAC is not allowed to operate until remedial action is taken by the operator. The PAC ON flag is latched to 0 and the PAC ON (*Actuator*) sub-flag is set.

7.4.4 The Divergent Flag

The DIVERGENT flag is set when the wind turbine operating point is unable to return to the normal operating strategy without either turning the PAC off and

entering recovery mode or altering the requested ΔP . An obvious example of this happening is when the PAC is switched on and an increase in power output is immediately requested in below rated operation. The operating point moves upwards and to the left on the torque speed plane. Because the pitch angle is already set to the minimum (and optimum) value, the aerodynamic torque cannot be raised above the generator torque to move the operating point back to the normal operational strategy without changing the ΔP provided.

The DIVERGENT flag has no effect on the operation of the PAC, it merely serves as a warning to the WFDC that the wind turbine will continue to move away from the normal operational strategy unless remedial action is taken.

The logic for the DIVERGENT flag is,

$$\begin{aligned}
 & \text{if } \frac{1}{2} \rho \pi R^2 V^3 C_p(\lambda, \beta_0) < (T_0 + \Delta T) \omega + B \omega + \text{Losses} & (7.1) \\
 & \text{then } \text{DIVERGENT} = 1 \\
 & \text{else } \text{DIVERGENT} = 0
 \end{aligned}$$

7.4.5 Limitations due to Specific Wind Turbine Design Issues

In addition to the limits that are typical for all wind turbines, there may be additional limitations introduced for specific wind turbines. For example, it may be the case that, due to poor controller/turbine design, a structural mode such as the tower frequency is within the operational envelope of the wind turbine. In this case there may already be measures in place that prevent the turbine from operating close to this frequency for prolonged periods of time. Because the PAC moves the operating point away from the normal operating strategy, care must be taken to ensure that the turbine does not operate at the undesirable frequency when the PAC is in operation.

Any additional limitation reduces the flexibility of operation by necessity; however, minimising additional loads that may be placed on the turbine through operation in undesirable operating regions takes priority.

The majority of the additional limits that may be imposed can be achieved through minor alterations to the maximum and minimum speed and torque limitations described previously. Hence, all the limits that are placed on the turbines operation can be thought of as either limiting the torque or limiting the speed of the turbine and can be achieved in a similar manner.

7.5 Design of the Flags and Limits

7.5.1 Diagrams of Limits for the 1.5MW and 5MW Wind Turbines

The limits for the 1.5MW wind turbine and for the 5MW wind turbine are shown in Figure 135 and Figure 136 respectively. Both wind turbine's upper torque limits are a safe distance away from the stall region. For the 1.5MW wind turbine, the shape of the curve of the upper torque limit changes as the rotor speed increases. This ensures that there is enough room either side of the constant speed section so that use of the PAC is not limited too greatly. The design of these limits is further discussed in the subsequent sections.

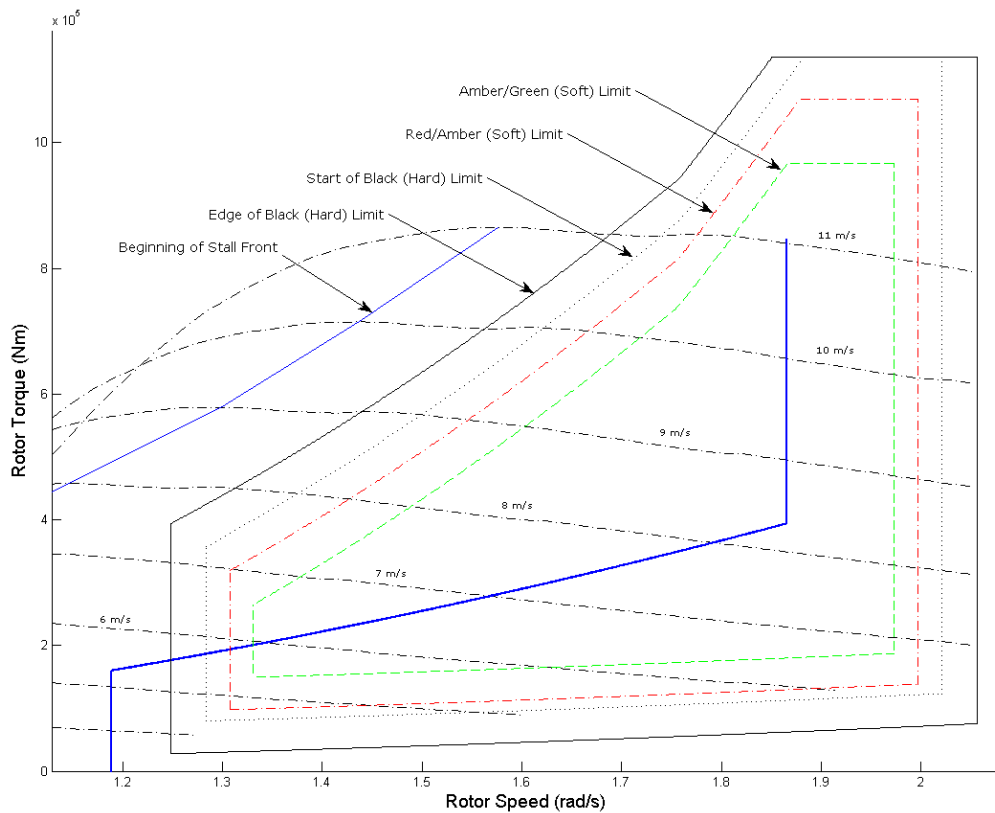


Figure 135: Operational Strategy and PAC Limits for the 1.5MW Wind Turbine

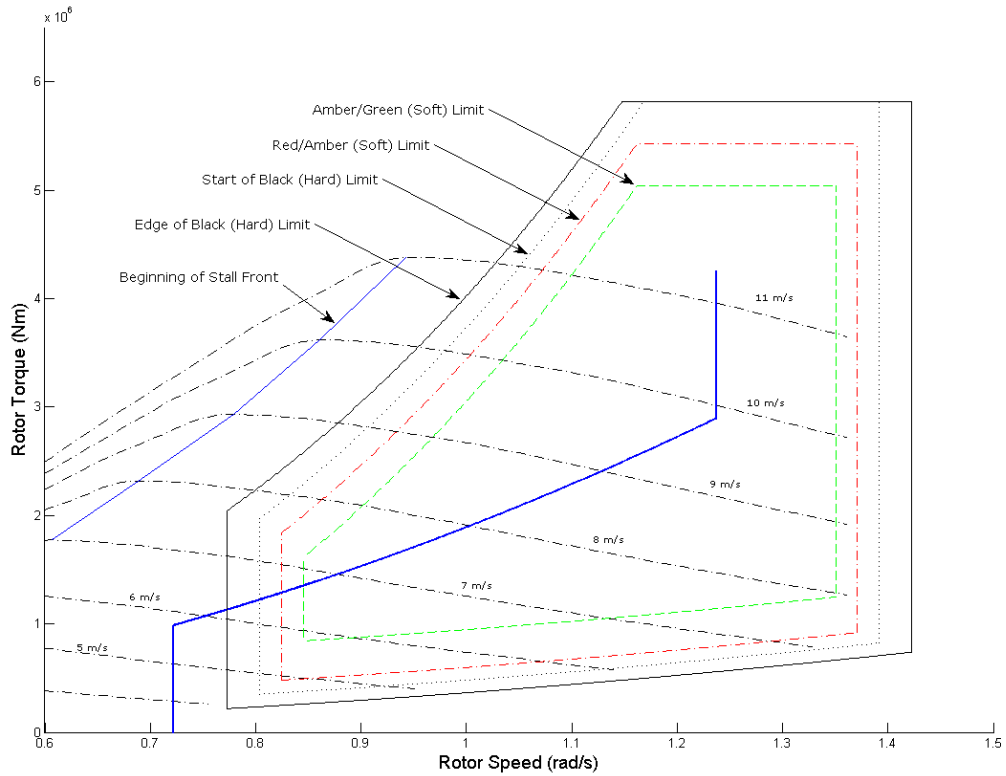


Figure 136: Operational Strategy and PAC Limits for the 5MW Wind Turbine

7.5.2 Hard Limit on the Speed of the Wind Turbine

As discussed in section 7.2 a hard limit is used to prevent the generator speed exceeding a maximum or minimum generator speed. The limit acts via an amendment to the change in torque demand from the PAC (ΔT).

For ease of explanation, the following paragraphs refer to the minimum speed limit.

A simple limit consists of a switch that sets ΔT to a value less than zero if ω becomes less than or equal to the minimum speed ω_{min} . With a negative change in torque output the operating point of the wind turbine moves back towards the normal operating strategy. This alone however, results in both a large step in the torque output and chattering of the switch. As such, ΔT is instead linearly reduced towards a set value as the minimum speed (ω_{min}) is approached. The reduction in torque starts at a set speed of $\omega_{min} + \omega_{offset}$, resulting in the wind turbine operating point being kept to the right of the minimum speed limit.

The logic used is,

$$\begin{aligned}
 & \mathbf{if} \ \omega < \omega_{min} + \omega_{Offset} & (7.2) \\
 & k_{min} = \frac{(\omega - \omega_{min})}{\omega_{Offset}} \\
 & \mathbf{else} \ k_{min} = 1
 \end{aligned}$$

The value k_{min} is used in the generation of the change in torque ΔT , whereby the new value of ΔT is given by,

$$\Delta T_{new} = \Delta T k_{min} + \Delta T_{Low}(1 - k_{min}) \quad (7.3)$$

where ΔT_{Low} is a large negative value. Using this logic, the value for ΔT tends towards ΔT_{Low} as the generator speed tends towards ω_{min} . The values of ΔT_{min} , ΔT_{Low} , and ω_{gap} are chosen carefully so that the generator speed does not chatter but is prevented from dropping lower than ω_{min} .

The REJECTION flag and a sub-flag (*limit*) are set when the limit is activated.

For the maximum speed limit the logic is similar,

$$\begin{aligned}
 & \mathbf{if} \ \omega > \omega_{max} - \omega_{Offset} & (7.4) \\
 & k_{max} = \frac{(\omega_{max} - \omega)}{\omega_{Offset}} \\
 & \mathbf{else} \ k_{max} = 1
 \end{aligned}$$

The change in torque is then adjusted via,

$$\Delta T_{new} = \Delta T k_{max} + \Delta T_{High}(1 - k_{max}) \quad (7.5)$$

where ΔT_{High} is a large positive value.

The REJECTION flag and the (*limit*) sub-flag are set when the limit is activated.

7.5.3 Hard Upper and Lower Limits on the Torque of the Wind Turbine

The limit imposed on the total torque demand sent to the wind turbine cannot be applied directly as a limit to ΔT . If ΔT is limited directly then, because of the speed of response of the ΔT output and the requirement to measure the total torque T that includes the torque output from the full envelope controller, the full envelope controller is effectively by-passed. Bypassing the full envelope controller has a

highly detrimental effect on the wind turbine, as any protective measures built into the full envelope controller torque response (such as the drive-train filter) are therefore bypassed, leading to increased loads on the wind turbine and, in the worst case, instability of the controller. Instead, the total torque demand is limited indirectly by limiting the estimated change in generator speed $\Delta\omega$.

The $\Delta\omega$ signal is subtracted from the generator speed input fed into the full envelope controller in order to prevent the full envelope controller from countermanding the actions of the PAC, as explained in chapter 4. If the input to the $\Delta\omega$ transfer function $G(s) = \frac{1}{Js+B}$ is driven by a large value with the opposite sign to $\Delta\omega$ (i.e. with a positive sign for the upper torque limit or a negative sign for the lower torque limit), then the operating point moves away from the torque limit. The input to $G(s)$ is therefore linearly changed from its usual input ($\Delta Q - \Delta T$) to a large value with the opposite sign to $\Delta\omega$ as the operating point approaches the torque limit. The effect of this is to cause the full envelope controller to detect a large decrease/increase in speed as the upper/lower torque limit is approached, causing the full envelope controller to reduce its torque output (or if in above-rated operation, increase its demanded pitch angle). Because the upper torque limit typically prevents the operating point entering the stall front, the worst case out of the generator torque and the estimated aerodynamic torque is compared with the torque limit. For the lower torque limit only the generator speed is considered as a low aerodynamic torque is not a concern.

Careful tuning of the controller prevents the limit from being exceeded in most conditions. If the limit is exceeded however, then a secondary safety mechanism is activated that turns off the PAC and starts the recovery process. Good design of the upper limit prevents the limit from being exceeded in all but the most extreme conditions e.g. the maximum increase in torque being requested as the wind speed suddenly drops by a very large amount. Testing of the upper limit in section 7.6 considers these issues in more detail.

The logic for the limits is given below, firstly the upper torque limit and secondly the lower torque limit.

Let the upper torque limit be T_{upper} , the largest of either the total generator torque or the estimate of aerodynamic torque be T^* , the input to $G(s)$ be U , K_{minus} be a large negative value, and K_{offset} be T_{upper} minus the torque at which the limit should start to take effect.

$$\mathbf{if} \ T^* > T_{upper} - K_{offset} \tag{7.6}$$

$$\mathbf{then} \ K_{upper} = \min\left(1, \frac{T_{upper} - T^*}{K_{offset}}\right)$$

end if

$$U = (\Delta T - \Delta Q)K_{upper} + (1 - K_{upper})K_{minus} \tag{7.7}$$

For the lower torque limit:

Let the lower torque limit be T_{lower} , the total generator torque be T^* , the input to $G(s)$ be U , K_{plus} be a large positive value, and K_{offset} be T_{upper} minus the torque at which the limit should start to take effect.

$$\mathbf{if} \ T^* < T_{lower} + K_{offset} \tag{7.8}$$

$$\mathbf{then} \ K_{lower} = \min\left(1, \frac{T^* - T_{lower}}{K_{offset}}\right)$$

end if

$$U = (\Delta T - \Delta Q)K_{lower} + (1 - K_{lower})K_{plus} \tag{7.9}$$

If the upper torque limit is activated (i.e. $K_{upper} < 1$) or if the lower torque limit is activated (i.e. $K_{lower} < 1$), the REJECTION (*Limit*) flag and sub-flag are set. If the maximum or minimum torque limits are exceeded then the PAC ON flag is reset to 0, the REJECTION (*Limit*) flag is set, and the turbine enters recovery mode.

7.5.3.1 Amendment in Above-rated Wind Conditions

In above-rated wind conditions, the wind turbine speed is controlled by the full envelope controller via the blade pitch angle. As the pitch angle increases, the beginning of the stall region (the turning points of the constant wind speed lines on

the torque –speed plane) moves further upwards and to the left on the torque-speed curve.

This is shown in Figure 137 for the 5MW wind turbine.

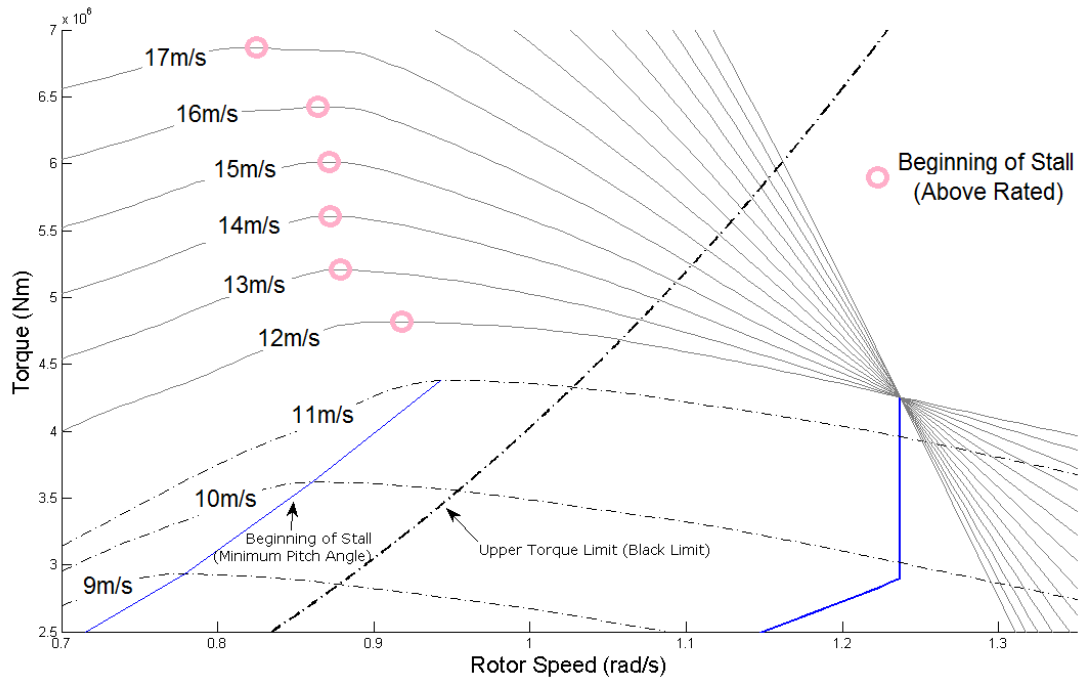


Figure 137: Beginning of Stall Region at Above-rated Wind Speeds

At 12m/s the pitch angle is approximately 3 degrees, at 13m/s it is approximately six degrees. As the beginning of the stall region has moved upwards and to the left it is reasonable to move the upper torque limit in the same direction. The upper torque limit is therefore scheduled on pitch angle, moving upwards and to the left as pitch angle increases whilst maintaining the same or larger gap between itself and the beginning of stall.

7.5.4 Maximum and Minimum Torque Limits

For the maximum and minimum torque limits (the horizontal limits described in section 7.2), the logic is very simple. If the total generator torque exceeds the maximum or minimum value then the REJECTION (*Limit*) flag and sub-flag combination are set, and the PAC ON flag is reset to 0.

7.5.5 Summary of Flags

Table 7 is a summary of all the flags and sub-flags discussed in this chapter.

Table 7: Summary of Flags and Sub-Flags used by the PAC

Flag Symbol	Sub-Flag	Purpose/Significance when set
PAC ON	-	The PAC is on
PAC ON	(<i>Turbulence</i>)	The PAC cannot be turned on as the turbulence level is too high
PAC ON	(<i>Wind Speed</i>)	The PAC cannot be turned on as the wind speed is too low
PAC ON	(<i>Actuator</i>)	The PAC cannot be turned on as the pitch demand signal from the full envelope controller has exceeded the actuator limits
RECOVERY	-	The wind turbine is recovering back to normal operation or has recovered
RECOVERY	(<i>Complete</i>)	The wind turbine has recovered back to normal operation
RECOVERY	(<i>Fast/Slow</i>)	If set then the recovery speed is fast (a 0 signal sets the speed to slow)
REJECTION	(<i>Limit</i>)	The requested ΔP cannot be provided as a black limit has been exceeded
REJECTION	(<i>Red/Amber/Green</i>)	The requested ΔP cannot be provided as it is of greater

		magnitude than the limit set for the relevant traffic light zone
REJECTION	(Recovery)	The requested ΔP cannot be provided as the PAC is in recovery mode
REJECTION	(Power Rate)	The requested ΔP cannot be provided due to the limits on the rate of change of power
REJECTION	(Power)	The requested ΔP cannot be provided as it exceeds the maximum/minimum power limit
RED	-	The turbine is in the red "traffic light" zone
AMBER	-	The turbine is in the amber "traffic light" zone
GREEN	-	The turbine is in the green "traffic light" zone
PRIORITY	-	A priority event (such as synthetic inertia) is occurring and so the traffic light limits and power rate limits are ignored
DIVERGENT	-	The turbine will continue to move further from the normal operating strategy unless the PAC enters recovery or a change to ΔP is made.

7.6 Demonstration of Recovery Flag and Sub-Flags

Eight simulations are conducted to demonstrate the recovery flags and sub-flags, covering above and below-rated wind speeds with both fast and slow recovery and in both constant and turbulent winds. For all the simulations a reduction in power of 0.15MW is used with the 1.5MW wind turbine. For the simulations with turbulent wind, "class A" high turbulence as defined in the IEC international standard 61400-1 (third edition) [76] is used.

The first simulations are at 8m/s (below-rated) constant wind speed. One simulation has the recovery speed set to fast, whilst the other has it set to slow. The results of these simulations are presented in Figure 138.

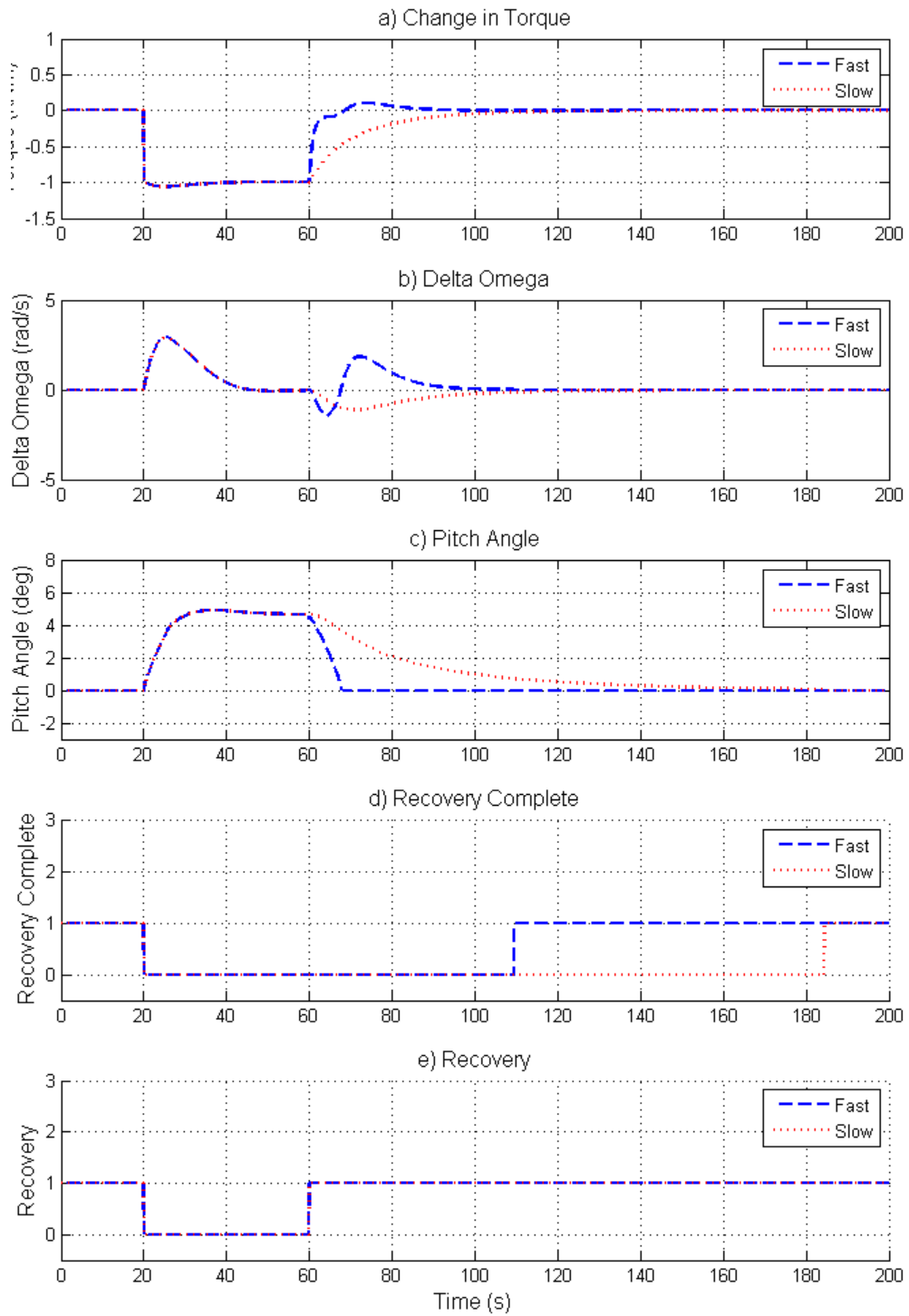


Figure 138: Recovery Process and Flags – 8m/s Constant Wind Speed

Both recovery speeds successfully return the wind turbine back to normal operation. When recovery is complete the RECOVERY (*Complete*) flag and sub flag are set, whilst the recovery is on-going the RECOVERY flag is set but the (*Complete*) sub-flag

is not set, and during operation of the PAC neither are set (see graph *d*) and graph *e*) of Figure 138).

The “fast” recovery quickly returns the change in torque (see graph *a*) of Figure 138) back towards zero, albeit with some overshoot. The “slow” recovery returns the change in torque back to zero more slowly – there is no overshoot.

The change in pitch angle (see graph *c*) of Figure 138) is quickly driven back to zero in the “fast” recovery, reaching zero within 10 seconds of the PAC being switched off. In the “slow” recovery the pitch angle is reduced more slowly and takes approximately 120 seconds to return to zero. The speed of the change in torque and pitch angle in the “fast” recovery causes a larger change in $\Delta\omega$ (see graph *b*) of Figure 138) during the recovery process than in the “slow” recovery.

A set of simulations are run at 15m/s (above-rated) constant wind speed. One simulation has the RECOVERY (*Fast/Slow*) sub-flag set to 1 (fast), the other has it set to 0 (slow). The results of these simulations are presented in Figure 139.

The same comments as for the below-rated simulations discussed previously apply here. Because the change in pitch angle is not as large in the above-rated simulations, the recovery is quicker in both the “fast” and “slow” cases compared to the below rated simulations, and the torque overshoot in the “fast” case is smaller.

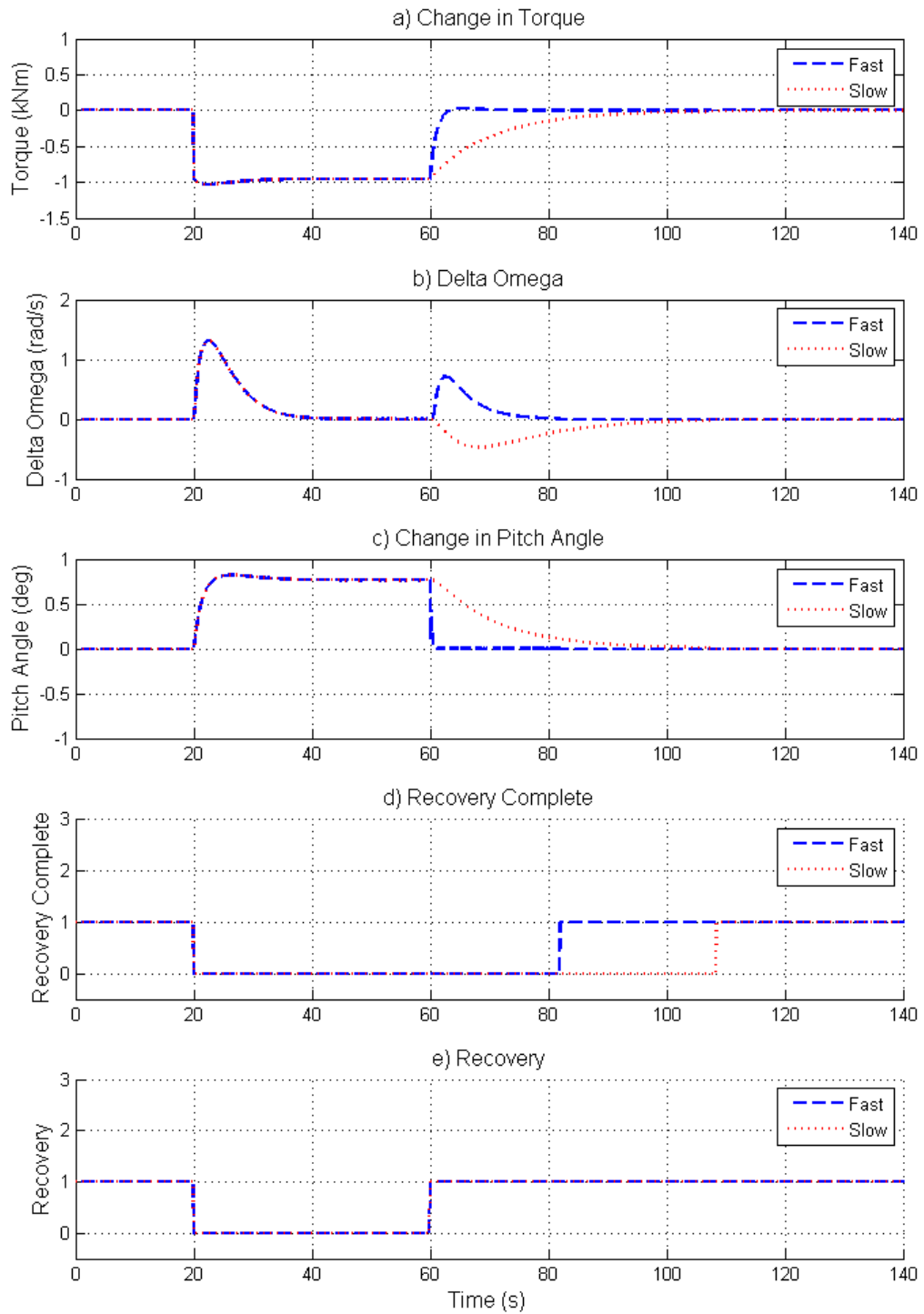


Figure 139: Recovery Process and Flags – 15m/s Constant Wind Speed

Additional simulations are shown in Figure 140 and Figure 141 using turbulent wind speed.

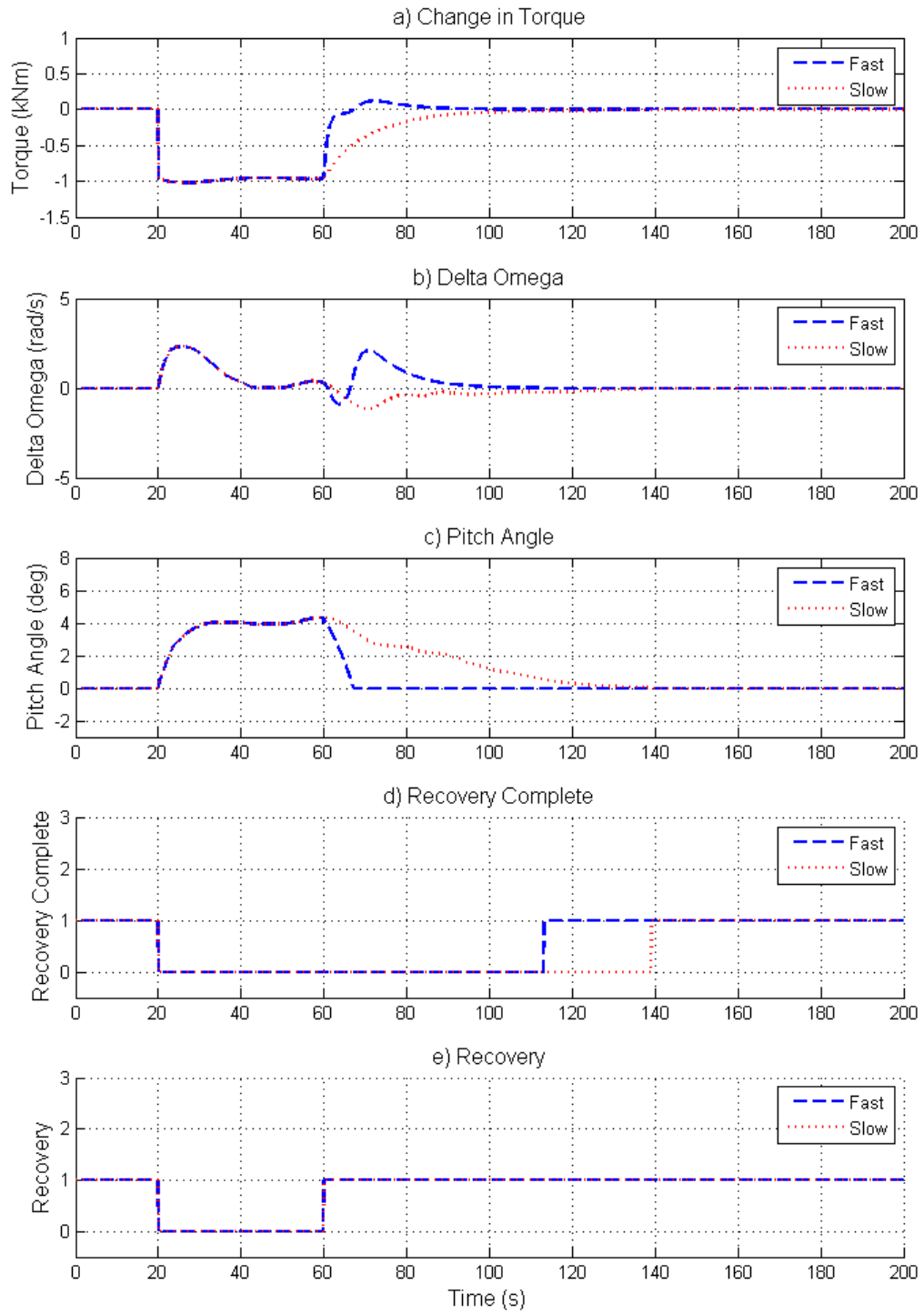


Figure 140: Recovery Process and Flags – 8m/s Variable Wind Speed

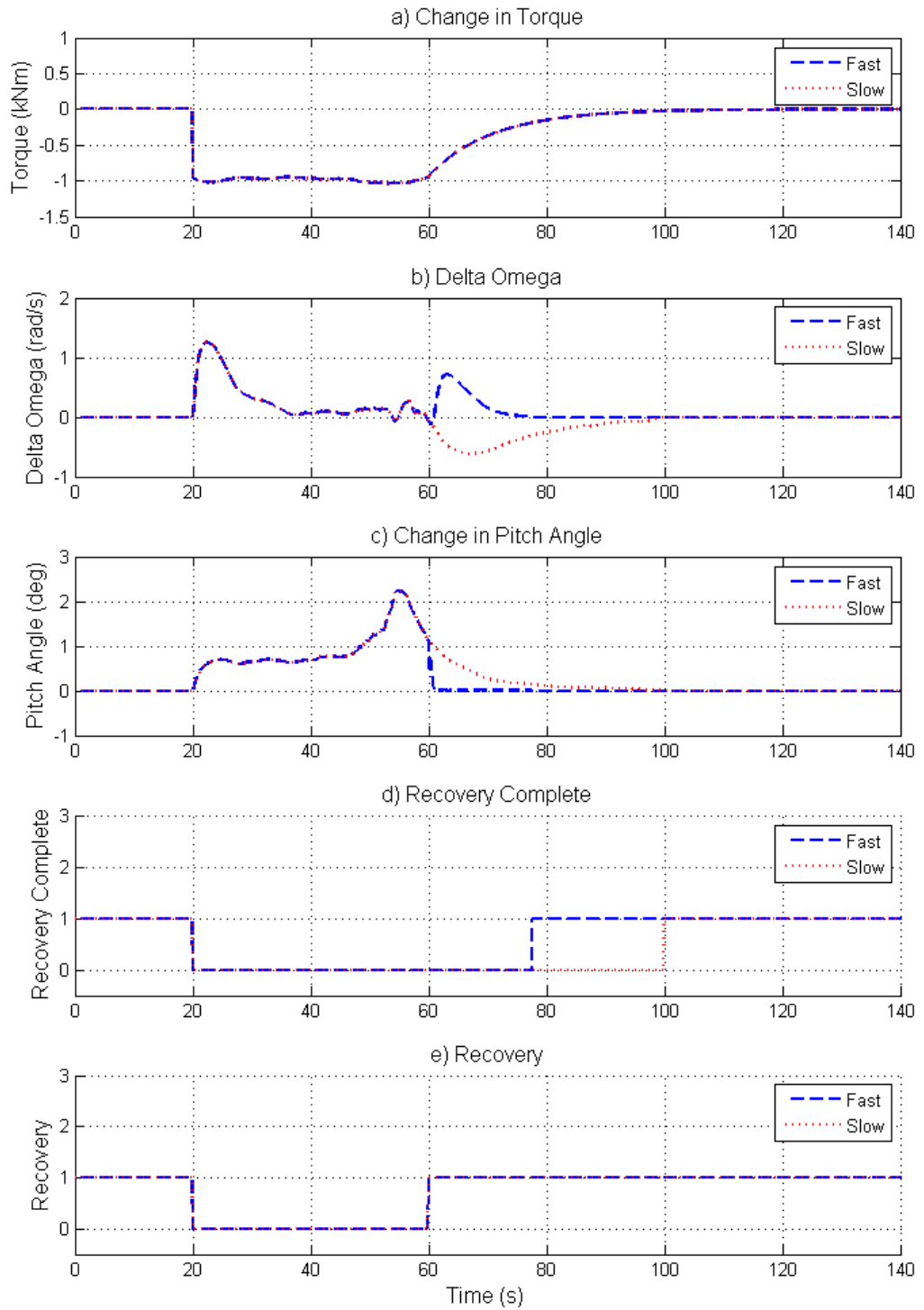


Figure 141: Recovery Process and Flags – 15m/s Variable Wind Speed

The turbulent wind simulations show that the recovery process still operates effectively in turbulent wind. The results are similar to the constant wind speed simulations and the same comments apply.

7.7 Testing of the Hard Limits

To demonstrate the hard limits, simulations are conducted that deliberately force the turbine's operating point far from its normal operating strategy. The limits demonstrated in this section are:

- The upper torque limit
- The lower torque limit
- The maximum speed limit
- The minimum speed limit
- The maximum torque limit
- The minimum torque limit.

7.7.1 Upper Torque Limit, Maximum Torque Limit and Minimum Speed Limit

In order to demonstrate the upper torque limit, the PAC is given a ΔP input of ΔP_{Max} . The simulations performed here are worst case, in that the change in power is at its maximum, the traffic light limits are not in use, and the PRIORITY flag is set to 1. The position of the turbine operating point on the torque-speed plane for three simulations with constant wind speed inputs is shown in Figure 142. The wind speeds used are 7.5m/s, 9m/s, and 10.5m/s. No simulations above-rated are completed as the turbine is highly unlikely to reach the limits. This is because the turbine is able to reduce the pitch angle of the blades to increase the aerodynamic torque and prevent the operating point moving far from the operational strategy, and the upper torque limit moves upward and to the left as the pitch angle increases, as discussed in section 7.5.3.1. The aerodynamic and generator torque are both shown with reference to the low speed shaft.

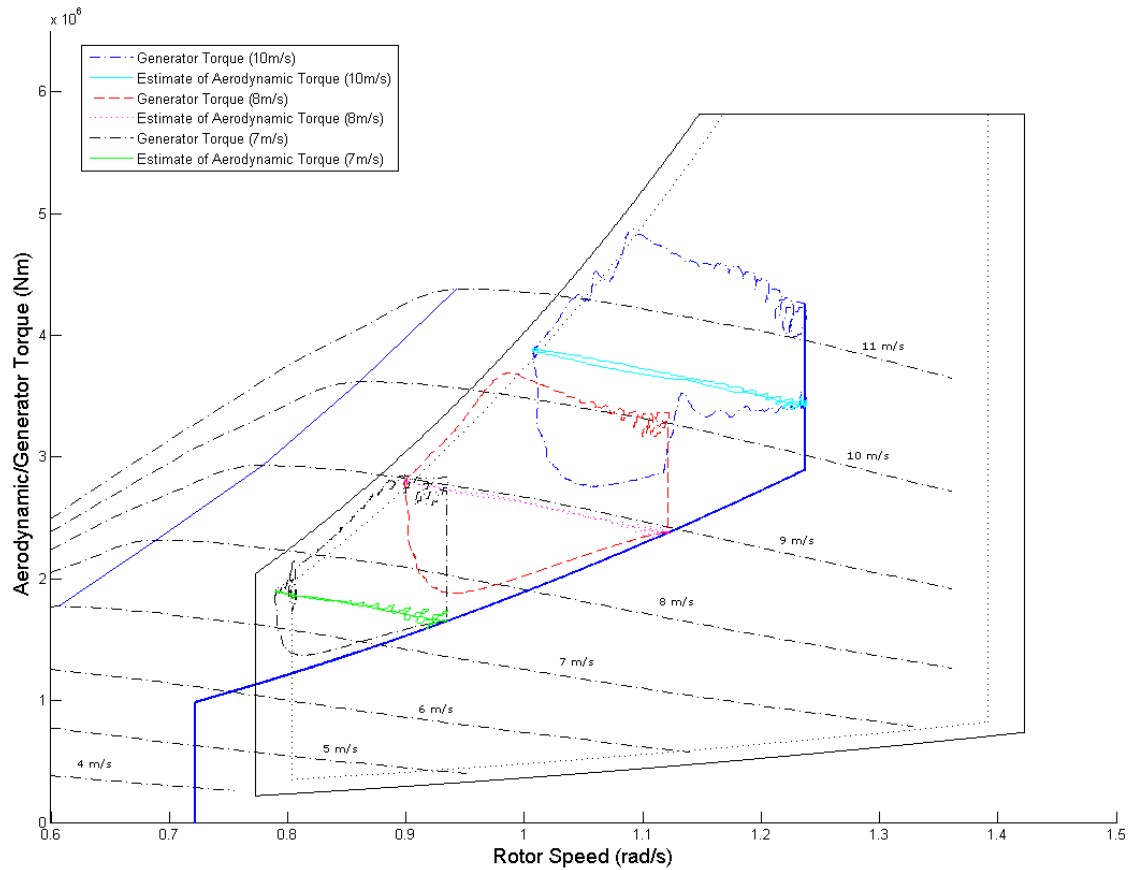


Figure 142: Activation of Upper Torque Limits – Constant Wind Speeds – 5MW Wind Turbine

In all the simulations the operating point moves upward and to the left as the torque increases and the generator speed decreases. As the operating point moves past the offset, the torque is reduced. The turbine is kept to the right of the limit and, after a set time limit of 20 seconds, the recovery mode is activated, returning the operating point to the normal operating strategy

In the case of the 7.5m/s simulation, the equilibrium point near the limit is at a speed below the minimum speed offset. As the operating point approaches the minimum speed limit the torque is therefore limited further, keeping the operating point within the safe operating zone. In the 10.5m/s and 9m/s simulations an equilibrium point is reached prior to activation of the minimum speed limit.

The simulation at 9m/s shows the behaviour of the limit when the full envelope controller is in the max power tracking region whereas the 10.5m/s simulation shows the behaviour of the limit when the wind turbine is in the second constant

speed region. Because the limit utilises a change in $\Delta\omega$ to affect a change in the torque output of the full envelope controller, the resultant behaviour differs for the two different simulations due to differences in the characteristics of the full envelope controller in different modes. Care must be taken when designing the limit to ensure that both cases are catered for. It should be noted that as an additional safety mechanism, if the upper torque limit is breached then the PAC will enter recovery.

Three further simulations are completed using turbulent winds at means of 7m/s, 8m/s, and 10m/s. The torque-speed curves are shown in Figure 143. These show that despite the wind having a turbulence of close to 15% and the change in power being at the maximum value, the upper limit still prevents the operating point moving outside of the safe operating envelope.

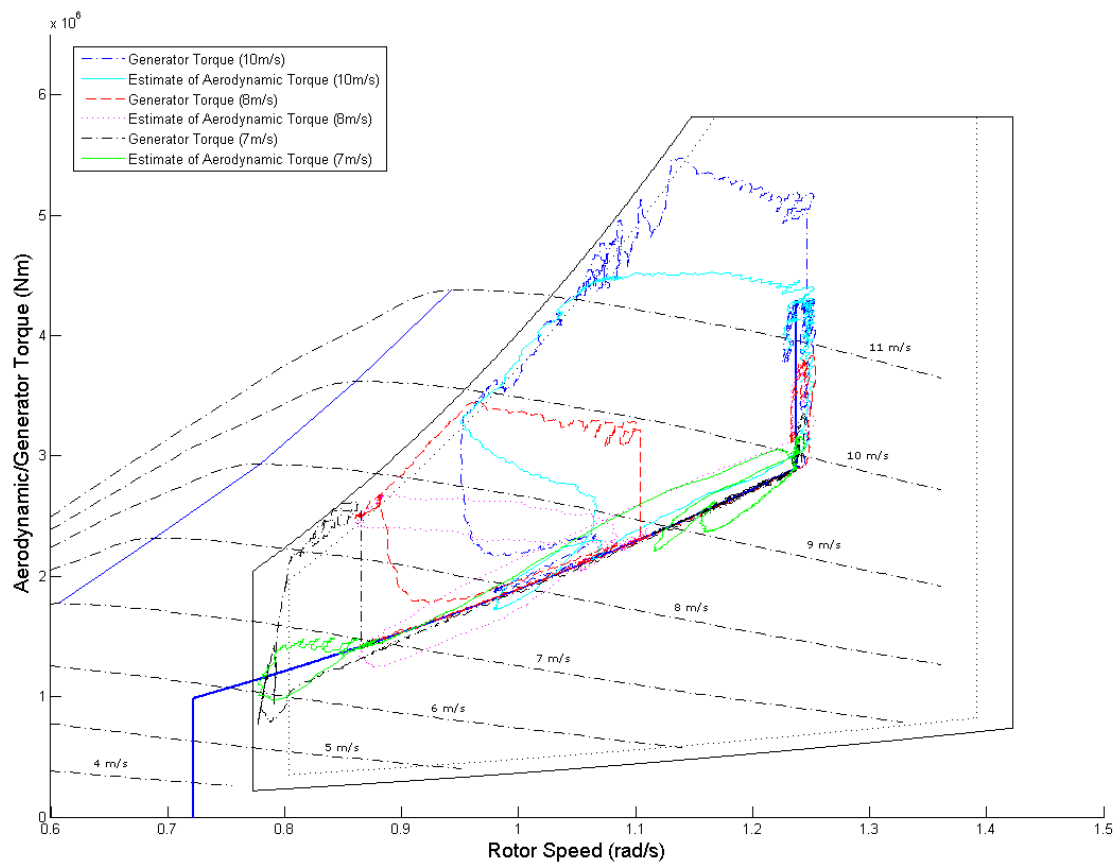


Figure 143: Activation of Upper Torque Limits – Variable Wind Speeds – 5MW Wind Turbine

Simulations are conducted with the upper torque limit deliberately detuned so that the operating point is not prevented from crossing the limit. Because the limit is not effective, the limit is exceeded, causing the wind turbine to recover back to the main strategy; as seen on the torque-speed curves presented in Figure 144. The simulations show that even if the upper torque limit is not effective, operation is prevented from moving further towards the stall region, keeping the operating point within a safe operating envelope. For the 10m/s simulation, the generator torque crosses the beginning of the upper torque region and nearly reaches the upper torque limit, however, the wind speed drops at this point and so the torque limit is not reached. Shortly after, the wind speed increases again and the upper torque limit is reached, causing the PAC to be turned off and to recover back to normal operation. In the 7m/s and 8m/s simulations the generator torque quickly reaches the upper torque limit and so the PAC is switched off and the wind turbine undergoes recovery.

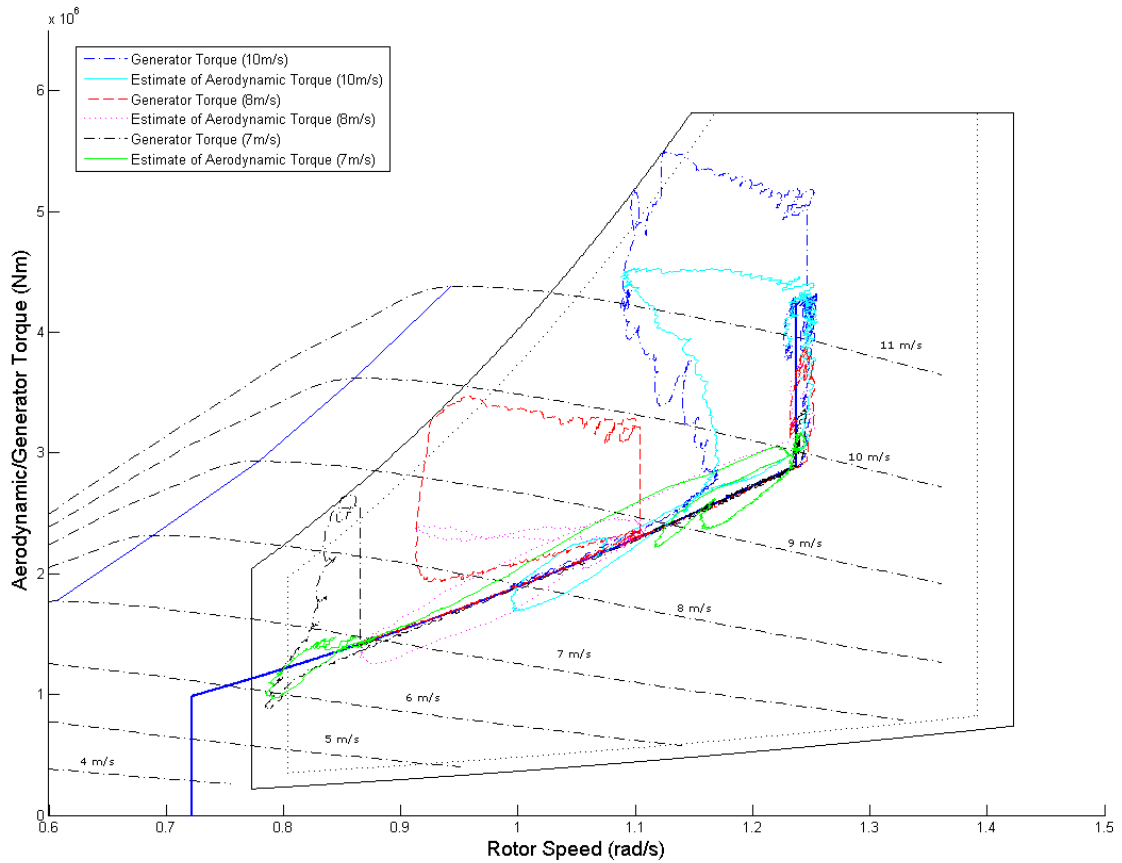


Figure 144: Activation of Maximum Torque Limits – Variable Wind Speeds – De-Turned Upper Torque Limit – 5MW Wind Turbine

7.7.2 Lower Torque Limit, Minimum Torque Limit and the Maximum Speed Limit

As the wind turbine is able to utilise blade pitch to reduce the aerodynamic torque, the minimum torque, lower torque and maximum speed limits are less likely to be activated. In the simulation presented here, the PRIORITY flag is set to 1 and so no soft limits are applied.

Two sets of simulations are completed – one using constant wind speeds, and one using variable wind speeds.

The operating point is plotted on the torque-speed plane for two simulations with constant wind speed inputs in Figure 145. The wind speeds used are 7m/s, and 10m/s and the ΔP requests are -0.3MW and -0.5MW respectively.

Chapter 7: PAC Supervisory Rules

For the 10m/s simulation the generator speed increases after the initial torque drop until it reaches the offset from the black limit. Here it is held below the maximum speed whilst the aerodynamic torque continues to be reduced by pitch action. This pitch action reduces the aerodynamic torque below the generator torque and the turbine is brought back to a stable operating point directly below the original operating point. The PAC is then turned off and the wind turbine recovers to the normal operating strategy.

For the 7m/s simulation the generator torque is held above the lower limit for torque. Because the stable operating point is betwixt the offset and the black limit, the turbine continues to be limited until the black timer reaches twenty seconds. At this point the wind turbine recovers back to its original operating point. Note that the aerodynamic torque is permitted to exceed the lower torque limit as described in section 7.5.3.

It should also be noted that these limits are less likely to be reached in normal operation as the soft limits are normally in use and so a well-designed WFDC is likely to alter the requested ΔP before the limits are reached.

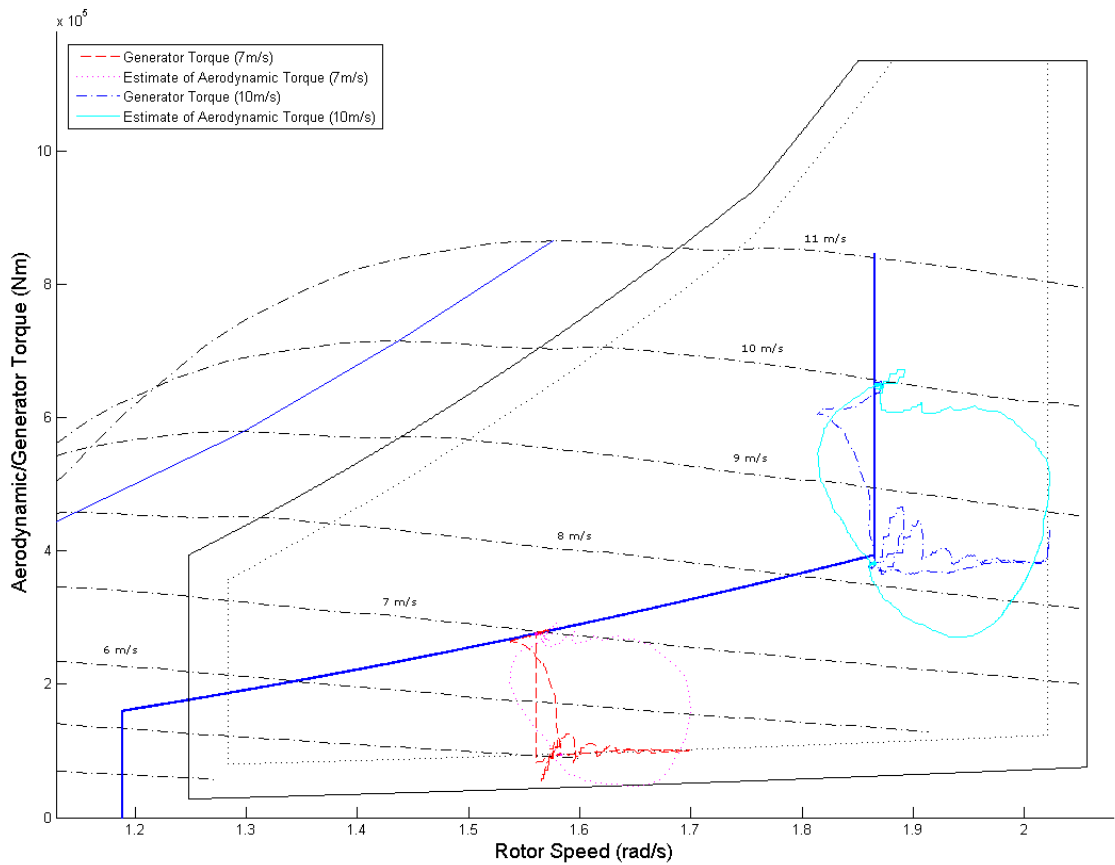


Figure 145: Activation of Lower Torque Limits – Constant Wind Speeds – 1.5MW Wind Turbine

The results of simulations activating the lower torque and/or maximum speed limits with variable wind speeds are shown in Figure 146. The wind speeds used have means of 8m/s and 10m/s.

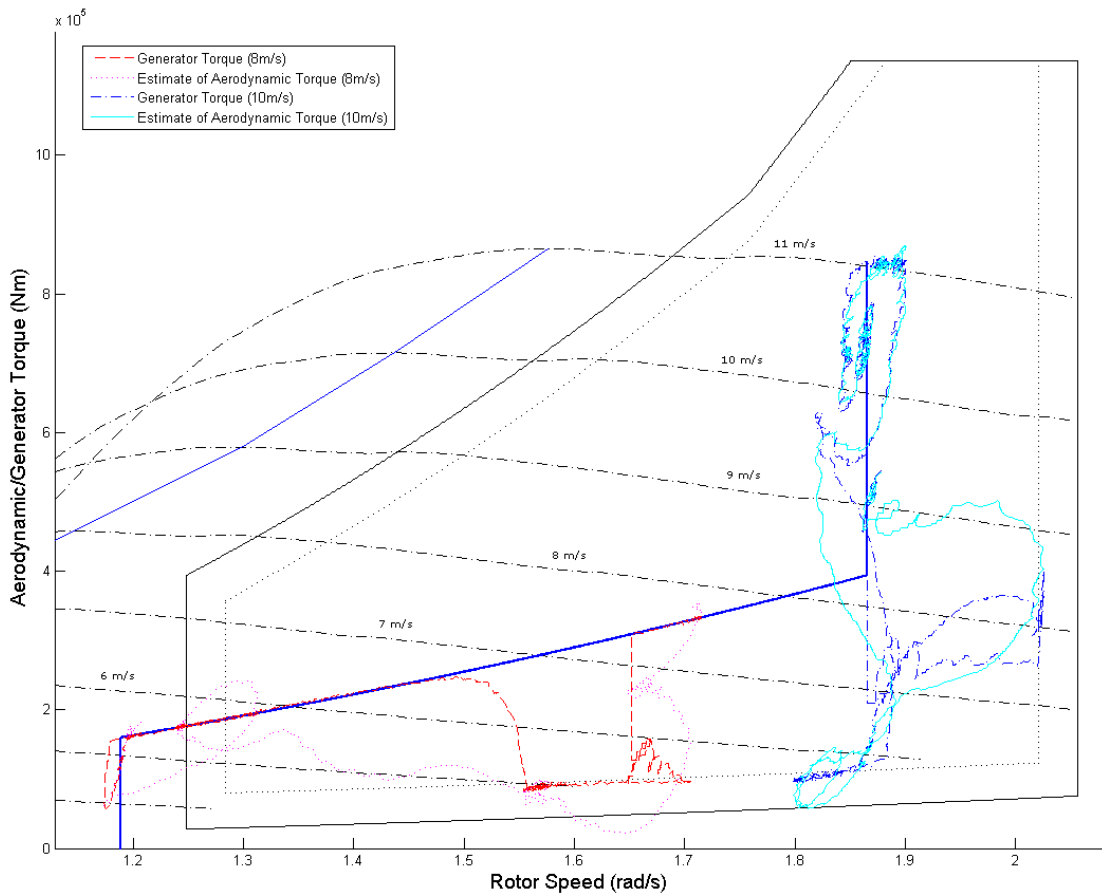


Figure 146: Activation of Lower Torque Limits – Variable Wind Speeds – 1.5MW Wind Turbine

In the 10m/s simulation, the maximum speed limit is reached shortly after the initial reduction in torque. After being limited for a few seconds, the pitch action of the PAC brings the generator speed back towards the strategy. The wind speed drops and so the generator torque reduces and the lower torque limit is activated. The operating point is held within the limit until the black timer reaches the set time limit, at which point the turbine recovers back to the normal operating strategy.

In the 8m/s simulation the lower torque limit is activated, preventing the generator torque from reducing below the lower limit. The aerodynamic torque is allowed below the limit. Once the black limit timer reaches the set time limit, the turbine recovers back to the normal operating point. During the recovery the rotor speed drops below the lower speed limit, however, because the turbine is in recovery, the limit has moved below the minimum speed of the operational strategy and is therefore not activated.

7.8 Concluding Remarks

The PAC necessarily moves the operating point away from the normal operating strategy, and, as such, without limitations on the action of the PAC it is possible for the operating point to move to undesirable locations. Hard limits on the operation of the PAC are therefore required to prevent operation in locations that are undesirable for the wind turbine. These limits are set in consultation with the wind turbine manufacturer and cannot be altered by the operator. They are in effect at all times and keep the operating point within a safe operating envelope.

The PAC is designed to operate in conjunction with a hierarchical wind farm control system, as described in chapter 3. It is therefore necessary for the PAC to communicate the condition of the wind turbine to the higher level WFDC. A system of flags and sub-flags is developed to facilitate communication between the PAC and the WFDC.

In addition to the hard limits described, the operator may wish to impose their own limits on the operation of the PAC. The safe operational envelope is therefore divided into three zones; a green zone, an amber zone, and a red zone. Flags are sent to the WFDC to communicate which zone the turbine is in. It is then at the discretion of the WFDC to decide if the requested change in power should be altered in light of the turbine's operating point.

The hard limits are designed such that, for most cases, the operating point is held between the limit and an offset from the limit for a set time period if the limit is activated. In the event that the limit is exceeded the wind turbine is automatically set to recover back to the operational strategy.

The recovery process is conducted at either a fast or a slow speed, as selected by the WFDC.

The limits are shown to be effective, even in turbulent wind conditions, keeping the wind turbine in a safe operational envelope. The flags and hard limits allow the WFDC to be more easily designed, as the designer has, via the flags, access to information regarding the condition of each turbine within the farm and knows that

Chapter 7: PAC Supervisory Rules

it is not possible for the WFDC to cause a turbine to move to an unsafe operating point.

Chapter 8:

Using the PAC to Provide Grid Frequency Support

ONE OF THE possible uses for the PAC is to provide support to the grid via a change in power output in order to maintain the grid frequency. This chapter concerns the provision of two types of frequency support through the operation of the PAC. The first of these is known as synthetic inertia, whilst the second is droop control. A description of these processes was provided in chapter 3, section 3.2, but, briefly put; synthetic inertia is the provision of additional power proportional to the rate of change of grid frequency, whilst droop control is the provision of additional power proportional to the error in grid frequency measured from the reference value.

When operated in the conventional manner, variable speed, asynchronous wind turbines do not provide any form of grid support (see chapter 3, section 3.2). Whilst the number of wind turbines connected to the grid is small, this does not pose a significant problem, as the inertial characteristics of the connected conventional generation combined with the primary and secondary response provided by the same are still adequate to control the frequency. As the percentage of electricity production provided by variable speed, asynchronous wind turbines increases however, this may no longer be the case. As such, the ability of wind turbines and/or wind farms to provide frequency support becomes a higher priority.

8.1 Using the PAC to Provide Synthetic Inertia

Synthetic inertia is the provision of an increase in the power output of a wind turbine decoupled from the grid in order to provide a similar effect upon the grid dynamics as the natural inertial response of a synchronous machine. The grid frequency is directly linked to the sum of the power generated on the power system and the power demanded from the power system via the equation,

$$Jf \frac{df}{dt} = P_{sup} - P_{dem} \quad (8.1)$$

where J is the combined inertia of all the synchronous plant, f is the grid frequency, P_{sup} is the power supplied and P_{dem} is the power demanded. Variable speed wind turbines do not contribute towards the grid inertia and so the grid frequency changes more quickly for a given imbalance of power generation and demand if there are large numbers of variable speed wind turbines attached to the grid. The effect of inertia in slowing the rate of change of frequency for a given imbalance in power can be emulated by providing an increased power output proportional to the rate of change of grid frequency.

Because the action of inertia is instantaneous (as it is a physical effect caused by the large rotating masses of synchronous generators) it is essential that synthetic inertia is provided very quickly (typically in less than 200ms). The PAC is well suited to this requirement, as the power output of the turbine is altered through the torque demand at the generator, which has very fast dynamics. In addition, the PAC is capable of providing an increase in power for a limited time without reducing the power output prior to the event; instead kinetic energy in the rotating blades is converted into electrical energy, slowing the rotational speed of the machine. Because the PAC does not require prior reduction of power output, any wind turbine with the PAC installed is capable of providing synthetic inertia quickly when demanded without reducing the power capture of the machine during normal operation.

After provision of synthetic inertia in below rated wind conditions, a reduction in the power output is required to allow the rotor to speed back up to the normal operating speed. When a wind farm provides synthetic inertia response, the timing and speed of this recovery process can be staggered to prevent a large drop in power output immediately following a grid frequency event.

Conventional, synchronous plant have an inertia constant H (kinetic energy per apparent power unit) of approximately 6s. The inertia constant is related to the rate of change of frequency by (8.2).

$$\frac{df}{dt} = \frac{\Delta P f}{2HS} \quad (8.2)$$

where ΔP is the change in power output, f is the grid frequency, and S is the rated power. For a wind turbine to produce an equivalent inertial response, the change in power for a given change in frequency is therefore calculated by a constant multiplied by the rate of change of frequency (assuming the total change in frequency is small). This constant is given by (8.3).

$$K_{inertia} = \frac{-\Delta P}{\frac{df}{dt}} = \frac{-2SH}{f_{nominal}} \quad (8.3)$$

When the grid frequency is recovering from a frequency drop the rate of change of frequency will be positive. Providing a reduction in power when the frequency is returning towards the nominal value is undesirable, and so the change in power output requested as a result of synthetic inertia is bounded by a minimum value of zero. A maximum value is not required, as the PAC already limits the maximum requested change in power as part of the limits defined in chapter 7.

8.1.1 Alteration to the PAC Laws when providing Synthetic Inertia

In the case of a request to supply synthetic inertia it is required to alter the PAC laws through the use of the PRIORITY flag (described previously in chapter 7). In these situations, the power system takes precedence over the turbine, and so the traffic light laws are disabled and the black limits are the only restriction on operation. If the wind turbine reaches a black limit then it is held on the limit line

until after the frequency event has finished. In addition, any limit on the rate of change of ΔP is removed to allow a quick response. If farm control is used then recovery from synthetic inertia is staggered amongst the turbines to prevent a significant drop in the total farm output. The timing of the recoveries is defined by the wind farm controller as the required information is not available at the turbine level. If the PAC is operating without farm control then the recovery process is started when the frequency rises back above a set frequency.

8.1.2 Impact of Turbine Size and Operating Strategy on Provision of Synthetic Inertia

The potential for a wind turbine to provide synthetic inertia is dependent upon both the size of the turbine and the operating strategy of the full envelope controller. Larger turbines have larger blades and hence there is greater kinetic energy stored in the rotor during operation. Work by Jamieson on scaling wind turbines [79] is used to provide an estimate for the increase in kinetic energy stored as turbine size increases. Using a power law exponent for mass of 2.29 and for tip speed ratio of 0.28, a power law exponent for inertia of 4.58 and hence a power law exponent of 3.14 for the energy stored in the blades is calculated. Whilst this calculation is only an estimate, the potential for larger turbines to provide greater provision of synthetic inertia is clear.

Whilst larger wind turbines have greater potential to provide synthetic inertia due to their physical characteristics, their potential can be severely limited by the control strategy that they use. Specifically, if the strategy operates close to the onset of aerodynamic stall then the turbine's ability to provide synthetic inertia is greatly reduced compared to if the strategy keeps the operating point far from the onset of aerodynamic stall. Operating close to the onset of aerodynamic stall reduces the area on the torque-speed plane between the operating strategy and the upper torque limit, reducing the duration for which a given increase in power output can be maintained before it is limited to protect the turbine. Reducing the time that a given

power increase can be sustained for reduces the potential for a turbine to provide synthetic inertia.

It should be noted that the onset of aerodynamic stall can be moved further from the operating strategy by pitching the blades, however, the resultant reduction in aerodynamic torque would result in the operating point accelerating away from the operational strategy, and the task of recovering the turbine back to the operational strategy would be exceedingly difficult, and, in some cases, impossible.

The potential for a turbine to provide synthetic inertia is therefore strongly dependent upon the design of both the wind turbine in question, and the turbine full envelope controller's operational strategy.

8.1.3 Synthetic Inertia Simulations

In this section simulations in which the PAC is used to provide a synthetic inertia response to a drop in grid frequency are presented. All simulations are conducted using GL Bladed.

Two different frequency inputs are used to simulate synthetic inertia. The first is real data from a frequency event that happened at approximately 8:05 am on the 16th October 2014, recorded at Strathclyde University. The second set of data is artificially generated data designed to simulate a worst case drop in frequency, based on the suggested large frequency drop in [80]. Grid frequency is highly unlikely to drop faster or further than this in reality. Both sets of data are shown in. In [81] Wu and Infield modelled the drop in frequency on the UK power system given a sudden loss of 1.8GW of generation, equivalent to losing half the generating capacity of Drax power station, the largest in the UK. Without frequency support from wind turbines the peak rate of change of frequency (ROCOF) was -0.6 Hz/s, and the frequency nadir was approximately 49.3Hz assuming worst case conditions for type of generation mix and power demand. The most probable peak ROCOF was -0.3 Hz/s. The frequency drops modelled in Figure 147 can therefore be considered as being representative of a very large frequency drop and a small frequency drop for the artificial and measured data respectively. It is assumed that

the frequency is known via accurate measurement.

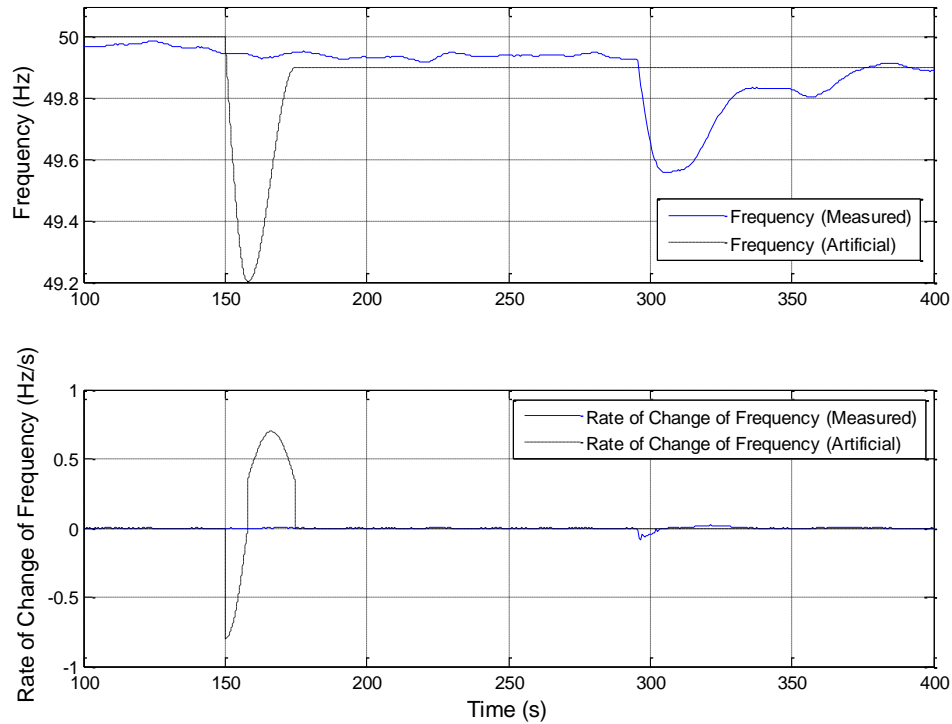


Figure 147: Frequency Data Used for Synthetic Inertia Simulations

Synthetic inertia is only required during large frequency drops and so synthetic inertia is only provided if the frequency drops below 49.9Hz. The recovery process is set to occur five seconds after the frequency returns above 49.8Hz (the lower limit for the National Grid [25]).

In Figure 148, power outputs for simulations of the 5MW wind turbine providing synthetic inertia at various constant wind speeds, with the smaller frequency drop in Figure 147 used as the input, are presented.

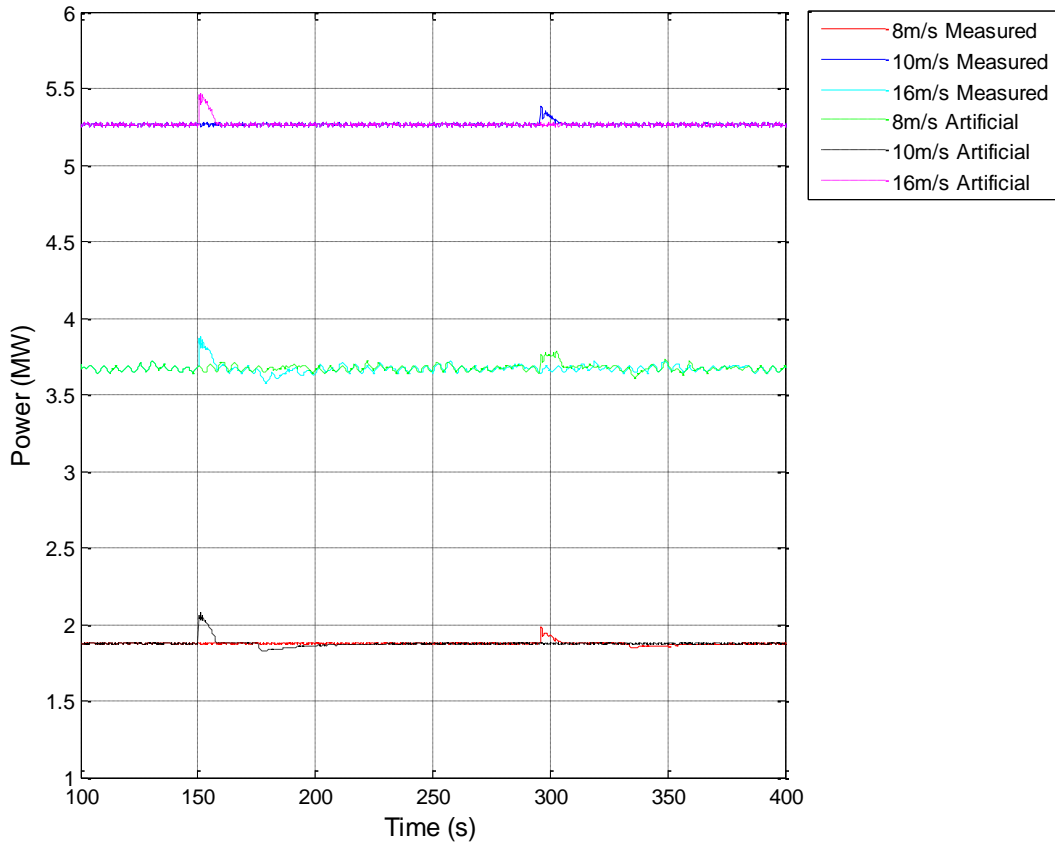


Figure 148: Synthetic Inertia Response of the 5MW Wind Turbine

Because the requested ΔP is a function solely of the rate of change of grid frequency, the change in power output is the same for all wind speeds. The maximum value of ΔP in Figure 148 is very small (only approximately 20% of the maximum ΔP for the 5MW turbine). As the ΔP is small, the deviation from the normal strategy on the torque-speed plane (shown for the larger, artificial frequency drop in Figure 149) is also small.

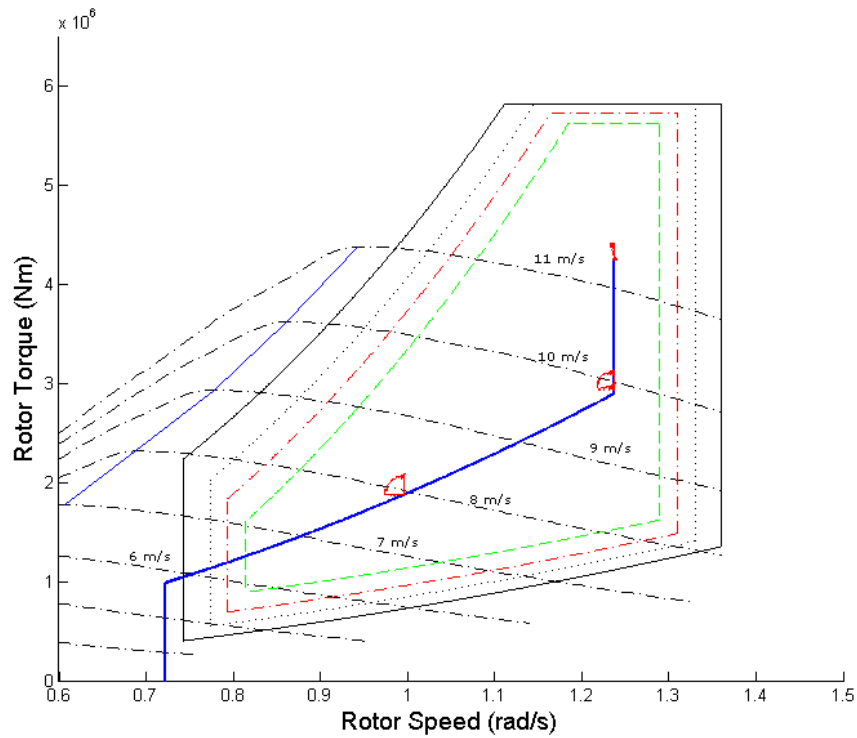


Figure 149: Torque-Speed Curve – 5MW Wind Turbine Providing Synthetic Inertia

It is clear therefore that the 5MW wind turbine is capable of providing greater amounts of grid support through synthetic inertia. To demonstrate this, the value for $K_{inertia}$ is increased so that the wind turbines provide the equivalent of a synchronous plant with an H value of 18s, triple the typical value. The results are presented in Figure 150.

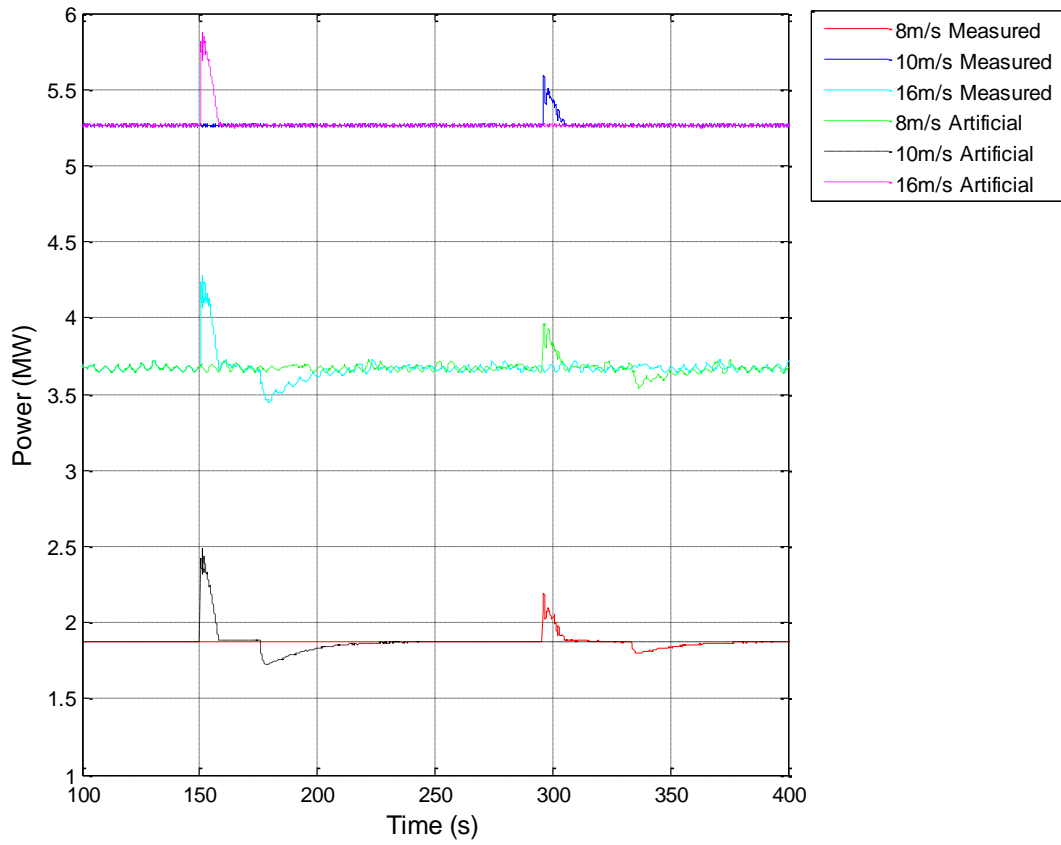


Figure 150: Increased Synthetic Inertia Response of the 5MW Wind Turbine

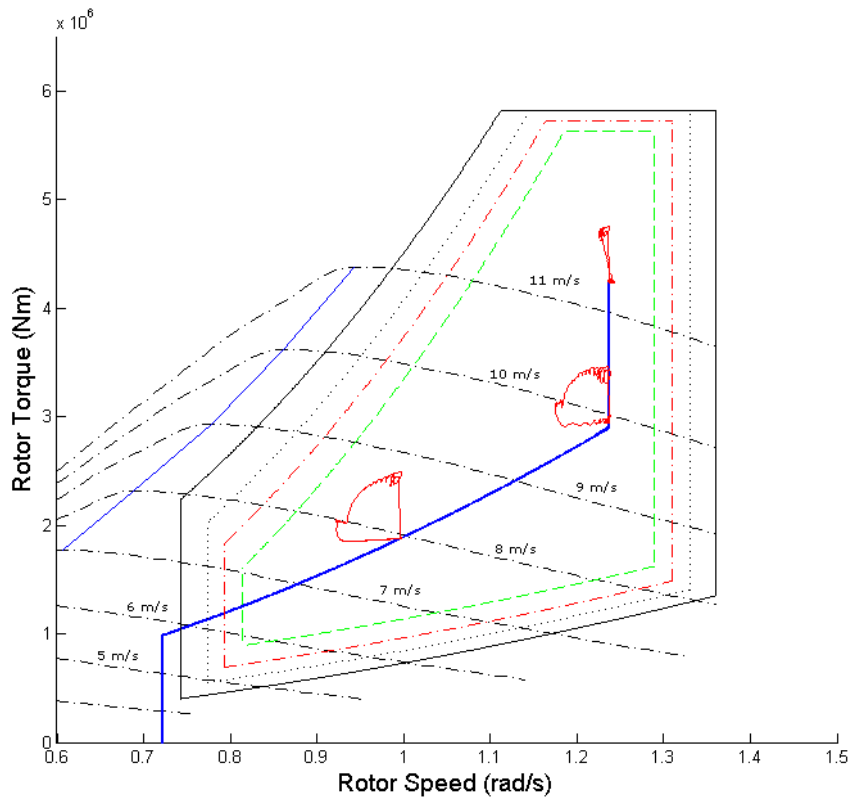


Figure 151: Torque-Speed Curve – 5MW Wind Turbine Providing Increased Synthetic Inertia

Chapter 8: Using the PAC to Provide Grid Frequency Support

Despite providing a synthetic inertia response of three times the magnitude of conventional plant for a very large drop in grid frequency, the operating point of the wind turbine does not move outside of the green “traffic light zone” (for an explanation of the traffic light zones refer to chapter 7). Simulations are run using the 1.5MW wind turbine with the same increased inertial constant of 18s. The results are presented in Figure 152 and Figure 153.

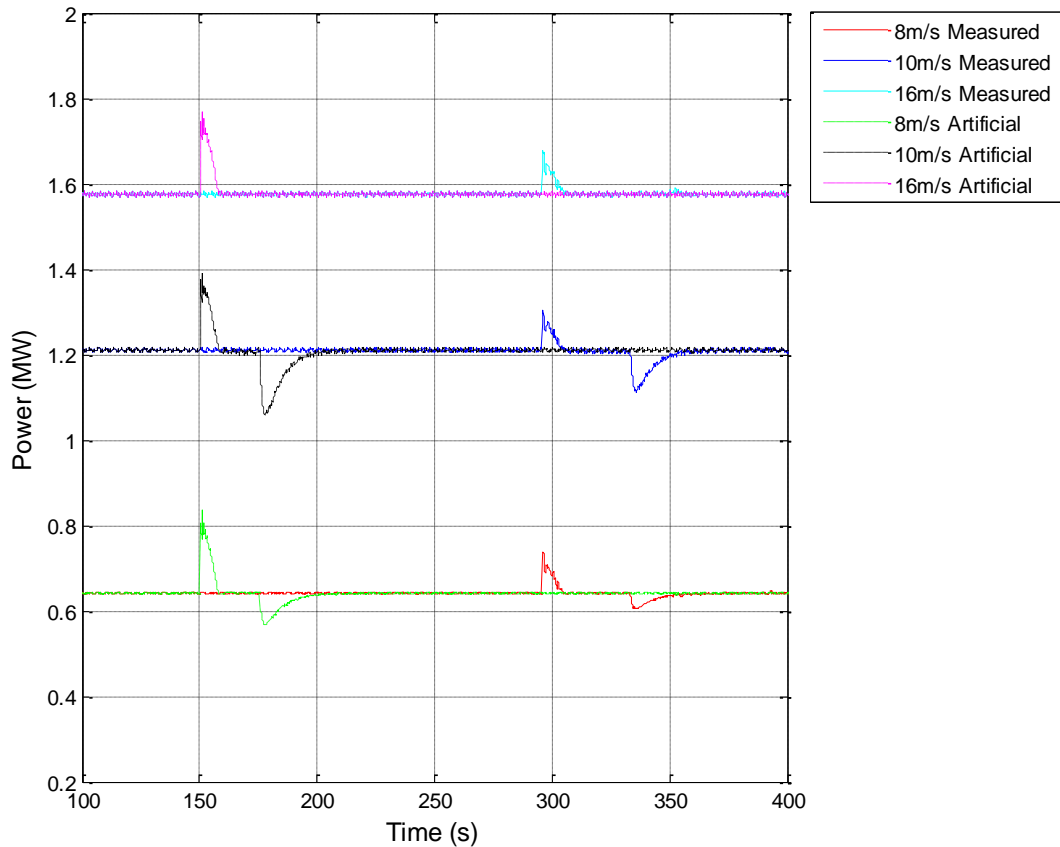


Figure 152: Increased Synthetic Inertia Response of the 1.5MW Wind Turbine

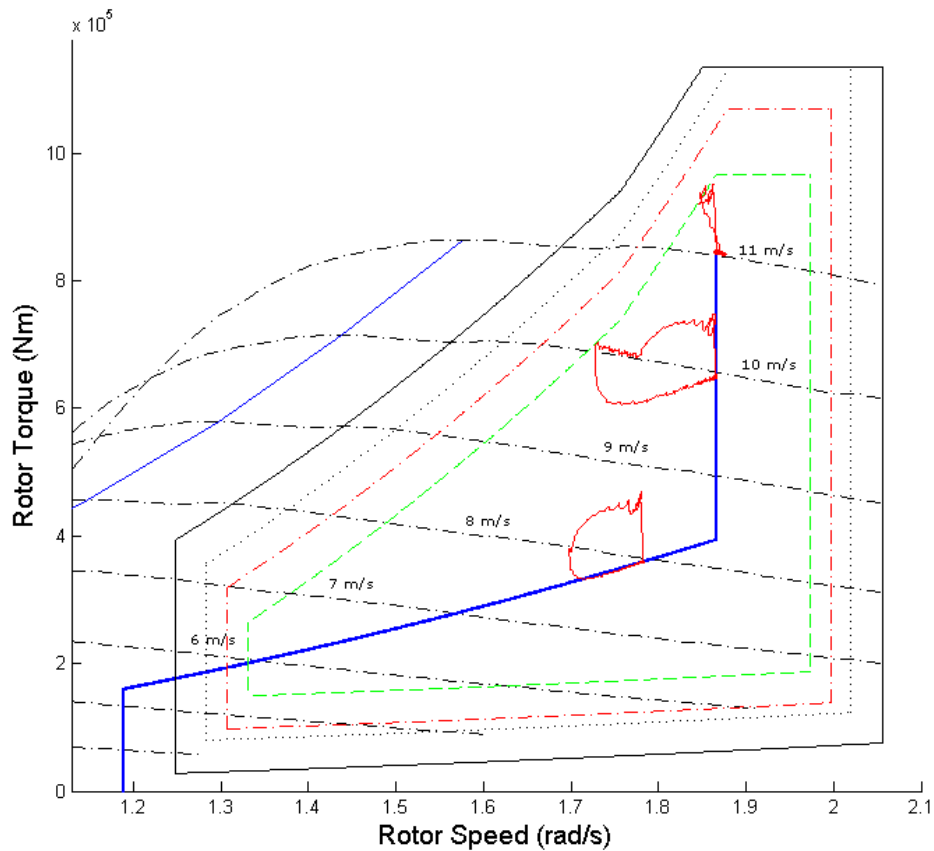


Figure 153: Torque-Speed Curve – 1.5MW Wind Turbine Providing Increased Synthetic Inertia

The 1.5MW wind turbine has less kinetic energy stored in its blades than the 5MW turbine, as its blades are less massive. Due to the 1.5MW wind turbine’s operational strategy and the aerodynamics of its rotor, the area to the left of the operational strategy is smaller than for the 5MW wind turbine. Despite these factors, the 1.5MW wind turbine is able to provide a synthetic inertia response equivalent to an inertial constant of 18s without exiting the green “traffic light” zone.

It is interesting that, due to the strategy and aerodynamics of the 1.5MW machine, the turbine is better placed to provide inertial response at wind speeds of 8m/s to 9m/s than it is at wind speeds from 10m/s to 11m/s as the area between the operating strategy and the upper torque limit is larger.

Simulations using an inertial constant of 18s are completed with the 5MW wind turbine with variable wind speed and with the 1.5MW wind turbine with variable wind speed. The results are shown in Figure 154 and Figure 155.

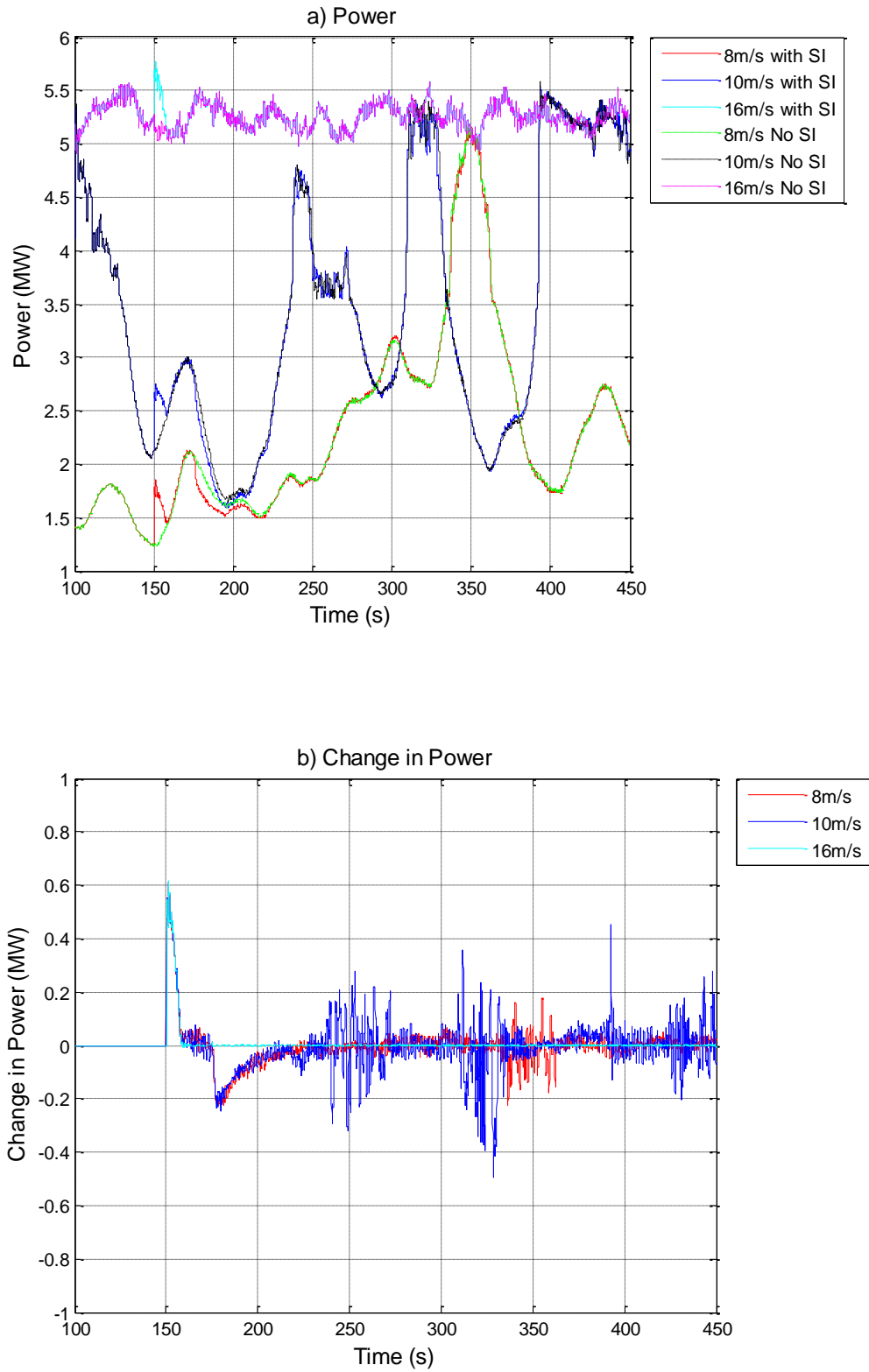


Figure 154: Increased Synthetic Inertia Response of the 5MW Wind Turbine – Variable Wind Speed

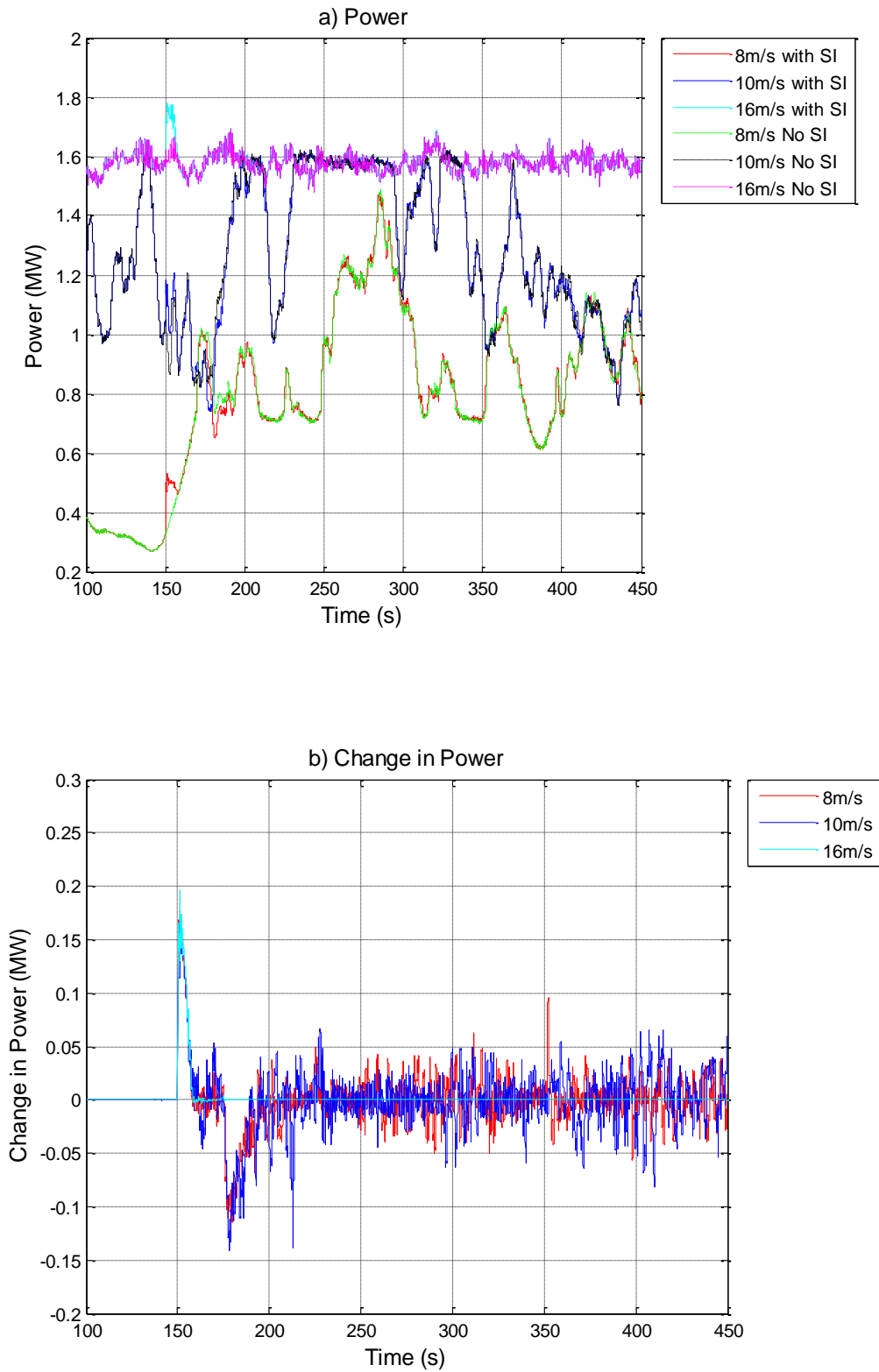


Figure 155: Increased Synthetic Inertia Response of the 1.5MW Wind Turbine – Variable Wind Speed

Figure 154 and Figure 155 show that the PAC delivers accurate synthetic inertia in variable wind speeds. There is some noise after synthetic inertia has been provided,

however this is due to the difference in the rotational sampling between the simulations with synthetic inertia and those without, caused by the change in rotor speed, as discussed in chapter 4.

It is clear that wind turbines equipped with the PAC are capable of providing excellent inertial response. Whilst the amount of inertial response that a turbine is capable of depends upon both the design of the turbine and its operational strategy, for the wind turbines studied, an inertial response of three times the magnitude provided by conventional plant is possible, even for an extreme event.

The ability to provide a larger inertial response is very useful when considering wind farm control. As well as the obvious advantage of being able to provide greater support to the grid, a wind farm is also able to provide the same inertial response as conventional synchronous plant without using all of the turbines in the plant to do so (for example one third of the turbines could provide inertial support equivalent to an inertia constant of 18s whilst the rest are not used for synthetic inertia).

8.1.3.1 Analysis of Loads

As synthetic inertia is only very rarely requested, only the ultimate loads on the turbine are investigated, specifically the loads on the tower, blades, and drive-train. The aforementioned loads are shown in Figure 156 and Figure 157 for variable wind speed simulations of the 1.5MW and 5MW machines providing increased synthetic inertia (i.e. with an equivalent inertia constant of 18s) with the artificial frequency input from Figure 147.

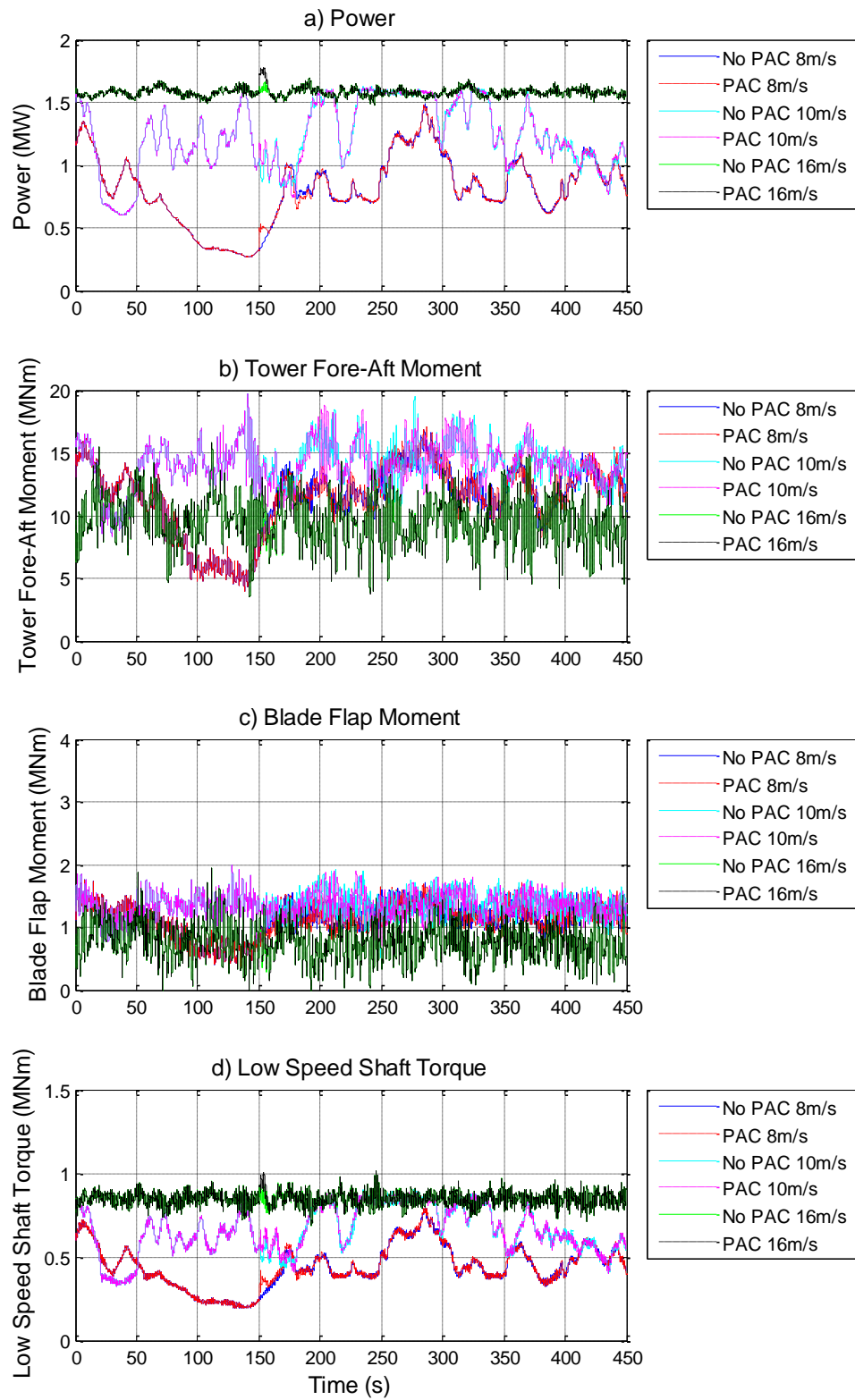


Figure 156: Power and Structural Loads for the 1.5MW Wind Turbine Providing Synthetic Inertia

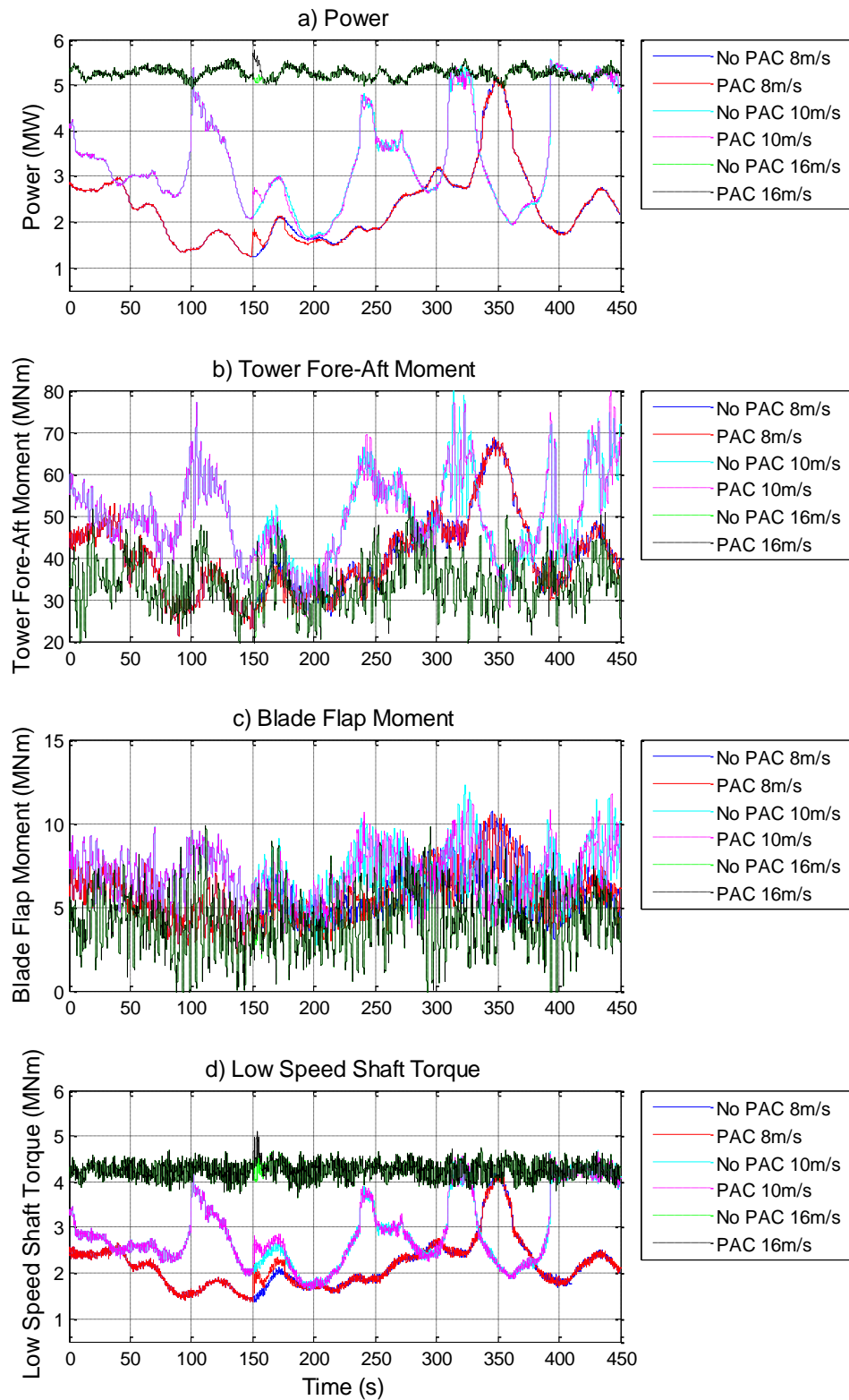


Figure 157: Power and Structural Loads for the 5MW Wind Turbine Providing Synthetic Inertia

In all cases, the PAC causes a modest increase in the drivetrain loads above normal operation and very small increases in the blade flap and tower fore-aft loads.

However, as discussed in chapter 6, this increase is expected to be within the design tolerances of the relevant components, and, as synthetic inertia is both short in duration and would be expected to be infrequent, only the instantaneous load is of concern (not the fatigue loads). If the loads were deemed to be of concern, the maximum power increase could be limited via the PAC rules discussed in chapter 7.

8.2 Using the PAC to Provide Droop Control

Whilst synthetic inertia provides a mechanism for reducing the magnitude of the rate of change of frequency (see section 8.1) it does not prevent the frequency from dropping, and so, with no additional remedial action, the frequency will continue to fall albeit at a slower rate than if synthetic inertia was not provided. In order to prevent the frequency from continuing to fall, the power supplied to the power system must be increased so that it matches or exceeds the power demanded. The method typically used by conventional generators to do this is known as droop control.

When the frequency reduces, generators increase their power output proportionally to the deviation in grid frequency from the set value (typically 50Hz). When operated in the conventional manner, neither wind turbines nor wind farms provide this response. As such, with increased penetration of wind generation in the power system comes a reduction in the grid system frequency stability.

The PAC is used to provide droop control from wind turbines by using the following method:

1. The output of the wind turbine is reduced by a set offset to provide “head room” for increases in power output. The value is denoted as ΔP_{offset}
2. A further adjustment is made to the change in power output that is proportional to the change in grid frequency. This value is $\Delta P_{freq} = K_{freq}(f_{nominal} - f)$
3. The total change in power output (ΔP) is then found by summing the values in 1. and 2.

Hence, the total change in power output is given by,

$$\Delta P = \Delta P_{offset} + \Delta P_{freq} = \Delta P_{offset} + K_{freq}(f_{nominal} - f) \quad (8.4)$$

The value of the offset and the variable K_{freq} is determined by the operator in order to meet the demands of the grid.

8.2.1 The Requirements for Droop Control

The UK grid code is fairly typical of grid codes for modern industrialised countries. It requires synchronous generation to have a droop capability of 3-5%. This means that a change in frequency of 3-5% will result in a change in power output of 100%. It is also a requirement that the frequency should be kept between 49.8 and 50.2Hz and so the maximum change in power output required during normal operation is 10% of output power.

8.2.2 Strategies for Implementation of Droop Control

By utilising a hierarchical structure such as that described in section 3.7 it is possible to dynamically vary the required response from each machine in a wind farm in order to provide droop control in as efficient a manner as possible (i.e. minimising the reduction in energy capture and/or reducing the overall loads on the wind turbines). Design of these higher level controllers and the required wind farm models are however, outside the scope of this work. In addition, it is possible for wind turbines that are not part of a hierarchical wind farm structure to provide droop control. It is both logical and useful therefore, to investigate methods of providing droop control without the use of a wind farm level controller and instead using just the PAC.

One of the first considerations is to decide in which wind conditions droop control is provided and in which conditions it is not. When the wind speed is very low the power output of a wind turbine is correspondingly also very low. In these conditions it is sensible to curtail provision of droop control, as if a reduction in power output is required then the wind turbine may end up demanding zero or even negative power. In addition, any response provided by the turbine is very

small in relation to the total power generation on the grid, and so not providing droop control from turbines experiencing very low wind speeds will not have a large effect on the grid stability.

Once a wind turbine reaches rated wind speed, there is no longer a requirement for an offset to provide head room. In above-rated conditions it is possible instead, to “over-rate” the machine for a limited time. When over-rating the turbine it is required to produce a power output higher than the rated value, which is possible in above-rated wind speeds without an offset as the PAC can utilise a negative $\Delta\beta$ value to increase the aerodynamic torque to match an increased generator torque. Droop control is provided at all above rated wind speeds up to the cut-out wind speed. At wind speeds close to rated it is important to avoid chattering between the above-rated offset of zero and the below-rated offset. As such, a simple hysteresis is used whereby the switch to zero offset occurs at a wind speed x m/s above-rated and the switch to the normal offset value occurs at a wind speed y m/s above-rated, where $y < x$. The wind speed is measured using the wind speed estimator in the PAC described in chapter 5.

Over-rating the turbine increases the cyclic thermal loads on the converter. However, it has been demonstrated [82], that the torque demand to the converter in above rated conditions would need to be raised to as much as 120% of rated torque for up to 20 minutes before the temperature limits are reached and thermal loads become a concern. Over-rating the converter by a maximum of 10% for periods of time generally well under 20 minutes, as would be typical for droop control, should therefore be sustainable.

Different strategies to provide droop control are investigated. The simplest strategy, referred to as strategy 1, is to provide an offset of 10% of rated power in all wind conditions. This ensures that the required change in power will be provided in all wind conditions above the minimum “cut out” speed.

Strategy 1 results in an offset far greater than 10% of the current power in below rated wind speeds. A more advanced strategy (referred to as strategy 2) therefore,

Chapter 8: Using the PAC to Provide Grid Frequency Support

is to determine the offset based on the estimate of wind speed in the PAC. In order to ensure that no strong feedback loop is induced the wind speed is measured every 5 seconds.

Graphs of these strategies for the 1.5MW and 5MW wind turbines are given in Figure 158. Both values for hysteresis are displayed; for both strategies and turbines, the offset is implemented when the wind speed rises above 8m/s, the PAC is switched off if the wind speed falls below 7m/s, the offset is reduced to zero if the wind speed rises above 15m/s, and the offset is implemented if the wind speed falls below 13m/s.

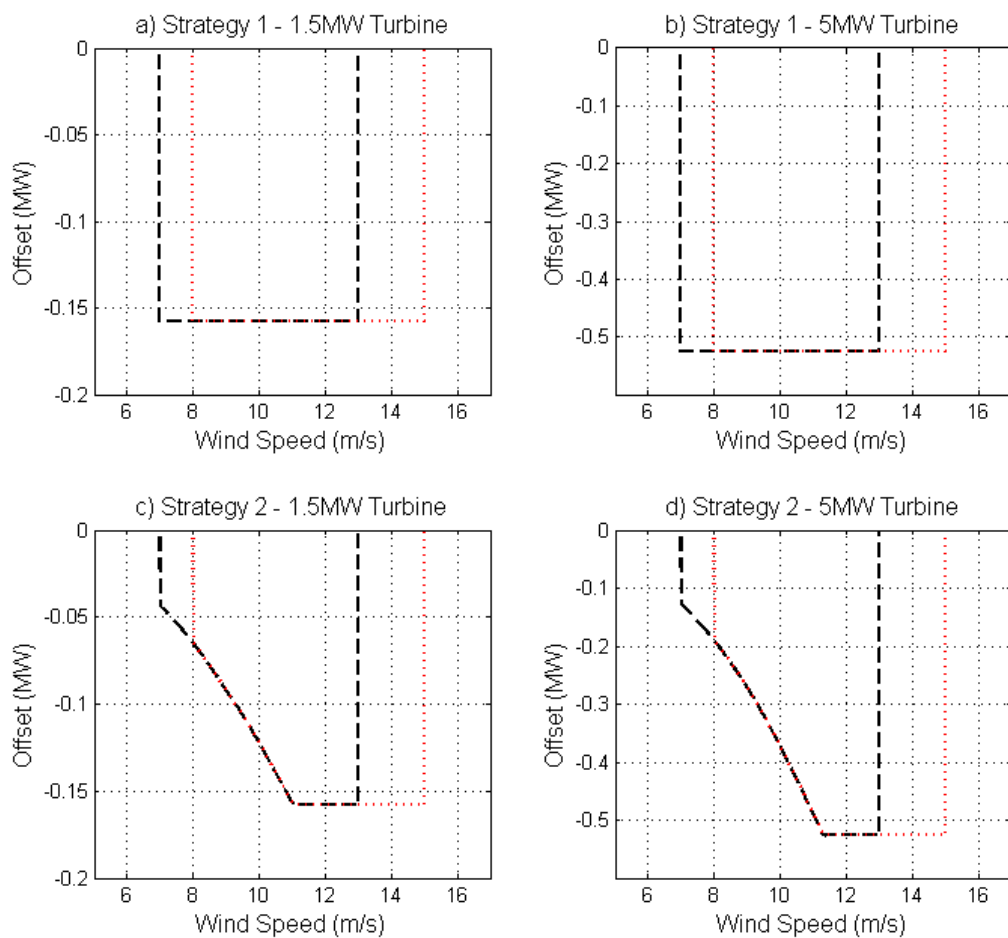


Figure 158: Two Strategies for Droop Control for the 1.5MW Wind Turbine and the 5MW Wind Turbine

8.2.3 Droop Control Simulations

Simulations are conducted using both the 1.5MW and 5MW wind turbines, with the PAC set to provide droop control as per strategy 1 and strategy 2 in Figure 158.

Eighteen simulations are conducted for each strategy, six at 8m/s, six at 10m/s and six at 14m/s, all with turbulence levels of class B as defined in the IEC international standard 61400-1 (third edition) [76], but with different turbulence seeds. The frequency input is a ten minute sample of measured grid frequency data and is the same for each 1.5MW wind turbine simulation and for each 5MW wind turbine simulation. The grid frequency data is shown in Figure 159.

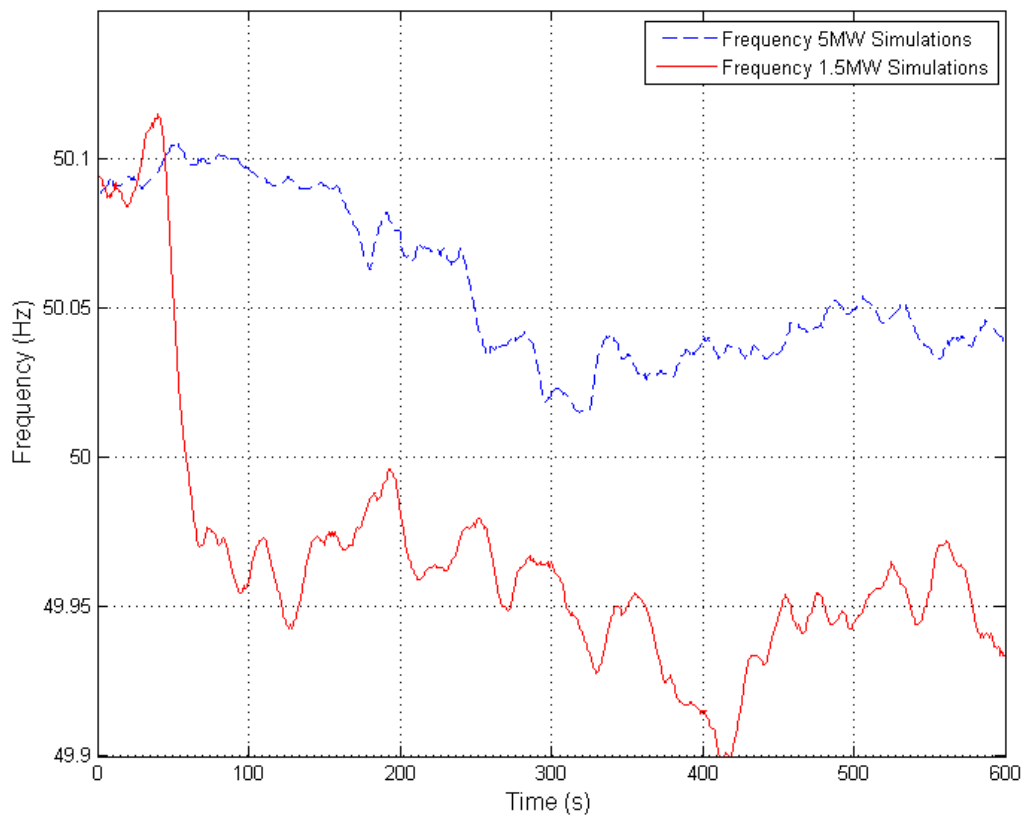


Figure 159: Frequency for Droop Control Simulations

The results for three of the simulations using the 1.5MW wind turbine with strategy 1, one simulation at each wind speed, are shown in Figure 160. In graph *a*) the power output with and without the PAC is plotted, in graph *b*) the ideal change in power request and the actual change in power request are plotted, and in graph *c*) the actual change in power request and the actual change in power are plotted.

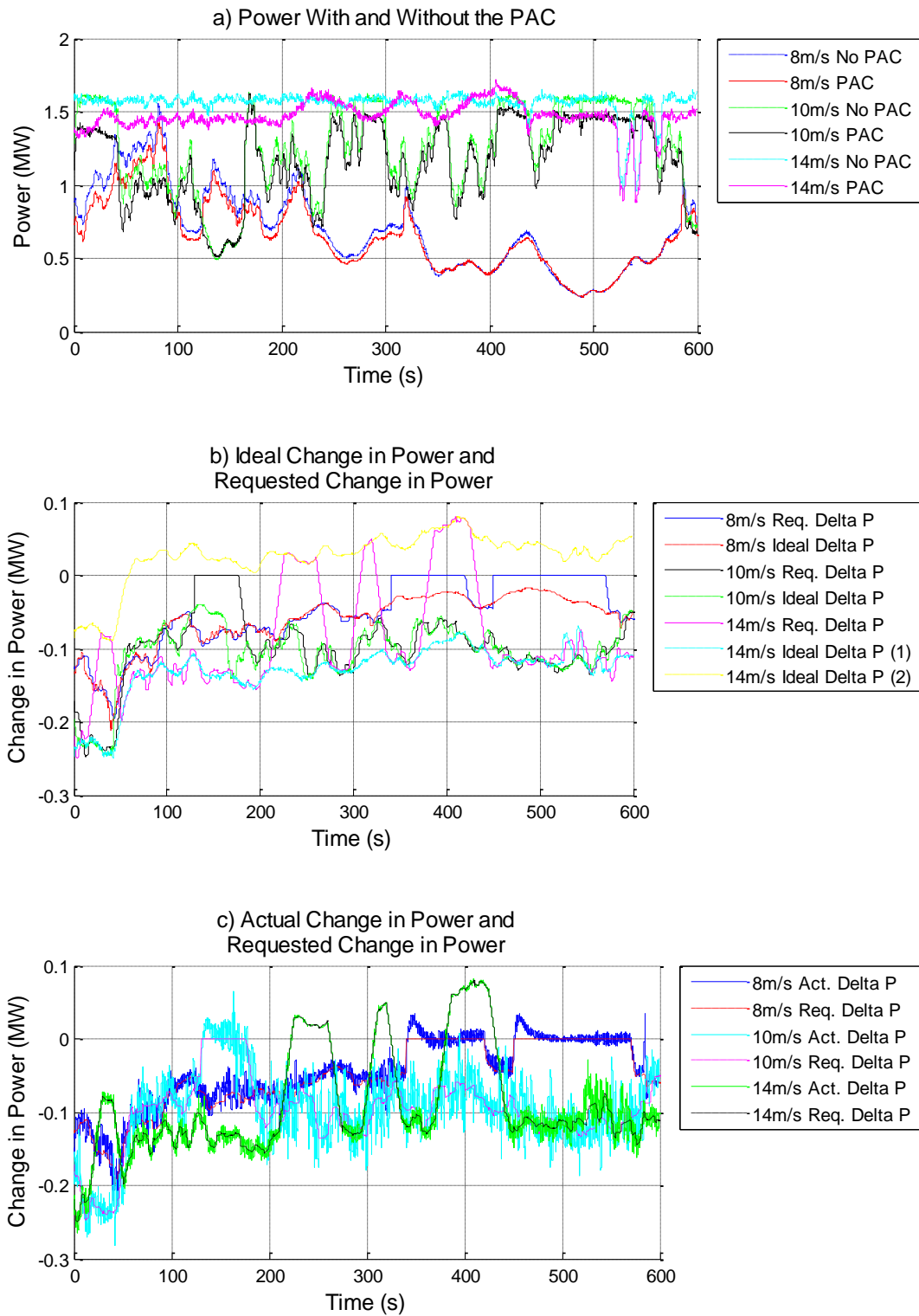


Figure 160: Droop Control Results - Single 1.5MW Wind Turbine (Strategy 1)

Graph *b)* in Figure 161 shows that ideal change in power specified by the strategy in Figure 158 is tracked by the requested change in power. In the 8m/s simulation the change in power reduces to zero at the start of the simulation, approximately 420

seconds and approximately 570 seconds as the wind speed drops below 7m/s. The change in power is reduced to zero once for the 10m/s at approximately 130 seconds for the same reason. For the 14m/s simulation, two ideal change in power curves are plotted; one with the offset and one without. The actual requested change in power moves between the two ideal change in power lines as the wind speed increases above 15m/s and drops below 13m/s.

Graph *c*) shows that the requested change in power is well matched by the actual change in power. There is noise in the signal, especially for the 10m/s simulation, however this is due to misalignment of the rotational sampling of the simulations with and without the PAC, and from slight differences in the timing of the full envelope controller switching between operational modes, both caused by the change in rotor speed (as explained in chapter 4).

The results for three of the simulations using the 5MW wind turbine with strategy 2, one simulation at each wind speed, are shown in Figure 161. In graph *a*) the power output with and without the PAC is plotted, in graph *b*) the ideal change in power request and the actual change in power request are plotted, and in graph *c*) the actual change in power request and the actual change in power are plotted.

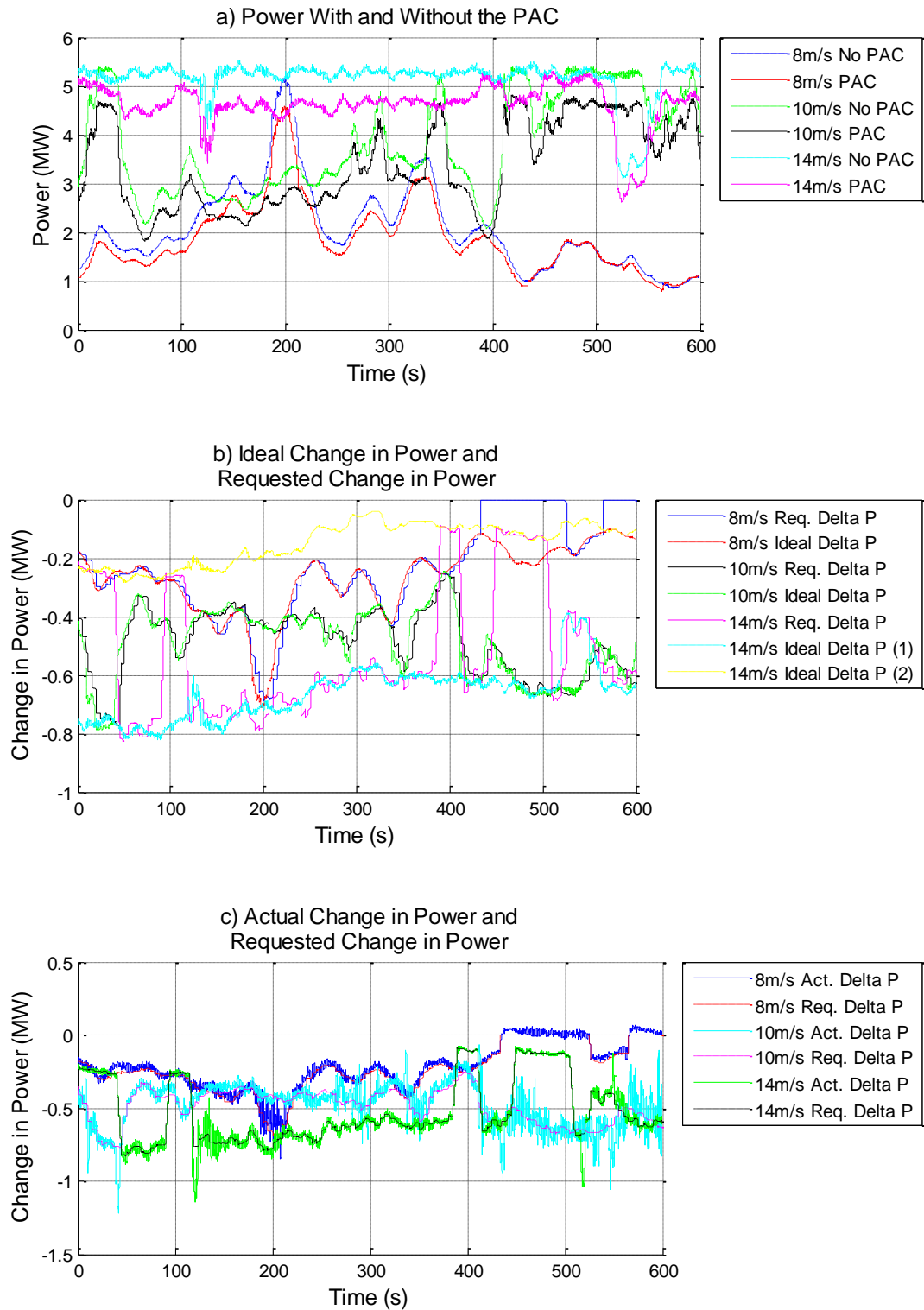


Figure 161: Droop Control Results - Single 5MW Wind Turbine (Strategy 2)

Graph *b)* in Figure 161 shows that ideal change in power specified by the strategy in Figure 158 is tracked by the requested change in power. In the 8m/s simulation the change in power reduces to zero at approximately 430 seconds and approximately

560 seconds as the wind speed drops below 7m/s. For the 14m/s simulation, two ideal change in power curves are plotted; one with the offset and one without. The actual requested change in power moves between the two ideal change in power lines as the wind speed increases above 15m/s and decreases below 13m/s.

Graph *c*) shows that the requested change in power is well matched by the actual change in power. There is noise in the signal, especially for the 10m/s simulation, however this is due to misalignment of the rotational sampling of the simulations with and without the PAC, and from slight differences in the timing of the full envelope controller switching between operational modes, both caused by the change in rotor speed (as explained in chapter 4).

It is clear that, unlike the simulations using strategy 1, the offset and change in power output are varied with the wind speed. Varying the offset and change in power output increases the energy capture of the turbine, however the droop response of the turbine less; it is proportional to the current power output as opposed to the rated power output.

In Figure 162 and Figure 163, the average effect of each strategy over six wind turbines is shown for each wind speed.

Chapter 8: Using the PAC to Provide Grid Frequency Support

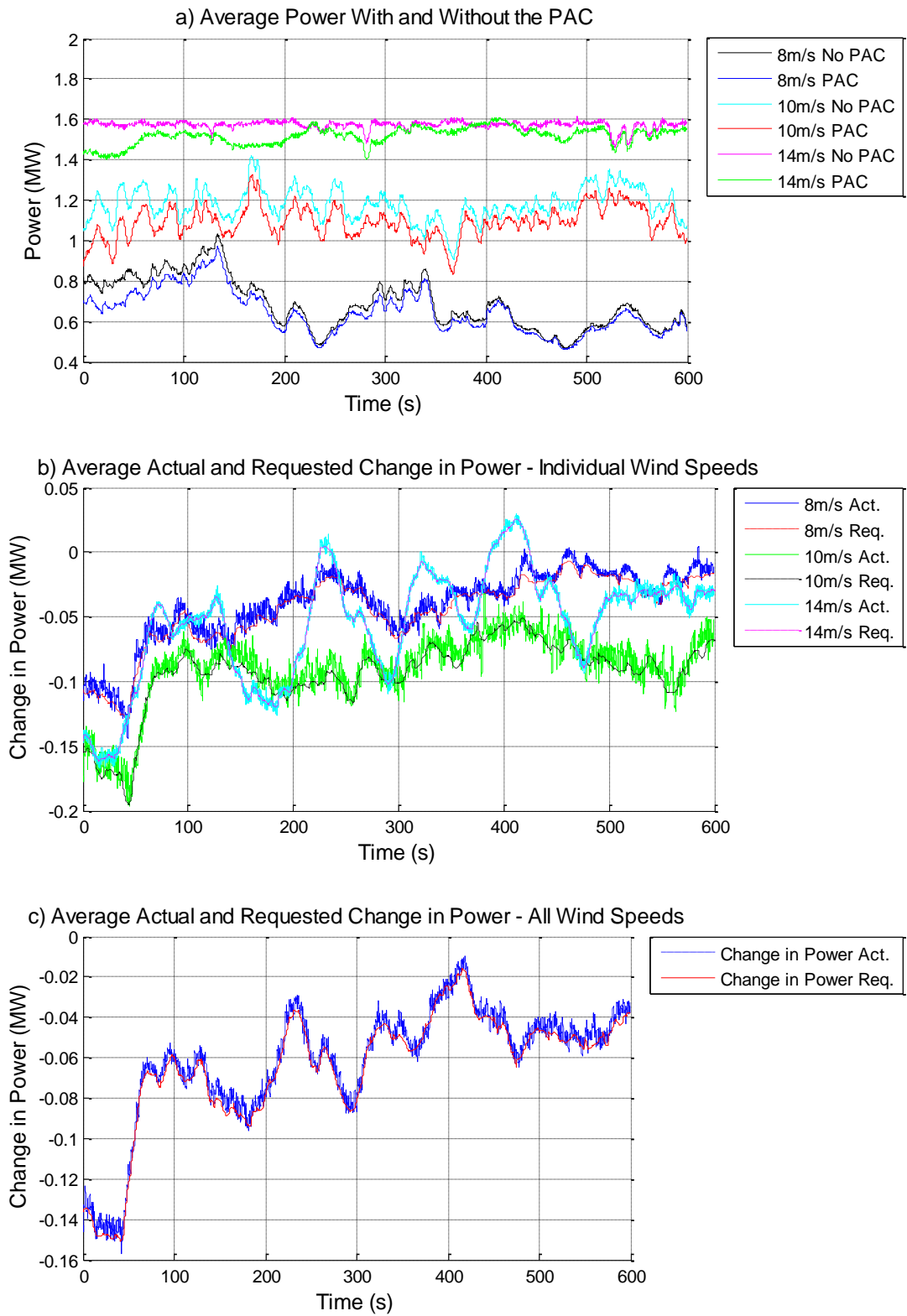


Figure 162: Droop Control Results – Six 1.5MW Wind Turbines (Strategy 1)

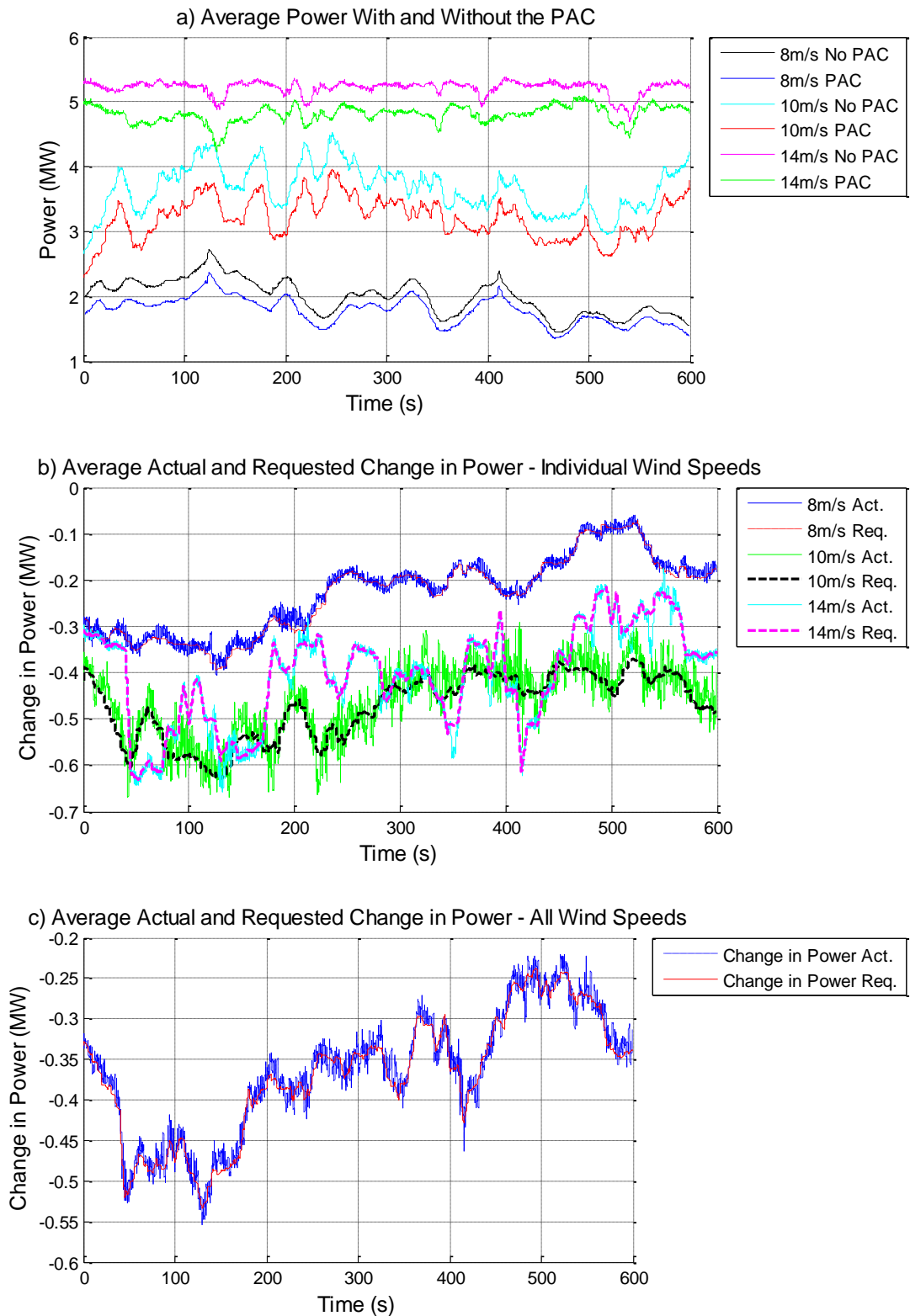


Figure 163: Droop Control Results – Six 5MW Wind Turbines (Strategy 2)

Graphs *a)* in Figure 162 and Figure 163 show the average power output for each of the six turbines at each mean wind speed. Graphs *b)* shows the average change in

power requested and the average change in power delivered for each wind speed. Graphs *c)* shows the average requested change in power and actual change in power across all 18 wind turbines.

Overall, the change in power requested is tracked accurately. The results presented show the effect of averaging on the change in power output. The noise on the signals is greatly reduced compared to the results for a single turbine. For larger wind farms this averaging effect is likely to be even greater, reducing noise further.

For the simulations at 8m/s, the change in power sometimes exceeds the requested change for a short time, such as at 120 seconds in graph *b)* Figure 162. The error in the change in power is a result of the recovery process. When the turbine recovers, ΔP is set to zero, however a wind turbine will often produce an increase in power output as it returns to the normal operating strategy. Recovery happens more often at lower wind speeds, hence the error being greater for the 8m/s simulations. The effect can also be seen in the total change in power across all 18 turbines in graph *c)* of Figure 162. Wind farm control could be used to alleviate this issue.

The results show that the PAC is capable of providing an accurate change in power proportional to the change in grid frequency suitable for droop control and that both strategy 1 and strategy 2 are effectively followed.

8.2.3.1 Impact on Fatigue Loads and Energy Capture

The PAC is set up to provide droop control for both the 1.5MW and the 5MW wind turbine, as outlined in the previous sections. Six simulations are conducted for each mean wind speed from 8m/s up to 24m/s for each turbine and for each strategy. It is assumed that at average wind speeds below 8m/s droop control would not be used, as the power output of the turbine is low. The turbulence levels are defined by following the IEC international standard 61400-1 (third edition) [76]. The wind is assumed to be class B as defined in these standards – that is medium turbulence levels. Each simulation uses a different randomly selected 600 second section of a 24 hour long sample of grid frequency (measured on the UK national grid on the

14th November 2014 at Strathclyde University) as an input. The 24 hours of frequency data are shown in Figure 164.

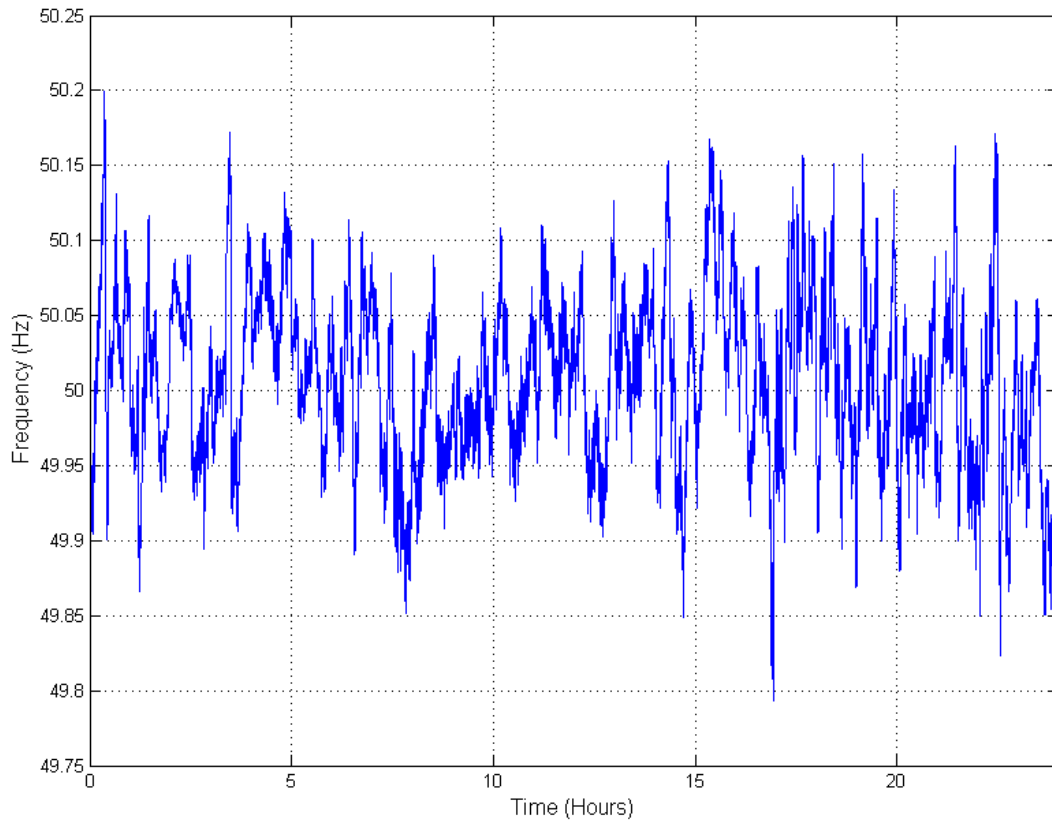


Figure 164: 24 Hours of Grid Frequency Data

For both the 1.5MW and 5MW simulations the combined change in power output across the six turbines is compared with the requested change in power output. The percentage reduction in energy capture across the six turbines is calculated assuming wind speed distributions class I, class II and class III in the IEC international standard 61400-1 (third edition) [76]. Using the same wind distributions, the impact of providing droop control on the fatigue loads of the turbines is calculated through comparison with simulations under the same conditions but with no droop control provided. The magnitude of the reduction in energy capture for each turbine for each of the three wind speed distributions is presented in Table 8. As would be expected, the reductions for strategy 1 using the two turbines are the same, however the reductions are different for strategy 2 as the turbines have differently shaped power curves and hence differently shaped offset

Chapter 8: Using the PAC to Provide Grid Frequency Support

curves for strategy 2. As the offset is a different percentage of the power output at a given wind speed, the reduction in energy capture differs.

Table 8: Percentage Reduction in Energy Capture Due to Droop Control

	1.5MW Wind Turbine (Class I, Class II, Class III)			5MW Wind Turbine (Class I, Class II, Class III)		
Strategy 1	-4.6	-4.7	-4.4	-4.6	-4.7	-4.4
Strategy 2	-3.6	-3.5	-3.3	-3.5	-3.4	-3.1

To calculate the impact of providing droop control using the PAC on the turbine fatigue loads the same method as that used in chapter 6 section 6.5.2 is used. The percentage change in tower fore-aft DELs, blade flap DELs, hub over-turning DELs, and hub yaw DELs for the 1.5MW and 5MW wind turbines for each strategy are shown in Figure 165, Figure 166, Figure 167, Figure 168, Figure 169, and Figure 170.

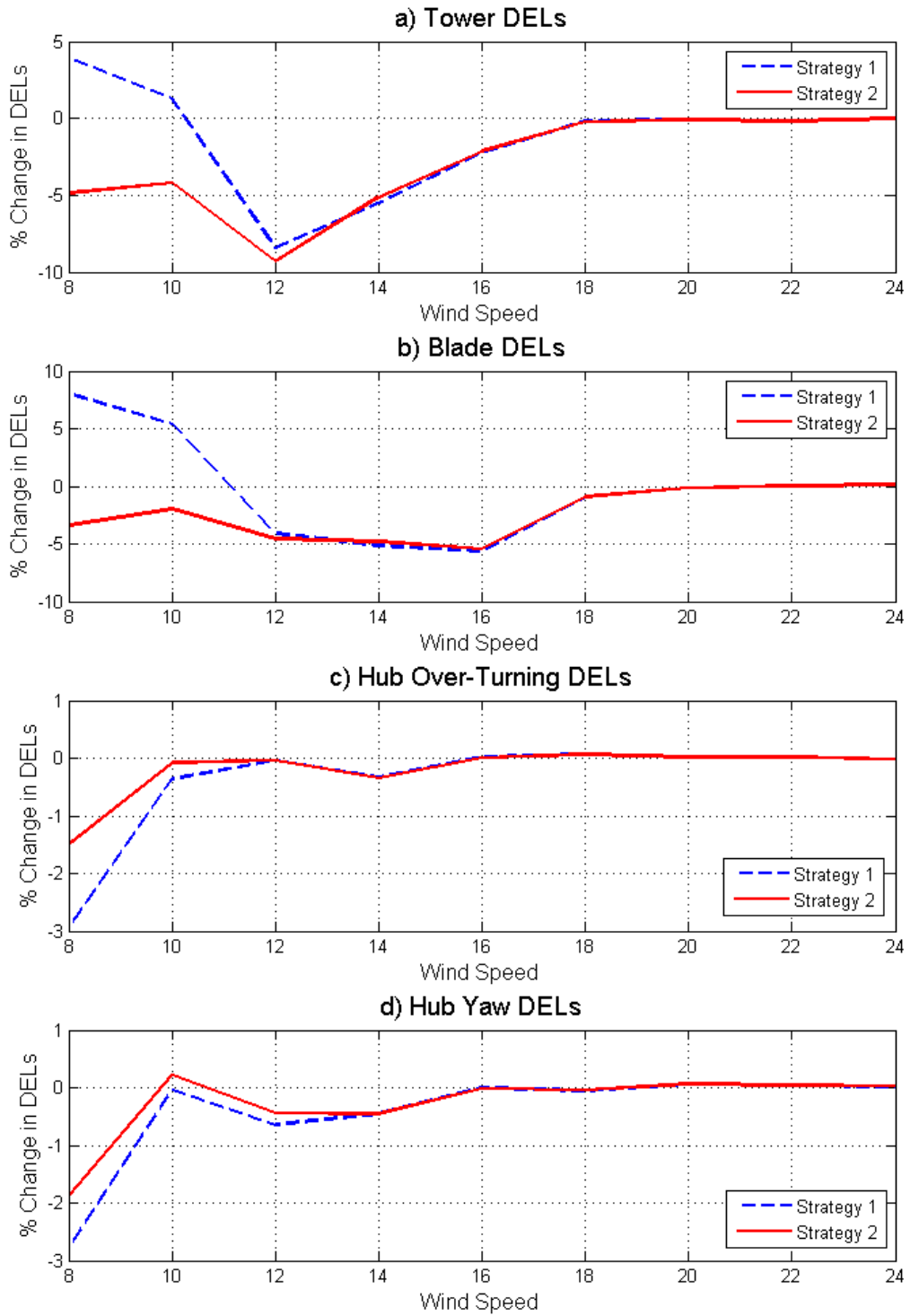


Figure 165: Tower Fore-Aft, Blade Flap, and Hub DELs for a Range of Wind Speeds When Providing Droop Control Using the PAC on the 1.5MW Wind Turbine

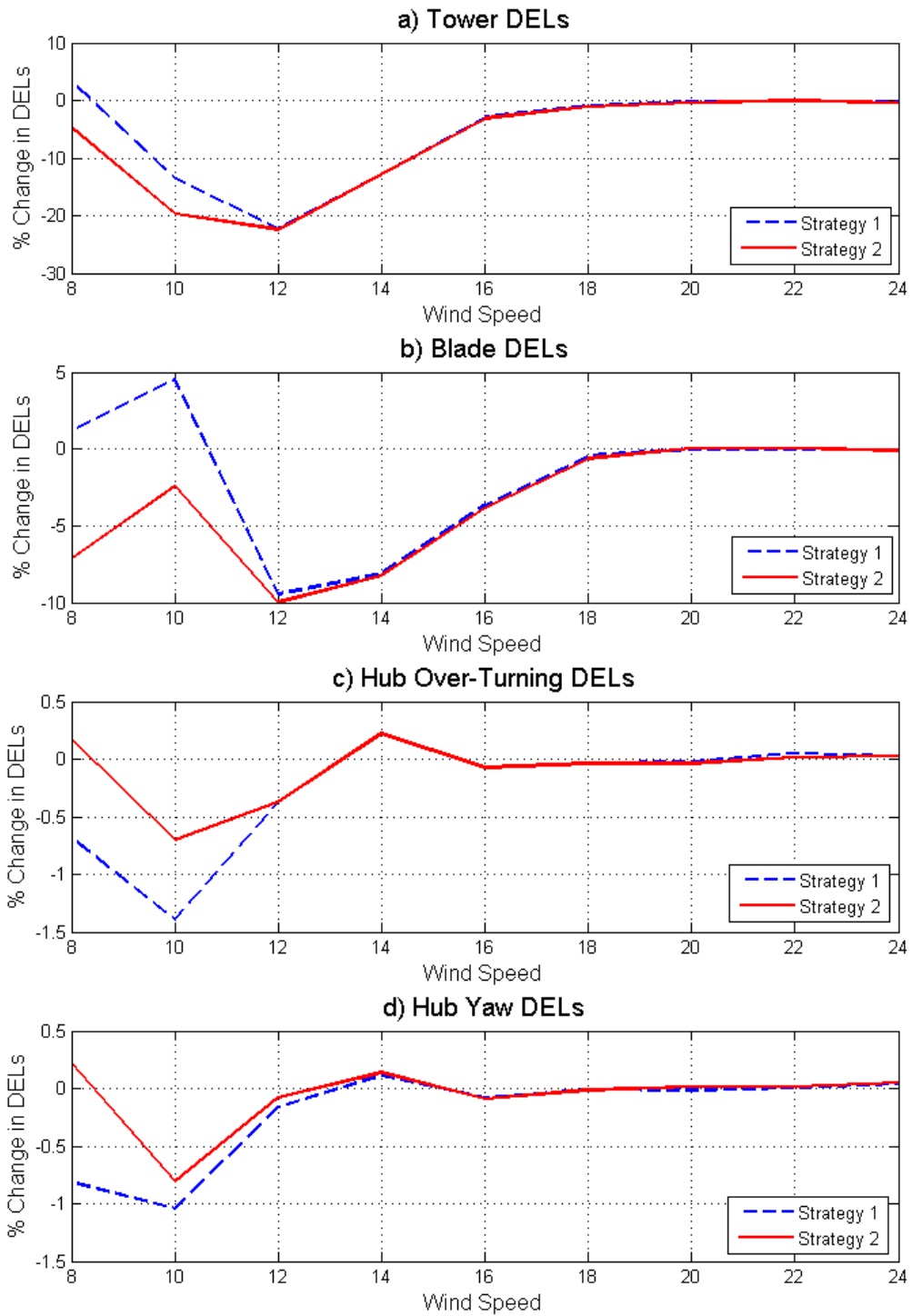


Figure 166: Tower Fore-Aft, Blade Flap, and Hub DELs for a Range of Wind Speeds When Providing Droop Control Using the PAC on the 5MW Wind Turbine

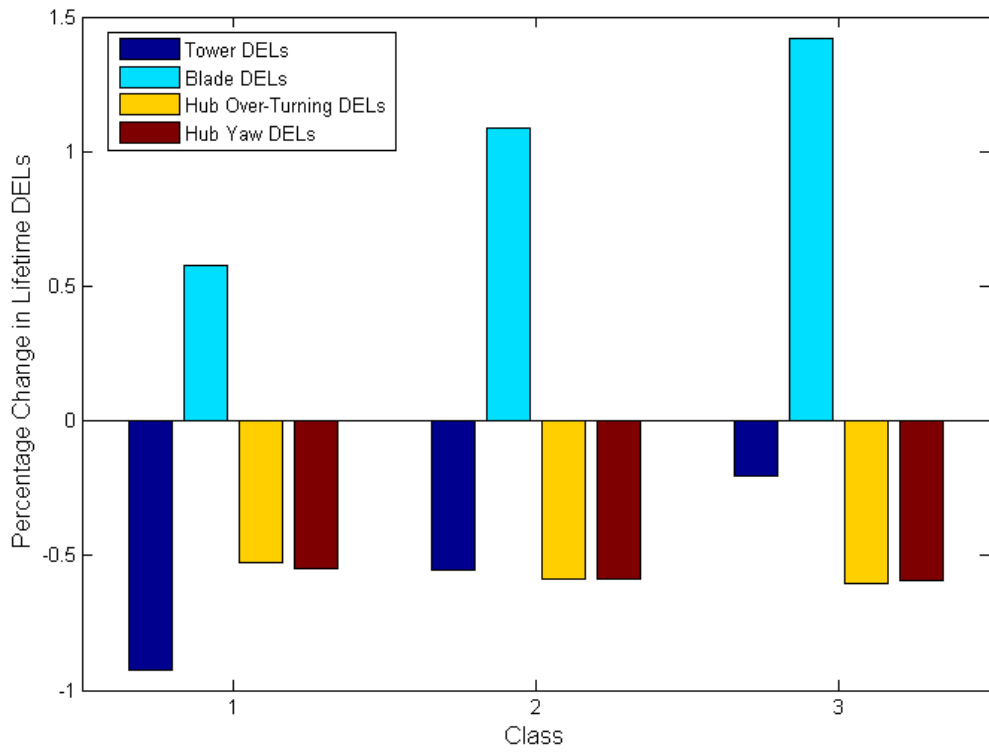


Figure 167: Impact on DELs of providing Droop Control Using the PAC on the 1.5MW Wind Turbine for Different Wind Distributions (Strategy 1)

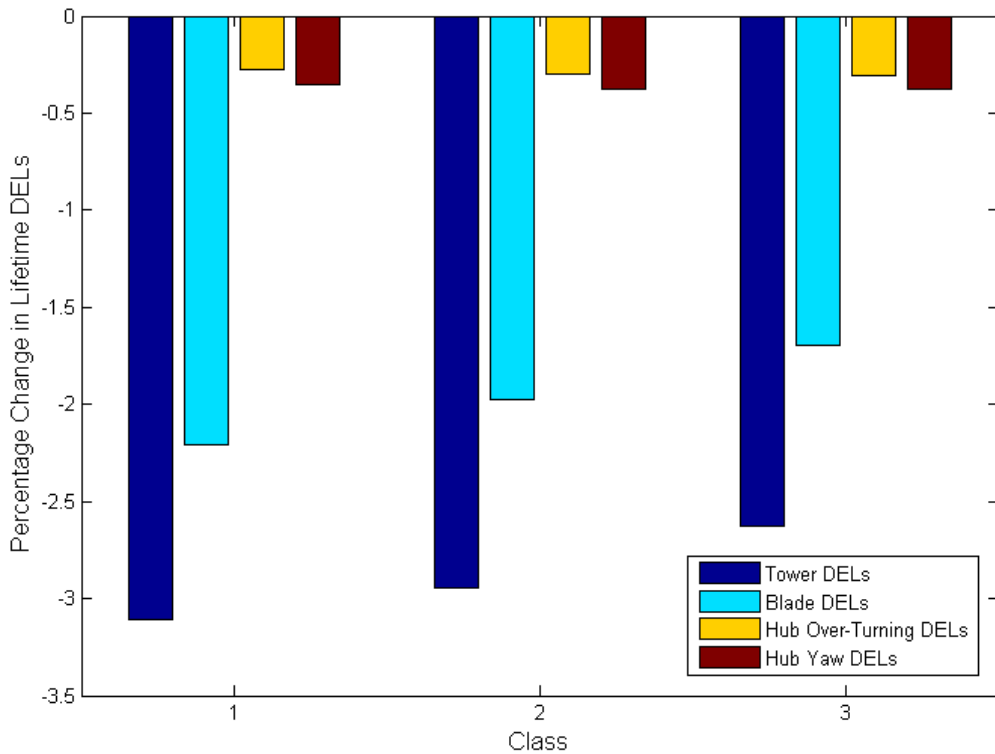


Figure 168: Impact on DELs of providing Droop Control Using the PAC on the 1.5MW Wind Turbine for Different Wind Distributions (Strategy 2)

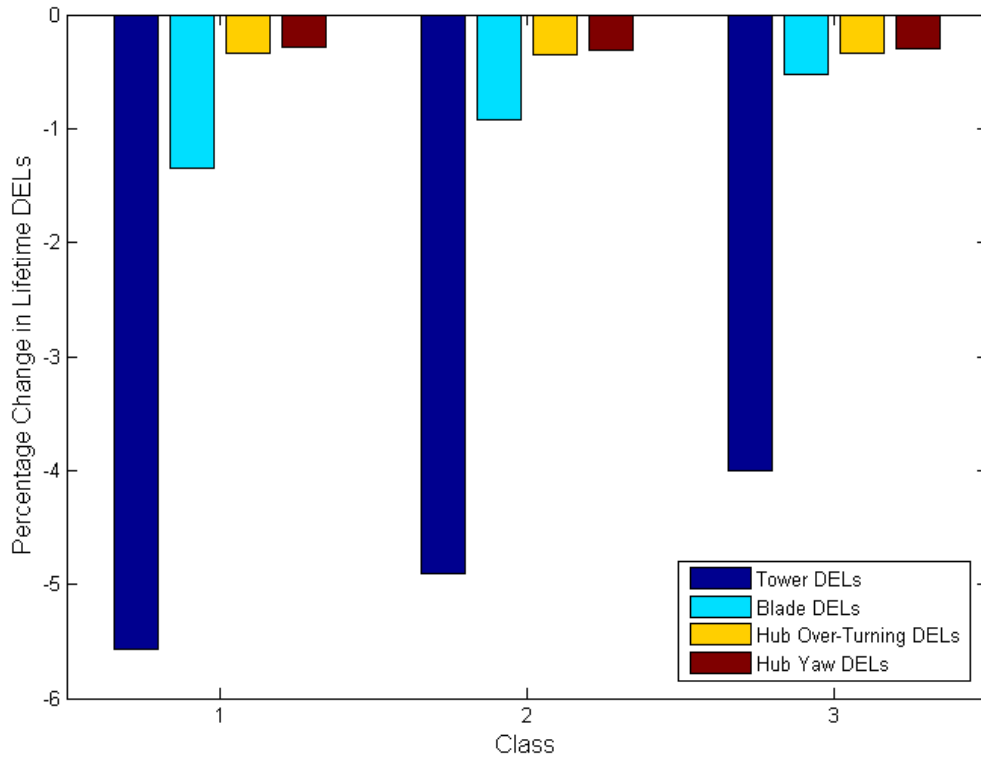


Figure 169: Impact on DELs of providing Droop Control Using the PAC on the 5MW Wind Turbine for Different Wind Distributions (Strategy 1)

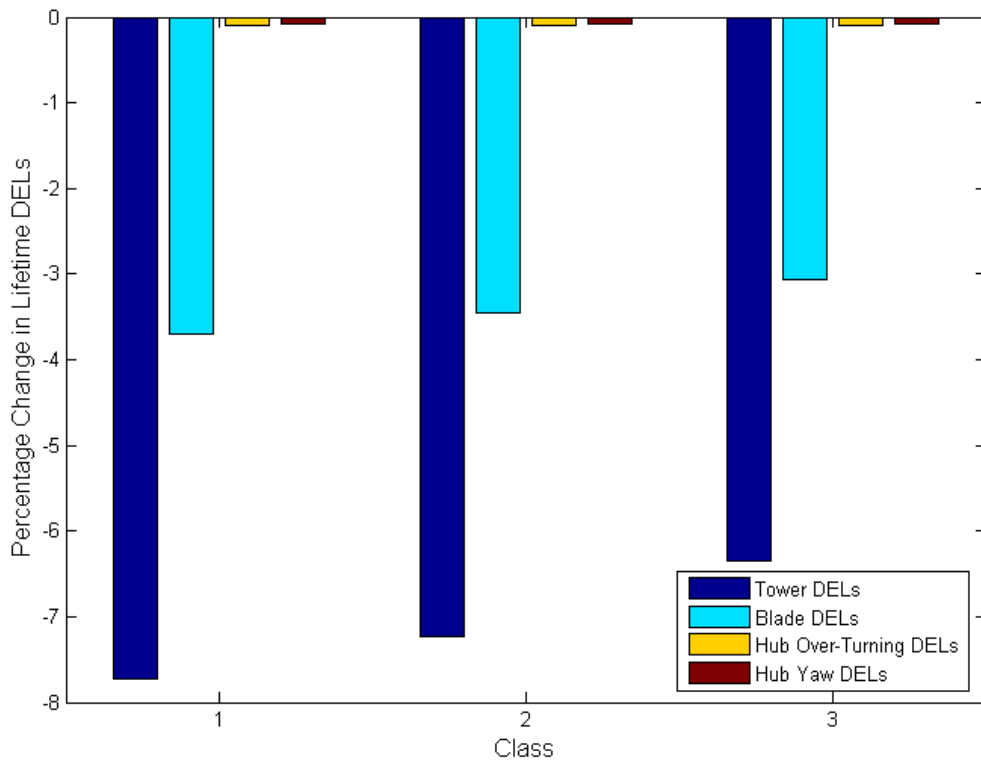


Figure 170: Impact on DELs of providing Droop Control Using the PAC on the 5MW Wind Turbine for Different Wind Distributions (Strategy 2)

It is clear that providing droop control causes a reduction in the turbine tower and hub DELs for all the simulations.

For strategy 1, as would be expected, the results are highly similar to the results presented for a constant offset at the end of chapter 6, and the same explanation for these loads applies.

For strategy 2, the change in the hub lifetime DELs is small, between nearly 0 and 0.34%. The blade flap lifetime DELs are reduced by between 1.7% and 3.7% and the tower fore-aft lifetime DELs are reduced by between 2.6% and 7.7%, both significant reductions. There are greater reductions in the blade and tower DELs for the 5MW machine than for the 1.5MW machine, indicating that the load reductions may increase with turbine size. Turbine size is identified as a probable factor as the spatial filtering of the wind increases with rotor size such that the turbulence of the effective wind speed is reduced, reducing the amount of pitch action required in below rated operation with the PAC. Further work studying more wind turbines would be required to validate this hypothesis.

It can be concluded however, that providing droop control using the PAC with strategy 2 does not increase the lifetime DELs on the turbines studied and causes large decreases in the tower fore-aft and blade flap DELs.

8.3 Combined Droop Control and Synthetic Inertia

Contributing to grid stability via droop control does not preclude a turbine from contributing synthetic inertia in the case of a rapid drop in the grid frequency. The turbine can quickly react with a fast increase in power output as long as the turbine is not at the upper limit for torque, nor the lower limit for speed (see chapter 7).

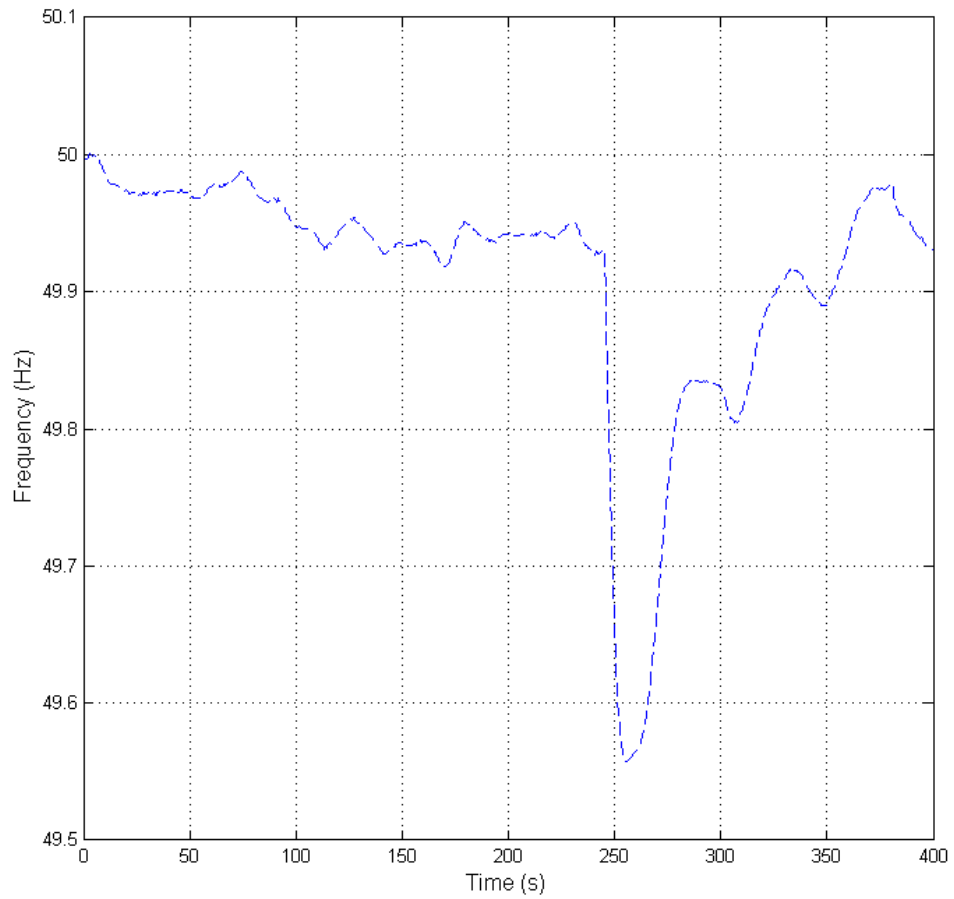


Figure 171: Grid Frequency Data for Combined Droop Control and Synthetic Inertia

Using the measured grid data shown in Figure 171, simulations are performed in which both synthetic inertia and droop control (using strategy 2) are provided. The results are presented in Figure 172 and Figure 173.

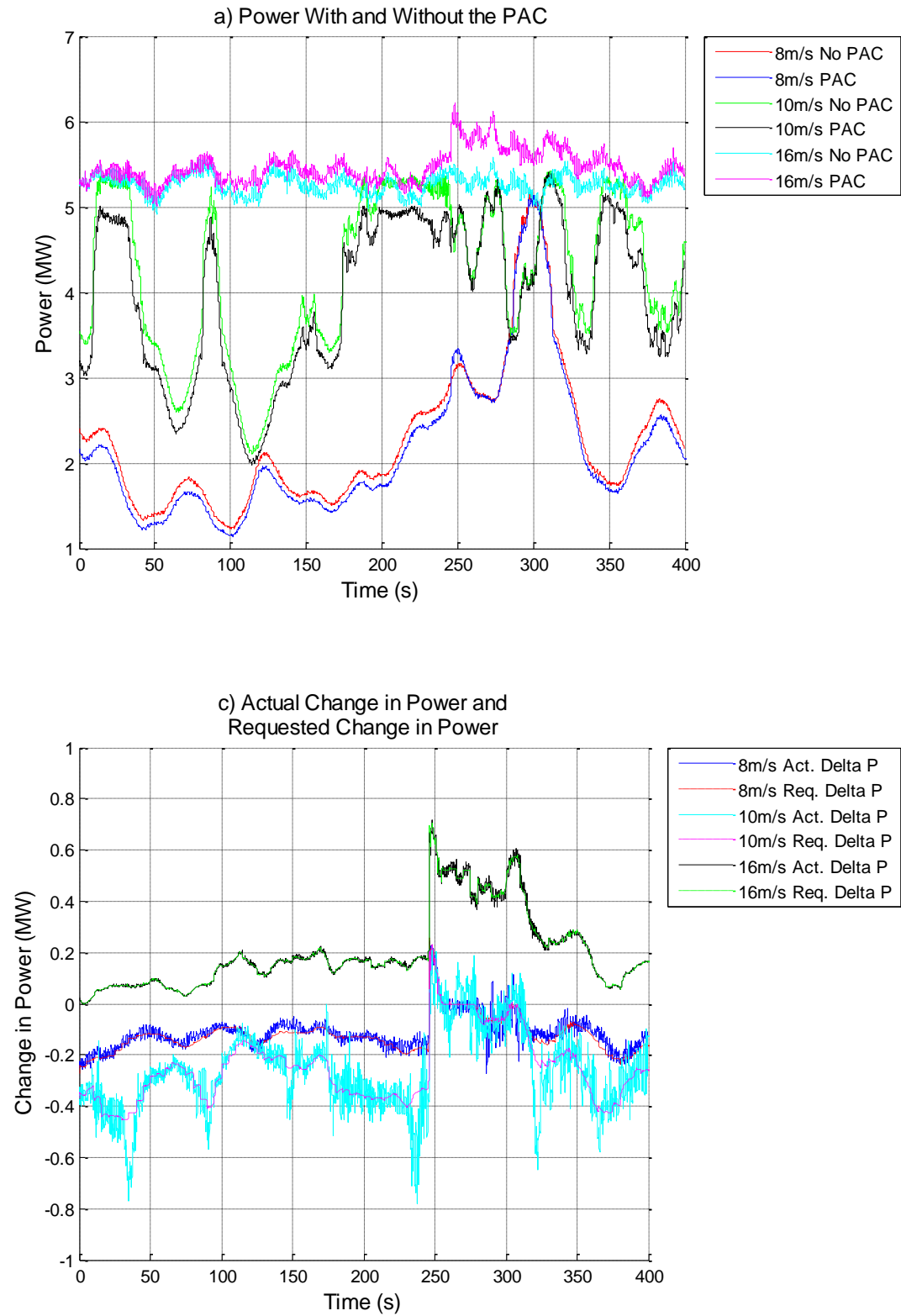


Figure 172: 5MW Wind Turbine Providing Synthetic Inertia and Droop Control Simultaneously

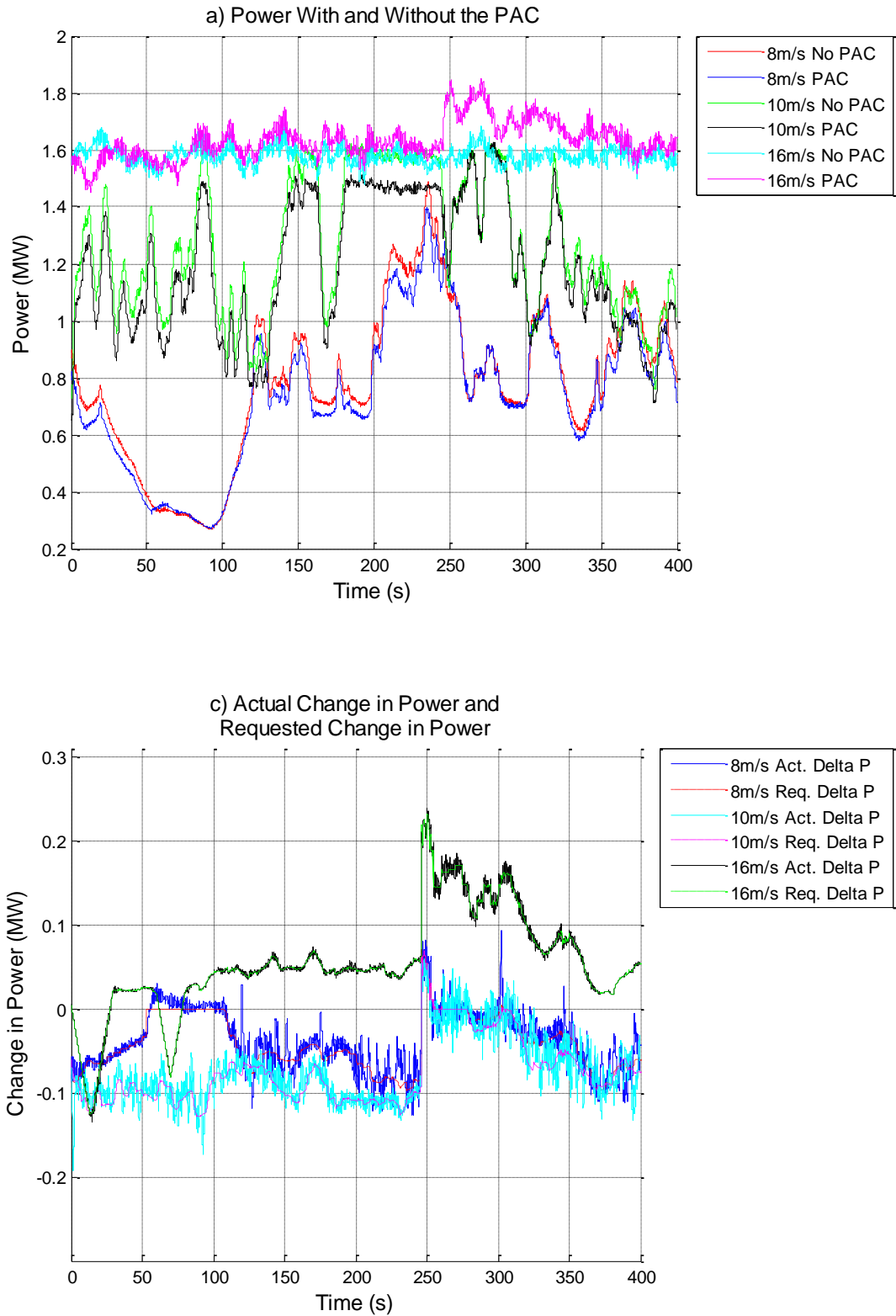


Figure 173: 1.5MW Wind Turbine Providing Synthetic Inertia and Droop Control Simultaneously

The provision of synthetic inertia does not prevent the provision of droop control and vice versa. Because of the offset used in droop control, the PAC does not need to recover after the provision of synthetic inertia.

8.4 Concluding Remarks

The PAC is used to provide synthetic inertia. It is possible to provide synthetic inertia equivalent to an inertial constant of 18s when using the 1.5MW and 5MW turbines studied in this work, effectively three times the inertia typically provided by synchronous plant. The 5MW and 1.5MW wind turbines used are typical of modern wind turbines and so, whilst the provision of synthetic inertia is dependent on both the wind turbine design and the wind turbine full envelope controller strategy used, most large modern wind turbines are expected to be able to provide synthetic inertia via the PAC. Future work studying more wind turbines would be required to validate this hypothesis.

Because the PAC allows the wind turbines studied to provide an equivalent inertial constant greater than the typical value of synchronous plant, there is potential for wind farm control to be used to distribute the required change in power amongst turbines in a farm. As a simple example; the farm may still provide the same effective inertial constant as synchronous plant, but only use one third of the turbines.

The increase in ultimate loads on the turbine caused by the provision of synthetic inertia via the use of the PAC are small and hence would not be expected to be of concern. If the loads are deemed to be large enough to be of concern then they can be limited via a limit on the maximum power increase allowable via the PAC rules. Grid frequency events requiring the provision of synthetic inertia are expected to be rare and so the fatigue loads induced are not considered.

Simulations conducted on the 1.5MW and 5MW wind turbines show that the PAC is capable of providing accurate changes in power output proportional to the grid frequency known as droop control.

Chapter 8: Using the PAC to Provide Grid Frequency Support

Droop control requires an offset in power to provide head room in low wind speeds, reducing energy capture. Two strategies for providing droop control are presented, one provides headroom via a constant offset in power (strategy 1) whilst the other uses a variable offset (strategy 2). The reduction in energy capture is between 4.4 and 4.7% for the strategy 1 and between 3.1% and 3.6% for strategy 2. Wind distributions with higher average wind speeds result in lower reductions in energy capture as more time is spent with no offset used. Note that the reductions stated are for the specific examples, the exact change in power capture for any given turbine is highly dependent upon the turbine design, the full envelope controller design, and the wind conditions at the operating site.

Droop control is demonstrated using both strategies for a range of wind speeds on both wind turbines and the change in damage equivalent loads (DELs) for tower fore-aft moment, blade flap root bending moment and hub nod moment are assessed. Using strategy 1 produces changes to the DELs similar to the simulations presented in chapter 6 for a constant offset; the same comments apply here. All lifetime DELs are reduced through the provision of droop control using strategy 2 for both wind turbines. The reductions in hub lifetime DELs are small, less than 0.5%. The reduction in Blade lifetime DELs are higher, between 0.5% and 3.8%. Finally, the tower lifetime DELs have the largest reductions in DELs of between 0.2% and 7.7%. The higher the mean wind speed of a wind distribution, the larger the reduction in the loads.

Finally, provision of both synthetic inertia and droop control using the PAC is presented. The PAC is able to provide both synthetic inertia and droop control without impacting the operation of either strategy.

Chapter 9:

Conclusion

THE ABILITY TO FLEXIBLY operate wind plant via an alteration to the power output is becoming increasingly desirable for various reasons; to improve the power system characteristics of wind turbines to meet the increasingly stringent requirements of transmission service operators, as a means of increasing the total power output of a wind farm, or as a means to reduce the loads and hence the operational and maintenance costs of the plant.

In this thesis, a novel method for flexibly operating a wind turbine via adjustment of the power output, called the Power Adjusting Controller (PAC) is presented. The thesis contributes new knowledge in the field of wind turbine dynamics and control.

- The development of a novel controller augmentation (the PAC) to vary the power output of a wind turbine in chapters 4 and 5.
- The development of a wind speed estimator that accounts for dynamic inflow effects in chapter 5.

In chapters 2 and 3 of this thesis, the requirement for the development of an augmentation to wind turbine control to provide flexible operation via adjustment of the power output of the turbine is identified. Flexible operation in this manner could be used for a wide variety of purposes, including but not limited to; providing grid services such as droop control, curtailment of the power output of wind farms, and increasing the power output of a wind farm.

Chapter 9: Conclusions

In chapter 4 the PAC is developed as a method of providing augmented control.

- The controller is designed for use with a lumped parameter model of a wind turbine
- It is shown that the PAC does not introduce any strong feedback loops around the full envelope controller and so the performance of the full envelope controller is unaffected by the PAC
- The PAC is shown to provide fast and accurate changes in power output across the operational envelope of the wind turbine
- As no knowledge of the design of the wind turbines full envelope controller is required in order to design the PAC, it can be applied to any variable speed, pitch regulated wind turbine and can be retrofitted to old machines

At the end of chapter 4 the requirement for an improved wind speed estimator that accounts for the effects of dynamic inflow is identified. Chapter 5 details the development of this improved estimator. In order to develop the wind speed estimator, Blade Element Momentum theory (BEM) is redefined in terms of the wind speed at the rotor, rather than the usual wind speed far upstream from the rotor. The wind speed estimator is applied to the PAC, improving the performance when used with a wind turbine model that incorporates dynamic inflow effects.

The complete PAC, including the improved wind speed estimator, is assessed to ensure stability and to investigate its effect on the full envelope controller. The PAC is found to be highly decoupled from the full envelope controller, causing little impact on the full envelope controller's performance; that is to say that no strong feedback loops are introduced around the full envelope controller by the PAC.

In chapter 6 the PAC is discretised for use with the aero-elastic simulation package GL Bladed. An assessment is made of the impact of the PAC on ultimate loads and fatigue loads. Operation of the PAC, even to temporarily increase the power output, does not cause ultimate loads outside of the bounds of normal operation. Operating the PAC with a reduced power demand is shown to improve the lifetime fatigue loads of the turbine for blade flap, tower fore-aft and hub moment.

Chapter 9: Conclusions

It is clear that the greater the reduction in power, the greater the reduction in the fatigue loads. This result suggests that it may be possible to use the PAC to limit the loads on a wind turbine.

In chapter 7 limits and flags to ensure that the turbine is kept within a predefined safe operational envelope are developed. These measures are shown to be effective across the operational envelope. A system of flags and sub-flags is developed along with a “traffic light” system to communicate the state of the turbine to a farm level controller. The flags, sub-flags and “traffic light” system are designed to allow easy integration of the PAC into a hierarchical wind farm control structure.

Finally, chapter 8 details the application of the PAC as a means for providing droop control and synthetic inertia using a wind turbine. Provision of these grid services allows a greater number of wind turbines to be connected to the power system without reducing its stability. Provision of synthetic inertia is shown to have a negligible effect on the wind turbine loads. The 1.5MW and 5MW wind turbines studied are shown to be capable of providing synthetic inertia equivalent to an inertial constant triple the typical value for conventional synchronous plant. Droop control is shown to decrease the damage equivalent loads on the turbine, with reductions in the tower fore-aft DELs of between 1.8% and 7.3% and reductions in the blade flap DELs of between 1% and 3.2% for operation in typical wind speed distributions. Droop control necessarily reduces the energy capture of the wind turbine by between 3.1% and 4.7%.

The development of the PAC opens up a wide range of possibilities for future work. Many of these possibilities stem from the development of wind farm control techniques utilising the hierarchical structure outlined at the end of chapter 3, a structure which is impossible to utilise without a turbine controller augmentation capable of altering the power output such as the PAC.

Possible areas for further future work based on farm control techniques include:

- Optimising wind farm performance via increased total power output and/or decreased turbine loads across the wind farm.

Chapter 9: Conclusions

- Distributing loads more evenly on the turbines within a wind farm in order to reduce operational and maintenance costs.
- More intelligent distribution of droop control amongst wind turbines in a wind farm.
- Extension of the PAC for use on directly fed induction generator (DFIG) wind turbines.
- Extension of the PAC to deliver a specified power rather than a change in power.
- Application of the PAC in order to control multi-rotor wind turbines; a multi-rotor machine can be thought of as a wind farm by itself.

In addition to the aforementioned farm control possibilities there is also scope for further research relating to the PAC itself. A more in depth study into the change in loads on a wind turbine through use of the PAC, across a broad range of different wind turbines, identifying trends could be conducted.

Blade element momentum theory is heavily utilised in the PAC to obtain an accurate wind speed estimate that takes into account dynamic inflow effects. Future work could be conducted into the accuracy of the various versions of BEM described in chapter 5.

Testing of the PAC on a real wind turbine would be an ideal progression of the work in this thesis, providing real-world validation of the simulation results presented here.

Chapter 10:

References

- [1] T. J. Price, "James Blyth – Britain's first modern wind power pioneer," *Wind Eng.*, vol. 29, no. 3, pp. 191–200, May 2005.
- [2] Intergovernmental Panel on Climate Change, "Climate Change 2007 : An Assessment of the Intergovernmental Panel on Climate Change - Synthesis Report," IPCC Report, 2007.
- [3] UK Government, *Climate Change Act 2008 (c.27)*. Great Britain, 2008.
- [4] Department of Energy and Climate Change (DECC), "Renewable Sources of Energy: Chapter 6, Digest of United Kingdom Energy Statistics (DUKES)," DECC Report, 2012.
- [5] N. Fichaux, J. Beurskens, and P. Jensen, "Upwind: Design limits and solutions for very large wind turbines," *Sixth Framew. Program.*, 2011.
- [6] E. A. Bossanyi, "Wind Turbine Control for Load Reduction," *Wind Energy*, vol. 6, no. 3, pp. 229–244, Jul. 2003.
- [7] W. E. Leithead, S. Dominguez, and C. J. Spruce, "Analysis of Tower/Blade interaction in the cancellation of the tower fore-aft mode via control," in *Proc. European Wind Energy Conference 2004*, 2004.
- [8] W. E. Leithead and S. Dominguez, "Coordinated Control Design for Wind Turbine Control Systems," in *Proc. European Wind Energy Conference 2006*, 2006.
- [9] A. P. Chatzopoulos, "Full Envelope Wind Turbine Controller Design for Power Regulation and Tower Load Reduction," 2011.
- [10] W. E. Leithead and S. Dominguez, "Controller Design for the Cancellation of the Tower Fore-aft Mode in a Wind Turbine," *Proc. 44th IEEE Conf. Decis. Control*, pp. 1276–1281, 2005.
- [11] E. A. Bossanyi, "Individual Blade Pitch Control for Load Reduction," *Wind Energy*, vol. 6, no. 2, pp. 119–128, Apr. 2003.

Chapter 10: References

- [12] E. A. Bossanyi, "Further load reductions with individual pitch control," *Wind Energy*, vol. 8, no. 4, pp. 481–485, Oct. 2005.
- [13] H. Yi and W. E. Leithead, "Alleviation of Extreme Blade Loads by Individual Blade Control During Normal Wind Turbine Operation," in *Proc. European Wind Energy Association Conference 2012*, 2012, pp. 90 – 94.
- [14] W. E. Leithead, V. Neilson, S. Dominguez, and A. Dutka, "A novel approach to structural load control using intelligent actuators," in *2009 17th Mediterranean Conference on Control and Automation*, 2009, vol. 1, pp. 1257–1262.
- [15] W. Leithead, D. Leith, F. Hardan, and H. Markou, "Global gain-scheduling control for variable speed wind turbines," in *Proceedings of the European Wind Energy Conference 1999*, 1999.
- [16] W. E. Leithead and D. J. Leith, "On the Separability of Wind Turbine Rotor Aerodynamics," University of Strathclyde Report, Glasgow, 2000.
- [17] P. Jamieson, W. Leithead, and M. Gala-Santos, "The Aerodynamic Basis of a Torque Separability Property," in *Proc. European Wind Energy Association Conference 2011*, 2011.
- [18] M. Gala-Santos, "Aerodynamic and Wind Field Models for Wind Turbine Control," University of Strathclyde, Thesis to be submitted.
- [19] D. J. Leith and W. E. Leithead, "Appropriate realization of gain-scheduled controllers with application to wind turbine regulation," *Int. J. Control*, vol. 65, no. 2, pp. 223–248, Sep. 1996.
- [20] T. Burton, N. Jenkins, D. Sharpe, and E. Bossanyi, *Wind Energy Handbook*. Chichester, UK: John Wiley & Sons, Ltd, 2011.
- [21] J. F. Manwell, J. G. McGowan, and A. L. Rogers, *Wind Energy Explained: Theory, Design and Application*, 2nd ed. Wiley, 2009.
- [22] V. W. Neilson, "Individual Blade Control for Fatigue Load Reduction of Large-scaled Wind Turbines: Theory and Modelling," University of Strathclyde, 2010.
- [23] GL Garrad Hassan, *Bladed Theory Manual*, 4.4 ed. Bristol, UK: Garrad Hassan & Partners Ltd, 2013.
- [24] J. M. Jonkman and M. L. Buhl Jr, "FAST User's Guide," 2005.
- [25] National Grid Electricity Transmission plc, "The Grid Code," 2013.

Chapter 10: References

- [26] M. Tsili and S. Papathanassiou, "A review of grid code technical requirements for wind farms," *IET Renew. Power Gener.*, vol. 3, no. 3, p. 308, 2009.
- [27] Elkraft and Eltra, "Wind Turbines Connected to Grids with Voltages above 100 kV," 2004.
- [28] EirGrid, "EirGrid Grid Code Version 5.0," 2013.
- [29] K. E. Johnson and N. Thomas, "Wind farm control: Addressing the aerodynamic interaction among wind turbines," in *2009 American Control Conference*, 2009, pp. 2104–2109.
- [30] K. E. Johnson and G. Fritsch, "Assessment of Extremum Seeking Control for Wind Farm Energy Production," *Wind Eng.*, vol. 36, no. 6, pp. 701–716, Dec. 2012.
- [31] T. Horvat and V. Spudic, "Quasi-stationary optimal control for wind farm with closely spaced turbines," in *MIPRO, 2012 Proceedings of the 35th International Convention*, 2012, pp. 829–834.
- [32] J. G. Schepers and S. P. Van Der Pijl, "Improved modelling of wake aerodynamics and assessment of new farm control strategies," *J. Phys. Conf. Ser.*, vol. 75, p. 012039, Jul. 2007.
- [33] L. A. H. Machielse, S. Barth, E. T. G. Bot, H. B. Hendriks, and J. G. Schepers, "Evaluation of 'Heat and Flux' Farm Control," ECN Wind Energy Report, 2008.
- [34] V. Spudic, J. Jelavic, and M. Baotic, "Wind Turbine Power References in Coordinated Control of Wind Farms," *Automatika*, vol. 52, no. 2, pp. 82–94, 2011.
- [35] V. Spudic, "Wind Farm Load Reduction via Parametric Programming Based Controller Design," in *Proc. 18th IFAC World Congress*, 2011, no. 2001, pp. 1704–1709.
- [36] D. Madjidian, K. Martensson, and A. Rantzer, "A distributed power coordination scheme for fatigue load reduction in wind farms," in *Proceedings of the 2011 American Control Conference*, 2011, pp. 5219–5224.
- [37] B. Biegel, D. Madjidian, V. Spudic, A. Rantzer, and J. Stoustrup, "Distributed low-complexity controller for wind power plant in derated operation," in *2013 IEEE International Conference on Control Applications (CCA)*, 2013, pp. 146–151.

Chapter 10: References

- [38] T. Knudsen, T. Bak, and M. Svenstrup, "Survey of wind farm control-power and fatigue optimization," *Wind Energy (Online Only)*, May 2014.
- [39] G. Lalor, A. Mullane, and M. O'Malley, "Frequency Control and Wind Turbine Technologies," *IEEE Trans. Power Syst.*, vol. 20, no. 4, pp. 1905–1913, Nov. 2005.
- [40] European Parliament and Council of the European Union, "Decision No 406/2009/EC of the European Parliament and of the Council of 23 April 2009 on the effort of Member States to reduce their greenhouse gas emissions to meet the Community's greenhouse gas emission reduction commitments up to 2020," *Off. J. Eur. Union*, vol. 52, no. L140, pp. 114 – 130, 2009.
- [41] European Commission, "Green Paper COM(2013) 169 - A 2030 framework for climate and energy policies," 2013.
- [42] European Wind Energy Association, "Wind in power - 2012 European Statistics," EWEA Report, 2013.
- [43] A. D. Hansen, M. Altin, I. D. Margaris, F. Iov, and G. C. Tarnowski, "Analysis of the short-term overproduction capability of variable speed wind turbines," *Renew. Energy*, vol. 68, pp. 326–336, Aug. 2014.
- [44] E. Muljadi, V. Gevorgian, M. Singh, and S. Santoso, "Understanding inertial and frequency response of wind power plants," in *2012 IEEE Power Electronics and Machines in Wind Applications*, 2012, pp. 1–8.
- [45] G. Tarnowski, P. Kjær, P. Sørensen, and J. Østergaard, "Study on variable speed wind turbines capability for frequency response," in *Proc. of the European Wind Energy Conf. 2009*, 2009.
- [46] I. D. Margaris, S. A. Papathanassiou, N. D. Hatzargyriou, A. D. Hansen, and P. Sorensen, "Frequency Control in Autonomous Power Systems With High Wind Power Penetration," *IEEE Trans. Sustain. Energy*, vol. 3, no. 2, pp. 189–199, Apr. 2012.
- [47] A. Buckspan, J. Aho, P. Fleming, Y. Jeong, and L. Pao, "Combining droop curve concepts with control systems for wind turbine active power control," in *2012 IEEE Power Electronics and Machines in Wind Applications*, 2012, pp. 1–8.
- [48] J. Morren, S. W. H. de Haan, W. L. Kling, and J. a. Ferreira, "Wind Turbines Emulating Inertia and Supporting Primary Frequency Control," *IEEE Trans. Power Syst.*, vol. 21, no. 1, pp. 433–434, Feb. 2006.
- [49] I. Erlich and M. Wilch, "Primary frequency control by wind turbines," in *IEEE PES General Meeting*, 2010, pp. 1–8.

Chapter 10: References

- [50] H. T. Ma and B. H. Chowdhury, "Working towards frequency regulation with wind plants: combined control approaches," *IET Renew. Power Gener.*, vol. 4, no. 4, p. 308, 2010.
- [51] G. Ramtharan, N. Jenkins, and J. B. Ekanayake, "Frequency support from doubly fed induction generator wind turbines," *IET Renew. Power Gener.*, vol. 1, no. 1, p. 3, 2007.
- [52] R. G. de Almeida and J. a. Pecas Lopes, "Participation of Doubly Fed Induction Wind Generators in System Frequency Regulation," *IEEE Trans. Power Syst.*, vol. 22, no. 3, pp. 944–950, Aug. 2007.
- [53] R. J. Nelson, "Frequency-responsive Wind Turbine Output Control," US 8301311, 2012.
- [54] A. Yasugi, "Wind Turbine Generator and Method of Controlling the Same," US 8355824, 2013.
- [55] A. Nyborg and S. Dalsgaard, "Power Curtailment of Wind Turbines," US 2010 0286835, 2010.
- [56] J. Morren, J. Pierik, and S. W. H. de Haan, "Inertial response of variable speed wind turbines," *Electr. Power Syst. Res.*, vol. 76, no. 11, pp. 980–987, Jul. 2006.
- [57] L. Zeni, A. J. Rudolph, J. Münster-Swendensen, I. Margaritis, A. D. Hansen, and P. Sørensen, "Virtual inertia for variable speed wind turbines," *Wind Energy*, vol. 16, no. 8, pp. 1225–1239, Sep. 2013.
- [58] R. G. de Almeida and J. A. Pecas Lopes, "Primary frequency control participation provided by doubly fed induction wind generators," in *Proc. 15th Power System Computation Conf.*, 2005, vol. 22, no. 3.
- [59] R. G. deAlmeida, E. D. Castronuovo, and J. A. PecasLopes, "Optimum Generation Control in Wind Parks When Carrying Out System Operator Requests," *IEEE Trans. Power Syst.*, vol. 21, no. 2, pp. 718–725, May 2006.
- [60] B. H. Chowdhury and H. T. Ma, "Frequency regulation with wind power plants," in *2008 IEEE Power and Energy Society General Meeting - Conversion and Delivery of Electrical Energy in the 21st Century*, 2008, pp. 1–5.
- [61] A. Diaz de Corcuera, L. Trilla, A. Pujana-Arresse, O. Gomis-Bellmunt, F. Bianchi, and J. Landaluze, "Mechanical Load Analysis of PMSG Wind Turbines in Primary Frequency Regulation," in *Proc. European Wind Energy Association Conference 2014*, 2014, pp. 61–67.

Chapter 10: References

- [62] A. D. de Corcuera, A. Pujana-Arrese, J. M. Ezquerro, E. Seguro, and J. Landaluze, "H ∞ Based Control for Load Mitigation in Wind Turbines," *Energies*, vol. 5, no. 12, pp. 938–967, Apr. 2012.
- [63] J. Aho, A. Buckspan, J. Laks, P. Fleming, Y. Jeong, F. Dunne, M. Churchfield, L. Pao, and K. Johnson, "A Tutorial of Wind Turbine Control for Supporting Grid Frequency through Active Power Control," in *2012 American Control Conference*, 2012, pp. 3120–3131.
- [64] J. Aho, A. Buckspan, L. Pao, and P. Fleming, "An Active Power Control System for Wind Turbines Capable of Primary and Secondary Frequency Control for Supporting Grid Reliability," in *Proc. of 51st AIAA Aerospace Sciences Meeting*, 2013, pp. 1–13.
- [65] A. Buckspan, L. Pao, J. Aho, and P. Fleming, "Stability Analysis of a Wind Turbine Active Power Control System," in *2013 American Control Conference (ACC)*, 2013, pp. 1418–1423.
- [66] E. Ela, V. Gevorgian, P. Fleming, Y. C. Zhang, M. Singh, E. Muljadi, A. Scholbrook, J. Aho, A. Buckspan, L. Pao, V. Singhvi, A. Tuohy, P. Pourbeik, D. Brooks, and N. Bhatt, "Active Power Controls from Wind Power: Bridging the Gaps," NREL Report, 2014.
- [67] K. Z. Østergaard, P. Brath, and J. Stoustrup, "Estimation of effective wind speed," *J. Phys. Conf. Ser.*, vol. 75, p. 012082, Jul. 2007.
- [68] S. Bhowmik and R. Spee, "Wind speed estimation based variable speed wind power generation," in *IECON '98. Proceedings of the 24th Annual Conference of the IEEE Industrial Electronics Society (Cat. No.98CH36200)*, 1998, vol. 2, pp. 596–601.
- [69] N. Kodama, T. Matsuzaka, and N. Inomata, "Power Variation Control of a Wind Turbine Generator using Probabilistic Optimal Control, including Feed-Forward Control from Wind Speed," *Wind Eng.*, vol. 24, no. 1, pp. 13–23, Jan. 2000.
- [70] W. Leithead and M. Rogers, "Drive-train characteristics of constant speed HAWT's: part I-representation by simple dynamic models," *Wind Eng.*, vol. 20, no. 3, pp. 149–174, 1996.
- [71] W. Leithead and M. Rogers, "Drive-train characteristics of constant speed HAWT's: part II-simple characterisation of dynamics," *Wind Eng.*, vol. 20, no. 3, pp. 175–201, 1996.
- [72] W. E. Leithead and B. Connor, "Control of variable speed wind turbines: Dynamic models," *Int. J. Control*, vol. 73, no. 13, pp. 1173–1188, 2000.

Chapter 10: References

- [73] W. E. Leithead and B. Connor, "Control of variable speed wind turbines: Design task," *Int. J. Control*, vol. 73, no. 13, pp. 1189–1212, Jan. 2000.
- [74] L. B. Tuckerman, "NACA Report No. 210 - Inertia Factors of Ellipsoids for use in Airship Design," NACA Report, 1925.
- [75] G. F. Franklin and J. D. Powell, *Digital Control of Dynamic Systems*, 1st ed. Addison-Wesley Publishing Company, 1980.
- [76] International Electrotechnical Commission, "2005 IEC 61400-1 3rd edn 2005-08 Wind Turbines - Part 1: Design Requirements," vol. 2005. International Electrotechnical Commission Standard, 2005.
- [77] C. Plumley, "The Smart Rotor Wind Turbine," University of Strathclyde, 2015.
- [78] H. F. Veldkamp, "Chances in Wind Energy," Delft University of Technology, 2006.
- [79] P. Jamieson, *Innovation in Wind Turbine Design*, 1st ed. John Wiley and Sons, 2011.
- [80] A. Johnson, "System Technical Performance Summary of Work to Date - The Effect of Inertia on the Transmission System," 2010.
- [81] L. Wu and D. Infield, "Power system frequency management challenges – a new approach to assessing the potential of wind capacity to aid system frequency stability," *IET Renew. Power Gener.*, vol. 8, no. 7, pp. 733–739, Sep. 2014.
- [82] T. Lei, M. Barnes, S. Smith, S. Hur, A. Stock, and W. E. Leithead, "Using Improved Power Electronics Modeling and Turbine Control to Improve Wind Turbine Reliability," *IEEE Trans. Energy Convers.*, vol. Pre-Print, 2015.

Appendix I.

Sample Code

I.A Recovery Torque Code

The following logic is used to avoid a step in the torque demand when recovering the turbine back to normal operation.

$$\begin{aligned} & \mathbf{if} \ F_{PAC} > 0 \\ & \Delta T[n] = \Delta T_{PAC}[n] \\ & Y[n] = \Delta T[n] \\ & \mathbf{else} \\ & \Delta T[n] = \Delta T_R[n] \\ & Y[n] = \frac{T_s \Delta T[n] + T_s \Delta T[n-1] - (T_s - 2\tau)Y[n-1]}{2\tau + T_s} \\ & \Delta T[n] = Y[n] \end{aligned}$$

where F_{PAC} is a flag with a value 1 when the PAC is on and a value 0 when the PAC is off, ΔT_{PAC} is the value for ΔT generated by the PAC when the PAC is in use (when $F_{PAC} = 1$), ΔT_R is the value of ΔT generated in recovery mode (when $F_{PAC} = 0$), Y is the output of the low pass filter $\frac{1}{\tau s + 1}$, τ is the time constant of said filter, T_s is the discrete time step.

I.B Simulink Model

This appendix contains the details of the Simulink model used in chapter 4. Screenshots from the Simulink model and the code of the m-files incorporated into the model are given. Note that for the example given, the 5MW wind turbine is used. The same model is used for the 1.5MW wind turbine, albeit with different variable values.

For the calculation of the change in torque ΔT , the model shown in Figure 174 is used.

Appendix I: Sample Code

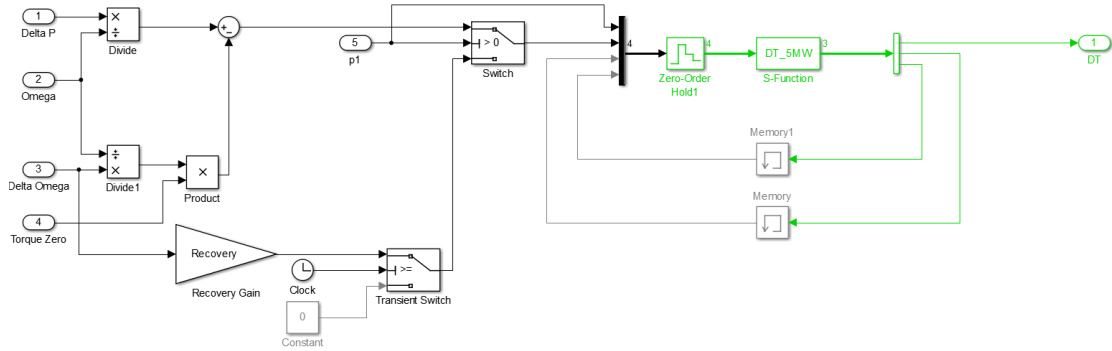


Figure 174: Simulink model - Calculation of Change in Torque ΔT

The model includes the Simulink function (S-Function) DT_5MW, the code for which is given below:

```
function [sys, x0, str, ts] = DT_5MW(~,~,u,flag)

switch flag,

case 0
    %%%%%%%%%%%%%%%
    % Initialization %
    %%%%%%%%%%%%%%%

    sizes = simsizes;
    sizes.NumContStates = 0;
    sizes.NumDiscStates = 0;
    sizes.NumOutputs = 3;
    sizes.NumInputs = 4;
    sizes.DirFeedthrough = 1;
    sizes.NumSampleTimes = 0;
    sys = simsizes(sizes);
    str = [];
    x0 = [];
    ts = [];

case 3

    p1 = u(1);
    D_T = u(2);
    D_Ttfold = u(3);
    D_Told = u(4);
    TT = 0.01;
    tfal = 5;

    if p1 > 0
        D_Ttf = D_T;
        D_T0 = D_T;
    else
        D_Ttf = (TT*D_T+TT*D_Told-(TT-2*tfal)*D_Ttfold)/(2*tfal+TT);
        D_T0 = D_Ttf;
    end
end
```

Appendix I: Sample Code

```
sys = [D_T0 D_Ttf D_T];
case { 1, 2, 4, 9}
```

end

For the estimate of aerodynamic torque the model shown in Figure 175 is used.

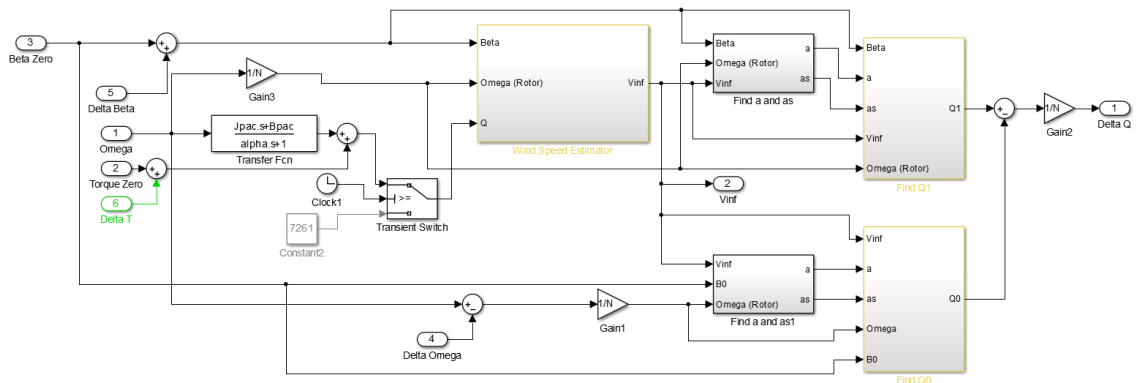


Figure 175: Simulink Model - Estimate of Aerodynamic Torque

The inside of the “Wind Speed Estimator” block is shown in Figure 176.

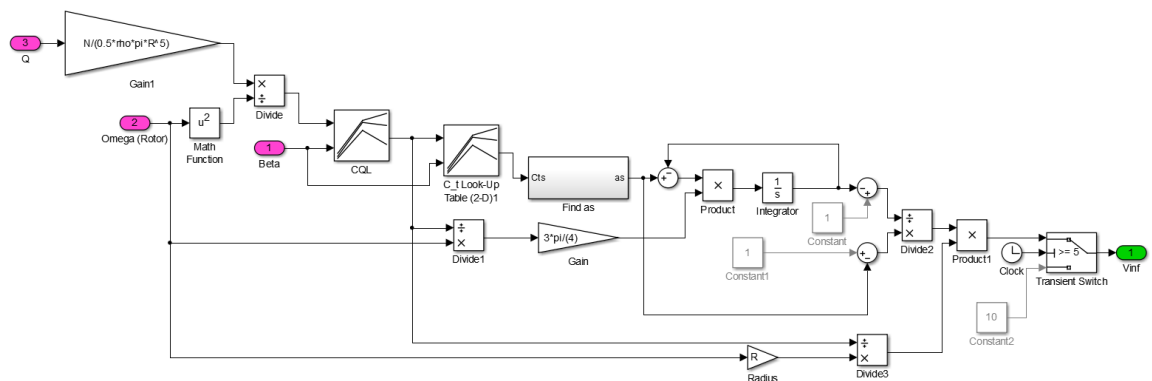


Figure 176: Simulink Model - Wind Speed Estimator

The inside of the “Find as” block is shown in Figure 177.

Appendix I: Sample Code

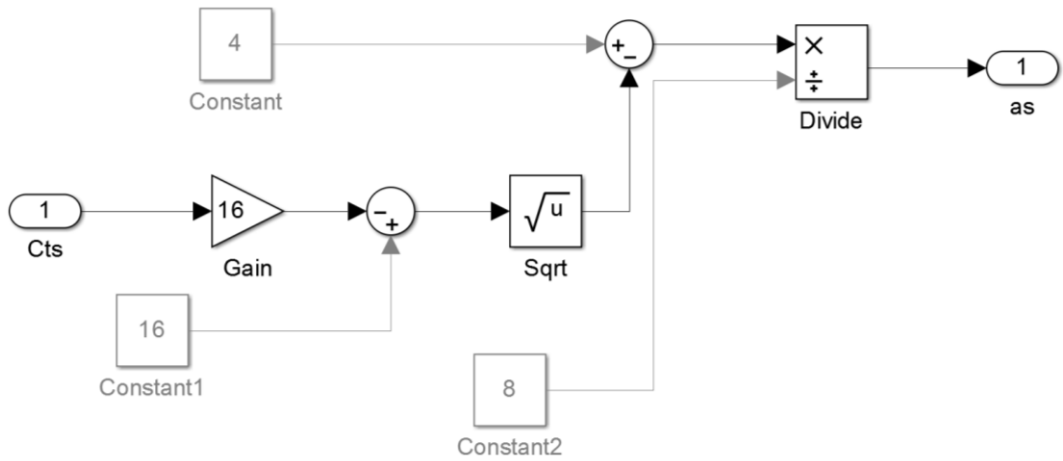


Figure 177: Simulink Model - "Find as" Block

There are two "Find a and as" blocks in Figure 175, which are identical (albeit with different inputs). The inside of a "Find a and as" block is shown in Figure 178.

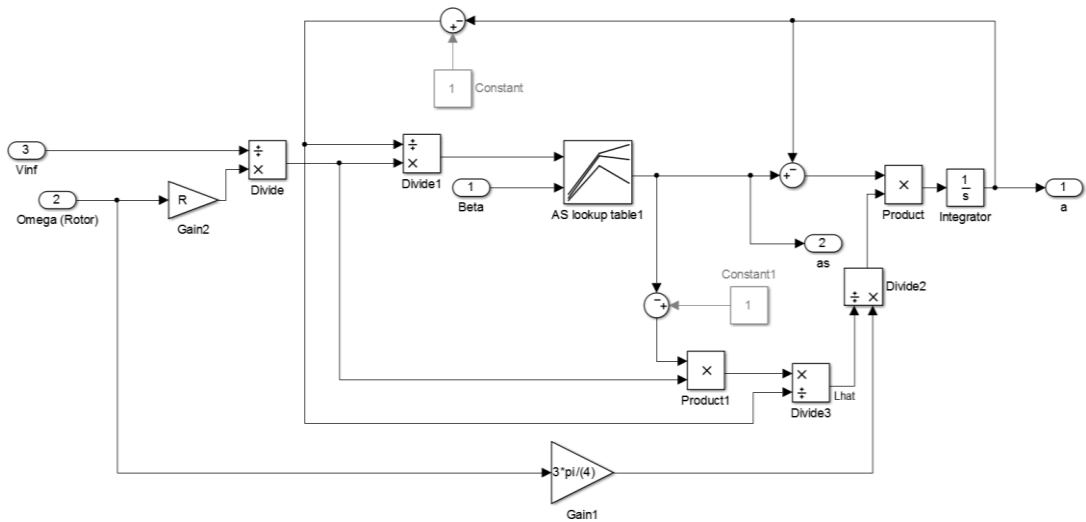


Figure 178: Simulink Model - "Find a and as" Block

There are two "Find Q" blocks in Figure 175, which are identical (albeit with different inputs). The inside of a "Find Q" block is shown in Figure 179.

Appendix I: Sample Code

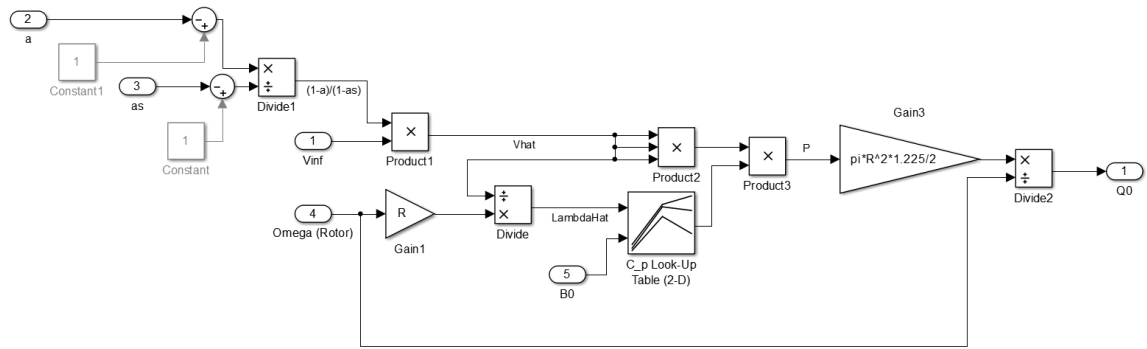


Figure 179: Simulink Model - "Find Q" Block

For the estimate of $\Delta\omega$, the model shown in Figure 180 is used.



Figure 180: Simulink Model - $\Delta\omega$ Estimator

Finally, the calculation of $\Delta\beta$, including anti-wind up, is performed using a Simulink function (S-Function). The code for the S-Function is given below:

```
function [sys, x0, str, ts] =
DB2_5MW3(~,~,u,flag,dcons,dslope,PITMIN,KiB,KpB,KGainB)

switch flag,

case 0
%%%%%%%%%%%%%%
% Initialization %
%%%%%%%%%%%%%%

sizes = simsizes;
sizes.NumContStates = 0;
sizes.NumDiscStates = 0;
sizes.NumOutputs = 12;
sizes.NumInputs = 28;
sizes.DirFeedthrough = 1;
sizes.NumSampleTimes = 0;
sys = simsizes(sizes);
str = [];
x0 = [];
ts = [];

case 3

TPitch = 0.05;
Kp = KpB; %% Proportional Gain for Pitch Controller
Ki = KiB; %% Integral Gain for Pitch Controller
M = dslope;
```

Appendix I: Sample Code

```
C = dcons;
KGain = u(1)*KGainB;
Input = u(2);
Inputd = u(3);
PAC_ON = u(4);
simTime = u(5);
D_B0d = u(6);
BetaDemand = u(7);
BetaDemandd = u(8);
Pbd = u(9);
Pbdd = u(10);
Pad = u(11);
Padd = u(12);
Pcld = u(13);
Pcldd = u(14);
Pbld = u(15);
Pbldd = u(16);
Input2d = u(17);
Input2dd = u(18);
Pxd = u(19);
Pxdd = u(20);
Pwld = u(21);
Pwlidd = u(22);
Pxdotd = u(23);
Pxdotdd = u(24);
Pw2d = u(25);
Pw2dd = u(26);
Recovery_Complete = u(27);
RECOVERY_SPEED = u(28);

c = 64;
b = 11.2;
PRmax = 0.13962634;
PRmin = -0.13962634;
Transient = 50;

if PAC_ON == 1
    D_B0 = (2 * D_B0d + (2 * KGain*Kp + KGain*Ki*TPitch)*Input +
(KGain*Ki*TPitch - 2 * KGain*Kp)*Inputd) / 2;
else
    if RECOVERY_SPEED == 1
        D_B0 = 0;

    else
        if D_B0d < 0.01 && D_B0d > -0.01
            D_B0 = 0;
        else
            D_B0 = (2 * D_B0d + (2 * KGain*Kp +
KGain*Ki*TPitch)*Input + (KGain*Ki*TPitch - 2 * KGain*Kp)*Inputd) /
2;
        end
    end
end

Dia = 0;
Dib = 0;
Dic = 64;
Did = 0;
Die = 1;
```

Appendix I: Sample Code

```
Dif = 11.2;
DiT = TPitch;

Dia0 = (4 * Dia + 2 * Dib*DiT + Dic*DiT*DiT) / (4 * Did + 2 *
DiT*Die + Dif*DiT*DiT);
Diq = (Dic - Dia0*Dif) / 2;
DiX = (Dib - Dia0*Die + Diq*DiT) / 2;

AA = 0;
BB = DiT*Diq;
CC = 2 * Diq;
DD = 0;
EE = Die;
FF = Dif;

aB1 = Dia0;

Pb1 = ((2*BB + CC*TPitch)*Pad + (CC*TPitch - 2*BB)*Padd + (2*EE -
FF*TPitch)*Pb1d)/(2*EE + FF*TPitch);

Dia = 0;
Dib = 0;
Dic = 1;
Did = 0;
Die = 1;
Dif = 0;

Dia0 = (4 * Dia + 2 * Dib*DiT + Dic*DiT*DiT) / (4 * Did + 2 *
DiT*Die + Dif*DiT*DiT);
Diq = (Dic - Dia0*Dif) / 2;
DiX = (Dib - Dia0*Die + Diq*DiT) / 2;

AA = 0;
BB = DiT*Diq;
CC = 2 * Diq;
DD = 0;
EE = Die;
FF = Dif;

aB2 = Dia0;

Pc1 = ((2*BB + CC*TPitch)*Pbd + (CC*TPitch - 2*BB)*Pbdd + (2*EE -
FF*TPitch)*Pc1d)/(2*EE + FF*TPitch);

Pc = (aB2*(Pb1 + aB1*BetaDemand) + Pc1) / (1 + aB1*aB2);
Pb = Pb1 + aB1*(BetaDemand - Pc);
Pa = BetaDemand - Pc;
Pd = M*Pc*Pc / 2 + C*Pc - M*PITMIN*PITMIN / 2 - C*PITMIN;
gneg1dot = 1 / (sqrt((C + M*PITMIN)*(C + M*PITMIN) + 2 * M*Pd));
gneg1dotdot = M^-1 / (((C + M*PITMIN)*(C + M*PITMIN) + 2 *
M*Pd)^1.5);
gamma1 = (BetaDemand - Pb*Pb*gneg1dotdot / (c*gneg1dot*gneg1dot) -
Pc) / gneg1dot;
```

Appendix I: Sample Code

```
Input2 = Pd + gamma1 + D_B0;

Dia = 0;
Dib = 0;
Dic = 64;
Did = 0;
Die = 1;
Dif = 11.2;

Dia0 = (4 * Dia + 2 * Dib*DiT + Dic*DiT*DiT) / (4 * Did + 2 *
DiT*Die + Dif*DiT*DiT);
Diq = (Dic - Dia0*Dif) / 2;
DiX = (Dib - Dia0*Die + Diq*DiT) / 2;

AA = 0;
BB = DiT*Diq;
CC = 2 * Diq;
DD = 0;
EE = Die;
FF = Dif;

aA3 = Dia0;

Pw1 = ((2*BB + CC*TPitch)*(Input2d - Pxd) + (CC*TPitch -
2*BB)*(Input2dd - Pxdd) + (2*EE - FF*TPitch)*Pw1d)/(2*EE +
FF*TPitch);

Dia = 0;
Dib = 0;
Dic = 1;
Did = 0;
Die = 1;
Dif = 0;

Dia0 = (4 * Dia + 2 * Dib*DiT + Dic*DiT*DiT) / (4 * Did + 2 *
DiT*Die + Dif*DiT*DiT);
Diq = (Dic - Dia0*Dif) / 2;
DiX = (Dib - Dia0*Die + Diq*DiT) / 2;

AA = 0;
BB = DiT*Diq;
CC = 2 * Diq;
DD = 0;
EE = Die;
FF = Dif;

aA4 = Dia0;

Pw2 = ((2*BB + CC*TPitch)*(Pxdotd) + (CC*TPitch - 2*BB)*(Pxdotdd) +
(2*EE - FF*TPitch)*Pw2d)/(2*EE + FF*TPitch);
Px = ((aA4*(Pw1 + aA3*Input2) + Pw2) / (1 + aA3*aA4));
Pxdot = Pw1 + aA3*(Input2 - Px);
sq3 = (C*C + 2 * M*(Px + C*PITMIN + 0.5*M*PITMIN*PITMIN);
if (sq3 > 0)
    Pz = (sqrt(sq3) - C) / M;
else
```

Appendix I: Sample Code

```
Pz = (0 - C)/M;
end
VLHiX = min(Pb + 0.0175, PRmax);
VLLoX = max(Pb - 0.0175, PRmin);

if (Pxdot - min(max(Pxdot, VLLoX*(M*Pz + C)), VLHiX*(M*Pz + C)) ~= 0
&& simTime > 5)
    sq4 = 4 * (C - M*aA4*VLHiX)*(C - M*aA4*VLHiX) + 4 * M*(PITMIN*(2
* C + M*PITMIN) + 2 * Pw2 + 2 * aA4*VLHiX*C);
    sq5 = 4 * (C - M*aA4*VLLoX)*(C - M*aA4*VLLoX) + 4 * M*(PITMIN*(2
* C + M*PITMIN) + 2 * Pw2 + 2 * aA4*VLLoX*C);
    if (sq4 < 0)
        sq4 = 0;
    end
    if (sq5 < 0)
        sq5 = 0;
    end
    AW3 = (-2 * (C - M*aA4*VLLoX) + sqrt(sq4)) / (2 * M);
    AW4 = (-2 * (C - M*aA4*VLHiX) + sqrt(sq5)) / (2 * M);
    minimum2 = min(abs(Pxdot - VLLoX*(C + M*AW3)), abs(Pxdot -
VLHiX*(C + M*AW4)));
    if (minimum2 == abs(Pxdot - VLHiX*(C + M*AW4)))
        Pz = AW4;
        pr2 = VLHiX;
    else
        Pz = AW3;
        pr2 = VLLoX;
    end
end

J2 = (1 / c)*(M*pr2*pr2 + b*pr2*(C + M*Pz));
Pxdot = J2*aA3 + Pw1;
Px = Pxdot*aA4 + Pw2;
Input2 = J2 + Px;
end

if (Px < 0 && simTime>Transient)
    Px = 0;
    sq3 = (C*C + 2 * M*(Px + C*PITMIN + 0.5*M*PITMIN*PITMIN));
    if (sq3 > 0)
        Pz = (sqrt(sq3) - C) / M;
    else
        Pz = (0 - C) / M;
    end
    Pxdot = (Px - Pw2) / aA4;
    Input2 = (Pxdot - Pw1) / aA3 + Px;
end

if (Px > (210) && simTime>Transient)
    Px = 210;
    sq3 = (C*C + 2 * M*(Px + C*PITMIN + 0.5*M*PITMIN*PITMIN));
    if (sq3 > 0)
        Pz = (sqrt(sq3) - C) / M;
    else
        Pz = (0 - C) / M;
    end
    Pxdot = (Px - Pw2) / aA4;
    Input2 = (Pxdot - Pw1) / aA3 + Px;
end
end
```

Appendix I: Sample Code

```
Pee = (Input2 - Px) / (M*Pz + C) - (Pxdot*Pxdot*M) / (c*(M*Pz +  
C)*(M*Pz + C)*(M*Pz + C)) + Pz - BetaDemand;  
D_B0 = Input2 - Pd - gammal;  
Input = (2 * D_B0 - (Ki*KGain*TPitch - 2 * KGain*Kp)*Inputd - 2 *  
D_B0d) / (2 * KGain*Kp + KGain*Ki*TPitch);  
sys = [D_B0 Pb Pa Pc1 Pb1 Input2 Px Pw1 Pxdot Pw2 Input Pee];  
case { 1, 2, 4, 9}
```

```
end
```

I.C Complete Pseudo-Code for the PAC

```
NN = Gearbox Ratio;  
RR = Rotor Radius;  
rho = Density of air;  
pi = pi;  
M = Slope of the gain scheduling function;  
C = Constant of the gain scheduling function;  
PAC_ON = 0;  
REJECTION = 0;  
D_T0d = D_T0;  
BlackLimit = 0;  
measuredSpeed = Measured Generator Speed  
TimeStep = Communication interval for controller  
PRIORITY = Priority Flag from Farm Controller  
simTime = Simulation Time  
PRmax = Maximum Pitch Rate  
PRmin = Minimum Pitch Rate  
  
If (Recovery_Complete)  
then MinimumTorque = 0;  
MaximumTorque = 0;  
end  
SPEED = (measuredSpeed* TimeStep + TimeStep *measuredSpeedd + (2 -  
TimeStep)*SPEEDd) / (2 + TimeStep);  
measuredSpeedd = measuredSpeed;  
SPEEDd = SPEED;  
DPmax = Max Change in Power;  
DPmin = Min Change in Power;  
D_P = Requested Change in Power  
if (D_P > DPmax)  
then D_P = DPmax;  
REJECTION = 1;  
MaxPower = 1;  
end  
if (D_P < DPmin)  
then D_P = DPmin;  
REJECTION = 1;  
MinPower = 1;  
end  
  
if (FECActuatorPositiond == 1 || FECActuatorSpeedd == 1 || BlackTimer > 20 ||  
Recovery_On_Going == 1)  
then PAC_ON = 0;  
end  
if (Vfil2 < 6.5)  
then Low_Wind_Counter = Low_Wind_Counter + TimeStep;  
else Low_Wind_Counter = 0;  
Low_Wind = 0;  
end
```

Appendix I: Sample Code

```
if (Low_Wind_Counter > 10)
then   PAC_ON = 0;
       Low_Wind = 1;
end

RATE = max rate of change per second of Change in Power;
D_P0old = D_P0;
D_P0 = D_P;
Power_Rate = 0;
if (PRIORITY)
then   D_P0 = D_P0;
else   if (D_P0 > D_P0old + RATE / 100 && PAC_ON == 1)
       then   D_P0 = D_P0old + RATE / 100;
              REJECTION = 1;
              Power_Rate = 1;
       end
       if (D_P0 < D_P0old - RATE / 100 && PAC_ON == 1)
       then   D_P0 = D_P0old - RATE / 100;
              REJECTION = 1;
              Power_Rate = 1;
       end
end
if (Recovery_Complete)
then   qq = 1;
else   if (PAC_ON == 1)
       then   qq = 1;
       else   qq = 0;
       end
end
PAC_ON = PAC_ON*qq;
PAC_ONold = PAC_ON;

if (PAC_ON == 0)
then   D_P = 0;
       D_P0 = D_P;
end
AT = Time step for calculating actuator wind up
if (Time step AT has passed || simTime == 0)
then   BPd = BP;
       BP = Actuator Transfer Function (PITCH);
       AWRated = AWRate;
       AWRate = (2 * BP - 2 * BPd - AT*AWRrated) / AT;
end

FECActuatorSpeedd = FECActuatorSpeed;
if (simTime > Transient && (AWRate > PRmax || AWRate < PRmin) ||
FECActuatorSpeedd == 1)
then   PAC_ON = 0;
       FECActuatorSpeed = 1;
end
FECActuatorPositiond = FECActuatorPosition;
if (simTime > Transient && (BP < -0.038 || BP > 1.57) || FECActuatorPositiond
== 1)
       PAC_ON = 0;
       FECActuatorPosition = 1;
end

if (simTime > Transient)
then   if (measuredSpeed - D_W0 > max_speed - MinOffset || TORQUE > TL1 ||
TURBULENCE == 1)
```

Appendix I: Sample Code

```
        then PAC_ON = 0;
           TURBULENCE = 1;
        end
    end
    if ((FECActuatorPosition || FECActuatorSpeed || TURBULENCE) &&
    Recovery_Complete)
    then FLAG_PAC = 0;
    end

    T_plus = -(TORQUE*D_W0) / (SPEED);
    T_add1 = (D_P0 / (SPEED));
    T2 = 1;
    T4 = 1;
    if (Recovery_On_Going)
    then min_speed = Value Lower than minimum speed of strategy;
    else min_speed = Minimum Speed (Black Limit);
    end
    max_speed = Maximum Speed (Black Limit);
    MinOffset = Offset from Minimum Speed;
    MaxOffset = Offset from Minimum Speed;
    Tee1 = (measuredSpeed - min_speed) / (MinOffset);
    if (measuredSpeed > min_speed + MinOffset)
    then T2 = 1;
    else T2 = Tee1;
    end
    T3 = -(measuredSpeed - max_speed) / (MinOffset);
    if (measuredSpeed < max_speed - MaxOffset)
    then T4 = 1;
    else T4 = T3;
    end
    if (simTime < Transient)
    then T2 = 1;
    end
    if (simTime < Transient + 1)
    then T4 = 1;
    end

    if (T2 < 1)
    then BlackLimit = 1;
       Limit = 1;
       REJECTION = 1;
    else Limit = 0;
    end

    if (T4 < 1)
    then Limit = 1;
       REJECTION = 1;
       BlackLimit = 1;
    else Limit = 0;
    end
    MaxTorque = Maximum Torque Allowable;
    MinTorque = Minimum Torque Allowable;
    MaximumTorqued = MaximumTorque;
    MinimumTorqued = MinimumTorque;
    T2 = MAX(T2, 0);
    T4 = MAX(T4, 0);
    KRecovery = Recovery Gain
    D_Told = D_T;
    if (Recovery_Complete == 1 && PAC_ON == 0)
    then D_T0 = 0;
    else if (PAC_ON > 0)
```

Appendix I: Sample Code

```

    then D_T = T_add1 + T_plus;
         D_T = D_T*T2*T4 + (1 - T2)*-LargeNumber + (1 - T4) *
LargeNumber;
    else D_T = KRecovery*D_W0*T2*T4 + (1 - T2)*- LargeNumber + (1 - T4) *
LargeNumber;
    end
    if (MAX((D_T + TORQUE), AeroT / NN) > TL1 && PAC_ON == 1)
    then if (simTime>Transient)
         then PAC_ON = 0;
              Limit = 1;
              REJECTION = 1;
         end
    end
    if ((D_T + TORQUE) < MAX(MinTorque, TL1L) && PAC_ON == 1)
    then if (simTime>Transient)
         then PAC_ON = 0;
              Limit = 1;
              REJECTION = 1;
         end
    end
    end

    if (RECOVERY_SPEED == 1)
    then tfa1 = 1;
    else tfa1 = 10;
    end
    TT = TimeStep
    if (PAC_ON > 0)
    then D_T0 = D_T;
         D_Ttfold = D_T;
    else D_Ttf = (TT*D_T + TT*D_Told - (TT - 2 * tfa1)*D_Ttfold) / (2 *
tfa1 + TT);
         D_Ttfold = D_Ttf;
         D_T0 = D_Ttf;
    end
    end

VT = Time Step for Wind Speed Estimator
if (Time step VT has passed || simTime == 0)
then RunPAC = 1;
else RunPAC = 0;
end
if (RunPAC == 1)
then B_plus_DB = measuredPitch;
     T_plus_DT = TORQUE + D_T0;
     TUNING = Factor to tune to Bladed (1 if not used)
     Jpac = Inertia of the system
     Bpac = Damping of the system
     FilCon = Time Constant for (J*s+B)/(FilCon*s+1)
     bb2 = bb1;
     bb1 = measuredSpeed;
     bb3 = bb4;
     bb4 = (Jpac*bb1 - (Jpac - Bpac*VT)*bb2 + (FilCon - VT)*bb3) / FilCon;
     bb5 = (bb4 + T_plus_DT)*NN;
     bb6 = bb5 / (0.5*1.225*pi*RR*RR*RR*RR*RR*measuredSpeed /
NN*measuredSpeed / NN);
     bb7 = Look up table value (CQL Look up table)
     V_est1 = measuredSpeed / NN*RR / bb7;
     CtsV = Look up table value (Ct Look up table)
     if (CtsV > 1)
     then CtsV = 1;
     end
end

```

Appendix I: Sample Code

```

asVd = asV;
asV = (4 - sqrt(16 - 16 * CtsV)) / 8;
mKd = mK;
mK = TUNING * 3 * pi*measuredSpeed / NN / (4 * bb7);
na = (asVd - nad)*mKd*VT + nad;
nad = na;
Vinfdd = Vinf;
Vinf = Vinf;
Vinf = (1 - asV) / (1 - na)*V_est1;
Filter1 = s^2 value for Notch Filter Numerator 1
Filter2 = s value for Notch Filter Numerator 1
Filter3 = units value for Notch Filter Numerator 1
Filter4 = s^2 value for Notch Filter Denominator 1
Filter5 = s value for Notch Filter Denominator 1
Filter6 = units value for Notch Filter Denominator 1
Filter7 = s^2 value for Notch Filter Numerator 2
Filter8 = s value for Notch Filter Numerator 2
Filter9 = units value for Notch Filter Numerator 2
Filter10 = s^2 value for Notch Filter Denominator 2
Filter11 = s value for Notch Filter Denominator 2
Filter12 = units value for Notch Filter Denominator 2

Fa1 = Filter1;
Fb1 = Filter2 * measuredSpeed / NN;
Fc1 = (Filter3 * measuredSpeed / NN)*(Filter3 * measuredSpeed / NN);
Fd1 = Filter4;
Fe1 = Filter5 * measuredSpeed / NN;
Ff1 = (Filter6 * measuredSpeed / NN)*(Filter6 * measuredSpeed / NN);
Fa2 = Filter7;
Fb2 = Filter8 * measuredSpeed / NN;
Fc2 = (Filter9 * measuredSpeed / NN)*(Filter9 * measuredSpeed / NN);
Fd2 = Filter10;
Fe2 = Filter11 * measuredSpeed / NN;
Ff2 = (Filter12 * measuredSpeed / NN)*(Filter12 * measuredSpeed / NN);
Vfil2dd = Vfil2;
Vfil2d = Vfil2;
Vfil1dd = Vfil1;
Vfil1d = Vfil1;
Vfil1 = (Vinf*(4 * Fa1 + 2 * Fb1*VT + Fc1*VT*VT) + Vinfd*(-8 * Fa1 + 2
* Fc1*VT*VT) + Vinfdd*(4 * Fa1 - 2 * Fb1*VT + Fc1*VT*VT) - Vfil1d*(-8 * Fd1 +
2 * Ff1*VT*VT) - Vfil1dd*(4 * Fd1 - 2 * Fe1*VT + Ff1*VT*VT)) / (4 * Fd1 + 2 *
Fe1*VT + Ff1*VT*VT);
Vfil2 = (Vfil1*(4 * Fa2 + 2 * Fb2*VT + Fc2*VT*VT) + Vfil1d*(-8 * Fa2 +
2 * Fc2*VT*VT) + Vfil1dd*(4 * Fa2 - 2 * Fb2*VT + Fc2*VT*VT) - Vfil2d*(-8 * Fd2
+ 2 * Ff2*VT*VT) - Vfil2dd*(4 * Fd2 - 2 * Fe2*VT + Ff2*VT*VT)) / (4 * Fd2 + 2
* Fe2*VT + Ff2*VT*VT);
Lfil2 = (measuredSpeed / NN)*RR / Vfil2;
Gpac_table_initialize(Lfil2, BETA);
CeePeeA = Gpac_table_step();
AeroTind = AeroTin;
AeroTin = Vfil2*Vfil2*Vfil2*CeePeeA*1.225 / 2 * pi*RR*RR /
(measuredSpeed / NN);
AeroT = (VT*AeroTin + VT*AeroTind - (VT - 2 * 0.5)*AeroTd) / (2 * 0.5 +
VT);
AeroTd = AeroT;
if (simTime>Transient)
then aq = qKd*VT + aq;
      aqd = aq;
      Lr = (measuredSpeed / NN*RR) / Vinf / (1 - aq);
      Gpac_table_initializeCa(Lr, BETA);

```

Appendix I: Sample Code

```

    asq = Gpac_table_stepCa();
    asqd = asq;
    qK = TUNING * 3 * pi / (4 * RR)*Vinf*(1 - aq) / (1 - asq)*(asq -
aq);
    qKd = qK;
    aq0 = qK0d*VT + aq0d;
    aq0d = aq0;
    Lr0 = ((measuredSpeed - D_w0) / NN*RR) / (Vinf / (1 - aq0));
    asq0 = Look up table value (As Look up table)
    asq0d = asq0;
    qK0 = BODGE * 3 * pi / (4 * RR)*Vinf*(1 - aq0) / (1 -
asq0)*(asq0 - aq0);
    qK0d = qK0;

    Vhat = (1 - aq) / (1 - asq)*Vinf;
    Lhat = (measuredSpeed / NN)*RR / Vhat;
    CeePee = Look up table value (Cp Look up table for Lhat and
BETA)
    TA1 = Vhat*Vhat*Vhat*CeePee*1.225 / 2 * 3.141592654*RR*RR /
(measuredSpeed / NN);
    Vhat0 = (1 - aq0) / (1 - asq0)*Vinf;
    Lhat0 = (measuredSpeed / NN - D_w0 / NN)*RR / Vhat0;
    CeePee0 = Look up table value (Cp Look up table for Lhat0 and
BETA0)
    TA0 = Vhat0*Vhat0*Vhat0*CeePee0*1.225 / 2 * 3.141592654*RR*RR /
(measuredSpeed / NN - D_w0 / NN);
    if (Recovery_Complete)
    then D_TA0 = 0;
    else D_TA0 = (TA0 - TA1) / NN;
    end
    else D_TA0 = 0;
    end
    Gpac_table_initialize(Lfil2, BETA0);
    CeePeeB = Look up table value (Cp Look up table for Lfil2 and BETA0);
    if (Vfil2*Vfil2*Vfil2*CeePeeA*1.225 *0.5 * 3.141592654*RR*RR / (SPEED /
NN) + Bpac*SPEED < (TORQUE + D_T0)*SPEED)
    then DIVERGENT = 1;
    end
end

KM = Offset for Black Torque Limit
KLimBeta = Variation in Black Limit as Beta Changes
MM = 1;
TL = Upper torque limit as a function of generator speed
TL1 = TL + KLimBeta;
TL2 = TORQUE + D_T0;
TL2 = TL1 - TL2;
if (simTime > Transient)
then TL3 = TL2;
else TL3 = 0;
end
MM = (TL3) / (KM);
if (simTime < Transient)
then MM = 1;
end

if (MM > 1)
then MM = 1;
end

if (MM != 1 && Minimum_Speed != 1)

```

Appendix I: Sample Code

```
then REJECTION = 1;
      Limit = 1;
      BlackLimit = 1;
else Limit = 0;
end

KML = Offset for the Lower Limit Line
TL1L = Limit for the lower torque line as a function of generator speed;
TL2L = TORQUE + D_T0;
TL2L = TL2L - TL1L;
if (simTime > Transient)
then TL3L = TL2L;
else TL3L = 0;
end
MMM = (TL3L) / (KML);
if (simTime < Transient)
then MMM = 1;
end
if (MMM > 1)
then MMM = 1;
end
if (MMM != 1 && Maximum_Speed != 1)
then REJECTION = 1;
      Limit = 1;
      BlackLimit = 1;
else Limit = 0;
end

if (BlackLimit == 1)
then BlackTimer = BlackTimer + 0.01;
      BlackTimer2 = 0;
else BlackTimer2 = BlackTimer2 + 0.01;
      BlackTimer = BlackTimer;
      if (BlackTimer2 > 20)
then BlackTimer2 = 20;
      BlackTimer = 0;
end

end

Amber1 = Green/Amber Upper Torque Boundary
Amber2 = MAX(TORQUE + D_T0, AeroT / NN);
Amber2b = TORQUE + D_T0;
Amber3 = Green/Amber Lower Torque Boundary
Amber4 = Green/Amber Maximum Torque Boundary
Amber5 = Green/Amber Minimum Torque Boundary
Amber6 = Green/Amber Upper Speed Boundary
Amber7 = Green/Amber Lower Speed Boundary
if (Amber2 > Amber1 || Amber2b < Amber3 || Amber2b > Amber4 || Amber2b <
Amber5 || measuredSpeed < Amber7 || measuredSpeed > Amber6)
then if (PAC_ON)
      then AMBER = 1;
      else AMBER = 0;
      end
else AMBER = 0;
end

Red1 = Amber/Red Upper Torque Boundary
Red2 = MAX(TORQUE + D_T0, AeroT / NN);
Red2b = TORQUE + D_T0;
```

Appendix I: Sample Code

```
Red3 = Amber/Red Lower Torque Boundary
Red4 = Amber/Red Maximum Torque Boundary
Red5 = Amber/Red Minimum Torque Boundary
Red6 = Amber/Red Upper Speed Boundary;
Red7 = Amber/Red Lower Speed Boundary;
if (Red2 > Red1 || Red2b < Red3 || TORQUE + D_T0 > Red4 || TORQUE + D_T0 <
Red5 || measuredSpeed < Red7 || measuredSpeed > Red6)
then   if (PAC_ON)
        then RED = 1;
        else  RED = 0;
        end
else
        RED = 0;
end

if (RED == 1)
then  AMBER = 0;
end
if (RED == 0 && AMBER == 0)
then  GREEN = 1;
else  GREEN = 0;
end

TPAC = Time Step for the Delta Omega Transfer Function
MM = MAX(MM, 0);
MMM = MAX(MMM, 0);
if (Time step TPAC has passed)
then  RunPAC = 1;
else  RunPAC = 0;
end
if (RunPAC == 1)
then  if (simTime > Transient)
        then  dd = D_TA0 + D_T0;
                dd = dd*MMM*MM + LargeNumber*(1 - MMM) - LargeNumber*(1 - MM);
        end
        D_Wd = D_W;
        D_W = (TPAC*dd0 + Jpac*D_Wd - (Bpac)*TPAC*D_Wd) / Jpac;
        dd0 = dd;
        D_W0 = -D_W;
        if (Recovery_Complete == 1 && PAC_ON == 0)
        then  dd = 0;
                dd0 = 0;
                D_Wd = 0;
                D_W0 = 0;
        end
end

if (D_W0 < A small positive number && Pee < A small positive number)
then  rec1 = D_W0;
else
        rec1 = -1;
end
if (rec1 > -0.01)
then
        rec2 = 1;
else
        rec2 = 0;
end
end
rec3old = rec3;
rec4old = rec4;
if (PAC_ON == 0)
```

Appendix I: Sample Code

```

then    rec3 = rec2;
else    rec3 = 0;
end
if (PAC_ON == 0)
then    rec4 = (TimeStep*rec3 + TimeStep*rec3old - (TimeStep - 2 *
0.5)*rec4old) / (2 * 0.5 + TimeStep);
else    rec4 = 0;
end
if (rec4>0.63)
then    RECOVERY = 1;
        Recovery_Complete = 1;
        Recovery_On_Going = 0;
else    Recovery_Complete = 0;
        RECOVERY = 0;
end
if (PAC_ON == 0 && Recovery_Complete == 0)
then    RECOVERY = 1;
        Recovery_On_Going = 1;
end

TPitch = Time Step for Pitch Control
if (Time step TPitch has passed)
then    RunPitch = 1;
else    RunPitch = 0;
end
Kp = Proportional Gain for Pitch Controller
Ki = Integral Gain for Pitch Controller
GSpac = Gain Scheduling of the Controller as a function of Wind Speed Estimate
KGain1 = Gain when Gain Scheduling = 1
KGain = KGain1*GSpac*((omega1 / NN)*(omega1 / NN)) / ((measuredSpeed /
NN)*(measuredSpeed / NN));

if (Vfil2 < 5)
then    KGain = KGain1*0.48*((omega1 / NN)*(omega1 / NN)) / ((measuredSpeed /
NN)*(measuredSpeed / NN));
end

if (Vfil2 > 25)
then    KGain = 0.008 * 2.13 * ((omega1 / NN)*(omega1 / NN)) / ((measuredSpeed
/ NN)*(measuredSpeed / NN));
end

if (RunPitch == 1)
then    Inputd = Input;
        Input = D_W0;
        if (PAC_ON == 1)
        then    D_B0d = D_B0;
                D_B0 = (2 * D_B0d + (2 * KGain*Kp + KGain*Ki*TPitch)*Input +
(KGain*Ki*TPitch - 2 * KGain*Kp)*Inputd) / 2;
        else    if (RECOVERY_SPEED == 1)
                then    D_B0d = D_B0;
                        D_B0 = 0;
                else    D_B0d = D_B0;
                        if (D_B0d < 0.001 && D_B0d > -0.001)
                        then    D_B0 = 0;
                        else    D_B0 = (2 * D_B0d + (2 * KGain*Kp +
KGain*Ki*TPitch)*Input + (KGain*Ki*TPitch - 2 * KGain*Kp)*Inputd) / 2;
                        end
                end
        end
        BetaDemandd = BetaDemand;

```

Appendix I: Sample Code

```

BetaDemand = PITCH;
Pbd = Pb;
Pad = Pa;
Pb1 = Pad through first half of actuator transfer function discretised;
Pc1 = Pbd through first half of actuator transfer function discretised;
Pc = (aB2*(Pb1 + aB1*BetaDemand) + Pc1) / (1 + aB1*aB2);
Pb = Pb1 + aB1*(BetaDemand - Pc);
Pa = BetaDemand - Pc;
Pd = M*Pc*Pc / 2 + C*Pc - M*PITMIN*PITMIN / 2 - C*PITMIN;
gneg1dot = 1 / (sqrt((C + M*PITMIN)*(C + M*PITMIN) + 2 * M*Pd));
gneg1dotdot = M*-1 / (pow(((C + M*PITMIN)*(C + M*PITMIN) + 2 * M*Pd), 3
/ 2));
gamma1 = (BetaDemand - Pb*Pb*gneg1dotdot / (c*gneg1dot*gneg1dot) - Pc)
/ gneg1dot;
Input2d = Input2;
Input2 = Pd + gamma1 + D_B0;
Pw1 = (Input2d - Pxd) through first half of actuator transfer function
discretised;
Pw2 = (Pxdotd) through first half of actuator transfer function
discretised;
Px = ((aA4*(Pw1 + aA3*Input2) + Pw2) / (1 + aA3*aA4));
ACTUATOR = 0;
Pxdot = Pw1 + aA3*(Input2 - Px);
sq3 = (C*C + 2 * M*(Px + C*PITMIN + 0.5*M*PITMIN*PITMIN))
if (sq3 > 0) /* this simply prevents complex numbers occurring*/
then Pz = (sqrt(sq3) - C) / M;
else Pz = (0 - C)/M;
end

if (Recovery_On_Going == 1)
then VLHiX = MIN(Pb + (max pitch rate in recovery),PRmax);
      VLLoX = MAX(Pb - (min pitch rate in recovery),PRmin);
else VLHiX = MIN(Pb + (max pitch rate in normal operation),PRmax);
      VLLoX = MAX(Pb - (min pitch rate in normal operation),PRmin);
end
Actuator_Velocity = 0;
if (Pxdot - MIN(MAX(Pxdot, VLLoX*(M*Pz + C)), VLHiX*(M*Pz + C)) != 0 &&
simTime > 5)
then sq4 = 4 * (C - M*aA4*VLHiX)*(C - M*aA4*VLHiX) + 4 * M*(PITMIN*(2
* C + M*PITMIN) + 2 * Pw2 + 2 * aA4*VLHiX*C);
      sq5 = 4 * (C - M*aA4*VLLoX)*(C - M*aA4*VLLoX) + 4 * M*(PITMIN*(2
* C + M*PITMIN) + 2 * Pw2 + 2 * aA4*VLLoX*C);
      if (sq4 < 0)
      then sq4 = 0;
      end
      if (sq5 < 0)
      then sq5 = 0;
      end
      AW3 = (-2 * (C - M*aA4*VLLoX) + sqrt(sq4)) / (2 * M);
      AW4 = (-2 * (C - M*aA4*VLHiX) + sqrt(sq5)) / (2 * M);
      minimum2 = MIN(absolute value of(Pxdot - VLLoX*(C + M*AW3)),
absolute value of(Pxdot - VLHiX*(C + M*AW4)));
      if (minimum2 == absolute value of (Pxdot - VLHiX*(C + M*AW4)))
      then Pz = AW4;
            pr2 = VLHiX;
      else Pz = AW3;
            pr2 = VLLoX;
      end
      J2 = (1 / c)*(M*pr2*pr2 + b*pr2*(C + M*Pz));
      Pxdot = J2*aA3 + Pw1;
      Px = Pxdot*aA4 + Pw2;

```

Appendix I: Sample Code

```

        Input2 = J2 + Px;
        Actuator_Velocity = 1;
        ACTUATOR = 1;
    end
    Actuator_Position = 0;
    if (Px < 0 && simTime>Transient)
    then    Px = 0;
           ACTUATOR = 1;
           Actuator_Position = 1;
           sq3 = (C*C + 2 * M*(Px + C*PITMIN + 0.5*M*PITMIN*PITMIN));
           if (sq3 > 0)
           then    Pz = (sqrt(sq3) - C) / M;
           else    Pz = (0 - C) / M;
           end
    Pxdot = (Px - Pw2) / aA4;
    Input2 = (Pxdot - Pw1) / aA3 + Px;
    end
    if (Px > (Max Pitch) && simTime>Transient)
    then    Px = 210;
           ACTUATOR = 1;
           Actuator_Position = 1;
           sq3 = (C*C + 2 * M*(Px + C*PITMIN + 0.5*M*PITMIN*PITMIN));
           if (sq3 > 0)
           then    Pz = (sqrt(sq3) - C) / M;
           else    Pz = (0 - C) / M;
           end
    Pxdot = (Px - Pw2) / aA4;
    Input2 = (Pxdot - Pw1) / aA3 + Px;
    end
    Pxd = Px;
    Pxdotd = Pxdot;
    Pee = (Input2 - Px) / (M*Pz + C) - (Pxdot*Pxdot*M) / (c*(M*Pz +
C)*(M*Pz + C)*(M*Pz + C)) + Pz - PITCH;
    D_B0 = Input2 - Pd - gamma1;
    Input = (2 * D_B0 - (Ki*KGain*TPitch - 2 * KGain*Kp)*Inputd - 2 *
D_B0d) / (2 * KGain*Kp + KGain*Ki*TPitch);
    end
    if (Recovery_Complete)
    then    Pee = 0;
    end

    PITCHPAC = PITCH + Pee;
    TORQUEPAC = TORQUE + D_T0;

    BETA = (PITCH + Pee) through the actuator transfer function
    BETA0 = (PITCH) through the actuator transfer function

```

Appendix II.

Turbine and Full Envelope Controller Variables

II.A Definition of the 1.5MW and 5MW Wind Turbines and Controllers

Variable	1.5MW Value	5MW Value
Tower Fore-Aft Frequency	2.5133 rad/s	1.7467 rad/s
Tower Fore-Aft Damping	0.005	0.01
Tower Side-Side Frequency	2.5133 rad/s	1.7593 rad/s
Tower Side-Side Damping	0.005	0.01
Ka (Tower Shape Factor)	1.4	1.2
Hub Inertia	12000 kgm ²	115926 kgm ²
Low Speed Shaft Damping	27000 Nms/rad	150000 Nms/rad

Appendix II: Turbine Variables

High Speed Shaft Damping	1.2 Nms/rad	5 Nms/rad
Low Speed Shaft Stiffness	1.9E+8 Nm/rad	4.45E+8 Nm/rad
High Speed Shaft Stiffness	1E+10 Nm/rad	1E+8 Nm/rad
Low Speed Shaft Material Damping	1.6E+6 Nms/rad	4.2E+6 Nms/rad
High Speed Shaft Material Damping	1000 Nms/rad	1000 Nms/rad
Gearbox Ratio	84.15	97
High Speed Shaft Inertia	5 kgm ²	5 kgm ²
Generator Inertia	130 kgm ²	534.116 kgm ²
Drive-train Efficiency Below-rated	1	1
Drive-train Efficiency Above-rated	1	1
Rotor Radius	37.5 m	63 m
Effective Blade Length	26.25 m	45 m
Distance of the Centre	11.94 m	20.5 m

Appendix II: Turbine Variables

One Blade Mass	5320 kg	17741 kg
Flap Natural Frequency	6.66 rad/s	4.1595 rad/s
Edge Natural Frequency	9.99 rad/s	6.7984 rad/s
Rotor Inertia	4.26849E+6 kgm ²	3.53715E+7 kgm ²
Hub Height	65 m	90m
Rotor and Nacelle Mass	97961 kg	350955 kg
Minimum Generator Speed	100 rad/s	70 rad/s
Maximum Generator Speed	157 rad/s	120 rad/s
Cut in Wind Speed	4 m/s	4m/s
Cut Out Wind Speed	25 m/s	25m/s
Nominal Generator Torque	10053 Nm	46372.7
Minimum Pitch Angle	-2 deg	0
Maximum Pitch Angle	90 deg	30 deg
Sampling Time	0.01s	0.01
Pitch Actuator Numerator	39.48	64

Appendix II: Turbine Variables

Pitch Actuator		
Denominator	$s^2 + 10.5s + 39.48$	$s^2 + 11.2s + 64$
Delay Time	0	0
Generator Actuator		
Numerator	1	1
Generator Actuator		
Denominator	1	1
Fluid Density	1.225 kg/m ³	1.225 kg/m ³
Pitch Controller	$-\frac{0.16482(s + 0.1)}{s(s + 2.2)}$	$\frac{-0.17238(s + 0.12024)}{s(s + 1.8)}$
Torque Controller	$-\frac{2163.8(s + 0.1)}{s(s + 2.2)}$	$\frac{-11743.2(s + 0.12024)}{s(s + 1.8)}$
Tower Damper		
Filter	$\frac{0.0711(s^2 + s + 6.24)}{s^2 + 1.32s^3 + 6.173s + 3.501}$	$\frac{0.002(s^2 + 7.65s + 2.89)}{s^3 + 1.82s^2 + 3.706s + 2.312}$
Drive-Train		
Damper Filter	$\frac{20000s}{(s + 8.4)(s + 18.9)}$	$\frac{45674s}{2.5s^2 + 35 + 199.21}$

Appendix III.

Linearisation – Without Induction

With reference to Figure 181, the state space equations for the linearisation of the Power Adjusting Controller are given below:

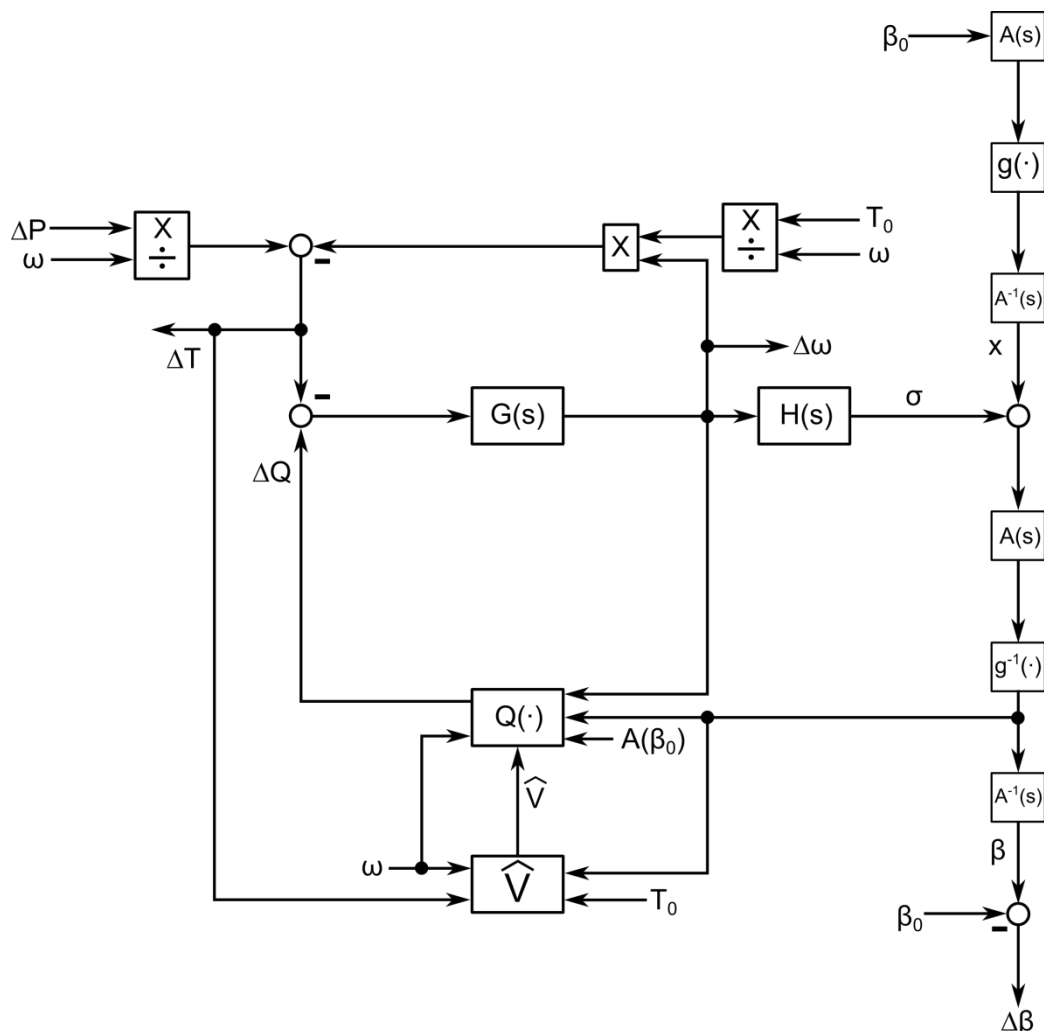


Figure 181: Diagram of the PAC

Appendix III: Linearisation (Without Induction)

Note that all variables correspond to the value at the equilibrium point. The values β and β_0 refer to the values passed through the dynamics of the pitch actuator.

Starting from $\delta\Delta\omega$:

$$[\delta\dot{x}] = [A_{11}][\delta x] + [B_{11}][\delta\Delta\omega]$$

$$[\delta\sigma] = [C_{11}][\delta x] + [D_{11}][\delta\Delta\omega]$$

$$A_{11} = 0$$

$$B_{11} = 1$$

$$C_{11} = K_G K_i;$$

$$D_{11} = K_G K_p$$

Finding the change in pitch angle $\Delta\beta$ and the total pitch β :

$$\begin{bmatrix} \delta\ddot{\varphi} \\ \delta\dot{\varphi} \end{bmatrix} = \begin{bmatrix} A_{11} & A_{12} \\ A_{21} & A_{22} \end{bmatrix} \begin{bmatrix} \delta\dot{\varphi} \\ \delta\varphi \end{bmatrix} + \begin{bmatrix} B_{11} & B_{12} \\ B_{21} & B_{22} \end{bmatrix} \begin{bmatrix} \delta H(\Delta\omega) \\ \delta\beta_0 \end{bmatrix}$$

$$\begin{bmatrix} \delta\beta \\ \delta\Delta\beta \end{bmatrix} = \begin{bmatrix} C_{11} & C_{12} \\ C_{21} & C_{22} \end{bmatrix} \begin{bmatrix} \delta\dot{\varphi} \\ \delta\varphi \end{bmatrix} + \begin{bmatrix} D_{11} & D_{12} \\ D_{21} & D_{22} \end{bmatrix} \begin{bmatrix} \delta H(\Delta\omega) \\ \delta\beta_0 \end{bmatrix}$$

$$A_{11} = 0$$

$$B_{11} = 0$$

$$A_{12} = 1$$

$$B_{12} = 0$$

$$A_{21} = -c$$

$$B_{21} = c$$

$$A_{22} = -b$$

$$B_{22} = 0$$

$$C_{11} = \frac{1}{g'(\beta)}$$

$$D_{11} = 0$$

$$C_{12} = 0$$

$$D_{12} = \frac{g'(\beta_0)}{g'(\beta)}$$

$$C_{21} = \frac{1}{g'(\beta)}$$

$$D_{21} = 0$$

$$C_{22} = 0$$

$$D_{22} = \frac{g'(\beta_0)}{g'(\beta)} - 1$$

Calculating $\delta\hat{V}$:

$$[\delta\dot{\zeta}] = [A_{11}][\delta\zeta] + [B_{11} \quad B_{12} \quad B_{13} \quad B_{14} \quad B_{15}] \begin{bmatrix} \delta\Delta\omega \\ \delta\beta_0 \\ \delta\Delta\beta \\ \delta T_0 \\ \delta\Delta T \end{bmatrix}$$

Appendix III: Linearisation (Without Induction)

$$[\delta\hat{V}] = [C_{11}][\delta\zeta] + [D_{11} \quad D_{12} \quad D_{13} \quad D_{14} \quad D_{15}] \begin{bmatrix} \delta\Delta\omega \\ \delta\beta_0 \\ \delta\Delta\beta \\ \delta T_0 \\ \delta\Delta T \end{bmatrix}$$

$$A_{11} = -\frac{1}{\alpha}$$

$$B_{11} = B - \frac{J}{\alpha}$$

$$B_{12} = 0$$

$$B_{13} = 0$$

$$B_{14} = 1$$

$$B_{15} = 1$$

$$C_{11} = -\frac{\delta C_{ql}}{\delta X} \frac{2N^3}{\rho\pi R^5} \frac{1}{(\omega^2\alpha)} \frac{\omega R}{N\hat{\lambda}^2}$$

$$D_{11} = \frac{\partial C_{ql}}{\partial X} \frac{\omega R}{N\hat{\lambda}^2} \frac{4QN^3}{\omega^3\rho\pi R^5} - \frac{\omega R}{N\hat{\lambda}^2} \frac{\partial C_{ql}}{\partial X} \frac{2N^3J}{\rho\pi R^5\omega^2\alpha} + \frac{R}{N\hat{\lambda}}$$

$$D_{12} = -\frac{\omega R}{N\hat{\lambda}^2} \frac{\delta C_{ql}}{\delta\beta}$$

$$D_{13} = -\frac{\omega R}{N\hat{\lambda}^2} \frac{\delta C_{ql}}{\delta\beta}$$

$$D_{14} = 0$$

$$D_{15} = 0$$

Calculating $\delta\Delta\omega$:

$$[\delta\Delta\omega] = [A_{11}][\delta\Delta\omega] + [B_{11} \quad B_{12} \quad B_{13} \quad B_{14} \quad B_{15} \quad B_{16}] \begin{bmatrix} \delta\Delta P \\ \delta T_0 \\ \delta\omega \\ \delta\hat{V} \\ \delta\beta \\ \delta\beta_0 \end{bmatrix}$$

$$\begin{bmatrix} \delta\Delta\omega \\ \delta\Delta T \end{bmatrix} = [C_{11} \quad C_{12}][\delta\Delta\omega] + \begin{bmatrix} D_{11} & D_{12} & D_{13} & D_{14} & D_{15} & D_{16} \\ D_{21} & D_{22} & D_{23} & D_{24} & D_{25} & D_{26} \end{bmatrix} \begin{bmatrix} \delta\Delta P \\ \delta T_0 \\ \delta\omega \\ \delta\hat{V} \\ \delta\beta \\ \delta\beta_0 \end{bmatrix}$$

Appendix III: Linearisation (Without Induction)

$$A_{11} = \frac{1}{J} \left(\frac{T_0}{w} - \frac{\frac{1}{2} \rho \pi R^2 \hat{V}^3 C_p(\hat{\lambda}_0, \beta_0)}{(\omega - \Delta\omega)^2} + \frac{1}{2} \rho \pi R^2 \hat{V}^3 \frac{\partial C_p}{\partial \hat{\lambda}_0} \frac{1}{\omega - \Delta\omega} \frac{R}{N\hat{V}} + B \right)$$

$$B_{11} = -\frac{1}{J\omega}$$

$$B_{12} = \frac{\Delta\omega}{\omega J}$$

$$B_{13} = \frac{1}{J} \left(\frac{\Delta P}{\omega^2} - \frac{\Delta\omega T_0}{\omega^2} - \hat{V}^3 \frac{C_p(\hat{\lambda}, \beta)}{w^2} \frac{1}{2} \rho \pi R^2 + \frac{1}{2} \rho \pi R^2 \hat{V}^3 \frac{\partial C_p}{\partial \hat{\lambda}} \frac{1}{\omega} \frac{R}{N\hat{V}} \right. \\ \left. - \frac{1}{2} \rho \pi R^2 \hat{V}^3 \frac{\partial C_p}{\partial \hat{\lambda}_0} \frac{1}{\omega - \Delta\omega} \frac{R}{N\hat{V}} + \hat{V}^3 \frac{C_p(\hat{\lambda}_0, \beta_0)}{(\omega - \Delta\omega)^2} \frac{1}{2} \rho \pi R^2 \right)$$

$$B_{14} = \frac{1}{J} \left(\frac{\frac{3}{2} \rho \pi R^2 \hat{V}^2 C_p(\lambda, \beta)}{\omega} - \frac{\frac{3}{2} \rho \pi R^2 \hat{V}^2 C_p(\hat{\lambda}_0, \beta_0)}{\omega - \Delta\omega} - \frac{1}{2} \rho \pi R^2 \hat{V}^3 \frac{\partial C_p}{\partial \hat{\lambda}} \frac{R}{N\hat{V}^2} \right. \\ \left. + \frac{1}{2} \rho \pi R^2 \hat{V}^3 \frac{\partial C_p}{\partial \hat{\lambda}_0} \frac{R}{N\hat{V}^2} \right)$$

$$B_{15} = \frac{1}{J} \left(\frac{1}{2} \rho \pi R^2 \hat{V}^3 \frac{\partial C_p}{\partial \beta} \frac{1}{\omega} \right)$$

$$B_{16} = -\frac{1}{J} \left(\frac{1}{2} \rho \pi R^2 \hat{V}^3 \frac{\partial C_p}{\partial \beta_0} \frac{1}{\omega - \Delta\omega} \right)$$

$$C_{11} = 1;$$

$$C_{12} = -\frac{T_0}{\omega}$$

$$D_{11} = 0$$

$$D_{12} = 0$$

$$D_{13} = 0$$

$$D_{14} = 0$$

$$D_{15} = 0$$

$$D_{16} = 0$$

Appendix III: Linearisation (Without Induction)

$$D_{21} = \frac{1}{\omega}$$

$$D_{22} = -\frac{\Delta\omega}{\omega}$$

$$D_{23} = -\frac{\Delta P}{\omega^2} + \frac{\Delta\omega}{\omega^2} T_0$$

$$D_{24} = 0$$

$$D_{25} = 0$$

$$D_{26} = 0$$

Appendix IV.

Linearisation with Induction

With reference to Figure 182, the state space equations for the linearisation of the Power Adjusting Controller are given below:

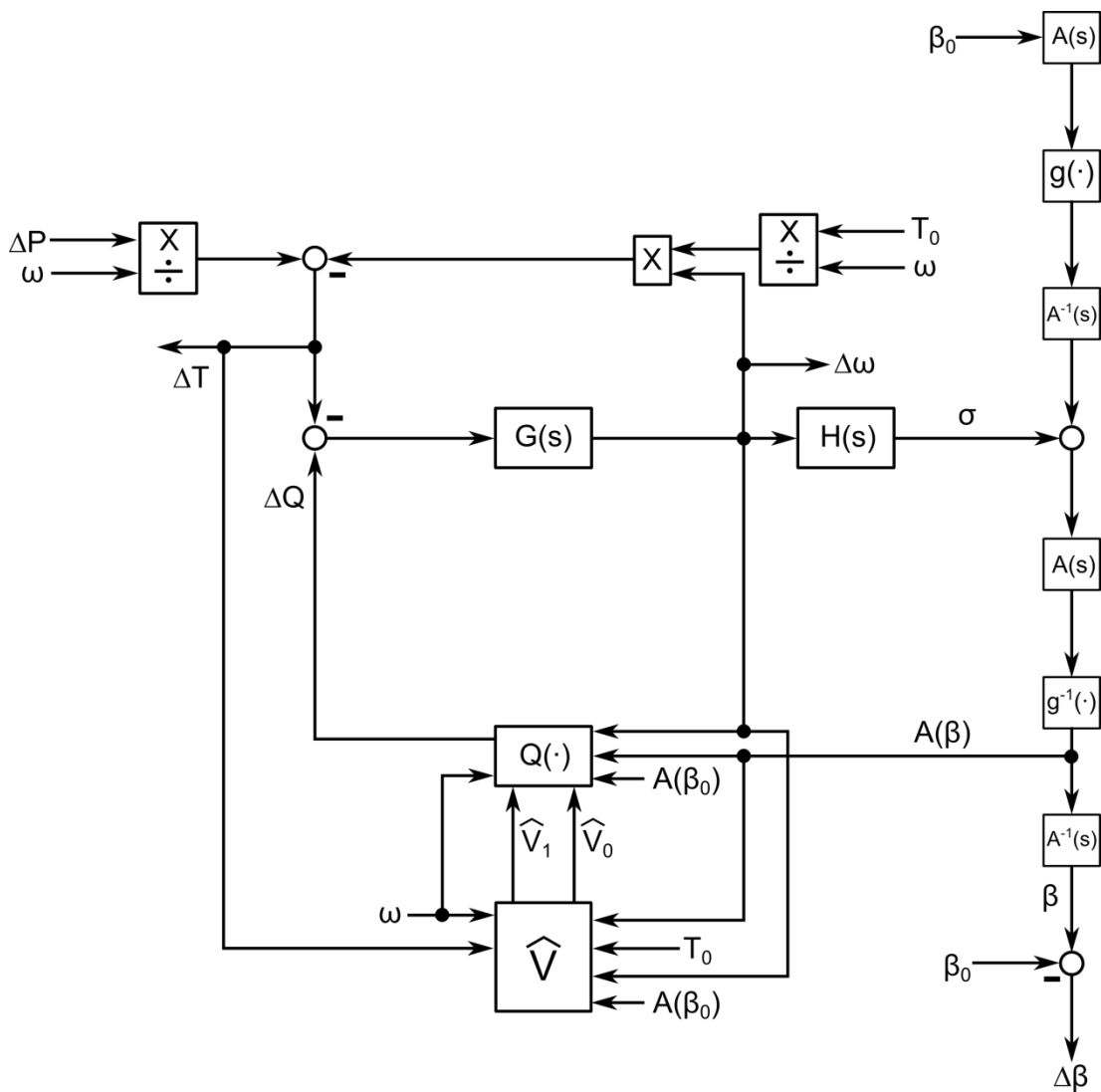


Figure 182: PAC Layout with Induction

Appendix IV: Linearisation (With Induction)

Note that all variables correspond to the value at the equilibrium point. The values β and β_0 refer to the values passed through the dynamics of the pitch actuator. At an equilibrium point, $\hat{V}_\infty = \hat{V}_1 = \hat{V}_0$ and so for ease of notation the symbol V is used for them all.

Define:

$$K_1 = \frac{1}{\omega - \Delta\omega} \left(\frac{C_p(\lambda_0, \beta_0)}{\omega - \Delta\omega} - \left(\frac{\partial C_p}{\partial \lambda_0} \frac{R}{NV} - \frac{3C_p(\lambda_0, \beta_0)}{V} \frac{1}{(1-a_0)^2} \frac{\partial A_s}{\partial \lambda_{R0}} \frac{R}{N} + \frac{\partial C_p}{\partial \lambda_0} \frac{R\omega}{NV^2} \frac{1}{(1-a_0)^2} \frac{\partial A_s}{\partial \lambda_{R0}} \frac{R}{N} \right) + B_{PAC} \right)$$

$$K_2 = \frac{1}{\omega - \Delta\omega} \left(\frac{\partial C_p}{\partial \beta_0} + 3C_p(\lambda_0, \beta_0) \frac{1}{1-a_0} \frac{\partial A_s}{\partial \beta_0} - \frac{\partial C_p}{\partial \beta_0} \frac{R(\omega - \Delta\omega)}{NV} \frac{1}{1-a_0} \frac{\partial A_s}{\partial \beta_0} \right)$$

$$K_3 = \frac{1}{\omega - \Delta\omega} \left(-3C_p(\lambda_0, \beta_0) \frac{1}{1-a_0} + 3C_p(\lambda_0, \beta_0) \frac{1}{(1-a_0)^3} \frac{\partial A_s}{\partial \lambda_{R0}} \lambda_0 - \frac{\partial C_p}{\partial \lambda_0} \lambda_0 \frac{1}{a_0 - 1} - \frac{\partial A_s}{\partial \lambda_{R0}} \frac{\lambda_0}{(1-a_0)^3} \frac{\partial C_p}{\partial \lambda_0} \lambda_0 \right)$$

$$K_4 = \frac{3\pi}{4R} V \left(1 - \frac{\partial C_p}{\partial \lambda_0} \frac{\lambda_0}{(1-a_0)^2} \right)$$

$$K_5 = \frac{3\pi}{4R} V \frac{\partial A_s}{\partial \beta_0}$$

$$K_6 = \frac{3\pi}{4R} \left(\frac{\partial A_s}{\partial \lambda_{R0}} \frac{1}{1-a_0} \frac{R}{N} \right)$$

$$K_7 = \frac{1}{\omega} \frac{\rho\pi R^2 V^3}{\omega} \left(\frac{C_p(\lambda, \beta)}{\omega} - \frac{\partial C_p}{\partial \lambda} \frac{R}{NV} - 3 \frac{C_p(\lambda, \beta)}{V} \frac{1}{(1-a)^2} \frac{\partial A_s}{\partial \lambda_R} \frac{R}{N} + \frac{\partial C_p}{\partial \lambda} \frac{R\omega}{NV^2} \frac{1}{(1-a)^2} \frac{\partial A_s}{\partial \lambda_R} \frac{R}{N} \right) + B_{PAC}$$

$$K_8 = \frac{1}{\omega} \frac{\rho\pi R^2 V^3}{\omega} \left(\frac{\partial C_p}{\partial \beta} + 3C_p(\lambda, \beta) \frac{1}{1-a} \frac{\partial A_s}{\partial \beta} - \frac{\partial C_p}{\partial \lambda} \frac{R\omega}{NV} \frac{1}{1-a} \frac{\partial A_s}{\partial \beta} \right)$$

Appendix IV: Linearisation (With Induction)

$$K_9 = \frac{1}{2} \frac{\rho \pi R^2 V^3}{\omega} \left(-3C_p(\lambda, \beta) \frac{1}{1-a} + 3C_p(\lambda, \beta) \frac{1}{(1-a)^3} \frac{\partial A_s}{\partial \lambda_R} \lambda - \frac{\partial C_p}{\partial \lambda} \lambda \frac{1}{a-1} - \frac{\partial A_s}{\partial \lambda_R} \frac{\lambda}{(1-a)^3} \frac{\partial C_p}{\partial \lambda} \lambda \right)$$

$$K_{10} = \frac{3\pi}{4R} V \left(1 - \frac{\partial A_s}{\partial \lambda_R} \frac{\lambda}{(1-a)^2} \right)$$

$$K_{11} = \frac{3\pi}{4R} V \frac{\partial A_s}{\partial \beta}$$

$$K_{12} = \frac{3\pi}{4R} \frac{\partial A_s}{\partial \lambda_R} \frac{1}{1-a} \frac{R}{N}$$

Starting from $\delta\Delta\omega$:

$$[\delta\dot{x}] = [A_{11}][\delta x] + [B_{11}][\delta\Delta\omega]$$

$$[\delta\sigma] = [C_{11}][\delta x] + [D_{11}][\delta\Delta\omega]$$

$$A_{11} = 0$$

$$B_{11} = 1$$

$$C_{11} = K_G K_i$$

$$D_{11} = K_G K_p$$

Finding the change in pitch angle $\Delta\beta$ and the total pitch β :

$$\begin{bmatrix} \delta\dot{\varphi} \\ \delta\dot{\varphi} \end{bmatrix} = \begin{bmatrix} A_{11} & A_{12} \\ A_{21} & A_{22} \end{bmatrix} \begin{bmatrix} \delta\dot{\varphi} \\ \delta\varphi \end{bmatrix} + \begin{bmatrix} B_{11} & B_{12} \\ B_{21} & B_{22} \end{bmatrix} \begin{bmatrix} \delta H(\Delta\omega) \\ \delta\beta_0 \end{bmatrix}$$

$$\begin{bmatrix} \delta\beta \\ \delta\Delta\beta \end{bmatrix} = \begin{bmatrix} C_{11} & C_{12} \\ C_{21} & C_{22} \end{bmatrix} \begin{bmatrix} \delta\dot{\varphi} \\ \delta\varphi \end{bmatrix} + \begin{bmatrix} D_{11} & D_{12} \\ D_{21} & D_{22} \end{bmatrix} \begin{bmatrix} \delta H(\Delta\omega) \\ \delta\beta_0 \end{bmatrix}$$

$$A_{11} = 0$$

$$B_{11} = 0$$

$$A_{12} = 1$$

$$B_{12} = 0$$

$$A_{21} = -c$$

$$B_{21} = c$$

$$A_{22} = -b$$

$$B_{22} = 0$$

Appendix IV: Linearisation (With Induction)

$$C_{21} = \frac{1}{g'(\beta)}$$

$$C_{22} = 0$$

$$D_{21} = 0$$

$$D_{22} = \frac{g'(\beta_0)}{g'(\beta)} - 1$$

Calculating δV_∞ :

$$\begin{bmatrix} \delta \dot{a} \\ \delta \dot{\zeta} \end{bmatrix} = \begin{bmatrix} A_{11} & A_{12} \\ A_{21} & A_{22} \end{bmatrix} \begin{bmatrix} \delta a \\ \delta \zeta \end{bmatrix} + \begin{bmatrix} B_{11} & B_{12} & B_{13} & B_{14} & B_{15} & B_{16} \\ B_{21} & B_{22} & B_{23} & B_{24} & B_{25} & B_{26} \end{bmatrix} \begin{bmatrix} \delta \omega \\ \delta \beta_0 \\ \delta \Delta \beta \\ \delta T_0 \\ \delta \Delta \omega \\ \delta \Delta P \end{bmatrix}$$

$$[\delta V_\infty] = \begin{bmatrix} C_{11} \\ C_{21} \end{bmatrix} \begin{bmatrix} \delta a \\ \delta \zeta \end{bmatrix} + \begin{bmatrix} D_{11} & D_{12} & D_{13} & D_{14} & D_{15} & D_{16} \\ D_{21} & D_{22} & D_{23} & D_{24} & D_{25} & D_{26} \end{bmatrix} \begin{bmatrix} \delta \omega \\ \delta \beta_0 \\ \delta \Delta \beta \\ \delta T_0 \\ \delta \Delta \omega \\ \delta \Delta P \end{bmatrix}$$

Where:

$$K = \frac{3\pi}{4R}$$

$$A_{11} = -K\hat{V}$$

$$A_{12} = \frac{K}{\alpha} \left(\hat{V} \frac{\partial C_t}{\partial \lambda} \frac{1}{\sqrt{(16 - 16C_t)}} \frac{\partial C_{ql}}{\partial X} \frac{2N^3}{\rho\pi R^5 \omega^2} - \frac{(a_s - a)\omega R}{N\hat{\lambda}^2} \frac{\partial C_{ql}}{\partial X} \frac{2N^3}{\rho\pi R^5 \omega^2} \right)$$

$$A_{21} = 0$$

$$A_{22} = -\frac{1}{\alpha}$$

$$\begin{aligned} B_{11} = K & \left(\frac{R}{\lambda N} (a_s - a) + \frac{\omega R}{\lambda^2 N} (a_s - a) \frac{\partial C_{ql}}{\partial X} \frac{4N^3 Q}{\rho\pi R^5 \omega^3} \right. \\ & - V \frac{\partial C_t}{\partial \lambda} \frac{1}{\sqrt{(16 - 16C_t(\lambda, \beta))}} \frac{\partial C_{ql}}{\partial X} \frac{4N^3 Q}{\rho\pi R^5 \omega^3} \\ & + \frac{J_{PAC}}{\alpha} V \frac{\partial C_t}{\partial \lambda} \frac{1}{\sqrt{(16 - 16C_t(\lambda, \beta))}} \frac{\partial C_{ql}}{\partial X} \frac{2N^3}{\rho\pi R^5 \omega^2} \\ & \left. - \frac{J_{PAC}}{\alpha} \frac{\omega R}{\lambda^2 N} (a_s - a) \frac{\partial C_{ql}}{\partial X} \frac{2N^3}{\rho\pi R^5 \omega^2} \right) \end{aligned}$$

Appendix IV: Linearisation (With Induction)

$$B_{12} = K \left(V \frac{\partial C_t}{\partial \lambda} \frac{1}{\sqrt{(16 - 16C_t(\lambda, \beta))}} \frac{\partial C_{ql}}{\partial \beta} + V \frac{\partial C_t}{\partial \beta} \frac{1}{\sqrt{(16 - 16C_t(\lambda, \beta))}} \right. \\ \left. - (a_s - a) \frac{\omega R}{N \lambda^2} \frac{\partial C_{ql}}{\partial \beta} \right)$$

$$B_{13} = K \left(V \frac{\partial C_t}{\partial \lambda} \frac{1}{\sqrt{(16 - 16C_t(\lambda, \beta))}} \frac{\partial C_{ql}}{\partial \beta} + V \frac{\partial C_t}{\partial \beta} \frac{1}{\sqrt{(16 - 16C_t(\lambda, \beta))}} \right. \\ \left. - (a_s - a) \frac{\omega R}{N \lambda^2} \frac{\partial C_{ql}}{\partial \beta} \right)$$

$$B_{14} = 0$$

$$B_{15} = 0$$

$$B_{16} = 0$$

$$B_{21} = B_{PAC} - \frac{J_{PAC}}{\alpha} - \frac{\Delta P}{\omega^2} + \frac{\Delta \omega T_0}{\omega^2}$$

$$B_{22} = 0$$

$$B_{23} = 0$$

$$B_{24} = 1 - \frac{\Delta \omega}{\omega}$$

$$B_{25} = -\frac{T_0}{\omega}$$

$$B_{26} = \frac{1}{\omega}$$

$$C_{11} = \frac{(1 - a_s)}{(1 - a)^2} V$$

$$C_{21} = -\frac{1 - a_s}{1 - a} \frac{\omega R}{\lambda^2 N} \frac{\partial C_{ql}}{\partial X} \frac{2N^3}{\rho \pi R^5 \omega^2} \frac{1}{\alpha} - \frac{V}{1 - a} \frac{\partial C_t}{\partial \lambda} \frac{1}{\sqrt{(16 - 16C_t)}} \frac{\partial C_{ql}}{\partial X} \frac{2N^3}{\rho \pi R^5 \omega^2} \frac{1}{\alpha}$$

Appendix IV: Linearisation (With Induction)

$$D_{11} = \frac{1 - a_s}{1 - a} \frac{R}{\lambda N} - \frac{\omega R}{\lambda^2 N} \frac{\partial C_{ql}}{\partial X} \frac{2N^3}{\rho \pi R^5 \omega^2} \frac{J_{PAC}}{\alpha} + \frac{\omega R}{\lambda^2 N} \frac{\partial C_{ql}}{\partial X} \frac{4QN^3}{\rho \pi R^5 \omega^3}$$

$$- \frac{V}{1 - a} \frac{\partial C_t}{\partial \lambda} \frac{1}{\sqrt{(16 - 16C_t)}} \frac{\partial C_{ql}}{\partial X} \frac{2N^3}{\rho \pi R^5 \omega^2} \frac{J_{PAC}}{\alpha}$$

$$+ \frac{V}{1 - a} \frac{\partial C_t}{\partial \lambda} \frac{1}{\sqrt{(16 - 16C_t)}} \frac{\partial C_{ql}}{\partial X} \frac{4QN^3}{\rho \pi R^5 \omega^3}$$

$$D_{12} = \frac{1 - a_s}{1 - a} \left(-\frac{\partial C_{ql}}{\partial \beta} \frac{\omega R}{\lambda^2 N} \right) - \frac{V}{1 - a} \frac{\partial C_t}{\partial \lambda} \frac{1}{\sqrt{(16 - 16C_t)}} \frac{\partial C_{ql}}{\partial \beta} - \frac{V}{1 - a} \frac{1}{\sqrt{(16 - 16C_t)}} \frac{\partial C_t}{\partial \beta}$$

$$D_{13} = \frac{1 - a_s}{1 - a} \left(-\frac{\partial C_{ql}}{\partial \beta} \frac{\omega R}{\lambda^2 N} \right) - \frac{V}{1 - a} \frac{\partial C_t}{\partial \lambda} \frac{1}{\sqrt{(16 - 16C_t)}} \frac{\partial C_{ql}}{\partial \beta} - \frac{V}{1 - a} \frac{1}{\sqrt{(16 - 16C_t)}} \frac{\partial C_t}{\partial \beta}$$

$$D_{14} = 0$$

$$D_{15} = 0$$

$$D_{16} = 0$$

Calculating $\delta \hat{V}_1$:

$$[\delta \hat{a}_1] = [A_{11}][\delta a_1] + [B_{11} \quad B_{12} \quad B_{13} \quad B_{14}] \begin{bmatrix} \delta w \\ \delta \beta_0 \\ \delta \Delta \beta \\ \delta V_\infty \end{bmatrix}$$

$$[\delta V_1] = [C_{11}][\delta a_1] + [D_{11} \quad D_{12} \quad D_{13} \quad D_{14}] \begin{bmatrix} \delta w \\ \delta \beta_0 \\ \delta \Delta \beta \\ \delta V_\infty \end{bmatrix}$$

Where:

$$A_{11} = -K_{10}$$

$$B_{11} = K_{12}$$

$$B_{12} = K_{11}$$

$$B_{13} = K_{11}$$

$$B_{14} = K \left(\frac{1 - a}{1 - a_s} (a_s - a) - \frac{V_\infty (a - 1)^2}{(a_s - 1)^2} \frac{\partial A_s}{\partial \lambda_R} \frac{1}{1 - a} \frac{R\omega}{V_\infty^2 N} \right)$$

Calculating $\delta \hat{V}_0$:

Appendix IV: Linearisation (With Induction)

$$[\delta \dot{a}_0] = [A_{11}][\delta a_0] + [B_{11} \quad B_{12} \quad B_{13} \quad B_{14}] \begin{bmatrix} \delta w \\ \delta \Delta \omega \\ \delta \beta_0 \\ \delta V_\infty \end{bmatrix}$$

$$[\delta V_0] = [C_{11}][\delta a_0] + [D_{11} \quad D_{12} \quad D_{13} \quad D_{14}] \begin{bmatrix} \delta w \\ \delta \beta_0 \\ \delta \Delta \beta \\ \delta V_\infty \end{bmatrix}$$

Where:

$$A_{11} = -K_4$$

$$B_{11} = K_6$$

$$B_{12} = -K_6$$

$$B_{13} = K_5$$

$$B_{14} = K \left(\frac{1 - a_0}{1 - a_{s0}} (a_{s0} - a_0) - \frac{V_\infty (a_0 - 1)^2}{(a_{s0} - 1)^2} \frac{\partial A_s}{\partial \lambda_{R0}} \frac{1}{1 - a_0} \frac{R(\omega - \Delta \omega)}{V_\infty^2 N} \right)$$

Calculating $\delta \Delta \omega$

$$[\delta \dot{\omega}] = [A_{11}][\delta \omega] + [B_{11} \quad B_{12} \quad B_{13} \quad B_{14} \quad B_{15} \quad B_{16} \quad B_{17}] \begin{bmatrix} \delta \Delta P \\ \delta T_0 \\ \delta w \\ \delta a_1 \\ \delta \beta \\ \delta a_0 \\ \delta \beta_0 \end{bmatrix}$$

$$[\delta \Delta T] = \begin{bmatrix} C_{11} \\ C_{21} \end{bmatrix} [\delta \omega] + \begin{bmatrix} D_{11} & D_{12} & D_{13} & D_{14} & D_{15} & D_{16} & D_{17} \\ D_{21} & D_{22} & D_{23} & D_{24} & D_{25} & D_{26} & D_{27} \end{bmatrix} \begin{bmatrix} \delta \Delta P \\ \delta T_0 \\ \delta w \\ \delta a_1 \\ \delta \beta \\ \delta a_0 \\ \delta \beta_0 \end{bmatrix}$$

Where:

$$A_{11} = \frac{1}{J_{PAC}} \left(\frac{T_0}{\omega} - K_1 \right);$$

$$B_{11} = -\frac{1}{J_{PAC} \omega}$$

$$B_{12} = \frac{\Delta \omega}{\omega J_{PAC}}$$

Appendix IV: Linearisation (With Induction)

$$B_{13} = \frac{1}{J_{PAC}} \left(\frac{\Delta P}{\omega^2} - \frac{\Delta \omega T_0}{\omega^2} + K_1 - K_7 \right)$$

$$B_{14} = \frac{1}{J_{PAC}} K_9$$

$$B_{15} = \frac{1}{J_{PAC}} K_8$$

$$B_{16} = \frac{1}{J_{PAC}} K_3$$

$$B_{17} = \frac{1}{J_{PAC}} K_2$$

$$C_{11} = 1$$

$$C_{21} = -\frac{T_0}{\omega}$$

$$D_{11} = 0$$

$$D_{12} = 0$$

$$D_{13} = 0$$

$$D_{14} = 0$$

$$D_{15} = 0$$

$$D_{16} = 0$$

$$D_{17} = 0$$

$$D_{21} = \frac{1}{\omega}$$

$$D_{22} = -\frac{\Delta \omega}{\omega}$$

$$D_{23} = -\frac{\Delta P}{\omega^2} + \frac{\Delta \omega}{\omega^2} T_0$$

$$D_{24} = 0$$

$$D_{25} = 0$$

$$D_{26} = 0$$

$$D_{27} = 0$$

Appendix V.

PAC Supervisory Rules

Summary

The PAC supervisory rules are implemented in the PAC to ensure that the turbine is kept in a safe operating regime. The occurrence of events triggered by these rules is communicated between the PAC and wind farm controller using flags residing in the PAC. (Capital letters are used to indicate flag names with sub-flags in bracketed italics) There are two sets of rules, black rules defined by a boundary on the torque/speed plane that act as a hard limit and traffic light rules, defined by two concentric boundaries contained within the black rules boundary, that act as soft limits. Maximum aerodynamic and drive-train torque boundaries apply. The regions inside the inner traffic light boundary, between the inner and outer traffic light boundaries and outside the outer traffic light boundary are designated green, amber and red, respectively.

General supervisory rules:

- The requested change in power, rate of change in power and pitch rates are subject to limits and the permissible turbulence intensity and wind speed are subject to upper and lower limits, respectively. These limits and events designated high priority, e.g. requests for synthetic inertia, are defined with agreement and cannot be changed without agreement of the OEM.
- The PAC is turned on when the PAC ON flag is set at a request from the wind farm controller.
- The PAC is turned off when the PAC ON flag is reset by either the PAC itself or by the PAC at a request from the wind farm controller. The PAC goes

Appendix V: PAC Supervisory Rules Summary

into recovery mode and the RECOVERY flag is set. The speed of recovery is fast or slow depending on the setting of the RECOVERY (*Fast/Slow*) flag and sub-flag. The sub-flag (*Fast/Slow*) can be reset at the request of the wind farm controller. The default setting is RECOVERY (*Fast*). During the recovery mode the PAC rejects any requested change in power. The REJECTION (*Recovery*) flag is set by the PAC. On completion of recovery mode the RECOVERY (*Complete*) flag and sub-flag are set and the PAC ON flag is reset.

- Only black supervisory rules apply to high priority events. The PRIORITY flag is set by the PAC at a request from the wind farm controller.
- If the limit for requested change in power is exceeded, the REJECTION (*Power*) flag is set by the PAC.
- If the limit for requested change of power rate limit is exceeded and the PRIORITY flag is not set, the rate limit applies and the REJECTION (*Power rate*) flag is set by the PAC.
- If the turbulence intensity limit is exceeded, the PAC ON flag is reset and latched and the PAC ON (*Turbulence*) sub-flag is set and latched by the PAC.
- If the actuator pitch rate limits are violated by the turbine full envelope controller, the PAC ON flag is reset indefinitely and the PAC ON (*Actuator*) sub-flag set indefinitely by the PAC.
- If the low wind speed limit is exceeded, the PAC ON flag is reset and latched and the PACON (*Wind Speed*) sub-flag is set and latched by the PAC.
- If the turbine state is divergent such that normal operation is unreachable, the DIVERGENT flag is set by the PAC.

Black supervisory rules:

- The boundary and maximum possible generator reaction torque are set with agreement and cannot be changed without agreement of the OEM.
- The boundary should not be crossed under any circumstances. If the turbine state is outside the boundary the PAC ON flag is reset by the PAC.

Appendix V: PAC Supervisory Rules Summary

- On the turbine state reaching the boundary, the REJECTION (*Limit*) flag and sub-flag are set by the PAC.
- If the turbine state remains on the boundary beyond a pre-set time limit, the PAC ON flag is reset by the PAC.
- On a section of the boundary corresponding to the maximum possible generator reaction torque, the permitted time limit before resetting the PAC ON flag is zero.

Traffic light supervisory rules:

- The boundaries can be set at a request from wind farm controller.
- The maximum magnitude of change of power in all regions can be set by the wind farm controller subject to the fixed upper limit, the maximum magnitude for the amber region being less than the maximum for the green region and the maximum/minimum change of power for that part of the red region to the left/right of the operating strategy being zero.
- When the turbine state is in the green/amber/red region, the corresponding GREEN/AMBER/RED flag is set by the PAC.
- When the demanded change in power exceeds the maximum or minimum, the corresponding REJECTION (*Green Limit*)/(*Amber Limit*)/(*Red Limit*) flag and sub-flag are set by the PAC.

Appendix VI.

PI Controller Gains and Gain Scheduling

The values for K_I , and K_P for the 1.5MW and 5MW wind turbines are shown in Table 9.

Table 9: Integral and Proportional Gains

Turbine	K_I	K_P
1.5MW	0.00064	0.02
5MW	0.00032	0.04

The gain scheduling for the 5MW wind turbine without the component dependent upon generator speed ($K_{GS} = \frac{\omega_{rated}^2}{\omega^2}$) is given in Table 10.

Table 10: Gain Scheduling for the 5MW Wind Turbine

Wind Speed	Gain Scheduling Value
6	1.75
6.5	1.66
7	1.58
7.5	1.53
8	1.47
8.5	1.42
9	1.38
9.5	1.34
10	1.28
10.5	1.17
11	1.08
11.5	1

Appendix VI: PI Controller Gains and Gain Scheduling

12	1.26
12.5	1.45
13	1.57
13.5	1.67
14	1.77
14.5	1.84
15	1.9
15.5	1.95
16	2.02
16.5	2.09
17	2.16
17.5	2.21
18	2.25
18.5	2.3
19	2.36
19.5	2.42
20	2.48
20.5	2.54
21	2.6
21.5	2.66
22	2.72
22.5	2.79
23	2.85
23.5	2.92
24	2.99
24.5	3.06
25	3.13

The gain scheduling for the 1.5MW wind turbine without the component dependent upon generator speed ($K_{GS} = \frac{\omega_{rated}^2}{\omega^2}$) is given in Table 11.

Table 11: Gain Scheduling for the 1.5MW Wind Turbine

Wind Speed	Gain Scheduling Value
6.5	1.58
7	1.57
7.5	1.59
8	1.62
8.5	1.46
9	1.37
9.5	1.3
10	1.36

Appendix VI: PI Controller Gains and Gain Scheduling

10.5	1.1
11	0.99
11.5	1
12	1.17
12.5	1.28
13	1.35
13.5	1.4
14	1.44
14.5	1.45
15	1.48
15.5	1.52
16	1.57
16.5	1.61
17	1.64
17.5	1.67
18	1.7
18.5	1.73
19	1.76
19.5	1.79
20	1.82
20.5	1.87
21	1.94
21.5	2
22	2.05
22.5	2.09
23	2.14
23.5	2.2
24	2.25
24.5	2.31
25	2.36